



UNIVERSITAT DE
BARCELONA

Role of carnitine palmitoyltransferase 1A as a downstream effector of ghrelin in cortical neurons and hypothalamus

Joan Francesc Mir Bonnín

ADVERTIMENT. La consulta d'aquesta tesi queda condicionada a l'acceptació de les següents condicions d'ús: La difusió d'aquesta tesi per mitjà del servei TDX (www.tdx.cat) i a través del Dipòsit Digital de la UB (diposit.ub.edu) ha estat autoritzada pels titulars dels drets de propietat intel·lectual únicament per a usos privats emmarcats en activitats d'investigació i docència. No s'autoritza la seva reproducció amb finalitats de lucre ni la seva difusió i posada a disposició des d'un lloc aliè al servei TDX ni al Dipòsit Digital de la UB. No s'autoritza la presentació del seu contingut en una finestra o marc aliè a TDX o al Dipòsit Digital de la UB (framing). Aquesta reserva de drets afecta tant al resum de presentació de la tesi com als seus continguts. En la utilització o cita de parts de la tesi és obligat indicar el nom de la persona autora.

ADVERTENCIA. La consulta de esta tesis queda condicionada a la aceptación de las siguientes condiciones de uso: La difusión de esta tesis por medio del servicio TDR (www.tdx.cat) y a través del Repositorio Digital de la UB (diposit.ub.edu) ha sido autorizada por los titulares de los derechos de propiedad intelectual únicamente para usos privados enmarcados en actividades de investigación y docencia. No se autoriza su reproducción con finalidades de lucro ni su difusión y puesta a disposición desde un sitio ajeno al servicio TDR o al Repositorio Digital de la UB. No se autoriza la presentación de su contenido en una ventana o marco ajeno a TDR o al Repositorio Digital de la UB (framing). Esta reserva de derechos afecta tanto al resumen de presentación de la tesis como a sus contenidos. En la utilización o cita de partes de la tesis es obligado indicar el nombre de la persona autora.

WARNING. On having consulted this thesis you're accepting the following use conditions: Spreading this thesis by the TDX (www.tdx.cat) service and by the UB Digital Repository (diposit.ub.edu) has been authorized by the titular of the intellectual property rights only for private uses placed in investigation and teaching activities. Reproduction with lucrative aims is not authorized nor its spreading and availability from a site foreign to the TDX service or to the UB Digital Repository. Introducing its content in a window or frame foreign to the TDX service or to the UB Digital Repository is not authorized (framing). Those rights affect to the presentation summary of the thesis as well as to its contents. In the using or citation of parts of the thesis it's obliged to indicate the name of the author.



UNIVERSITAT DE
BARCELONA

Departament de Bioquímica i Fisiologia
Facultat de Farmàcia

***Role of carnitine palmitoyltransferase 1A
as a downstream effector of ghrelin in
cortical neurons and hypothalamus***

Joan Francesc Mir Bonnín

2016



UNIVERSITAT^{DE}
BARCELONA

FACULTAT DE FARMÀCIA

Programa de doctorat en Biotecnologia

***Role of carnitine palmitoyltransferase 1A
as a downstream effector of ghrelin in cortical
neurons and hypothalamus***

Memòria presentada per Joan Francesc Mir Bonnín per optar al títol de Doctor per la Universitat de Barcelona.

Aquesta tesi s'ha realitzat sota la direcció de la Dra. Dolors Serra Cucurull i el Dr. Fausto García Hegardt, en la Secció de Bioquímica i Biologia Molecular, del Departament de Bioquímica i Fisiologia de la Facultat de Farmàcia de la Universitat de Barcelona.

Dra. Dolors Serra Cucurull

Dr. Fausto García Hegardt

Joan Francesc Mir

Barcelona, 2016

*A en Pep i na Joana,
perquè sempre he intentat que poguessin estar orgullosos del seu fill*

*A Alejandro,
porque tiene suficiente paciencia para ver en mí cosas buenas*

“Ciencia es todo aquello sobre lo cual siempre cabe discusión.”

José Ortega y Gasset

AGRAÏMENTS

En primera instància voldria agrair als meus directors de tesi la oportunitat que m'han brindat de fer la tesi en el nostre grup. Per una banda, em cal agrair a la Dra. Dolors Serra la paciència i els consells que m'ha anat donant a diari des que vaig trepitjar per primera vegada aquest laboratori, ja fa uns anys. Sempre se m'ha presentat com una persona de la que se'n pot aprendre cada dia i que en la seva implicació sempre ha anat un pas per endavant. D'altra banda, he d'agrair al Dr. Fausto García Hegardt la oportunitat que se'm va donar primer d'entrar al grup com a estudiant de llicenciatura i després en la obtenció del finançament per fer la tesi, sense el qual aquesta aventura no hagués començat. A part dels meus directors, he d'agrair a la Dra. Laura Herrero la seva capacitat de transmetre el seu entusiasme per la recerca i les seves ganes de millorar cada dia. També he de d'agrair a la Dra. Guillermina Asins els seus consells i les seves contagioses ganes de viure, i que a més em van atreure a jo per primera vegada al món de la recerca.

Després he d'agrair moltíssim a la Dra. Paula Mera les hores que va invertir en ensenyar-me moltes de les tècniques que he emprat a la tesi. A més d'esser una persona de la que val la pena aprendre científicament, ha estat una immillorable companya i amiga que vam enyorar molt quan va marxar del lab. D'altra banda, he d'agrair al Dr. Pep Orellana, el Dr. Kamil Makowski i la Dra. Mida Malandrino, per tots els bons moments que vam passar al laboratori i a fora del laboratori, durant els primers anys que vaig tenir al laboratori. A més voldria donar les gràcies a Mar Arasa per haver compartit durant els primers anys i el màster moltes hores de poiata. També voldria agrair a la futura Dra. Minéia Weber, perquè encara no n'és conscient de com l'estic enyorant i com l'enyoraré després de totes les aventures i desventures que hem passat plegats compartint aquests anys de la tesi. A la Dra. María Calderón-Domínguez i la Dra. Raquel Fucho els hi he de donar gràcies perquè m'han ensenyat que tan important és tenir bon criteri científic com tenir bon criteri per a la vida en general. M'ho he passat molt bé amb vosaltres, nines i vos enyoraré molt. Esper que ens tornem a trobar en el futur.

A més he d'agrair moltíssim a la Dra. Cristina Suñol i al Dr. Matthieu Lichtenstein, per haver tengut ganes d'ajudar-me amb la recerca de la tesi. Especialment a en Matthieu per haver-me ensenyat les tècniques que han permès fer gran part dels experiments amb els cultius primaris corticals. En el mateix sentit, voldria agrair a la Dra. Josefina Casas i la Dra. Gemma Fabriàs per la imprescindible ajuda que ens han donat per l'anàlisi lipídica del MBH i també a la Dra. Antònia Ribes i la Dra. Judit Garcia per l'inestimable ajuda que ens han donat per l'anàlisi dels intermediaris del cicle de Krebs. Certament sense aquestes anàlisis el plantejament dels resultats de la tesi serien diferents. També he d'agrair a la Dra. Núria Casals i a tothom del seu laboratori de la Universitat Internacional de Catalunya per les discussions de resultats que fèiem gairebé setmanalment per la valuable ajuda que m'ha suposat durant la tesi, especialment a la Dra. Sara Ramírez, la Dra. Macarena Pozo i la Dra. Rosalía Rodríguez.

D'altra banda voldria donar gràcies a na Nina Steiner, en Fran García, na Blanca Balañá, en Jordi Capdevila i na Sandra Recalde als que esper no haver fet embolicar massa la troca mentre els ajudava amb els seus projectes. També voldria agrair a tota la resta de persones que han passat pel lab, pels moments que hem passat plegats que t'enriqueixen d'una manera o una altra, especialment a Anna Orozco, Alessandra Piccoli, Natascia Caroccia, Eduviges Bustos, Iván Paz, Éilis Sutton, Júlia Vallvé, Lorea Valcárcel, la Dra. Sofia Costa, el Dr. David Santos, la Dra. Mar Romero i el Dr. Martín Alcalá-Díaz. Esper no haver-me deixat ningú, perquè no m'ho podria perdonar, ja que durant tots aquests anys han passat moltes persones que d'una manera o una altra han estat importants en el dia a dia.

Després voldria agrair especialment la paciència que han tengut amb jo 3 persones especialment. D'una banda, mon pare i ma mare, en Pep i na Joana, que sempre han estat a l'aguait dels èxits i dels fracassos dels seus fills i que han perdonat la comunicació poc freqüent amb el seu fill. Esper poder-vos-ho compensar qualche dia. D'altra banda he d'agrair especialment al meu company d'aventures i riures per tot el temps i la serenor que m'ha anat dedicant aquests anys. Alejandro, gràcies per haver-me sabut dur a bon port. T'estimo i passi el que passi sempre t'estimaré.

Moltes gràcies!

ABSTRACT

Role of carnitine palmitoyltransferase 1A as a downstream effector of ghrelin in cortical neurons and hypothalamus

Previous studies have reported the importance of carnitine palmitoyltransferase (CPT) 1A as an essential part of downstream ghrelin signaling in the central nervous system (CNS) for the control of food intake. Lipid metabolism in the ventromedial hypothalamus (VMH) has emerged as a crucial pathway in the regulation of feeding and energy homeostasis. However, the relationship between changes in CPT1A activity and the intracellular downstream effectors in the VMH that contribute to appetite modulation is not fully understood, nor its possible involvement in central extra-hypothalamic functions of ghrelin.

In this work, we examine the effect of long-term expression of a permanently activated CPT1A isoform (CPT1AM) by using an adeno-associated viral vector, injected into the VMH of rats. CPT1AM overexpression produces a sustained increase in food intake which leads to overweight. Mechanistically, CPT1AM alters the lipidomic profile of mediobasal hypothalamus, provoking an increase in ceramides and sphingolipids and a decrease in phospholipids. Furthermore, we detect increased vesicular γ -aminobutyric acid transporter (VGAT) and reduced vesicular glutamate transporter 2 (VGLUT2) expressions. These changes are noteworthy, since both GABA and glutamate have been proposed to be mediators in food intake control.

This signature led us to assess the effect of ghrelin in GABAergic neurons. Ghrelin reduces fatty acid oxidation, mitochondrial respiration and mitochondrial reactive oxygen species formation in GT1-7 cells. Moreover, ghrelin produces a reduction in GABA release from primary cortical neurons which is blocked by both pharmacological and genetic inhibition of CPT1A. In addition, ghrelin produces a reduction in: (1) mitochondrial oxygen consumption, (2) citrate and α -ketoglutarate cellular content and (3) GABA shunt connecting TCA cycle and releasable GABA pool.

Taken together, these observations indicate that CPT1A contributes to the regulation of feeding by modulating the expression of neurotransmitter transporters and lipid components that influence the orexigenic pathways in VMH. Moreover, it seems that ghrelin and changes in CPT1A activity modulate mitochondrial function, yielding changes in GABA metabolism, which affect eventually to GABAergic neurotransmission.

RESUM

Paper de la carnitina palmitoiltransferasa 1A com a efector subjacent de la grelina en neurones corticals i hipotàlem

Estudis previs havien destacat la importància de la carnitina palmitoiltransferasa (CPT) 1A com a part essencial de la senyalització de la grelina al sistema nerviós central (SNC) per al control de la ingesta alimentària. El metabolisme lipídic en el nucli ventromedial de l'hipotàlem (VMH) ha emergit com una via crucial per a la regulació de la ingesta i l'homeòstasi energètica. Això no obstant, la relació entre els canvis en l'activitat de la CPT1A i els efectors intracel·lulars subjacents en el VMH que contribueixen a la modulació de la gana no són totalment compresos, com tampoc la seva involucració en les funcions centrals extrahipotàlmiques de la grelina.

En aquest treball, hem examinat l'efecte a llarg termini de l'expressió d'una isoforma mutada permanentment activa de la CPT1A (CPT1AM), fent ús d'un vector víric adeno-associat, injectat en el VMH de rates. La sobreexpressió de la CPT1AM produeix un augment sostingut de la ingesta alimentària que hi promou sobrepès. En la descripció mecanística, la CPT1AM altera el perfil lipídomic del hipotàlem mediobasal, induint-hi un augment de ceramides i esfingolípid i alhora una reducció en fosfolípids. A més a més, hem detectat un augment en les expressions del transportador vesicular de l'àcid γ -aminobutíric (GABA) (VGAT, en les seves sigles en anglès) i una reducció del transportador vesicular de glutamat 2 (VGLUT2, en les seves sigles en anglès). Aquests canvis són destacables, ja que tant GABA como glutamat han sigut proposats com a mediadors en el control de la ingesta alimentària.

Aquestes observacions ens dugueren a estudiar l'efecte de la grelina en neurones GABAèrgiques. La grelina redueix l'oxidació d'àcids grassos, la respiració mitocondrial i la formació d'espècies reactives d'oxigen en cèl·lules GT1-7. D'afegitó, la grelina produeix una reducció en l'alliberament de GABA de neurones corticals primàries, la qual cosa és blocada tant per inhibició genètica i farmacològica de la CPT1A. A més a més, la grelina hi produeix una reducció: (1) del consum mitocondrial d'oxigen, (2) del contingut cel·lular de citrat i d' α -cetoglutarat i (3) de la via de desviació de GABA que connecta el cicle dels àcids tricarboxílics i el contingut alliberable de GABA.

En conjunt, aquestes observacions indiquen que la CPT1A contribueix a la regulació de la ingesta amb la modulació de l'expressió de transportadors involucrats en la neurotransmissió i la modulació de components lipídics que influencien les vies orexigèniques del VMH. A més a més, sembla que la grelina i els canvis en l'activitat CPT1A modulen la funció mitocondrial, obtenint-ne canvis al metabolisme del GABA, que afecten en darrera instància a la neurotransmissió GABAèrgica.

RESUMEN

Papel de la carnitina palmitoiltransferasa 1A como efector subyacente de la ghrelina en neuronas corticales e hipotálamo

Estudios previos habían destacado la importancia de la carnitina palmitoiltransferasa (CPT) 1A como parte esencial de la señalización de la ghrelina en el sistema nervioso central (SNC) para el control de la ingesta alimentaria. El metabolismo lipídico en el núcleo ventromedial del hipotálamo (VMH) ha surgido como una vía crucial para la regulación de la ingesta y la homeostasis energética. No obstante, la relación entre los cambios en la actividad de la CPT1A y los efectores intracelulares subyacentes en el VMH que contribuyen a la modulación del apetito no son comprendidos totalmente, como tampoco su involucración en las funciones centrales extrahipotálamicas de la ghrelina.

En este trabajo, hemos examinado el efecto a largo plazo de la expresión de una isoforma mutada permanentemente activa de la CPT1A (CPT1AM), mediante un vector vírico adeno-asociado, inyectado en el VMH de ratas. La sobreexpresión de la CPT1AM produce un aumento sostenido de la ingesta alimentaria que promueve a su vez sobrepeso. En la descripción mecanística, la CPT1AM altera el perfil lipídico del hipotálamo mediobasal, induciendo un aumento de ceramidas y esfingolípidos, y simultáneamente una reducción en fosfolípidos. Además, hemos detectado un aumento en las expresiones del transportador vesicular del ácido γ -aminobutírico (GABA) (VGAT, en sus siglas en inglés) y una reducción del transportador vesicular de glutamato 2 (VGLUT2, en sus siglas en inglés). Estos cambios son destacables, ya que tanto GABA como glutamato han sido propuestos como mediadores en el control de la ingesta alimentaria.

Estas observaciones nos llevaron a estudiar el efecto de la ghrelina en neuronas GABAérgicas. La ghrelina reduce la oxidación de ácidos grasos, la respiración mitocondrial y la formación de especies reactivas de oxígeno en células GT1-7. Asimismo, la ghrelina produce una reducción de la liberación de GABA de neuronas corticales primarias, lo cual se puede bloquear con la inhibición genética y farmacológica de la CPT1A. Además, la ghrelina produce una reducción: (1) del consumo mitocondrial de oxígeno, (2) el contenido celular de citrato y de α -cetoglutarato y (3) de la vía de desviación de GABA que conecta el ciclo de los ácidos tricarbóxicos y el contenido liberable de GABA.

En conjunto, estas observaciones indican que la CPT1A contribuye a la regulación de la ingesta con la modulación de la expresión de transportadores involucrados en la neurotransmisión y la modulación de componentes lipídicos que influyen en vías orexigénicas del VMH. Además, parece que la ghrelina y los cambios en la actividad CPT1A modulan la función mitocondrial, obteniendo de ella cambios en el metabolismo del GABA que afectan en última instancia a la neurotransmisión GABAérgica.

CONTENT

ABSTRACT	9
CONTENT	13
ABBREVIATIONS.....	19
INTRODUCTION	23
The central nervous system as a target for anti-obesity drugs.....	23
Central nervous system	25
Neurons and synaptic transmission.....	26
Hypothalamus: a metabolic signal integrator	28
Cerebrum.....	32
Energy metabolism and amino acid neurotransmitter metabolism in neurons.....	32
GABA shunt and glutamate-glutamine cycle.....	34
GABA metabolism and fasting	38
Ghrelin	40
Ghrelin receptor	42
Effect of ghrelin in the CNS.....	43
AMPK-ACC axis in VMH and ARC: the malonyl-CoA hypothesis.....	45
Carnitine palmitoyltransferase system as key element of fatty acid β -oxidation	47
CPT1AM overexpression in VMH	49
AIMS	53
EXPERIMENTAL PROCEDURES	55
1. Animals, viral vectors and cell cultures	55
1.1. Experimental procedures with rats	55
1.2. Stereotactic surgery.....	56
1.3. Bilateral ventromedial hypothalamus cannulation.....	56

1.4. Adeno-associated viruses microinjection in VMH	57
1.5. Cumulative Weekly Food Intake Measurement.....	57
1.6. Fast-refeeding satiety test.....	57
1.7. Body weight measurement.....	58
1.8. Glucose tolerance test.....	58
1.9. Pyruvate tolerance test	58
1.10. Serum preparation	59
1.11. Mediobasal hypothalamus dissection	59
1.12. Brain coronal sections for histological preparations.....	59
1.13. Potentially conditional CPT1A knockout mice generation.....	60
1.14. CPT1A ^(loxP/loxP) colony establishment	62
1.15. Adeno-associated viruses	63
1.16. Adenoviruses	65
1.16.1 Adenoviral constructions.....	65
1.16.2. CPT1AM-expressing adenovirus.....	65
1.16.3. shCPT1A-expressing adenovirus	66
2.16.4. CRE recombinase-expressing adenovirus.....	67
1.16.5. Adenoviral amplification.....	67
1.16.5. Adenoviral titration.....	68
1.17. Lentivirus	69
1.17.1. Lentiviral shCPT1A-expressing constructions.....	69
1.17.2. Lentiviral vector production.....	70
1.18. Cell cultures.....	71
1.18.1. Primary cortical neuronal cultures.....	72
1.18.2. Adenoviral infection of primary cortical neurons	73
1.18.3. Pharmacological treatments to primary neuronal cultures	74
1.19. Hypothalamic cell lines.....	74
1.19.1. mHypo-N41, mHypo-N29/4 and mHypo-N43/5 cells.....	75

1.19.2. GT1-7 cells.....	75
1.19.3. Adenoviral infection of hypothalamic cell lines.....	76
1.19.4. Lentiviral transduction and clonal selection in mHypo-N41	76
1.19.5. Pharmacological treatments to hypothalamic cell lines	77
1.20. HEK 293 derived cell lines	78
2. Molecular Biology Techniques.....	79
2.1. Genomic DNA extraction from mice ear tags	79
2.2. Phenol:chloroform pure genomic DNA extraction	79
2.3. Mice genotyping by polymerase chain reaction	80
2.4. CPT1A ^(+/frt) mice genotyping	81
2.5. CPT1A ^(+/loxP) and CPT1A ^(loxP/loxP) mice genotyping	82
2.6. Analysis by ddPCR of copy number in CPT1A ^(+/frt) mice.....	83
2.7. CPT1A ^{loxP} allele sequencing.....	86
2.8. RNA analysis techniques.....	87
2.9. Total RNA extraction from mediobasal hypothalamus.....	87
2.10. Total RNA extraction from cell cultures	88
2.11. cDNA synthesis by reverse transcription.....	88
2.12. Quantitative real time polymerase chain reaction.....	88
2.13. Total protein extraction	89
2.14. Bicinchoninic acid protein quantitation assay.....	90
3. Biochemical and functional assays	91
3.1. Radiometric fatty acid oxidation assay.....	91
3.2. Mitochondrial superoxide quantification in flow cytometry	92
3.3. Amino acid neurotransmitter release assay.....	92
3.4. GABA transaminase assay.....	93
3.5. Metabolic Extracellular Flux XF Analysis.....	94
3.6. Rat mediobasal hypothalamus lipidomic analysis.....	96
3.7. Rat plasma amino acid and thyroidal hormones analysis	96

3.8. Neuronal tricarboxylic acid cycle intermediates analysis	97
3.9. Acylcarnitines quantification.....	97
4. Bioinformatics and statistical analysis.....	98
RESULTS.....	99
PART 1. Evaluation of the hyperphagic phenotype in rats overexpressing CPT1AM in ventromedial hypothalamus	99
1.1. Analysis of infection and CPT1A activity in VMH.....	99
1.2. Effect on food intake and body weight	101
1.3. Lipidomic analysis on MBH	104
1.4. Analysis on hypothalamic gene expression.....	108
1.5. Analysis of circulating amino acids and thyroidal hormones	110
1.6. Analysis of glucose tolerance and gluconeogenesis.....	112
PART 2. Study of the role of CPT1AM as a downstream effector of ghrelin in hypothalamic cell lines	114
2.1. Selection of shCPT1A lentivirally transduced mHypo-N41 neuronal lines.....	114
2.2. Effect of ghrelin and etomoxir on gene expression in GT1-7	116
2.3. Effect of ghrelin on CPT1A activity and FAO in GT1-7	117
2.4. Effect of ghrelin on mitochondrial respiration in GT1-7 cells.....	119
2.4.1. Oxygen consumption rate of GT1-7 cells at physiological glycorrachia.....	120
2.4.2. Oxygen consumption rate of GT1-7 cells using palmitate.....	120
2.4.3. Oxygen consumption rate of GT1-7 cells with silenced CPT1A expression...	121
2.5. Effect of ghrelin on mitochondrial superoxide formation in GT1-7 cells.....	122
2.6. Effect of ghrelin on amino acid neurotransmitters in GT1-7 cells	123
PART 3. Study of the role of CPT1AM as a downstream effector of ghrelin in primary cortical neurons.....	125
3.1. Effect of intraperitoneal ghrelin on food intake	125
3.2. Effect of intraperitoneal ghrelin on cortical acylcarnitines	126
3.3. Effect of intraperitoneal ghrelin on cortical GABA metabolism.....	126

3.4. Appraisal of primary cortical neuronal cultures as a GABAergic ghrelin-responsive model.....	130
3.5. Effect of ghrelin on gene expression in primary cortical neurons	132
3.6. Effect of CPT1AM overexpression on mRNA expression in primary cortical neurons	134
3.7. Effect of CPT1AM on GABA release in primary cortical neurons.....	137
3.8. Genotyping of potentially conditional CPT1A knockout mice	138
3.9. Genotyping of CPT1A ^(loxP/loxP) mice generation.....	141
3.10. Effect of ghrelin and CPT1A deletion on mRNA levels of GABA metabolism enzymes in primary cortical neurons.....	144
3.11. Effect of ghrelin and CPT1A deletion on GABA release and GABAT activity in primary cortical neurons.....	145
3.12. Effect of ghrelin and CPT1A deletion on the intermediates of tricarboxylic acid cycle in primary cortical neurons.....	147
3.13. Effect of ghrelin and CPT1A deletion on mitochondrial respiration in primary cortical neurons.....	149
3.13.1 Oxygen consumption rate of primary cortical neurons at physiological glycorrachia.....	149
3.13.2 Oxygen consumption rate of primary cortical neurons at high glucose.....	150
3.13.3 Oxygen consumption rate primary cortical neurons using palmitate	151
3.14. Effect of ghrelin and CPT1A deletion on mitochondrial superoxide in primary cortical neurons.....	152
DISCUSSION	153
CPT1AM overexpression in VMH causes hyperphagia and overweight	153
CPT1AM overexpression in VMH modifies hypothalamic lipidomic profile and vesicular amino acid transporters transcription.....	154
Hypothalamic neuronal cell lines have limited validity as hypothalamic GABAergic neuronal models.....	158
Ghrelin reduces fatty acid oxidation, mitochondrial oxygen consumption rate and mitochondrial ROS formation in GT1-7 cells.....	159

Intraperitoneal ghrelin causes differential effects in CPT1A activity in cortex and hypothalamus and reduces GABA metabolism gene expression in cortex	162
Ghrelin reduces GABA release in primary cortical neurons.....	163
CPT1AM expression does not reduce GABA release in primary cortical neurons..	164
CPT1A deletion blunts ghrelin-induced reduction of GABA release and both ghrelin and CPT1A deletion reduce α -ketoglutarate and citrate in cortical neurons	167
Ghrelin reduces mitochondrial oxygen consumption in cortical neurons	169
CONCLUSIONS.....	175
REFERENCES.....	179
ANNEXES.....	209
PUBLICATIONS	215

ABBREVIATIONS

AAV	Adeno-associated virus
ACC	Acetyl-CoA carboxylase
Ad	Adenovirus
AgRP	Agouti-related protein
AMPK	AMP-dependent protein kinase
ANLS	Astrocyte-neuron lactate shuttle
ARC	Arcuate nucleus of hypothalamus
ATP	Adenosine triphosphate
BBB	Blood-brain barrier
CACT	Carnitine/acylcarnitine translocase
CART	Cocaine- and amphetamine-regulated transcript
CNS	Central nervous system
CoA	Coenzyme A
COT	Carnitine octanoyltransferase
CPT	Carnitine palmitoyltransferase
CPT1AM	Mutant malonyl-CoA-insensitive CPT1A
CrAT	Carnitine acetyltransferase
CSF	Cerebrospinal fluid
ddPCR	Digital droplet PCR
DMH	Dorsomedial nucleus of hypothalamus
ETC	Electron transport chain
FAO	Fatty acid β -oxidation
FBS	Fetal bovine serum
GABA	γ -Aminobutyric acid
GABAT	GABA transaminase

GAD	Glutamic acid decarboxylase
GFP	Green fluorescent protein
GH	Growth hormone
GHB	γ -Hydroxybutyrate
GHRPs	Growth hormone releasing peptide
GHSR	GH secretagogue receptor
GOAT	Ghrelin O-acyltransferase
GS	Glutamine synthetase
GTP	Guanosine triphosphate
GTT	Glucose tolerance test
HMGCS2	Mitochondrial 3-hydroxy-3-methylglutaryl-CoA synthase 2
ICV	Intracerebroventricular
IP	Intraperitoneal
α-KG	α -Ketoglutarate
LCFA	Long chain fatty acid
LH	Lateral hypothalamus
MBH	Mediobasal hypothalamus
MC3R	Melanocortin receptor 3
MC4R	Melanocortin receptor 4
α-MSH	α -Melanocyte-stimulating hormone
NAG	Neuropeptide Y/Agouti-related protein/ γ -Aminobutyric acid
NPY	Neuropeptide Y
OCR	Oxygen consumption rate
OCT	Optimal Cutting Temperature
OXPHOS	Oxidative phosphorylation
PCR	Polymerase chain reaction
pfu	Plaque-forming unit

PGC1α	Peroxisome proliferator-activated receptor γ coactivator 1 α
POA	Preoptic area
POMC	Proopiomelanocortin
PVH	Paraventricular nucleus of hypothalamus
qRT-PCR	Quantitative real time PCR
ROS	Reactive oxygen species
SF1	Steroidogenic factor 1
shRNA	Small hairpin RNA
siRNA	Small interfering RNA
SSA	Succinic semialdehyde
SSADH	Succinic semialdehyde dehydrogenase
SSV	Small synaptic vesicles
TCA	Tricarboxylic acid
UCP	Uncoupling protein
VGAT	Vesicular GABA transporter
VGLUT	Vesicular glutamate transporter
VMH	Ventromedial nucleus of hypothalamus

INTRODUCTION

The central nervous system as a target for anti-obesity drugs

Obesity and overweight, together with their associated pathologies, have become one of the most important challenges for national healthcare systems worldwide. The prevalence of obesity and associated metabolic diseases is rising exponentially, jointly with their sanitary costs. There are more than 600 million obese people worldwide and obesity-related pathologies have debunked malnourishment when it comes to number of deaths (World Health Organization, 2015).

Behavioral modifications, including healthy eating and exercise, seem to have limited success when it comes to long-term maintenance of weight loss. Bariatric surgery achieves a sustained weight loss over the years, but its cost and associated dangers reduce its clinical indication to morbidly obese patients (Schneider & Mun, 2005). Moreover, the endocrine effects of bariatric surgery seem to be more important than the mechanically induced food restriction, which has led many researchers to assess obesity treatments based on the endocrine modifications derived from it (Mumphrey, Patterson, Zheng, & Berthoud, 2013).

Even though the list of potential anti-obesity drugs is increasing, the approval of new anti-obesity drugs has been limited. This is due to the history of withdrawals of anti-obesity drugs from the market due to serious adverse effects (*e.g.*, dinitrophenol, fenfluramine, dexfenfluramine, phenylpropanolamine, sibutramine and rimonabant) (Hurt, Edakkanambeth Varayil, & Ebbert, 2014; Jackson, Price, & Carpino, 2014). This has led US Food and Drug Administration (FDA) and European Medicines Agency (EMA) to make it even harder for pharmaceutical corporations to market new anti-obesity drugs, especially in the case of the European regulator (European Medicines Agency (EMA), 2014). The enteric lipase inhibitor orlistat is the only weight-management drug approved with over-the-counter and prescription doses by both FDA and EMA. However, it has shown limited long-term effectiveness (Derosa & Maffioli, 2012). In the US, the serotonergic lorcaserin is also approved (Khan et al., 2012; O'Neil et al., 2012), but its European marketing authorization application has been withdrawn because of the lack of evidence regarding safety in tumorigenesis in long-term use (European Medicines Agency (EMA), 2013). Liraglutide, a previously approved antidiabetic drug, has recently been approved by both regulators for an anti-obesity indication (European Medicines Agency (EMA),

2015; US Food and Drug Administration (FDA), 2014). Nonetheless, the fixed-dose combination of bupropion/naltrexone, which is described to act in the central nervous system (CNS) by increasing proopiomelanocortin (POMC) neuron activity, has obtained marketing approval as an anti-obesity drug by the FDA (Jeon & Park, 2014), but the EMA seems to be much more conservative regarding the approval of weight-management drug with effect on the CNS (Caixàs, Albert, Capel, & Rigla, 2014).

The mechanisms of action of obesity-management drugs are classified into three groups (Hamdy, Uwaifo, & Oral, 2015): 1) centrally acting medications impairing dietary intake (including bupropion/naltrexone and lorcaserin); 2) medications that act peripherally to impair dietary absorption (*e.g.* orlistat); and 3) medications that increase energy expenditure, whose effect is often mediated by CNS.

Most of the more successful drugs for food intake management had their focus on central modulation of food intake, but they were withdrawn because of the many side effects related to their central action as well. In most of the cases, amphetamine derivatives used as first generation weight loss drugs, had this off-label indication prescribed at a time when little knowledge about central mechanisms for food intake control were achieved, around late 1930's and early 1940's (Rasmussen, 2008). The first indication for benzedrine as a weight loss drug was approved at 1947, a few years after the seminal publication of the ventromedial hypothalamus (VMH) lesions experiments reporting the importance of hypothalamus in the control of food intake (Hetherington & Ranson, 1942).

From that time on, many drugs for weight management involving CNS have been approved and withdrawn. Even though it has been in relatively recent times when the two main endocrine central modulators of food intake have been described: leptin (Y. Zhang et al., 1994) and ghrelin (Tschöp, Smiley, & Heiman, 2000). Moreover, the insulin role in this issue has been revisited and studied extensively (Bruning, 2000; Silvana Obici, Zhang, Karkanias, & Rossetti, 2002). Nonetheless, the discrete hypothalamic molecular mechanisms involved in the control of food intake have been assessed in the last two decades and they are still being disclosed. The discovery of new central mechanisms and targets involved in the control of food intake can boost the necessary efforts for the design of new weight management drugs and it can shed light in the mechanism of action which would minimize the side effects of the potential drugs.

Central nervous system

The **encephalon** is the part of the CNS where perceptions are integrated with previously registered information to eventually take decisions and trigger actions. It hosts intellectual insight, emotions, behavior and memory. The different parts which compose the encephalon act in an integrative way to achieve shared actions. Adult encephalon is composed out of 4 parts: The *brainstem*, which connects to spinal cord, is composed by the rachial bulb, the pons Varolii and the midbrain. The *cerebellum* can be found behind the brainstem. The *diencephalon* lays on the brainstem which is formed by the thalamus, the epithalamus and the hypothalamus, which will be further discussed. On the diencephalon and the brainstem, one can find the *cerebrum*, also known as telencephalon, the largest part of the encephalon, which will be further discussed as well. The cranial bones and the meninges protect the encephalon and act as a continuum of spinal meninges protecting the whole system. The three meninges are *dura mater*, the one that is attached to the skull, *pia mater*, in the middle, and *arachnoid mater*, closer to the neural tissue.

Blood reaches the encephalon mainly through inner carotid and vertebral arteries and flows back to the heart through the inner jugular veins. The blood flow to the brain is a capstone process, highly controlled due to its high energy needs. The **blood-brain barrier** (BBB) protects neurons from toxic substances and microorganisms, since it blocks the entrance of such elements from the blood to the neural tissue. BBB is formed out of two elements: The *tight junctions*, which block the endothelial intercellular space in encephalic capillaries, and the *basal membrane* which surrounds them. Many astrocytes, which are the support cells for neurons, have projection surrounding the capillaries and release chemicals into the bloodstream, keeping the aforementioned tight junctions to impede water-soluble substances to reach the brain. The hydrophilic substances, such as glucose, needed to reach the brain cells, go across the BBB in an ATP-dependent manner. Many substances such as creatinine, urea, most of the ions and many proteins or exogenous drugs, can go through the BBB following a low rate. On the contrary, liposoluble substances, such as oxygen, carbon dioxide, alcohol, fatty acids and many CNS-targeting drugs, such as anesthesia, can cross BBB easily.

The **cerebrospinal fluid** (CSF) is a colorless fluid which protects the encephalon and the spinal cord from physical and chemical events. It drives oxygen and glucose from blood to neurons and neuroglia. CSF circulation continues along the spine and all the cavities in the

brain, namely ventricles, and in the subarachnoid space, found between the arachnoid and pia matres. The total CSF in humans oscillates between 80 and 150 mL and it is secreted by choroid plexuses, which are located in the lateral, third and fourth ventricles, which follow a natural flux from the lateral ventricles into the third ventricle via the foramen of Munro and then to the fourth ventricle via the aqueduct of Sylvius, which connects to the subarachnoid space. CSF reabsorption into the blood takes place in the arachnoid villi found in the superior sagittal sinus, following the same CSF formation rate 20 mL per hour to maintain the intracranial pressure. CSF is a product of plasma filtration and membrane secretion, which makes its composition different from that of plasma. CSF is almost acellular (Meinkoth & Crystal, 1999) and has a low protein concentration, mainly albumin (Chan & Fishman, 1980), but various ions, enzymes and other substances can be found there, like nutrients, such as glucose. CSF general composition, and concretely glycorrhachia (*i.e.* CSF glucose levels) are relatively constant with time, but it depends on plasma composition which can vary along the day and depending on feeding state.

Neurons and synaptic transmission

Nervous tissue is the main element of the CNS. It is composed basically of two types of cells, **neurons**, which are responsible for most of the functions of the CNS, such as sensitivity, thinking, memory, motor control and endocrine regulation, and **glial cells**, which nurture, protect and hold the neurons in a suitable environment. Neuroglia can be classified according to their size, intracellular organization and cytoplasmic shape into 4 types: astrocytes, oligodendrocytes, microglia and ependyma. Astrocytes, which are star-shaped, are the most common cell type amongst neuroglia and are responsible for most of the functions attributable to neuroglia: physical scaffolding, isolation from toxic substances, neuronal growth regulation during embryonic development and synaptogenesis and stabilizing chemical environment for correct neuronal function. Oligodendrocytes are responsible for the formation of the myelin sheaths to speed up electric transmission along axons. Microglia have phagocytic functions and make up the primary immune system in the CNS. And ependymal cells are responsible for the formation and circulation of the CSF along the ventricles and are part of the BBB. The neuron:astrocyte ratio varies between different brain regions, but it is close to 1:10 (Bignami, 1991). Amongst cortical neurons, one finds two main types of neurons: excitatory neurons, which are 85% of total cortical neurons and are mostly glutamatergic; and inhibitory neurons, which are GABAergic and are 15% of total cortical neurons (Attwell & Laughlin, 2001;

Braitenberg, 1992; Niciu, Kelmendi, & Sanacora, 2012). They depolarize or hyperpolarize postsynaptic neurons, respectively.

Neurons are excitable cells that can produce electrical signals to which can react as well. Neurons have a specific morphology adapted to its function with two characteristic parts: the soma, also known as cell body, and the neurites, which are projected from the soma to connect with other neurons. Neurites can be differentiated into two types: dendrites, which receive signals from other neurons, and axons, which can be up to 1 meter long and project onto other neurons. The stimulus from one neuron to another is produced in the synaptic cleft, where neurotransmitters stored in vesicles found in the axonal nerve endings are released in order to affect neighboring cells. Lipids compose up to a 50% of the dry weight of neurons, with a high proportion of phospholipids, glycolipids and phospholipids.

When an action potential reaches the presynaptic membrane, voltage-dependent Ca^{++} channels in the membrane open to trigger neurotransmitter vesicles exocytosis. Classically and according to Dale's principle, it was proposed that each neuron uses the same neurotransmitter at all its synapses (Eccles, Fatt, & Koketsu, 1954), although this hypothesis seems to be outdated, as we will further discuss in this manuscript. The neurotransmitters diffuse through the synaptic cleft and bind eventually to their postsynaptic receptors, which can be classified in ionotropic receptors, which are ligand-gated ion channels which can produce both depolarization or hyperpolarization of the postsynaptic membrane depending on the ions controlled; or metabotropic receptors, often interacting with G proteins which will lead to activate or inhibit the synthesis of secondary messengers. Depolarizing processes are highly energy demanding, which explains that 85% of brain mitochondria are located in neurons, while only 5% are in glial cells (Wong-Riley, 1989).

Neurotransmitters can be classified according to their structure into several groups: **Neuropeptides** are the largest group amongst the transmitters; they are made of between 3 to 40 residues, with specific sequences. **Amino acid neurotransmitters**; besides neuropeptides, several proteinogenic amino acids act as neurotransmitters. Glutamate is the most important stimulatory neurotransmitters found in the CNS, since more than a half of the synapses in the brain are glutamatergic. Glycine can be a neurotransmitter as well, but it has inhibitory effect. Not only α -amino acids can act as amino acid neurotransmitters: glutamate-derived γ -aminobutyric acid (GABA) is the most important inhibitory neurotransmitter found in the CNS. **Acetylcholine** acts triggering muscle contraction at neuromuscular junctions and in certain

parts of the brain and autonomous nervous system. **Biogenic amines** include catecholamines, serotonin and histamine, which are also derived from α -amino acids deamination and act as hormones and transmitters.

Dale's law was proposed at a time when only two neurotransmitters were known, but with time, the CNS is apparently more complex than previously thought. It has been stated that multiple peptides, generated out of a common prepropeptide can be packed in a differential manner and released out of different dendrites, which suggests that neurons do not always release the same neurotransmitters from all the endings (Fisher, Sossin, Newcomb, & Scheller, 1988; Sossin, Sweet-Cordero, & Scheller, 1990). To complicate this even further, neurons are able to co-release not only peptidergic neurotransmitters, but also amino acid neurotransmitters (Dicken, Tooker, & Hentges, 2012; Schöne & Burdakov, 2012).

Hypothalamus: a metabolic signal integrator

The **hypothalamus** is one of the parts of the diencephalon, together with the thalamus and the epithalamus. It is located in the ventral part of the thalamus at both sides of the third ventricle and it is composed of about a dozen of nuclei. The hypothalamus is a complex brain area which forms a network integrating peripheral and central signals. The hypothalamus controls many organic functions and is the key body homeostasis regulator. Hypothalamus integrates both somatic and visceral information, besides sensorial information to promote the best response to modulate a wide range of physiological processes. The hypothalamus acts as a sensor itself, controlling constantly parameters such as osmotic pressure, glycaemia, levels of certain hormones, body temperature and blood pressure (Schwartz, Woods, Porte, Seeley, & Baskin, 2000). The hypothalamus is connected to the pituitary gland, to produce hormones with peripheral and central effects. Some functions have been attributed to concrete hypothalamic nuclei, but for some of them, its precise location is unknown. The main functions of the hypothalamus are the regulation of sleep/wakefulness, heart rate, body temperature, water and food intake, emotional patterns and behavior (together with the limbic system), hormone production and control of autonomous nervous system (Schwartz et al., 2000) The hypothalamus is the only area which is considered part of both the CNS and the endocrine system.

VMH is an important hypothalamic region for central energy homeostasis and food intake control, since it integrates nutrient availability information from peripheral tissues via arcuate nucleus, with information from other brain areas. Other hypothalamic areas modulate VMH signalling, such as DMH and paraventricular hypothalamus (PVH, found in the supraoptic region), but their roles have not been completely elucidated (Woods & D'Alessio, 2008)

Electric stimulation and many substances, such as norepinephrine (Sakaguchi & Bray, 1989), glutamate (Amir, 1990) and β -hydroxybutyrate (Sakaguchi, Arase, & Bray, 1988), modulate energy homeostasis, when administered to the VMH parenchyma. Besides existing pharmacological approaches to study the VMH function, genetic models are also widely used to study this hypothalamic nucleus. Steroidogenic factor 1 (SF1) is a specific marker for the VMH area which is important for the development of this hypothalamic area. The lack of VMH produces in SF1 defective mice reduces uncoupling protein (UCP) 1 levels in brown adipose tissue, and thus affecting the correct thermogenic regulation (K. W. Kim et al., 2011). Furthermore, estrogen receptor SF1-specific KO mice present a hyperphagic phenotype, with hyperghrelinemia, increased body weight and reduced thermogenesis (Xu et al., 2011). Another example can be found in insulin receptor SF1-specific KO mice, which also have shown an impaired control of energy homeostasis (Klöckener et al., 2011).

The *arcuate nucleus of hypothalamus* (ARC) is considered as the key food intake regulating area. It is located nearby the median eminence and the BBB fenestrated capillaries which allow ARC to directly sense circulating nutrients. It contains two different neuronal subpopulations named after the neuromodulators they produce: Neuropeptide Y(NPY)/Agouti-related protein (AgRP)/GABA (NAG) neurons and pro-opiomelanocortin (POMC)/ Cocaine and amphetamine regulated transcript (CART) neurons. These neuronal populations project into other hypothalamic areas such as VMH, PVH and DMH (Bouret, Draper, & Simerly, 2004).

NAG neurons produce the NPY which increases substantially food intake (Clark, Kalra, Crowley, & Kalra, 1984; Tatemoto, 1982). Its expression depends on the nutritional state, increasing during fasting and being reduced when sated (Sanacora, Kershaw, Finkelstein, & White, 1990; Swart, Michael Overton, & Houpt, 2001). Moreover, these neurons coexpress the AgRP, which acts as orexigenic signal as well. AgRP acts as an antagonist of melanocortin system, since it blocks melanocortin receptors MC3R and MC4R, activated by α -MSH produced in the other POMC/CART neuronal population (Asakawa et al., 2001) (**Fig 2**). Besides the aforementioned neuropeptides, GABA is co-released from NAG neurons and it has been recently

discovered that its release acutely stimulates food intake in a neuropeptide-independent manner (Krashes, Shah, Koda, & Lowell, 2013; Tong, Ye, Jones, Elmquist, & Lowell, 2008). The sole activation of NAG neurons using optogenetic approaches can trigger a voracious feeding behavior (Aponte, Atasoy, & Sternson, 2011).

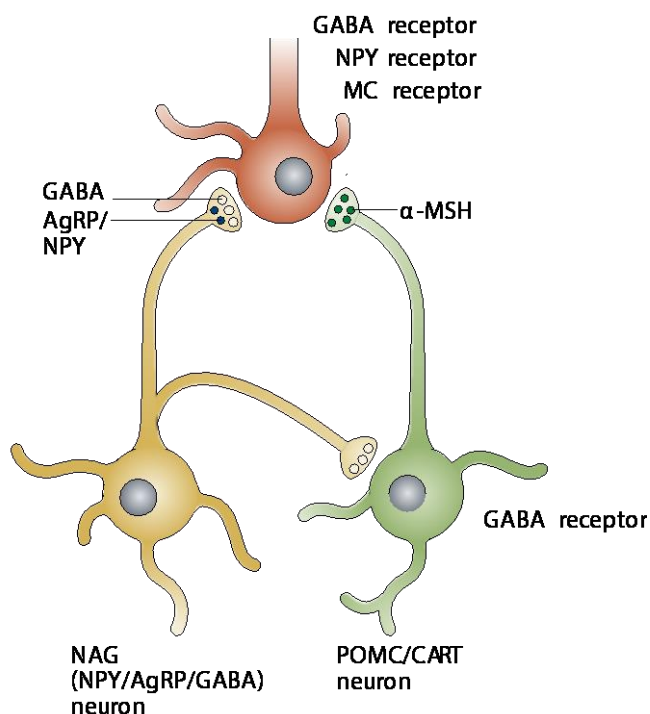


Fig 2. Relationship between NAG and POMC/CART neuronal populations in ARC. NAG neurons in ARC send inhibitory projections to secondary neurons and the anorexigenic primary POMC/CART neurons. Activation of POMC/CART cells by leptin triggers the release of α -MSH which binds to MC4R and promotes satiety. NAG neurons are inhibited by leptin but stimulated by ghrelin, which promotes feeding and silences firing of POMC/CART neurons. The effect of the NAG cells is mediated by GABA, NPY and AgRP. Adapted from (Bell, Walley, & Froguel, 2005).

POMC/CART neurons exert an anorexigenic effect since they produce α -melanocyte stimulating hormone (α -MSH) out of POMC peptide processing. α -MSH activates MC3R and MC4R in lateral hypothalamus, which promotes satiety and reduces food intake (Cone et al., 2001). AgRP and α -MSH are two counteracting parts of the melanocortin system controlling food intake, since they are released to neurons in other hypothalamic nuclei such as dorsomedial, lateral and ventromedial hypothalamus, to orchestrate an adaptive response of the organism, by regulating energy expenditure and food intake to balance energy homeostasis (Elmquist, 2001).

Cerebrum

The cerebrum (or named as its original prenatal structure *telencephalon* in most of the Romance languages) is the brain structure found on the diencephalon. In mammals, the cerebrum is the area which directs the conscious voluntary motor functions of the body in the motor cortex. It also receives and processes visual, auditory, somatosensory, gustatory and olfactory information in the primary sensory areas of the cerebral cortex, which with the association cortical areas generate the perception of our environment. Communication, language, learning and memory are related to the cerebrum. Broca's and Wernicke's areas control to communication and language. Hippocampus and regions of the medial temporal lobe are needed for learning processes and memory.

The cerebrum is composed out of two hemispheres, separated by the falx cerebri, which is in the longitudinal fissure. Both hemispheres have a gray matter external part, which is 2 to 4 mm wide and contains millions of neurons despite the reduced space, and a white matter inner part engulfing gray nuclei within. The **cerebral cortex** is formed by this gray matter external part, and presents gyri and sulci which increase the total surface of the cerebral cortex creating more space to contain neurons. It contains highly specialized areas which process specific signals: *sensory areas*, located mainly in the posterior part of both hemispheres; *motor areas*, whose efferences flow from the anterior part of both hemispheres, and amongst many others it includes the Broca's area; and *association areas*, which allow to produce a meaningful perceptual experience and encompass some motor and sensory areas, together with a large portion on the lateral surface of occipital, parietal and temporal lobe, and the frontal lobe before the motor areas

Energy metabolism and amino acid neurotransmitter metabolism in neurons

The brain and the CNS in general have high energy needs. Actually the 20% of the metabolized oxygen and around the 60% of the glucose is metabolized by the brain, which only represents a 2% of the whole body mass. This energy is used mainly by the adenosine triphosphate (ATP)-dependent ion pumps and other active transport processes needed to keep nerve conduction.

Glucose is often regarded as the only metabolite from which the brain is able to obtain adequate amounts of ATP through aerobic glycolysis and subsequent terminal oxidation to carbon dioxide and water (G A Dienel & Hertz, 2001). As neurons only have minor glycogen reservoir, they depend on a constant supply of glucose from the blood. A severe drop in the blood glucose or oxygen levels rapidly leads to a drop in the ATP level in the brain. This results in loss of consciousness and neurological deficits that can lead to death. The effects of a brief period of hypoxia are still reversible, but as time progresses irreversible damage increasingly occurs and eventually a complete loss of function. During starvation, the brain can use ketone bodies in addition to glucose to form ATP. This saves glucose and reduces the breakdown of muscle protein that maintains gluconeogenesis in the liver during prolonged starvation.

Nonetheless, mitochondria do not oxidize and obtain energy from a single substrate, but from a mixture of substrates depending on the metabolic situations, hormonal status and cell type. Because of the basic mitochondrial function, most of cells can obtain energy from different nutrient functions: carbohydrates, fatty acids and amino acids, but in the case of neurons and astrocytes, the variations in basic biochemistry are important for the adaptation of mitochondrial metabolism to cell specialization. In neurons, the role of fatty acids seems to be limited, despite being described as crucial for certain processes (Panov, Orynbayeva, Vavilin, & Lyakhovich, 2014). Nutrient availability in brain is an extremely controlled process, since it is necessary to keep a tightly regulated microenvironment for a reliable neuronal signaling (Ballabh, Braun, & Nedergaard, 2004; Kasser, Deutch, & Martin, 1986). The BBB is the structure responsible for this control, which acts as a metabolic border and inactivates many circulating neuroactive compounds (el-Bacha & Minn, 1999; Kasser et al., 1986). Nonetheless, hypothalamic nuclei have a relatively easy access for many circulating nutrients and peptide hormones, since it presents the fenestrated capillaries in the BBB (Lam, Schwartz, & Rossetti, 2005). Actually, hypothalamic fatty acid metabolism is regarded as a sensor for nutrient availability which modulates whole body energy homeostasis through the control of nutritional, hormonal and neurotransmitter signals (Lam et al., 2005)

However, glucose is regarded as the most important circulating substrate used as a source of energy by the adult regular brain (G A Dienel & Hertz, 2001). At most, glutamate-stimulated aerobic glycolysis in astrocytes yields lactate to be further oxidized in neuronal mitochondria. This system is known as the astrocyte-neuron lactate shuttle (ANLS) (Pellerin & Magistretti, 2012). Nevertheless, phosphorylative oxidation produces up to 3 times more ATP

than glycolytic pathway in astrocytes and should be regarded as a major source of energy for the complex astrocytic energy demands (Gerald A Dienel & Cruz, 2004). The stoichiometric mismatch between oxygen consumption and glucose and glycogen oxidation suggest that other sources of carbon are oxidized to obtain energy (Gerald A Dienel & Cruz, 2004).

Fatty acids and carnitine can go through BBB to oxidize fatty acids, generating about 20% of total energy expenses in adult brain (Ebert, Haller, & Walton, 2003; Schönfeld & Reiser, 2013; Spitzer, 1973). Nonetheless, fatty acid β -oxidation (FAO) in brain energy metabolism is often dismissed and generally it is believed to occur almost exclusively in astrocytes (Ebert et al., 2003). Besides glucose and fatty acids, amino acid neurotransmitters, such as glutamate and GABA may enter into tricarboxylic acid (TCA) cycle in both neurons and astrocytes to be oxidized, and in the case of glutamate, it is responsible for easing to reach maximal oxidative phosphorylation rates (Panov et al., 2009; Tillakaratne, Medina-Kauwe, & Gibson, 1995). More than 50% of synaptic cleft-released glutamate is removed by postsynaptic transporters in cerebellum, forebrain and midbrain (Auger & Attwell, 2000; Massie et al., 2008). Since postsynaptic glutamate reuptake occurs in hippocampus as well (Furness et al., 2008), this suggests this processes may happen in most brain regions. Consequently, mitochondria found in neurites may metabolize significant amounts of glutamate, besides pyruvate (Panov et al., 2009).

When it comes to GABAergic neurons, GABA reuptake betides even in a greater extent than glutamatergic reuptake (Bak, Schousboe, & Waagepetersen, 2006). Moreover, GABA degradation can happen in both neurons and astrocytes, through the entrance in tricarboxylic acid (TCA) cycle in the form of succinate, which is formed by the action of the GABA shunt enzymes (Bak et al., 2006; Tillakaratne et al., 1995).

GABA shunt and glutamate-glutamine cycle

As we mentioned before, besides glutamate role as a major excitatory neurotransmitter, it is an important metabolite in several metabolic pathways, including amino acid metabolism, energy metabolism and GABA synthesis. Both glutamate and GABA are synthesized in the brain itself, using both neurons and neuroglia to do so.

Since glutamate and GABA as neurotransmitters must not appear in the extracellular space in an unregulated manner, the astrocytes supply glutamatergic and GABAergic neurons with glutamine as a precursor for both (Reubi, Van Der Berg, & Cuénod, 1978), produced by the action of glutamine synthetase on glutamate in astrocytes (Riepe & Norenberg, 1978; Sonnewald et al., 1993) (Fig 3).

Unactive glutamine is transported into the neuron. There it is hydrolyzed by glutaminase to form glutamate again. In glutamatergic neurons, this is stored in small synaptic vesicles (SSV) by the action of vesicular glutamate transporters (VGLUT) to be released when stimulated. In GABAergic neurons, glutamate is recovered through a glutaminase as well, but subsequently it is decarboxylated into GABA, by glutamic acid decarboxylase (GAD). GABA to be released is stored into SSV as well, by vesicular GABA transporter (VGAT).

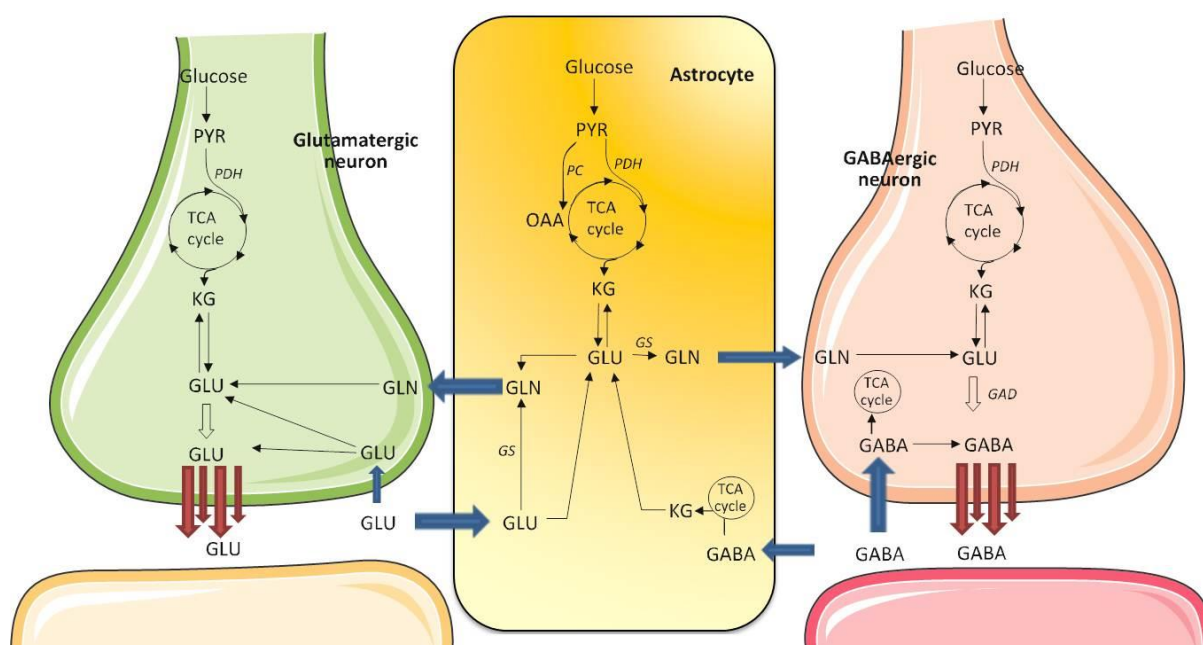


Fig 3. Release and uptake of neurotransmitters in glutamatergic and GABAergic synapses interacting with an astrocyte. GAD glutamate decarboxylase, GLN glutamine, GLU glutamate, GS glutamine synthetase, KG α -ketoglutarate, PC pyruvate carboxylase, PDH pyruvate dehydrogenase, TCA tricarboxylic acid. PYR pyruvate. OAA oxaloacetate. Adapted from (Walls, Waagepetersen, Bak, Schousboe, & Sonnewald, 2015)

Most of the GABA found in the synaptic cleft is recovered by transporters found in presynaptic neurons, and to a lesser extent into astrocytes (Hertz & Schousboe, 1987; Arne Schousboe, Bak, & Waagepetersen, 2013). Actually this recovered GABA is the predominantly found in the vesicular GABA quantum (Gram, Larsson, Johnsen, & Schousboe, 1988). Thus, the

loss of carbon skeletons from GABAergic neurons to astrocytes is reduced compared to glutamatergic neurons, which rely more in glutamine transfer (Walls et al., 2015). When new glutamate or GABA have to be generated, neurons preferentially use pyruvate as the anaplerotic substrate for its generation, via TCA cycle α -ketoglutarate (Cesar & Hamprecht, 1995; Yu, Drejer, Hertz, & Schousboe, 1983).

There are three pathways controlling cytoplasmic GABA content, besides GABA reuptake: GABA transport into small synaptic vesicles to be released, via vesicular GABA transporter (VGAT); glutamic acid decarboxylase (GAD) activity which is the canonical pathway to generate GABA from glutamate, and GABA shunt, which is an alternative pathway to supply carboxylic acids to TCA cycle and to enhance energy production in situations in which classical glucose/lactate pathway is compromised (Fig 4).

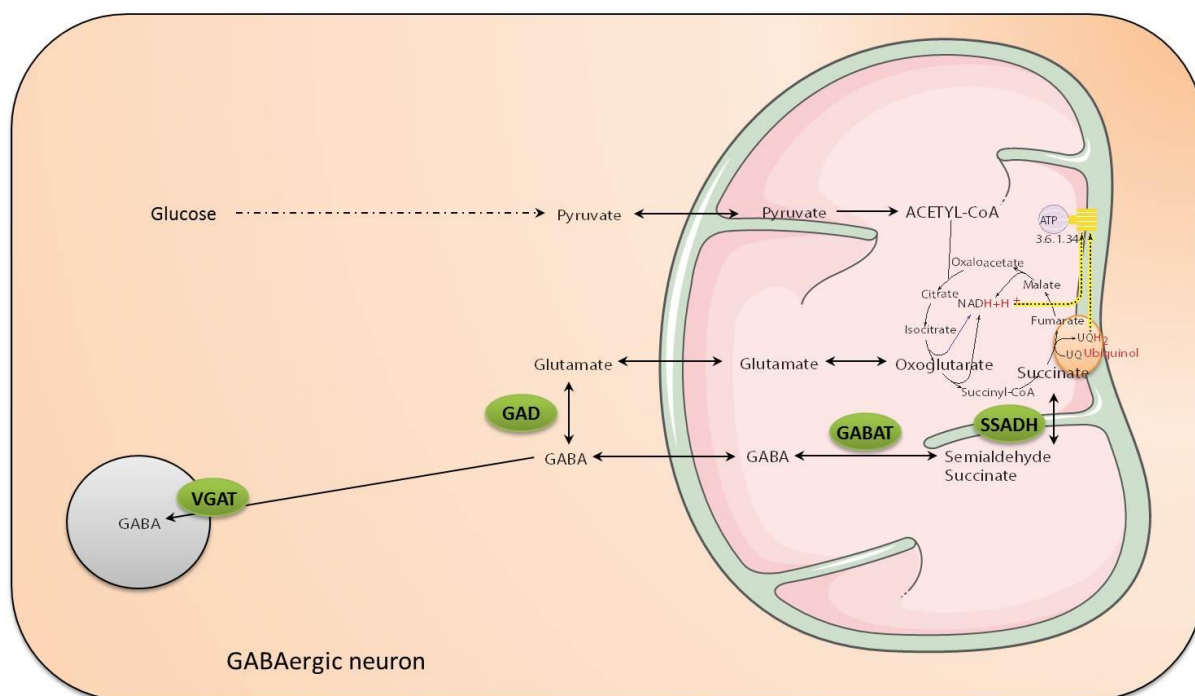


Fig 4. Processes involved in GABA metabolism. GABA content is controlled by three pathways; GABA transport into small synaptic vesicles controlled by vesicular GABA transporter (VGAT); glutamic acid decarboxylase (GAD) activity which is the canonical pathway to generate GABA from glutamate, and GABA shunt, catalyzed by succinate semialdehyde dehydrogenase (SSADH) and GABAT (GABA transaminase).

GABA shunt has been described to be activated after brain ischemia (Kang et al., 2002; Seo et al., 2009), epileptic seizures (Kang et al., 2003; Yogeewari, Sriram, & Vaigundaragavendran, 2005) and in Alzheimer's disease (Lanctôt, Herrmann, Mazzotta, Khan, & Ingber, 2004). GABA shunt is a well-characterized pathway found in plants, microorganisms and

vertebrates, which is highly conserved amongst them (Fait, Fromm, Walter, Galili, & Fernie, 2008; Mamelak, 2012; Michaeli et al., 2011). It consists of two enzymes, GABA transaminase (GABAT) and succinic semialdehyde dehydrogenase (SSADH), which are located both in mitochondria (Hearl & Churchich, 1984; A Schousboe, Hertz, & Svenneby, 1977).

GABAT catalyzes the reaction in which GABA and α -ketoglutarate are converted into succinic semialdehyde and glutamate (A. Schousboe, Wu, & Roberts, 1974). This enzyme is an already druggable target, whose irreversible inhibition by vigabatrin is used to treat epilepsy (Hammond & Wilder, 1985). GABAT activity and expression regulation are not completely elucidated, but ketone bodies are responsible for the reduction of both in rat primary astrocytes (Suzuki et al., 2009), which would explain the reduction in epileptic seizures in patients following ketogenic diets (Hartman, Gasior, Vining, & Rogawski, 2007). GABAT deficiency in humans is extremely rare and causes elevated levels of GABA along severe psychomotor retardation, seizures, hypotonia and hyperreflexia (Jaeken et al., 1984; Tsuji et al., 2010). Recently, in GABAT deficient patients, it has been reported to be essential for mitochondrial nucleoside metabolism, since it facilitates the conversion of dNDPs to dNTPs in the nucleoside salvage pathway (Besse et al., 2015). In this study, they show that vigabatrin is able to cause mitochondrial DNA depletion, which is rescued with dNTPs media supplementation.

The succinic semialdehyde formed by GABAT is rapidly converted to succinate by SSADH, generating NADH (Albers & Koval, 1961; Chambliss, Zhang, Rossier, Vollmer, & Gibson, 1995). Its deficiency has been extensively studied in humans, with several mutations characterized (Akaboshi et al., 2003; Malaspina, Picklo, Jakobs, Snead, & Gibson, 2009). Clinically, patients with reduced SSADH activity present high levels GABA and γ -hydroxybutyrate (GHB) in brain and even GHB aciduria. This provokes severe neurological disorders, such as ataxia and seizures, caused by disturbances in neuronal energy metabolism and increased oxidative stress. The mouse models of SSADH deficiency show similar defects to those present in SSADH-deficient patients (Pearl, Gibson, & Cortez, 2009). SSADH activity is highly sensitive to reactive oxygen species (ROS), since lipid peroxidation products, such as 4-hydroxynonenal, act as potent inhibitors of SSADH in rat brain mitochondria (Nguyen & Picklo, 2003).

In *Drosophila melanogaster*, the lack of GABAT promotes an accumulation of GABA which increases sleep and surprisingly, it also disrupts mitochondrial bioenergetic activity, since there is a reduction in TCA intermediates, NAD⁺/NADH and ATP levels (Maguire et al.,

2015). All these effects are reversed with glutamate supplementation, but not with semialdehyde succinate.

In neurons and astrocytes, anaplerotic pathways are essential for replenish losses of TCA intermediates. It has been calculated that around a 60% of astrocytic TCA cycle intermediates are continuously lost as glutamine (Hassel, Westergaard, Schousboe, & Fonnum, 1995). Besides glial cells, neurons may lose TCA intermediates through an export of citrate to the extracellular fluid (Hassel et al., 1995; Westergaard et al., 1994). A net loss of TCA cycle intermediates would reduce the oxidative capacity of the cell. With the less α -ketoglutarate, the less ATP is formed, because of the reduction in citrate needed in TCA cycle (Gatfield, Lowry, Schulz, & Passonneau, 1966).

GABA metabolism and fasting

Several researchers have approached to assess changes in GABA metabolism in different areas due to fasting. Three rat models had their GABA shunt and GAD activity assessed in hypothalamic nuclei: hyperphagic leptin receptor-deficient *fa/fa* Zucker rats, hyperphagic streptozotocin-induced diabetic rats and diet-restricted rats (Beverly & Martin, 1989). All the models show increased GAD activity in VMH and no changes in LH. Moreover, GABA shunt activities are increased in VMH from diet-restricted rats and *fa/fa* Zucker rats; but streptozotocin-induced diabetic rats show reduced GABA shunt in contrast. GABA shunt in LH seems to be unaffected, just like GAD activity (Beverly & Martin, 1989). Ghrelin raise and insulin drop are two of the events which appear in diet-restricted rats. Insulin production loss appears in streptozotocin-induced diabetic rats (Rerup, 1970). And leptin sensitivity due to a mutation in leptin receptor is the key characteristic of *fa/fa* Zucker rats (K Takaya et al., 1996). All these suggest that GABA metabolism can be modulated in hypothalamus in endocrine way. Nonetheless, one can wonder whether the definition of VMH for Beverly et al referred to MBH, encompassing both VMH and arcuate nucleus, since GABAergic neurons have been described only in ARC and VMH has been described to be mainly glutamatergic (Schöne & Burdakov, 2012).

The reduction of testis size and testosterone due to food restriction was explained by an increase in GABA metabolism in VMH (Leonhardt, Shahab, Luft, Wuttke, & Jarry, 1999). Male

rats, with a daily intake reduced to 8 g of normal chow, show a 35% reduction in body weight and 15% in testis weight. The authors claim that food restriction induces a 90% reduction of luteinizing hormone secretion, which produces a similar testosterone decrease. The researchers assess the expression of several GABA metabolism enzymes in MBH and preoptic area (POA). They observed a 2-fold increase in GAD1 mRNA and a similar increase in astrocytocal glutaminase, with no changes in the POA (Leonhardt et al., 1999).

A mild caloric restriction to a 90% of recommended intake can increase around 45% in GAD expression in several brain areas (Cheng, Hicks, Wang, Eagles, & Bondy, 2004). Inferior and superior colliculus show a 1.4-fold increase in GAD67 expression due to caloric restriction. A 1.75-fold increase in GAD67 in cerebellum is described as well. Moreover, GAD65 is increased in 1.5-fold in temporal cortex and 1.2 fold in superior colliculus. The authors expected to see more changes due to ketogenic calorie-restricted diets in GAD expression, but only mild increases in GAD67 were found in striatum, differentially (Cheng et al., 2004).

Some years ago, the effect of food restriction was assessed in cortical GABAergic neurons from adult rats (Spolidoro et al., 2011). Rats were given divided into two groups one of which was given *ad libitum* access to normal chow diet only every two days for 24h, while the control group was fed *ad libitum stricto sensu*. Their daily mean food intake was reduced in a 25%, which translated in a 83% reduction in body weight and a 2-fold increase in circulating corticosterone. Interestingly, this intervention causes a 84% reduction of GABA release in cortical tissue and a 20% reduction in GAD65 expression in visual cortex. The authors prove that this produces an increase in synaptic plasticity in a BDNF-independent manner (Spolidoro et al., 2011).

More recently, GAD1 mRNA which codifies for GAD67 has been described as a good indicator of GABA release in arcuate nucleus of the hypothalamus (ARC) in mice (Dicken, Hughes, & Hentges, 2015). GAD1 mRNA and GABA release from NAG neurons is increased after fasting in mice. It promotes a reduction of POMC/CART neurons activation, due to an increase of readily releasable GABA pool from NAG neurons (Dicken et al., 2015). Moreover as we explained previously, GAD1 mRNA, which codifies for GAD67 to produce GABA out of glutamate in neurons, seems to be a good indicator of GABA release in hypothalamus. GAD1 mRNA and GABA release from NAG neurons is increased after fasting in mice. It promotes a reduction of POMC/CART neurons activation, due to an increase of readily releasable GABA pool from NAG neurons (Dicken et al., 2015).

Even more recently, a 70% caloric restriction has been reported to promote a 3-fold increase in circulating octanoyl-ghrelin (J. A. Bayliss et al., 2016) The authors affirm that caloric restriction-driven ghrelin increase is the main neuroprotective factor of caloric restriction in Parkinson's disease. Moreover they affirm that it requires activation of AMPK due to ghrelin for this neuroprotective benefits (J. A. Bayliss et al., 2016; Jacqueline A. Bayliss & Andrews, 2013).

Ghrelin

Ghrelin (whose INN as exogenous drug is lenomorelin) is an octanoylated 28 amino acid peptide expressed mainly in stomach. It was first described in 1999 as the endogenous ligand of growth hormone stimulating receptor (GHSR) (Kojima et al., 1999). GHRL gene encodes a preprohormone, preproghrelin with 117 amino acids, which can be cleaved in two regions which become two different hormones: ghrelin (28 residues in the most common variant) and obestatin (23 residues) (Kanamoto et al., 2004) (**Fig 5**). When discovered, obestatin was described to antagonize the effects of ghrelin, promoting a reduction in intestinal motility and a decrease in food intake (J. V Zhang et al., 2005), but the receptor mediating in this effect is a source of discussion.

Ghrelin is the only peripheral hormone described to the date with orexigenic effects. (Nakazato et al., 2001; Sun, Wang, Zheng, & Smith, 2004; Wren et al., 2001). To do so, it needs to be in an activated form as octanoyl-ghrelin, whose formation is controlled by ghrelin O-acyltransferase (GOAT). GOAT actually can use as substrate hexanoyl-CoA, octanoyl-CoA and decanoyl-CoA as acylating agents on Ser3 (Hosoda, Kojima, Mizushima, Shimizu, & Kangawa, 2003; Kojima et al., 1999), but octanoyl-ghrelin is the most abundant variety, despite hexanoyl-ghrelin is thermodynamically most efficient product (Ohgusu et al., 2009). The length of the fatty acid used to acylate ghrelin alters GHSR activation and affects its physiological effects. Both octanoyl- and decanoyl-ghrelin are activators of GHSR (Heppner et al., 2012). The synthesis of octanoyl-ghrelin is produced mainly in endoplasmic reticulum of stomachal X/A-like cells in which both ghrelin/obestatin preprohormone gene and GOAT are expressed (Gutierrez et al., 2008; Yang, Brown, Liang, Grishin, & Goldstein, 2008). Dietary medium-chain triacylglycerols seem to be the origin of octanoyl-CoA used for acylation (Kirchner et al., 2009), since these can be directly absorbed with no need of intestinal lipases action. Actually, an

increase in medium-chain triacylglycerols dietary intake, promotes an increase in circulating acyl-ghrelin levels (Nishi, Mifune, & Kojima, 2012) and this could be used as an strategy to modulate ghrelin's effect. Interestingly, there is a 9 to 1 ratio between desacyl-ghrelin and active ghrelin in blood, probably due to the shorter half-life of active ghrelin (Akamizu et al., 2005). Recent evidence indicates that desacyl-ghrelin to be a functional inhibitor of active ghrelin (Delhanty et al., 2015).








Feature	Position	Length	Description	Graphical view
Signal peptide	1-23	23	Removed in mature form	
Peptide	24-51	28	Ghrelin (28 aa)	
Peptide	24-50	27	Ghrelin (27 aa)	
Propeptide	52-75	24	Removed in mature form	
Peptide	76-98	23	Obestatin	
Propeptide	99-117	19	Removed in mature form	
Lipidation	26	1	O-acyl serine; alternate	

Fig 5. Scheme of GHRL processing to form octanoyl-ghrelin and obestatin. Adapted from UniProtKB - Q9UBU3 (GHRL_HUMAN)

Strikingly, despite ghrelin and GOAT colocalize, their expression is not simultaneous: prolonged fasting increases ghrelin expression, but decreases GOAT at the same time, promoting a high desacyl-ghrelinemia (Kirchner et al., 2009). Thus GOAT-ghrelin system acts as a nutrient sensor by using dietary absorbable TAG, leading to a careful regulation of growth signals and nutrient use (Kirchner et al., 2009; Nishi et al., 2012).

Ghrelin receptor

Ghrelin is an example of a hormone whose receptor, GHSR, was discovered before the hormone itself. In 1980s, exogenous synthetic methionine-enkephalin derivatives were synthesized and show an effect stimulating growth hormone (GH) release (Bowers et al., 1980; Momany et al., 1981), independently to somatostatin/somatoliberin pathway (Bowers et al., 1990). These molecules promote GH release by acting in pituitary and arcuate hypothalamus. Because of that they are called growth hormone releasing peptides (GHRPs).

One of these GHRPs, ibutamoren, was used to identify its receptor, GHSR1a (Howard et al., 1996). GHSR1a is a 366 residue variant encoded by the GHSR gene, found in humans in the third chromosome. A splicing process can befall GHSR mRNA, producing two proteins: GHSR1a, the sole active ghrelin receptor, and GHSR1b, a 289 amino acid variant, which lacks a third intracellular loop which blunts its capacity of coupling G-proteins (C. R. Y. Cruz & Smith, 2008; McKee et al., 1997).

GHSR1a activation triggers phospholipase C producing inositol triphosphate and subsequently opening of calcium channels from endoplasmic reticulum for signal transduction (Guan et al., 1997; Smith et al., 2011). This occurs only by the docking of octanoyl-ghrelin, with no effect from desacyl-ghrelin at physiological concentrations (Broglia et al., 2003; Gauna et al., 2007). This medium chain acyl may favor ghrelin to interact with GHSR1a, by attracting the hormone to the lipidic cell surface (Staes et al., 2010).

The expression of GHSR1a is located predominantly in pituitary gland, hypothalamus (mainly ventromedial and arcuate, but also dorsomedial, lateral and paraventricular hypothalamus), hippocampus, ventral tegmental area and raphe nuclei, and when it comes to peripheral expression GHSR1a mRNA has been detected in pancreatic islets, adrenal glands, thyroids and myocardium (Guan et al., 1997; Zigman, Jones, Lee, Saper, & Elmquist, 2006). Recent studies using transgenic mice expressing eGFP controlled by GHSR promoter suggest that the receptor is expressed in more areas in the brain than the described before (Mani et al., 2014). Concretely, GHSR promoter-driven eGFP expression is found in several regions of neocortex, olfactory bulb, basal ganglia and cerebellum. The authors discuss that these differences appear due to sensitivity differences in probes used to detect mRNA and the longer half-life of eGFP (Mani et al., 2014). Moreover, primary cortical neurons show GHSR expression along their *in vitro* culture, being GHSR1a-positive a 76% of them (Stoyanova & le Feber, 2014).

Effect of ghrelin in the CNS

Ghrelin's main function is related to the central control of energy homeostasis and use: promotion of food intake (Druce et al., 2005; Hotta et al., 2009; Mericq et al., 2003), increase in body weight (Nagaya et al., 2005; Nass et al., 2008), control of glucose homeostasis (Egido, Rodríguez-Gallardo, Silvestre, & Marco, 2002; Tassone et al., 2003) and control of GH secretion (Kazuhiko Takaya et al., 2000). However actions on higher areas with the modulation of anxiety, stress and sleep (Chuang et al., 2011; Lutter et al., 2008; Tolle et al., 2002) have been increasingly studied. Moreover ghrelin has direct effects on peripheral tissues, whose effects are synergistic with those exerted in the CNS: promotion of adiposity (Tschöp et al., 2000).

Ghrelin has been shown to have an important role in the regulation of other central processes such as cognition (Zane B. Andrews, 2011), sleep (Kluge et al., 2008), reward circuits (Jerlhag et al., 2009) and mood (Chuang & Zigman, 2010). Moreover, it has been suggested to be involved in disorders related to addiction (Jerlhag et al., 2006; Vengeliene, 2013), anxiety (Steiger, Dresler, Schüssler, & Kluge, 2011), neurodegeneration (Frago et al., 2002; Gahete, Córdoba-Chacón, Kineman, Luque, & Castaño, 2011) and eating disorders (Atalayer, Gibson, Konopacka, & Geliebter, 2013). The action of ghrelin in such processes implies it to reach extra-hypothalamic areas, away from hypothalamic fenestrated capillaries. To do so, ghrelin is actively transported through the BBB (Banks, Tschop, Robinson, & Heiman, 2002). This transport between plasma and CSF is not fast and it actually seems to be delayed in time (Grouselle et al., 2008).

The protective effect of ghrelin in neurodegenerative diseases was proposed soon after its discovery (Frago et al., 2002). Ghrelin has been described to enter the hippocampus and promote dendritic spine synapse formation there (Diano et al., 2006). Hippocampal neurogenesis is promoted by ghrelin both in *in vivo* and *in vitro* experiments (Davis, Choi, Clegg, & Benoit, 2011; Stoyanova & le Feber, 2014). The physiological implication of such observations implies that ghrelin can enhance memory and spatial learning in rodents (Davis et al., 2011; Diano et al., 2006). The molecular mechanisms of ghrelin neuroprotective and antiapoptotic properties seem to be related to mitochondrial metabolism modulation (Zane B Andrews et al., 2009). This agrees with mitochondrial dysfunction implicated in pathogenesis of neurodegenerative diseases (Ghavami et al., 2014).

Besides its orexigenic effect in hypothalamus, ghrelin has been described to enhance motivation for food intake, since it mediates in the rewarding effect of palatable food (Egecioglu et al., 2010; Jerlhag et al., 2006; Perello et al., 2010). Ghrelin mediates stress-induced food reward and several authors hypothesize about an overlap between physiological mechanisms regulating food and drug reward (Morganstern, Barson, & Leibowitz, 2011). Systemic administration of ghrelin causes dopamine release in nucleus accumbens, which leads to hedonic feeling of reward needed for addiction development (Jerlhag et al., 2006; Ross & Peselow, 2009). Moreover, GABAergic neurotransmission in amygdala is increased after local application of ghrelin in rats, which mimics in alcoholism process (M. T. Cruz, Herman, Cote, Ryabinin, & Roberto, 2013). Mechanistically, GHSR1a seems to be mediating such effects (Jerlhag, Janson, Waters, & Engel, 2012) and ghrelin reinforces behaviors, since promotes learning effects involved in addictive behavior in rodents (Egecioglu et al., 2010). In humans, ghrelinemia is elevated in early abstinent alcohol-dependent patients (D. J. Kim et al., 2005). Moreover, certain polymorphisms in GHSR1a are associated to alcoholism (Landgren et al., 2008).

Ghrelin relationship with anxiety processes is controversial, since some studies suggest an anxiolytic effect for ghrelin (Alvarez-Crespo et al., 2012; Lutter et al., 2008; Spencer et al., 2012), while others propose anxiogenic effect for this hormone (Asakawa et al., 2001; Carlini et al., 2002; Currie, Schuette, Wauson, Voss, & Angeles, 2014; C. Hansson et al., 2011). Some authors state that ghrelin exerts a dual effect, both anxiogenic and anxiolytic depending on the conditions (Meyer, Burgos-Robles, Liu, Correia, & Goosens, 2014). Actually some aspects, such as the way of administration may explain this dissonance in observations: most of the studies showing anxiolytic effects had ghrelin administered peripherally (Lutter et al., 2008; Spencer et al., 2012), while centrally injected ghrelin seems to exert an anxiogenic effect (Carlini et al., 2002; Currie et al., 2014; Meyer et al., 2014). Parallely, central administration impairs sleep (Szentirmai, Hajdu, Obal, & Krueger, 2006) and peripheral administration promotes it (Kluge et al., 2010). Moreover, variations may occur depending the dose, timing and concrete place of central administration (Chuang & Zigman, 2010). Moreover, a polymorphism in GHRL gene has been associated to panic disorder in humans (Caroline Hansson et al., 2013).

Ghrelin orexigenic effect has been proposed to be exerted mainly in a GHSR1a-mediated manner, by its stimulation in arcuate and ventromedial hypothalamus, to increase expression of AgRP and NPY, orexigenic neuropeptide (Z B Andrews et al., 2008; Kamegai et al., 2001; R Lage et al., 2010; Nakazato et al., 2001; Ramírez et al., 2013). Moreover, ghrelin has been reported to

inhibit the firing of postsynaptic POMC neurons by increasing the release of GABA (Tong et al., 2008). To support that, a reduction of GABA output has been reported in *ex vivo* hypothalamic cells from fasted animals as well, which correlates with changes in GADs (Dicken et al., 2015, 2012).

AMPK-ACC axis in VMH and ARC: the malonyl-CoA hypothesis

Brain lipid metabolism has emerged to be one of the important elements in the central regulation of food intake control (Z B Andrews et al., 2008; Gao, Serra, Keung, Hegardt, & Lopaschuk, 2013; Miguel López et al., 2008; S Obici, Feng, Arduini, Conti, & Rossetti, 2003; Silvana Obici et al., 2002; Ramírez et al., 2013) and it seems to be a clear downstream element for ghrelin's effect on food intake and energy homeostasis, especially when it comes to the control of neuropeptide orexigenic signalling. Moreover, some of these hormones, such as ghrelin, have been described to have central extra-hypothalamic functions which can be related directly or indirectly with the food intake modulation, but also with other pathologies (Zane B. Andrews, 2011; Wittekind & Kluge, 2014). The molecular mechanisms involved in ghrelin orexigenic effects are not completely understood, but hypothalamic AMP-dependent protein kinase (AMPK) has a key role (Andersson et al., 2004; Kola et al., 2008; Ricardo Lage, Diéguez, Vidal-Puig, & López, 2008). The importance of VMH and ARC in energy homeostasis resides in their role as a metabolic sensor, which allows the adaptation of body to respond to changes in metabolic state. To this end, AMPK is the key hub for this metabolic sensing, since it is activated by high AMP levels in low energy situations (Ferrer, Caelles, Massot, & Hegardt, 1985). In most tissues, AMPK triggers the metabolic switch to FA use for ATP production (Hardie, Corton, Ching, Davies, & Hawley, 1997). In the VMH and ARC, it modulates energy expenditure and food intake, when activated both by high AMP or direct phosphorylation. Its role has been thoroughly explored, since a decrease in AMPK activity in VMH activates thermogenesis via an increased sympathetic activity onto BAT (Martínez de Morentin et al., 2014). Moreover, overexpression of downstream effectors of AMPK, such as CPT1A, in VMH produces hyperphagia and overweight in rats (Mera, 2012). Downstream AMPK activation promotes acetyl-CoA carboxylase (ACC) inactivation, which produces two effects: on the one hand, it halts lipogenesis since its precursor formation, namely malonyl-CoA, is blocked with by ACC phosphorylation (Kahn, Alquier, Carling, & Hardie, 2005). While on the other hand the less malonyl-CoA is produced, the less neuronal CPT1 isoforms are inhibited (Zammit, 2008) (**Fig 6**).

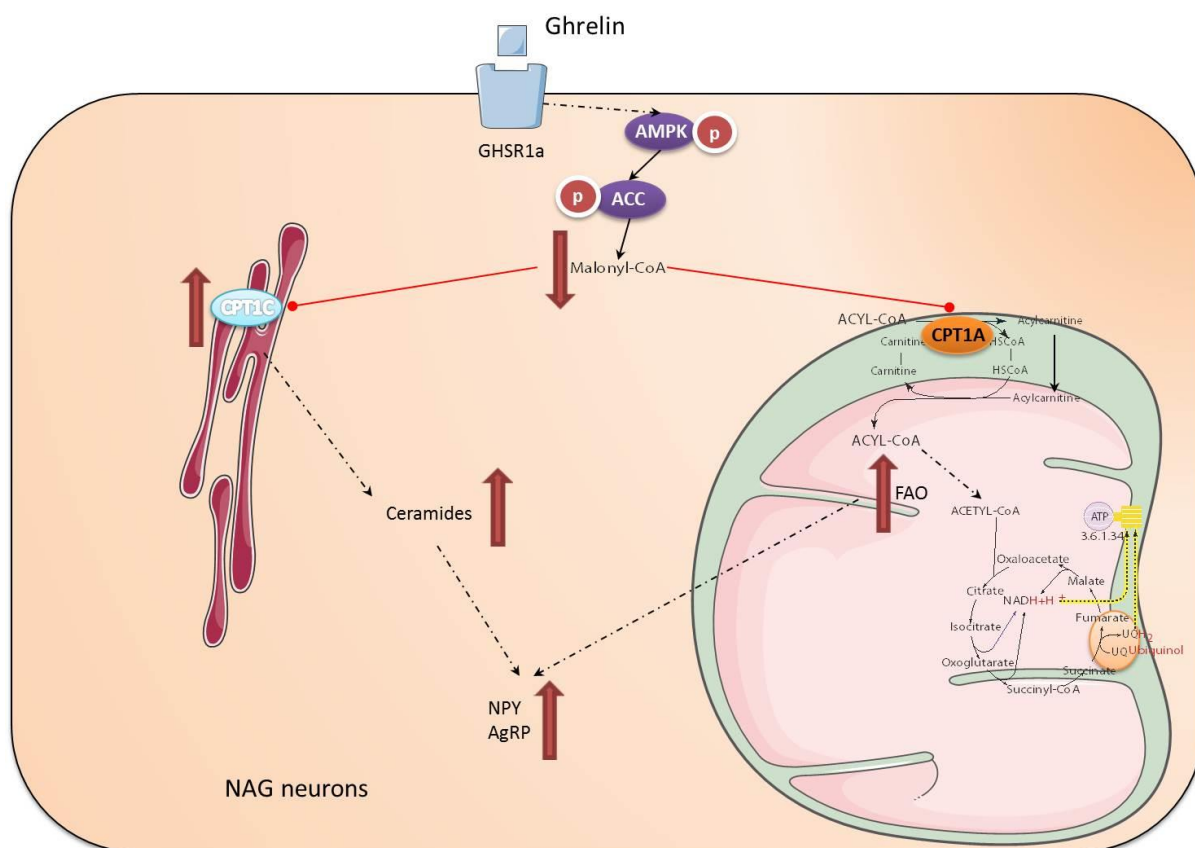


Fig 6. GHSR1a downstream activation pathway in arcuate NAG neurons. Ghrelin stimulates the AMPK-ACC-malonyl-CoA axis, leading to decreased levels of hypothalamic malonyl-CoA, the CPT1 brain isoforms. GHSR1a activation promotes disinhibition of CPT1A and CPT1C, which increases FAO and promotes ceramides increase, respectively. These metabolic changes increase mRNA expression of AgRP and NPY genes, which are involved in the orexigenic effect of ghrelin. Adapted from (Ramírez et al., 2013)

This is the basis for the malonyl-CoA hypothesis for the regulation of the food intake. This hypothesis suggests that an increase in the concentration of malonyl-CoA in hypothalamus act as a satiety intracellular signalling, which reduces food intake. Consequently, a reduction in malonyl-CoA triggers hyperphagia (Hu, Cha, van Haasteren, Wang, & Lane, 2005; Hu, Dai, Prentki, Chohnan, & Lane, 2005; Wolfgang & Lane, 2006). Malonyl-CoA levels change in hypothalamus depending on the nutritional state, which suggests that malonyl-CoA could have something to do with feeding behavior control (Hu, Cha, Chohnan, & Lane, 2003). Fatty acid synthase (FAS) inhibitors, which promote its substrate malonyl-CoA accumulation, have anorexigenic effects (Loftus et al., 2000; M. López et al., 2006). Moreover, overexpression of malonyl-CoA decarboxylase (MCD), which reduces malonyl-CoA levels, promotes hyperphagia (Hu et al., 2003). And leptin anorexigenic effect seems to be related to ACC activation, which increases malonyl-CoA (Gao, Keung, et al., 2011).

Carnitine palmitoyltransferase system as key element of fatty acid β -oxidation

The CPT system is made up of two enzymes which catalyze two transesterification reactions by which long chain fatty acyl (LCFA)-CoA are converted into LCFA-carnitine, to ease their entrance into mitochondrial matrix via carnitine/acylcarnitine translocase (CACT), and then it is transesterified back to LCFA-CoA in the mitochondrial matrix. There LCFA-CoA can proceed to ongoing FAO (McGarry & Brown, 1997). The two transesterification enzymes, namely CPT1 and CPT2, are located in the outer mitochondrial membrane and in the inner mitochondrial membrane, respectively (**Fig 7**). The three aforementioned enzymes ease the translocation of LCFA-CoA into mitochondria, which avoids futile processes between fatty acid synthesis and FAO (Ramsay, Gandour, & van der Leij, 2001).

CPT1 is tightly regulated by its physiological inhibitor malonyl-CoA, thus CPT1 is the key regulation point of FAO. Malonyl-CoA is generated as the first intermediate in lipogenesis, which is another way to avoid futile processes in the lipid generation and oxidation.

Mammals express three CPT1 isoforms, which are encoded in different genes and present differential biochemical characteristics as well as different tissue distribution. Nonetheless, only two CPT1 isoforms are expressed in the brain, both putatively inhibitable by malonyl-CoA: CPT1A and CPT1C.

CPT1A is the most widely distributed isoform, which can be found in liver, lungs, pancreas, bowel, kidneys, ovaries and brain (McGarry & Brown, 1997). Its gene is located in chromosome 11 and codifies for a 773 residues protein whose molecular mass is 88 kDa (Britton et al., 1997; Esser, Britton, Weis, Foster, & McGarry, 1993). It resides in mitochondria in neurons and astrocytes. It is responsible for translocation of LCFA-CoA into the mitochondrial matrix in brain (Zammit, 2008) and its malonyl-CoA IC₅₀ is around 3-30 μ M (McGarry, Mills, Long, & Foster, 1983).

CPT1B, which is the non-neural isoform, is expressed in rat in skeletal muscle, heart, BAT, WAT and testis (Gao, Keung, et al., 2011; Lavrentyev, Matta, & Cook, 2004). Its sensitivity to malonyl-CoA is around 30-fold higher than the other isoforms (McGarry et al., 1983).

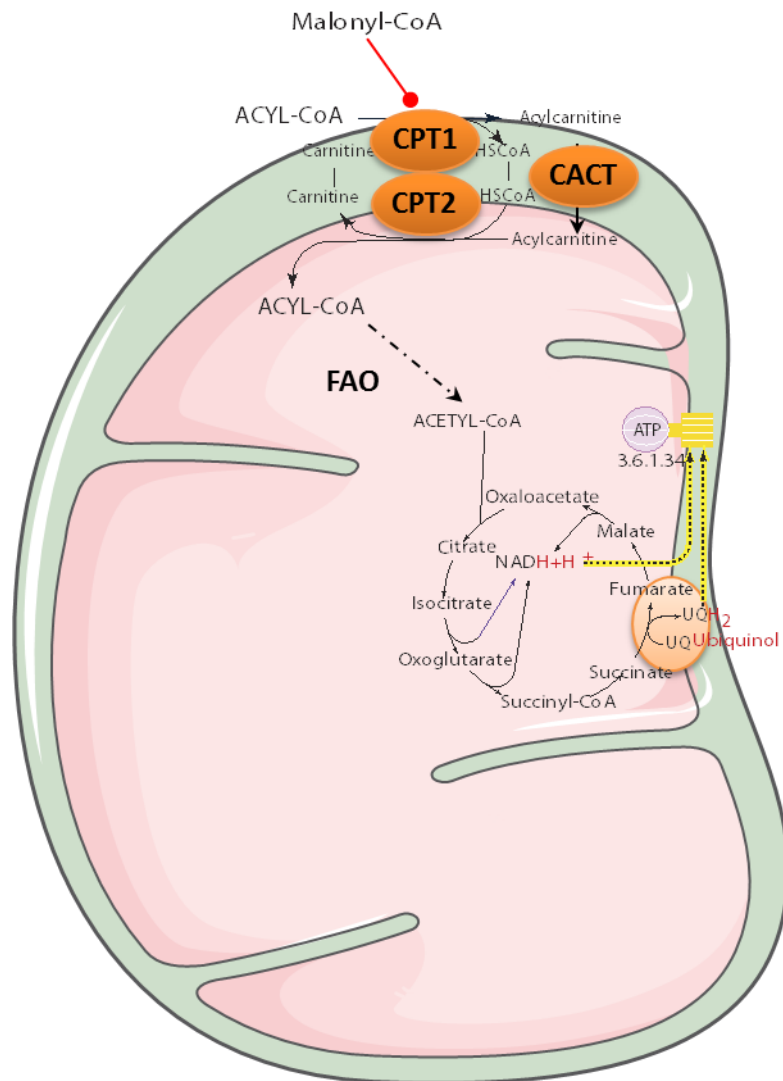


Fig 7. The carnitine palmitoyltransferase system in mitochondria. CoA-activated fatty acids are transesterified by CPT1, which generates fatty acylcarnitines. Those can be transported by CACT, so fatty acyl-CoA can be regenerated by CPT2, to go on with FAO in mitochondrial matrix.

CPT1C is mainly found in the brain, but also in testis. It is encoded by a gene in the chromosome 19, which was described as a CPT1 gene because of its similitude with CPT1A (70%) and CPT1B (66%) (Price et al., 2002). No orthologous sequences of CPT1C can be found in other species but mammals, which suggests a specific function in more evolved brains (Price et al., 2002; Sierra et al., 2008). Despite having all the residues conferring CPT1 catalytic activity and malonyl-CoA sensitivity, it was described to lack any carnitine acyltransferase activity (Price et al., 2002; Wolfgang & Lane, 2006). Nonetheless, an affinity constant for malonyl-CoA was described (0.3 μM) which is within the hypothalamic malonyl-CoA concentration range (0.1-1.4 μM) (Wolfgang & Lane, 2006). CPT1C is embedded in endoplasmic reticulum with a

really low transesterification catalytic activity *in vitro* (Sierra et al., 2008). The fact that previous studies tried to find CPT1C activity in mitochondria might explain the unsuccessful results to detect it (Price et al., 2002; Wolfgang & Lane, 2006).

In any case, AMPK, through CPT1A as well as CPT1C, seems to be involved in downstream ghrelin signaling in brain (Lane, Wolfgang, Cha, & Dai, 2008). Moreover, both isoforms have been reported to affect peripheral tissues, including BAT amongst others (Mera, 2012; Wolfgang & Lane, 2006). Ghrelin has been described to modulate ceramide metabolism in hypothalamus through CPT1C, which is moreover responsible for changes in NPY and AgRP expression (Ramírez et al., 2013). Ghrelin was previously described to depend on UCP2 to trigger NPY and AgRP expression as well (Z B Andrews et al., 2008). In this case, the authors suggest that downstream events to GHSR1a activation are sequentially AMPK activation, ACC phosphorylation and subsequent malonyl-CoA reduction. This would increase CPT1A activity and FAO. The increased FAO in neurons would trigger UCP2 activation in order to buffer ROS, which would let NAG neurons to obtain enough energy from FAO to activate its firing and thus promote food intake through NPY and AgRP release (Z B Andrews et al., 2008). This work became controversial, when proposing that neurons would oxidize fatty acids to obtain energy. Moreover, other works appeared, suggesting AgRP release to be dependent on autophagy derived fatty acids, but independent from FAO (S Kaushik et al., 2011). They proved that CPT1A inhibition by etomoxir did not affect AgRP release provoked by increased autophagy. Nonetheless, this work was focused in a starvation ghrelin-independent model of AgRP release (Singh, 2012).

CPT1AM overexpression in VMH

The role of CPT1A in VMH had preliminary studies in our group, as a part of a previous thesis (Mera, 2012). We focused mainly on the peripheral effects of CPT1A long-term overexpression, as well as some hypothalamic feeding control elements (**Fig 8**). For this experiments we use adeno-associated viral vectors to express a malonyl-CoA-insensitive and permanently activated CPT1A isoform, which was developed and studied extensively in our group (Herrero et al., 2005; López-Viñas et al., 2007; Malandrino et al., 2015; Mera et al., 2014; Morillas et al., 2003; Orellana-Gavalda et al., 2011).

A hyperphagic phenotype is observed due to CPT1AM overexpression in VMH (Fig 8A,B). This hyperphagia promoted a non-significant increase in body weight (Fig 8C), with increased adiposity (Fig 8D,E). The overexpression of CPT1AM induces insulin increase and hyperglycemia (Fig 8F,G), which is accompanied by an increase in gluconeogenic enzymes expression in liver (Mera, 2012). Surprisingly, an increase in fasting octanoyl-ghrelin is produced by CPT1AM overexpression in VMH, suggesting some kind of positive feedback produced by ghrelin signalling downstream activation (Fig 8H). Strikingly, the increase in adiposity was not accompanied with an increase in circulating leptin (Fig 8I).

When hypothalamic mechanisms were assessed, no changes are observed in the expression of any of the feeding control hypothalamic neuropeptides during fasting (Fig 9J). Nonetheless, an increase in ghrelin and NPY receptors expression in MBH is induced by CPT1AM overexpression, reinforcing in the case of GHSR1a the notion of a feedback signaling (Fig 9J). The thesis results of Dr. Mera, together with the ones shown in the first part of the results of the present thesis, conformed a co-authored research paper, found in Publications section (Mera et al., 2014).

Dr. Mera assessed in her thesis not only the overexpression of CPT1AM in VMH, but also pharmacological inhibition by C75-CoA of CPT1A in hypothalamus (Makowski et al., 2013; Mera, 2012; Mera et al., 2009). Moreover, C75 enantiomers show differential effects, since (+)-C75 is the only capable of inhibiting hypothalamic CPT1A, when converted to (+)-C75-CoA, and therefore it produces an anorexic effect (Makowski et al., 2013).

In this work, we focus with more depth on the mechanistic insight of ghrelin action in the modulation of neurotransmission in hypothalamus and cortex and the involvement of CPT1A in it.

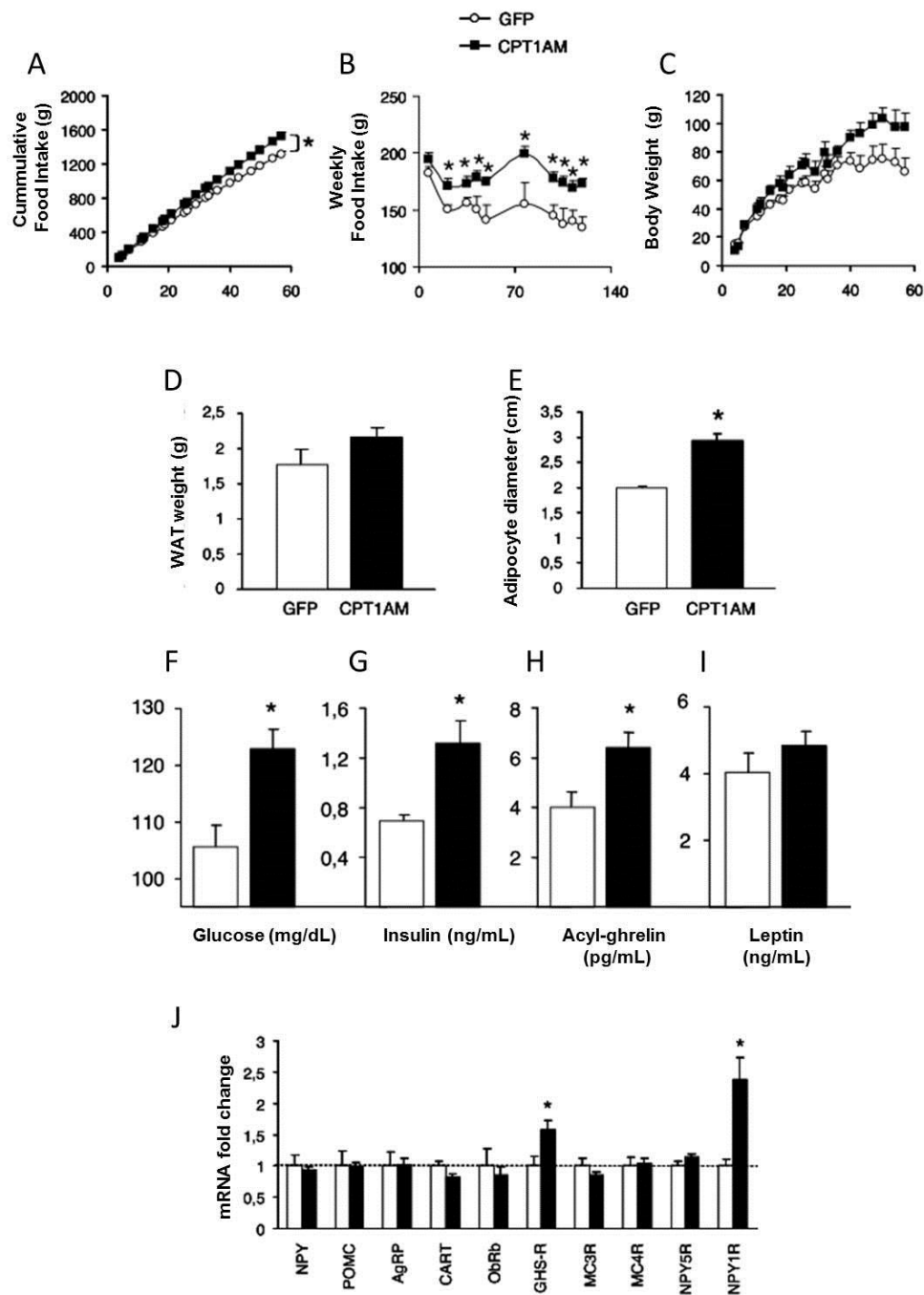


Fig. 8. Effect of CPT1AM overexpression in VMH on food intake (A, B), body weight (C), adiposity (D, E), serum levels of glucose (F), insulin (G), acyl-ghrelin (H) and leptin (I) and mRNA levels of hypothalamic neuropeptides and receptors (J). Adapted from (Mera, 2012). Average \pm SEM, * $p < 0.05$.

AIMS

The main aim of this doctoral dissertation is the study of the **role of carnitine palmitoyltransferase 1A (CPT1A)** as a downstream effector of **ghrelin** in **hypothalamus** and **cerebral cortex** and to examine the mechanisms by which it modulates **neurotransmission** in these brain areas. To this end, we have assessed several approaches to get a mechanistic insight, through different specific objectives:

1. Evaluation of the hyperphagic phenotype in rats overexpressing CPT1AM in ventromedial hypothalamus.
2. Study of the role of CPT1A as a downstream effector of ghrelin in hypothalamic cell lines.
3. Study of the role of CPT1A as a downstream effector of ghrelin in primary cortical neurons.

EXPERIMENTAL PROCEDURES

1. Animals, viral vectors and cell cultures

1.1. Experimental procedures with rats

We used 10-12 weeks old male Sprague-Dawley rats (*Rattus norvegicus*) which were purchased from Charles River, with weights of 260-290 grams. They were maintained with a 12h-light/dark cycle, with *ad libitum* water and food (Harlan Ibérica, ref. 2014) in the *Unitat d'Experimentació Animal* Facilities of the *Universitat de Barcelona* School of Pharmacy and Food Sciences, where environmental conditions are controlled at $22\pm 2^{\circ}\text{C}$ and 60% humidity. All the experiments with rats were previously approved by the *Comité Ètic d'Experimentació Animal* of the *Universitat de Barcelona* (CEEA-UB), whose procedures obtained the DAAM Permits #4058 and #5471.

We assessed the effect of CPT1AM overexpression in VMH on weight, food intake, glucose metabolism, circulating amino acids and thyroidal hormones, MBH lipid composition, MBH ROS-buffering enzymes and ER stress proteins transcripts, as well as MBH neuropeptides and glutamate and GABA metabolism genes mRNA. To do so, we cannulated the animals after at least 1-week post arrival quarantine to reach VMH with ongoing microinjection. 1 week later, AAV vectors were microinjected into rats' VMH and after another week, body weight and food intake was monitored along their lives. 8 weeks before rats' termination, a fast-refeeding satiety test was performed and 4 weeks previous their sacrifice glucose tolerance test (GTT) and pyruvate tolerance test (PTT), each to two different sets of animals, were performed (**Fig 9**).



Fig 9. Scheme of the time course of the experiment.

1.2. Stereotactic surgery

Stereotactic surgery allows reaching regions deep inside the brain with the use of cannulae or needles in a region-specific manner. To do so, 3-dimensional coordinates referring to Bregma point in rat's skull had to be defined previously using Paxinos and Watson's *The Rat Brain in Stereotaxic Coordinates* (Paxinos & Watson, 1998)

1.3. Bilateral ventromedial hypothalamus cannulation

Once rats were completely anesthetized with ketamine (90 mg/kg) and xylazine (11 mg/kg), they were set in a stereotactic apparatus (Kopf Instrument, Model 900 Small Animal Stereotactic Instrument). Once its head was shaved using an electric trimmer, a longitudinal cut was made on the head using a scalpel to find the rat's skull. Then Bregma point was found in the perpendicular intersection between sagittal and coronal synarthroses. Its coordinates were set on the apparatus and used as a reference to find the area where a trephining was performed with a thin and sharp microdriller to allow brain cannulation. In all this process it was key to keep the area free from any connective tissue and unmoisturized. Once the burr hole was open, a set of four smaller holes were performed, to set 4 stainless steel screws (Plastics One, ref. screw 0-80x1-16 1212 080x062). These screws allowed fixing the cannula using dental cement. Then the bilateral cannula (Plastics One, ref. C235G-1.5-SPC Guide DBL 26GA 1.5 mm C-C/9 mm Below Pedestal) was introduced at a 9-mm depth and is fixed first with cyanoacrylate liquid (Loctite, Super Glue 3 Pincel 5 g) and then permanently with high-speed drying dental cement (Plastics One, ref. cere-AD Cerebond/cere-Tub Cerebond Mixing Tube). The coordinates for VMH are from Bregma -2.8 mm posterior, ± 0.7 mm lateral and -10 mm ventral (Paxinos & Watson, 1998). Once dried, an obturer (Plastics One, ref. C235-SPC/fit 9 mm C235-1.5 W-O Proj.) was introduced into the cannula to avoid any obstruction. Both the cannula and the obturer were protected with a plastic dust cap (Plastics One, ref. 303DCFT Dust Cap). Once the procedure was finished, the animals were individually caged with *ad libitum* food and post surgical drug-supplemented water, containing enrofloxacin (10%) and buprenorfin (0.3 g/400 mL) as antibiotic and analgesic, respectively. Daily monitoring was performed to follow up the general state of the operated rats for a week.

1.4. Adeno-associated viruses microinjection in VMH

After a post surgical quarantine of a week, the animals were once again anesthetized to be set in the stereotactic apparatus, as previously stated. Thanks to a 5- μ L microsyringe (Hamilton, ref. 7633-01) adeno-associated viruses, described in following parts of this dissertation, were injected into VMH bilaterally through the previously set cannula at a 10-mm depth, from the skull surface. The injected volume was 1 μ L in total at a 0.2 μ L/min rate, with a 10-minute preinjection wait, once set the needle into the VMH parenchyma, and a 10 min wait, once finished the injection, to avoid any reflux. The final dose was $2.5 \cdot 10^9$ pfu per injection site in 1 μ L. Once the procedure was finished, the animals were individually caged with *ad libitum* food and post surgical drug-supplemented water, containing enrofloxacin (10%) and buprenorphine (0.3 g/400 mL). Daily monitoring was performed to follow up the general state of the operated rats for a week. The correct cannulation and infection was assessed postmortem in sagittal brain sections, taking advantage of GFP expressing AAVs microinjected as control.

1.5. Cumulative Weekly Food Intake Measurement

A week after AAV microinjection, the food to be eaten by the individually caged AAV-injected animals was monitored. To do so, the initial amount of compound pelleted fodder was weighed at the beginning of every week, using a precision scale. At the following week, remaining pellets were measured again with the same scale, and food was added up to the same amount given the last week. In any case, all rats had *ad libitum* food supply and its consumption was tightly monitored during the 108 days after infection until the animals' termination.

1.6. Fast-refeeding satiety test

10 weeks after the AAV microinjection, the fast-refeeding studies were performed to assess whether the changes in food intake were dependent or independent to sated state in our model. To do so, animals were overnight fasted for 12 h and then refeed with a preweighed amount of pellets. Food intake was measured at 1 h, 2 h, 4 h, 8 h and 24 h after refeeding. All measurements were weighed using the same precision scale.

1.7. Body weight measurement

A week after AAV microinjection, the body weight of the AAV-injected animals was monitored weekly during the 108 days after infection until the rats' sacrifice, using every week the same precision scale.

1.8. Glucose tolerance test

14 weeks after AAV microinjection, we assessed insulin sensitivity performing a glucose tolerance test (GTT) in a set of animals. This test was performed after 12 h fasting, when the rats were injected 20% glucose (Baxter, ref. 2B0124P) intraperitoneally to a final dose of 2 g/kg. Caudal glycaemia was measured 0 min, 15 min, 30 min, 60 min 90 min and 120 min after the glucose bolus. The glycaemia assessment was measured using a hand glucometer (Bayer, Contour XT, ref. 83415194) and its test strips (Bayer, Contour next, ref. 84191389).

1.9. Pyruvate tolerance test

14 weeks after AAV microinjection, we assessed hepatic gluconeogenesis performing a PTT in another set of animals. This test was performed after 12 h fasting, when the rats were injected 0.2g/mL pyruvate (Sigma-Aldrich, ref. P5280) in phosphate-buffered solution intraperitoneally to a final dose of 2 g/kg. Caudal glycaemia was measured 0 min, 15 min, 30 min, 60 min 90 min and 120 min after the pyruvate bolus. The glycaemia assessment was measured using a hand glucometer (Bayer, Contour XT, ref. 83415194) and its test strips (Bayer, Contour next, ref. 84191389).

1.10. Serum preparation

Blood from sacrifice terminated rats was obtained after cervical dislocation using a rodent guillotine (Kent Scientific Corporation, ref. DCAP). It was collected within 50 mL tubes and then aliquoted into smaller volumes. The blood was kept for at least 30 min at room temperature. Following that, it was centrifuged at $10\,000 \times g$ for 5 min at 4°C. Then the supernatant serum was aliquoted and kept at -20°C for ongoing hormones and metabolites measurements.

1.11. Mediobasal hypothalamus dissection

Once decapitated, the implanted cannula was gently detached and removed from the skull, taking care of not damaging the brain tissue. Then the skull was open using surgical equipment and the brain was extracted. Phosphate-buffered solution was used to gently rinse and remove any remaining blood. Then, the brain was gently placed in a plastic rat brain matrix (Kent Scientific Corporation, ref. RMC1), which allows to obtain sagittal cuts with a width starting from 1 mm. Sharp matrix blades (Kent Scientific Corporation, ref. BLADE) were used to cut a 2-mm sagittal section encompassing most of the ventromedial hypothalamus, taking as a reference the optical chiasm to set them for the dissection. Once the section was cut, the remaining brain was carefully removed outside the matrix and the section was extracted and horizontally positioned. Avoiding smashing the tissue, the blade in the most rostral part was removed exposing the section, to proceed to cut the mediobasal hypothalamus. This area is found bilaterally in the most basal part of the brain and dissected with a crosswise cut starting and enclosing two thirds of the 3rd ventricle up to 1.5 mm to each side of it, to obtain two wedges. See figure 1 in Introduction for rat brain coronal section depicting hypothalamic nuclei.

1.12. Brain coronal sections for histological preparations

We proceeded to extract the brain as explained in the former paragraph. After a gentle phosphate-buffered solution rinse, brain was fixed overnight in neutral-buffered 10% formalin solution (Sigma-Aldrich, ref. HT5012) at 4°C. Next, the brain was immersed in a phosphate-buffered 20% sucrose solution at 4°C for 18-36 h. Coronal sections with 50 µm width were

obtained using a sledge microtome-cryostat (Leika, SM2000R), using Tissue-Tek Optimal Cutting Temperature (OCT) compound (Sakura Finetek, ref. 4583) to immobilize the brain and give it enough rigidity to cut the sections. The different sagittal sections were gently ordered in phosphate-buffered solution from rostral to caudal part of the brain and then mounted onto microscope slides (Thermo Scientific, Superfrost Plus ref. #4951PLUS-001) with Shandon Immu-Mount (Thermo Scientific, ref. 9990402) to prevent fluorescence fading and 24x60 mm coverslips (Knittel Gläser, ref. VD1 2460 Y100A).

1.13. Potentially conditional CPT1A knockout mice generation

An important tool to find molecular mechanisms in which CPT1A might be involved is the use of knockout mice (*Mus musculus*) for its gene. Due to the importance of this enzyme in general metabolism, animals lacking both *cpt1a* alleles are not born and only heterozygous CPT1A^(+/-) survive (Nyman et al., 2005). To overcome this, cell-specific CRE recombinase-driven knockout mice have emerged as a solution for mechanistic studies, but no inducible knockout model for CPT1A had been developed to the moment.

In our case, we took advantage of the European Conditional Mouse Mutagenesis (EUCOMM) program whose mutant embryonic stem cells and vectors can be obtained from the European Mouse Mutant Cell Repository (EuMMCR) and even mutant mice, from European Mouse Mutant Archive (EMMA).

We obtained from the repository two heterozygous clones, whose reference number is HEPD0727_3_H09 and HEPD0727_3_E10, which had a potentially conditional knockout for CPT1A. In both cases, they had been obtained by homologous recombination, in a construct in which the 5' homology arm included the area around exon 3 and the 3' homology arm, the area around exon 5 (**Fig 10**). In any case, exon 4 is flanked by two loxP regions in what has been called the critical region in the construct. Upstream this area, the construct includes a FRT-flanked region which contains a NEO gene as well as a LACZ gene, for clone selection. In the latter, it is separated with an IRES region from an alternative deletion Exon Del, which truncates the expression of wild type CPT1A from this allele, unless it is processed by a FLP recombinase, also known as flipase. The deletion of the FRT-flanked region makes the allele to regain CPT1A

expression, but in a conditional knockout manner, depending on CRE recombinase activity to lose its function again.

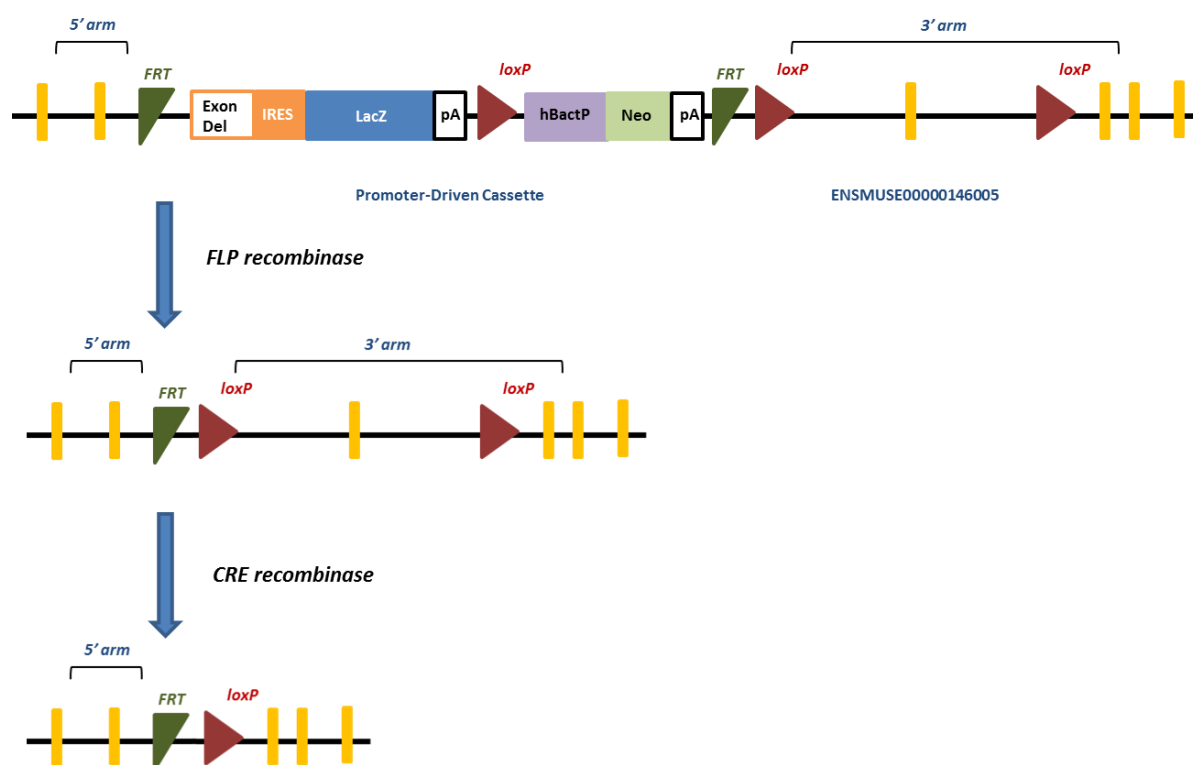


Fig 10. Scheme of the construction present in $CPT1A^{f/t}$ mice (top), $CPT1A^{(loxP/loxP)}$ mice (middle) and $CPT1A^{(loxP/loxP)}$; CRE mice (bottom). FRT: Target sequence for FLP recombinase; Exon Del: Internal Exon Deletion which blocks wildtype CPT1A translation; IRES: Internal ribosome entry site; LACZ: β -galactosidase gene; pA: Polyadenylation sequence; loxP: Target sequence for CRE recombinase; hBactP: Human β -actin promoter; NEO: Neomycin resistance gene.

The two embryonic stem cells containing a $CPT1A^{tm1a(EUCOMM)Hmgu}$ (simplified as $CPT1A^{f/t}$) allele from the parental cell line JM8A3.N1 were sent to the *Centre de Biotecnologia Animal i Teràpia Gènica* (CBATEG) at the *Universitat Autònoma de Barcelona* to go on with the chimeric mice generation. At CBATEG, karyotype and morphology studies were performed in growing stem cells to assess the fittest clone to be injected:

<i>Clone</i>	<i>Euploidy</i>	<i>Growth</i>	<i>Morphology</i>
HEPD0727_3_H09	92%	Good	Good
HEPD0727_3_E10	85%	Good	Good

The clone HEPD0727_3_H09 was the chosen one to be microinjected to obtain the chimeric mice. Its parental cell line JM8A3.N1 confers a agouti-fur phenotype, so this clone was injected into black-fur phenotype C57BL/6J.Ola.Hsd blastocyst, which will produce chimeric mice with agouti upon black background.

These injected blastocysts were transferred into foster mothers, which gave birth to 8 chimerae:

<i>Transfer</i>	<i>Chimera #</i>	<i>Sex</i>	<i>Birth</i>	<i>Chimerism</i>
B80	1	♂	2013.11.25	30%
B80	2	♀	2013.11.25	80%
B80	3	♂	2013.11.25	75%
B81	4	♂	2013.11.25	70%
B81	5	♂	2013.11.25	10%
B81	6	♀	2013.12.22	60%
B93	7	♂	2014.01.06	90%

1.14. CPT1A^(loxP/loxP) colony establishment

All the chimerae were shipped to the *Unitat d'Experimentació Animal* Facilities of the *Universitat de Barcelona* School of Pharmacy where we got the permit to establish a colony for the subsequent breeding. The chimerae and all their descendants lived in controlled environmental conditions at 22±2°C and 60% humidity with a 12h-light/dark cycle, with *ad libitum* water and food (Harlan Ibérica). Chimeric mice #2, #3, #4 and #7 were mated with C57BL/6J mice purchased from Charles Rivers. Only chimera #2 gave birth to descendants. These animals were genotyped and those carrying the potentially conditional knockout *cpt1a* allele in heterozygosis (CPT1A^(+/ftr)) were mated with heterozygous FLP recombinase-expressing mouse (Kranz et al., 2010) gently provided by Dr. Barbara Tondelli. Some of their descendants had the genotype CPT1A^{(+/ftr);FLP^(+/-), whose expression of FLP recombinase}

allowed to have CPT1A^(+/loxP) mice. These descendants were mated to obtain CPT1A^(loxP/loxP), avoiding litter inbreeding when possible. gDNA was obtained from all these animals and their descendants to be genotyped and this procedure is available on *DNA techniques* section of this typescript.

1.15. Adeno-associated viruses

Adeno-associated viruses (AAV) were used to overexpress CPT1AM in rat VMH, due to its low immunogenicity and its long-term expression (Vandenberghe, Wilson, & Gao, 2009). They belong to *Parvoviridae* family within the *Dependovirus* genre. This kind of virus needs a helper virus, such as an adenovirus, to be able to infect the host cell and to replicate. When no coinfection occurs, the AAV remain latently integrated specifically in the nucleus of chromosome 19q13.4. The AAV contain a single-stranded DNA genome with *circa* 4 700 nucleotides. It contains two open reading frames (ORF), flanked by two inverted terminal repeats (ITR), being the latter the only elements essential for the genome to be replicated and packed. The different capsid protein composition allows AAV to have a wide range of serotypes, which are also defined with different cell entrance mechanisms determining cell-specificity when it comes to infection. When it comes to transduce CNS cells, AAV serotypes 1, 4, 5, 7 and 8 have been used to successfully infect several neuronal types in different brain areas (Allocca et al., 2007; Davidson et al., 2000). Glial cell transduction has been performed mainly with AAV1 and AAV5 (Davidson et al., 2000; Wang, Wang, Clark, & Sferra, 2003). AAV9 has been described as a potential tool to overcome blood-brain barrier (Manfredsson, Rising, & Mandel, 2009) and infect brain cells without injecting the viral particles in the parenchyma or the CSF.

The adeno-associated viruses used for this project were produced at UniQure NV facilities in Amsterdam, NL since our research group tied a collaboration agreement with this company. UniQure NV, formerly known as Amsterdam Molecular Therapeutics (AMT), is a biotechnological company focused in the production of AAV aimed to gene therapy. Actually, it has been the first pharmaceutical company ever to have the approval in 2012 from the European Medicines Agency to market alipogene tiparvovec (marketed as Glybera®), as a treatment for lipoprotein lipase deficiency in humans.

The procedure followed to produce the AAV (Urabe, Ding, & Kotin, 2002) is based in the obtaining of 3 baculoviruses to infect insect Sf9 cell line, where AAV particles are produced. One of the baculovirus contains *rep*, which codifies proteins involved in replication; the second, *cap*, for the capsid proteins, and lastly the third baculovirus codifies for our gene of interest.

In our case, our third baculovirus contained the *cytomegalovirus* (CMV) promoter to drive the expression of *green fluorescent protein* (GFP) cDNA, in our control group, or rat malonyl-CoA insensitive *carnitine palmitoyltransferase 1A* (CPT1AM) cDNA, to act as constitutively active downstream effector of ghrelin signalling. Besides, the *woodchuck posttranscriptional regulatory element* (WPRE) [GenBank acc AY468 486] is added to enhance the transcription process, and the *bovine growth hormone polyadenylation* (bGH) signal [GenBank acc M57764, 2326-2533 bp], to set transcription end. All these elements are encasted between two *inverted terminal repeats* (ITR) regions, from AAV2. The baculovirus for *rep* and *cap*, were supplied by UniQure NV and confere a AAV1 capsid, which enhances neuronal infection in CNS (**Fig 11**)

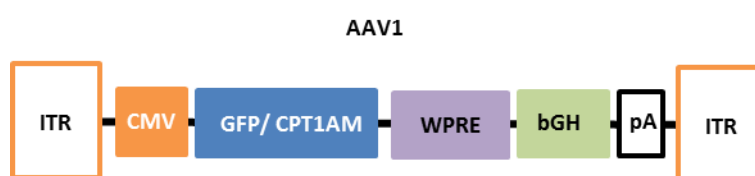


Fig 11. Structural scheme of the AAV1 used to overexpress GFP and CPT1AM in rats. ITR: Inverted terminal repeats; CMV: cytomegalovirus promoter; GFP: green fluorescent protein; CPT1Am: Mutant malonyl-CoA-insensitive CPT1A; WPRE: woodchuck posttranscriptional regulatory element; bGH: growth hormone polyadenylation sequence.

The titration of the AAV used was:

Adenoviral vector

Titration

AAV-CPT1AM

2.5·10¹² pfu/mL

AAV-GFP

5.0·10¹² pfu/mL

1.16. Adenoviruses

Adenoviral vectors have been used in this work with the aim to overexpress, silence and delete CPT1A in different neuronal cell types. They confer a rapid and efficient DNA transference in a wide range of mammalian cells, so they have become one of the key vectors used in gene function studies and transgenesis. They have the advantage to deliver up to 36 000 bp, but they usually do not integrate into the genomic DNA. Since they remain in an episomal state, this causes a transient expression of the transgene, with its maximum at 48 h after infection. The Adenoviruses belong to the *Adenoviridae* family and they contain a double-stranded DNA genome. In our project, we have used serotype-5 human adenovirus (Ad5). The adenoviral vector design is based on the deletion of certain genes found in the *wild type* vector, such as E1 and E3, to maximize the exogenous DNA which can fit into the genome from 2 000 bp to 7 000 bp. This strategy has another aim as well, thus the adenovirus become replication-defective, which makes cells to be infected without major perturbation of the normal functions, which allows to study the functional properties of the transgene. Nonetheless, E1 gene is essential for the amplification and propagation of the virus. To overcome this, the amplification is performed in HEK 293A cell line, which contains gDNA-integrated E1 region in its cellular gDNA.

1.16.1 Adenoviral constructions

The adenoviral vectors have been used in this work with the aim to overexpress the permanently active malonyl-CoA-insensitive CPT1A isoform (CPT1AM), to silence the endogenous CPT1A using a small hairpin RNA (shRNA) and to express CRE recombinase in *cpt1a^(loxP/loxP)* cells to delete CPT1A.

1.16.2. CPT1AM-expressing adenovirus

Our laboratory has been working for several years with a mutated isoform of CPT1A, which we developed by site-directed mutagenesis (M593S). This isoform is insensitive to malonyl-CoA, which confers a permanently active state. Its constant expression is driven by the

CMV promoter. The control adenoviral vector used in this case had the same structure, but expressing GFP instead.

<i>Adenoviral vector</i>	<i>Titration</i>
Ad-CPT1AM	1.20·10 ¹¹ pfu/mL
Ad-GFP	6.20·10 ¹⁰ pfu/mL

1.16.3. shCPT1A-expressing adenovirus

Small hairpin RNA (shRNA) is an artificial RNA which can be used to silence a targeted gene expression. Once expressed, shRNAs are processed by DICER system to become a small interfering RNA (siRNA) which diminishes the mRNA of a certain gene, with the consequent protein translation reduction. In our case, we took advantage of the MISSION® shRNA repository, which we had also used for lentiviral shRNA expression, to find a sequence to knockdown CPT1A both in rats and mice. The plasmid whose sequence was used, was obtained from the plasmid of MISSION® shRNA Bacterial Glycerol Stock (Sigma-Aldrich, ref. SHCLNG-NM_013495.1-1766s1c1; TRC0000110597) which had a 73% validated knockdown in Hepa 1-6 cells:

5' CCGGGCTCGCACATTACAAGGACATCTCGAGATGTCCTTGTAATGTGCGAGCTTTTTG 3'

This sequence was subcloned in a vector for adenoviral amplification. The construction had CMV promoter to drive the hairpin expression and an IRES region to promote the expression of GFP as well. The control adenoviral vector used in this case had the same structure, but expressing a scramble shRNA sequence instead.

<i>Adenoviral vector</i>	<i>Titration</i>
Ad-shCPT1A	7.88·10 ¹⁰ pfu/mL
Ad-scramble	4.76·10 ¹⁰ pfu/mL

2.16.4. CRE recombinase-expressing adenovirus

Our generated CPT1A^(loxP/loxP) mice let us study molecular mechanisms involving CPT1A in primary cultures, if expressing CRE recombinase. To this end, we purchased an adenoviral vector expressing constitutively CRE recombinase, besides GFP controlled by an independent promoter. The viral vector, namely Ad-CRE-GFP (Vector Biolabs, ref. 1700) was amplified upon arrival, as well as Ad-GFP to be used as its control vector.

<i>Adenoviral vector</i>	<i>Titration</i>
Ad-CRE-GFP	4.22·10 ⁹ pfu/mL
Ad-GFP	3.32·10 ⁹ pfu/mL

1.16.5. Adenoviral amplification

The adenoviral amplification was performed in 2 subsequent amplifications: For the first amplification, HEK 293A cells were cultured in 10-cm plates. With a confluency around 70%, the medium was removed to wash the cells with PBS and 5 mL of fresh 25 mM glucose pyruvate- and glutamine-included Dulbecco's Modified Eagle Medium (DMEM) (Biowest, ref. L0104-500) supplemented with 5% fetal bovine serum (FBS) (GIBCO, ref. 102070-106) and 1% penicillin/streptomycin (100 U/mL final concentration) (GIBCO, ref. 15140122) was added carefully not to detach the cells. Then 50 µL of the adenoviral stock per plate were used to infect the cells. After overnight infection, 5 mL of high-glucose pyruvate- and glutamine-included DMEM (Biowest, ref. L0104-500) supplemented with 10% FBS (GIBCO, ref. 102070-106) and 1% penicillin/streptomycin were added to the infection medium in each plate. When the cytopathic effects were complete, *i.e.* all the cells were detached which occurs 48 h after infection; cells were collected within the medium to a 15-mL sterile polypropylene tube. Then a series of 3 freeze/thaw cycles were applied to the cells using liquid nitrogen and a 37°C water bath to release the viral particles still remaining in the cells. Eventually, all the debris were pelleted at 2 000 x *g* for 5 min at 4°C and the supernatant was recovered for the second amplification. In case this would not take place in the same day, the infectious supernatant might be stored at -80°C, once refrozen in liquid nitrogen.

For the second amplification, HEK 293A cells were cultured in ten 15-cm plates. With a confluency around 70%, the medium was removed to wash the cells with PBS and 5 mL of fresh high-glucose pyruvate- and glutamine-included DMEM (Biowest, ref. L0104-500) supplemented with 5% fetal bovine serum (FBS) (GIBCO, ref. 102070-106) and 1% penicillin/streptomycin (final concentration 100 U/mL) (GIBCO, ref. 15140122) was added carefully not to detach the cells and verifying all the cells have medium on them. Then 400 μ L of the adenoviral infectious supernatant from the first amplification were added to infect the cells in each plate. 2 hours after infection, 10 mL of high-glucose pyruvate- and glutamine-included DMEM (Biowest, ref. L0104-500) supplemented with 10% fetal bovine serum (FBS) (GIBCO, ref. 102070-106) and 1% penicillin/streptomycin were added to the infection medium in each plate. Cell detachment was monitored in each plate around 20-30 h after infection. At the initial stage of detachment, cells were gently scraped and collected into a 50-mL sterile polypropylene tube. Cells containing the virus are pelleted at 200 $\times g$ for 5 min at room temperature. Supernatant is removed and all the cells infected with the same virus in different plates are resuspended in 5 mL of medium. Then a series of 3 freeze/thaw cycles were applied to the cells using liquid nitrogen and a 37 $^{\circ}$ C water bath to release the viral particles. Finally, all the debris were pelleted at 2 000 $\times g$ for 5 min at 4 $^{\circ}$ C and the supernatant was recovered and aliquoted as adenoviral stocks for following titration and infection use.

1.16.5. Adenoviral titration

The adenoviral titration is important to ensure consistency between infections and to reach the right transient expression. To do so, we have used *Adeno-X Rapid Titer Kit* (Clontech, ref. 632250), which takes advantage of the detection of viral hexon proteins for the quantification of the adenoviral stocks. Cultured HEK 293A cells are infected with adenoviral serial dilutions of our stocks. 48 h later, the infected cells are fixed with methanol and incubated with a mouse monoclonal anti-hexon antibody. Then, they are incubated with a secondary horseradish peroxidase-conjugated anti-mouse IgG antibody. After several rinsing steps, fixed cells are incubated with 3,3'-diaminobenzidine, which is a peroxidase substrate and turns hexon-containing (*i.e.* infected) cells into dark brown. The titer of the stock can be determined by counting the dark brown cells in a given area, since each stained cell corresponds to a single infectious plaque-forming unit (pfu).

1.17. Lentivirus

Lentiviral vectors are useful to infect both dividing and nondividing cells in a stable manner. Their cytopathic effects usually appear after a long incubation period during which the viral single-stranded RNA genome gets adapted and integrated into the host cell genome, thanks to the action of a reverse transcriptase and an integrase (lysogenic cycle). After the incubation, a natural lentivirus can reactivate and initiate the lytic cycle to generate new viral particles. Lentiviruses belong to the *Retroviridae* family, the same which includes the *Human Immunodeficiency Virus 1* (HIV1), which is the actual base for the recombinant lentiviruses used in this project. These recombinant vectors have been deprived of their lentiviral replicative machinery, so once they have infected a cell they integrate the recombinant gene but no longer progress into the lytic cycle, unless their host cells express the other essential genes which allow the lentiviral particles generation.

1.17.1. Lentiviral shCPT1A-expressing constructions

The lentiviral vectors have been used in this work with the aim to silence the endogenous CPT1A using a small hairpin RNA (shRNA) in a stable way. Small hairpin RNA (shRNA) is an artificial RNA which can be used to silence a targeted gene expression. Once expressed, shRNAs are processed by DICER system to become a small interfering RNA (siRNA) which diminishes the mRNA of a certain gene, with the consequent protein translation reduction. In our case, we took advantage of the MISSION® shRNA repository, which we had also used for lentiviral shRNA expression, to find a sequence to knockdown CPT1A both in rats and mice. The plasmid used from MISSION® shRNA Bacterial Glycerol Stock (Sigma-Aldrich, ref. SHCLNG-NM_013495.1-1766s1c1; TRC0000110597) contained the following shRNA coding sequence which had a 73% previously validated knockdown in Hepa 1-6 cells:

5' CCGGGCTCGCACATTACAAGGACATCTCGAGATGTCCTTGTAATGTGCGAGCTTTTTG 3'

The plasmid used is the TRC pLKO.1-Puro, whose features are exposed in the following scheme:

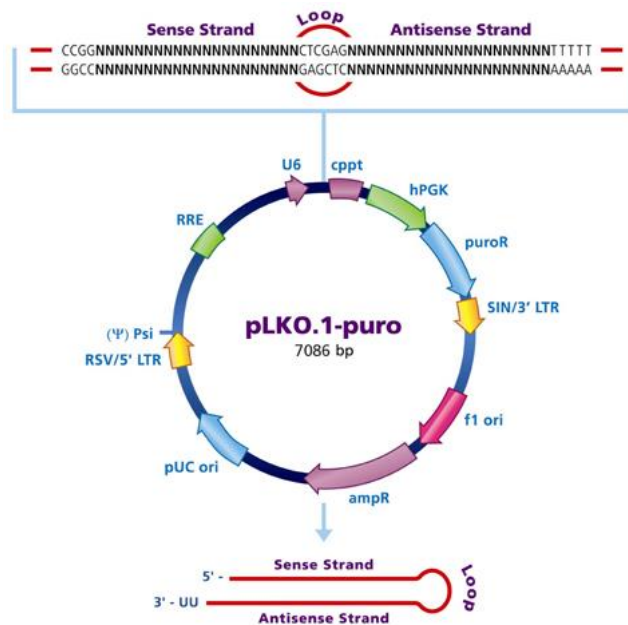


Fig 12. Plasmid used for the lentivirus production. U6: U6 Promoter; cppt: Central polypurine tract; hPGK: Human phosphoglycerate kinase eukaryotic promoter; puroR: Puromycin resistance gene for mammalian selection; SIN/3' LTR: 3' self-inactivating long terminal repeat; f1 ori: f1 origin of replication; ampR: Ampicillin resistance gene for bacterial selection; pUC ori: pUC origin of replication; 5' LTR: 5' long terminal repeat; (ψ) Psi: RNA packaging signal; RRE: Rev response element.

Besides de LV-shCPT1A, we used a LV-scramble as the control vector in this. It case has the same structure, but expressing a scramble shRNA sequence instead (Sigma-Aldrich, ref. SHC002).

1.17.2. Lentiviral vector production

The lentiviral vectors are produced in HEK 293T cells which are a variant of common HEK 293 that has been clonally selected to be easily transfected and support high expression levels of viral proteins. These cells are transfected following a protocol based in the use of calcium phosphate; concretely we used the CalPhos Mammalian Transfection Kit (Clontech, ref. 631312) to produce LV-shCPT1A and LV-scramble. To this end, besides pLKO.1-Puro-shCPT1A and pLKO.1-Puro-scramble, we needed pVSV-G, which codifies for envelop proteins, and pCMVAR8.91, which codifies proteins involved in the lentiviral packaging.

In the first day, HEK 293T were plated at $3.5 \cdot 10^6$ cells per 10-cm plate. Around 30 h later, medium was replaced with fresh medium. Endotoxin-free DNA vectors were mixed in a

50-mL sterile polypropylene tube as it follows: 3.4 µg/plate envelope plasmid (pVSV-G), 6.3 µg packaging plasmid (pCMVAR8.91) and 9.8 µg/plate transfer plasmid (pLKO.1-Puro-shCPT1A or pLKO.1-Puro-scramble). While vortexing the mix, 86.8 µL of 2M CaCl₂ was added to the mixture dropwise. Then included sterile water was added qsp 700µL/plate, after the manner of a drop while vortexing as well. After that, 700 µL/plate of 2x HEPES-buffered solution (HBS) was added dropwise while vortexing. After that, the mix was incubated at room temperature for 15 min. This transfection mix was added in the form of drops on the medium of each plate, stirring the plate gently meanwhile. Cells were incubated at 37°C and 5% CO₂, for around 15 h. Then medium with calcium phosphate precipitate was removed and fresh medium, replaced.

This medium with infectious lentivirus was collected 24 h later and replaced with fresh medium. The collected infectious medium was centrifuged at 1200 *x g* for 10 min at room temperature, to pellet the cell debris. The supernatant was filtered with a 0.45 µm membrane and kept at 4°C for 24h in agitation. After 24 h, the second collection of infectious medium was harvested. The collected infectious medium was spun at 1200 *x g* for 10 min at room temperature and filtered with a 0.45 µm membrane. The two days' collection were mixed, aliquoted and kept -80°C, unless it was meant to be use the same day in previously prepared cells to be transduced to generate stable cell lines expressing the shRNA.

1.18. Cell cultures

This project has been based in a large part on different neuronal models, both based in primary cultures or in stable cell lines, for the study of metabolic mechanisms involved in ghrelin action on amino acid neurotransmission. Hypothalamic neuronal cell lines are commonly used as a good model for neuropeptidergic transmission, since they express some neuropeptides with a physiological response to different hormones and stimuli. Nevertheless, they do not express the complete range of neuropeptides and when it comes to execute physiological functional studies involving amino acid neurotransmission, they are useless, since they do not exhibit some of their essential features. Primary neuronal cultures seem to be more adequate for this purpose, since their amino acid neurotransmitters metabolism and release gimmicks are intact. However, in the case of cortical neurons, they do not necessarily meet the same regulatory control than in the case of neurons in hypothalamic nuclei. Those are the main grounds why we use both systems to figure out the physiological mechanisms involved.

1.18.1. Primary cortical neuronal cultures

The methodologies are based in the protocols learnt in Dr. Cristina Suñol's laboratory at *Institut d'Investigació Biomèdica de Barcelona (IIBB-CSIC)* (Solà, Cristòfol, Suñol, & Sanfeli, 2011). Primary neurons are directly obtained from fresh tissue and maintain during several days or even weeks their specific physiological characteristics, which is useful for the study of the neuronal mechanisms of different substances, such as metabolic inhibitors or hormones. The strains used in this project have been CD1, C57BL/6J and CPT1A^(loxP/loxP) mice. All the experiments with mice to obtain primary cultures were previously approved by the *Comité Ètic d'Experimentació Animal* of the *Universitat de Barcelona* (CEEAA-UB), whose procedures obtained the DAAM Permit #8173.

The general procedure is based on the dissection of a selected brain area from the animal postmortem. The tissue is mechanically disaggregated and enzymatically digested. Then the cells are washed and seeded on an appropriately coated surface for their attachment. During the whole process, cells are kept in sterile physiological conditions and are seeded with a culture medium that mimics the blood bicarbonate buffering system. The culture is kept at 37°C with 5% CO₂ in a humidified incubator.

Within cortical neurons both GABAergic and glutamatergic neurons can be found. To prepare the primary culture, cerebral cortices are harvested from unborn pups in embryonic days from 15 to 17. All the solutions' composition can be found in annexes. The pregnant mouse was terminated by cervical dislocation. Then it was located upside-down and 70% ethanol solution was used to clean the abdomen. A lengthwise incision was performed in the middle and the abdomen was open. Then the uterus was transferred to a 10-cm polystyrene plate containing a glucose-enriched phosphate-buffered solution (namely PBE) kept on ice. The embryos were taken out and transferred to a new plate with PBE on ice. Following that, the embryos' heads were cut off and their skulls were open using a fine #7 curved watchmaker's tweezer (Quirumed, ref. 002-BA-331-12). Then, using the same tweezers, both cortices were dissected and placed in another plate with fresh PBS on ice, dissecting and removing meninges, under a stereoscopic microscope if needed. The cortices obtained from the entire litter were chopped using a sterile scalpel. The minced tissue was then transferred to a 50-mL sterile polypropylene tube and pelleted within the PBE solution at 500 x *g* for 1 min at 4°C. Supernatant was carefully discarded and 5 mL solution 1 was used to resuspend and rinse the

tissue. The cortices were pelleted as stated before. Solution 1 was then removed and replaced with 5 mL solution 2, containing trypsin, to resuspend the minced cortices, which were incubated for 10 min at 37°C in a water bath. Following that, 5 mL solution 4, which contains diluted DNase and a trypsin inhibitor) was added onto the suspension and a sterile Pasteur pipette was used to help tissue disaggregation. Then, 5 mL solution 3, containing concentrated DNase and trypsin inhibitor, is added onto the suspension and thoroughly mixed with the Pasteur pipette. A 5-min incubation at 37°C followed, before passing the suspension through a sterile 250- μ m nylon mesh (Filter-lab, ref. FMNY250) several times into a sterile beaker. The already translucent suspension is then collected and pelleted at 500 x *g* for 5 min. The supernatant is removed and replaced with 7 mL 30 mM glucose-enriched pyruvate- and glutamine-included Dulbecco's Modified Eagle Medium (DMEM) (Biowest, ref. L0104-500) supplemented with 10% fetal bovine serum (FBS) (GIBCO, ref. 102070-106) and 1% penicillin/streptomycin (100 U/mL final concentration) (GIBCO, ref. 15140122). The suspension had its cells and their viability quantified using Countess Automated Cell Counter (Invitrogen, ref. C10227). No isolation with less than 60% viability was used. Then 8·10⁵ living cells per well (in 6-well plates) were seeded. Each litter yielded around 6 to 8 plates, which were precoated with 4°C overnight incubation with 0.005% poly-L-lysine, prepared from 2x solution (Sigma-Aldrich, ref. P4707). 3 h after seeding, cells were attached and the medium was replaced with Neurobasal Medium (GIBCO, ref. 21103-049) supplemented at 1x with B27 (GIBCO, ref. 17504-044) and GlutaMax (GIBCO, ref. 35050-038), as well as 1% penicillin/streptomycin (100 U/mL final concentration) (GIBCO, ref. 15140122). Two days after culturing the cells, 2 μ M cytosine β -D-arabinofuranoside (Sigma-Aldrich, ref. C1768) is added to avoid proliferation of non-neuronal cells to the medium. Every two days, medium had to be changed, removing a half of the previous medium, which was replaced with fresh medium. Cells were avoided to dry out without any medium upon them.

1.18.2. Adenoviral infection of primary cortical neurons

The infection of cortical neurons was made using the following adenoviruses: Ad-CPT1AM (and Ad-GFP as its control) for CPT1A overexpression, described on Experimental procedures 1.16.2; Ad-shCPT1A (and Ad-scramble as its control) to knock down CPT1A in wild type cortical neurons, described on Experimental procedures 1.16.3; and Ad-CRE-GFP (and Ad-GFP as its control) in cortical neurons obtained from CPT1A^(loxP/loxP) embryos to knockout CPT1A, described on Experimental procedures 1.16.4. The multiplicity of infection has been of

100 pfu per cell and applied in medium volume reduced to a half for overnight infection. The medium was replenished to its full the next day. The medium used was the same used for the regular culture: Neurobasal Medium (GIBCO, ref. 21103-049) supplemented at 1x with B27 (GIBCO, ref. 17504-044) and GlutaMax (GIBCO, ref. 35050-038), as well as 1% penicillin/streptomycin (100 U/mL final concentration) (GIBCO, ref. 15140122) and 2 μ M cytosine β -D-arabinofuranoside (Sigma-Aldrich, ref. C1768).

1.18.3. Pharmacological treatments to primary neuronal cultures

Neurons in different regions in the brain have been described to have ghrelin receptors, also known as *growth hormone secretagogue receptor* (GHSR). We wanted to assess whether its activation by its endogenous ligand, octanoylated ghrelin, would exert some effect on amino acid metabolism through CPT1A as we hypothesized. A 30-min treatment with 100 nM ghrelin (Sigma-Aldrich, ref. G8903) was used. The glucose concentration used in maintenance primary neuronal culture medium is far beyond the cerebrospinal fluid concentration: complete Neurobasal medium contains 25 mM glucose, despite glycorrhachia, which is the glucose concentration in CSF, oscillates between 3-5 mM. To this end, we tested several conditions regarding glucose concentration. We set a 3 h pretreatment before ghrelin treatment with the same maintenance medium with 0 mM, 5 mM and 25 mM glucose. Taking into account the results, as well as the fact that 5 mM is the closest to physiological glycorrhachia, we performed most of the experiments with a 5 mM glucose pretreatment.

To pharmacologically inhibit CPT1A, we added 40 μ g/mL etomoxir in the 30 min ghrelin treatment. In order to block tricarboxylic cycle by inhibiting isocitrate dehydrogenase, we added 700 μ M 2-hydroxyglutarate.

1.19. Hypothalamic cell lines

Several hypothalamic neuronal cell lines exist at the moment obtained by immortalization of hypothalamic primary cultures. These succeed to reproduce some of the physiological features they have *in vivo*, but not them all. The most widely used is GT1-7, since it was one of the first cell lines obtained, which expresses AgRP in a ghrelin-responsive manner,

although it was not dissected specifically from arcuate nucleus. Later on, the Canadian company CELLutions Biosystems Inc. has developed a wide range of hypothalamus-derived embryonic neurons which respond to physiological stimuli unevenly. A complete gene expression comparison between hypothalamus and hypothalamic cell lines can be found in Annexes.

1.19.1. mHypo-N41, mHypo-N29/4 and mHypo-N43/5 cells

Hypothalamic cell lines obtained by CELLutions Biosystems Inc are embryonic mouse hypothalamus cell lines that have been immortalized from embryonic days 15, 17 and 18 hypothalamic primary cultures by retroviral transfer of SV40 T antigen oncogene, which is the same method previously used for GT1-7 generation. We tried to validate mHypo-N29/4 and mHypo-N43/5 as hypothalamic neuronal models for our purpose, but we concluded we had to discard them for our purposes.

Later, they let us to test mHypo-N41 cell line, which actually expresses AgRP and NPY. Nonetheless, only AgRP has an expression dependent on ghrelin pathway activation, but seems to have most of the amino acid neurotransmission metabolism intact.

The medium used to culture this line is 25 mM glucose pyruvate- and glutamine-enriched Dulbecco's Modified Eagle Medium (DMEM) (Biowest, ref. L0104-500) supplemented with 10% fetal bovine serum (FBS) (GIBCO, ref. 102070-106) and 1% penicillin/streptomycin (100 U/mL final concentration) (GIBCO, ref. 15140122). Subcultures have to be done every 2 to 3 days at 1:10.

1.19.2. GT1-7 cells

GT1-7 is one of the first embryonic mouse hypothalamus cell lines that had been immortalized by Dr. Pamela Mellon's laboratory at the University of California, San Diego (UCSD). They transferred hypothalamic primary cultures from embryonic days 15, 17 and 18 expressing *gonadotropin-releasing hormone* (GnRH) with lentivirus expressing SV40 T antigen oncogene (Mellon et al., 1990). They were not meant to be arcuate neurons, but they do express AgRP (but not NPY) in a ghrelin-dependent manner, so this cell line has been used extensively

as a cellular model for arcuate NAG neurons, when studying molecular mechanisms involved in food intake control and energy homeostasis. Moreover, this line seems to have most of the amino acid neurotransmission metabolism intact.

We cultured $2 \cdot 10^5$ cells per well in 6-well plates, if not stated otherwise. The medium used to culture this line is the same described for the other hypothalamic cell lines: 25 mM glucose pyruvate- and glutamine-enriched Dulbecco's Modified Eagle Medium (DMEM) (Biowest, ref. L0104-500) supplemented with 10% fetal bovine serum (FBS) (GIBCO, ref. 102070-106) and 1% penicillin/streptomycin (100 U/mL final concentration) (GIBCO, ref. 15140122). Subcultures have to be done every 4 days at 1:4.

1.19.3. Adenoviral infection of hypothalamic cell lines

The infection of hypothalamic cell lines (both GT1-7 and mHypo-N41) was made using the adenoviruses previously described: Ad-CPT1AM (and Ad-GFP as its control) for CPT1A overexpression, described on Experimental procedures 1.16.2; and Ad-shCPT1A (and Ad-scramble as its control) to knock down CPT1A, described on Experimental procedures 1.16.3. The cells, unless stated otherwise in certain procedures, were plated at $2 \cdot 10^5$ cells per well in 6-well plates and infected 3 to 5 after seeding, when cells were already attached.

The multiplicity of infection was of 100 pfu per cell and applied in medium volume reduced to a half for overnight infection. The medium was replenished to its full the next day. The infection medium used has its FBS content reduced to 5% compared to regular culture: 25mM-glucose pyruvate- and glutamine-included Dulbecco's Modified Eagle Medium (DMEM) (Biowest, ref. L0104-500) supplemented with 5% fetal bovine serum (FBS) (GIBCO, ref. 102070-106) and 1% penicillin/streptomycin (100 U/mL final concentration) (GIBCO, ref. 15140122). The ongoing treatments and sample collection were performed 48 h after infection, unless stated otherwise.

1.19.4. Lentiviral transduction and clonal selection in mHypo-N41

We took advantage of lentiviral integration to generate a stable polyclonal hypothalamic cell line derived from mHypo-N41 with a CPT1A knock down. To this end, we had to determine

a puromycin kill curve to select transduced clones, infect the cells and perform a clonal selection at using the minimum concentration that causes complete cell death after 5 days. In the case of mHypo-N41 seeded at $1.6 \cdot 10^4$ cells/well in a 96-well plate the concentration was 5 $\mu\text{g}/\text{mL}$ puromycin (Sigma-Aldrich, ref. P9620).

For the lentiviral transduction, $1.6 \cdot 10^6$ cells per 10-cm plate were seeded. The following day, medium was removed and changed with infectious medium obtained from the lentiviral productions (both LV-scramble and LV-shCPT1A, described on Experimental procedures 1.17.1). They were supplemented with polybrene (Sigma-Aldrich, ref. H9268) up to 8 $\mu\text{g}/\text{mL}$, which enhances transduction. After 24h infection, infectious media were replaced with maintenance 25mM-glucose pyruvate- and glutamine-included Dulbecco's Modified Eagle Medium (DMEM) (Biowest, ref. L0104-500) supplemented with 10% fetal bovine serum (FBS) (GIBCO, ref. 102070-106) and 1% penicillin/streptomycin (100 U/mL final concentration) (GIBCO, ref. 15140122). The next day, fresh maintenance medium with 5 $\mu\text{g}/\text{mL}$ puromycin (Sigma-Aldrich, ref. P9620) was used to replace previous-day medium to start clonal selection. The medium with fresh puromycin was replaced every 3-4 days until resistant colonies were identified. These clones were expanded and characterized to perform ongoing experiments.

1.19.5. Pharmacological treatments to hypothalamic cell lines

Ghrelin treatments in hypothalamic cell lines, both GT1-7 and mHypo-N41, were performed like in primary cortical neurons: a 30-min treatment with 100 nM ghrelin (Sigma-Aldrich, ref. G8903) after a 3 h pretreatment with 5 mM glucose pyruvate- and glutamine-enriched Dulbecco's Modified Eagle Medium (DMEM) (Biowest, ref. L0060-500) supplemented with 10% fetal bovine serum (FBS) (GIBCO, ref. 102070-106) and 1% penicillin/streptomycin (100 U/mL final concentration) (GIBCO, ref. 15140122).

To pharmacologically inhibit CPT1A, we added 40 $\mu\text{g}/\text{mL}$ etomoxir in the 30 min ghrelin treatment. In order to block tricarboxylic cycle by inhibiting isocitrate dehydrogenase, we added 700 μM 2-hydroxyglutarate.

1.20. HEK 293 derived cell lines

HEK 293 is a cell line obtained from human embryonic kidney cells from a Dutch legally aborted foetus which were cultured and immortalized in 1973 (Graham, Smiley, Russell, & Nairn, 1977). This cell line is easy to grow and transfect, which makes it essential in Cell Biology research and Biotechnology to produce therapeutic proteins and viral vectors for gene therapy. In this project we have used two variants: HEK 293A, which is a line enhanced for adenoviral production, and HEK 293T, a variant selected for easy calcium-phosphate transfection and lentiviral production. In both cases, the maintenance medium used is 25 mM glucose glutamine-enriched Dulbecco's Modified Eagle Medium (DMEM) (Biowest, ref. L0102-500) supplemented with 10% fetal bovine serum (FBS) (GIBCO, ref. 102070-106) and 1% penicillin/streptomycin (100 U/mL final concentration) (GIBCO, ref. 15140122).

2. Molecular Biology Techniques

The techniques learnt to characterize, isolate, and manipulate the molecular components of cells and organisms have been developed from the latter half of the 20th century to the present days. These components include DNA, as the repository of genetic information; RNA, another polynucleotide whose functions range from serving as a temporary working copy of DNA to actual structural and enzymatic functions as well as a functional and structural part of the ribosome; and proteins, the major structural and enzymatic type of molecule in cells.

2.1. Genomic DNA extraction from mice ear tags

When it came to use gDNA for conventional polymerase chain reaction (PCR), low quantity and purity gDNA was obtained from mice ear tags using QuickExtract DNA solution (Epicenter, ref. QE09050). It is a fast and convenient procedure which allows extracting gDNA with enough purity to be processed for genotyping.

A week after weaning, mice were tagged for identification on their ears. Remaining tissue from the ear was carefully collected from each mouse and properly identified in a sterile 500 μ L microcentrifuge tube. Then 50 μ L QuickExtract DNA solution was added to each tube. The tubes were given a quick spin, to ensure contact between the ear tags and the solution. A 6-min incubation at 65°C and vigorous vortexing for mechanical disruption were applied to ease the polynucleotide liberation into the solution. Following that, the tubes were incubated again for 2 min at 92°C. An overnight incubation at 4°C was applied before any other processing of the sample. If not used at the following day, the extraction liquid was stored at -20°C. Before any supernatant sampling for PCR, tubes were centrifuged at maximum speed for 5 min to pellet any remaining ear debris. This protocol can be used with pelleted cells for a fast gDNA preparation for conventional PCR purposes.

2.2. Phenol:chloroform pure genomic DNA extraction

Once the carriers of the CPT1A^(+/ftrt) by PCR from gDNA obtained from the ear tags, new purer and more concentrated gDNA preparation had to be obtained in order to determine the

construct copy number using droplet digital PCR (ddPCR). To this end, we opted to prepare the gDNA with a phenol:chloroform extraction protocol. 1-cm tail cuts from F1 CPT1A^(+/firt) mice detected by conventional PCR were incubated overnight in 2-mL microcentrifuge tubes at 55°C with 700 μ L proteinase K digestion solution: 0.5mg/mL proteinase K; 1% SDS; 100 mM NaCl and 15 mM EDTA. Once digested, 10 μ L RNase A (10 mg/mL) is added into each tube and incubated at 37°C for 1 h for RNA degradation. Extraction is started by adding 700 μ L phenol (100 mM, Tris-buffered pH 8.0) and vigorous 10-min shaking. Vortexing should be avoided to keep DNA integrity. Tubes were centrifuged at maximum speed for 15 min and upper phase was placed into a new tube. 700 μ L Phenol:Chloroform:Isoamyl alcohol (25:24:1) was added to each tube, which were vigorously shaken for 10 min. Tubes were centrifuged again at maximum speed for 15 min and upper phase was placed into a new tube. 700 μ L Chloroform:Isoamyl alcohol (24:1) was added to each tube, which were vigorously shaken for 5 min. Tubes were centrifuged again at maximum speed for 15 min and upper phase was placed into a new tube. At this point gDNA was isolated and had to be precipitated. To this end, 700 μ L Isopropanol and 15 NaCl (5M) were added to each tube and vigorously mixed. After 10 min rest, gDNA was precipitated by centrifugation at maximum speed for 15 min. Supernatant was removed avoiding any gDNA pellet disturbance. 100 μ L Ethanol (70%) was added to each tube for washing and after 15 min centrifugation at maximum speed, ethanol supernatant was removed and the gDNA was left to dry out. Once it was dry, the gDNA pellet was resuspended with 100 μ L Tris-EDTA (10 mM - 5 mM) solution and stored at 4°C at least overnight before any further processing. gDNA yield was quantified using NanoDrop 1000 Spectrophotometer (Thermo Scientific, ref. ND-1000).

Pure gDNA is needed as well for DNA dot blot analysis. In this case, treated cells are scraped and pelleted with PBS 1x at 1 500 $\times g$ for 5 min at 4°C. Then supernatant is removed and proteinase K digestion is performed only for 2 h at 55°C. The rest of the protocol is the same previously described.

2.3. Mice genotyping by polymerase chain reaction

For this project, two specific polymerase chain reaction protocols had to be designed for the genotype identification of CPT1A^(+/firt), CPT1A^(+/loxP) and CPT1A^(loxP/loxP) mice.

2.4. CPT1A^(+/frt) mice genotyping

In this case, we designed an experiment in which three oligonucleotides were used: a common forward primer (namely, ComAKO For) which anneals to both wild-type CPT1A and CPT1 *tm1a(EUCOMM)Hmgu* alleles, and two reverse primers, which one anneals to wild-type *cpt1a* (namely, SpWT Rev) and the other to CPT1A *tm1a(EUCOMM)Hmgu* allele (called, SpAKO Rev). The amplicon expected in CPT1A^(+/+) is 900 bp long approximately; and in CPT1A^(+/frt), two 900 bp and 500 bp amplicons approximately are expected at the amplification set conditions.

The primers used were the following:

Oligonucleotide	Sequence	Melting temperature
<i>ComAKO For</i>	5'- TAACCCCTCAAATAGCAGCAC -3'	58.00 °C
<i>SpAKO Rev</i>	5'- ATAGGAACTTCGGTCCGGC -3'	59.82 °C
<i>SpWT Rev</i>	5'- AGTCATGATGATCGCCACCC -3'	59.89 °C

The reaction mixed used was based in the REExtract-N-Amp PCR ReadyMix (Sigma-Aldrich, ref. R4775) which contains all the reagents needed for PCR amplification as well as for the 1% agarose gel electrophoresis (with 0.008% GelRED Nucleic Acid Gel Stain - Biotium, ref. 41003) to visualize the amplicons:

	Final concentration	Volume (1x)
<i>ddH₂O</i>	qsp 20 uL	3 µL
<i>REExtract-N-Amp PCR ReadyMix 2x</i>	1x	10 µL
<i>ComAKO For 10 µM</i>	1 µM	2 µL
<i>SpAKO Rev 10 µM</i>	1 µM	2 µL
<i>SpWT Rev 10 µM</i>	1 µM	2 µL
<i>gDNA</i>	n/a	1 µL

The program set in the thermocycler was:

Initial dehybridization	94°C	5 min	
Dehybridization	94 °C	30 s	} 25 cycles
Annealing	60 °C	30 s	
Elongation	72 °C	1 min	
Final elongation	72 °C	5 min	

2.5. CPT1A^(+/loxP) and CPT1A^(loxP/loxP) mice genotyping

In this case, we designed an experiment in which two oligonucleotides annealed in the common homology arms, found both in wild-type CPT1A allele and in the floxed CPT1A^{loxP} allele, but depending on the allele, the amplicons have different longitude: wild-type CPT1A allele amplicon is 990 bp long and CPT1A^{loxP} allele is 1030 bp long. In the case of CPT1A^(+/loxP) mice two 1030 and 990 bp amplicons result and in CPT1A^(loxP/loxP) only one 1030 bp amplicon is found.

Moreover, this PCR design allowed us to test CRE recombinase activity when infecting CPT1A^(loxP/loxP) cells with Ad-CRE, since infected cells presented a 219 bp amplicon.

The primers used were the following:

Oligonucleotide	Sequence	Melting temperature
<i>HomArm For</i>	5'- CAGGATCCCTTTGAGCAGCAG -3'	61.10 °C
<i>HomArm Rev</i>	5'- CAAAGTGGCCCTAAGGCTAC -3'	61.10 °C

The reaction mixed used was also based in the REExtract-N-Amp PCR ReadyMix (Sigma-Aldrich, ref. R4775) which contains all the reagents needed for PCR amplification as well as for the 1% agarose gel electrophoresis (with 0.008% GelRED Nucleic Acid Gel Stain - Biotium, ref. 41003) to visualize the amplicons:

	Final concentration	Volume (1x)
<i>ddH₂O</i>	qsp 20 uL	5 μL
<i>REExtract-N-Amp PCR ReadyMix 2x</i>	1x	10 μL
<i>HomArm For 10 μM</i>	1 μM	2 μL
<i>HomArm Rev 10 μM</i>	1 μM	2 μL
<i>gDNA</i>	n/a	1 μL

The program set in the thermocycler was:

Initial dehybridization	94°C	5 min	
Dehybridization	94 °C	30 s	} 25 cycles
Annealing	56 °C	30 s	
Elongation	72 °C	1 min	
Final elongation	72 °C	5 min	

2.6. Analysis by ddPCR of copy number in CPT1A^(+/firt) mice

In our CPT1A^(+/firt) mice we had to check if the integration of the construct had only taken place by homologous recombination at the targeted area (*i.e.* around exon 4 in *cpt1a* gene) or if it had integrated more than one time, in a non-homologous way. To this end, we assessed the number of copies of our construct present in the gDNA of several CPT1A^(+/firt) mice of the F1, used later for CPT1A^(+/loxP) and CPT1A^(loxP/loxP) generation. Instead of using other old-fashioned radiometric technologies, such as Southern blot, we opted for digital PCR analysis.

Droplet digital PCR (ddPCR) is a digital PCR method, in which a water-oil emulsion is used to form the partitions which separate the template DNA molecules within the droplets. The sample partition into thousands of nanoliter droplets and their separate PCR amplification carried out within each droplet allows one to estimate the number of copies of the targeted template DNA by assuming that the molecule population follows the Poisson distribution. As a

result, each part will contain 0 or 1 molecule, being the PCR positive or negative, respectively. By counting the positive PCR products in relation the total count and by applying mathematical models, one can estimate the number of copies present in the sample originally. We used a QX100 Droplet Digital PCR System (BioRad, ref. QX100) which had been adapted for the use of QX200 ddPCR EvaGreen Supermix dsDNA binding dye (BioRad, ref. 186-4035) which was our election, instead of fluorescent probes. All the equipment was available from Dr. Salvador Bartolomé Piñol *Laboratori de Luminiscència i Espectroscòpia de Biomolècules* from the *Servei Científicotècnic de la Universitat Autònoma de Barcelona (UAB)*.

To confirm this, we designed two pairs of primers to amplify both genes:

Oligonucleotide	Sequence	Melting temperature
<i>Tert For</i>	5'- CCTCTGTGTCCGCTAGTTACA -3'	61.10 °C
<i>Tert Rev</i>	5'- TCTTTGTACCTCGAGATGGCA -3'	61.10 °C
<i>LacZ For</i>	5'- GCTGGAGTGACGGCAGTTAT -3'	60.11 °C
<i>LacZ Rev</i>	5'- TACCCGTAGGTAGTCACGCA -3'	60.04 °C

The amplicons sizes are 137 bp for TERT and 197 bp for LACZ. Moreover, to ensure a correct distribution of all the putative copies present in the genome, even if the might be in the same chromosome, we had to perform an enzymatic digestion with a restriction enzyme, before proceeding to ddPCR. We eventually opted for EcoRI, since it is a convenient enzyme for gDNA digestion.

gDNA from a wild type mouse and several F1 CPT1A^(+/frt) mice was extracted from their tails using the phenol:chloroform methodology previously described. Next, we digested 1 µg gDNA from each mice using 5 U EcoRI/µg gDNA in 100 µL of volume reaction for 1 h at 37°C. The enzyme was then inactivated at 65°C for 20 min. Correct digestion was analyzed by 0.8% agarose gel electrophoresis of 5 µL digested gDNA, by looking at repetition bands presence. Conventional PCR and qRT-PCR are performed to double check correct amplification with designed primers, testing different digested gDNA quantities (10 ng, 2 ng and 1 ng).

Due to specific characteristics of ddPCR a temperature gradient has to be performed to test the best temperature around the theoretically optimal annealing temperature of the pair of

primers, which was around 60°C. The annealing temperatures (T_{ann}^*) tested are 58.9°C, 60.1°C, 61.0°C and 61.6°C.

The reaction mix is the following for each pair of primers:

	Final concentration	Volume (1x)
<i>EvaGreen SuperMix 2x</i>	1x	11 µL
<i>Oligonucleotide For 10 µM</i>	0.5 µM	1 µL
<i>Oligonucleotide Rev 10 µM</i>	0.5 µM	1 µL
<i>gDNA 1.22 ng/µL</i>	0.5 ng/µL	9 µL

Then 20 µL of each reaction mix were transferred to the sample wells of the emulsifier. In the corresponding oil wells, 70 µL EvaGreen Droplet Generation Oil were added in the DG8 cartridge (BioRad, ref. 186-3006) as well. The bubbles were removed from the system, since they can interfere in the emulsification. The cartridge was then placed in the QX100 droplet generator (BioRad, ref. 186-3002) which was activated.

Once emulsification was done, the emulsified reaction mixes had to be transferred into a 96-well plate and covered with a thermal aluminum seal. Then we proceeded to amplification using a thermocycler which allowed us to test the four temperatures with the two pairs of primers, using the following program:

The program set in the thermocycler was:

Initial dehybridization	95°C	5 min	} 39 cycles
Dehybridization	95 °C	30 s	
Annealing and Elongation	T_{ann}^*	1 min	
Cooling and Standby	4°C	5 min	
	90°C	5 min	
Hold	25°C		

The chosen temperature (T_{ann}^*) was 59.0°C, which was the one with better results.

Once finished the program, the samples are analyzed using QX100 Droplet Reader (BioRad, ref. 186-3003) and QuantaSoft Software, which allows to absolutely quantify the copy number for *TERT* and *LACZ*.

2.7. CPT1A^{loxP} allele sequencing

In order to confirm the integrity of the exon 4 and the loxP regions flanking it in the CPT1A^(loxP/loxP), we assessed the sequence found in their alleles. To do so, we took advantage of a variation of DNA sequencing technologies developed in mid-1970's (Sanger, Nicklen, & Coulson, 1977), materialized in our case in the BigDye Terminator v3.1 Cycle Sequencing Kit (Applied Biosystems, ref. 4337455). This method requires chain-terminating dideoxynucleotides (ddNTPs) which cause DNA polymerase to stop DNA extension, when one of these ddNTPs is incorporated. Each of the four ddNTPs is labelled with a different fluorescent dye which allows assessing the nucleotide incorporated in a particular position in the DNA polymer along the whole sequence.

The oligonucleotides used as primers in this case are the following:

Oligonucleotide	Sequence	Melting temperature
<i>HomArm For</i>	5'- CAGGATCCCTTTGAGCAGCAG -3'	61.10 °C
<i>HomArm Rev</i>	5'- CAAAGTGGCCCCTAAGGCTAC -3'	61.10 °C
<i>BGLII CPT1 For</i>	5'- CTACTCGCTGAAGGTGCTGC - 3'	60.40 °C
<i>SpWT Rev</i>	5'- AGTCATGATGATCGCCACCC -3'	59.89 °C

The reaction mix used for each primer was the following:

		Volume (1x)
<i>ddH₂O</i>	qsp 20 µL	8.65 µL
<i>Ready BigDye Reaction Mix</i>		1 µL
<i>BigDye Sequencing Buffer</i>		3 µL
<i>Oligonucleotide 10 µM</i>		2 µL
<i>gDNA</i>	70 µg	7 µL

The program set in the thermocycler was:

Initial dehybridization	96°C	1 min	
Dehybridization	96 °C	10 s	} 25 cycles
Annealing	50 °C	5 s	
Elongation	60 °C	4 min	
Hold	4 °C		

The reactions were further processed at the Genomic Services Unit from the *Centres Científics i Tecnològics de la Universitat de Barcelona* (CCiT-UB) to obtain the sequence chromatograms.

2.8. RNA analysis techniques

The changes in transcripts were studied for coding mRNA, snoRNA, pre-microRNA and microRNA in cellular cultures as well as in MBH. A specific RNA extraction kit was used to obtain the RNA, which was adapted to the tissular/cellular characteristics. Nonetheless, both kits are based in the use of a monophasic phenol:guanidinium isocyanate solution designed to ease the cellular lysis and RNase inhibition. This lysis is complemented with a RNA purification using silica membrane columns.

2.9. Total RNA extraction from mediobasal hypothalamus

Total RNA was extracted from one half of mediobasal hypothalamus (MBH) dissected from the studied rats using the RNeasy Lipid Tissue Mini kit (QIAGEN, ref. 25-0500-71) following the manufacturer's indications with minor modifications. The previously ultrafrozen dissected tissue was homogenized in 1 mL Lysis QIAzol solution using an ultrasound homogenizer. During the extraction, the Rnase-free DNase I (QIAGEN, ref. 79254) optional digestion was performed in all cases. RNA elution was performed with 35 µL RNase-free water, and its yield was quantified using NanoDrop 1000 Spectrophotometer (Thermo Scientific, ref. ND-1000).

2.10. Total RNA extraction from cell cultures

Total RNA was extracted from cultured cells using the Illustra Mini RNAspin kit (GE Lifesciences, ref. 25-0500-71) following the manufacturer's indications with minor modifications. Cells were directly lysed by adding 350 μ L RA1 lysis buffer with 3.5 μ L β -mercaptoethanol to each well in a 6-well plate. RNA elution was performed with 35 μ L RNase-free water, and its yield was quantified using NanoDrop 1000 Spectrophotometer (Thermo Scientific, ref. ND-1000).

2.11. cDNA synthesis by reverse transcription

cDNA was obtained using TaqMan Reverse Transcription Kit (Applied Biosystems, ref. N8080234), from 1 μ g total RNA from MBH or 400 μ g from cell cultures, because of the different RNA extraction yields. The protocol from the manufacturer was used with hexamer primers to obtain cDNA from all the mRNA. The tissular cDNA was diluted to 2.5 ng/ μ L and cellular cDNA to 3.33 ng/ μ L in RNase-free water, to ease the relative quantification by quantitative real time PCR.

2.12. Quantitative real time polymerase chain reaction

Quantitative real time polymerase chain reaction (qRT-PCR) was performed using Power SYBR Green PCR Master Mix adapted for LightCycler 480 (Applied Biosystems, ref. 4367659), according to the manufacturer's indications in the LightCycler 480 Instrument II (Roche, ref. 05015243001).

Gene expression quantification by qRT-PCR was made in a relative manner, using Roche Software *E-Method*, which is based in the comparison between the mRNA expression of our target gene and a reference or normalizer gene, taking into account the crossing point (Cp) cycle, in which fluorescence reaches a threshold defined value, and the reaction efficiency. The reference transcript is usually from a housekeeping gene, whose expression has to be constant and constitutive regardless of the treatments in the experiments. For overexpression *in vivo* experiments in rats, β -actin gene (*BACTIN*) was our reference, although for *in vitro* and *in vivo*

experiments with mice, TATA box binding protein transcript (*TBP*), was a better choice when it came to stability of its expression. The sequences of all the oligonucleotides and their efficiencies used for qRT-PCR can be found in Annexes.

The reaction mix for each well was the following:

		Volume (1x)
<i>ddH₂O</i>	qsp 10 μ L	2.5 μ L
<i>Primer Mix, containing:</i>		0.5 μ L
- <i>Oligonucleotide For</i> 10 μ M		
- <i>Oligonucleotide Rev</i> 10 μ M		
<i>Power SYBR Green PCR Master Mix 2x</i>		5 μ L
<i>cDNA</i> (2.5 or 3.33 ng/ μ L stock)		2.5 μ L

The program set in the thermocycler was:

Initial dehybridization	95°C	10 min	} 45 cycles
Dehybridization	95 °C	15 s	
Annealing	60 °C	1 min	
- Capture			
Melting curve	95 °C	5 min	
	65°C	1 min	
- Increase to	97°C		at 0.11°C/s

The melting curve allowed verifying the number of amplicons obtained after the PCR end point. The relative quantification was expressed referred to fold change from the control group in each gene and each group had 4 samples or more which were analyzed in duplicate each one.

2.13. Total protein extraction

Cells to have their proteins extracted after the treatment were washed with phosphate-buffered solution and put on ice. Then 50 μ L cold protein lysis buffer was applied to each well in

a 6-well plate and cells were scraped. Cells were kept on ice with gentle orbital agitation for 5 min and then collected into a 1.5 mL microcentrifuge tube. Samples were homogenized during 10 min by alternating vigorous vortexing with ice incubation. Lysates are centrifuged for 10 min at 4°C at maximum speed and collected in the supernatant for further processing.

The lysis buffer composition was the following for 10 mL:

30 mM HEPES, 150 NaCl, pH 7.4	8 mL
100% Glycerol	1 mL
20% Triton X-100	0.5 mL
10% Deoxycholate	0.5 mL
cOmplete Mini Protease Inhibitor Tablets (Roche, ref. 11836153001)	1 tablet
PhosSTOP Phosphatase Inhibitor Tablets (Roche, ref. 04906837001)	1 tablet

2.14. Bicinchoninic acid protein quantitation assay

Bicinchoninic acid (BCA) protein quantitation assay allows quantifying total protein with a colorimetric assay and with no disturbances due to lysis buffer detergents and lipids within the sample. The purple colored product of the assay exhibits a strong absorbance at 562 nm and is nearly linear up to 2 mg/mL. We have used Pierce BCA Protein Assay kit (Thermo Scientific, ref. 23225) according to manufacturer's indications, mixing reagents A:B (50:1). We used 2 mg/mL BSA stock for protein standard curve, ranging 0.018 mg/mL up to 0.181 mg/mL in a final volume of 220 µL (200 µL of the reaction mix and 20 µL of the standard). Samples were quantified with 2-5 µL, brought up to 20 µL to which 200 µL of the reagent mix was added. The overall reaction took place at 37°C for 30 min and absorbance was then read.

3. Biochemical and functional assays

3.1. Radiometric fatty acid oxidation assay

The radiometric fatty acid oxidation assay allows studying the capacity of cells to β -oxidizing fatty acids. Cells are incubated with a radioactively tagged long chain fatty acid, such as [^{14}C]oleate or [^{14}C]palmitate in our case, and the released $^{14}\text{CO}_2$ and [^{14}C]acid-soluble products, which are mainly amino acids and tricarboxylic acid intermediates in brain tissue (Kawamura & Kishimoto, 1981). This method uses a hermetically closed T-flasks system in which the carbon dioxide generated in a 3 h period from a fix amount of [^{14}C] palmitate is trapped in a KOH soaked paper with overnight incubation, after the reaction is stopped by the addition to the cells of perchloric acid. Then, both radiolabeled CO_2 and acid-soluble products are quantified.

Cells were seeded adapting the confluence used in 6-well plate to a T25 flask (2:5). Then cells were infected and treated as described before. After that, cells were washed with 2 mL 0.1% BSA KRBH per flask and then incubated at 37°C for 30 min with 3 mL 1% BSA KRBH per flask; this allowed to remove most of the remaining fatty acids from the medium. Then cells are washed again with 2 mL 0.1% BSA KRBH per flask. Then 2 mL reaction mix per flask is added. The reaction mix is made of 200 μM BSA-conjugated [^{14}C] palmitate, 11 mM glucose and 800 μM carnitine in KRBH. The system was closed with a rubber stopper (Fisher Scientific, ref. 14-126-BB) which held a 3 cm PVC tube (Fisher Scientific, ref. 14-169-7B) containing a 4 cm^2 Whatman paper soaked with 100 μL 0.1 N KOH. All the system was sealed with parafilm and the flasks were incubated at 37°C for 3 h. After that 200 μL 40% perchloric acid is injected into each flask using a needle to stop the reaction. The system is left overnight at room temperature, to allow the carbon dioxide to be trapped into the KOH. The following day, the system was open and the papers left to dry out, before putting them into 5 mL scintillation fluid (Perkin Elmer, ref. 6013159). Then 1 mL of the reaction mix with perchloric acid is taken and centrifuged at maximum speed for 10 min. 800 μL of the supernatant, which contains the acid-soluble products, is placed into 5 mL scintillation fluid. After 2 h stabilization, samples are analyzed and the results for carbon dioxide are expressed as:

$$\frac{\text{nmol palmitate}}{\text{mg prot} \cdot \text{h}} = \frac{(\text{cpm}_{\text{sample}} - \text{cpm}_{\text{blank}}) \cdot 500}{\text{cpm}_{50\mu\text{L}} \cdot \text{prot} \cdot t}$$

The results for acid-soluble products are expressed as:

$$\frac{\text{nmol palmitate}}{\text{mg prot} \cdot \text{h}} = \frac{(\text{cpm}_{\text{sample}} - \text{cpm}_{\text{blank}}) \cdot 500}{\text{cpm}_{50\mu\text{L}} \cdot \text{prot} \cdot \text{t}} \cdot \frac{2200}{800}$$

3.2. Mitochondrial superoxide quantification in flow cytometry

To detect superoxide generation changes due to ghrelin and CPT1A, MitoSOX Red (Life Technologies, M36008) fluorescence was measured by flow cytometry. Neuronal cells were infected and treated as described previously. Medium was removed, and cells were incubated for 30 min with PBS containing 5 μM MitoSOX Red. The labeled cells were washed three times with HBSS-Ca-Mg, pelleted, resuspended in 300 μl of HBSS-Ca-Mg, and fixed by adding 1.2 ml of absolute ethanol and keeping them at -20°C for 5 min. Cells were pelleted again and resuspended in HBSS-Ca-Mg containing 3 μM DAPI to mark their nuclei. Then macrophages were analyzed using a Gallios Cytometer (Beckman-Coulter). The fluorescence intensity of MitoSOX Red was measured using excitation at 510 nm and emission at 580 nm.

3.3. Amino acid neurotransmitter release assay

The *in vivo* changes observed with the overexpression of CPT1AM in MBH vesicular amino acid neurotransmitter transporters led us to hypothesize a possible effect of ghrelin mediated by CPT1A on glutamate and GABA release. To test this fact, we set a series of experiments with neuronal cultures exposed to depolarizing potassium chloride concentrations (25 mM KCl), alternated with 5 mM KCl, to prove if there were changes in amino acid release due to ghrelin and how this was affected when inhibiting CPT1A pharmacologically and genetically.

We carried out the experiments with cultured primary neurons in the 8th day of *in vitro* (8 DIV) culture, when they are mature enough. If an infection had to be made, *e.g.* to delete CPT1A with Ad-CRE or to silence it with Ad-shCPT1A, cells were infected on 6 DIV, to have its maximum expression on 8DIV. On that day, any pretreatment (5 mM glucose reduction for 3 h)

and treatment (100 nM ghrelin, 40 µg/mL etomoxir for 30 min) was done just after the amino acid neurotransmitter release assay.

For this assay we need two buffers at least: Basal 5 mM KCl Hank's buffer (K5) and depolarizing 90 mM KCl Hank's buffer (K90). To prepare them Hank's buffer solution was prepared without any NaCl, KCl nor glucose, whose composition in this case would be 1.3 mM CaCl₂, 0.4 mM KH₂PO₄, 0.5 mM MgCl₂, 0.4 mM MgSO₄, 4.2 mM NaHCO₃, 0.3 mM Na₂HPO₄·2H₂O, 8 mM HEPES at pH 7.4. Then, for basal 5 mM KCl Hank's buffer 5 mM KCl and 136.4 mM NaCl were added; and for depolarizing 90 mM KCl Hank's buffer, 90 mM KCl and 51.4 mM NaCl.

After treatments, the wells were washed with pre-warmed Hank's Buffer (K5). The 1 mL K5 buffer was added per well and incubated for 10 min at 37°C, so that neurons could stabilize in the buffer. The buffer was aspirated and cells were incubated with 1 mL K5 for 2 min and the supernatant was kept in a microcentrifuge tube. Then cells were incubated with 1 mL K90 for 2 min and the supernatant was kept in a microcentrifuge tube. This process was done up to 6 times, alternating K5 and K90 solutions and keeping the neurotransmitters released into the Hank's solution for posterior analysis. As a control of non-vesicular neurotransmitter efflux an incubation for 2 min in 1 mL K90 without Ca²⁺ and 3 mM EGTA was done and its supernatant was kept as well to be analyzed. All the samples were stored at -20°C until analysis and the cells in the plate were lysed with 0.2 mL NaOH 0.2N to quantify the protein content for normalization.

Amino acid neurotransmitters content was then measured from the samples HPLC-MS/MS at the *Institut d'Investigació Biomèdica de Barcelona (IIBB-CSIC)*

3.4. GABA transaminase assay

To detect changes due to ghrelin and CPT1A in GABA metabolism, we wanted to assess the activity of one of the main enzymes involved in the GABA shunt pathway, GABA transaminase, which connects the releasable GABA pool with tricarboxylic acid cycle intermediates (**Fig 13**). Concretely, with succinate, since it converts GABA into semialdehyde succinate, which is later converted into succinate in the Krebs Cycle.

We took advantage of a GABA aminotransferase (GABAT) Assay Kit (BMRService, ref. E134) which is based on sequential GABA transamination reaction and glutamate oxidation,

which couples the reduction of iodonitrotetrazolium (INT) into INT-formazan ($\epsilon=18 \text{ mM}^{-1}\cdot\text{cm}^{-1}$ at 492 nm).

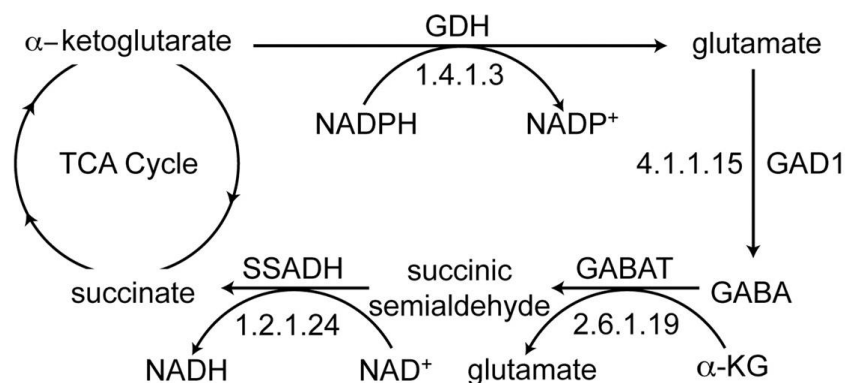


Fig 13. GABA shunt and GAD reactions are responsible for the synthesis, conservation and metabolism of GABA. GABAT, GABA transaminase; GAD, glutamic acid decarboxylase; SSADH, succinic semialdehyde dehydrogenase.

This method allows an indirect sensitive detection of GABA transaminase activity in cell/tissue samples. The manufacturer's instructions were followed, using 100 μL 1x cell lysis buffer for $2 \cdot 10^5$ cells/well in mHypo-N41 and for $8 \cdot 10^5$ cells/well in primary cortical neurons. To perform the assay 10 μL of each sample lysate was used. The optical density measurement was done in a Benchmark Plus microplate spectrophotometer (BioRad, ref. 170-6930) at 492 nm.

3.5. Metabolic Extracellular Flux XF Analysis

The extracellular flux XF analysis is the first *in vitro* technology which grants a non-invasive method to understand the metabolism key role in cell physiology, pathology and etiology. The cause of mitochondrial dysfunction can be easily assessed to reach a thorough understanding of metabolic pathways, signals and phenotypes. The SeaHorse XF24 Metabolic Flux Analysis measures key parameters of mitochondrial function by directly measuring the oxygen consumption rate (OCR), in the presence of different respiration modulators targeting the components of the electron transport chain, which are sequentially injected to measure basal respiration, ATP production, maximal respiration and non-mitochondrial respiration.

Besides mitochondrial respiration, this technology allows to study glycolysis, the other energy producing pathway, as well as it allows to indirectly measure the fatty acid oxidation (FAO), both from endogenous and exogenous fatty acid sources. Nevertheless, only the latter, exogenous FAO is assessed

The compounds injected are oligomycin, FCCP and antimycin A, which target specific components of the electron transport chain (ETC) (**Fig 14**).

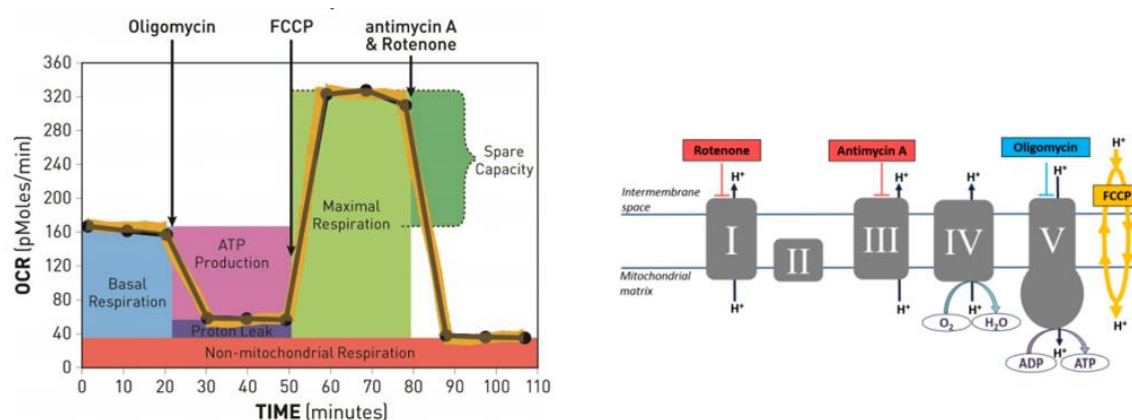


Fig 14. Bioenergetic profile to test the key parameters of mitochondrial respiration. Sequential compound injections measure basal respiration, ATP production, proton leak, maximal respiration, spare respiratory capacity, and non-mitochondrial respiration. Oligomycin inhibits ATP synthase (also known as complex V), FCCP uncouples oxygen consumption from ATP production, and antimycin A inhibits complex III.

Oligomycin inhibits ATP synthase and the decrease in OCR due to its injection correlates to the mitochondrial respiration associated to ATP production. FCCP, namely carbonyl cyanide-p-trifluoromethoxyphenylhydrazone, is an uncoupling agent that collapses the proton gradient and disrupts the mitochondrial membrane potential. All this provokes complex IV to maximally consume oxygen. This value can be used to calculate spare respiratory capacity, as the difference between maximal respiration and basal respiration. Nonetheless, in certain cell types with low respiratory capacity this value is hard to be assessed since they do not have spare respiratory capacity. The third injection, with antimycin A, acts inhibiting complex III, to shut down mitochondrial respiration and enables the calculation of non-mitochondrial respiration driven by processes outside the mitochondria.

Cells were differentiated in customized Seahorse 24-well plates and infected as described above. Before the measurement, cells treated for 3 h with 25 mM glucose medium, 5 mM glucose medium or FAO assay medium. In the last 30 min the pharmacological treatments

were made as previously explained. Then they were assayed for 1 hour in XF Assay Medium (Seahorse Bioscience) plus 5 mM glucose. During the assay, we injected the following at the final concentrations shown: 2 µg/mL oligomycin, 0.16 µM FCCP and 2 µM antimycin A (Sigma-Aldrich). OCR was calculated by plotting the oxygen tension of media as a function of time (pmol/min), and data were normalized by the protein concentration measured in each individual well. The results were quantified as the average of 8-10 wells +/- SEM per time point in at least three independent experiments.

3.6. Rat mediobasal hypothalamus lipidomic analysis

MBH wedges were quickly removed, frozen in liquid nitrogen, and stored at -80 °C prior to lipid analysis. Sphingolipid extraction and analysis by UPLC-TOF was carried out as described (Canals et al., 2009). Phospholipid extracts were obtained using the same procedure but without the saponification step. Lipids were analysed by UPLC-TOF in positive or negative mode. The two mobile phases were 1 mM ammonium formate in methanol (phase A) and 2 mM ammonium formate in H₂O (phase B), both phases with 0.05 mM formic acid. The following gradient was programmed: 0 min, 80% A; 3 min, 90% A; 6 min, 90% A; 15 min, 99% A; 18 min, 99% A; 20 min, 80% A, and a flow rate of 0.3 mL/min. The ratio between the areas was normalized by the protein concentration of the sample (µg/µl).

3.7. Rat plasma amino acid and thyroidal hormones analysis

Blood collected from rats and processed to provide plasma and serum. An ELISA commercial kit was used to measure T3, T4 and TSH (DRG Diagnostics). For the measurement of plasma amino acids, distilled water (100 µL), 1000 µM NLE (50 µL) and 10% trifluoroacetic acid (100 µL) were added to 100 µL plasma sample. After 10 min incubation, tubes were centrifuged at 10 000 *x g*. The supernatant was filtered (Ultracel membrane 10 kDa filter, Milipore), dried under nitrogen stream and resuspended in lithium citrate pH 2.2 (100 µL). Amino acids were measured using an auto analyzer at *Centres Científics i Tecnològics de la Universitat de Barcelona* (CCiT-UB).

3.8. Neuronal tricarboxylic acid cycle intermediates analysis

Analysis of tricarboxylic acids was carried out by gas chromatography-mass spectrometry (GC-MS) detection with a method adapted from the literature (Ribes et al., 1992; Serra-Pérez et al., 2010; Tanaka, West-Dull, Hine, Lynn, & Lowe, 1980). Experiments were performed on cell cultures. At the end of the incubations, cells were washed with PBS, and the cell pellet was resuspended in 500 μl of milli-Q water and frozen at $-20\text{ }^{\circ}\text{C}$ until assayed (a separate fraction was set aside for protein quantification). For the preparation of extracts, the 500- μl samples were taken to a volume of 2 ml with water, and further added 1 ml of 8 M NaOH and 1 ml of 25 mg/ml hydroxylamine. The sample was then heated at $60\text{ }^{\circ}\text{C}$ for 30 min, and pH was adjusted by adding 1 ml of 6 N HCl. Sequential extractions were carried out as described (Ribes et al., 1992) with the exception that samples were extracted twice with 2 ml of diethyl ether and twice with 2 ml of ethyl acetate. 6 μl of 5 mM undecanoic acid was added at the collection tube to serve as an internal standard of the procedure. Once completely evaporated with nitrogen gas, the final dry residue was resuspended in 75 μl of trimethylsilyl, incubated at $60\text{ }^{\circ}\text{C}$ for 30 min to derivatize the keto acids, and kept at $-20\text{ }^{\circ}\text{C}$ until injected. 2- μl samples were injected into a 7890A-5975C GC-MS (Agilent Technologies), with an HP-5MS $60 \times 0.25 \times 0.25$ capillary column using a splitless method and pressure ramp, and results were analyzed by using the ChemStation GC/MSD software. The ratio between the areas was normalized by the protein concentration of the sample ($\mu\text{g}/\mu\text{l}$).

3.9. Acylcarnitines quantification

Acylcarnitines were obtained from MBH wedges and cell cultures. Samples were homogenized each in 200 μL PBS 1x, from which 20 μL are taken for protein content analysis. Then deuterated palmitoylcarnitine is added to get a final concentration of 50 ppb. Sequential extractions were performed using Folch reagent and methanol:dH₂O:chloroform (48:47:3). Once completely evaporated with nitrogen gas, samples were resuspended in 300 μL methanol to be analyzed. Acylcarnitines quantification was performed in an Acquity UPLC-TOF system (Waters) with a BEH C8 column (1.7 μm particle size, 100 mm x 2.1 mm, Waters). The two mobile phases were 1 mM ammonium formate in methanol (phase A) and 2 mM ammonium formate in H₂O (phase B), both phases with 0.05 mM formic acid. The following gradient was programmed: 0 min, 65% A; 10 min, 90% A; 15 min, 99% A; 20 min 65% A, and a flow rate of

0.3 mL/min. Quantification was carried out using the extracted ion chromatogram of each compound using 50 mDa window. The linear dynamic range was determined by injecting standard mixtures. Positive identification of compounds was based on the accurate mass measurement with an error lower than 50 ppm and their LC retention time compared to that of a standard ($\pm 2\%$). The ratio between the areas was normalized by the protein concentration of the sample ($\mu\text{g}/\mu\text{l}$).

4. Bioinformatics and statistical analysis

Statistical significance was determined using Prism 6 software from GraphPad, by two-way ANOVA, followed by post-hoc analysis with Tukey-Kramer test in the multiple comparison analysis. In some cases Student's T test was performed in the analysis of two groups. Data is expressed as mean \pm SEM. P value lower than 0.05 is considered significant. Association between lipid species within each experimental group was evaluated using Pearson correlation coefficients (r) were computed using the PROC CORR of SAS. Metabolic extracellular flux XF analysis to evaluate oxygen consumption rate was performed using Wave Desktop software 2.2 from Seahorse Bioscience. Digital PCR experiments were analyzed using QuantaSoft software 1.7.4 from BioRad. Sequencing experiments were analyzed using Chromas Lite software 2.5.1 from Technelysum and CLC Sequence Viewer 7 from CLC Bio. Oligonucleotide design for qRT-PCR experiments was performed using Universal Probe Library on-line software from Roche. Management of scientific references has been performed using Mendeley Desktop 1.16 from Mendeley Ltd.

RESULTS

PART 1. Evaluation of the hyperphagic phenotype in rats overexpressing CPT1AM in ventromedial hypothalamus

CPT1A has been described to have increased activity in fasting state due to the activation of GHSR by ghrelin. We assessed the effect of CPT1AM overexpression in VMH on weight, food intake, glucose metabolism, circulating amino acids and thyroidal hormones, MBH lipid composition, MBH ROS-buffering enzymes and ER stress proteins transcripts, as well as MBH neuropeptides and glutamate and GABA metabolism genes mRNA. To do so, we cannulated the animals after at least 1-week post arrival quarantine to reach VMH with ongoing microinjection (see Fig 10 in Experimental procedures 1.1). 1 week later, AAV vectors were microinjected into rats VMH and after another week, body weight and food intake was monitored along their lives. 8 weeks before rats termination, a fast-refeeding satiety test was performed and 4 weeks previous their sacrifice GTT and PTT assays, each to two different sets of animals, were performed.

1.1. Analysis of infection and CPT1A activity in VMH

We injected bilaterally a set of cannulated rats with AAV-CPT1AM, and another with AAV-GFP as control, using the coordinates to reach the ventromedial nucleus of the hypothalamus (VMH), following the directions found in the Experimental procedures 1.3 and 1.4. Firstly, the nucleus-specific infection was confirmed by histological analysis of coronal sections of 18-week AAV-GFP injected rats, taking advantage of the green fluorescence found in the cells infected. Results showed that infection was primarily limited to the VMH area (**Fig 15**).

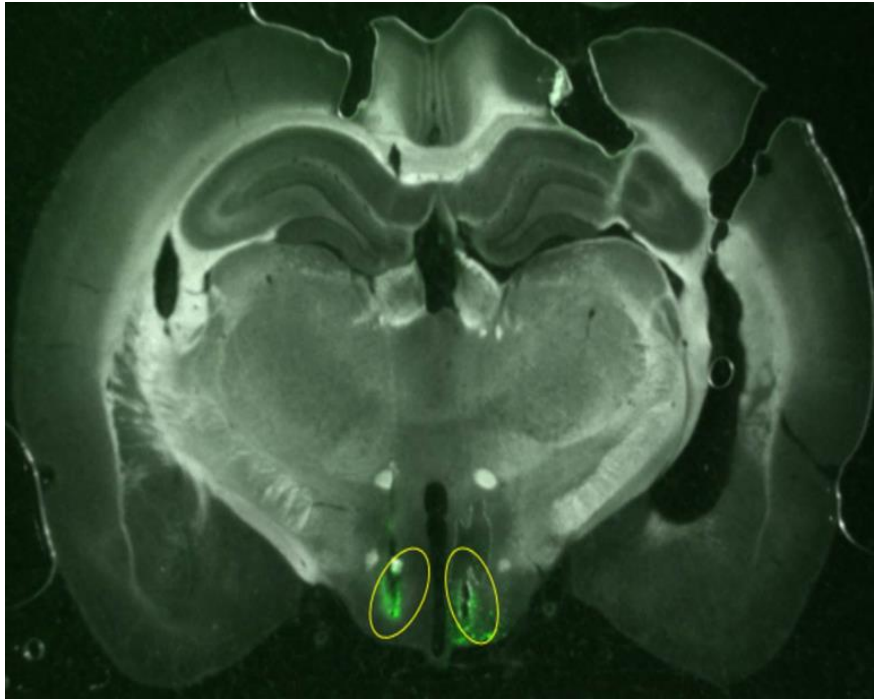


Fig 15. Representative histological coronal section showing GFP in the VMH of AAV-GFP infected rats after the bilateral injection of AAV vectors.

Secondly, we wanted to assess whether AAV-CPT1AM actually increased CPT1A activity in the infected area. To this end, we analyzed the levels of long-chain acylcarnitines, as direct products of CPT1A activity, and the levels of long chain fatty acyl (LCFA)-CoA, its direct substrate, in mediobasal hypothalamus (MBH). VMH specific dissection has some technical issues, thus we opted to analyze CPT1A products in a broader area, *i.e.* MBH, encompassing both VMH and arcuate nucleus, which does not substantially dilute VMH acylcarnitines and LCFA-CoA pools. To this end, rats were sacrificed at 18 weeks after infection, they had their MBH dissected and lipids specifically extracted and analyzed as previously on Experimental procedures 3.9. On the one hand, the levels of C18:0 acylcarnitines are 3.3-fold higher (298.4 ± 72.65 pmol/ μ g) in rats infected with AAV-CPT1A (from now on referred as CPT1A rats) compared to AAV-GFP infected rats (GFP rats, 90.46 ± 12.69 pmol/ μ g, $p < 0.05$). C14:0 and C16:0 acylcarnitines levels were not significantly higher, but showed a tendency to increase (**Fig 16**).

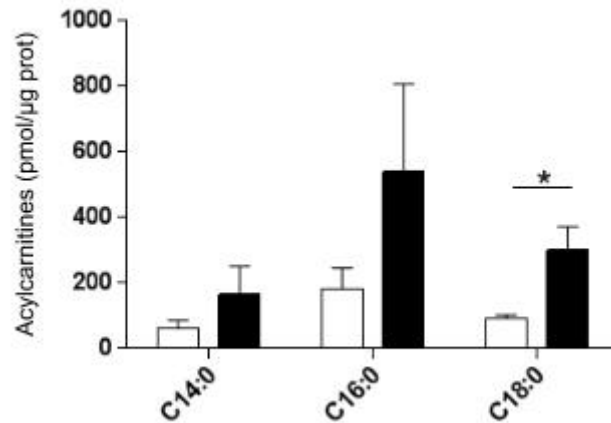


Fig 16. Quantification of acylcarnitines found in MBH of overnight fasted rats. Samples were obtained 18 weeks after AAV injection. White bars, GFP rats, and black bars, CPT1AM rats. Error bars represent SEM $*p < 0.05$.

On the other hand, we analyzed the levels of the long chain fatty acyl (LCFA)-CoA to assess if they were decreased in our model like some of our collaborators stated, with a short-term VMH CPT1AM adenovirally driven overexpression (Gao et al., 2013). In our model, based in long-term overexpression, LCFA-CoA were not decreased in the overall pool, but increased in the case of C18:0 acyl-CoA (0.19 ± 0.04 pg/mg, in GFP rats, $n=5$; 0.3 ± 0.02 pg/mg, in CPT1AM rats, $n=7$; $p=0.02$).

These results, added to the previously found in our group (Mera, 2012) regarding CPT1A mRNA increase due to AAV-CPT1A infection, show that stereotactic bilateral cannulation in VMH allows a delimited infection mainly in this nucleus. And following the viral injection, the infection triggers an increase in CPT1A activity, as shown due to the higher levels of long chain acylcarnitines in CPT1AM rats, but the hyperphagic phenotype to be described appears regardless there is no reduction in the total pool of LCFA-CoA. All these confirm the effectivity and function of the viral vectors used to overexpress GFP and CPT1AM in the VMH.

1.2. Effect on food intake and body weight

We assessed the effect of CPT1AM overexpression in VMH on food intake, both in satiety test and long term cumulative food intake. We found that CPT1AM rats show significant hyperphagia in their weekly food intake when fed *ad libitum*, compared to GFP rats, from the

day 21 after infection along almost all the weeks until their sacrifice (**Fig 17**). Consequently, cumulative food intake along this period is statistically higher in CPT1AM rats (**Fig 18**)

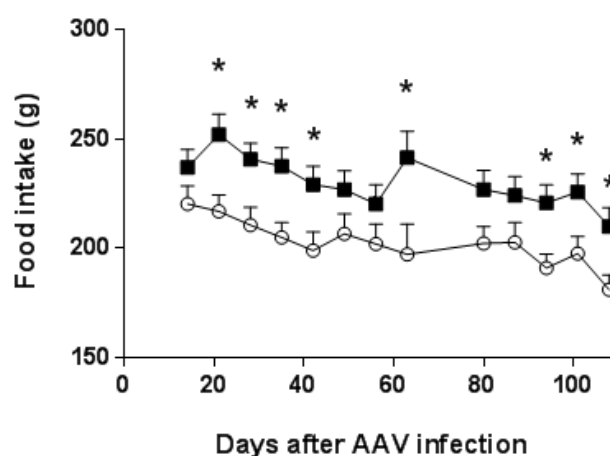


Fig 17. Weekly food intake of CPT1AM and GFP rats. White circles, GFP rats, and black squares, CPT1AM rats. n=11. Error bars represent SEM, $p < 0.05$.

We wanted to assess if CPT1A rats have higher food intake regardless the satiety state. To this end we performed a satiety test, 10 weeks after AAV injection, following a refeeding after fasting scheme. When refed, CPT1AM rats are hyperphagic after 1, 2, 4 8 and 24 h which confirms an increase in food intake regardless to the satiety state (**Fig 19**).

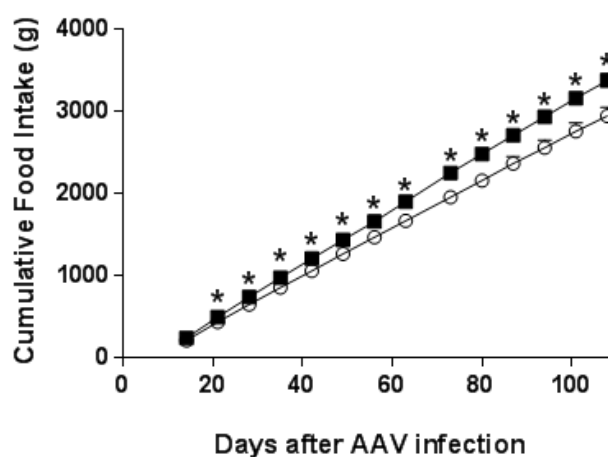


Fig. 18. Cumulative food intake of CPT1AM and GFP rats. White circles, GFP rats, and black squares, CPT1AM rats. n=11. Error bars represent SEM, $p < 0.05$.

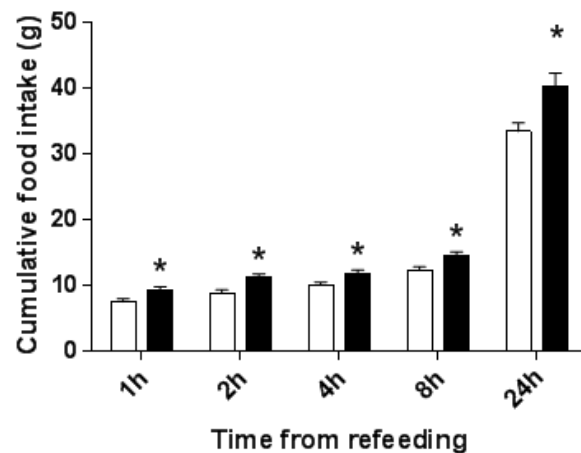


Fig 19. Analysis of cumulative food intake for 24 h after an overnight fasting to test the satiety state of CPT1AM and GFP rats. Analysis was performed 10 weeks after AAV injection. White bars, GFP rats, and black bars, CPT1AM rats. n=11. Error bars represent SEM, * $p < 0.05$.

This hyperphagia was accompanied by an increase in total body weight measured weekly, which was significant starting at the 21 days after injection (**Fig 20**).

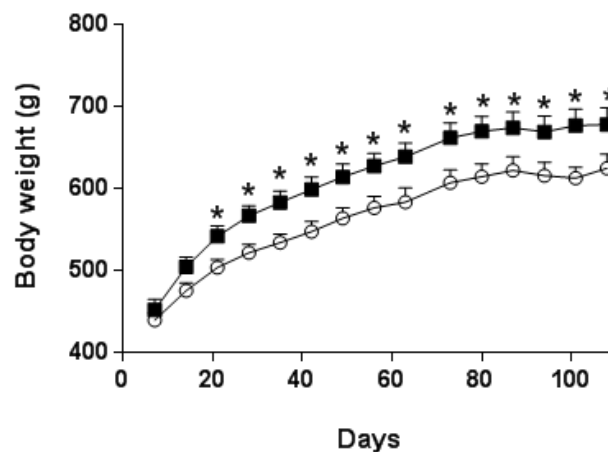


Fig 20. Analysis of body weight changes in CPT1AM and GFP rats. White circles, GFP rats, and black squares, CPT1AM rats. n=11. Error bars represent SEM, * $p < 0.05$.

These results indicate that CPT1AM overexpression in VMH causes hyperphagia regardless the satiety state and we have shown that there is an increase in body weight as well, not detected in previous studies. Moreover, we have actually evaluated the CPT1A activity in MBH, since we were able to detect an increase in long chain acylcarnitines, but there was no reduction in LCFA-CoA after long term overexpression. This suggests that CPT1A activity per se is important for the control of food intake.

1.3. Lipidomic analysis on MBH

We wanted to assess the extent of bioactive lipid changes, beyond variation in direct substrate and product levels in CPT1AM rats, so we performed a lipidomic analysis in collaboration with Dr. Josefina Casas and Dr. Gemma Fabriàs, from *Institut de Química Avançada de Catalunya* (IQAC - CSIC). These lipidomic modifications in MBH might shed some light to check its ulterior involvement in the hyperphagic phenotype. Other collaborators of our group have shown that some lipids, such as ceramides, are linked to appetite modulation (Gao, Zhu, et al., 2011; Ramírez et al., 2013). In our model, total ceramide levels are not significantly different in MBH (**Fig. 7**). Nonetheless, an analysis by species show an increase in levels of C14:0 ceramide (5.3 ± 0.7 pmol/mg, GFP rats; 8.3 ± 1.0 pmol/mg, CPT1AM rats, $p < 0.01$) and C18:1 ceramide (170.4 ± 18.8 pmol/mg, GFP rats; 250.5 ± 31.9 pmol/mg, CPT1AM rats, $p < 0.02$) (**Table. 1**).

	GFP-expressing rats	CPT1AM-expressing rats	
Ceramides (pmol/mg protein)	n = 10	n = 10	p value
14:0	5.3±0.7	8.3±1	0.01
14:1	2.7±0.4	4±0.7	ns
16:0	66.3±9.6	84.9±13.1	ns
16:1	7.3±1.1	9.5±1	ns
18:0	1479.9±177.9	1880.8±165.9	ns
18:1	170.4±18.8	250.5±31.9	0.02
20:0	246.9±41.3	312.4±23.9	ns
22:0	40.3±6.9	51±7.1	ns
22:1	10.6±1.3	12.5±1.2	ns
24:0	61.2±9.4	67.1±13.5	ns
24:1	65±7.8	67.5±10.5	ns
24:2	24.3±3.5	29.1±3.6	ns

Table 1. Analysis of ceramide levels in MBH from CPT1AM and GFP rats after overnight fasting. Analysis performed from samples obtained 18 weeks after AAV injection. Ceramide levels in MBH from CPT1AM and GFP rats. Data indicated as Mean ± SEM.

We also observe a 36.1% increase in total lactosylceramide (LacCer) in CPT1AM rats (**Fig 21**). Moreover, other sphingolipids related to ceramides, such as sphingomyelin (SM) and dihydrosphingomyelin (DHSM) were analyzed. Their total concentrations are increased in MBH from CPT1A rats by 30.8% and 30.6%, respectively (**Fig 21**).

Membrane traffic and vesicular fusion are especially sensitive to the amount of phosphatidylethanolamine (PE) (Thai et al., 2001). We determined the total levels of

lysophosphatidylethanolamine (LPE), plasmalogen phosphatidylethanolamine (PlasPE) and lysoplasmalogen phosphatidylethanolamine (LPlasPE), which are decreased by 38.5%, 29.0% and 45.8% respectively in CPT1AM rats, with respect to controls (**Fig 22**).

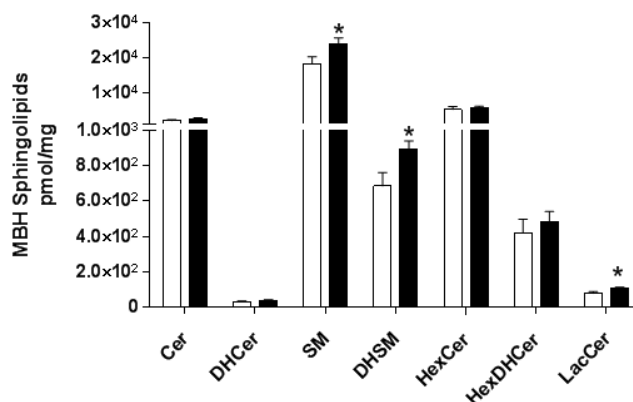


Fig 21. Analysis of spingolipids in MBH from CPT1AM and GFP rats after overnight fasting. Analysis performed in samples taken 18 weeks after AAV injection. White bars, GFP rats, and black bars, CPT1AM rats. n=10. Error bars represent SEM, $p < 0.05$.

The concentration of lysophosphatidylserine (LPS) was also analyzed in the MBH, which was decreased by 39.0% in CPT1AM rats compared to control rats (**Fig 22**). Interestingly, the amount of lysophosphatidylcholine (LPC) was 30.0% higher in CPT1AM rats group, despite no changes are observed in total phosphatidylcholine (PC) and plasmalogen phosphatidylcholine (PlasPC).

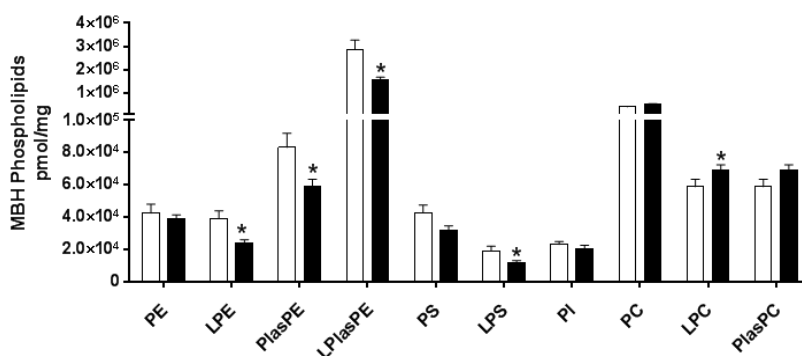


Fig 22. Analysis of phospholipids in MBH from CPT1AM and GFP rats after overnight fasting. Analysis performed in samples taken 18 weeks after AAV injection. White bars, GFP rats, and black bars, CPT1AM rats. n=10. Error bars represent SEM, $p < 0.05$.

Neutral lipids, such as triacylglycerols (TAG), diacylglycerols (DAG) and cholesterol esters (Chol-E) show a tendency to increase (**Fig 23**).

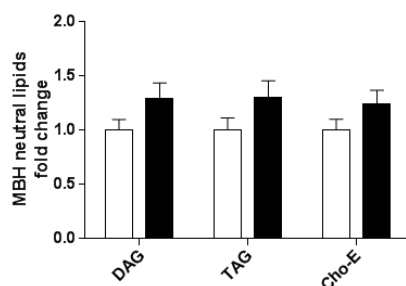


Fig 23. Analysis of neutral lipids in MBH from CPT1AM and GFP rats. Analysis performed in samples taken 18 weeks after AAV injection after overnight fasting. White bars, GFP rats, and black bars, CPT1AM rats. n=10. Error bars represent SEM.

In addition to the total amount of lipid species, we studied the correlations between the lipid compounds in each group (**Fig 24**). The lipidomic correlation signature in CPT1AM rats has many traits in common with control GFP animals (shown in yellow). Nonetheless, some differ from the signature exclusive for control animals (green): we observe strong positive correlations between most of the phospholipids -namely, phosphatidylethanolamine (PE), lysophosphatidylethanolamine (LPE), phosphatidylserine (PS), lysophosphatidylserine (LPS), some phosphatidylcholines (PC) and lysophosphatidylcholine (LPC)- and many sphingolipids - such as sphingomyelin (SM), dihydro sphingomyelin (DHSM), hexosyl ceramide (HexCer), hexosyl dihydroceramide (HexDHCer), lactosyl ceramide (LCer)- in the GFP rats. These positive correlations were not observed in CPT1AM animals. These rats also lost the positive correlations between the phospholipid group composed by PE, LPE, PS and LPS and the phosphatidylcholine derivatives (PC and LPC), despite most of the correlations within the phospholipid group being kept. On the other hand, new correlations were detected in CPT1AM animals, which were not observed in GFP counterparts. Given the activity of CPT1A, positive correlations between acylcarnitines (mostly C16:0, C18:0 and C20:0) and phospholipids (PE, LPE, PEP, LPEP, PS, LPS, PC and LPC) were found. Moreover, new correlations were detected between triacylglycerols, diacylglycerols, phospholipids, and ceramides.

All these observations indicate that CPT1A expression in the VMH changes lipid metabolic flows and alters the profile of structural and bioactive complex lipids in the MBH, which may be involved in the hyperphagic phenotype observed.



Fig 24. Integration of lipid correlations in the MBH from CPT1AM and GFP rats. Analysis performed in samples taken 18 weeks after AAV injection. The pixel map is derived from correlation analyses between the lipids in MBH. Green pixels indicate the correlations only in GFP rats. Red pixels indicate the correlations in CPT1AM rats. Yellow pixels indicate the correlations in both groups.

1.4. Analysis on hypothalamic gene expression

To discern the molecular mechanisms involved in the hyperphagia produced in CPT1AM rats, compared to GFP counterparts, we analyzed the levels of different transcripts of MBH neurotransmission elements involved in the control of food intake.

Our group had previously reported that neither orexigenic (*i.e.* AgRP and NPY) nor anorexigenic neuropeptides (*i.e.* POMC and CART) have their transcripts changed when producing a long-term overexpression of CPT1AM (Mera, 2012). We reproduced this once again, showing that none of the food intake-related neuropeptides are changed in our model (**Fig 25**).

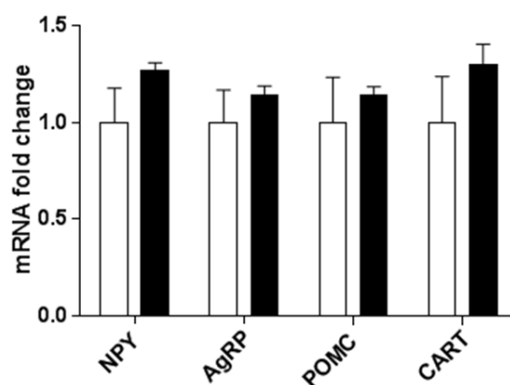


Fig 25. Analysis of mRNA levels of arcuate neuropeptides controlling food intake, from MBH samples obtained from CPT1AM and GFP rats. Analysis performed by qRT-PCR from mRNA samples obtained 18 weeks after AAV injection, after overnight fasting (n=6-7). White bars, GFP rats, and black bars, CPT1AM rats. Error bars represent SEM, $p < 0.05$.

Since CPT1AM rats show unaltered food intake neuropeptidergic profile, we assessed changes in the expression of some genes which are related to amino acid neurotransmission and have been described to be involved in food intake and energy homeostasis (Dicken et al., 2015; Krashes et al., 2013; Tong et al., 2007, 2008). We observed an 82% decrease ($p < 0.05$) in vesicular glutamate transporter 2 (VGLUT2) transcript in CPT1AM rats, with no changes in VGLUT1 and VGLUT3. VGLUT family allows glutamate to get into small synaptic vesicles (SSV) to be released due to depolarization to the synaptic cleft, being VGLUT2 the most expressed in VMH. Vesicular GABA transporter (VGAT), which has a similar role with γ -aminobutyric acid (GABA), showed a 2.2 ± 0.4 fold increase ($p < 0.05$) in CPT1A rats' MBH (**Fig 26**). GABAergic neurons found in this area are present mainly in arcuate nucleus (Tong et al., 2008). All these

data suggest amino acid neurotransmission disturbances in MBH of CPT1A rats, which may be related to the hyperphagic phenotype.

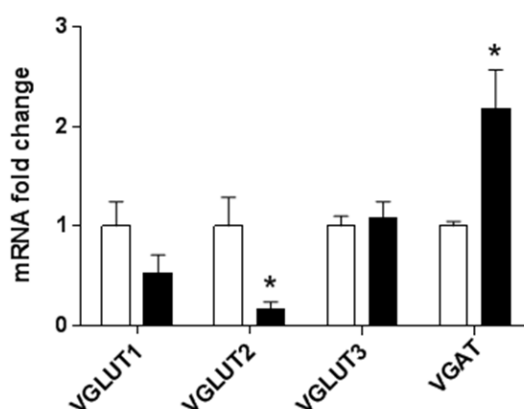


Fig 26. Analysis of mRNA levels of vesicular neurotransmitter transporters from MBH samples obtained from CPT1AM and GFP rats. Analysis performed by qRT-PCR from mRNA samples obtained 18 weeks after AAV injection, after overnight fasting (n=6-7). White bars, GFP rats, and black bars, CPT1AM rats. Error bars represent SEM, $p < 0.05$.

AgRP neurons and GABAergic neurotransmission can be modulated by reactive oxygen species (ROS) (Z B Andrews et al., 2008; Tarasenko, Krupko, & Himmelreich, 2012). Given that CPT1A activity putatively increases mitochondrial FAO and ROS, we measured the mRNA levels of antioxidant enzymes and UCP2 (**Fig 27**). A slight increase in catalase (CAT), glutathione peroxidase 3 (Gpx3) and superoxide dismutase (SOD) was detected in CPT1AM rats' MBH (1.2 ± 0.04 , 1.5 ± 0.1 and 1.2 ± 0.03 -fold increase respectively, $p < 0.01$). Furthermore, UCP2 was increased as well (1.4 ± 0.1 -fold increase, $p < 0.05$) in MBH from CPT1AM rats.

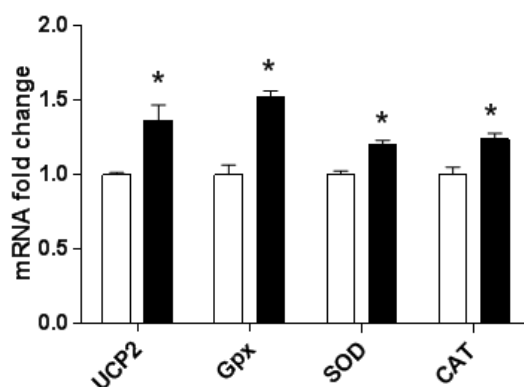


Fig 27. Analysis of mRNA levels of ROS-buffering enzymes from MBH samples obtained from CPT1AM and GFP rats. Analysis performed by qRT-PCR from mRNA samples obtained 18 weeks after AAV injection, after overnight fasting (n=6-7). White bars, GFP rats, and black bars, CPT1AM rats. Error bars represent SEM, $p < 0.05$.

We wanted to assess whether this ROS might be inducing endoplasmic reticulum (ER) stress or changes in the expression of unfolded protein response (UPR) genes, so we checked several markers related to it in MBH of CPT1AM and GFP rats, but no significant changes are found in their expression (**Fig 28**).

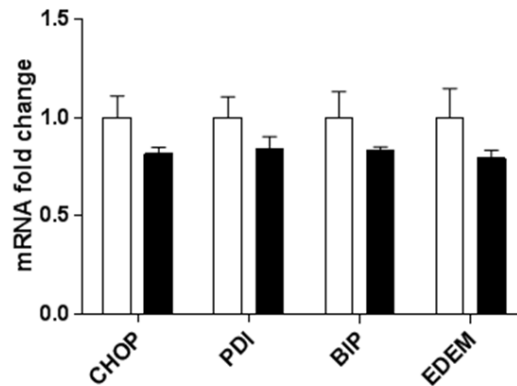


Fig 28. Analysis of mRNA levels of ER stress elements from MBH samples obtained from CPT1AM and GFP rats. Analysis performed by qRT-PCR from mRNA samples obtained 18 weeks after AAV injection, after overnight fasting (n=6-7). White bars, GFP rats, and black bars, CPT1AM rats. Error bars represent SEM, $p < 0.05$.

1.5. Analysis of circulating amino acids and thyroidal hormones

To complement the previously described increased in fasting glucose, insulin and octanoyl ghrelin observed in CPT1AM rats and unchanged serum levels of leptin (Mera, 2012) we studied other serum parameters, which might be related to the obesogenic phenotype.

We evaluated the plasma aminogram and interestingly, specific branched-chain amino acids (BCAA), such as Val and Ile, which are considered obesity markers, are increased by 18.8% and 19.8% respectively in CPT1AM rats compared to control rats. Nonetheless, Leu remained unchanged. Moreover, Gly is reduced and Orn and His are increased in CPT1AM rats (**Table 2**).

	GFP-expressing rats	CPT1AM-expressing rats	
Amino acids (μM)	<i>n</i> = 6	<i>n</i> = 6	<i>p</i> value
Taur	132 \pm 9	128 \pm 10.1	<i>ns</i>
Asp	23.7 \pm 0.8	26.7 \pm 1.2	<i>ns</i>
Hypro	1.6 \pm 0.2	1.7 \pm 0.1	<i>ns</i>
Thr	198.5 \pm 11.1	216.7 \pm 9.6	<i>ns</i>
Ser	216.2 \pm 6	221.4 \pm 5.6	<i>ns</i>
Asn	30.4 \pm 1.1	30.5 \pm 2.3	<i>ns</i>
Glu	192.4 \pm 15.8	265.1 \pm 12.3	<i>ns</i>
Gln	103.1 \pm 9.8	91.3 \pm 10.1	<i>ns</i>
Pro	70.8 \pm 1.5	67.5 \pm 2.7	<i>ns</i>
Gly	251 \pm 7.4	223.1 \pm 8.3	0.04
Ala	335 \pm 11.3	324.3 \pm 10.7	<i>ns</i>
Citr	66.4 \pm 3.5	71.2 \pm 3.8	<i>ns</i>
Val	159.4 \pm 6.2	189 \pm 5.8	0.006
Cyst	50 \pm 1.4	57.1 \pm 3.1	<i>ns</i>
Met	78.5 \pm 2.4	77.1 \pm 4.5	<i>ns</i>
Ile	66.1 \pm 2.5	79.2 \pm 2.2	0.003
Leu	194.3 \pm 6.9	204.9 \pm 3	<i>ns</i>
Tyr	127.5 \pm 8.4	144.7 \pm 8	<i>ns</i>
Phe	75 \pm 2.8	79.7 \pm 0.9	<i>ns</i>
Orn	115.5 \pm 3.2	163 \pm 7.1	0.004
Lys	632 \pm 9.1	696.1 \pm 25	0.05
His	101.3 \pm 2.7	122.4 \pm 2.8	0.001
Trp	21.9 \pm 1.5	20.8 \pm 2	<i>ns</i>
Arg	215.4 \pm 9.4	225.9 \pm 6.3	<i>ns</i>

Table 2. Analysis of plasma aminogram from CPT1AM and GFP rats. Analysis performed from samples obtained 18 weeks after AAV injection and overnight fasting. Data indicated as Mean \pm SEM.

Levels of thyroid hormones (T3, T4 and TSH) were evaluated, since alterations in thyroidal function have been related to overweight. In our model, thyroid hormones remained unaltered between the two groups (**Fig 29**)

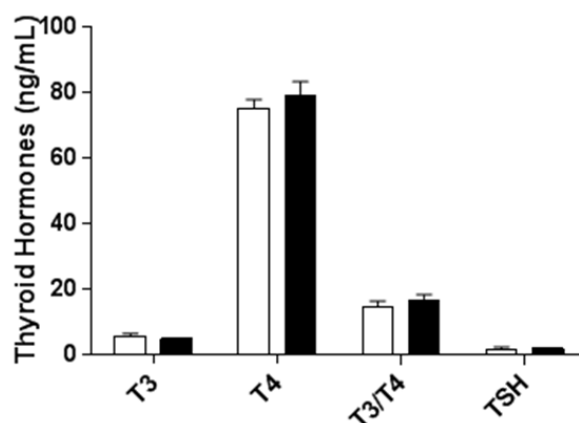


Fig 29. Analysis of serum thyroidal hormones from CPT1AM and GFP rats. Analysis performed from samples obtained 18 weeks after AAV injection after overnight fasting (*n*=6). White bars, GFP rats, and black bars, CPT1AM rats. Error bars represent SEM.

This data discards any thyroidal disturbances due to the CPT1AM overexpression and show a typical increase in BCAA observed in other obese models.

1.6. Analysis of glucose tolerance and gluconeogenesis

Our group had previously reported that CPT1AM rats showed altered glucose tolerance and moreover, increased hepatic phosphoenolpyruvate carboxykinase, which is a marker for gluconeogenesis (Mera, 2012).

We confirmed the previous results in a glucose tolerance test performed at 14 weeks after AAV injection. Glycaemia was higher at 30, 90 and 120 min after intraperitoneal (IP) glucose bolus, and the area under the curve was higher in CPT1AM rats, which is a sign for impaired glucose tolerance (**Fig 30**).

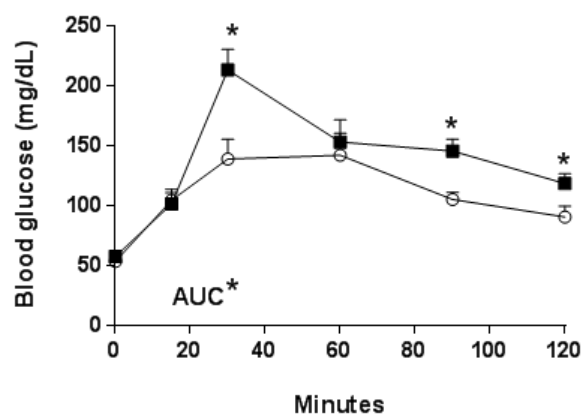


Fig 30. Analysis of glucose tolerance in CPT1AM and GFP rats. Analysis performed 14 weeks after AAV injection after overnight fasting (n=6). White circles, GFP rats, and black squares, CPT1AM rats. Error bars represent SEM. * $p < 0.05$

In another of the experimental sets of rats we further assessed the hepatic gluconeogenesis by checking the glucose de novo formation, after an intraperitoneal pyruvate bolus. Surprisingly, we observed that the glycaemia was only increased significantly at the beginning and 120 min in CPT1AM rats, and the overall area under the curve is not significantly higher in one group compared to the other (**Fig 31**), despite we had previously reported increased hepatic PEPCK mRNA levels in CPT1A rats. However, if glycaemic values had been

recorded beyond the 120 min, the AUC would probably be greater in CPT1AM rats, despite not having a higher peak due to gluconeogenesis.

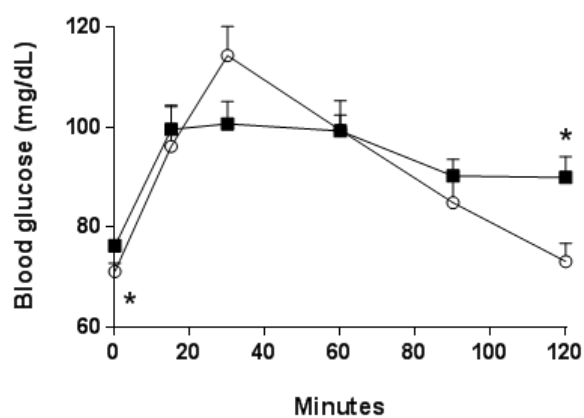


Fig 31. Analysis of gluconeogenesis in CPT1AM and GFP rats. Analysis performed 14 weeks after AAV injection, after overnight fasting (n=6). White circles, GFP rats, and black squares, CPT1AM rats. Error bars represent SEM. * $p < 0.05$

PART 2. Study of the role of CPT1A as a downstream effector of ghrelin in hypothalamic cell lines

We used several hypothalamic neuronal cell lines which had been obtained by immortalization of hypothalamic primary cultures to assess if ghrelin was able to modulate amino acid neurotransmission and if CPT1A was in the signaling pathway downstream GHSR in this effect. These succeed to reproduce some of the physiological features they have *in vivo*, but not them all. The most widely used is GT1-7, since it was one of the first cell lines obtained, which expresses AgRP in a ghrelin-responsive manner, although it was not dissected specifically from arcuate nucleus. Later on, the Canadian company CELLutions Biosystems Inc. has developed a wide range of hypothalamus-derived embryonic neurons which respond to physiological stimuli unevenly.

We tested mHypo-N29/4 and mHypo-N43/5 as models for NAG neurons and CART/POMC neurons I ARC. Unfortunately, the expression of the four neuropeptides was almost inexistent in our hands. Then we used mHypo-N41 cell line, which actually expresses AgRP only to perform experiments to analyze its ghrelin-responsiveness and GABAergic nature.

2.1. Selection of shCPT1A lentivirally transduced mHypo-N41 neuronal lines

To study the implication of CPT1A in ghrelin effect on amino acid neurotransmitter metabolism, we pursued to obtain a clonally selected mHypo-N41 neuronal line expressing a shRNA which knocks down CPT1A. To this end, we obtained two lentiviral vectors, one containing shRNA against CPT1A and the other a scramble sequence as a control, following the previously described procedure.

We performed a puromycin kill curve experiment to determine the lowest puromycin concentration to clonally select mHypo-N41 neurons infected by the lentiviral vectors conferring puromycin resistance, as well as the expression of the shRNA. The concentration finally used was 1 µg/mL puromycin. After almost 8 days exposed to puromycin, remaining cells expressing both lentiviral elements, were grown in a puromycin-free complete medium to

expand them. Cells were subcultured to confirm the reduction of CPT1A mRNA due to shRNA expression and the effect on expression of AgRP as a control, one of the orexigenic neuropeptides present in the hypothalamic cell line. The clonally selected mHypo-N41-shCPT1A reduces significantly CPT1A mRNA levels to a 59% ($p=3\cdot 10^{-7}$) and AgRP expression is reduced to a half as well ($p=0.02$), compared to its control, clonally selected mHypo-N41-scramble (**Fig 32**).

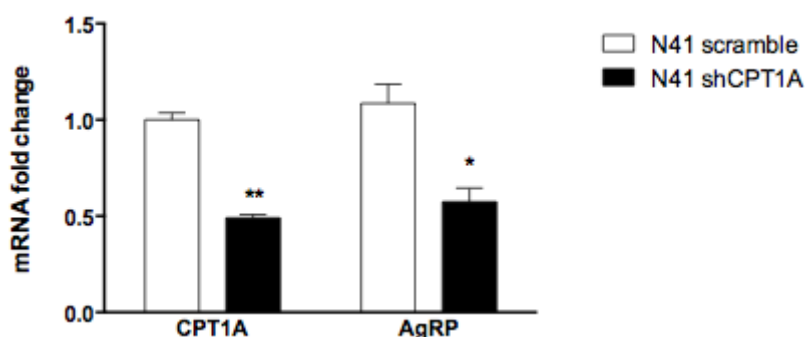


Fig 32. Analysis of mRNA levels of CPT1A and AgRP in clonally selected mHypo-N41-shCPT1A and mHypo-N41-scramble. Analysis performed by qRT-PCR. Error bars represent SEM, n=4, ** $p=3\cdot 10^{-7}$, * $p=0.02$

Nonetheless, when we wanted to assess the effect of ghrelin on the selected lines, mHypo-N41 infected with LV-scramble, namely mHypo-N41-scramble, showed no changes in CPT1A and AgRP expression, even though some effect on their transcripts was observed in CPT1A and AgRP, but none on NPY in wild type mHypo-N41 cells (**Fig 33**).

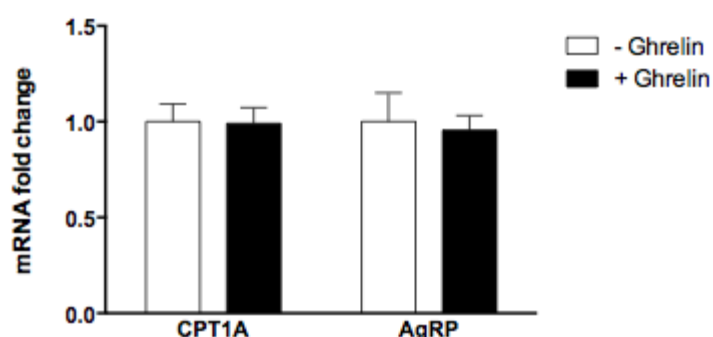


Fig 33. Analysis of mRNA levels of CPT1A and AgRP in clonally selected mHypo-N41-scramble after ghrelin treatment. Analysis performed by qRT-PCR. Error bars represent SEM, n=4,

The lack of NPY and ArGP responsiveness to ghrelin led us to discard mHypo-N41 as a good hypothalamic cell line. We opted to change to GT1-7 cell lines, because their response to ghrelin was more established and seemed to be a more reliable model to focus on a mechanistic

insight. Moreover, we designed another viral vector containing both CPT1A and scramble shRNA for an acute infection with adenovirus, instead of clonally select cells infected by lentivirus.

2.2. Effect of ghrelin and etomoxir on gene expression in GT1-7

Firstly, we wanted to confirm the effect of ghrelin on CPT1A, CPT1C and AgRP transcripts with a physiological glucose concentration. In the three cases, ghrelin produces around of a 50% increase in their expression compared to basal levels in the hypothalamic cell line: CPT1A, 1.53 ± 0.10 -fold increase, $p=0.001$; CPT1C, 1.60 ± 0.09 -fold increase, $p=0.0002$; and AgRP, 1.47 ± 0.14 -fold increase, $p=0.01$. Interestingly, these effects are reverted when the neurons are co treated with CPT1A inhibitor etomoxir. We also measured HMGCS2 expression, key enzyme of ketone body formation, which can be used as an indirect marker of CPT1A activity. Its expression is increased due to ghrelin, which is reversed by etomoxir, as well (**Fig 34**).

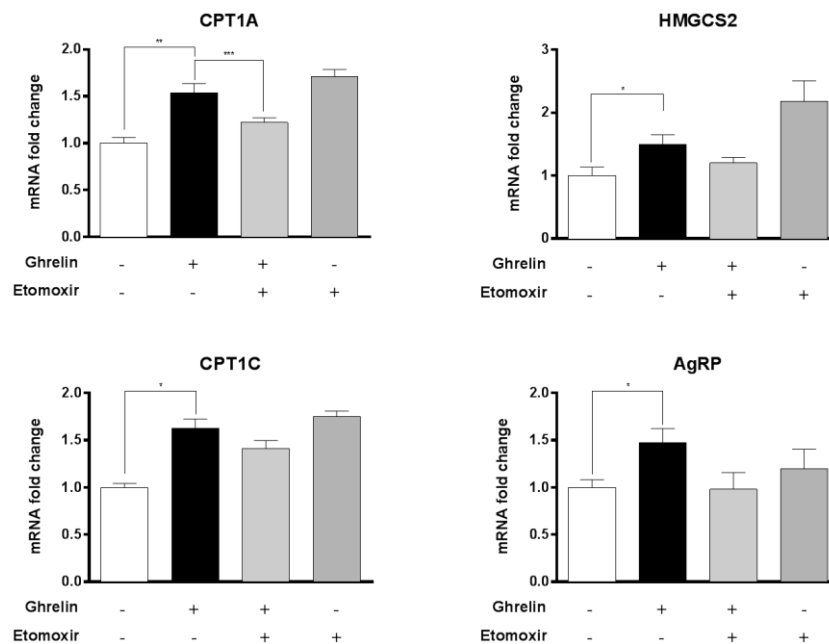


Fig 34. Analysis of mRNA levels of CPT1A, CPT1C, HMGCS2 and AgRP in GT1-7 cells after ghrelin treatment. Analysis performed by qRT-PCR. Error bars represent SEM, $n=4$. $p<0.05$.

Secondly, we analyzed whether ghrelin would affect to the expression of enzymes related to GABA metabolism and release. We observed that ghrelin produces an increase as well in the 3 enzymes controlling GABA pool in this hypothalamic neuronal line: GAD1, 1.56 ± 0.16 -fold increase, $p < 0.05$; GABAT, 1.64 ± 0.04 -fold increase, $p = 0.02$; SSADH, 1.50 ± 0.07 -fold increase, $p = 0.013$ (**Fig 35**). GAD2 and VGAT are not detectable in this cell line, which may suggest an impaired or at least incomplete GABA metabolic system.

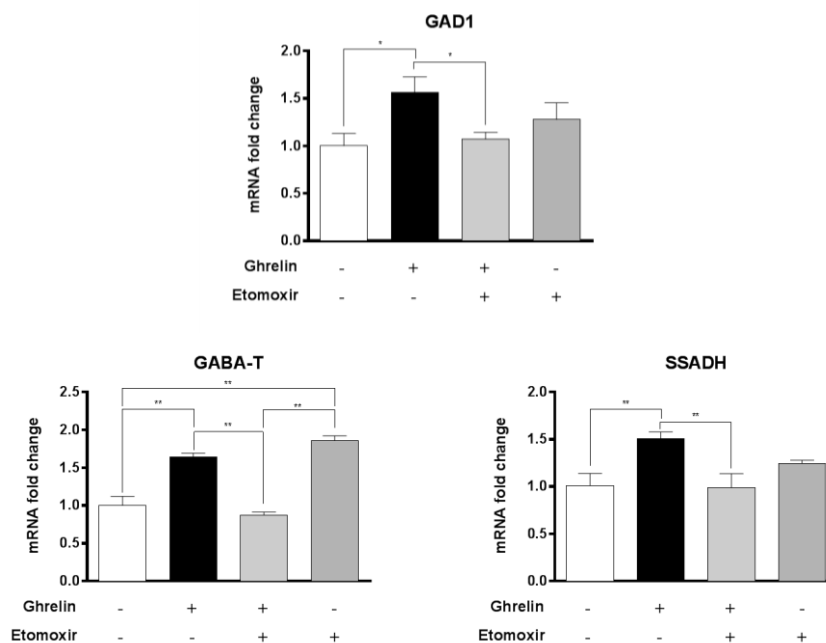


Fig 35. Analysis of mRNA levels of GAD1, GABAT and SSADH in GT1-7 cells after ghrelin treatment. Analysis performed by qRT-PCR. Error bars represent SEM, $n=4$. $p < 0.05$.

2.3. Effect of ghrelin on CPT1A activity and FAO in GT1-7

Since ghrelin induces AMPK phosphorylation in hypothalamus, this hormone putatively produces an increase of CPT1A activity due to a reduction of its physiological inhibitor, malonyl-CoA (Miguel López et al., 2008). To confirm that, we followed two approaches as a secondary measure of CPT1A activity in intact cells: we performed a fatty acid oxidation assay with hypothalamic GT1-7 neurons, and we measured the total acylcarnitines formed in the same cell line. A proper CPT1A assay with a mitochondria-enriched extract would not show changes due to malonyl-CoA, since its endogenous levels would be diluted during the purification process (Zammit & Arduini, 2008). We infected GT1-7 cells with 100 moi Ad-shCPT1A, or Ad-scramble

as control, and performed the assay with [¹⁴C]palmitic acid or we proceeded to extract the acylcarnitines pool from the cells.

We first measured the levels of acylcarnitines, we observed that ghrelin reduces the pool of acylcarnitines to a half ($p=0.00019$), which may imply a reduction in CPT1A activity. When CPT1A is genetically inhibited, we reach a reduction up to a half as well ($p=0.01$) of basal acylcarnitine levels. Surprisingly, when these CPT1A genetically inhibited neurons are treated with ghrelin, acylcarnitines have a 3-fold increase ($p=0.01$) (**Fig 36**).

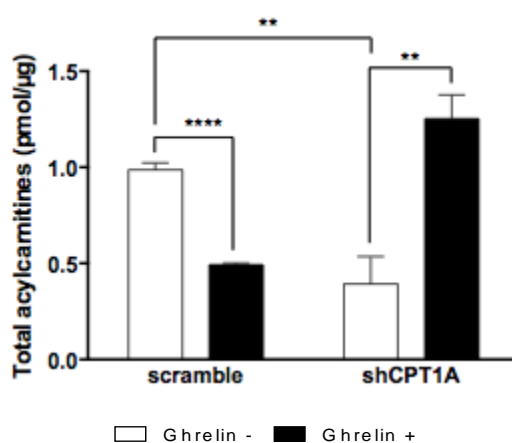


Fig 36. Analysis of acylcarnitines content as a measure for CPT1A activity after ghrelin treatment and CPT1A silencing. Error bars represent SEM, n=4. ** $p=0.01$ **** $p=0.0001$ in Student's T test. Two-way ANOVA Interaction**, CPT1A factor (ns), ghrelin factor (ns)

Moreover, when we measured carbon dioxide, produced from [¹⁴C]palmitic acid and the acid soluble products (ASP) formed from it, remaining in the media after stopping the 3 h reaction. The results showed there is a non-significant tendency to increase total carbon dioxide due to ghrelin ($p=0.08$) in control cells, but at the same time their acid soluble products (ASP) from [¹⁴C]palmitic acid are reduced to a 13% of ASP from control basal cells ($p<0.05$). Surprisingly, the genetic reduction in CPT1AM mRNA, blocks the effect of ghrelin on ASP, but not in carbon dioxide, whose increase due to ghrelin is significant. (**Fig 37**).

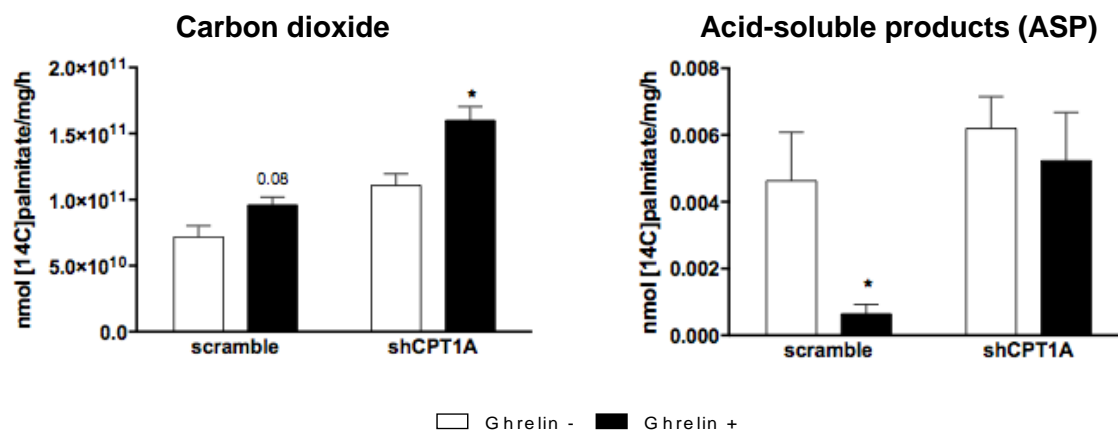


Fig 37. Analysis of FAO in GT1-7 after ghrelin treatment and CPT1A silencing. Error bars represent SEM, n=4. * $p < 0.05$ in Student's T test. Two-way ANOVA; CO₂= Interaction (ns), CPT1A factor ***, ghrelin factor **; Acid-soluble products (ASP)= Interaction (ns), CPT1A factor *, ghrelin factor (ns)

All this results seem to contradict the premise that, in hypothalamus *in vivo*, ghrelin provokes an increase of CPT1A activity due to a malonyl-CoA reduction, or at least the validity of GT1-7 as a model which faithfully reproduces hypothalamic ghrelin response.

2.4. Effect of ghrelin on mitochondrial respiration in GT1-7 cells

We wanted to assess the mitochondrial function through measuring the oxygen consumption rate (OCR) performing an extracellular flux analysis with an XF SeaHorse Analyzer. We wanted to do so, because we observed a drop in acid-soluble products of β -oxidation due to ghrelin and a reduction in acylcarnitines. These ASP are mostly related to mitochondria, which are in an 80% amino acids, such as glutamate and aspartate, and in a 20% organic acids, mainly citrate, when analyzed in brain mitochondrial extracts (Kawamura & Kishimoto, 1981). We set three different conditions to study the OCR in hypothalamic GT1-7 cells described as follows.

2.4.1. Oxygen consumption rate of GT1-7 cells at physiological glycorrachia

We wanted to analyze the effect of ghrelin on OCR in the closest conditions to physiology. Cells were pretreated with 5 mM glucose medium for 3h, to mimic physiological glucose levels in CSF, previous to perform the extracellular flux analysis. 100 nM ghrelin was added to half of the wells to assess its effect. Oligomycin and antimycin A were sequentially injected to measure mitochondrial, non-mitochondrial and ATP-linked OCR, as well as proton leak, taking into account basal initial OCR, and OCR after each drug injection, as explained in Experimental procedures 3.5. In this assay, ghrelin reduces the OCR along the whole experiment compared to basal OCR in GT1-7 cells. Consequently, mitochondrial, non-mitochondrial and ATP-linked OCR, as well as basal OCR and proton leak, are significantly reduced because of ghrelin effect (Fig 38).

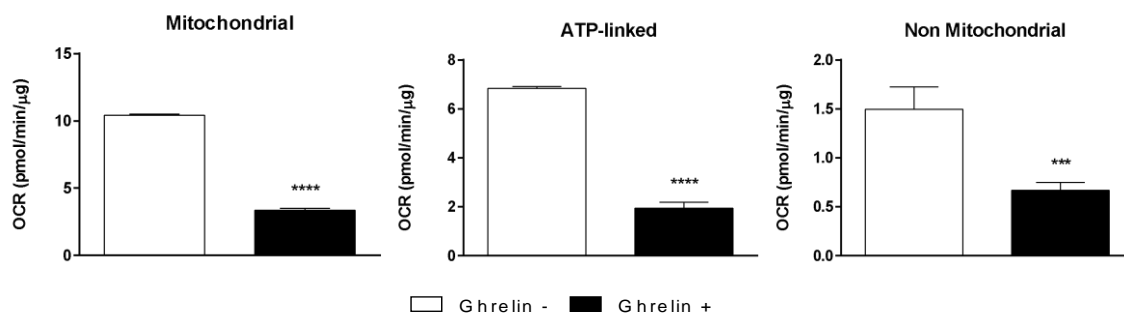


Fig 38. Analysis of mitochondrial, ATP-linked and non-mitochondrial OCR in GT1-7 neurons after ghrelin treatment. Error bars represent SEM, n=4. *** $p < 0.005$ **** $p < 0.001$

This mitochondrial function reduction due to ghrelin matches the previous results regarding fatty acid oxidation and acylcarnitines content, even though fatty acids are not the main source of carbon for ATP synthesis.

2.4.2. Oxygen consumption rate of GT1-7 cells using palmitate

We wanted to assess how changing substrate to fatty acids would affect to the response of GT1-7 to ghrelin. To this end, cells were pretreated with 5 mM glucose medium for 3h, to mimic physiological glucose levels in CSF, previous to perform the extracellular flux analysis. To the assay medium 100 nM ghrelin and/or 40 μg/mL etomoxir, a CPT1A inhibitor, was added to

the corresponding wells. All the wells contained the FAO reaction medium with BSA-conjugated palmitic acid. Oligomycin and antimycin A were sequentially injected to perform the measurements of OCR due to different subcellular elements. In this experiment, ghrelin reduced in basal state mitochondrial, ATP-linked and non-mitochondrial OCR. By inhibiting CPT1A with etomoxir, non-mitochondrial OCR drop as well, but it is noteworthy to point out significant increases in mitochondrial and ATP-linked OCR due to ghrelin (**Fig 39**).

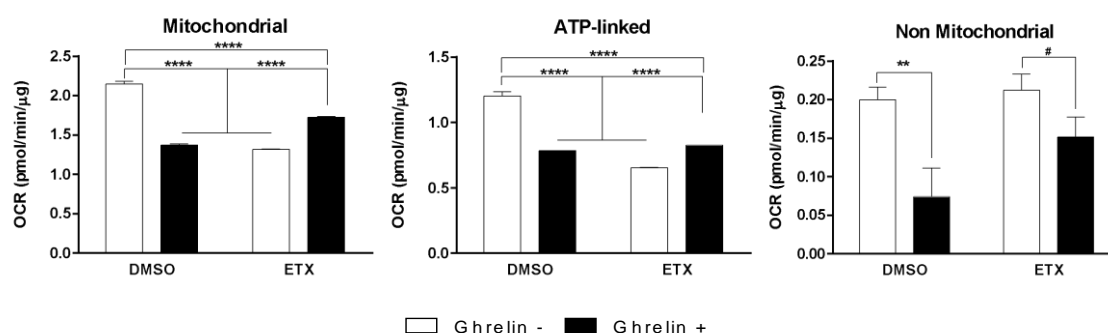


Fig 39. Analysis of mitochondrial, ATP-linked and non-mitochondrial OCR in GT1-7 neurons after ghrelin treatment and CPT1A pharmacological inhibition by etomoxir (ETX) in a palmitate rich medium. Error bars represent SEM, n=4. ** $p < 0.01$ **** $p < 0.0001$ in two-way ANOVA. # $p < 0.05$ in Student's T test.

These results are similar to the ones observed in fatty acid oxidation radiometric assay and acylcarnitines quantification, in which ghrelin effect is not only reversed but takes the opposite sign, increasing instead of decreasing mitochondrial activity due to ghrelin.

2.4.3. Oxygen consumption rate of GT1-7 cells with silenced CPT1A expression

In this experiment, we did not analyze ghrelin effect on OCR, but the effect on OCR of CPT1A genetic inhibition, depending on the substrate used (endogenous fatty acid and glucose or exogenous palmitic acid). Cells were infected with 100 moi Ad-shCPT1A (or Ad-scramble). On the day of the assay, they were pretreated with 5 mM glucose medium for 3h, to mimic physiological glucose levels in CSF, previous to perform the extracellular flux analysis. To the fatty acid oxidation reaction medium BSA-conjugated palmitic acid, or BSA as control, was added to the corresponding wells. Oligomycin and antimycin A were sequentially injected to perform the measurements of OCR due to different subcellular compartments. In this experiment, CPT1A inhibition by shRNA is primarily detected when cells are forced to use

palmitic acid as fuel, with a significant reduction of mitochondrial and ATP-linked OCR. Curiously, BSA-conjugated palmitic acid was able to reduce non mitochondrial OCR regardless the changes in CPT1A expression. In scramble-expressing cells, BSA-conjugated palmitic acid do not show any change in either mitochondrial or ATP-linked OCR (**Fig 40**).

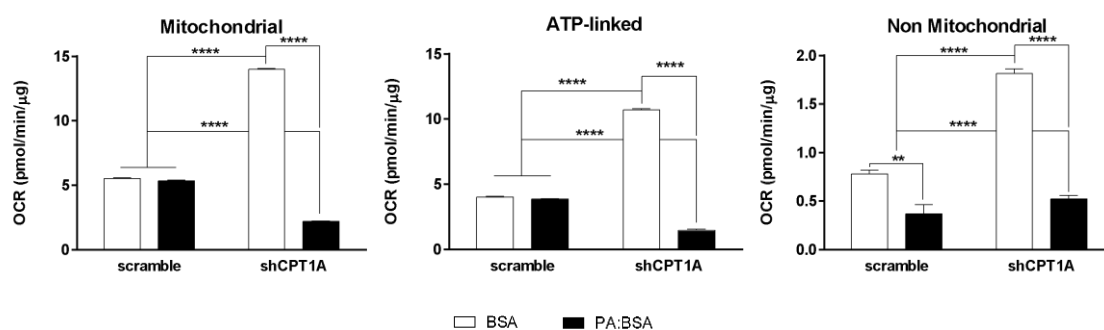


Fig 40. Analysis of mitochondrial, ATP-linked and non-mitochondrial OCR in GT1-7 neurons after CPT1A silencing in a palmitate rich medium. Analysis performed after 16h infection with adenovirus, Ad-scramble and Ad-shCPT1A. Error bars represent SEM, n=4. **** $p < 0.001$ in two-way ANOVA.

The complete set of results regarding mitochondrial function on GT1-7 with ghrelin seems to contradict the basic metabolic changes described in hypothalamic nuclei. Ghrelin does not increase CPT1A or fatty acid oxidation, but moreover it reduces mitochondrial function in hypothalamic GT1-7 cell line.

2.5. Effect of ghrelin on mitochondrial superoxide formation in GT1-7 cells

Ghrelin has been reported to mediate neuronal function by controlling reactive oxygen species formation (Z B Andrews et al., 2008). We wanted to assess if CPT1A would be involved in ROS generation, so we measured mitochondrial superoxide formation in GT1-7 cells treated with ghrelin and when CPT1A was genetically silenced. We observed that ghrelin significantly decreases superoxide formation in mitochondria upto a 61% of the basal levels (Student's T test, $p = 0.0009$). Moreover, this effect was blunted with a significant interaction in GT1-7 neurons infected with Ad-shCPT1A (Two-way ANOVA, $p = 0.0009$) (**Fig 41**).

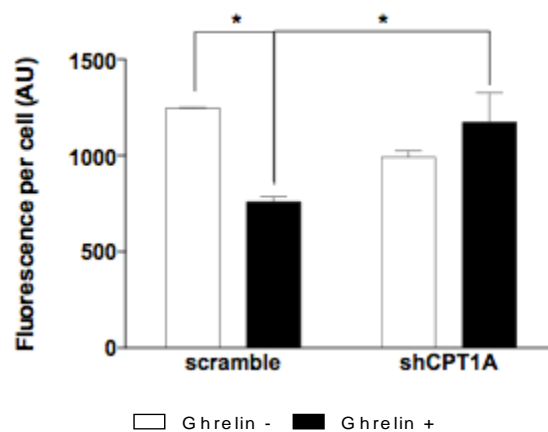


Fig 41. Analysis of superoxide formation in GT1-7 neurons after ghrelin treatment and CPT1A silencing. Superoxide formation measured by MitoSOX derived fluorescence in GT1-7 cells after 16h infection with adenovirus Ad-scramble and Ad-shCPT1A. Error bars represent SEM, n=4. Interaction $p < 0.001$ in two-way ANOVA.

The initial premise that ROS reduction is due to an increase UCP2 in whole hypothalamus should be argued extensively, taking into account our results in hypothalamic GT1-7 neuronal line. Ghrelin seems to produce an overall reduction of mitochondrial activity, promoting a reduction in CPT1A activity, in fatty acid oxidation, in ATP formation and presumably in tricarboxylic acid cycle. In this case, the reduction of ROS formation due to ghrelin would appear due to the reduction in mitochondrial processes, but not because of an increase in ROS-buffering mechanisms.

2.6. Effect of ghrelin on amino acid neurotransmitters in GT1-7 cells

We assessed the integrity of amino acid neurotransmission by performing an amino acid neurotransmitters release assay with hypothalamic GT1-7 neurons. We hypothesize that the overall reduction in mitochondrial capacity would eventually affect the pool of tricarboxylic acid cycle intermediates, which through α -ketoglutarate and/or succinic acid could form GABA eventually and effect to the GABA pool to be release.

We took advantage of the release assay to analyze if ghrelin produced any change in neurotransmitters release depending on CPT1A, by treating the cells with ghrelin and etomoxir in the previously explained fashion. We observed that hypothalamic cell lines do not respond to depolarizing stimulus (90 mM KCl), with unchanged levels of GABA and glutamate, regardless the treatments and membrane polarization state (Data not shown).

We assessed as well GABAT activity, using the methodology described on Experimental procedures 3.4, and we observed that GT1-7 cells have negligible activity (Data not shown), at least not detectable with the methodology used.

All the results found led us to wonder whether ghrelin inhibits CPT1A instead of activating it, at least in this GT1-7 cell line. AMPK phosphorylation due to ghrelin has been thoroughly described in hypothalamus (Miguel López et al., 2008). This would eventually activate CPT1A activity in hypothalamic nuclei, although this effect due to a malonyl-CoA reduction would be uneasy to confirm with a classical radiometric assay (Zammit & Arduini, 2008). Moreover, GABA output has been described to be increased due fasting in hypothalamic arcuate GABA neurons, promoting hyperphagia (Dicken et al., 2015). Since GT1-7 is not a good model to evaluate GABAergic response changes due to ghrelin, we opt to approach to ghrelin effect in other neurons which are responsive to ghrelin.

PART 3. Study of the role of CPT1AM as a downstream effector of ghrelin in primary cortical neurons

Ghrelin has been described to have neuroprotective effects and GHSR activation mediates in neurite formation in cortical neurons (Mani et al., 2014; Stoyanova, le Feber, & Rutten, 2013). To this end, we wanted to assess the effect of ghrelin on cortical neurons, both *in vivo* and *in vitro*, on fatty acid oxidation and on GABA metabolism and release. Furthermore, we hypothesize differential effects of ghrelin depending on neuronal type and region.

3.1. Effect of intraperitoneal ghrelin on food intake

In order to analyze the effects of ghrelin in several cortical parameters, we injected two doses of 10 μg ghrelin (or the equivalent volume of phosphate-buffered solution, *i.e.* 300 μL) intraperitoneally (IP) every 30 min (Sun et al., 2004) and monitored their food intake for 1 h in mice which had been food-deprived for 2 hours after the dark period. The food intake in PBS-injected mice was almost negligible (0.0025 ± 0.0025 g/mice/h), while the average food intake in ghrelin-injected mice was significantly higher compared to control mice (0.0333 ± 0.012 g/mice/h, $p < 0.045$) (Fig 42).

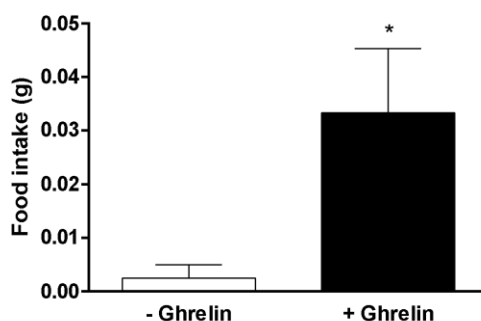


Fig 42. Analysis of food intake after an acute intraperitoneal ghrelin bolus. Two IP ghrelin (or PBS) bolus were injected with 30 min difference and food was monitored for 1h. Error bars represent SEM, $n=3-4$, $p=0.0045$.

This data validated ghrelin central effects to study further details of ghrelin effect on cerebral cortex.

3.2. Effect of intraperitoneal ghrelin on cortical acylcarnitines

We wanted to assess whether intraperitoneal ghrelin actually increased CPT1A activity in cortex and in whole hypothalamus. To this end, we analyzed the levels of long-chain acylcarnitines, as direct products of CPT1A activity, in cortical and hypothalamic dissections. To this end, mice were sacrificed at 1 h after ghrelin or PBS injection, they had their brain tissues dissected and lipids specifically extracted and analyzed as previously explained. Surprisingly, ghrelin has a region specific effect on CPT1A activity. Cortex and hypothalamus have similar basal levels of total acylcarnitines (4.03 pmol/ μ g and 5.30 pmol/ μ g, respectively), but when treated with ghrelin, cortical acylcarnitines drop to a 48% (1.97 pmol/ μ g, $p=0.034$) and hypothalamic pool increases 3-fold (15.50 pmol/ μ g, $p=0.003$) (Fig 43)

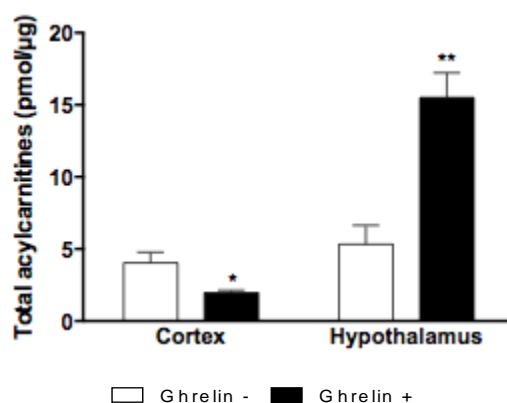


Fig 43. Analysis of cortical and hypothalamic acylcarnitine levels as a measure of CPT1A activity after an intraperitoneal ghrelin bolus. Two IP ghrelin (or PBS) bolus were injected with 30 min difference and samples were obtained at that time to be analyzed. White bars, PBS-treated mice, and black bars, ghrelin-treated mice. Error bars represent SEM, n=4.

3.3. Effect of intraperitoneal ghrelin on cortical GABA metabolism

We evaluated the effects of IP ghrelin on cortical mRNA levels of different genes related to lipid, carnitine and amino acid neurotransmitter metabolism. Both isoforms CPT1A and CPT1C have been extensively described to have upregulated mRNA levels in mediobasal hypothalamus due to ghrelin treatment after 2 h, as well as increased activity due to malonyl-CoA reduction (Miguel López et al., 2008; Ramírez et al., 2013). We found that at 1 h after ghrelin injection CPT1A mRNA levels remains unchanged, but CPT1C mRNA is reduced 20% compared to basal ($p=0.0007$), as well as carnitine acetyltransferase (CrAT) in 24.5% ($p=0.001$) and carnitine octanoyltransferase (COT) in 14.6% ($p=0.04$) (Fig 44).

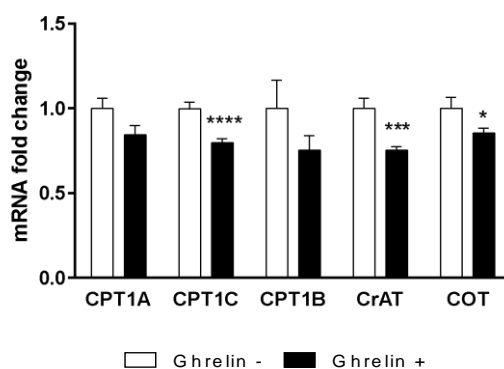


Fig 44. Analysis of cortical mRNA levels of different carnitine acyltransferases after an intraperitoneal ghrelin bolus. Two IP ghrelin (or PBS) bolus were injected with 30 min difference and samples were obtained at that time to be analyzed by qRT-PCR. White bars, PBS-treated mice, and black bars, ghrelin-treated mice. Error bars represent SEM, n=3-4, **** $p=0.0007$, *** $p=0.001$, * $p=0.04$.

We evaluated the cortical effects of ghrelin on FAS and ACC mRNA levels, from lipid anabolism, and HMGCS2, related to ketone body formation, and mitochondrial biogenic, PGC1 α (Fig 45).

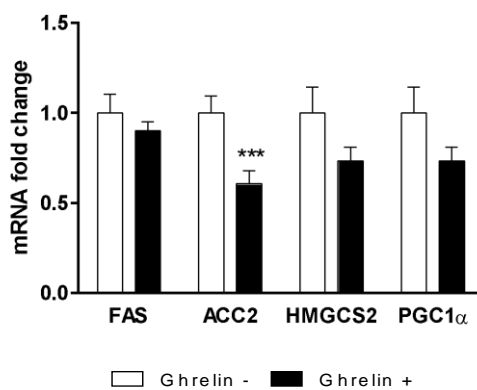


Fig 45. Analysis of cortical mRNA levels of enzymes involved in lipid and ketone bodies metabolism and mitochondrial biogenesis markers after an intraperitoneal ghrelin bolus. Two IP ghrelin (or PBS) bolus were injected with 30 min difference and samples were obtained at that time to be analyzed by qRT-PCR. White bars, PBS-treated mice, and black bars, ghrelin-treated mice. Error bars represent SEM, n=3-4, *** $p=0.007$.

Surprisingly, ACC2 is the only aforementioned gene to be significantly reduced (39.2% reduction, $p=0.007$) in cortex from ghrelin-treated mice. If this reduction is sustained, it would lead to reduced ACC2 protein levels and eventually reduced malonyl-CoA and increased CPT1A activity, which however would happen at the long term, making it compatible with the sudden reduced acetylcarnitine levels in cortex due to intraperitoneal ghrelin injection.

Since the overexpression of CPT1AM in MBH, which is a putative downstream effector of ghrelin, showed changes in the mRNA levels pattern of glutamate and GABA vesicular transporters, we evaluated the effect of ghrelin on their vesicular transporters and metabolic enzymes. Only VGLUT3 shows a 35.3% reduction ($p=0.01$), there are no changes in neocortical VGLUT1 and a non-significant tendency to reduced thalamocortical VGLUT2 ($p=0.057$). VGLUT3 mRNA levels is clustered in different brain regions and in cortex it is often associated to GABAergic neurons among others (Herzog et al., 2004; Liguz-Leczna & Skangiel-Kramska, 2007). When it comes to GABA, vesicular GABA transporter (VGAT) mRNA levels is reduced in 26.8% ($p=0.01$). Moreover, both glutamic acid decarboxylase (GAD) 1 and GAD2, which are responsible for generating GABA from glutamate, have their mRNA levels significantly reduced (in 20.9% $p=0.005$ and in 25.7% $p=0.01$, respectively). Furthermore, GABA transaminase (GABAT) is also reduced in 18.9% ($p=0.04$). GABAT is part of an alternative GABA generating pathway, known as GABA shunt, responsible of GABA synthesis from succinic acid, together with semialdehyde succinic acid dehydrogenase (SSADH), which shows a non-significant tendency to be reduced in cortex ($p=0.07$) (Fig 46).

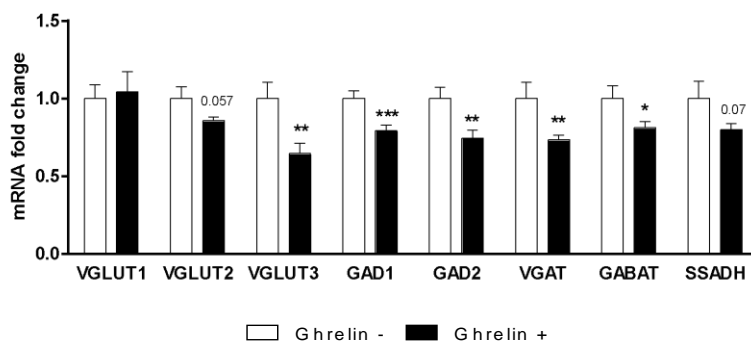


Fig 46. Analysis of cortical mRNA levels of amino acid neurotransmitters metabolic enzymes and vesicular transporters after an intraperitoneal ghrelin bolus. Two IP ghrelin (or PBS) bolus were injected with 30 min difference and samples were obtained at that time to be analyzed by qRT-PCR. White bars, PBS-treated mice, and black bars, ghrelin-treated mice. Error bars represent SEM, $n=3-4$, * $p=0.04$, ** $p=0.01$ *** $p=0.005$.

We measured GABAT activity in cortical samples obtained from PBS- and ghrelin-injected mice using the methodology explained in Experimental procedures 3.4. We observed that the subtle reduction in GABAT mRNA was accompanied with an evident reduction in GABAT activity to around 16% of basal activity ($p=0.01$), due to ghrelin (Fig 47).

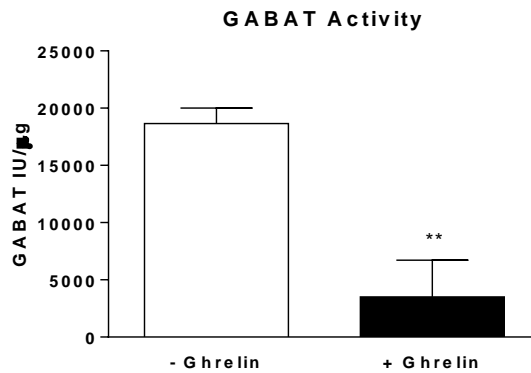


Fig 47. Analysis of cortical GABAT activity after an intraperitoneal ghrelin bolus. Two IP ghrelin (or PBS) bolus were injected with 30 min difference and samples were obtained at that time to be analyzed. White bars, PBS-treated mice, and black bars, ghrelin-treated mice. Error bars represent SEM, n=3-4, ** $p=0.01$

All these results suggest that ghrelin is modulating the cortical gene expression of enzymes and transporters of GABA metabolism enzymes and vesicular transporters. This modulation may be involved in behavioral effects of ghrelin in cortex.

3.4. Appraisal of primary cortical neuronal cultures as a GABAergic ghrelin-responsive model

Since ghrelin showed effects in cortical tissue *in vivo*, we decided to discern the mechanism involved in its effect on mitochondrial function and GABA metabolism and release. We decided to evaluate whether ghrelin has some effect on primary cortical neurons, because they have been described to contain GSHR, *i.e.* ghrelin receptor (Mani et al., 2014), and when cultured, ghrelin affects to synaptic growth (Stoyanova et al., 2013).

We learnt the procedure to obtain the embryonic primary cortical cultures from the Dr. Suñol's group and managed to replicate it in our laboratory, following their protocol described elsewhere in this typescript (Solà et al., 2011). This procedure, allows obtaining mature and functional neurons, keeping non-neuronal cells in the culture up to 2-5% approximately. The viability and complete physiological function starts at 5 days *in vitro* (DIV) and they have been viable in our hands up to 16 DIV, but some authors even state that primary cortical neuronal cultures are viable until 60 DIV (Lesuisse & Martin, 2002). The morphology and growth of the cultures was correct and similar from one culture to another with a confluence of $8 \cdot 10^5$ cells per well in 6-well plates (**Fig 48**).

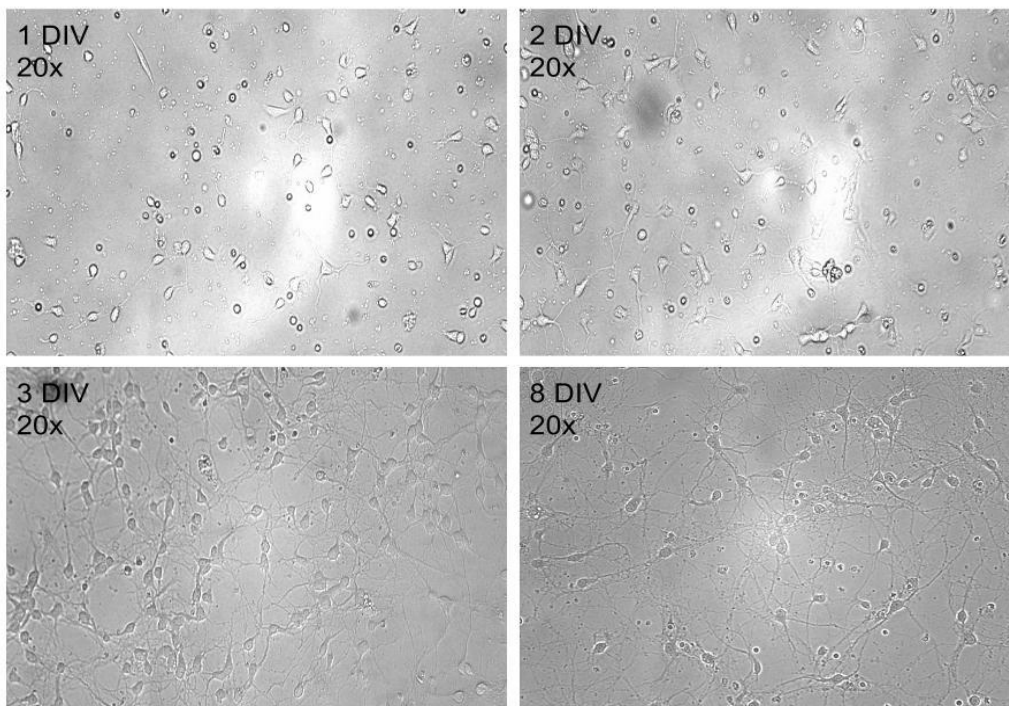


Fig 48. Representative micrographs at 20 x in phase-contrast microscope of primary cortical neuronal cultures at 1 day *in vitro* (DIV), 2 DIV, 3 DIV and 8 DIV.

Every experiment performed to pursue this work has been performed in primary cortical neurons cultured up to 8 DIV. When adenoviral infection was needed, they were infected at 6 DIV to have the maximum expression on 8 DIV to perform the experiments.

We first assessed whether ghrelin would affect to amino acid neurotransmitter release, when the neurons were pretreated for 3 h at different glucose concentrations: 25 mM glucose, which is the basal culture medium concentration; 5 mM glucose, which is similar to physiological glycorrachia; and in total glucose depletion. We observed, that released GABA at depolarizing 90 mM KCl is significantly reduced upto a 55% compared to 5 mM KCl in ghrelin-treated neurons at physiological glucose levels and in glucose-depleted medium (**Fig 49**). Moreover, basal depolarized levels of released GABA are 4-fold higher at 5 mM glucose, compared to those at 0 and 25 mM glucose. Cortical neurons present both GABAergic and glutamatergic types. In the conditions assayed, glutamate was reduced due to ghrelin only in glucose-depleted medium (data not shown). We assessed if there would be changes in GABA release in a purely glutamatergic culture such as cerebellar granular neurons and no changes were produced (data not shown). Due to this and the fact that glutamate related genes in GT1-7 remained unchanged, we decided to go on studying the effects on GABA metabolism in primary cortical neurons.

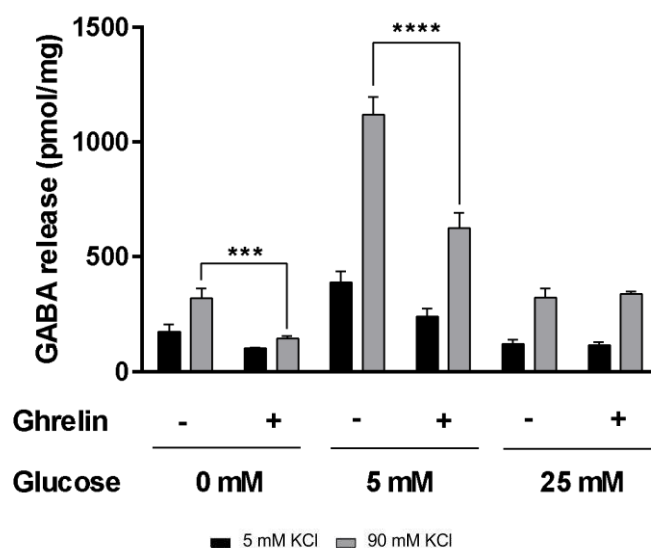


Fig 49. Analysis of GABA release in 8 DIV cortical neurons after ghrelin treatment. GABA release at 5 mM and 90 mM KCl in primary cortical neurons pretreated with 0 mM, 5 mM and 25 mM glucose treated with 100 nM ghrelin. Error bars represent SEM. Student's T test *** $p < 0.005$ **** $p < 0.001$.

We analyzed if this ghrelin effect could be blunted by inhibiting CPT1A. To this end we added etomoxir to block CPT1A activity. We observed that in the presence of 40 $\mu\text{g}/\text{mL}$ etomoxir, the

reduction of GABA release due to 100 nM ghrelin is blunted when co-treated for 30 min (**Fig 50**).

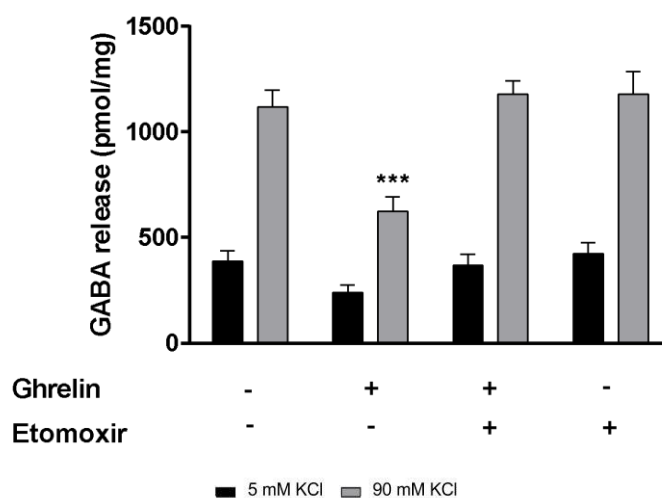


Fig 50. Analysis of GABA release in 8 DIV cortical neurons after ghrelin and etomoxir treatment. GABA release at 5 mM and 90 mM KCl in primary cortical neurons pretreated with 5 mM glucose treated with 100 nM ghrelin and/or 40 µg/mL for 30 min. Error bars represent SEM. Student's T test *** $p < 0.005$ **** $p < 0.001$.

3.5. Effect of ghrelin on gene expression in primary cortical neurons

We wanted to confirm if there is any effect of ghrelin on CPT1A, CPT1C, HMGCS2 and VGAT mRNA levels in primary cortical neurons. We found that CPT1A, CPT1C and VGAT are upregulated when co-treated with ghrelin for 30 min: CPT1A has 1.38 ± 0.14 -fold increase; CPT1C, 1.29 ± 0.08 -fold increase; and VGAT, 1.35 ± 0.07 -fold increase ($p < 0.01$, in all cases). Moreover, when co-treated with ghrelin and etomoxir for 30 min, neurons have an even higher increase in their transcripts: CPT1A has 1.45 ± 0.04 -fold increase; CPT1C, 1.47 ± 0.06 -fold increase; and VGAT, 1.43 ± 0.09 -fold increase ($p < 0.01$, in all cases). When it comes to HMGCS2, there is a 1.47 ± 0.08 -fold increase ($p < 0.01$), but no changes when CPT1A is pharmacologically inhibited (**Fig 51**).

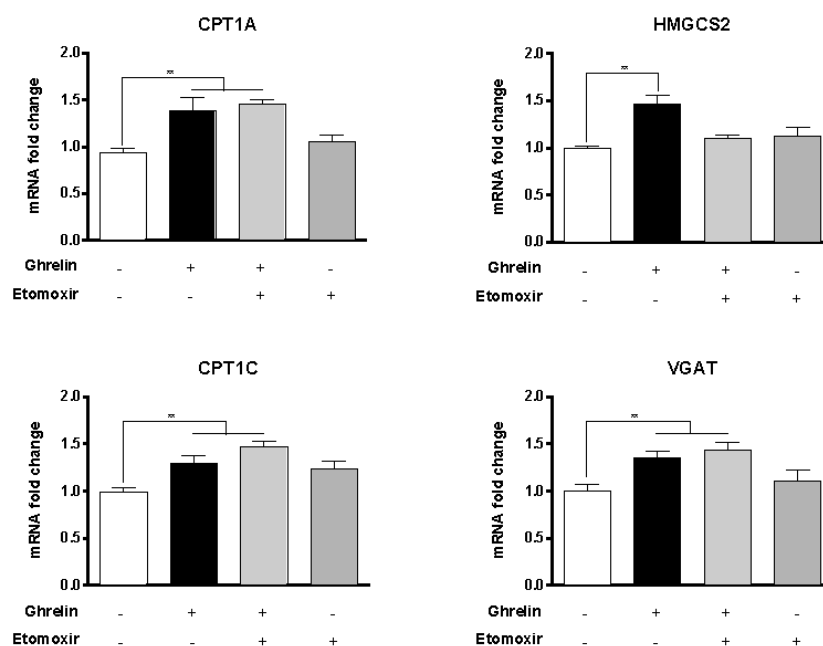


Fig 51. Analysis of mRNA levels of CPT1A, CPT1C, HMGCS2 and VGAT in 8 DIV cortical neurons after ghrelin and etomoxir treatment. Analysis performed by qRT-PCR from samples of primary cortical neurons pretreated with 5 mM glucose medium for 3h and 20 min of 100 nM ghrelin and/or 40 µg/mL etomoxir. Error bars represent SEM, n=4. ** $p<0.01$.

Secondly, we studied whether ghrelin would affect to the expression of enzymes related to GABA metabolism and release. We observed that ghrelin produces an increase in 2 of the enzymes controlling GABA pool in the primary cortical neurons, like we observed in GT1-7: GAD1, 1.19 ± 0.06 -fold increase ($p<0.01$) and SSADH, 1.26 ± 0.09 -fold increase, $p=0.03$ (**Fig. 42**). GAD2 was unchanged due to ghrelin, but when combined with etomoxir, produces a 1.25 ± 0.07 -fold increase ($p=0.02$). Nonetheless, the changes in GAD1 and SSADH due to ghrelin were not reversed by etomoxir, but even higher: GAD1, 1.31 ± 0.08 -fold increase ($p<0.01$) and SSADH, 1.32 ± 0.12 -fold increase ($p=0.04$) (**Fig 52**).

All these results suggest that ghrelin produces changes in primary cortical neurons which eventually can affect GABAergic neurons function. Amongst others, ghrelin reduced GABA release in depolarizing conditions. This effect is blunted by etomoxir, which suggests that CPT1A, its pharmacological target, may be mediating this effect. Moreover, ghrelin shows a clear effect on the modulation of many of the genes implicated in the control of releasable GABA pool.

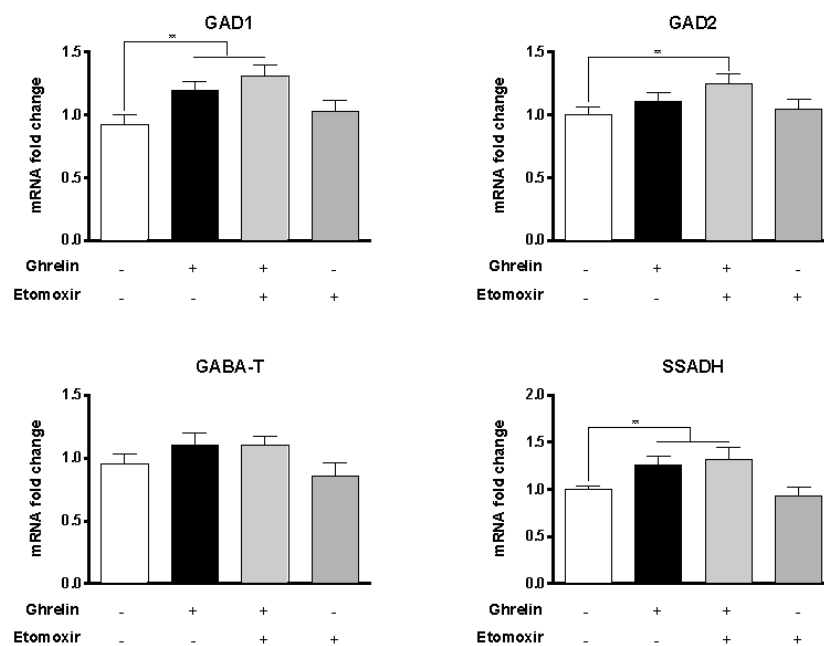


Fig 52. Analysis of mRNA levels of GAD1 and GAD2 and GABA shunt genes in 8 DIV cortical neurons after ghrelin and etomoxir treatment. Analysis performed by qRT-PCR from samples of primary cortical neurons pretreated with 5 mM glucose medium for 3h and 20 min of ghrelin and/or etomoxir. Error bars represent SEM, n=4. ** $p < 0.01$.

3.6. Effect of CPT1AM overexpression on mRNA expression in primary cortical neurons

The hypotheses regarding CPT1A as a downstream effector of ghrelin are based in the putative activation of CPT1A due to a reduction in malonyl-CoA produced by ghrelin (Z B Andrews et al., 2008; Miguel López et al., 2008). We first assessed whether overexpression of a permanently active CPT1A would trigger the same transcriptional changes observed due to ghrelin. To this end we performed a time course experiment, infecting with 100 moi Ad-CPT1AM (or Ad-GFP) to have at 8 DIV, 12h, 24h or 48h of infection, with a 3h 5 mM glucose pretreatment after mRNA sample collection. We observe that with a 24 h infection the transcriptional pattern is similar to that observed due to ghrelin effect. With a 149-fold increase in CPT1A mRNA levels (both endogenous and CPT1AM) ($p=0.01$), we observe a 2-fold increase in HMGCS2 transcript ($p=0.002$) and a non-significant tendency for CPT1C to increase (1.45-fold, $p=0.19$) (Fig 53).

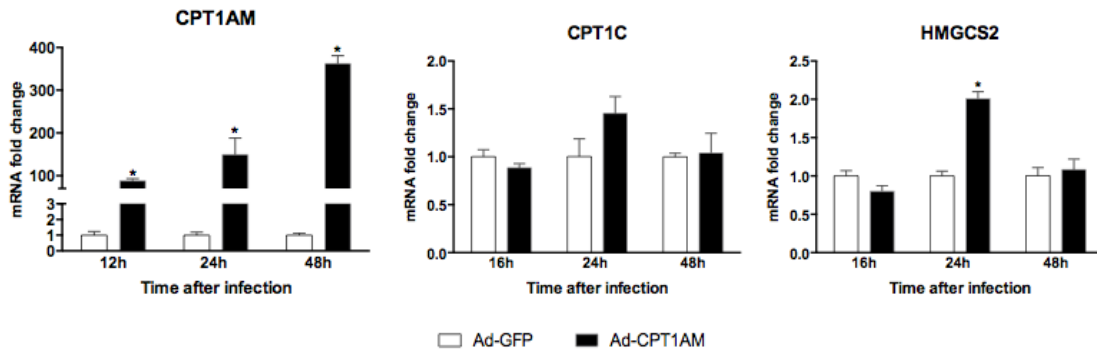


Fig 53. Time course analysis of mRNA levels of CPT1A, CPT1C and HMGCS2 in 8 DIV cortical neurons after CPT1AM overexpression. Effect of CPT1AM overexpression at 12 h, 24 h and 48 h infection on mRNA levels of total CPT1A, CPT1C and HMGCS2 in primary cortical neurons pretreated with 5 mM glucose medium for 3h. Error bars represent SEM, n=4. $p < 0.01$.

When it comes to vesicular amino acid neurotransmitter transporters, we observe a 1.5-fold increase in VGAT at 24 h ($p < 0.03$) (**Fig. 54**), similar to that observed when treated with ghrelin (**Fig. 41**). Moreover, at 12 h, both VGAT and VGLUT are slightly but significantly reduced to around 80% of basal ($p < 0.05$); and at 48 h, both VGLUT1 and VGLUT3 are significantly increased, around 15-fold and 70-fold respectively.

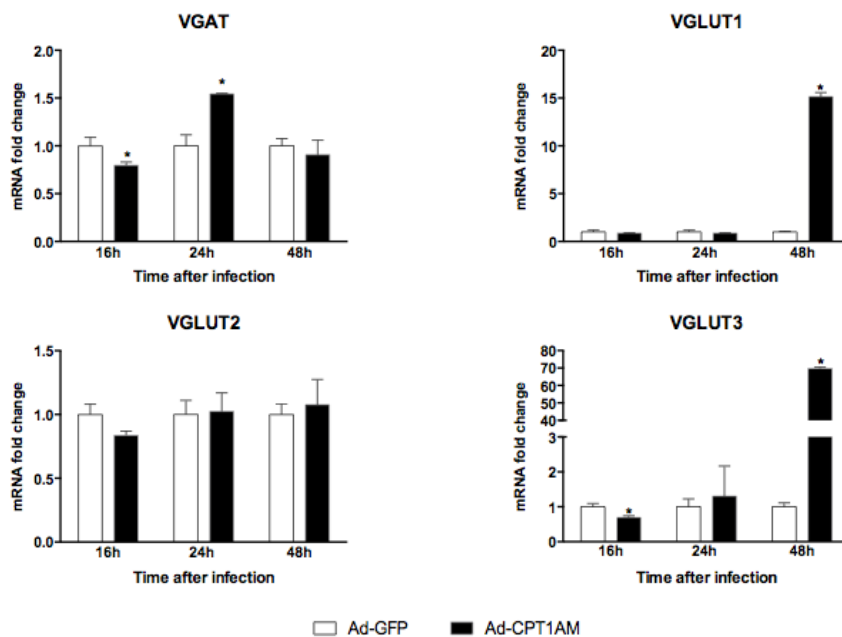


Fig 54. Time course analysis of mRNA levels of vesicular neurotransmitter transporters in 8 DIV cortical neurons after CPT1AM overexpression. Analysis performed by qRT-PCR to assess the effect of CPT1AM overexpression at 12 h, 24 h and 48 h infection on mRNA levels of vesicular amino acid neurotransmitter transporters in primary cortical neurons pretreated with 5 mM glucose medium for 3h. Error bars represent SEM, n=4. $p < 0.05$.

We further assessed if there was glucose dependence to this effect, so we infected primary cortical neurons at 7 DIV with 100 moi Ad-CPT1AM and Ad-GFP for 24h. At 8DIV, cells were treated with 5 mM and 25 mM glucose for 3 h to mimic physiological and culture glucose concentrations. CPT1AM overexpression reached around a 200-fold increase, which promotes a 1.75-fold increase in HMGCS2 and 1.4-fold increase in VGAT (Two-way ANOVA, $p < 0.05$). When treated in a high glucose medium, VGAT was significantly reduced to a 78% of mRNA in its GFP control (Student's T test, $p < 0.05$) (Fig 55).

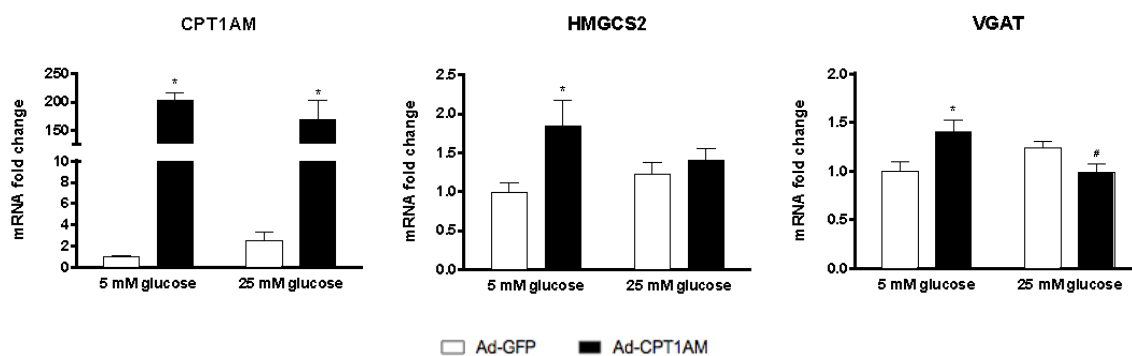


Fig 55. Analysis of mRNA levels of CPT11A, HMGCS2 and VGAT in 8 DIV cortical neurons after CPT1AM overexpression in different glucose concentrations. Analysis performed by qRT-PCR from samples obtained after 24h infection, 8 DIV. Error bars represent SEM, n=4. *Two-way ANOVA $p < 0.05$. #Student's T test $p < 0.05$.

We decided to assess this condition also in transcripts of GABA metabolic enzymes: glutamic acid deaminases and GABA shunt genes. Both GAD1 and GAD2 are increased at 5 mM glucose when CPT1AM is overexpressed in 1.26- and 1.35-fold increase, respectively (Two-way ANOVA, $p < 0.05$) (Fig 56).

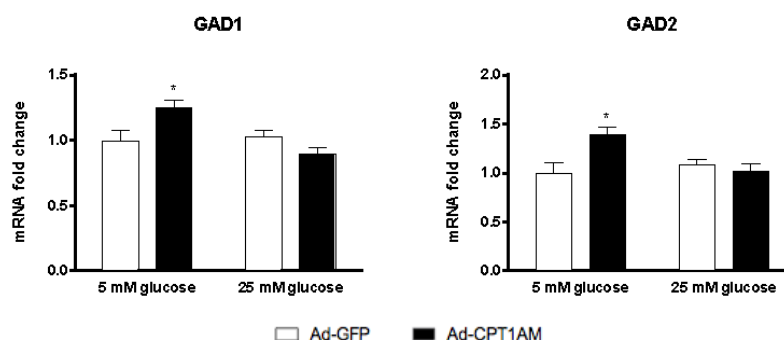


Fig 56. Analysis of mRNA levels of glutamic acid decarboxylase isoforms in 8 DIV cortical neurons after CPT1AM overexpression in different glucose concentrations. Analysis performed by qRT-PCR from samples obtained after 24h infection,, 8 DIV. Error bars represent SEM, n=4. *Two-way ANOVA $p < 0.05$.

In GABA shunt enzymes, there is a 1.30-fold increase in both, GABAT (Two-way ANOVA, $p<0.05$) and SSADH (Student's T test, $p<0.05$). Surprisingly, CPT1AM overexpression produces a reduction to 80% of its basal GFP control, in a 25 mM glucose medium (Two-way ANOVA, $p<0.05$) (Fig 57).

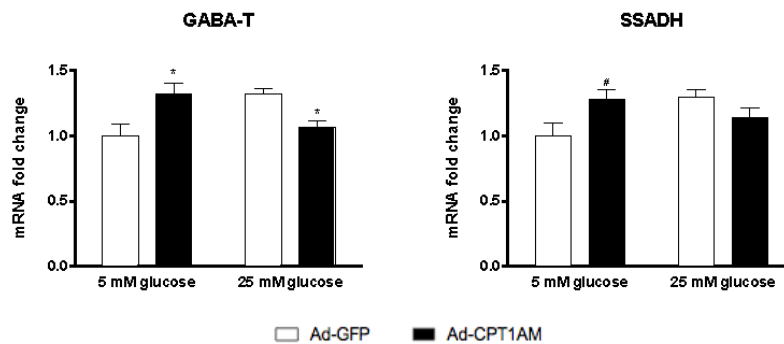


Fig 57. Analysis of mRNA levels of GABA shunt genes in 8 DIV cortical neurons after CPT1AM overexpression in different glucose concentrations. Analysis performed with samples obtained after 24h infection, 8 DIV. Error bars represent SEM, n=4. *Two-way ANOVA $p<0.05$. #Student's T test $p<0.05$.

These results show the ability of CPT1A to modulate the expression of different genes involved in GABA metabolism and the dependence on the glucose metabolic state of the system.

3.7. Effect of CPT1AM on GABA release in primary cortical neurons

To assess the impact of these changes found in mRNA expression in GABA release, we performed an amino acid neurotransmitter release assay. In this case, overexpression of CPT1AM in primary cortical neurons at 5 mM glucose does not promote any change in the pool of GABA to be released, nor in glutamate (Data not shown). Contrarily, CPT1AM overexpression promotes a 1.2-fold increase in GABA release, when the cells are kept in a high-glucose maintenance medium (25 mM) (Fig 58).

All these results suggest that CPT1A modulation is one of the upstream elements involved in changes in GABA release, but other factors, including substrate availability, cell typology and anatomical cell distribution may affect the actual GABA output. Since CPT1AM overexpression is not able to mimic ghrelin effect on GABA output, but contrarily when overexpressed at 25 mM glucose produces an increase in GABA, we suggest other mechanisms involved. Moreover, the net effect seems to include a reduction of CPT1A activity in cortical brain. To this end, we propose the use of primary cortical cultures, whose CPT1A has been completely genetically deleted to assess the involvement of CPT1A in the effect of ghrelin on GABA release and metabolism.

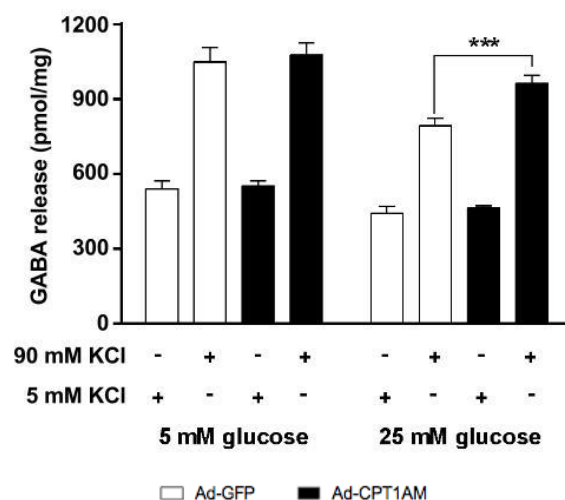


Fig 58. Analysis of GABA release in 8 DIV cortical neurons overexpressing CPT1A in different glucose concentrations Error bars represent SEM. Student's T test *** $p < 0.005$.

3.8. Genotyping of potentially conditional CPT1A knockout mice

Instead of infecting primary neurons with adenovirus expressing short hairpins to silence CPT1A, we decided to eliminate completely CPT1A to avoid any compensatory expression of the gene. To this end, we needed to generate CPT1A^(loxP/loxP) mice from whose embryos we could obtain primary cortical neurons. We opted to follow a strategy starting from a potentially conditional CPT1A knockout mice. We took advantage of two clones from the European Conditional Mouse Mutagenesis (EUCOMM) program. We obtained two heterozygous clones from the cell repository, whose reference numbers are HEPD0727_3_H09 and HEPD0727_3_E10, which have a potentially conditional knockout for CPT1A. In both cases, they had been obtained by homologous recombination, in a construct in which the 5' homology arm includes the area around exon 3 and the 3' homology arm, the area around exon 5 (Fig. 59).

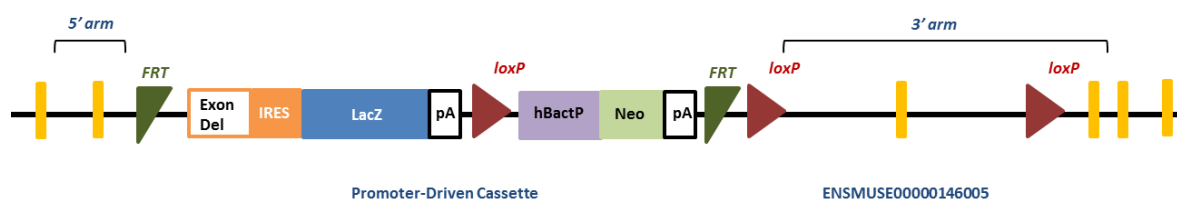


Fig. 59. Scheme of the construction present in CPT1A^{fl} mice. FRT: Target sequence for FLP recombinase; Exon Del: Internal Exon Deletion which blocks wildtype CPT1A translation; IRES: Internal ribosome entry site; LACZ: β -galactosidase gene; pA: Polyadenylation sequence; loxP: Target sequence for CRE recombinase; hBactP: Human β -actin promoter; NEO: Neomycin resistance gene.

In any case, exon 4 is flanked by two loxP regions in what has been called the critical region in the construct. Upstream this area, the construct includes a FRT-flanked region which contains a NEO gene as well as a LACZ gene, for clone selection. In the latter, it is separated with an IRES region from an alternative deletion Exon Del, which truncates the expression of wild type CPT1A from this allele, unless it is processed by a FLP recombinase, also known as flipase. The deletion of the FRT-flanked region makes the allele to regain CPT1A expression, but in a conditional knockout manner, depending on CRE recombinase activity to lose its function again.

The two embryonic stem cells containing a CPT1A^{tm1a(EUCOMM)Hmgu} (simplified as CPT1A^{frt}) allele from the parental cell line JM8A3.N1 were sent to the *Centre de Biotecnologia Animal i Teràpia Gènica* (CBATEG) at the *Universitat Autònoma de Barcelona* to go on with the chimeric mice generation.

At CBATEG, karyotype and morphology studies were performed in growing stem cells to assess the fittest clone to be injected (**Table 4**). The clone HEPD0727_3_H09 was the chosen one to be microinjected to obtain the chimeric mice. Its parental cell line JM8A3.N1 confers a agouti-fur phenotype, so this clone was injected into black-fur phenotype C57BL/6J.Ola.Hsd blastocyst, which would produce chimeric mice with agouti upon black background.

<i>Clone</i>	<i>Euploidy</i>	<i>Growth</i>	<i>Morphology</i>
HEPD0727_3_H09	92%	Good	Good
HEPD0727_3_E10	85%	Good	Good

Table 4. Karyotype and morphology evaluation of CPT1A^{frt} clones from EUCOMM

These injected blastocysts were transferred into foster mothers, which gave birth to 8 chimerae (**Table 5**). They were shipped to the *Unitat d'Experimentació Animal* Facilities of the *Universitat de Barcelona* School of Pharmacy and Food Sciences where we got the permit to establish a colony for the subsequent breeding. Chimeric mice #2, #3, #4 and #7 were mated with C57BL/6J mice purchased from Charles Rivers. Only chimera #2 gave birth to descendants, which were putatively CPT1A^(+/frt). These animals were genotyped by analyzing the number of constructs present in them, by Digital Droplet PCR (ddPCR) following the previously described procedure (See Experimental procedures chapter XXXX). We assessed the number of copies of

lacz gene, present in our construct, compared to the number of copies of *tert* gene, which codifies for telomerase reverse transcriptase.

<i>Transfer</i>	<i>Chimera #</i>	<i>Sex</i>	<i>Birth</i>	<i>Chimerism</i>
B80	1	Male	2013.11.25	30%
B80	2	Female	2013.11.25	80%
B80	3	Male	2013.11.25	75%
B81	4	Male	2013.11.25	70%
B81	5	Male	2013.11.25	10%
B81	6	Female	2013.12.22	60%
B93	7	Male	2014.01.06	90%

Table 5. Chimerism percentage present in the mice born from injected blastocysts.

If the construct was present in heterozygosis, as we expected, the copy number ratio between *TERT* and *LACZ* would be 2:1 (*TERT*:*LACZ*). In our samples, we could easily distinguish *CPT1A*^(+/frt), since *LacZ* gene was only detected in *CPT1A*^(+/frt) mice and not in wild type control mice (**Fig 60**).

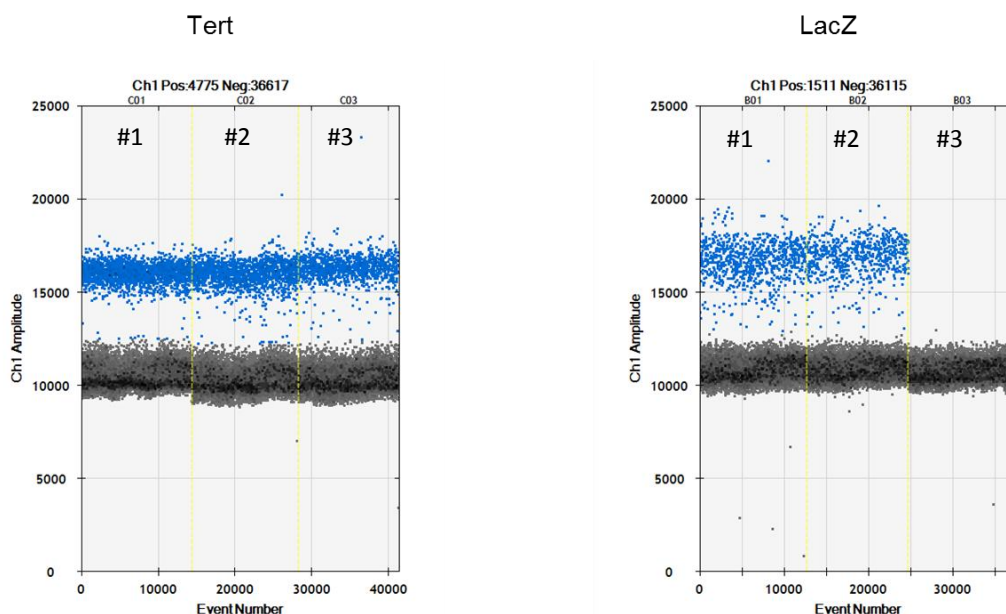


Fig 60. Analysis by ddPCR of *TERT* and *LACZ* amplification to genotype *CPT1A*^(+/frt) mice. Fluorescence amplitude detected in droplet analysis in ddPCR of *TERT* and *LACZ*. Positive events, in blue dots; negative/background events, in gray. gDNA #1 and #2, from C57BL/6j *CPT1A*^(+/frt) AKO-462 and AKO-465 mice; #3, from C57BL/6j wt mice.

The absolute number of copies in each sample can be known by applying a Poisson modelling to the number of events detected in each samples (**Fig 61**). When this absolute number is normalized by dividing it by the number of copies of a reference gene (in our case TERT, which has 2 copies in diploid cells), CPT1A^(+/frt) cells present 1 LACZ copy per 2 TERT copies, since LACZ/TERT ratio is 0.478 and TERT/LACZ ratio is 2.09.

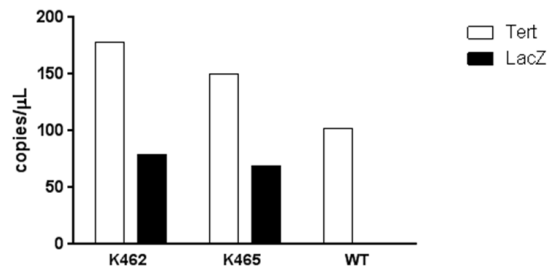


Fig 61. Analysis by ddPCR of absolute concentration of copies in each sample of TERT and LACZ genes in C57BL/6J CPT1A^(+/frt) AKO-462 and AKO-465 mice and C57BL/6J wt mice.

3.9. Genotyping of CPT1A^(loxP/loxP) mice generation

Those mice carrying the potentially conditional knockout CPT1A allele in heterozygosis (CPT1A^(+/frt)) were mated with heterozygous FLP recombinase-expressing mouse (Kranz et al., 2010) gently provided by Dr. Barbara Tondelli, from the *Institut de Recerca Biomèdica de Barcelona* Mouse Mutant Core Facility. Some of their descendants had the genotype CPT1A^{(+/frt);FLP^(+/-)}, whose expression of FLP recombinase allowed to have CPT1A^(+/loxP) mice. These descendants were mated to obtain CPT1A^(loxP/loxP), avoiding litter inbreeding when possible.

To genotype CPT1A^(loxP/loxP) and CPT1A^(+/loxP) mice, their gDNA was obtained from as described on Experimental procedures 2.5. We used a set of oligonucleotides to amplify the homology arms regions used to introduce our construct in the genetically modified mice (**Fig. 59**). When PCR is performed, we obtain a 1030 bp amplicon in wild type CPT1A allele and a 990 bp amplicon in CPT1A^{loxP} allele. Thus, CPT1A^(+/loxP) mice present two bands (990 and 1030 bp), while CPT1A^(loxP/loxP) mice have only the 1030 bp amplicon (**Fig 62 - left side**). gDNA from CPT1A^(loxP/loxP) mice was obtained to sequence the critical region containing the loxP-flanked exon 4 to confirm its immutability. The results show that the region remains unchanged, as it was designed in the original construct (**Fig. 63**).

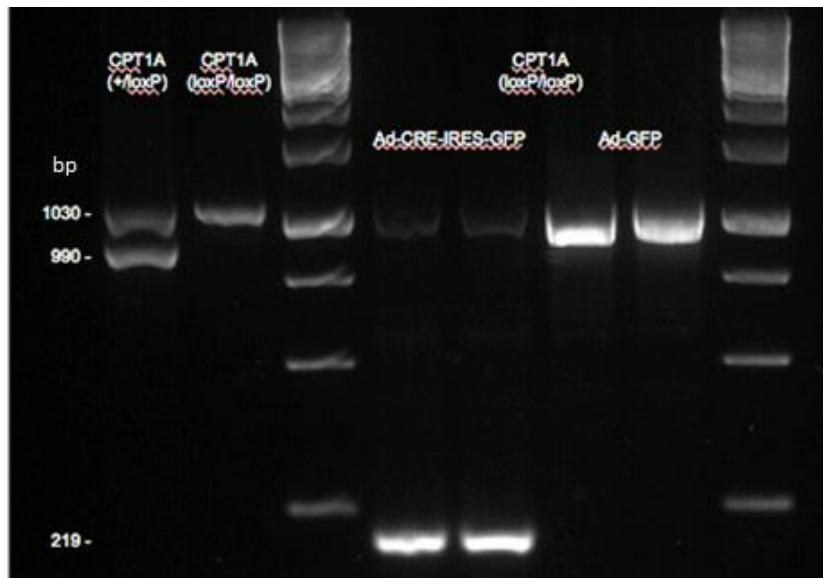


Fig 62. Amplicons from homology arms in a 1% agarose gel, from CPT1A^(+/loxP) and CPT1A^(loxP/loxP) tail gDNA and CPT1A^(loxP/loxP) hepatocytes gDNA infected by Ad-CRE or Ad-GFP.

CPT1A^(loxP/loxP) colony was expanded and one of the mice was used to obtain primary hepatocytes with a collagenase infusion method (Moldéus, 1978). These primary hepatocytes were infected with CRE recombinase-expressing adenovirus, to double check loxP sequences integrity, as direct substrates of the recombinase and to evaluate the deletion of exon 4 in gDNA. After 24 h infection with 50 moi, the 1030 bp is barely detectable by PCR using gDNA from CRE recombinase expressing hepatocytes. Moreover, a new band with a 219 bp length appeared, absent in control infected hepatocytes (**Fig 62 - right side**). This 219 bp band was predicted to be amplified in CPT1A^(loxP/loxP) hepatocytes expressing CRE recombinase, due to the deletion of the loxP-flanked exon 4.

To assess the integrity of loxP-flanked critical region even further and the ability of CRE recombinase to delete CPT1A exon 4, we confirmed by PCR the elimination of exon 4 in cDNA obtained from CPT1A^(loxP/loxP) hepatocytes expressing CRE recombinase. The primers used in this case hybridize on the exon 3 and 5, producing a 288 bp amplicon, and when the recombination takes place, it was predicted to drop to a 116 bp amplicon. The products of amplification show the 288 bp amplicon in control cDNA, which disappears in CRE-expressing cells cDNA, but in this case, the 116 bp band is barely detectable (**Fig. 64A**). This probably happens due to a reduction of mRNA stability when exon 4 is deleted. We assessed the drop in CPT1A mRNA in primary cortical neurons after 16h infection with Ad-CRE, which produced a reduction of CPT1A mRNA levels (**Fig. 64B**).

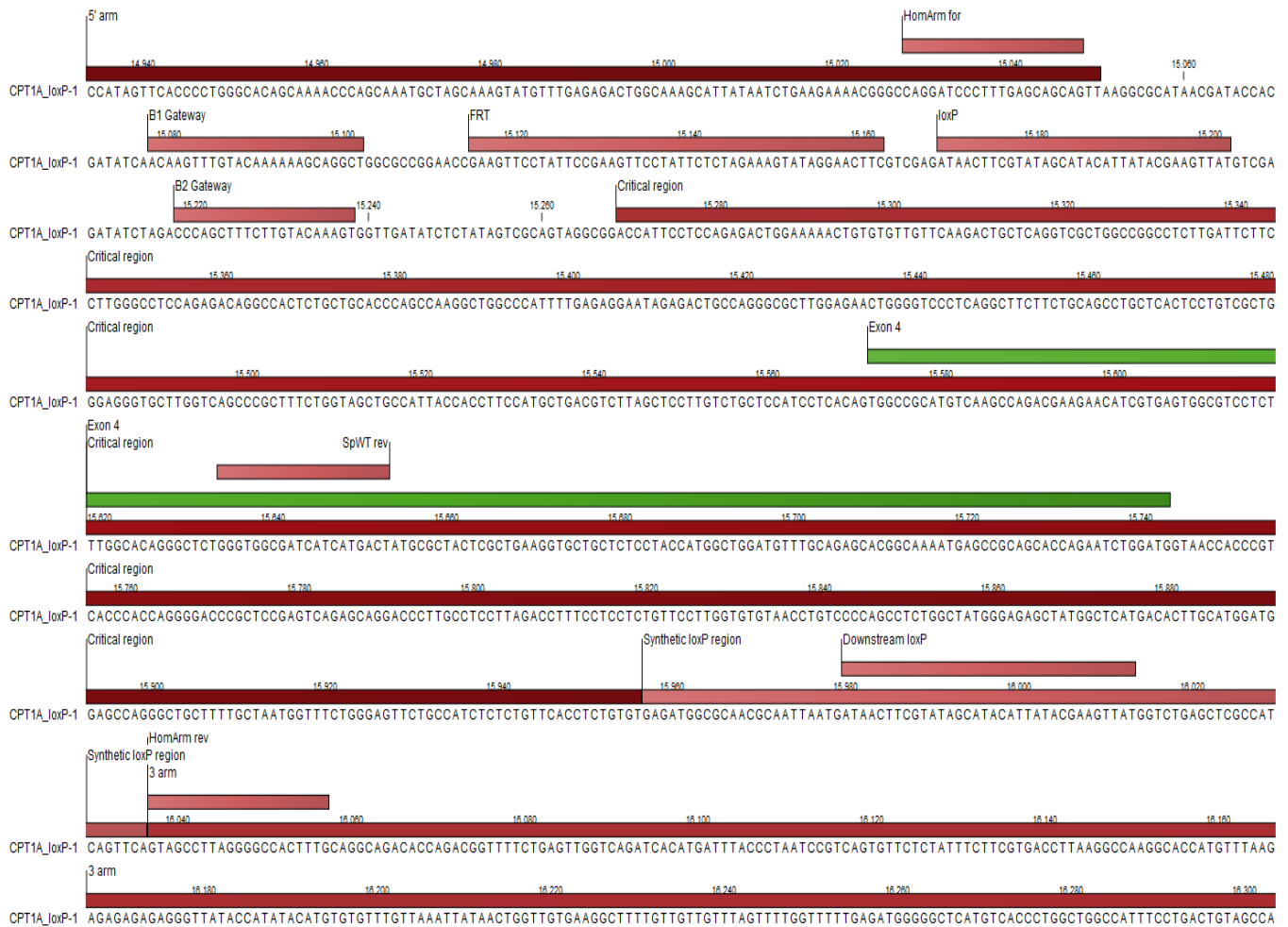


Fig. 63. Confirmed sequence found in the critical region of CPT1A^(loxP/loxP) mice. FRT: Target sequence for FLP recombinase; Exon Del: Internal Exon Deletion which blocks wildtype CPT1A translation; IRES: Internal ribosome entry site; LACZ: β -galactosidase gene; pA: Polyadenylation sequence; loxP: Target sequence for CRE recombinase; hBactP: Human β -actin promoter; NEO: Neomycin resistance gene. HomArm for: Oligonucleotide on 5' homology arm for PCR genotyping. HomArm rev: Oligonucleotide on 3' homology arm for PCR genotyping. SpWT rev: Oligonucleotide for alternative amplification in wild type mice for PCR genotyping.

All these results indicate that CPT1A^(loxP/loxP) mice have intact CPT1A mRNA transcription, but when infected its cells are infected by CRE recombinase-expressing viral vector and CPT1A exon 4 is successfully deleted.

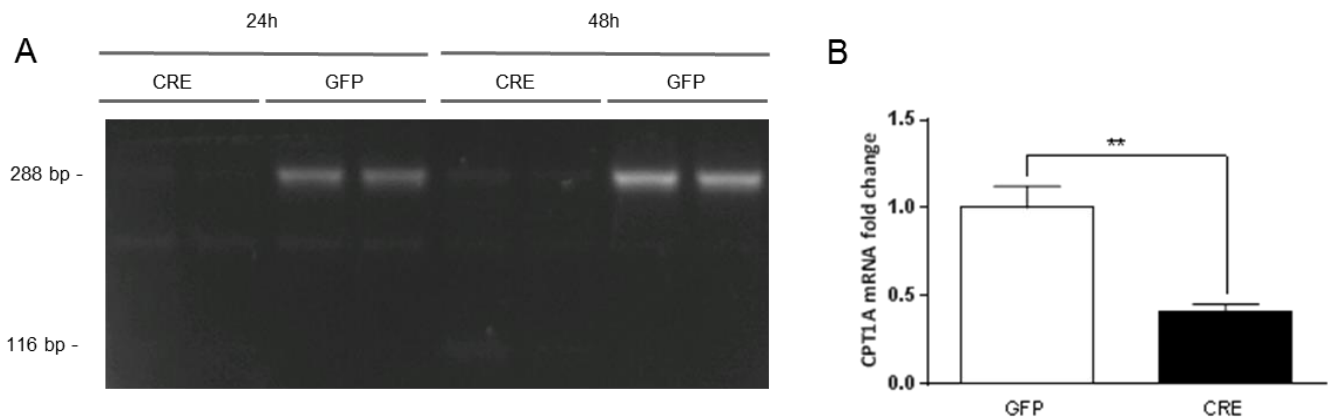


Fig. 64. Analysis of CPT1A deletion of after Ad-CRE infection in CPT1A^(loxP/loxP) primary cultures. (A) Amplicons from exon 3 to exon 5 in a 1.5% agarose gel, from cDNA from CPT1A^(loxP/loxP) hepatocytes infected by Ad-CRE or Ad-GFP after 24h and 48h and analysis by qRT-PCR of mRNA of CPT1A from primary cortical neurons obtained after 16h infection (B). Error bars represent SEM, n=4. Student's T test. ***p<0.01*.

3.10. Effect of ghrelin and CPT1A deletion on mRNA levels of GABA metabolism enzymes in primary cortical neurons

Since we had previously observed the impact of CPT1A overexpression and inhibition on mRNA levels of GABA shunt enzymes, glutamic acid decarboxylases and VGAT, we wanted to assess the consequences of CPT1A deletion and the treatment with ghrelin in their mRNA levels.

We found that after the genetic deletion of CPT1A, GABAT, SSADH, GAD1 and VGAT had their mRNA levels reduced to around the 50% (Two-way ANOVA, *p<0.05* in most cases, *p<0.01* in VGAT), but the cells seemed unresponsive when it comes to mRNA changes to ghrelin, since the reduction in GFP-infected cells was not significant in any of the genes, since control GFP group had greater variability (Fig 65).

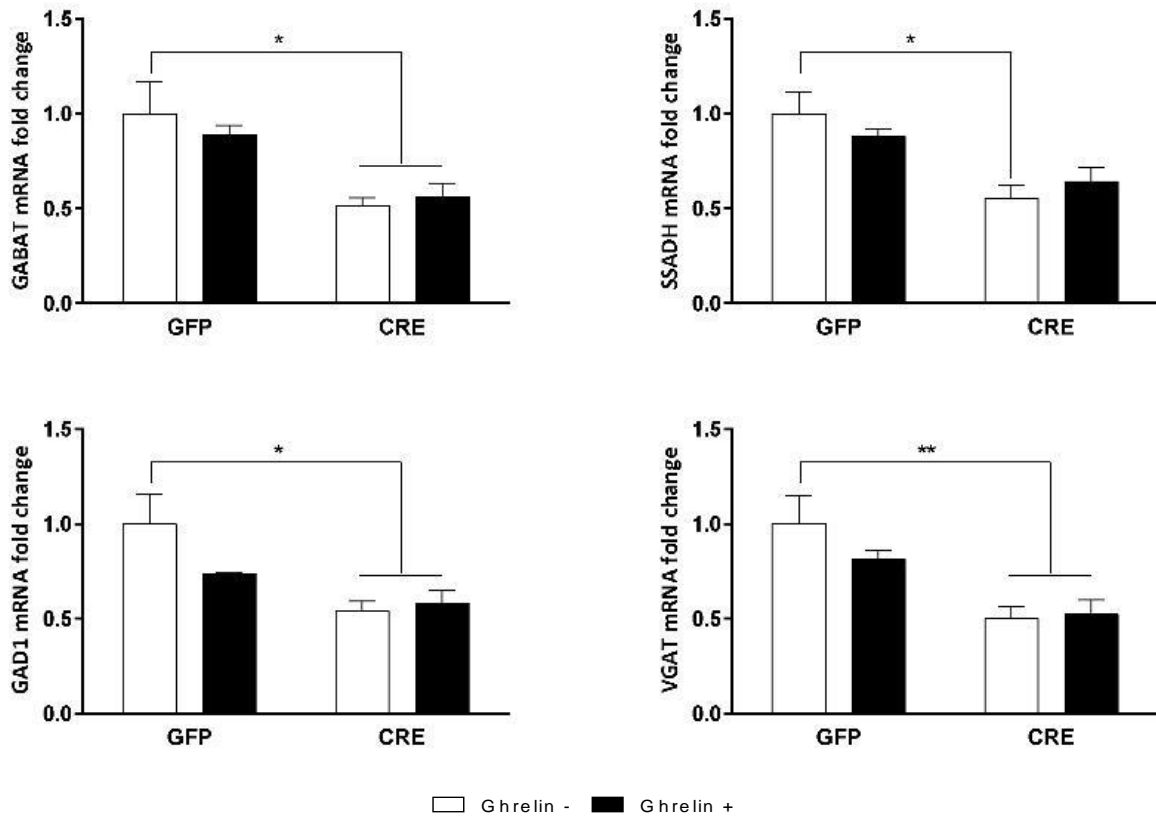


Fig 65. Analysis of mRNA levels of GABA metabolism genes in 8 DIV primary cortical neurons after CPT1A deletion and ghrelin treatment. Analysis performed by qRT-PCR with samples obtained at 8 DIV after 16h infection with Ad-CRE and Ad-GFP. Error bars represent SEM, n=4. Two-way ANOVA * $p < 0.05$, ** $p < 0.01$

The results on mRNA changes due to CPT1A modulation or ghrelin treatment, have been highly dependent on the metabolic situation of the cells. For example, with CPT1A overexpression at 5 mM glucose the changes are similar to those observed when cortical cells are treated with ghrelin at 5 mM. Nonetheless, the effect on GABA output is dissimilar, pointing out the existence of other factors modulating GABA pool and its release.

3.11. Effect of ghrelin and CPT1A deletion on GABA release and GABAT activity in primary cortical neurons

Since we had previously experienced that changes in mRNA of GABA metabolic enzymes do not necessarily have a direct effect on GABA release, we performed an amino acid neurotransmitter release experiment on cortical neurons with and without CPT1A deletion. Besides exposing them to ghrelin, we tested the effect of inhibiting tricarboxylic acid cycle to see

whether the effect obtained was the same observed with ghrelin treatment. We used 2-hydroxyglutarate (2-HOglu), which acts inhibiting isocitrate dehydrogenase. Both ghrelin and 2-HOglu cause a similar decrease in GABA release (to 58% and 67%, respectively. $p < 0.01$), but when combined, both compounds offset their effects, with a GABA release similar to basal. When CPT1A is deleted, neither ghrelin nor 2-HOglu cause any change in GABA release (**Fig 66**).

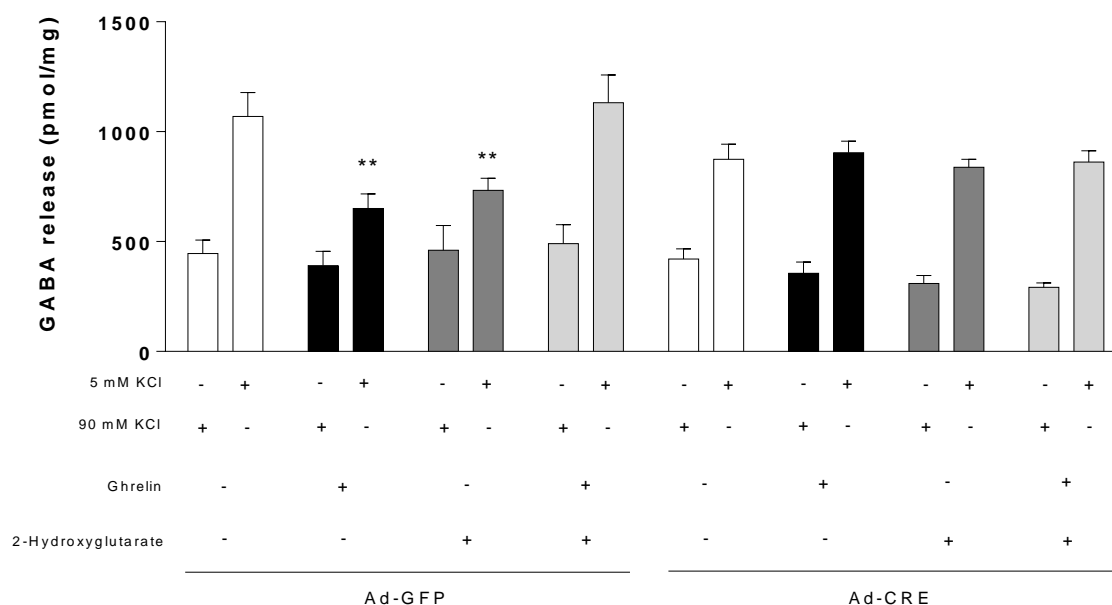


Fig 66. Analysis of GABA release in 8 DIV primary cortical neurons after CPT1A deletion and ghrelin and 2-hydroxyglutarate treatment. Analysis performed with cells at 8 DIV after 16h infection with Ad-CRE and Ad-GFP. Error bars represent SEM, n=4. Student's T test $**p < 0.01$

Moreover, we took a look on GABA transaminase activity, to check whether the reduction in its mRNA due to CPT1A deletion would actually affect its activity. We observed that both CPT1A deletion and ghrelin reduce GABA transaminase activity detected in neuronal extracts: ghrelin reduces it to a 50% and CPT1A deletion reduces it to around the 30% of basal GABAT activity (**Fig 67**). All these results point out the involvement of ghrelin and CPT1A in the modulation of mitochondrial function, which eventually leads to changes in GABA metabolism and release.

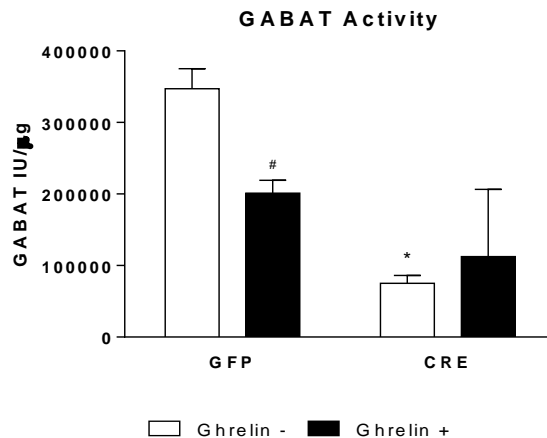


Fig 67. Analysis of GABAT activity in 8 DIV primary cortical neurons after CPT1A deletion and ghrelin treatment. Analysis performed with samples obtained at 8 DIV after 16h infection with Ad-CRE and Ad-GFP. Error bars represent SEM, n=3. #Two-way ANOVA $p < 0.05$ *Student's T test $p < 0.05$, referred to GFP, Ghrelin -

3.12. Effect of ghrelin and CPT1A deletion on the intermediates of tricarboxylic acid cycle in primary cortical neurons

The results obtained with ghrelin treatments on primary cortical neurons, as well as GT1-7 neurons, suggest that its effect is not only produced in fatty acid oxidation, but also in the mitochondria as a whole. Krebs cycle, which acts as main metabolic hub in the mitochondria, could be easily a target of this effect, moreover taking into account the observed effect of tricarboxylic acid (TCA) cycle inhibition with 2-hydroxyglutarate. We assessed the levels of many of the TCA cycle intermediates using HPLC in primary cortical neurons treated with ghrelin, with and without CPT1A deletion.

Both ghrelin and CPT1A deletion promote a significant reduction in citrate, the main TCA cycle intermediate (around a 70% reduction, $p < 0.01$) and in α -ketoglutarate (around an 80% reduction, $p < 0.01$), which through becoming glutamate can form GABA. Besides the other intermediates assessed, succinate, fumarate and malate are unchanged (**Fig 68**).

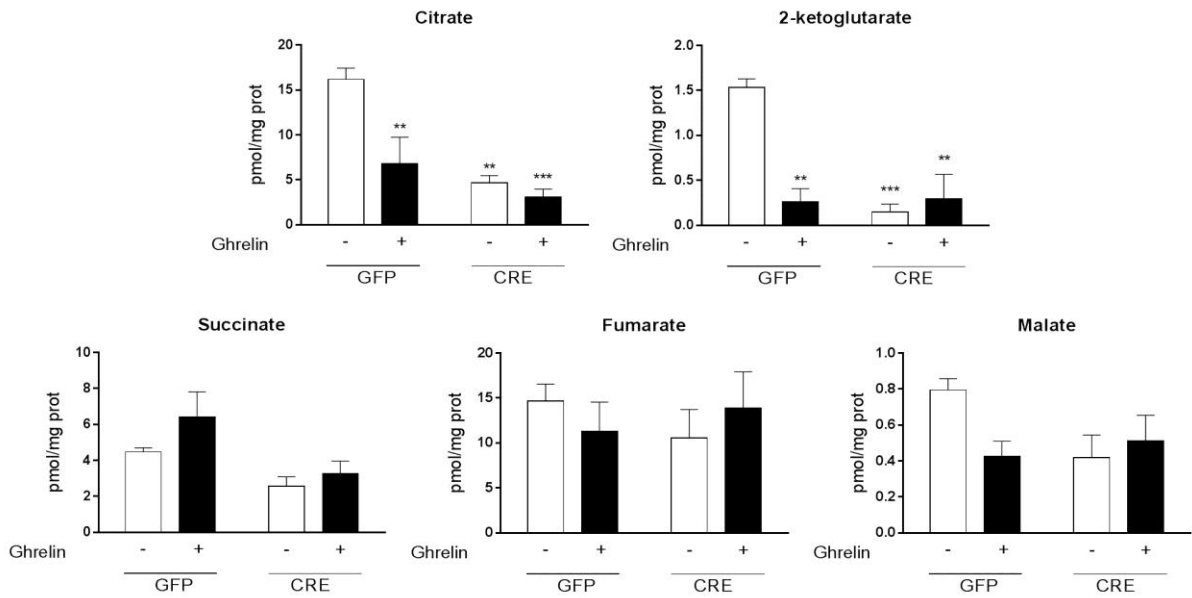


Fig 68. Effect of ghrelin and CPT1A deletion on TCA cycle intermediates. Samples were collected from 8 DIV primary cortical neurons after 16 h infection with Ad-CRE and Ad-GFP and 30 min ghrelin treatment. Error bars represent SEM, n=4. ** $p < 0.01$, *** $p < 0.001$

Since we had described that 2-hydroxyglutarate is able to inhibit GABA release as well, we checked its effect on TCA cycle intermediates. We observed that only in the case of citrate, it was able to revert its reduction (**Fig 69**)

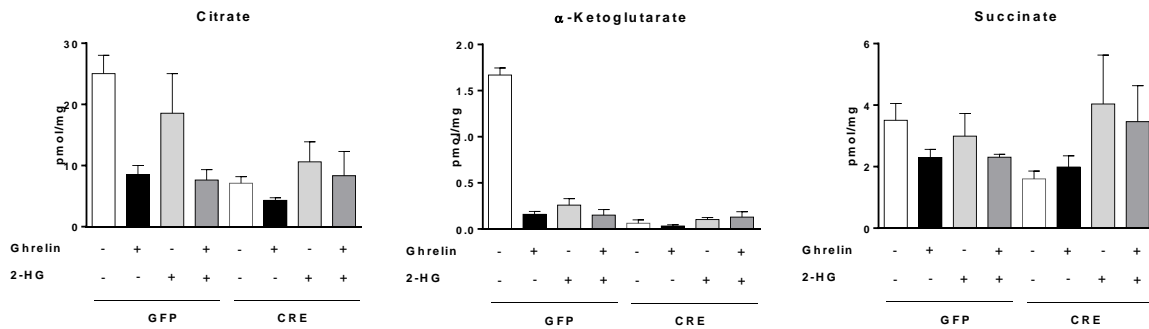


Fig 69. Effect of ghrelin, 2-hydroxyglutarate and CPT1A deletion on TCA cycle intermediates. Samples were collected from 8 DIV primary cortical neurons after 16 h infection with Ad-CRE and 30 min ghrelin and/or 2-hydroxyglutarate (2-HG) treatment. Error bars represent SEM, n=4

To sum up, it seems that total pool of TCA cycle intermediates is an important factor to take into account for the modulation of GABA release. Moreover, both ghrelin and CPT1A deletion produce a drop in TCA intermediates, which suggests that sudden ghrelin treatment mimics the effect of CPT1A deletion.

3.13. Effect of ghrelin and CPT1A deletion on mitochondrial respiration in primary cortical neurons

Since we had different results when it came to GABA response to ghrelin in different glucose concentrations, we wanted to assess the mitochondrial function through measuring the oxygen consumption rate (OCR) in primary cortical cells using different substrates as fuel. We analyzed mitochondrial function at 5 mM glucose and at 25 mM glucose. We assessed it using a reaction medium in which we forced the use of exogenous palmitic acid, similar to a radioametric fatty acid oxidation assay. All these data would give us information about the capacity of neuronal mitochondria to adapt to different fuel availability and to let us know if there is actually a reduction in fatty acid oxidation due to ghrelin in cortical neurons.

3.13.1 Oxygen consumption rate of primary cortical neurons at physiological glycorrachia

We wanted to analyze the effect of ghrelin on OCR in the closest conditions to physiology. Cells were pretreated with 5 mM glucose medium for 3h, to mimic physiological glucose levels in CSF, previous to perform the extracellular flux analysis. 100 nM ghrelin was added to half of the wells to assess its effect. Oligomycin and antimycin A were sequentially injected to measure mitochondrial, non-mitochondrial and ATP-linked OCR, as well as proton leak, taking into account basal initial OCR, and OCR after each drug injection, as explained on Experimental procedures 3.5.

Both ghrelin and CPT1A deletion produce a reduction in non-mitochondrial oxygen consumption to a 50-45%. Strikingly, ghrelin reduces mitochondrial respiration independently to CPT1A deletion. However, this reduction is only significant in total mitochondrial respiration of CPT1A deleted neurons, while only in mitochondrial ATP-linked oxygen consumption is affected when CPT1A is intact (**Fig 70**).

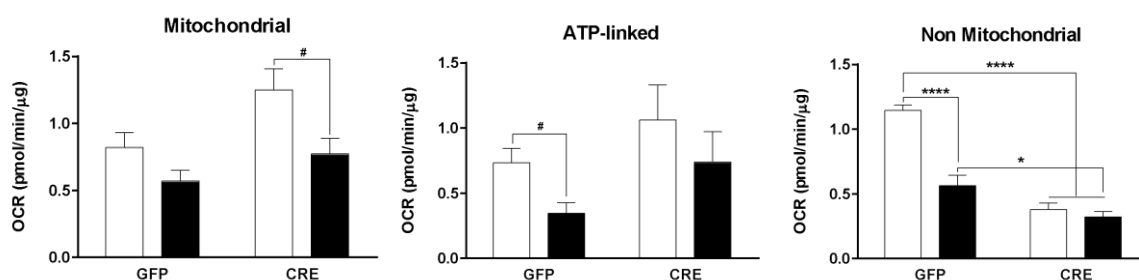


Fig 70. Analysis of mitochondrial, ATP-linked and non-mitochondrial OCR in 8DIV primary cortical neuronal cultures after ghrelin treatment CPT1A deletion at 5 mM glucose. Cells were analyzed after 16 h infection with Ad-CRE and Ad-GFP at 5 mM glucose. Error bars represent SEM, n=4. Two-way ANOVA *p<0.05 ****p<0.0001 Student's T test #p<0.05

3.13.2 Oxygen consumption rate of primary cortical neurons at high glucose

Cells were pretreated with 25 mM glucose medium for 3h, the same concentration used when subcultured, previous to perform the extracellular flux analysis. 100 nM ghrelin was added to half of the wells to assess its effect. Oligomycin and antimycin A were sequentially injected to measure mitochondrial, non-mitochondrial and ATP-linked OCR, as well as proton leak, taking into account basal initial OCR, and OCR after each drug injection, as explained on Experimental procedures 3.5.

Interestingly, ghrelin produces an increase in mitochondrial respiration regardless CPT1A deletion. Nonetheless, both ghrelin and CPT1A deletion produce a drop in non-mitochondrial oxygen consumption (**Fig 71**).

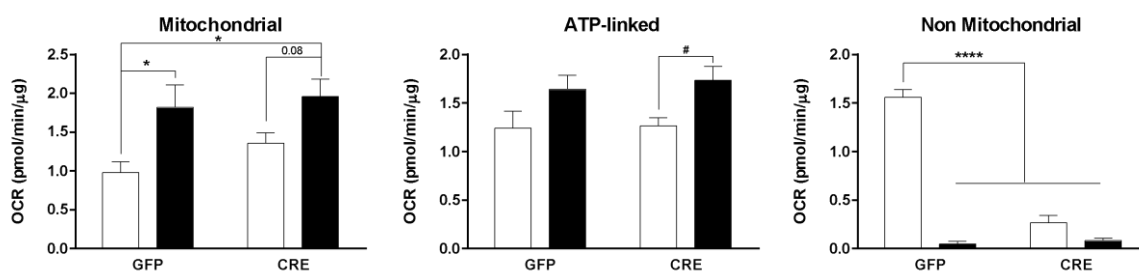


Fig 71. Analysis of mitochondrial, ATP-linked and non-mitochondrial OCR in 8DIV primary cortical neuronal cultures after ghrelin treatment CPT1A deletion at 25 mM glucose. Cells were analyzed after 16 h infection with Ad-CRE and Ad-GFP at 25 mM glucose. Error bars represent SEM, n=4. Two-way ANOVA *p<0.05 ****p<0.0001 Student's T test #p<0.05

3.13.3 Oxygen consumption rate primary cortical neurons using palmitate

Cells were pretreated with 5 mM glucose medium for 3h, to mimic physiological glucose levels in CSF, previous to perform the extracellular flux analysis. 100 nM ghrelin was added to half of the wells to assess its effect and the medium used was the same used during the radiometric fatty acid oxidation assay, using in this case cold palmitic acid instead. Oligomycin and antimycin A were sequentially injected to measure mitochondrial, non-mitochondrial and ATP-linked OCR, as well as proton leak, taking into account basal initial OCR, and OCR after each drug injection, as explained on Experimental procedures 3.5.

Ghrelin produces a drop in mitochondrial oxygen consumption, but interestingly, neurons lacking CPT1A forced to use palmitate show unchanged OCR due to ghrelin. The results obtained in this experiment are similar to those found in the radiometric assay with GT1-7: in that case acid-soluble products were reduced due to ghrelin and in this case mitochondrial and ATP-linked OCR are reduced; while CPT1A deletion (or silencing with GT1-7) brings a compensatory effect with an OCR increase. Surprisingly, non-mitochondrial OCR seems to increase when CPT1A is deleted and cells are forced to use exogenous palmitic acid as fuel (**Fig 72**).

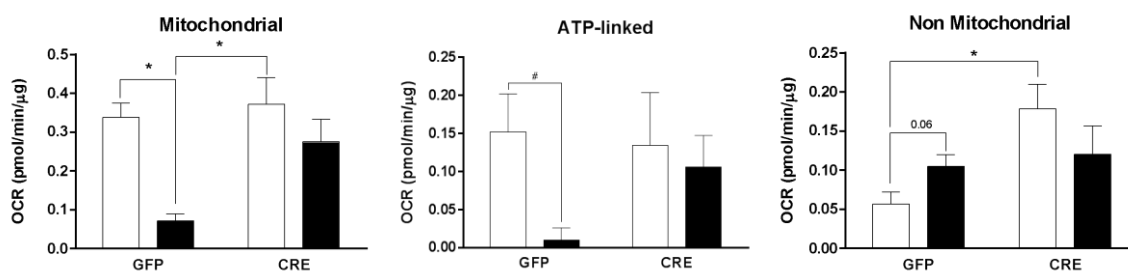


Fig 72. Analysis of mitochondrial, ATP-linked and non-mitochondrial OCR in 8DIV primary cortical neuronal cultures after ghrelin treatment CPT1A deletion with palmitate-rich medium. Cells were analyzed after 16 h infection with Ad-CRE. Error bars represent SEM, n=4. Two-way ANOVA *p<0.05 Student's T test #p<0.05

3.14. Effect of ghrelin and CPT1A deletion on mitochondrial superoxide in primary cortical neurons

We wanted to assess if we could reproduce the effects of ghrelin and CPT1A silencing in GT1-7 in the primary neuronal culture, since CPT1A would be also involved in ROS generation, so we measured mitochondrial superoxide formation in primary cortical neurons treated with ghrelin and when CPT1A was genetically deleted. In this case, we were not able to reproduce the same effects observed in GT1-7 with no apparent changes in superoxide formation (**Fig 73**). This happens probably due to the variability found in primary cortical neuronal cultures.

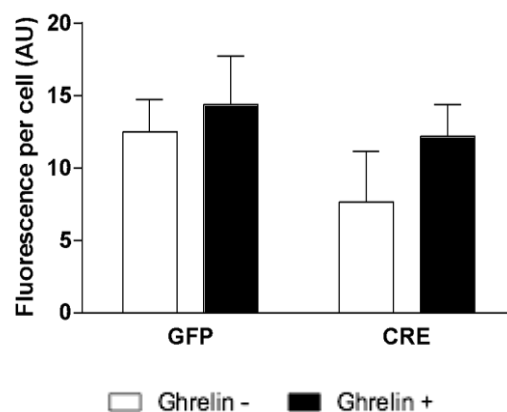


Fig 73. Analysis of superoxide formation in 8 DIV primary cortical neurons after ghrelin treatment and CPT1A deletion. Superoxide formation measured by MitoSOX derived fluorescence in primary cortical cells. Cells were analyzed after 16 h infection with Ad-CRE by FACS. Error bars represent SEM, n=4.

All the results obtained in this third part suggest an important role of ghrelin in mitochondrial activity modulation, which seems to be crucial to produce changes in amino acid neurotransmission. Modulation of CPT1A seems to be one of the changes produced, but we cannot categorically affirm that of the observed changes are due to this downstream effector, but it is clear that its modulation changes the reactivity of the model to ghrelin.

DISCUSSION

In this work, we focus on the modulation of neurotransmission by CPT1A, as a downstream effector of ghrelin, in both cortical neurons and hypothalamus. We assess whether CPT1A has a metabolic role in the direct control of amino acid neurotransmitters metabolism, besides being part of the signaling for orexigenic neuropeptide expression.

CPT1AM overexpression in VMH causes hyperphagia and overweight

Previous experiments in our group pursuing the CPT1AM overexpression in VMH show that CPT1A activity promotes a hyperphagic phenotype (Mera, 2012). Thanks to the fluorescence shown in GFP rats, we observed that the infection is circumscribed mainly in VMH, with no GFP-expressing cells beyond MBH. If we assume that AAV-GFP and AAV-CPT1AM have infected similarly the rats, we can attribute the observed phenotype to the CPT1AM overexpression in VMH. By measuring the formation of acylcarnitines in MBH, we confirmed that CPT1AM can actually raise its activity in VMH, which we had not previously assessed directly. This increase of acylcarnitines is not accompanied with a reduction in LCFA-CoA, but actually there is an increase in C18:0 acyl-CoA. This fact collides with the outdated hypothesis regarding LCFA-CoA levels in the control of food intake. This initial hypothesis stated that LCFA-CoA might act as a signal in the pathways to modulate food intake, since its increase, due to CPT1A genetic inhibition, using ribozymes, or a direct oleate injection promoted a decrease in food intake (S Obici et al., 2003). Nonetheless, with long-term CPT1AM expression in VMH, rats did not show a reduction of total LCFA-CoA, contrarily to the previous reports of some of our collaborators (Gao et al., 2013). The fact that in our case the permanent activation of CPT1A lasted longer may explain the divergent results compared to short-term overexpression. Nonetheless, this suggests that increased food intake is independent from LCFA-CoA levels.

Another important hypothesis for the control of food intake involves malonyl-CoA (Miguel López et al., 2008; Nogueiras, López, & Diéguez, 2010). The importance of malonyl-CoA in the AMPK-ACC-CPT1 signaling axis for the food intake control is confirmed by our experiments, since the overexpression of a malonyl-CoA-insensitive CPT1A isoform can promote hyperphagia, independently of the satiety and metabolic state and the consequent changes in malonyl-CoA levels. We have confirmed that this CPT1AM-induced hyperphagia is

independent from satiety state, since refeeding-after-fasting satiety tests show that CPT1AM rats have increased food intake, regardless being fasted or fed. In conclusion, it would be due to CPT1AM insensitivity to malonyl-CoA.

In this new set of experiments, we confirm the hyperphagic phenotype and conclude that it can eventually lead to an obese phenotype, probably due to the hyperphagia itself, but we cannot discard a direct effect of VMH on the organism's capacity to store and consume energy.

This hyperphagia-driven overweight is accompanied with an increase in circulating BCAA, which are considered obesity biomarkers. Moreover, CPT1AM rats show an impaired glucose tolerance, which is usual in many overweight animal models and was previously described as well in our previous reports (Mera, 2012). We tested pyruvate tolerance, since hepatic phosphoenolpyruvate carboxykinase (PEPCK) is increased in CPT1AM rats. We have detected no changes in gluconeogenesis in CPT1AM rats, despite initial glucose levels during PTT were increased in CPT1AM rats, as well as at the end of the experiment, but overall AUC is not different in CPT1AM rats. We cannot discard we could have detected an increased AUC if the assay had measures later than 120 min, since the tendency of GFP was to decrease glycaemia, while CPT1AM rats had higher levels.

CPT1AM overexpression in VMH modifies hypothalamic lipidomic profile and vesicular amino acid transporters transcription

To deepen our knowledge and our understanding in the mechanisms by which hypothalamic CPT1A is involved in the control of food intake, we analyzed the transcription of the different hypothalamic neuropeptides. POMC and CART expression remains unaltered, in agreement with an unactivated anorexigenic response. However, when we assessed orexigenic neuropeptides, no changes are observed. Surprisingly, both NPY and, α -MSH antagonist, AgRP remain unaltered as well. Nonetheless, these results confirm the previously observed in our group (Mera, 2012). In both cases, we analyzed the mRNA expression in MBH from rats sacrificed after an overnight fasting, which may mask the changes produced by CPT1AM overexpression. Nonetheless, the levels of octanoyl-ghrelin are increased in CPT1AM rats regardless their fasting state (Mera, 2012) and interestingly, we have shown in this work that CPT1AM rats are hyperphagic independently to their fasting in the satiety test. All these results

suggest that the hyperphagia observed is not necessarily mechanistically controlled only by hypothalamic neuropeptidergic signaling. Here we show that CPT1AM overexpression in VMH triggers the expression of BSX, CREB and FoxO1, which are transcription factors of NPY and AgRP. However, they are not able to promote orexigenic neuropeptides expression in fasted animals. These transcription factors have been described to be triggered by ghrelin in response to a ROS-buffering enzymes formation (Z B Andrews et al., 2008). In our studies, CPT1AM overexpression triggers UCP2 and antioxidant enzymes expression in MBH and this is not accompanied by a production of ER stress. In our model, ROS formation and buffering may be involved in the hyperphagic phenotype as well, but in a mechanism independent from neuropeptidergic signaling.

NAG neurons have been described to act in a biphasic fashion when it comes to feeding (Krashes et al., 2013): on the one hand, AgRP modulates feeding chronically, but not quickly; and on the other hand, either GABA or NPY are required for rapid feeding. Moreover, some authors have described a compensatory GABAergic output increase in mice models lacking NPY (Atasoy, Betley, Su, & Sternson, 2012). Furthermore, VMH neurotransmission has been described as primarily glutamatergic and this neurotransmission is involved in the control of food intake and energy homeostasis (Amir, 1990; Fu & van den Pol, 2008; K. W. Kim et al., 2011; Tejas-Juárez et al., 2014; Tong et al., 2007). Therefore, amino acid neurotransmission appears as an important player in the control of food intake. In our model of rats overexpressing CPT1AM in VMH, the animals show unaltered expression of ARC-expressed neuropeptides. Thus, we assessed the effect of CPT1AM overexpression in amino acid neurotransmission. We evaluated the effect on the mRNA expression of the vesicular amino acid neurotransmitter transporters found in MBH: VGAT, which controls vesicular GABA in NAG neurons in ARC, and VGLUT2, controlling glutamate quantal size in VMH. Moreover, we evaluated the mRNA levels of other minority vesicular glutamate transporters which can be putatively found in MBH, *i.e.* VGLUT1 and VGLUT3. In the case of VGLUT3, it is related to GABA/glutamate co-release in GAD+ neurons. The results showed potential alterations in both glutamate and GABA quantal size, due to changes in their vesicular transporters. VGLUT2 expression is reduced in CPT1AM rats, while the same animals show increased VGAT expression in MBH. Although, text book descriptions often oversee amino acid neurotransmission and focus on well-established neuropeptidergic circuitry, its importance is being increasingly highlighted by researchers worldwide. Glutamatergic outputs from VMH have been described to activate anorexigenic POMC/CART neurons to stimulate satiety signaling (Sternson, Shepherd, & Friedman, 2005). A decrease in VGLUT2 in VMH, where it is mainly located in MBH, may lead to a reduction in glutamate

quantal size, which would attenuate the activation of anorexigenic neurons. Furthermore, optogenetic stimulation on NAG neurons produces an orexigenic effect that is blocked using GABA antagonists (Atasoy et al., 2012). This finding indicates that the orexigenic signaling is not dependent on hypothalamic neuropeptides. The VGAT mRNA increase may eventually lead to a rise in GABAergic signaling. This inhibitory signaling may come from VMH (Zhu et al., 2010) and/or from NAG neurons (Wu & Palmiter, 2011) to anorexigenic POMC/CART neurons. This notion is consistent with the experiments showing that muscimol injections, which is a GABA agonist, markedly increases food intake (Kelly, Rothstein, & Grossman, 1979). Although we do not know how the vesicular transporters are modulated in our model, ROS signaling has been reported to boost GABA release (Tarasenko et al., 2012). For this reason, we hypothesize that CPT1AM expression in VMH, which increases ROS, might be responsible for this higher inhibitory output. Although we did not monitor ROS directly, we observed an increase in the transcription of ROS-buffering enzymes.

Alternatively, the CPT1AM-driven lipidomic profile changes could be responsible for the increased food intake. CPT1A alters lipid turnover and consequently the lipidomic profile in neurons (Arduini et al., 1994). Lipid membrane composition is crucial to keep the structure and functionality of embedded proteins (Lundbæk, 2006; Schug, Frezza, Galbraith, & Gottlieb, 2012; Sprong, van der Sluijs, & van Meer, 2001; Takamori et al., 2006). In some physiopathological states, neurotransmission is modified by changes in membrane lipid composition (du Bois, Deng, & Huang, 2005). In the synaptic vesicular model developed by Takamori et al., transmembrane proteins encompass one fourth of the whole vesicular surface (Takamori et al., 2006). Amongst them, vesicular amino acid neurotransmitter transporters, such as VGAT or VGLUT2, need phospholipidic rims to be anchored to the lipid bilayer and to work properly (Lundbæk, 2006; Takamori et al., 2006). The reduction in phospholipids observed in our model may affect the functionality of these transporters. Therefore, VGLUT2 may have compromised its anchorage to the vesicular membrane, affecting eventually to its transcription. Nonetheless, we hypothesize that the putatively increase VGAT expression occurs as a result of indirect effect on other regions such as ARC. Both changes in lipid composition and expression of vesicular amino acid transporters might be implicated in the increase in food intake in CPT1AM rats.

Moreover, hypothalamic ceramides have been demonstrated to be involved in feeding regulation. Concretely, CPT1C is required by the ghrelin-induced increase in hypothalamic ceramides, which triggers the expression of NPY and AgRP in NAG neurons (Ramírez et al., 2013). We show that CPT1A expression modifies ceramide metabolism, as CPT1AM rats show

an increase in C18:1 and C14:0 ceramides. Sphingolipids act as signaling molecules in a variety of physiological processes, including neuronal development and plasticity. The formation and transport of specific axonal vesicles has been reported to be coupled to sphingolipid synthesis (Chang, Wisco, Ewers, Norden, & Winckler, 2006). CPT1AM rats have increased sphingomyelin and dihydrosphingomyelin, which may lead to changes in hypothalamic synaptic plasticity and energy balance. Moreover, CPT1AM overexpression reduces phospholipids in MBH, which may act as substrates for the increased FAO in CPT1AM-expressing cells.

To sum up, with previous and current results, CPT1A expression in the VMH plays a key role in the regulation of food intake and glucose homeostasis (**Fig 74**). Mechanistically, our findings suggest that CPT1A modulates the expression of GABA and glutamate transporters, which control their quantal sizes. We cannot discard the involvement of phospholipids, sphingolipids and ROS in the mechanisms controlling appetite. Mitochondrial FAO in hypothalamus is revealed as a potential target for the control of food intake.

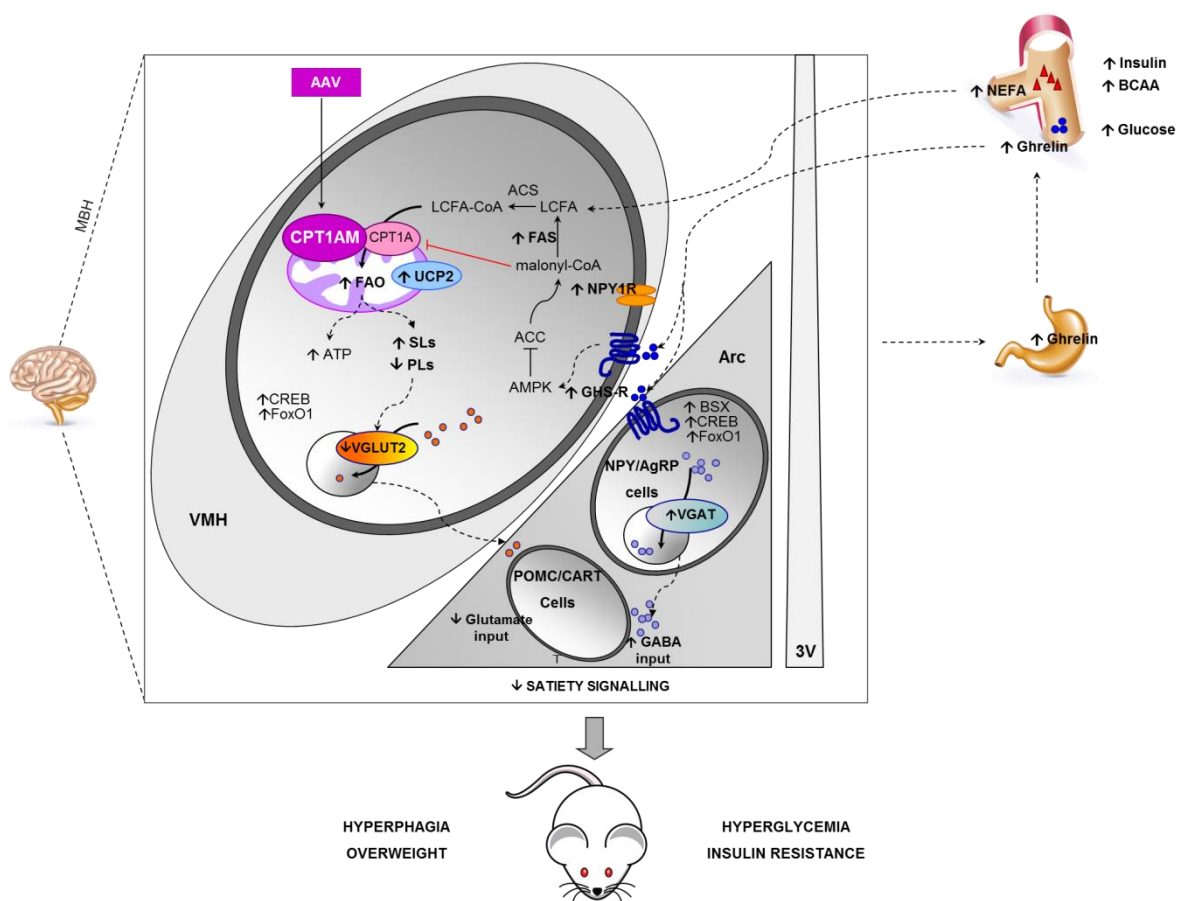


Fig 74. Proposed role of VMH CPT1A in the hypothalamic control of satiety. Adapted from (Mera et al., 2014)

Hypothalamic neuronal cell lines have limited validity as hypothalamic GABAergic neuronal models

The long-term expression of CPT1A in VMH of rat is both strength and limitation in these experiments. This is therefore, since we take advantage of an animal model, which is more complex and closer to physiological system, but at the same time, the long-term overexpression lets the system to create compensatory mechanisms which mask the physiological gimmick involved in the control of food intake in ghrelin signaling, downstream CPT1A. Nonetheless, they gave us a clue to go on investigating on amino acid neurotransmission in the hypothalamus. To this end, we carried on a series of validation experiments using several hypothalamic cell lines, to find a valid amino acid neurotransmitting hypothalamic model.

To this end, we evaluated at first mHypo-N29/4 and mHypo-N43/5 as arcuate neuronal models. When purchased, mHypo-N29/4 was claimed to be an AgRP/NPY-expressing hypothalamic neuronal line and mHypo-N43/5, a CART/POMC-expressing hypothalamic neuronal line. Unfortunately, the expression of the four neuropeptides was almost inexistent in our hands, as it was confirmed later on by the company which retracted their claims. CELLutions actually stated later on that mHypo-N43/5 expressed both orexigenic AgRP and anorexigenic CART, claim that we cannot confirm. Later on, we evaluated mHypo-N41 cell line. It actually expresses AgRP and NPY. Nonetheless, only AgRP expression is ghrelin-dependent, but seems to have most of the amino acid neurotransmission metabolism intact. We infected mHypo-N41 neurons with LV-shCPT1A (and LV-scramble) and selected a clone with reduced CPT1A expression and a control clone, to test the effect of ghrelin in both clones and the involvement of CPT1A in ghrelin control of neurotransmission. The mHypo-N41-shCPT1A clone has a reduction to a half of CPT1A mRNA, compared to control. Therefore, the expression of AgRP is reduced to a half as well. However, when we test their responsiveness to ghrelin, mHypo-N41-scramble control clone has no changes in the expression of the orexigenic AgRP.

The clonal selection shows that this cell line easily loses some of the neuronal features of the hypothalamic cell line, such as the responsiveness to ghrelin, after several subcultures. This fact was known from other hypothalamic neuronal cell lines as well, such as GT1-7, but we chose to test mHypo-N41 first, since it seemed to be a fitter model for hypothalamic neurons. However, we decided to change our approach and opted to use a hypothalamic cell model better studied, in this case hypothalamic GT1-7, which had been extensively used as ARC NAG

neuronal model (Hu, Dai, et al., 2005; Susmita Kaushik et al., 2012; Morrison, Xi, White, Ye, & Martin, 2007; Ramírez, 2014). We first validated GT1-7 responsiveness to ghrelin, and we observed that ghrelin produces increased AgRP expression, as well as increased CPT1A and CPT1C mRNA levels, which can produce an increase in FAO. When FAO is activated, excessive acetyl-CoA tends to induce the formation of ketone bodies, by the induction of the expression of HMGCS2. In this model, HMGCS2 mRNA is increased in ghrelin treated cells and the co-treatment with etomoxir, a CPT1 inhibitor, reverses this induction. Moreover, etomoxir blunts ghrelin-induced AgRP, CPT1C and CPT1A mRNA raises. Since GT1-7 expresses AgRP, but not NPY, we tested the expression of several GABA metabolism enzymes in this model. We could not detect GAD2 and VGAT, but we were able to detect GAD1 and GABA shunt genes. Interestingly, the three aforementioned GABA metabolism genes have their expression induced due to ghrelin. Moreover, etomoxir reverses the ghrelin-induced changes in GABA metabolism genes, which suggests an involvement of CPT1A in this effect.

Notwithstanding, despite the expression of GABAT mRNA in GT1-7, when we assessed its activity, our experiments show it is negligible. The signal attributable to GABAT activity is not higher than the background. Moreover, when we tested whether GABA release from these cells was possible, we observed that in depolarizing KCl concentration, GT1-7 cells release neither GABA nor glutamate. However, we decided to evaluate other downstream effects of ghrelin involving lipid degradation and mitochondrial activity, as putative upstream elements to GABA neurotransmission in real GABAergic neurons.

Ghrelin reduces fatty acid oxidation, mitochondrial oxygen consumption rate and mitochondrial ROS formation in GT1-7 cells

Ghrelin has been extensively described to putatively promote an increase in FAO, due to an increased CPT1A activity because of a reduction in malonyl-CoA levels and an increase in CPT1A expression (Z B Andrews et al., 2008; Gao et al., 2013; Miguel López et al., 2008; S Obici et al., 2003; Silvana Obici et al., 2002; Ramírez et al., 2013). We have shown that GT1-7 cells are ghrelin-responsive when it comes to AgRP, CPT1A and CPT1C mRNA increases. Nonetheless, we wanted to assess the actual effects of ghrelin on CPT1A in this cells line. However, we had to discard the use of CPT1 radiometric assay. Malonyl-CoA, which is mainly responsible for the changes in CPT1A activity due to ghrelin, could be diluted during the assay and it may mask this

physiological mechanism (Zammit & Arduini, 2008). To this end we opted to analyze CPT1A metabolic products, acylcarnitines, as well as the actual FAO occurring due to the CPT1A expression.

We wanted to assess if CPT1A silencing might affect ghrelin's signaling, since this hormone increases CPT1A activity in hypothalamus, via AMPK-ACC axis. CPT1A silencing in GT1-7, using 48h adenoviral infection, efficiently reduces CPT1A activity, which is shown with a reduction to more than a half of produced acylcarnitines. Strikingly, ghrelin produces a reduction in acylcarnitines in GT1-7 cells as well. This fact contradicts the described effect of ghrelin on hypothalamic lipid metabolism. We wanted to confirm these results by testing the effect of ghrelin on final products of FAO. Surprisingly, ghrelin reduces acid-soluble products of FAO, which are mainly amino acids and intermediates of TCA cycle (Kawamura & Kishimoto, 1981), but at the same time the final product of mitochondrial respiration, carbon dioxide, has a non-significant tendency to increase. It is noteworthy that CPT1A silencing triggers some kind of compensatory effects which do not reduce acid-soluble products or carbon dioxide produced out of [¹⁴C] palmitic acid. Actually, ghrelin increases both carbon dioxide and acylcarnitines formation in CPT1A-silenced GT1-7 cells. We wonder whether this compensatory elements involve very long-chain fatty acid oxidation machinery in peroxisomes, which allow peroxisomal FAO to take place until the formation of octanoyl-CoA, which would be further transformed in mitochondria thanks to the action of peroxisomal carnitine octanoyltransferase (COT). However, acylcarnitines detected in our experimental setting are C16:0 and C18:0 acylcarnitines, none of which is product of COT.

We decided to approach to FAO with a different strategy, assessing oxygen consumption rate (OCR) in GT1-7 cells forced to use palmitic acid as source of carbon. To this end, we took advantage of a metabolic extracellular flux analyzer (XF Seahorse). The first thing we observed was a reduction of OCR when cells were forced to use palmitic acid as fuel: mitochondrial OCR dropped from 10 pmol/min/μg to 2 pmol/min/μg. Then ghrelin treatment produces a reduction in both mitochondrial and ATP-linked OCR in palmitate-fueled GT1-7. Surprisingly, when inhibiting CPT1A with etomoxir, ghrelin promotes a slight but significant increase in mitochondrial and ATP-linked OCR, which resembles carbon dioxide and acylcarnitine increases due to ghrelin in CPT1A-silenced GT1-7 cells. This effect on oxygen use might depend on the source of carbon used in the cell. To this end, we tested ghrelin effect basal conditions for GT1-7 cells. Ghrelin produces a reduction in basal OCR, which translates in a reduction in mitochondrial, ATP-linked and even in non-mitochondrial OCR. These data suggest that ghrelin

reduces in a certain way the ability of GT1-7 cells to use oxygen by the mitochondria. However, non-mitochondrial OCR, which proceeds mainly from cytosolic ROS formation, is reduced regardless of the fuel used. The reduction in mitochondrial OCR due to ghrelin could have several origins: a reduced ATP demand, some kind of damage in the electron transport chain or a drop in substrate availability. Nonetheless, ghrelin has been described traditionally to promote a switch from glucose consumption to FAO. However, this switch can be harsh in a cell type which is unprepared to oxidize fatty acids (Panov et al., 2014; Schönfeld & Wojtczak, 2012). Ghrelin had been described to increase UCP2 to buffer FAO-originated ROS formation, we tested the mitochondrial superoxide formation and we found it is decreased due to ghrelin. However, it is more probable to have this reduction due to the diminished mitochondrial activity than because of an increase in UCP2.

Therefore, all these results point out the unsuitability of GT1-7 cells as a model of hypothalamic NAG neurons because of the following three reasons: (1) GT1-7 cells respond to ghrelin increasing AgRP expression, as well as CPT1A and CPT1C mRNA, but lack NPY and GABAergic neurotransmission. (2) Ghrelin decreases CPT1A activity, measured as acylcarnitines formation and FAO, contrarily to the increase described physiologically in hypothalamus. (3) Ghrelin decreases mitochondrial activity, measured as mitochondrial OCR, contrarily to what we would expect in hypothalamus due to FAO increase. These differences in metabolic response *in vitro* and *in vivo* suggest a key role of glial cells in the effect of ghrelin in hypothalamus.

Often cell lines have limited success in mimicking neuronal physiologic responses (Gordon, Amini, & White, 2013). Neuronal cultures often lack any glial support and they have to be cultured in media which are often dissimilar to the physiological conditions in which they are nurtured *in vivo*. Moreover, the differences found between *in vitro* culture and *in vivo* neurons is not only due to the lack of glial cells to give support to the neurons, but also from the inherent characteristics of immortalized cells which sets neuronal cell lines apart from neuronal physiological responses. Furthermore, GT1-7 is serendipitously used as a model of AgRP neurons. Because of the AgRP expression it has been used as an ARC neuronal model, but this cell line was developed as a GnRH+ hypothalamic cell line (Mellon et al., 1990).

Intraperitoneal ghrelin causes differential effects in CPT1A activity in cortex and hypothalamus and reduces GABA metabolism gene expression in cortex

Since we want to assess the effects of ghrelin on amino acid neurotransmission, we opt to use a primary neuronal model, which is more likely to behave in a more physiological way than neuronal cell lines. We decide to go for primary cortical neurons, which are ghrelin-responsive and have been used to study the neuroprotective effects of ghrelin (Stoyanova et al., 2013; Stoyanova & le Feber, 2014). Moreover, cortical neurons are known to express GHSR1a (Mani et al., 2014).

Firstly, we assessed the effect of intraperitoneal ghrelin on CPT1A activity in cortex and hypothalamus. We proceeded with a double injection with 1 h treatment, as described in the seminal paper regarding GHR1a-mediated ghrelin's effect on food intake (Sun et al., 2004). We monitored the food intake of PBS- and ghrelin-injected mice and we confirmed that the latter show hyperphagia. After 1h, we sacrificed the animals and obtained samples of cortical tissue and the hypothalamus. We analyzed the acylcarnitine content in hypothalamus and cortex of both groups. Ghrelin produces an increase in acylcarnitines found in hypothalamus, while in the same mice, cortical acylcarnitines are reduced. The raise in acylcarnitines was expected due to the increase in CPT1A activity in hypothalamus. However, the reduction in cortical acylcarnitines, was a result completely unannounced. The effect of ghrelin in cortical CPT1A activity and FAO has not been previously assessed. This surprising reduction in cortical acylcarnitines due to ghrelin follows a similar trend to the effect of ghrelin on acylcarnitines of GT1-7 cells. Notwithstanding, the reduction in hypothalamic GT1-7 neuronal cell line differs from the increased acylcarnitines observed in hypothalamus after intraperitoneal injection and it does not follow the AMPK-ACC-malonyl-CoA-CPT1 axis hypothesis in the control of food intake and energy homeostasis (Andersson et al., 2004; Z B Andrews et al., 2008; Cha, Hu, Chohnan, & Lane, 2005; Hu, Dai, et al., 2005; Kola et al., 2008; Lane et al., 2008; Loftus et al., 2000; Miguel López et al., 2008). Once again, GT1-7 cells are revealed as a neuronal cell line with limited success to reproduce metabolic mechanisms found in hypothalamus *in vivo*, but intriguingly GT1-7 cells seem to reproduce a pattern more similar to primary cortical neurons. This suggest that astrocytes in cortex and hypothalamus may have a different role in modulating the metabolism in the two areas, promoting a differential response to ghrelin.

Then we assessed the effect of ghrelin on cortical mRNA levels of several lipid metabolism genes. We observe a reduction of almost a third in ACC2 and also slight but significant reductions in CPT1C, CrAT and COT mRNA levels. With this data it becomes evident that not only CPT1A activity is reduced by ghrelin, but also other lipid metabolism genes expression and interestingly in an opposite sign compared to ghrelin's effect in hypothalamic lipid metabolism. Since ghrelin modulates neuropeptides and other neurotransmitters in hypothalamus, we wanted to assess its effect in cortical amino acid neurotransmitters metabolism in neurons. Ghrelin produces a significant reduction around 20-25% in all the genes involved in GABAergic quantal size control (GAD1, GAD2, VGAT and GABAT), with the exception of SSADH, which shows a non-significant tendency to decrease as well. Moreover, VGLUT3, which is a vesicular glutamate transporter related to GABAergic neurons (Herzog et al., 2004), is also significantly reduced. All these results suggest a reduction in GABA metabolism genes which would imply a reduction in GABA quantal size to be released. Hypothalamic GAD1 has been described to be a reliable marker for GABAergic release (Dicken et al., 2015). The mRNA reduction found in many of the genes involved in GABA metabolism may be indicative of a reduction in GABAergic output, but it should be further assessed.

To sum up, intraperitoneal ghrelin seems to modulate *in vivo* cortical CPT1A activity, as well as GABA metabolism in cortex, which in some cases would explain part of the central extra-hypothalamic effects of ghrelin (Zane B. Andrews, 2011; Atalayer et al., 2013; Caroline Hansson et al., 2013; Kent et al., 2015; Kluge et al., 2011; Meyer et al., 2014; Perello et al., 2010; Spencer et al., 2012; Stoyanova & le Feber, 2014). Due to these results, in order to deepen in the role of ghrelin and CPT1A in the control of GABA neurotransmission in cortex, we decide to use primary cortical neurons as a model to study their effects.

Ghrelin reduces GABA release in primary cortical neurons

Primary cortical neuronal cultures have a mixture of GABAergic and glutamatergic neurons. We tested the effect of ghrelin on GABA release at different glucose concentrations. These neuronal cultures need 25 mM glucose for maintenance, but this concentration is far from physiological. CSF glucose concentration oscillates between 2.5-4 mM glucose and since glucose is essential for the formation of the neurotransmitters' backbone, we decided to study the effect of ghrelin at different glucose concentrations. Only at 5 mM glucose and with no glucose at all,

released GABA with depolarizing stimuli was reduced significantly. Glutamate release was also reduced due to ghrelin in glucose-deprived conditions. Interestingly, the maximum GABA and glutamate released was observed at 5 mM glucose. Therefore, we decided to carry on the experiments with this concentration which was the closest to glycorrachia amongst the tested concentrations. Moreover, 5 mM glucose was the concentration tested in GT1-7 cells, because of the same reasons.

To have a first approach to CPT1A involvement in the effect of ghrelin on GABA release, we inhibited pharmacologically it by using etomoxir. The CPT1A pharmacological inhibition blunts ghrelin reduction of GABA release, suggesting some kind of involvement of the enzyme in this process. We further checked the changes produced by ghrelin and etomoxir in the mRNA expression of several genes involved in CPT1A activity and GABA metabolism. Ghrelin produces an increase in CPT1A, CPT1C and HMGCS2 mRNA expression, as well as an increase in GAD1 and SSADH. Interestingly, the expression pattern differs from the one observed in cortex after intraperitoneal ghrelin injection, in which GABA metabolic enzymes expression was diminished.

CPT1AM expression does not reduce GABA release in primary cortical neurons

Then we approached to the role of CPT1A in GABA metabolism by overexpressing it in primary cortical neurons. We performed a time course experiment to analyze the effect of the infection at different times. After 24h of infection, the mRNA expression pattern is similar to the one observed due to ghrelin treatment, so we performed ongoing experiments at that infection time. The experiments were performed using 5 mM and 25 mM glucose media. Thus we studied whether the effect is dependent on the glucose concentration as well, in an overexpression situation in which mimics ghrelin's effect. At 5 mM glucose, CPT1AM overexpression causes an increase in HMGCS2, VGAT, GAD1, GAD2 and GABAT and SSADH. Interestingly, these increases do not happen at 25 mM glucose, but contrarily, GABAT and VGAT have their mRNA levels reduced. All these data suggest that mRNA changes due to ghrelin and CPT1A are not exclusively ghrelin-dependent, but rely in other factors, such as glucose availability.

GABA release was tested using the same conditions. Surprisingly, CPT1AM overexpression does not cause any changes in GABA release in depolarizing conditions at 5 mM

glucose. More strikingly, at 25 mM glucose, the overexpression triggers an increase in GABA release. On the one hand, the higher glucose concentration and the increased FAO would lead to an increase in TCA cycle intermediates, given the increase in pyruvate used to generate oxaloacetate and the increase in acetyl-CoA from fatty acids degradation. Given the disruption of the switch mechanism composed by malonyl-CoA and CPT1A's malonyl-CoA-sensitivity, the overexpression generates a non-physiological process in which both glycolysis and FAO are activated at the same time, contrarily to a neuronal reinterpretation of Randle's hypothesis (Randle, Garland, Hales, & Newsholme, 1963). Physiologically, when glycolysis is active, part of the acetyl-CoA might be used in fatty acid biosynthesis to generate malonyl-CoA. This fatty acid precursor would in turn block FAO via inhibiting CPT1A to block any futile cycle. However, when overexpressing a malonyl-CoA-insensitive CPT1A, both processes are active, promoting an increase in TCA cycle intermediates. This raise would in turn activate anabolic/cataplerotic processes in order to control the excess of reductive power generated by the excess of carbon backbones from both processes. In GABAergic neurons, the increase in α -ketoglutarate and succinate would lead to an increase in glutamate and GABA formation. This agrees with the increased GABA release observed due to CPT1AM overexpression in 25 mM glucose medium. Nonetheless, this glucose concentration is far from being physiological, but it shows there is a direct link between GABA production and release and lipid metabolism (**Fig 75**).

On the other hand, these data suggest that other factors are involved in the control of GABA release besides CPT1A as a downstream ghrelin effector in the AMPK-ACC-CPT1 axis. Ghrelin, which hypothetically activates CPT1A activity, is able to reduce GABA release at 5 mM glucose. However, CPT1AM overexpression does not render the same result at 5 mM glucose. Here we have several factors to take into account. Firstly, the overexpression is measured after a 24 h infection, which may trigger some adaptation in the system. Ghrelin-driven activation of CPT1A is fastly promoted by the decrease in malonyl-CoA. Nonetheless, CPT1A increased activity in CPT1AM-overexpressing neurons is not so sudden, it starts after the virus-contained genes are expressed, with its maximum at 48 h. Moreover, since FAO-originated acetyl-CoA may saturate TCA cycle, it could trigger the expression of HMGCS2 which may leak excessive acetyl-CoA into the generation of ketone bodies if neurons were neat ketogenic cells, which are not. However, in our astrocyte-less neuronal culture, we do observe an increase in HMGCS2 when overexpressing CPT1AM in low glucose medium. Probably, neurons could reroute *in vivo* this excess of acetyl-CoA into glial cells somehow. Moreover, we should take into account postranslational inactivation of HMGCS2 due to succinylation (Hegardt, 1999; Lowe & Tubbs, 1985), which is likely to occur in the tested high glucose situation. To sum up, the putative

reduction in TCA cycle intermediates discards the possibility of using them in GABA biosynthesis and GABA shunt.

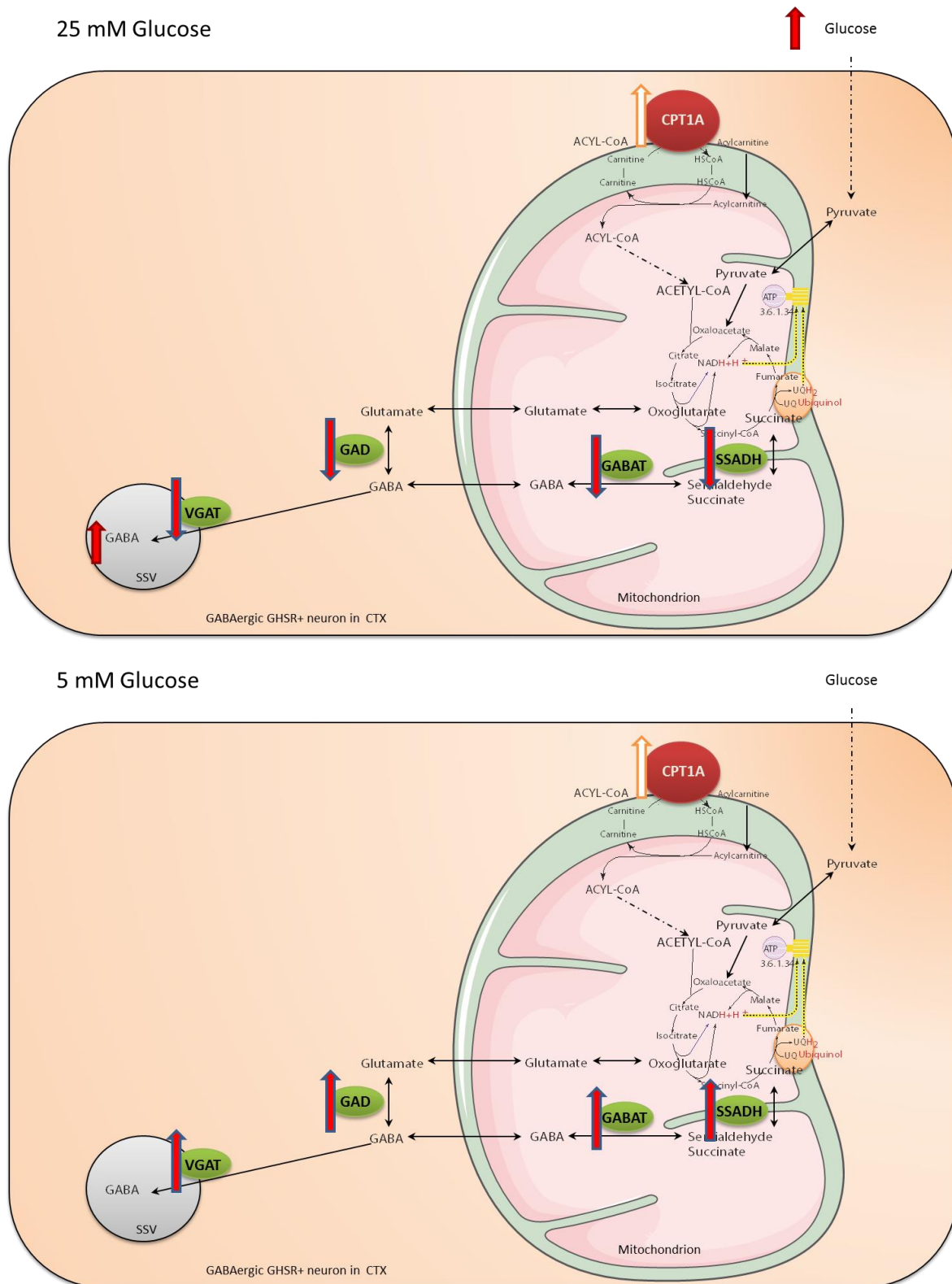


Fig 75. Effect of CPT1AM overexpression on GABA metabolism depending on glucose concentration in the medium

When analyzing mRNA expression patterns, VGAT and GABAT are downregulated in a situation in which GABA release is increased, when overexpressing CPT1AM with 25 mM glucose medium. This would suggest some kind of compensatory effect trying to reverse the metabolic changes produced on GABA pool due to the overexpression. However, with higher glucose concentration, most of GABA metabolism genes are upregulated in CPT1AM-overexpressing neurons, but no reduction in GABA release takes place. However, we cannot discard that it may reduce mitochondrial GABA pool, which may affect releasable GABA pool at the long term. Moreover, ghrelin may exert the reduction in GABA release not only by reducing its pool, but also affecting neurotransmitter vesicular exocytosis, which may explain the lack of reduction on GABA release.

CPT1A deletion blunts ghrelin-induced reduction of GABA release and both ghrelin and CPT1A deletion reduce α -ketoglutarate and citrate in cortical neurons

Instead of silencing CPT1A expression with a shRNA against it, we decided to eliminate it completely. Thus we would avoid any compensatory effects on CPT1A expression. To do so, we obtained a mouse whose CPT1A exon 4 is flanked by two loxP sequences. Nevertheless, at the end of the development of this project we knew that another research groups had generated mice with floxed CPT1A sequence successfully (Schoors et al., 2015). Despite this, we carried on obtaining our model. We obtained potentially conditional knockout mice which were obtained using homology recombination in the EUCOMM program. We eventually used the HEPD0727_3_H09 clone, which was the fittest to be injected in the blastocysts. We analyzed the chimerae obtained by using ddPCR technology to validate that the only recombination given in the clones was in homology. Thus, we validated that only a copy of the construct was introduced, and we proceeded to obtain CPT1A^(+/loxP) mice from the heterozygous. We obtained the sequence of the recombined critical region and confirmed that the elements within have not mutated. Primary cells were obtained from CPT1A^(loxP/loxP) mice and they were infected with CRE recombinase adenovirus. The expression of CRE recombinase produced a successful elimination of exon 4 and a reduction in wildtype CPT1A mRNA. Interestingly, the elimination of exon 4 seems to produce a reduced viability of the mRNA outcome of CPT1A.

We evaluated the changes in mRNA expression in different GABA metabolism genes due to the elimination of CPT1A. This appraisal show there is direct link between CPT1A activity and GABA metabolism, since mRNA expression in GABA shunt genes, GAD1 and VGAT drop substantially with CPT1A deletion. Interestingly, no significant changes appear due to ghrelin treatment. This fact suggests that GABA metabolism gene expression changes observed in basal state are due to counter regulatory effects given after metabolic changes. It becomes clear that changes in GABA metabolism mRNA depend on other factors such as substrate availability in CPT1AM overexpression. In this model, factors like glycolysis activation or CPT1A activation or deletion seem to be involved in the activation of GABA metabolism. These processes yield the carbon backbones needed for the generation of GABA, especially out of pyruvate. However, in our model both changes in acetyl-CoA (from glycolysis and FAO) and pyruvate (from glycolysis) would be responsible for the modification of TCA intermediates amounts needed for the generation of GABA. This is evident with the activation of both FAO and glycolysis by the overexpression of CPT1AM in a high glucose medium. The importance of TCA cycle intermediates as carbon backbone donors for the GABA biosynthesis is clear when we study the changes in GABA release. The isocitrate dehydrogenase inhibitor, 2-hydroxyglutarate, which stops TCA cycle, produces a significant decrease in GABA release. Intriguingly, ghrelin produces exactly the same effect and the deletion of CPT1A blunts it. These data suggests that ghrelin produces changes in substrate availability for GABA biosynthesis. We have not assessed the metabolism of other amino acids, that could be modified due to effect of ghrelin and explain the drop of some of the TCA intermediates. Moreover, we should assess whether this modulation may be controlled by the changes in CPT1A activity promoted by ghrelin.

Due to the clues given by TCA cycle inhibition effect on GABA release, we decided to evaluate the effect of ghrelin and CPT1A deletion on cellular content of the different TCA cycle intermediates and mitochondrial activity and oxygen consumption to shed more light on the mechanistic insight of the observed phenomena. When treated with ghrelin in a 5 mM glucose medium, primary cortical neurons have their citrate and α -ketoglutarate content reduced. Interestingly, CPT1A deletion reduces these two TCA as well, which are two of the initial Krebs cycle intermediates. However, neither malate nor fumarate have their levels significantly reduces, and interestingly succinate, which is the intermediate involved in GABA shunt has a non-significant tendency to increase. Somehow, both ghrelin and CPT1A seem to reduce the initial TCA intermediates but since subsequent steps tend to be unchanged, let us wonder whether anaplerotic pathways are replenishing the TCA intermediates. The tendency of succinate to be increased due to ghrelin would suggest that maybe GABA shunt is active at this

point. However, our results with GABAT activity suggest that this anaplerotic pathway is reduced.

Ghrelin reduces mitochondrial oxygen consumption in cortical neurons

Furthermore, we assessed oxygen consumption changes due to ghrelin in primary cortical neurons (Table 6). We have tested OCR at three different conditions: with a medium which contains glucose as main fuel, the closest to a physiological state; with a medium containing high glucose concentration; and with a medium which contains palmitate as main fuel. The use of different fuel sources and the actual impact in ATP synthesis and the extra mitochondrial oxygen consumption has given valuable information about the bioenergetic processes taking place. Ghrelin seems to have a direct impact on the ATP biosynthesis, since ghrelin reduces ATP production in a glucose concentration closer to glycorrachia and in a medium containing physiological glucose levels but with palmitate as main source of carbon. Interestingly, ghrelin increases mitochondrial OCR in a high glucose medium. It is noteworthy, that ATP-linked mitochondrial OCR has a tendency to increase due to ghrelin, but it is non-significant. However, the deletion of CPT1A increases ATP-linked OCR due to ghrelin. This suggests that a high glucose medium promotes a ghrelin-dependent activation of mitochondrial respiration. This effect is boosted by the deletion of CPT1A to enhance ATP biosynthesis. The differential effects depending on glucose concentration suggest once again that ghrelin acts as a metabolic switch.

Fuel	Ghrelin	CPT1A	ATP-linked OCR		Non-mitochondrial OCR	
			+	-	+	-
Glucose	-		c	=	c	↓
	+		↓	=	↓	↓
High Glucose	-		c	=	c	↓
	+		=	↑	↓	↓
Palmitate	-		c	=	c	↑
	+		↓	=	↑	↑

Table 6. Effect of CPT1A deletion and ghrelin in primary cortical neurons on mitochondrial respiration and non-mitochondrial oxygen consumption. The table shows summarizes changes in OCR referred to each control(c): increased (↑), decreased (↓) or similar (=) OCR

However, FAO has not been taken into account as a metabolic modulator for other neuronal processes. Interestingly, the changes in ATP production in a high glucose medium due to ghrelin are lost. Unless CPT1A is deleted, which actually produces the contrary effect: ghrelin increases ATP production when CPT1A is not present.

Despite some of our experimental results are surprising, they agree with most of the previous literature. Ghrelin, whose effect is mediated in most of the cases by AMPK triggers an activation of FAO and glycolysis. AMPK activation, which is a counter regulatory mechanism to fight low energy states, enhances catabolic processes in order to obtain energy. Amongst them, FAO and glycolysis are activated in most of the tissues. However, FAO as a main process for energy production in brain has been classical dismissed due to the multiple side effects which may appear with it: increased risk of hypoxia, increased ROS generation and difficulties matching ATP requirements and production to sustain neuronal electrical activity. In this project we have tried to discern the importance of CPT1A as a downstream effector of ghrelin in a neuronal context (Schönfeld & Reiser, 2013). Nonetheless, the involvement of AMPK-ACC-CPT1 axis in ghrelin modulation of orexigenic neuropeptides expression has been repeatedly validated, but in a more physiological context in which neurons have astrocytic support.

On the one hand, the expression of a constitutively active isoform of CPT1A in VMH promotes an increase in VGAT, which may putatively promote an increase in GABA vesicular quantal size and release. Moreover, we have again confirmed the increase in CPT1A activity in hypothalamus due to ghrelin intraperitoneal injection.

On the other hand, ghrelin reduces CPT1A activity in cortex, which is confirmed with a reduced capacity of palmitate oxidation in primary cortical neurons. Intriguingly, hypothalamic GT1-7 cells show reduced CPT1A activity due to ghrelin. This happens contrarily to the *in vivo* cortical results and the results of primary cortical neuronal cultures. Besides the reduction in CPT1A activity, it promotes in cortical neurons a reduction in citrate and succinate, a reduction in mitochondrial respiration, a reduction *in vivo* of the mRNA expression of GADs, SSADH, GABAT and VGAT, a reduction in GABAT activity and a reduction in GABA release (**Fig 76**).

2016). This fact agrees with the reduction in oxygen consumption observed due to ghrelin both in primary cortical neurons and GT1-7 cells, which suggests a similar phenomenon in our models, which should be assessed. That study is mainly focused on astrocyte glutamate metabolism. They show that glucose uptake is reduced in astrocytes as well. However, glutamate uptake and protein expression of glutamate transporters is increased. Interestingly, glutamine synthetase, which facilitates neuronal reuptake of glutamate carbon backbones from astrocytes, has its protein levels reduced. Moreover, lactate formation remains unchanged, which suggests a sequestration of astrocytes as fuel donors to neurons in hypothalamus. Interestingly, we have observed intraperitoneal ghrelin increases CPT1A activity in hypothalamus, which may use fatty acids as a substitutive fuel for energy generation. However, we cannot discern in this context the cell types which show CPT1A activation, since we collected the whole hypothalamus. Intriguingly, ICV ghrelin injection increases hypothalamic GAD65, codified by GAD2 gene in neurons (Fuente-Martín et al., 2016). This agrees with the increased GABA output shown in fasted mice and increased GAD1, which has been presented as a proxy marker of increased GABAergic transmission (Dicken et al., 2015).

Another intriguing factor worth-studying is the mechanism by which ghrelin produces the differential effects in both GABA metabolism and FAO depending on the brain region. The hypothalamic proximity to fenestrated capillaries may light this issue, since makes neurons less dependent on the carbon sources found in CSF. Hypothalamic cells could use more easily the scarce nutritional resources found in blood when ghrelin increases during fasting. Moreover, a hypothetical differential responsiveness to ghrelin of the astrocytes found in hypothalamus and cortex may explain the dissimilar results in the two brain areas.

From the hypothalamic perspective, our in vivo model highlights the importance of CPT1A and amino acid neurotransmission for the modulation of the food intake. Interestingly, our animal model shows hyperphagia independently from its satiety state. Moreover, NPY and AgRP remain unchanged. One may suggest that the sacrifice of the animals after fasting would influence the orexigenic neuropeptides expression. However, the satiety test shows that CPT1A rats' food intake is higher independently if they have been fasted or fed. This shows that their hyperphagia was not necessarily regulated by the expression of NPY and AgRP, since their mRNA levels were similar in both hyperphagic and normophagic rats, when fasted. The importance of GABA regulation of food intake is increasing in the last years. However, little is known about the influence of the glutamate output. On the one hand, scientific literature suggests that GABA neurotransmission in MBH comes mainly from arcuate NAG neurons

(Dicken et al., 2015; Krashes et al., 2013; Tong et al., 2008). On the other hand, the most abundant glutamatergic population of neurons in MBH is located mainly in VMH (Cheung et al., 2015; Tejas-Juárez et al., 2014), where precisely we have performed our intervention. However, the changes in vesicular transporters have been observed both in glutamatergic and GABAergic neurotransmission. How can the latter, which putatively proceeds from ARC be influenced by an increase in CPT1A performed in VMH? This fact suggests some kind of regulation of NAG neurons from VMH neurons. Another option would be the presence of GABAergic neurons in VMH specifically in our model, which is possible but unlikely. This point needs further assessment.

When setting our focus on cortical neurons, ghrelin reduction of GABAergic output in cortex could explain some of the central extra-hypothalamic effects of this gastric hormone. Starting from the anxiogenic and alertness effect needed to complement hypothalamic effects for foraging in animals (Thomas MA et al 2015) and to block sleep (Szentirmai et al 2006), which become evident in a paradigm in which inhibitory neurotransmitters, such as GABA, have reduced output. Furthermore, ghrelin's neuroprotective effect with enhanced memory and spatial learning in mice (Davis et al 2011; Diano et al 2006) has been described to be tightly related to mitochondrial metabolism modulation (Andrews et al 2009). Here we show that mitochondrial respiration is also related to mitochondrial capacity of biosynthesizing GABA in cortical neurons, and both processes seem to be related to ghrelin's capacity of modulating mitochondrial activity. It becomes evident that CPT1A acts as a part of the mechanism by which ghrelin can modulate mitochondrial processes, since the deletion of its gene promotes deep changes in the metabolic responsiveness of the neuron to ghrelin. Interestingly, CPT1A deletion seems to trigger extra-mitochondrial metabolic processes, which become evident when forcing the neurons to use palmitate as a source of carbon. However, the relationship of those processes to the blunting of ghrelin modulation of GABA neurotransmission remains to be uncovered.

One of the strengths, and also a weakness of our neuronal model, is the lack of astrocytes interrelationship. However, some authors undertone the importance of astrocytes in GABAergic neurotransmission, since they suggest that GABA reuptake from the synaptic cleft is performed mainly into the presynaptic neuron, unlike glutamate, which is recovered by the astrocyte and sent back to the neuron in the form of glutamine. Moreover, they state that GABA has barely no bioenergetic implication in astrocytes (Chatton, Pellerin, & Magistretti, 2003). Nonetheless, this hypothesis is currently discussed, but the released GABA does not originate from the glutamate pool recovered from glutamine uptaken from the synaptic cleft. Contrarily, it

is formed out of the TCA cycle intermediates. Therefore, ghrelin-dependent changes in released GABA appear due to changes in succinate and α -ketoglutarate. Thus, ghrelin triggers a reduction in mitochondrial respiration and TCA intermediates, which eventually affects the releasable pool of GABA.

Therefore, our data, together with previously published literature, suggests that mitochondrial activation mediates ghrelin modulation of GABA neurotransmission from a metabolic point of view. In the hypothalamus, this effect is added to the modulation of arcuate neuropeptides expression. Both neuropeptides and amino acid neurotransmitters are responsible for the modulation of the food intake. Moreover, this metabolic and mitochondrial modulation triggered by ghrelin might be involved in the central extra-hypothalamic processes in which it has been described to be involved.

CONCLUSIONS

1. CPT1AM overexpression in VMH of Sprague-Dawley rats causes hyperphagia and overweight. CPT1AM rats are hyperphagic regardless their satiety state.
2. Mechanistically, hyperphagia in CPT1AM rats seems to be independent from changes in NPY, AgRP, POMC and CART expression. However, it triggers ROS-buffering enzymes and UCP2 which have been described to be involved in AgRP and NPY expression.
3. CPT1AM overexpression in VMH reduces VGLUT2 and increases VGAT mRNA levels. This suggests that CPT1A may be involved in the modulation of amino acid neurotransmission.
4. CPT1AM overexpression in VMH promotes important changes in lipidomic profile. It produces a reduction in phospholipids and an increase in sphingolipids found in MBH, such as ceramides C18:1 and C14:0, which have been described to control food intake. Moreover, these lipidomic changes may affect the vesicular lipid composition and modify neurotransmitters release in hypothalamus.
5. Ghrelin reduces CPT1 activity and acid-soluble products of fatty acid oxidation in GT1-7. This lipid catabolism reduction is accompanied by a reduction in ROS formation and a reduction in mitochondrial respiration. These data suggest that GT1-7 cells behave differently than neurons in hypothalamus.
6. Hypothalamic neuronal cell lines, such as mHypo-N29/4, mHypo-N43/5, mHypo-N41 and GT1-7, have limited validity as hypothalamic GABAergic neuronal models. In particular, GT1-7 lacks key GABA metabolism enzymes (VGAT and GAD2) and they do not release GABA in depolarizing conditions.
7. Intraperitoneal ghrelin administration produces an increase in acylcarnitines in mice hypothalamus, but surprisingly, acylcarnitines are reduced in cortical tissue. This fact suggests a differential action of ghrelin when it comes to fatty acid oxidation in the two brain areas.

8. The expression of genes in GABA metabolism is reduced in cortex after intraperitoneal ghrelin administration. GABAT activity in cortex is reduced as well. This does not match the increase in GABA output observed in hypothalamus of mice after fasting, which suggest also a differential effect of ghrelin in both brain areas.
9. Ghrelin increases the mRNA levels of genes involved in GABA metabolism. Moreover, ghrelin reduces GABA release in primary cortical neurons which is reversed by both pharmacological inhibition and genetic deletion of CPT1A. This reduction is glucose dependent, since high glucose medium reduces GABAergic output and blunts any effect of ghrelin.
10. CPT1A overexpression in primary cortical neurons at low glucose, promotes an expression pattern of GABA genes similar to the one observed due to ghrelin treatment. However, the appraisal of GABA release shows no changes due to CPT1A overexpression at low glucose. These data suggest that ghrelin effect on GABA release is not entirely dependent on CPT1A modulation, but it may rely on other factors.
11. Both ghrelin and CPT1A deletion in primary cortical neurons produce a reduction in citrate and α -ketoglutarate content. Ghrelin reduces mitochondrial respiration in primary cortical neurons and availability of fatty acids triggers non-mitochondrial oxygen consumption.
12. Ghrelin and CPT1A deletion and overexpression modulate mitochondrial function in primary cortical neurons, yielding changes in GABA metabolism, which affect eventually to GABAergic neurotransmission.

REFERENCES

- Akaboshi, S., Hogema, B. M., Novelletto, A., Malaspina, P., Salomons, G. S., Maropoulos, G. D., ... Gibson, K. M. (2003). Mutational spectrum of the succinate semialdehyde dehydrogenase (ALDH5A1) gene and functional analysis of 27 novel disease-causing mutations in patients with SSADH deficiency. *Human Mutation*, *22*(6), 442–50. doi:10.1002/humu.10288
- Akamizu, T., Shinomiya, T., Irako, T., Fukunaga, M., Nakai, Y., Nakai, Y., & Kangawa, K. (2005). Separate measurement of plasma levels of acylated and desacyl ghrelin in healthy subjects using a new direct ELISA assay. *The Journal of Clinical Endocrinology and Metabolism*, *90*(1), 6–9. doi:10.1210/jc.2004-1640
- Albers, R. W., & Koval, G. J. (1961). Succinic semialdehyde dehydrogenase: Purification and properties of the enzyme from monkey brain. *Biochimica et Biophysica Acta*, *52*(1), 29–35. doi:10.1016/0006-3002(61)90900-3
- Allocca, M., Mussolino, C., Garcia-Hoyos, M., Sanges, D., Iodice, C., Petrillo, M., ... Auricchio, A. (2007). Novel adeno-associated virus serotypes efficiently transduce murine photoreceptors. *Journal of Virology*, *81*(20), 11372–80. doi:10.1128/JVI.01327-07
- Alvarez-Crespo, M., Skibicka, K. P., Farkas, I., Molnár, C. S., Egecioglu, E., Hrabovszky, E., ... Dickson, S. L. (2012). The Amygdala as a Neurobiological Target for Ghrelin in Rats: Neuroanatomical, Electrophysiological and Behavioral Evidence. *PLoS ONE*, *7*(10). doi:10.1371/journal.pone.0046321
- Amir, S. (1990). Intra-ventromedial hypothalamic injection of glutamate stimulates brown adipose tissue thermogenesis in the rat. *Brain Research*, *511*(2), 341–4. Retrieved from <http://www.ncbi.nlm.nih.gov/pubmed/1970749>
- Andersson, U., Filipsson, K., Abbott, C. R., Woods, A., Smith, K., Bloom, S. R., ... Small, C. J. (2004). AMP-activated protein kinase plays a role in the control of food intake. *The Journal of Biological Chemistry*, *279*(13), 12005–8. doi:10.1074/jbc.C300557200
- Andrews, Z. B. (2011). The extra-hypothalamic actions of ghrelin on neuronal function. *Trends in Neurosciences*. doi:10.1016/j.tins.2010.10.001
- Andrews, Z. B., Erion, D., Beiler, R., Liu, Z.-W., Abizaid, A., Zigman, J., ... Horvath, T. L. (2009). Ghrelin promotes and protects nigrostriatal dopamine function via a UCP2-dependent mitochondrial mechanism. *The Journal of Neuroscience: The Official Journal of the Society for Neuroscience*, *29*(45), 14057–65. doi:10.1523/JNEUROSCI.3890-09.2009
- Andrews, Z. B., Liu, Z. W., Wallingford, N., Erion, D. M., Borok, E., Friedman, J. M., ... Diano, S. (2008). UCP2 mediates ghrelin's action on NPY/AgRP neurons by lowering free radicals.

- Nature*, 454(7206), 846–851. Retrieved from http://www.ncbi.nlm.nih.gov/entrez/query.fcgi?cmd=Retrieve&db=PubMed&dopt=Citation&list_uids=18668043
- Aponte, Y., Atasoy, D., & Sternson, S. M. (2011). AGRP neurons are sufficient to orchestrate feeding behavior rapidly and without training. *Nature Neuroscience*, 14(3), 351–5. doi:10.1038/nn.2739
- Arduini, A., Denisova, N., Virmani, A., Avrova, N., Federici, G., & Arrigoni-Martelli, E. (1994). Evidence for the involvement of carnitine-dependent long-chain acyltransferases in neuronal triglyceride and phospholipid fatty acid turnover. *Journal of Neurochemistry*, 62(4), 1530–8. Retrieved from <http://www.ncbi.nlm.nih.gov/pubmed/8133280>
- Asakawa, A., Inui, A., Kaga, T., Yuzuriha, H., Nagata, T., Fujimiya, M., ... Kasuga, M. (2001). A role of ghrelin in neuroendocrine and behavioral responses to stress in mice. *Neuroendocrinology*, 74(3), 143–147. doi:10.1159/000054680
- Atalayer, D., Gibson, C., Konopacka, A., & Geliebter, A. (2013). Ghrelin and eating disorders. *Progress in Neuro-Psychopharmacology & Biological Psychiatry*, 40, 70–82. doi:10.1016/j.pnpbp.2012.08.011
- Atasoy, D., Betley, J. N., Su, H. H., & Sternson, S. M. (2012). Deconstruction of a neural circuit for hunger. *Nature*, 488(7410), 172–7. doi:10.1038/nature11270
- Attwell, D., & Laughlin, S. B. (2001). An energy budget for signaling in the grey matter of the brain. *Journal of Cerebral Blood Flow and Metabolism: Official Journal of the International Society of Cerebral Blood Flow and Metabolism*, 21(10), 1133–1145. doi:10.1097/00004647-200110000-00001
- Auger, C., & Attwell, D. (2000). Fast Removal of Synaptic Glutamate by Postsynaptic Transporters. *Neuron*, 28(2), 547–558. doi:10.1016/S0896-6273(00)00132-X
- Bak, L. K., Schousboe, A., & Waagepetersen, H. S. (2006). The glutamate/GABA-glutamine cycle: aspects of transport, neurotransmitter homeostasis and ammonia transfer. *Journal of Neurochemistry*, 98(3), 641–53. doi:10.1111/j.1471-4159.2006.03913.x
- Ballabh, P., Braun, A., & Nedergaard, M. (2004). The blood-brain barrier: An overview: Structure, regulation, and clinical implications. *Neurobiology of Disease*. doi:10.1016/j.nbd.2003.12.016
- Banks, W. A., Tschop, M., Robinson, S. M., & Heiman, M. L. (2002). Extent and direction of ghrelin transport across the blood-brain barrier is determined by its unique primary structure. *Journal of Pharmacology and Experimental Therapeutics*, 302(2), 822–827. doi:10.1124/jpet.102.034827
- Bayliss, J. A., & Andrews, Z. B. (2013). Ghrelin is neuroprotective in Parkinson's disease:

- molecular mechanisms of metabolic neuroprotection. *Therapeutic Advances in Endocrinology and Metabolism*, 4(1), 25–36. doi:10.1177/2042018813479645
- Bayliss, J. A., Lemus, M. B., Stark, R., Santos, V. V., Thompson, A., Rees, D. J., ... Andrews, Z. B. (2016). Ghrelin-AMPK Signaling Mediates the Neuroprotective Effects of Calorie Restriction in Parkinson's Disease. *Journal of Neuroscience*, 36(10), 3049–3063. doi:10.1523/JNEUROSCI.4373-15.2016
- Bell, C. G., Walley, A. J., & Froguel, P. (2005). The genetics of human obesity. *Nature Reviews. Genetics*, 6(3), 221–34. doi:10.1038/nrg1556
- Besse, A., Wu, P., Bruni, F., Donti, T., Graham, B. H., Craigen, W. J., ... Bonnen, P. E. (2015). The GABA transaminase, ABAT, is essential for mitochondrial nucleoside metabolism. *Cell Metabolism*, 21(3), 417–27. doi:10.1016/j.cmet.2015.02.008
- Beverly, J. L., & Martin, R. J. (1989). Increased GABA shunt activity in VMN of three hyperphagic rat models. *The American Journal of Physiology*, 256(6 Pt 2), R1225–31. Retrieved from <http://ajpregu.physiology.org/content/256/6/R1225.abstract>
- Bignami, A. (1991). Glial cells in the central nerve system. *Discussions in Neuroscience*, 8, 1–45.
- Bouret, S. G., Draper, S. J., & Simerly, R. B. (2004). Formation of projection pathways from the arcuate nucleus of the hypothalamus to hypothalamic regions implicated in the neural control of feeding behavior in mice. *The Journal of Neuroscience: The Official Journal of the Society for Neuroscience*, 24(11), 2797–2805. doi:10.1523/JNEUROSCI.5369-03.2004
- Bowers, C. Y., Momany, F., Reynolds, G. A., Chang, D., Hong, A., & Chang, K. (1980). Structure-activity relationships of a synthetic pentapeptide that specifically releases growth hormone in vitro. *Endocrinology*, 106(3), 663–667. doi:10.1210/endo-106-3-663
- Bowers, C. Y., Reynolds, G. A., Durham, D., Barrera, C. M., Pezzoli, S. S., & Thorner, M. O. (1990). Growth hormone (GH)-releasing peptide stimulates GH release in normal men and acts synergistically with GH-releasing hormone. *Journal of Clinical Endocrinology and Metabolism*, 70(4), 975–982.
- Braitenberg, V. (1992). *Corticonics: Neural Circuits of the Cerebral Cortex. Trends in Neurosciences* (Vol. 15). doi:10.1016/0166-2236(92)90361-B
- Britton, C. H., Mackey, D. W., Esser, V., Foster, D. W., Burns, D. K., Yarnall, D. P., ... McGarry, J. D. (1997). Fine chromosome mapping of the genes for human liver and muscle carnitine palmitoyltransferase I (CPT1A and CPT1B). *Genomics*, 40(1), 209–11. doi:10.1006/geno.1996.4539
- Broglio, F., Gottero, C., Benso, A., Prodam, F., Destefanis, S., Gauna, C., ... Ghigo, E. (2003). Effects of ghrelin on the insulin and glycemic responses to glucose, arginine, or free fatty acids load in humans. *Journal of Clinical Endocrinology and Metabolism*, 88(9), 4268–4272.

doi:10.1210/jc.2002-021940

- Bruning, J. C. (2000). Role of Brain Insulin Receptor in Control of Body Weight and Reproduction. *Science*, 289(5487), 2122–2125. doi:10.1126/science.289.5487.2122
- Caixàs, A., Albert, L., Capel, I., & Rigla, M. (2014). Naltrexone sustained-release/bupropion sustained-release for the management of obesity: review of the data to date. *Drug Design, Development and Therapy*, 8, 1419–27. doi:10.2147/DDDT.S55587
- Canals, D., Mormeneo, D., Fabriàs, G., Llebaria, A., Casas, J., & Delgado, A. (2009). Synthesis and biological properties of Pachastrissamine (jaspine B) and diastereoisomeric jaspines. *Bioorganic & Medicinal Chemistry*, 17(1), 235–41. doi:10.1016/j.bmc.2008.11.026
- Caraty, A., Fabre-Nys, C., Delaleu, B., Locatelli, A., Bruneau, G., Karsch, F. J., & Herbison, A. (1998). Evidence that the mediobasal hypothalamus is the primary site of action of estradiol in inducing the preovulatory gonadotropin releasing hormone surge in the ewe. *Endocrinology*, 139(4), 1752–60. doi:10.1210/endo.139.4.5904
- Carlini, V. P., Monzón, M. E., Varas, M. M., Cragolini, A. B., Schiöth, H. B., Scimonelli, T. N., & De Barioglio, S. R. (2002). Ghrelin increases anxiety-like behavior and memory retention in rats. *Biochemical and Biophysical Research Communications*, 299(5), 739–743. doi:10.1016/S0006-291X(02)02740-7
- Cesar, M., & Hamprecht, B. (1995). Immunocytochemical examination of neural rat and mouse primary cultures using monoclonal antibodies raised against pyruvate carboxylase. *Journal of Neurochemistry*, 64(5), 2312–8. Retrieved from <http://www.ncbi.nlm.nih.gov/pubmed/7722517>
- Cha, S. H., Hu, Z., Chohnan, S., & Lane, M. D. (2005). Inhibition of hypothalamic fatty acid synthase triggers rapid activation of fatty acid oxidation in skeletal muscle. *Proceedings of the National Academy of Sciences of the United States of America*, 102(41), 14557–62. doi:10.1073/pnas.0507300102
- Chambliss, K. L., Zhang, Y. A., Rossier, E., Vollmer, B., & Gibson, K. M. (1995). Enzymatic and immunologic identification of succinic semialdehyde dehydrogenase in rat and human neural and nonneural tissues. *Journal of Neurochemistry*, 65(2), 851–5. Retrieved from <http://www.ncbi.nlm.nih.gov/pubmed/7616245>
- Chan, P. H., & Fishman, R. A. (1980). Transient formation of superoxide radicals in polyunsaturated fatty acid-induced brain swelling. *Journal of Neurochemistry*, 35(4), 1004–7. Retrieved from <http://www.ncbi.nlm.nih.gov/pubmed/6256498>
- Chang, M. C., Wisco, D., Ewers, H., Norden, C., & Winckler, B. (2006). Inhibition of sphingolipid synthesis affects kinetics but not fidelity of L1/NgCAM transport along direct but not transcytotic axonal pathways. *Molecular and Cellular Neurosciences*, 31(3), 525–38.

doi:10.1016/j.mcn.2005.11.006

- Chatton, J.-Y., Pellerin, L., & Magistretti, P. J. (2003). GABA uptake into astrocytes is not associated with significant metabolic cost: implications for brain imaging of inhibitory transmission. *Proceedings of the National Academy of Sciences of the United States of America*, *100*(21), 12456–61. doi:10.1073/pnas.2132096100
- Cheng, C. M., Hicks, K., Wang, J., Eagles, D. A., & Bondy, C. A. (2004). Caloric restriction augments brain glutamic acid decarboxylase-65 and -67 expression. *Journal of Neuroscience Research*, *77*(2), 270–6. doi:10.1002/jnr.20144
- Cheung, C. C., Krause, W. C., Edwards, R. H., Yang, C. F., Shah, N. M., Hnasko, T. S., & Ingraham, H. A. (2015). Sex-dependent changes in metabolism and behavior, as well as reduced anxiety after eliminating ventromedial hypothalamus excitatory output. *Molecular Metabolism*, *4*(11), 857–866. doi:10.1016/j.molmet.2015.09.001
- Chuang, J. C., Perello, M., Sakata, I., Osborne-Lawrence, S., Savitt, J. M., Lutter, M., & Zigman, J. M. (2011). Ghrelin mediates stress-induced food-reward behavior in mice. *Journal of Clinical Investigation*, *121*(7), 2684–2692. doi:10.1172/JCI57660
- Chuang, J. C., & Zigman, J. M. (2010). Ghrelin's roles in stress, mood, and anxiety regulation. *International Journal of Peptides*. doi:10.1155/2010/460549
- Clark, J. T., Kalra, P. S., Crowley, W. R., & Kalra, S. P. (1984). Neuropeptide Y and human Pancreatic polypeptide stimulate feeding behavior in rats. *Endocrinology*, *115*(1), 427–429. doi:10.1017/CBO9781107415324.004
- Cone, R. D., Cowley, M. A., Butler, A. A., Fan, W., Marks, D. L., & Low, M. J. (2001). The arcuate nucleus as a conduit for diverse signals relevant to energy homeostasis. *International Journal of Obesity and Related Metabolic Disorders: Journal of the International Association for the Study of Obesity*, *25 Suppl 5*, S63–S67. doi:10.1038/sj.ijo.0801913
- Cruz, C. R. Y., & Smith, R. G. (2008). The growth hormone secretagogue receptor. *Vitamins and Hormones*, *77*, 47–88. doi:10.1016/S0083-6729(06)77004-2
- Cruz, M. T., Herman, M. A., Cote, D. M., Ryabinin, A. E., & Roberto, M. (2013). Ghrelin increases GABAergic transmission and interacts with ethanol actions in the rat central nucleus of the amygdala. *Neuropsychopharmacology: Official Publication of the American College of Neuropsychopharmacology*, *38*(2), 364–75. doi:10.1038/npp.2012.190
- Currie, P. J., Schuette, L. M., Wauson, S. E. R., Voss, W. N., & Angeles, M. J. (2014). Activation of urocortin 1 and ghrelin signaling in the basolateral amygdala induces angiogenesis. *Neuroreport*, *25*(1), 60–4. doi:10.1097/WNR.0000000000000047
- Davidson, B. L., Stein, C. S., Heth, J. A., Martins, I., Kotin, R. M., Derksen, T. A., ... Chiorini, J. A. (2000). Recombinant adeno-associated virus type 2, 4, and 5 vectors: transduction of

- variant cell types and regions in the mammalian central nervous system. *Proceedings of the National Academy of Sciences of the United States of America*, 97(7), 3428–32. doi:10.1073/pnas.050581197
- Davis, J. F., Choi, D. L., Clegg, D. J., & Benoit, S. C. (2011). Signaling through the ghrelin receptor modulates hippocampal function and meal anticipation in mice. *Physiology & Behavior*, 103(1), 39–43. doi:10.1016/j.physbeh.2010.10.017
- Delhanty, P. J. D., Huisman, M., Julien, M., Mouchain, K., Brune, P., Themmen, A. P. N., ... van der Lely, A. J. (2015). The acylated (AG) to unacylated (UAG) ghrelin ratio in esterase inhibitor-treated blood is higher than previously described. *Clinical Endocrinology*, 82(1), 142–6. doi:10.1111/cen.12489
- Derosa, G., & Maffioli, P. (2012). Anti-obesity drugs: a review about their effects and their safety. *Expert Opinion on Drug Safety*, 11(3), 459–71. doi:10.1517/14740338.2012.675326
- Diano, S., Farr, S. A., Benoit, S. C., McNay, E. C., da Silva, I., Horvath, B., ... Horvath, T. L. (2006). Ghrelin controls hippocampal spine synapse density and memory performance. *Nature Neuroscience*, 9(3), 381–8. doi:10.1038/nn1656
- Dicken, M. S., Hughes, A. R., & Hentges, S. T. (2015). Gad1 mRNA as a reliable indicator of altered GABA release from orexigenic neurons in the hypothalamus. *The European Journal of Neuroscience*. doi:10.1111/ejn.13076
- Dicken, M. S., Tooker, R. E., & Hentges, S. T. (2012). Regulation of GABA and glutamate release from proopiomelanocortin neuron terminals in intact hypothalamic networks. *The Journal of Neuroscience: The Official Journal of the Society for Neuroscience*, 32(12), 4042–8. doi:10.1523/JNEUROSCI.6032-11.2012
- Dienel, G. A., & Cruz, N. F. (2004). Nutrition during brain activation: does cell-to-cell lactate shuttling contribute significantly to sweet and sour food for thought? *Neurochemistry International*, 45(2-3), 321–51. doi:10.1016/j.neuint.2003.10.011
- Dienel, G. A., & Hertz, L. (2001). Glucose and lactate metabolism during brain activation. *Journal of Neuroscience Research*, 66(5), 824–38. Retrieved from <http://www.ncbi.nlm.nih.gov/pubmed/11746408>
- Druce, M. R., Wren, A. M., Park, A. J., Milton, J. E., Patterson, M., Frost, G., ... Bloom, S. R. (2005). Ghrelin increases food intake in obese as well as lean subjects. *International Journal of Obesity (2005)*, 29(9), 1130–6. doi:10.1038/sj.ijo.0803001
- du Bois, T. M., Deng, C., & Huang, X.-F. (2005). Membrane phospholipid composition, alterations in neurotransmitter systems and schizophrenia. *Progress in Neuro-Psychopharmacology & Biological Psychiatry*, 29(6), 878–88. doi:10.1016/j.pnpbp.2005.04.034
- Ebert, D., Haller, R. G., & Walton, M. E. (2003). Energy Contribution of Octanoate to Intact Rat

- Brain Metabolism Measured by ¹³C Nuclear Magnetic Resonance Spectroscopy. *The Journal of Neuroscience*, 23(13), 5928–5935. Retrieved from <http://www.jneurosci.org/content/23/13/5928.abstract>
- Eccles, J. C., Fatt, P., & Koketsu, K. (1954). Cholinergic and inhibitory synapses in a pathway from motor-axon collaterals to motoneurons. *The Journal of Physiology*, 126(3), 524–562. doi:10.1113/jphysiol.1954.sp005226
- Egecioglu, E., Jerlhag, E., Salomé, N., Skibicka, K. P., Haage, D., Bohlooly-Y, M., ... Dickson, S. L. (2010). Ghrelin increases intake of rewarding food in rodents. *Addiction Biology*, 15(3), 304–311. doi:10.1111/j.1369-1600.2010.00216.x
- Egido, E. M., Rodríguez-Gallardo, J., Silvestre, R. A., & Marco, J. (2002). Inhibitory effect of ghrelin on insulin and pancreatic somatostatin secretion. *European Journal of Endocrinology*, 146(2), 241–244. doi:146241 [pii]
- el-Bacha, R. S., & Minn, A. (1999). Drug metabolizing enzymes in cerebrovascular endothelial cells afford a metabolic protection to the brain. *Cellular and Molecular Biology (Noisy-Le-Grand, France)*, 45(1), 15–23. Retrieved from <http://www.ncbi.nlm.nih.gov/pubmed/10099836>
- Elmqvist, J. K. (2001). Hypothalamic pathways underlying the endocrine, autonomic, and behavioral effects of leptin. In *Physiology and Behavior* (Vol. 74, pp. 703–708). doi:10.1016/S0031-9384(01)00613-8
- Esser, V., Britton, C. H., Weis, B. C., Foster, D. W., & McGarry, J. D. (1993). Cloning, sequencing, and expression of a cDNA encoding rat liver carnitine palmitoyltransferase I. Direct evidence that a single polypeptide is involved in inhibitor interaction and catalytic function. *J Biol Chem*, 268(8), 5817–5822. Retrieved from http://www.ncbi.nlm.nih.gov/entrez/query.fcgi?cmd=Retrieve&db=PubMed&dopt=Citation&list_uids=8449948
- European Medicines Agency (EMA). (2013). *Withdrawal of the marketing authorisation application for Belviq (lorcaserin)*. London. Retrieved from http://www.ema.europa.eu/docs/en_GB/document_library/Medicine_QA/2013/05/WC500143811.pdf
- European Medicines Agency (EMA). (2014). *Guideline on clinical evaluation of medicinal products used in weight control*. London. Retrieved from http://www.ema.europa.eu/docs/en_GB/document_library/Scientific_guideline/2014/07/WC500170278.pdf
- European Medicines Agency (EMA). (2015). *Saxenda recommended for approval in weight management in adults Medicine to be used in addition to reduced-calorie diet and physical*

- activity. London. Retrieved from http://www.ema.europa.eu/docs/en_GB/document_library/Press_release/2015/01/WC500180857.pdf
- Fait, A., Fromm, H., Walter, D., Galili, G., & Fernie, A. R. (2008). Highway or byway: the metabolic role of the GABA shunt in plants. *Trends in Plant Science*, *13*(1), 14–19. doi:10.1016/j.tplants.2007.10.005
- Ferrer, A., Caelles, C., Massot, N., & Hegardt, F. G. (1985). Activation of rat liver cytosolic 3-hydroxy-3-methylglutaryl coenzyme A reductase kinase by adenosine 5'-monophosphate. *Biochemical and Biophysical Research Communications*, *132*(2), 497–504. Retrieved from <http://www.ncbi.nlm.nih.gov/pubmed/4062938>
- Fisher, J. M., Sossin, W., Newcomb, R., & Scheller, R. H. (1988). Multiple neuropeptides derived from a common precursor are differentially packaged and transported. *Cell*, *54*(6), 813–822. doi:10.1016/S0092-8674(88)91131-2
- Frago, L. M., Pañeda, C., Dickson, S. L., Hewson, A. K., Argente, J., & Chowen, J. A. (2002). Growth Hormone (GH) and GH-releasing peptide-6 increase brain insulin-like growth factor-I expression and activate intracellular signaling pathways involved in neuroprotection. *Endocrinology*, *143*(10), 4113–4122. doi:10.1210/en.2002-220261
- Fu, L.-Y., & van den Pol, A. N. (2008). Agouti-related peptide and MC3/4 receptor agonists both inhibit excitatory hypothalamic ventromedial nucleus neurons. *The Journal of Neuroscience: The Official Journal of the Society for Neuroscience*, *28*(21), 5433–49. doi:10.1523/JNEUROSCI.0749-08.2008
- Fuente-Martín, E., García-Cáceres, C., Argente-Arizón, P., Díaz, F., Granado, M., Freire-Regatillo, A., ... Chowen, J. A. (2016). Ghrelin Regulates Glucose and Glutamate Transporters in Hypothalamic Astrocytes. *Scientific Reports*, *6*, 23673. doi:10.1038/srep23673
- Furness, D. N., Dehnes, Y., Akhtar, A. Q., Rossi, D. J., Hamann, M., Grutle, N. J., ... Danbolt, N. C. (2008). A quantitative assessment of glutamate uptake into hippocampal synaptic terminals and astrocytes: new insights into a neuronal role for excitatory amino acid transporter 2 (EAAT2). *Neuroscience*, *157*(1), 80–94. doi:10.1016/j.neuroscience.2008.08.043
- Gahete, M. D., Córdoba-Chacón, J., Kineman, R. D., Luque, R. M., & Castaño, J. P. (2011). Role of ghrelin system in neuroprotection and cognitive functions: Implications in Alzheimer's disease. *Peptides*. doi:10.1016/j.peptides.2011.09.019
- Gao, S., Keung, W., Serra, D., Wang, W., Carrasco, P., Casals, N., ... Lopaschuk, G. D. (2011). Malonyl-CoA mediates leptin hypothalamic control of feeding independent of inhibition of CPT-1a. *American Journal of Physiology. Regulatory, Integrative and Comparative*

- Physiology*, 301(1), R209–17. doi:10.1152/ajpregu.00092.2011
- Gao, S., Serra, D., Keung, W., Hegardt, F. G., & Lopaschuk, G. D. (2013). Important role of ventromedial hypothalamic carnitine palmitoyltransferase-1a in the control of food intake. *American Journal of Physiology. Endocrinology and Metabolism*, 305(3), E336–47. doi:10.1152/ajpendo.00168.2013
- Gao, S., Zhu, G., Gao, X., Wu, D., Carrasco, P., Casals, N., ... Lopaschuk, G. D. (2011). Important roles of brain-specific carnitine palmitoyltransferase and ceramide metabolism in leptin hypothalamic control of feeding. *Proceedings of the National Academy of Sciences of the United States of America*, 108(23), 9691–6. doi:10.1073/pnas.1103267108
- Gatfield, P. D., Lowry, O. H., Schulz, D. W., & Passonneau, J. V. (1966). Regional energy reserves in mouse brain and changes with ischaemia and anaesthesia. *Journal of Neurochemistry*, 13(3), 185–95. Retrieved from <http://www.ncbi.nlm.nih.gov/pubmed/5939991>
- Gauna, C., Uitterlinden, P., Kramer, P., Kiewiet, R. M., Janssen, J. A. M. J. L., Delhanty, P. J. D., ... van der Lely, A. J. (2007). Intravenous glucose administration in fasting rats has differential effects on acylated and unacylated ghrelin in the portal and systemic circulation: a comparison between portal and peripheral concentrations in anesthetized rats. *Endocrinology*, 148(11), 5278–87. doi:10.1210/en.2007-0225
- Ghavami, S., Shojaei, S., Yeganeh, B., Ande, S. R., Jangamreddy, J. R., Mehrpour, M., ... Łos, M. J. (2014). Autophagy and apoptosis dysfunction in neurodegenerative disorders. *Progress in Neurobiology*. doi:10.1016/j.pneurobio.2013.10.004
- Gordon, J., Amini, S., & White, M. K. (2013). General overview of neuronal cell culture. *Methods in Molecular Biology (Clifton, N.J.)*, 1078, 1–8. doi:10.1007/978-1-62703-640-5_1
- Graham, F. L., Smiley, J., Russell, W. C., & Nairn, R. (1977). Characteristics of a Human Cell Line Transformed by DNA from Human Adenovirus Type 5. *Journal of General Virology*, 36(1), 59–72. doi:10.1099/0022-1317-36-1-59
- Gram, L., Larsson, O. M., Johnsen, A. H., & Schousboe, A. (1988). Effects of valproate, vigabatrin and aminooxyacetic acid on release of endogenous and exogenous GABA from cultured neurons. *Epilepsy Research*, 2(2), 87–95. Retrieved from <http://www.ncbi.nlm.nih.gov/pubmed/3143560>
- Grouselle, D., Chaillou, E., Caraty, a, Bluet-Pajot, M.-T., Zizzari, P., Tillet, Y., & Epelbaum, J. (2008). Pulsatile cerebrospinal fluid and plasma ghrelin in relation to growth hormone secretion and food intake in the sheep. *Journal of Neuroendocrinology*, 20(10), 1138–1146. doi:10.1111/j.1365-2826.2008.01770.x
- Guan, X.-M., Yu, H., Palyha, O. C., McKee, K. K., Feighner, S. D., Sirinathsinghji, D. J. S., ... Howard, A. D. (1997). Distribution of mRNA encoding the growth hormone secretagogue receptor in

- brain and peripheral tissues. *Molecular Brain Research*, 48(1), 23–29. doi:10.1016/S0169-328X(97)00071-5
- Gutierrez, J. A., Solenberg, P. J., Perkins, D. R., Willency, J. A., Knierman, M. D., Jin, Z., ... Hale, J. E. (2008). Ghrelin octanoylation mediated by an orphan lipid transferase. *Proceedings of the National Academy of Sciences of the United States of America*, 105(17), 6320–5. doi:10.1073/pnas.0800708105
- Hamdy, O., Uwaifo, G. I., & Oral, E. A. (2015). Obesity Medication. Retrieved March 23, 2015, from <http://emedicine.medscape.com/article/123702-medication>
- Hammond, E. J., & Wilder, B. J. (1985). Gamma-vinyl GABA: a new antiepileptic drug. *Clinical Neuropharmacology*, 8(1), 1–12. Retrieved from <http://www.ncbi.nlm.nih.gov/pubmed/3884148>
- Hansson, C., Annerbrink, K., Nilsson, S., Bah, J., Olsson, M., Allgulander, C., ... Dickson, S. L. (2013). A possible association between panic disorder and a polymorphism in the preproghrelingene. *Psychiatry Research*, 206(1), 22–25. doi:10.1016/j.psychres.2012.09.051
- Hansson, C., Haage, D., Taube, M., Egecioglu, E., Salomé, N., & Dickson, S. L. (2011). Central administration of ghrelin alters emotional responses in rats: Behavioural, electrophysiological and molecular evidence. *Neuroscience*, 180, 201–211. doi:10.1016/j.neuroscience.2011.02.002
- Hardie, D. G., Corton, J., Ching, Y. P., Davies, S. P., & Hawley, S. (1997). Regulation of lipid metabolism by the AMP-activated protein kinase. *Biochemical Society Transactions*, 25(4), 1229–31. Retrieved from <http://www.ncbi.nlm.nih.gov/pubmed/9449981>
- Hartman, A. L., Gasior, M., Vining, E. P. G., & Rogawski, M. A. (2007). The Neuropharmacology of the Ketogenic Diet. *Pediatric Neurology*. doi:10.1016/j.pediatrneurol.2007.02.008
- Hassel, B., Westergaard, N., Schousboe, A., & Fonnum, F. (1995). Metabolic differences between primary cultures of astrocytes and neurons from cerebellum and cerebral cortex. Effects of fluorocitrate. *Neurochemical Research*, 20(4), 413–420. doi:10.1007/BF00973096
- Hearl, W. G., & Churchich, J. E. (1984). Interactions between 4-aminobutyrate aminotransferase and succinic semialdehyde dehydrogenase, two mitochondrial enzymes. *J. Biol. Chem.*, 259(18), 11459–11463. Retrieved from <http://www.jbc.org/content/259/18/11459.short>
- Hegardt, F. G. (1999). Mitochondrial 3-hydroxy-3-methylglutaryl-CoA synthase: a control enzyme in ketogenesis. *Biochemical Journal*, 338(3), 569–582. doi:10.1042/bj3380569
- Heppner, K. M., Chaudhary, N., Müller, T. D., Kirchner, H., Habegger, K. M., Ottaway, N., ... Tschöp, M. H. (2012). Acylation type determines Ghrelin's effects on energy homeostasis in rodents. *Endocrinology*, 153(10), 4687–4695. doi:10.1210/en.2012-1194

- Herrero, L., Rubí, B., Sebastián, D., Serra, D., Asins, G., Maechler, P., ... Hegardt, F. G. (2005). Alteration of the malonyl-CoA/carnitine palmitoyltransferase I interaction in the beta-cell impairs glucose-induced insulin secretion. *Diabetes*, *54*(2), 462–471.
- Hertz, L., & Schousboe, A. (1987). Primary Cultures of Gabaergic and Glutamatergic Neurons as Model Systems to Study Neurotransmitter Functions I. Differentiated Cells. In A. Vernadakis, A. Privat, J. M. Lauder, P. S. Timiras, & E. Giacobini (Eds.), *Model Systems of Development and Aging of the Nervous System* (pp. 19–31). Boston, MA: Springer US. doi:10.1007/978-1-4613-2037-1
- Herzog, E., Gilchrist, J., Gras, C., Muzerelle, A., Ravassard, P., Giros, B., ... El Mestikawy, S. (2004). Localization of VGLUT3, the vesicular glutamate transporter type 3, in the rat brain. *Neuroscience*, *123*(4), 983–1002. doi:10.1016/j.neuroscience.2003.10.039
- Hetherington, A., & Ranson, S. (1942). The spontaneous activity and food intake of rats with hypothalamic lesions. *American Journal of Physiology*. Retrieved from <http://www.cabdirect.org/abstracts/19421402515.html>
- Hosoda, H., Kojima, M., Mizushima, T., Shimizu, S., & Kangawa, K. (2003). Structural divergence of human ghrelin: Identification of multiple ghrelin-derived molecules produced by post-translational processing. *Journal of Biological Chemistry*, *278*(1), 64–70. doi:10.1074/jbc.M205366200
- Hotta, M., Ohwada, R., Akamizu, T., Shibasaki, T., Takano, K., & Kangawa, K. (2009). Ghrelin increases hunger and food intake in patients with restricting-type anorexia nervosa: a pilot study. *Endocrine Journal*, *56*(9), 1119–1128. doi:10.1507/endocrj.K09E-168
- Howard, A. D., Feighner, S. D., Cully, D. F., Arena, J. P., Liberatore, P. A., Rosenblum, C. I., ... Van der Ploeg, L. H. (1996). A receptor in pituitary and hypothalamus that functions in growth hormone release. *Science (New York, N.Y.)*, *273*(5277), 974–7. doi:10.1126/science.273.5277.974
- Hu, Z., Cha, S. H., Chohann, S., & Lane, M. D. (2003). Hypothalamic malonyl-CoA as a mediator of feeding behavior. *Proc Natl Acad Sci U S A*, *100*(22), 12624–12629. Retrieved from http://www.ncbi.nlm.nih.gov/entrez/query.fcgi?cmd=Retrieve&db=PubMed&dopt=Citation&list_uids=14532332
- Hu, Z., Cha, S. H., van Haasteren, G., Wang, J., & Lane, M. D. (2005). Effect of centrally administered C75, a fatty acid synthase inhibitor, on ghrelin secretion and its downstream effects. *Proceedings of the National Academy of Sciences of the United States of America*, *102*(11), 3972–7. doi:10.1073/pnas.0500619102
- Hu, Z., Dai, Y., Prentki, M., Chohann, S., & Lane, M. D. (2005). A role for hypothalamic malonyl-CoA in the control of food intake. *The Journal of Biological Chemistry*, *280*(48), 39681–3.

doi:10.1074/jbc.C500398200

- Hurt, R. T., Edakkanambeth Varayil, J., & Ebbert, J. O. (2014). New pharmacological treatments for the management of obesity. *Current Gastroenterology Reports*, 16(6), 394. doi:10.1007/s11894-014-0394-0
- Jackson, V. M., Price, D. A., & Carpino, P. A. (2014). Investigational drugs in Phase II clinical trials for the treatment of obesity: implications for future development of novel therapies. *Expert Opinion on Investigational Drugs*, 23(8), 1055–66. doi:10.1517/13543784.2014.918952
- Jaeken, J., Casaer, P., de Cock, P., Corbeel, L., Eeckels, R., Eggermont, E., ... Brucher, J. M. (1984). Gamma-aminobutyric acid-transaminase deficiency: a newly recognized inborn error of neurotransmitter metabolism. *Neuropediatrics*, 15(3), 165–9. doi:10.1055/s-2008-1052362
- Jeon, W. S., & Park, C. Y. (2014). Antiobesity pharmacotherapy for patients with type 2 diabetes: focus on long-term management. *Endocrinology and Metabolism (Seoul, Korea)*, 29(4), 410–7. doi:10.3803/EnM.2014.29.4.410
- Jerlhag, E., Egecioglu, E., Dickson, S. L., Andersson, M., Svensson, L., & Engel, J. A. (2006). Ghrelin stimulates locomotor activity and accumbal dopamine-overflow via central cholinergic systems in mice: Implications for its involvement in brain reward. *Addiction Biology*, 11(1), 45–54. doi:10.1111/j.1369-1600.2006.00002.x
- Jerlhag, E., Egecioglu, E., Landgren, S., Salomé, N., Heilig, M., Moechars, D., ... Engel, J. A. (2009). Requirement of central ghrelin signaling for alcohol reward. *Proceedings of the National Academy of Sciences of the United States of America*, 106(27), 11318–23. doi:10.1073/pnas.0812809106
- Jerlhag, E., Janson, A. C., Waters, S., & Engel, J. A. (2012). Concomitant Release of Ventral Tegmental Acetylcholine and Accumbal Dopamine by Ghrelin in Rats. *PLoS ONE*, 7(11). doi:10.1371/journal.pone.0049557
- Kahn, B. B., Alquier, T., Carling, D., & Hardie, D. G. (2005). AMP-activated protein kinase: ancient energy gauge provides clues to modern understanding of metabolism. *Cell Metabolism*, 1(1), 15–25. doi:10.1016/j.cmet.2004.12.003
- Kamegai, J., Tamura, H., Shimizu, T., Ishii, S., Sugihara, H., & Wakabayashi, I. (2001). Chronic central infusion of ghrelin increases hypothalamic neuropeptide Y and Agouti-related protein mRNA levels and body weight in rats. *Diabetes*, 50(11), 2438–43. Retrieved from <http://www.ncbi.nlm.nih.gov/pubmed/11679419>
- Kanamoto, N., Akamizu, T., Tagami, T., Hataya, Y., Moriyama, K., Takaya, K., ... Nakao, K. (2004). Genomic structure and characterization of the 5'-flanking region of the human ghrelin gene. *Endocrinology*, 145(9), 4144–4153. doi:10.1210/en.2003-1718

- Kang, T.-C., Park, S.-K., Hwang, I. K., An, S.-J., Choi, S. Y., Kwon, O.-S., ... Won, M. H. (2003). The altered expression of GABA shunt enzymes in the gerbil hippocampus before and after seizure generation. *Neurochemistry International*, 42(3), 239–49. Retrieved from <http://www.ncbi.nlm.nih.gov/pubmed/12427478>
- Kang, T.-C., Park, S.-K., Hwang, I.-K., An, S.-J., Choi, S. Y., Cho, S.-W., & Won, M. H. (2002). Spatial and temporal alterations in the GABA shunt in the gerbil hippocampus following transient ischemia. *Brain Res*, 944(1-2), 10–18.
- Kasser, T. R., Deutch, A., & Martin, R. J. (1986). Uptake and utilization of metabolites in specific brain sites relative to feeding status. *Physiology and Behavior*, 36(6), 1161–1165. doi:10.1016/0031-9384(86)90494-4
- Kaushik, S., Arias, E., Kwon, H., Lopez, N. M., Athonvarangkul, D., Sahu, S., ... Singh, R. (2012). Loss of autophagy in hypothalamic POMC neurons impairs lipolysis. *EMBO Reports*, 13(3), 258–65. doi:10.1038/embor.2011.260
- Kaushik, S., Rodriguez-Navarro, J. A., Arias, E., Kiffin, R., Sahu, S., Schwartz, G. J., ... Singh, R. (2011). Autophagy in hypothalamic AgRP neurons regulates food intake and energy balance. *Cell Metab*, 14(2), 173–183. Retrieved from http://www.ncbi.nlm.nih.gov/entrez/query.fcgi?cmd=Retrieve&db=PubMed&dopt=Citation&list_uids=21803288
- Kawamura, N., & Kishimoto, Y. (1981). Characterization of Water-Soluble Products of Palmitic Acid beta-Oxidation by a Rat Brain Preparation. *Journal of Neurochemistry*, 36(5), 1786–1791. doi:10.1111/j.1471-4159.1981.tb00432.x
- Kelly, J., Rothstein, J., & Grossman, S. P. (1979). GABA and hypothalamic feeding systems. I. Topographic analysis of the effects of microinjections of muscimol. *Physiology & Behavior*, 23(6), 1123–34. Retrieved from <http://www.ncbi.nlm.nih.gov/pubmed/542523>
- Kent, B. A., Beynon, A. L., Hornsby, A. K. E., Bekinschtein, P., Bussey, T. J., Davies, J. S., & Saksida, L. M. (2015). The orexigenic hormone acyl-ghrelin increases adult hippocampal neurogenesis and enhances pattern separation. *Psychoneuroendocrinology*, 51, 431–9. doi:10.1016/j.psyneuen.2014.10.015
- Khan, A., Raza, S., Khan, Y., Aksoy, T., Khan, M., Weinberger, Y., & Goldman, J. (2012). Current updates in the medical management of obesity. *Recent Pat Endocr Metab Immune Drug Discov*, 6(2), 117–128.
- Kim, D. J., Yoon, S. J., Choi, B., Kim, T. S., Woo, Y. S., Kim, W., ... Jeong, J. (2005). Increased fasting plasma ghrelin levels during alcohol abstinence. *Alcohol and Alcoholism*, 40(1), 76–79. doi:10.1093/alcalc/agh108
- Kim, K. W., Zhao, L., Donato, J., Kohno, D., Xu, Y., Elias, C. F., ... Elmquist, J. K. (2011).

- Steroidogenic factor 1 directs programs regulating diet-induced thermogenesis and leptin action in the ventral medial hypothalamic nucleus. *Proceedings of the National Academy of Sciences of the United States of America*, *108*(26), 10673–8. doi:10.1073/pnas.1102364108
- Kirchner, H., Gutierrez, J. A., Solenberg, P. J., Pfluger, P. T., Czyzyk, T. A., Willency, J. A., ... Tschöp, M. H. (2009). GOAT links dietary lipids with the endocrine control of energy balance. *Nature Medicine*, *15*(7), 741–5. doi:10.1038/nm.1997
- Klökener, T., Hess, S., Belgardt, B. F., Paeger, L., Verhagen, L. A. W., Husch, A., ... Brüning, J. C. (2011). High-fat feeding promotes obesity via insulin receptor/PI3K-dependent inhibition of SF-1 VMH neurons. *Nature Neuroscience*, *14*(7), 911–8. doi:10.1038/nn.2847
- Kluge, M., Gazea, M., Schüssler, P., Genzel, L., Dresler, M., Kleyer, S., ... Steiger, A. (2010). Ghrelin increases slow wave sleep and stage 2 sleep and decreases stage 1 sleep and REM sleep in elderly men but does not affect sleep in elderly women. *Psychoneuroendocrinology*, *35*(2), 297–304. doi:10.1016/j.psyneuen.2009.07.007
- Kluge, M., Schüssler, P., Bleninger, P., Kleyer, S., Uhr, M., Weikel, J. C., ... Steiger, A. (2008). Ghrelin alone or co-administered with GHRH or CRH increases non-REM sleep and decreases REM sleep in young males. *Psychoneuroendocrinology*, *33*(4), 497–506. doi:10.1016/j.psyneuen.2008.01.008
- Kluge, M., Schüssler, P., Dresler, M., Schmidt, D., Yassouridis, A., Uhr, M., & Steiger, A. (2011). Effects of ghrelin on psychopathology, sleep and secretion of cortisol and growth hormone in patients with major depression. *Journal of Psychiatric Research*, *45*(3), 421–6. doi:10.1016/j.jpsychires.2010.09.002
- Kojima, M., Hosoda, H., Date, Y., Nakazato, M., Matsuo, H., & Kangawa, K. (1999). Ghrelin is a growth-hormone-releasing acylated peptide from stomach. *Nature*, *402*(6762), 656–660. doi:10.1038/45230
- Kola, B., Farkas, I., Christ-Crain, M., Wittmann, G., Lolli, F., Amin, F., ... Korbonits, M. (2008). The orexigenic effect of ghrelin is mediated through central activation of the endogenous cannabinoid system. *PloS One*, *3*(3), e1797. doi:10.1371/journal.pone.0001797
- Kranz, A., Fu, J., Duerschke, K., Weidlich, S., Naumann, R., Stewart, A. F., & Anastassiadis, K. (2010). An improved Flp deleter mouse in C57Bl/6 based on Flpo recombinase. *Genesis (New York, N.Y. : 2000)*, *48*(8), 512–20. doi:10.1002/dvg.20641
- Krashes, M. J., Shah, B. P., Koda, S., & Lowell, B. B. (2013). Rapid versus delayed stimulation of feeding by the endogenously released AgRP neuron mediators GABA, NPY, and AgRP. *Cell Metabolism*, *18*(4), 588–95. doi:10.1016/j.cmet.2013.09.009
- Lage, R., Diéguez, C., Vidal-Puig, A., & López, M. (2008). AMPK: a metabolic gauge regulating whole-body energy homeostasis. *Trends in Molecular Medicine*, *14*(12), 539–49.

doi:10.1016/j.molmed.2008.09.007

- Lage, R., Vázquez, M. J., Varela, L., Saha, A. K., Vidal-Puig, A., Nogueiras, R., ... López, M. (2010). Ghrelin effects on neuropeptides in the rat hypothalamus depend on fatty acid metabolism actions on BSX but not on gender. *FASEB J*, 24(8), 2670–2679. Retrieved from http://www.ncbi.nlm.nih.gov/entrez/query.fcgi?cmd=Retrieve&db=PubMed&dopt=Citation&list_uids=20335227
- Lam, T. K., Schwartz, G. J., & Rossetti, L. (2005). Hypothalamic sensing of fatty acids. *Nat Neurosci*, 8(5), 579–584. Retrieved from http://www.ncbi.nlm.nih.gov/entrez/query.fcgi?cmd=Retrieve&db=PubMed&dopt=Citation&list_uids=15856066
- Lanctôt, K. L., Herrmann, N., Mazzotta, P., Khan, L. R., & Ingber, N. (2004). GABAergic function in Alzheimer's disease: evidence for dysfunction and potential as a therapeutic target for the treatment of behavioural and psychological symptoms of dementia. *Canadian Journal of Psychiatry. Revue Canadienne de Psychiatrie*, 49(7), 439–453.
- Landgren, S., Jerlhag, E., Zetterberg, H., Gonzalez-Quintela, A., Campos, J., Olofsson, U., ... Engel, J. A. (2008). Association of pro-ghrelin and GHS-R1A gene polymorphisms and haplotypes with heavy alcohol use and body mass. *Alcoholism: Clinical and Experimental Research*, 32(12), 2054–2061. doi:10.1111/j.1530-0277.2008.00793.x
- Lane, M. D., Wolfgang, M., Cha, S.-H., & Dai, Y. (2008). Regulation of food intake and energy expenditure by hypothalamic malonyl-CoA. *International Journal of Obesity (2005)*, 32 Suppl 4, S49–54. doi:10.1038/ijo.2008.123
- Lavrentyev, E. N., Matta, S. G., & Cook, G. A. (2004). Expression of three carnitine palmitoyltransferase-I isoforms in 10 regions of the rat brain during feeding, fasting, and diabetes. *Biochemical and Biophysical Research Communications*, 315(1), 174–8. doi:10.1016/j.bbrc.2004.01.040
- Leonhardt, S., Shahab, M., Luft, H., Wuttke, W., & Jarry, H. (1999). Reduction of Luteinizing Hormone Secretion Induced by Long-Term Feed Restriction in Male Rats Is Associated with Increased Expression of GABA-Synthesizing Enzymes Without Alterations of GnRH Gene Expression. *Journal of Neuroendocrinology*, 11(8), 613–619. doi:10.1046/j.1365-2826.1999.00377.x
- Lesuisse, C., & Martin, L. J. (2002). Long-term culture of mouse cortical neurons as a model for neuronal development, aging, and death. *Journal of Neurobiology*, 51(1), 9–23. Retrieved from <http://www.ncbi.nlm.nih.gov/pubmed/11920724>
- Liguz-Leczna, M., & Skangiel-Kramska, J. (2007). Vesicular glutamate transporters VGLUT1 and VGLUT2 in the developing mouse barrel cortex. *International Journal of Developmental*

- Neuroscience: The Official Journal of the International Society for Developmental Neuroscience*, 25(2), 107–14. doi:10.1016/j.ijdevneu.2006.12.005
- Loftus, T. M., Jaworsky, D. E., Frehywot, G. L., Townsend, C. A., Ronnett, G. V., Lane, M. D., & Kuhajda, F. P. (2000). Reduced Food Intake and Body Weight in Mice Treated with Fatty Acid Synthase Inhibitors. *Science*, 288(5475), 2379–2381. doi:10.1126/science.288.5475.2379
- López, M., Lage, R., Saha, A. K., Pérez-Tilve, D., Vázquez, M. J., Varela, L., ... Vidal-Puig, A. (2008). Hypothalamic fatty acid metabolism mediates the orexigenic action of ghrelin. *Cell Metabolism*, 7(5), 389–99. doi:10.1016/j.cmet.2008.03.006
- López, M., Lelliott, C. J., Tovar, S., Kimber, W., Gallego, R., Virtue, S., ... Vidal-Puig, A. J. (2006). Tamoxifen-induced anorexia is associated with fatty acid synthase inhibition in the ventromedial nucleus of the hypothalamus and accumulation of malonyl-CoA. *Diabetes*, 55(5), 1327–1336. doi:10.2337/db05-1356
- López-Viñas, E., Bentebibel, A., Gurunathan, C., Morillas, M., de Arriaga, D., Serra, D., ... Gómez-Puertas, P. (2007). Definition by functional and structural analysis of two malonyl-CoA sites in carnitine palmitoyltransferase 1A. *The Journal of Biological Chemistry*, 282(25), 18212–24. doi:10.1074/jbc.M700885200
- Lowe, D. M., & Tubbs, P. K. (1985). Succinylation and inactivation of 3-hydroxy-3-methylglutaryl-CoA synthase by succinyl-CoA and its possible relevance to the control of ketogenesis. *The Biochemical Journal*, 232(1), 37–42. Retrieved from <http://www.pubmedcentral.nih.gov/articlerender.fcgi?artid=1152835&tool=pmcentrez&rendertype=abstract>
- Lundbæk, J. A. (2006). Regulation of membrane protein function by lipid bilayer elasticity—a single molecule technology to measure the bilayer properties experienced by an embedded protein. *Journal of Physics. Condensed Matter: An Institute of Physics Journal*, 18(28), S1305–44. doi:10.1088/0953-8984/18/28/S13
- Lutter, M., Sakata, I., Osborne-Lawrence, S., Rovinsky, S. a, Anderson, J. G., Jung, S., ... Zigman, J. M. (2008). The orexigenic hormone ghrelin defends against depressive symptoms of chronic stress. *Nature Neuroscience*, 11(7), 752–753. doi:10.1038/nn.2139
- Maguire, S. E., Rhoades, S., Chen, W.-F., Sengupta, A., Yue, Z., Lim, J. C., ... Sehgal, A. (2015). Independent Effects of GABA Transaminase (GABAT) on Metabolic and Sleep Homeostasis. *The Journal of Biological Chemistry*, 290(33), 20407–16. doi:10.1074/jbc.M114.602276
- Makowski, K., Mera, P., Paredes, D., Herrero, L., Ariza, X., Asins, G., ... Serra, D. (2013). Differential pharmacologic properties of the two C75 enantiomers: (+)-C75 is a strong anorectic drug; (-)-C75 has antitumor activity. *Chirality*, 25(5), 281–7. doi:10.1002/chir.22139

- Malandrino, M. I., Fucho, R., Weber, M., Calderon-Dominguez, M., Mir, J. F., Valcarcel, L., ... Herrero, L. (2015). Enhanced fatty acid oxidation in adipocytes and macrophages reduces lipid-induced triglyceride accumulation and inflammation. *American Journal of Physiology. Endocrinology and Metabolism*, *ajpendo.00362.2014*. doi:10.1152/ajpendo.00362.2014
- Malaspina, P., Picklo, M. J., Jakobs, C., Snead, O. C., & Gibson, K. M. (2009). Comparative genomics of aldehyde dehydrogenase 5a1 (succinate semialdehyde dehydrogenase) and accumulation of gamma-hydroxybutyrate associated with its deficiency. *Human Genomics*, *3*(2), 106–120. doi:10.1186/1479-7364-3-2-106
- Mamelak, M. (2012). Sporadic Alzheimer's disease: the starving brain. *Journal of Alzheimer's Disease : JAD*, *31*(3), 459–74. doi:10.3233/JAD-2012-120370
- Manfredsson, F. P., Rising, A. C., & Mandel, R. J. (2009). AAV9: a potential blood-brain barrier buster. *Molecular Therapy : The Journal of the American Society of Gene Therapy*, *17*(3), 403–5. doi:10.1038/mt.2009.15
- Mani, B. K., Walker, A. K., Lopez Soto, E. J., Raingo, J., Lee, C. E., Perelló, M., ... Zigman, J. M. (2014). Neuroanatomical characterization of a growth hormone secretagogue receptor-green fluorescent protein reporter mouse. *The Journal of Comparative Neurology*, *522*(16), 3644–66. doi:10.1002/cne.23627
- Martínez de Morentin, P. B., González-García, I., Martins, L., Lage, R., Fernández-Mallo, D., Martínez-Sánchez, N., ... López, M. (2014). Estradiol Regulates Brown Adipose Tissue Thermogenesis via Hypothalamic AMPK. *Cell Metabolism*, *1*, 41–53. doi:10.1016/j.cmet.2014.03.031
- Massie, A., Cnops, L., Smolders, I., McCullumsmith, R., Kooijman, R., Kwak, S., ... Michotte, Y. (2008). High-affinity Na⁺/K⁺-dependent glutamate transporter EAAT4 is expressed throughout the rat fore- and midbrain. *The Journal of Comparative Neurology*, *511*(2), 155–72. doi:10.1002/cne.21823
- McGarry, J. D., & Brown, N. F. (1997). The mitochondrial carnitine palmitoyltransferase system. From concept to molecular analysis. *Eur J Biochem*, *244*(1), 1–14. Retrieved from http://www.ncbi.nlm.nih.gov/entrez/query.fcgi?cmd=Retrieve&db=PubMed&dopt=Citation&list_uids=9063439
- McGarry, J. D., Mills, S. E., Long, C. S., & Foster, D. W. (1983). Observations on the affinity for carnitine, and malonyl-CoA sensitivity, of carnitine palmitoyltransferase I in animal and human tissues. Demonstration of the presence of malonyl-CoA in non-hepatic tissues of the rat. *The Biochemical Journal*, *214*(1), 21–8. Retrieved from <http://www.pubmedcentral.nih.gov/articlerender.fcgi?artid=1152205&tool=pmcentrez&rendertype=abstract>

- McKee, K. K., Tan, C. P., Palyha, O. C., Liu, J., Feighner, S. D., Hreniuk, D. L., ... Van der Ploeg, L. H. (1997). Cloning and characterization of two human G protein-coupled receptor genes (GPR38 and GPR39) related to the growth hormone secretagogue and neurotensin receptors. *Genomics*, *46*(3), 426–34. doi:10.1006/geno.1997.5069
- Meinkoth, J., & Crystal, M. (1999). Cerebrospinal fluid analysis. In *Diagnostic Cytology and Hematology of the Dog and Cat* (2nd ed.).
- Mellon, P. L., Windle, J. J., Goldsmith, P. C., Padula, C. A., Roberts, J. L., & Weiner, R. I. (1990). Immortalization of hypothalamic GnRH neurons by genetically targeted tumorigenesis. *Neuron*, *5*(1), 1–10. Retrieved from <http://www.ncbi.nlm.nih.gov/pubmed/2196069>
- Mera, P. (2012). *Papel de la carnitina palmitoiltransferasa 1A hipotalámica en el control de la ingesta*. Universitat de Barcelona. Retrieved from <http://tdx.cat/handle/10803/78903>
- Mera, P., Bentebibel, A., López-Viñas, E., Cordente, A. G., Gurunathan, C., Sebastián, D., ... Hegardt, F. G. (2009). C75 is converted to C75-CoA in the hypothalamus, where it inhibits carnitine palmitoyltransferase 1 and decreases food intake and body weight. *Biochem Pharmacol*, *77*(6), 1084–1095. doi:10.1016/j.bcp.2008.11.020
- Mera, P., Mir, J. F., Fabriàs, G., Casas, J., Costa, A. S. H., Malandrino, M. I., ... Serra, D. (2014). Long-term increased carnitine palmitoyltransferase 1A expression in ventromedial hypothalamus causes hyperphagia and alters the hypothalamic lipidomic profile. *PLoS One*, *9*(5), e97195. doi:10.1371/journal.pone.0097195
- Mericq, V., Cassorla, F., Bowers, C. Y., Avila, A., Gonen, B., & Merriam, G. R. (2003). Changes in appetite and body weight in response to long-term oral administration of the ghrelin agonist GHRP-2 in growth hormone deficient children. *Journal of Pediatric Endocrinology & Metabolism : JPEM*, *16*(7), 981–5. Retrieved from <http://www.ncbi.nlm.nih.gov/pubmed/14513874>
- Meyer, R. M., Burgos-Robles, A., Liu, E., Correia, S. S., & Goosens, K. A. (2014). A ghrelin-growth hormone axis drives stress-induced vulnerability to enhanced fear. *Molecular Psychiatry*, *19*(12), 1284–94. doi:10.1038/mp.2013.135
- Michaeli, S., Fait, A., Lagor, K., Nunes-Nesi, A., Grillich, N., Yellin, A., ... Fromm, H. (2011). A mitochondrial GABA permease connects the GABA shunt and the TCA cycle, and is essential for normal carbon metabolism. *The Plant Journal : For Cell and Molecular Biology*, *67*(3), 485–98. doi:10.1111/j.1365-3113.2011.04612.x
- Moldéus, P. (1978). Paracetamol metabolism and toxicity in isolated hepatocytes from rat and mouse. *Biochemical Pharmacology*, *27*(24), 2859–63. Retrieved from <http://www.ncbi.nlm.nih.gov/pubmed/736978>
- Momany, F. A., Bowers, C. Y., Reynolds, G. A., Chang, D., Hong, A., & Newlander, K. (1981). Design,

- synthesis, and biological activity of peptides which release growth hormone in vitro. *Endocrinology*, 108(1), 31–39. doi:10.1210/endo-108-1-31
- Morganstern, I., Barson, J. R., & Leibowitz, S. F. (2011). Regulation of drug and palatable food overconsumption by similar peptide systems. *Current Drug Abuse Reviews*, 4(3), 163–73. doi:BSP/CDAR/E-Pub/000042 [pii]
- Morillas, M., Gomez-Puertas, P., Bentebibel, A., Selles, E., Casals, N., Valencia, A., ... Serra, D. (2003). Identification of conserved amino acid residues in rat liver carnitine palmitoyltransferase I critical for malonyl-CoA inhibition. Mutation of methionine 593 abolishes malonyl-CoA inhibition. *J Biol Chem*, 278(11), 9058–9063. Retrieved from [http://www.ncbi.nlm.nih.gov/entrez/query.fcgi?cmd=Retrieve&db=PubMed&dopt=Citation&list_uids=12499375](http://www.ncbi.nlm.nih.gov/entrez/query.fcgi?cmd=Retrieve&db=PubMed&dopt= Citation&list_uids=12499375)
- Morrison, C. D., Xi, X., White, C. L., Ye, J., & Martin, R. J. (2007). Amino acids inhibit Agrp gene expression via an mTOR-dependent mechanism. *American Journal of Physiology. Endocrinology and Metabolism*, 293(1), E165–71. doi:10.1152/ajpendo.00675.2006
- Mumphrey, M. B., Patterson, L. M., Zheng, H., & Berthoud, H.-R. (2013). Roux-en-Y gastric bypass surgery increases number but not density of CCK-, GLP-1-, 5-HT-, and neurotensin-expressing enteroendocrine cells in rats. *Neurogastroenterology and Motility: The Official Journal of the European Gastrointestinal Motility Society*, 25(1), e70–9. doi:10.1111/nmo.12034
- Nagaya, N., Itoh, T., Murakami, S., Oya, H., Uematsu, M., Miyatake, K., & Kangawa, K. (2005). Treatment of cachexia with ghrelin in patients with COPD. *Chest*, 128(3), 1187–1193. doi:10.1378/chest.128.3.1187
- Nakazato, M., Murakami, N., Date, Y., Kojima, M., Matsuo, H., Kangawa, K., & Matsukura, S. (2001). A role for ghrelin in the central regulation of feeding. *Nature*, 409(6817), 194–8. doi:10.1038/35051587
- Nass, R., Pezzoli, S. S., Oliveri, M. C., Patrie, J. T., Harrell, F. E., Clasey, J. L., ... Thorner, M. O. (2008). Effects of an oral ghrelin mimetic on body composition and clinical outcomes in healthy older adults: a randomized trial. *Annals of Internal Medicine*, 149(9), 601–11. Retrieved from <http://www.pubmedcentral.nih.gov/articlerender.fcgi?artid=2757071&tool=pmcentrez&rendertype=abstract>
- Nguyen, E., & Picklo, M. J. (2003). Inhibition of succinic semialdehyde dehydrogenase activity by alkenal products of lipid peroxidation. *Biochimica et Biophysica Acta (BBA) - Molecular Basis of Disease*, 1637(1), 107–112. doi:10.1016/S0925-4439(02)00220-X
- Niciu, M. J., Kelmendi, B., & Sanacora, G. (2012). Overview of glutamatergic neurotransmission in

- the nervous system. *Pharmacology, Biochemistry, and Behavior*, 100(4), 656–64. doi:10.1016/j.pbb.2011.08.008
- Nishi, Y., Mifune, H., & Kojima, M. (2012). Ghrelin acylation by ingestion of medium-chain fatty acids. *Methods in Enzymology*, 514, 303–15. doi:10.1016/B978-0-12-381272-8.00019-2
- Nogueiras, R., López, M., & Diéguez, C. (2010). Regulation of lipid metabolism by energy availability: a role for the central nervous system. *Obesity Reviews: An Official Journal of the International Association for the Study of Obesity*, 11(3), 185–201. doi:10.1111/j.1467-789X.2009.00669.x
- Nyman, L. R., Cox, K. B., Hoppel, C. L., Kerner, J., Barnoski, B. L., Hamm, D. A., ... Wood, P. A. (2005). Homozygous carnitine palmitoyltransferase 1a (liver isoform) deficiency is lethal in the mouse. *Molecular Genetics and Metabolism*, 86(1-2), 179–87. doi:10.1016/j.ymgme.2005.07.021
- O'Neil, P. M., Smith, S. R., Weissman, N. J., Fidler, M. C., Sanchez, M., Zhang, J., ... Shanahan, W. R. (2012). Randomized Placebo-Controlled Clinical Trial of Lorcaserin for Weight Loss in Type 2 Diabetes Mellitus: The BLOOM-DM Study. *Obesity (Silver Spring)*, 20(7), 1426–1436.
- Obici, S., Feng, Z., Arduini, A., Conti, R., & Rossetti, L. (2003). Inhibition of hypothalamic carnitine palmitoyltransferase-1 decreases food intake and glucose production. *Nat Med*, 9(6), 756–761. Retrieved from <http://www.ncbi.nlm.nih.gov/pubmed/12754501>
- Obici, S., Zhang, B. B., Karkanias, G., & Rossetti, L. (2002). Hypothalamic insulin signaling is required for inhibition of glucose production. *Nature Medicine*, 8(12), 1376–82. doi:10.1038/nm798
- Ohgusu, H., Shirouzu, K., Nakamura, Y., Nakashima, Y., Ida, T., Sato, T., & Kojima, M. (2009). Ghrelin O-acyltransferase (GOAT) has a preference for n-hexanoyl-CoA over n-octanoyl-CoA as an acyl donor. *Biochemical and Biophysical Research Communications*, 386(1), 153–158. doi:10.1016/j.bbrc.2009.06.001
- Olney, J. W. (1969). Brain lesions, obesity, and other disturbances in mice treated with monosodium glutamate. *Science (New York, N.Y.)*, 164(880), 719–721. doi:10.1126/science.164.3880.719
- Orellana-Gavaldá, J. M., Herrero, L., Malandrino, M. I., Paneda, A., Sol Rodríguez-Pena, M., Petry, H., ... Sol Rodríguez-Peña, M. (2011). Molecular therapy for obesity and diabetes based on a long-term increase in hepatic fatty-acid oxidation. *Hepatology*, 53(3), 821–832. doi:10.1002/hep.24140
- Panov, A., Orynbayeva, Z., Vavilin, V., & Lyakhovich, V. (2014). Fatty acids in energy metabolism of the central nervous system. *BioMed Research International*, 2014, 472459. doi:10.1155/2014/472459

- Panov, A., Schonfeld, P., Dikalov, S., Hemendinger, R., Bonkovsky, H. L., & Brooks, B. R. (2009). The neuromediator glutamate, through specific substrate interactions, enhances mitochondrial ATP production and reactive oxygen species generation in nonsynaptic brain mitochondria. *Journal of Biological Chemistry*, 284(21), 14448–14456. doi:10.1074/jbc.M900985200
- Paxinos, G., & Watson, C. (1998). *The Rat Brain in Stereotaxic Coordinates* (5th ed.). New York, NY: Academic.
- Pearl, P., Gibson, K., & Cortez, M. (2009). Succinic semialdehyde dehydrogenase deficiency: lessons from mice and men. *Journal of Inherited ...* Retrieved from <http://link.springer.com/article/10.1007/s10545-009-1034-y>
- Pellerin, L., & Magistretti, P. J. (2012). Sweet sixteen for ANLS. *Journal of Cerebral Blood Flow and Metabolism: Official Journal of the International Society of Cerebral Blood Flow and Metabolism*, 32(7), 1152–66. doi:10.1038/jcbfm.2011.149
- Perello, M., Sakata, I., Birnbaum, S., Chuang, J. C., Osborne-Lawrence, S., Rovinsky, S. A., ... Zigman, J. M. (2010). Ghrelin Increases the Rewarding Value of High-Fat Diet in an Orexin-Dependent Manner. *Biological Psychiatry*, 67(9), 880–886. doi:10.1016/j.biopsych.2009.10.030
- Price, N., van der Leij, F., Jackson, V., Corstorphine, C., Thomson, R., Sorensen, A., & Zammit, V. (2002). A novel brain-expressed protein related to carnitine palmitoyltransferase I. *Genomics*, 80(4), 433–442. Retrieved from http://www.ncbi.nlm.nih.gov/entrez/query.fcgi?cmd=Retrieve&db=PubMed&dopt=Citation&list_uids=12376098
- Ramírez, S. (2014). *Hypothalamic ceramide levels regulated by CPT1C mediate the orexigenic effect of ghrelin*. Universitat Internacional de Catalunya.
- Ramírez, S., Martins, L., Jacas, J., Carrasco, P., Pozo, M., Clotet, J., ... Casals, N. (2013). Hypothalamic ceramide levels regulated by CPT1C mediate the orexigenic effect of ghrelin. *Diabetes*, 62(7), 2329–37. doi:10.2337/db12-1451
- Ramsay, R. R., Gandour, R. D., & van der Leij, F. R. (2001). Molecular enzymology of carnitine transfer and transport. *Biochimica et Biophysica Acta*, 1546(1), 21–43. Retrieved from <http://www.ncbi.nlm.nih.gov/pubmed/11257506>
- Randle, P. J., Garland, P. B., Hales, C. N., & Newsholme, E. A. (1963). The glucose fatty-acid cycle. Its role in insulin sensitivity and the metabolic disturbances of diabetes mellitus. *The Lancet*, 281(7285), 785–789. doi:10.1016/S0140-6736(63)91500-9
- Rasmussen, N. (2008). America's first amphetamine epidemic 1929-1971: a quantitative and qualitative retrospective with implications for the present. *American Journal of Public*

- Health*, 98(6), 974–85. doi:10.2105/AJPH.2007.110593
- Rerup, C. C. (1970). Drugs producing diabetes through damage of the insulin secreting cells. *Pharmacological Reviews*, 22(4), 485–518. Retrieved from <http://www.ncbi.nlm.nih.gov/pubmed/4921840>
- Reubi, J.-C., Van Der Berg, C., & Cuénod, M. (1978). Glutamine as precursor for the GABA and glutamate transmitter pools. *Neuroscience Letters*, 10(1-2), 171–174. doi:10.1016/0304-3940(78)90030-7
- Ribes, A., Riudor, E., Briones, P., Christensen, E., Campistol, J., & Millington, D. S. (1992). Significance of bound glutarate in the diagnosis of glutaric aciduria type I. *Journal of Inherited Metabolic Disease*, 15(3), 367–70. Retrieved from <http://www.ncbi.nlm.nih.gov/pubmed/1405471>
- Riepe, R. E., & Norenberg, M. D. (1978). Glutamine synthetase in the developing rat retina: An immunohistochemical study. *Experimental Eye Research*, 27(4), 435–444. doi:10.1016/0014-4835(78)90022-2
- Ross, S., & Peselow, E. (2009). The neurobiology of addictive disorders. *Clinical Neuropharmacology*. doi:10.1097/WNF.0b013e3181a9163c
- Sakaguchi, T., Arase, K., & Bray, G. A. (1988). Effect of intrahypothalamic hydroxybutyrate on sympathetic firing rate. *Metabolism: Clinical and Experimental*, 37(8), 732–5. Retrieved from <http://www.ncbi.nlm.nih.gov/pubmed/3405090>
- Sakaguchi, T., & Bray, G. A. (1989). Effect of norepinephrine, serotonin and tryptophan on the firing rate of sympathetic nerves. *Brain Research*, 492(1-2), 271–80. Retrieved from <http://www.ncbi.nlm.nih.gov/pubmed/2752301>
- Sanacora, G., Kershaw, M., Finkelstein, J. A., & White, J. D. (1990). Increased hypothalamic content of preproneuropeptide Y messenger ribonucleic acid in genetically obese Zucker rats and its regulation by food deprivation. *Endocrinology*, 127(2), 730–7. doi:10.1210/endo-127-2-730
- Sanger, F., Nicklen, S., & Coulson, A. R. (1977). DNA sequencing with chain-terminating inhibitors. *Proceedings of the National Academy of Sciences of the United States of America*, 74(12), 5463–7. Retrieved from <http://www.ncbi.nlm.nih.gov/pubmed/271968>
- Schneider, B. E., & Mun, E. C. (2005). Surgical Management of Morbid Obesity. *Diabetes Care*, 28(2), 475–480. doi:10.2337/diacare.28.2.475
- Schöne, C., & Burdakov, D. (2012). Glutamate and GABA as rapid effectors of hypothalamic “peptidergic” neurons. *Frontiers in Behavioral Neuroscience*, 6(November), 81. doi:10.3389/fnbeh.2012.00081
- Schönfeld, P., & Reiser, G. (2013). Why does brain metabolism not favor burning of fatty acids to

- provide energy? Reflections on disadvantages of the use of free fatty acids as fuel for brain. *Journal of Cerebral Blood Flow and Metabolism : Official Journal of the International Society of Cerebral Blood Flow and Metabolism*, 33(10), 1493–9. doi:10.1038/jcbfm.2013.128
- Schönfeld, P., & Wojtczak, L. (2012). Brown adipose tissue mitochondria oxidizing fatty acids generate high levels of reactive oxygen species irrespective of the uncoupling protein-1 activity state. *Biochimica et Biophysica Acta*, 1817(3), 410–8. doi:10.1016/j.bbabi.2011.12.009
- Schoors, S., Bruning, U., Missiaen, R., Queiroz, K. C. S., Borgers, G., Elia, I., ... Carmeliet, P. (2015). Fatty acid carbon is essential for dNTP synthesis in endothelial cells. *Nature*, 520(7546), 192–7. doi:10.1038/nature14362
- Schousboe, A., Bak, L. K., & Waagepetersen, H. S. (2013). Astrocytic control of biosynthesis and turnover of the neurotransmitters glutamate and GABA. *Frontiers in Endocrinology*. doi:10.3389/fendo.2013.00102
- Schousboe, A., Hertz, L., & Svenneby, G. (1977). Uptake and metabolism of GABA in astrocytes cultured from dissociated mouse brain hemispheres. *Neurochemical Research*, 2(2), 217–29. doi:10.1007/BF00964098
- Schousboe, A., Wu, J.-Y., & Roberts, E. (1974). Subunit structure and kinetic properties of 4-aminobutyrate-2-ketoglutarate transaminase purified from mouse brain. *Journal of Neurochemistry*, 23(6), 1189–1195. doi:10.1111/j.1471-4159.1974.tb12216.x
- Schug, Z. T., Frezza, C., Galbraith, L. C. A., & Gottlieb, E. (2012). The music of lipids: how lipid composition orchestrates cellular behaviour. *Acta Oncologica (Stockholm, Sweden)*, 51(3), 301–10. doi:10.3109/0284186X.2011.643823
- Schwartz, M. W., Woods, S. C., Porte, D., Seeley, R. J., & Baskin, D. G. (2000). Central nervous system control of food intake. *Nature*, 404(6778), 661–71. doi:10.1038/35007534
- Seo, J. Y., Lee, C. H., Cho, J. H., Choi, J. H., Yoo, K.-Y., Kim, D. W., ... Won, M.-H. (2009). Neuroprotection of ebselen against ischemia/reperfusion injury involves GABA shunt enzymes. *Journal of the Neurological Sciences*, 285(1-2), 88–94. doi:10.1016/j.jns.2009.05.029
- Serra-Pérez, A., Planas, A. M., Núñez-O'Mara, A., Berra, E., García-Villoria, J., Ribes, A., & Santalucía, T. (2010). Extended ischemia prevents HIF1 α degradation at reoxygenation by impairing prolyl-hydroxylation: role of Krebs cycle metabolites. *The Journal of Biological Chemistry*, 285(24), 18217–24. doi:10.1074/jbc.M110.101048
- Sierra, A. Y., Gratacós, E., Carrasco, P., Clotet, J., Ureña, J., Serra, D., ... Casals, N. (2008). CPT1c is localized in endoplasmic reticulum of neurons and has carnitine palmitoyltransferase activity. *The Journal of Biological Chemistry*, 283(11), 6878–85.

doi:10.1074/jbc.M707965200

- Singh, R. (2012). Autophagy in the control of food intake. *Adipocyte*, 1(2), 75–79. doi:10.4161/adip.18966
- Smith, R. G., Ploeg, L. H. T. Van der, Howard, A. D., Feighner, S. D., Cheng, K., Hickey, G. J., ... Patchett, A. A. (2011). Peptidomimetic Regulation of Growth Hormone Secretion. *Endocrine Reviews*, 18(5), 621–45. Retrieved from <http://www.ncbi.nlm.nih.gov/pubmed/9331545>
- Solà, C., Cristòfol, R., Suñol, C., & Sanfeli, C. (2011). Primary Cultures for Neurotoxicity Testing. In M. Aschner (Ed.), *Cell Culture Techniques* (Vol. 56, pp. 281–296). Springer New York. doi:10.1016/B978-0-12-374849-2.00013-7
- Sonnewald, U., Westergaard, N., Schousboe, A., Svendsen, J. S., Unsgård, G., & Petersen, S. B. (1993). Direct demonstration by [¹³C]NMR spectroscopy that glutamine from astrocytes is a precursor for GABA synthesis in neurons. *Neurochemistry International*, 22(1), 19–29. doi:10.1016/0197-0186(93)90064-C
- Sossin, W. S., Sweet-Cordero, a, & Scheller, R. H. (1990). Dale's hypothesis revisited: different neuropeptides derived from a common prohormone are targeted to different processes. *Proceedings of the National Academy of Sciences of the United States of America*, 87(June), 4845–4848. doi:10.1073/pnas.87.12.4845
- Spencer, S. J., Xu, L., Clarke, M. A., Lemus, M., Reichenbach, A., Geenen, B., ... Andrews, Z. B. (2012). Ghrelin regulates the hypothalamic-pituitary-adrenal axis and restricts anxiety after acute stress. *Biological Psychiatry*, 72(6), 457–465. doi:10.1016/j.biopsych.2012.03.010
- Spitzer, J. J. (1973). CNS and fatty acid metabolism. *The Physiologist*, 16(1), 55–68. Retrieved from <http://www.ncbi.nlm.nih.gov/pubmed/4693712>
- Spolidoro, M., Baroncelli, L., Putignano, E., Maya-Vetencourt, J. F., Viegli, A., & Maffei, L. (2011). Food restriction enhances visual cortex plasticity in adulthood. *Nature Communications*, 2, 320. doi:10.1038/ncomms1323
- Sprong, H., van der Sluijs, P., & van Meer, G. (2001). How proteins move lipids and lipids move proteins. *Nature Reviews. Molecular Cell Biology*, 2(7), 504–13. doi:10.1038/35080071
- Staes, E., Absil, P.-A., Lins, L., Bresseur, R., Deleu, M., Lecouturier, N., ... Pr eat, V. (2010). Acylated and unacylated ghrelin binding to membranes and to ghrelin receptor: towards a better understanding of the underlying mechanisms. *Biochimica et Biophysica Acta*, 1798(11), 2102–13. doi:10.1016/j.bbamem.2010.07.002
- Steiger, A., Dresler, M., Sch ussler, P., & Kluge, M. (2011). Ghrelin in mental health, sleep, memory. *Molecular and Cellular Endocrinology*. doi:10.1016/j.mce.2011.02.013
- Sternson, S. M., Shepherd, G. M. G., & Friedman, J. M. (2005). Topographic mapping of VMH -->

- arcuate nucleus microcircuits and their reorganization by fasting. *Nature Neuroscience*, 8(10), 1356–63. doi:10.1038/nn1550
- Stoyanova, I. I., & le Feber, J. (2014). Ghrelin accelerates synapse formation and activity development in cultured cortical networks. *BMC Neuroscience*, 15, 49. doi:10.1186/1471-2202-15-49
- Stoyanova, I. I., le Feber, J., & Rutten, W. L. C. (2013). Ghrelin stimulates synaptic formation in cultured cortical networks in a dose-dependent manner. *Regulatory Peptides*, 186, 43–8. doi:10.1016/j.regpep.2013.07.004
- Sun, Y., Wang, P., Zheng, H., & Smith, R. G. (2004). Ghrelin stimulation of growth hormone release and appetite is mediated through the growth hormone secretagogue receptor. *Proceedings of the National Academy of Sciences of the United States of America*, 101(13), 4679–84. doi:10.1073/pnas.0305930101
- Suzuki, Y., Takahashi, H., Fukuda, M., Hino, H., Kobayashi, K., Tanaka, J., & Ishii, E. (2009). Beta-hydroxybutyrate alters GABA-transaminase activity in cultured astrocytes. *Brain Research*, 1268, 17–23. doi:10.1016/j.brainres.2009.02.074
- Swart, I., Michael Overton, J., & Hout, T. A. (2001). The effect of food deprivation and experimental diabetes on orexin and NPY mRNA levels. *Peptides*, 22(12), 2175–2179. doi:10.1016/S0196-9781(01)00552-6
- Szentirmai, E., Hajdu, I., Obal, F., & Krueger, J. M. (2006). Ghrelin-induced sleep responses in ad libitum fed and food-restricted rats. *Brain Research*, 1088(1), 131–140. doi:10.1016/j.brainres.2006.02.072
- Takamori, S., Holt, M., Stenius, K., Lemke, E. A., Grønborg, M., Riedel, D., ... Jahn, R. (2006). Molecular anatomy of a trafficking organelle. *Cell*, 127(4), 831–46. doi:10.1016/j.cell.2006.10.030
- Takaya, K., Ariyasu, H., Kanamoto, N., Iwakura, H., Yoshimoto, A., Harada, M., ... Nakao, K. (2000). Ghrelin strongly stimulates growth hormone (GH) release in humans. *Journal of Clinical Endocrinology and Metabolism*, 85(12), 4908–4911. doi:10.1210/jc.85.12.4908
- Takaya, K., Ogawa, Y., Isse, N., Okazaki, T., Satoh, N., Masuzaki, H., ... Nakao, K. (1996). Molecular cloning of rat leptin receptor isoform complementary DNAs--identification of a missense mutation in Zucker fatty (fa/fa) rats. *Biochemical and Biophysical Research Communications*, 225(1), 75–83. doi:10.1006/bbrc.1996.1133
- Tanaka, K., West-Dull, A., Hine, D. G., Lynn, T. B., & Lowe, T. (1980). Gas-chromatographic method of analysis for urinary organic acids. II. Description of the procedure, and its application to diagnosis of patients with organic acidurias. *Clinical Chemistry*, 26(13), 1847–53. Retrieved from <http://www.ncbi.nlm.nih.gov/pubmed/7438430>

- Tarasenko, A., Krupko, O., & Himmelreich, N. (2012). Reactive oxygen species induced by presynaptic glutamate receptor activation is involved in [(3)H]GABA release from rat brain cortical nerve terminals. *Neurochemistry International*, 61(7), 1044–51. doi:10.1016/j.neuint.2012.07.021
- Tassone, F., Broglio, F., Destefanis, S., Rovere, S., Benso, a, Gottero, C., ... Maccario, M. (2003). Neuroendocrine and metabolic effects of acute ghrelin administration in human obesity. *The Journal of Clinical Endocrinology and Metabolism*, 88(11), 5478–5483. doi:10.1210/jc.2003-030564
- Tatemoto, K. (1982). Neuropeptide Y: complete amino acid sequence of the brain peptide. *Proceedings of the National Academy of Sciences of the United States of America*, 79(18), 5485–5489. doi:10.1073/pnas.79.18.5485
- Tejas-Juárez, J. G., Cruz-Martínez, A. M., López-Alonso, V. E., García-Iglesias, B., Mancilla-Díaz, J. M., Florán-Garduño, B., & Escartín-Pérez, R. E. (2014). Stimulation of dopamine D4 receptors in the paraventricular nucleus of the hypothalamus of male rats induces hyperphagia: involvement of glutamate. *Physiology & Behavior*, 133, 272–81. doi:10.1016/j.physbeh.2014.04.040
- Thai, T. P., Rodemer, C., Jauch, A., Hunziker, A., Moser, A., Gorgas, K., & Just, W. W. (2001). Impaired membrane traffic in defective ether lipid biosynthesis. *Human Molecular Genetics*, 10(2), 127–36. Retrieved from <http://www.ncbi.nlm.nih.gov/pubmed/11152660>
- Tillakaratne, N. J. K., Medina-Kauwe, L., & Gibson, K. M. (1995). Gamma-aminobutyric acid (GABA) metabolism in mammalian neural and nonneural tissues. *Comparative Biochemistry and Physiology -- Part A: Physiology*. doi:10.1016/0300-9629(95)00099-2
- Tolle, V., Bassant, M. H., Zizzari, P., Poindessous-Jazat, F., Tomasetto, C., Epelbaum, J., & Bluet-Pajot, M. T. (2002). Ultradian rhythmicity of ghrelin secretion in relation with gh, feeding behavior, and sleep-wake patterns in rats. *Endocrinology*, 143(4), 1353–1361. doi:10.1210/en.143.4.1353
- Tong, Q., Ye, C., McCrimmon, R. J., Dhillon, H., Choi, B., Kramer, M. D., ... Lowell, B. B. (2007). Synaptic glutamate release by ventromedial hypothalamic neurons is part of the neurocircuitry that prevents hypoglycemia. *Cell Metabolism*, 5(5), 383–93. doi:10.1016/j.cmet.2007.04.001
- Tong, Q., Ye, C.-P., Jones, J. E., Elmquist, J. K., & Lowell, B. B. (2008). Synaptic release of GABA by AgRP neurons is required for normal regulation of energy balance. *Nature Neuroscience*, 11(9), 998–1000. doi:10.1038/nn.2167
- Tschöp, M., Smiley, D. L., & Heiman, M. L. (2000). Ghrelin induces adiposity in rodents. *Nature*, 407(6806), 908–913. doi:10.1038/35038090

- Tsuji, M., Aida, N., Obata, T., Tomiyasu, M., Furuya, N., Kurosawa, K., ... Osaka, H. (2010). A new case of GABA transaminase deficiency facilitated by proton MR spectroscopy. *Journal of Inherited Metabolic Disease*, 33(1), 85–90. doi:10.1007/s10545-009-9022-9
- Urabe, M., Ding, C., & Kotin, R. M. (2002). Insect cells as a factory to produce adeno-associated virus type 2 vectors. *Human Gene Therapy*, 13(16), 1935–43. doi:10.1089/10430340260355347
- US Food and Drug Administration (FDA). (2014). *NDA 206321 - Liraglutide Injection, 3 mg - Novo Nordisk*.
- Vandenbergh, L. H., Wilson, J. M., & Gao, G. (2009). Tailoring the AAV vector capsid for gene therapy. *Gene Therapy*, 16(3), 311–9. doi:10.1038/gt.2008.170
- Vengeliene, V. (2013). The role of ghrelin in drug and natural reward. *Addiction Biology*, 18(6), 897–900. doi:10.1111/adb.12114
- Walls, A. B., Waagepetersen, H. S., Bak, L. K., Schousboe, A., & Sonnewald, U. (2015). The glutamine-glutamate/GABA cycle: function, regional differences in glutamate and GABA production and effects of interference with GABA metabolism. *Neurochemical Research*, 40(2), 402–9. doi:10.1007/s11064-014-1473-1
- Wang, C., Wang, C.-M., Clark, K. R., & Sferra, T. J. (2003). Recombinant AAV serotype 1 transduction efficiency and tropism in the murine brain. *Gene Therapy*, 10(17), 1528–34. doi:10.1038/sj.gt.3302011
- Westergaard, N., Sonnewald, U., Unsgård, G., Peng, L., Hertz, L., & Schousboe, a. (1994). Uptake, release, and metabolism of citrate in neurons and astrocytes in primary cultures. *Journal of Neurochemistry*, 62(5), 1727–33. Retrieved from <http://www.ncbi.nlm.nih.gov/pubmed/7908943>
- Wittekind, D. A., & Kluge, M. (2014). Ghrelin in psychiatric disorders—a review. *Psychoneuroendocrinology*, 52C, 176–194. doi:10.1016/j.psyneuen.2014.11.013
- Wolfgang, M. J., & Lane, M. D. (2006). Control of energy homeostasis: role of enzymes and intermediates of fatty acid metabolism in the central nervous system. *Annual Review of Nutrition*, 26, 23–44. doi:10.1146/annurev.nutr.25.050304.092532
- Wong-Riley, M. T. (1989). Cytochrome oxidase: an endogenous metabolic marker for neuronal activity. *Trends in Neurosciences*, 12(3), 94–101. Retrieved from <http://www.ncbi.nlm.nih.gov/pubmed/2469224>
- Woods, S. C., & D'Alessio, D. a. (2008). Central control of body weight and appetite. *The Journal of Clinical Endocrinology and Metabolism*, 93(11 Suppl 1), S37–50. doi:10.1210/jc.2008-1630
- World Health Organization. (2015). Obesity and overweight. Fact sheet N° 311. Retrieved April 20, 2015, from <http://www.who.int/mediacentre/factsheets/fs311/en/> (accessed 29

April 2015)

- Wren, A. M., Seal, L. J., Cohen, M. A., Brynes, A. E., Frost, G. S., Murphy, K. G., ... Bloom, S. R. (2001). Ghrelin enhances appetite and increases food intake in humans. *Journal of Clinical Endocrinology and Metabolism*, *86*(12), 5992–5995. doi:10.1210/jc.86.12.5992
- Wu, Q., & Palmiter, R. D. (2011). GABAergic signaling by AgRP neurons prevents anorexia via a melanocortin-independent mechanism. *European Journal of Pharmacology*, *660*(1), 21–7. doi:10.1016/j.ejphar.2010.10.110
- Xu, Y., Nedungadi, T. P., Zhu, L., Sobhani, N., Irani, B. G., Davis, K. E., ... Clegg, D. J. (2011). Distinct hypothalamic neurons mediate estrogenic effects on energy homeostasis and reproduction. *Cell Metabolism*, *14*(4), 453–65. doi:10.1016/j.cmet.2011.08.009
- Yang, J., Brown, M. S., Liang, G., Grishin, N. V., & Goldstein, J. L. (2008). Identification of the Acyltransferase that Octanoylates Ghrelin, an Appetite-Stimulating Peptide Hormone. *Cell*, *132*(3), 387–396. doi:10.1016/j.cell.2008.01.017
- Yogeeswari, P., Sriram, D., & Vaigundaragavendran, J. (2005). The GABA shunt: an attractive and potential therapeutic target in the treatment of epileptic disorders. *Current Drug Metabolism*, *6*(2), 127–139. doi:10.2174/1389200053586073
- Yu, A. C., Drejer, J., Hertz, L., & Schousboe, A. (1983). Pyruvate carboxylase activity in primary cultures of astrocytes and neurons. *Journal of Neurochemistry*, *41*(5), 1484–7. Retrieved from <http://www.ncbi.nlm.nih.gov/pubmed/6619879>
- Zammit, V. A. (2008). Carnitine palmitoyltransferase 1: central to cell function. *IUBMB Life*, *60*(5), 347–54. doi:10.1002/iub.78
- Zammit, V. A., & Arduini, A. (2008). The AMPK-malonyl-CoA-CPT1 axis in the control of hypothalamic neuronal function. *Cell Metabolism*, *8*(3), 175; author reply 176. doi:10.1016/j.cmet.2008.07.009
- Zhang, J. V., Ren, P.-G., Avsian-Kretchmer, O., Luo, C.-W., Rauch, R., Klein, C., & Hsueh, A. J. W. (2005). Obestatin, a peptide encoded by the ghrelin gene, opposes ghrelin's effects on food intake. *Science (New York, N.Y.)*, *310*(5750), 996–9. doi:10.1126/science.1117255
- Zhang, Y., Proenca, R., Maffei, M., Barone, M., Leopold, L., & Friedman, J. M. (1994). Positional cloning of the mouse obese gene and its human homologue. *Nature*, *372*(6505), 425–32. doi:10.1038/372425a0
- Zhu, W., Czyzyk, D., Paranjape, S. A., Zhou, L., Horblitt, A., Szabó, G., ... Chan, O. (2010). Glucose prevents the fall in ventromedial hypothalamic GABA that is required for full activation of glucose counterregulatory responses during hypoglycemia. *American Journal of Physiology. Endocrinology and Metabolism*, *298*(5), E971–7. doi:10.1152/ajpendo.00749.2009
- Zigman, J. M., Jones, J. E., Lee, C. E., Saper, C. B., & Elmquist, J. K. (2006). Expression of ghrelin

receptor mRNA in the rat and the mouse brain. *The Journal of Comparative Neurology*, 494(3), 528–48. doi:10.1002/cne.20823

ANNEXES

Gene expression comparison between hypothalamus and hypothalamic cell lines

MARKER	N29/4	N43/5	Hypothalamus	GT1-7	N41
<i>Adiponectin receptor 1</i>	+	+	+	+	+
<i>Adiponectin receptor 2</i>	+	+	+	+	+
<i>Adiponutrin (cDNA)</i>	+	+	+	+	+
<i>Adiponutrin (one-step)</i>	+	+	+	+	-
<i>Agrp</i>	-	+	+	+	+
<i>Ahr</i>	+	+	+	weak	+
<i>Angiotensinogen</i>	weak	weak	+	+	strong
<i>Angiotensin Receptor 1</i>	-	-	N/A	strong	strong
<i>Angiotensin Receptor 2</i>	strong	-	N/A	-	-
<i>AR</i>	-	+	+	+	+
<i>Arnt2</i>	+	+	+	+	+
<i>Aromatase</i>	-	-	+	-	+
<i>Avp</i>	N/A	-	+	+	-
<i>AVPR1a</i>	+	+	+	weak	+
<i>AVPR1b</i>	+	+	+	+	+
<i>BDNF</i>	+	+	+	weak	+
<i>Calcium Receptor (CaR)</i>	strong	+	strong	strong	+
<i>CART</i>	-	+	+	+	?
<i>CB1 receptor</i>	-	N/A	+	weak	+
<i>cc1ab</i>	N/A	N/A	+	+	N/A
<i>cc1ac</i>	N/A	N/A	+	+	N/A
<i>ChAT</i>	+	-	+	+	-
<i>chemerin</i>	-	weak	+	+	+
<i>chemerinR</i>	+	+	+	+	+
<i>CNTFR</i>	-	+	+	+	+
<i>CRFR1</i>	N/A	N/A	+	+	N/A
<i>CRFR1</i>	+	-	+	N/A	+
<i>CRFR2</i>	N/A	N/A	+	+	N/A
<i>CRFR2</i>	+	+	strong	strong	+
<i>CRH/CRF</i>	-	weak	strong	-	weak
<i>CRLR</i>	-	+	+	-	+
<i>DAT</i>	-	+	+	+	+
<i>Dpp4</i>	-	-	+	+	-
<i>Dynorphin</i>	-	-	+	N/A	-
<i>ER α</i>	-	+	+	+	+
<i>ER β</i>	+	+	+	+	+
<i>FIAF</i>	+	+	+	+	+
<i>Gad1 (Gad 67)</i>	+	+	+	+	+
<i>Gad2 (Gad 65)</i>	?	+	+	+	+

MARKER	N29/4	N43/5	Hypothalamus	GT1-7	N41
<i>Gal</i>	-	+	+	-	+
<i>GALP</i>	+	-	+	N/A	+
<i>GCK</i>	+	+	+	+	+
<i>GFAP</i>	N/A	N/A	+	-	N/A
<i>Ghrelin</i>	+	+	+	+	+
<i>Ghrelin variant</i>	+	-	+	+	+
<i>GHRH (southern)</i>	+	N/A	+	+	+
<i>GHSR1a</i>	+	weak	N/A	+	strong
<i>Glp1R</i>	-	-	strong	strong	+
<i>Glp2R</i>	-	-	strong	-	weak
<i>Glucagon receptor</i>	-	weak	weak	-	+
<i>Glucocorticoid receptor (GR)</i>	+	+	+	+	+
<i>GLUT1</i>	+	+	+	+	+
<i>GLUT2</i>	-	-	+	strong	-
<i>GLUT3</i>	+	+	+	+	+
<i>GLUT4</i>	+	+	+	+	+
<i>GMR alpha</i>	+	+	+	weak	+
<i>GnIH (Rfrp)</i>	weak	+	strong	strong	strong
<i>GnRH</i>	N/A	N/A	N/A	+	very weak
<i>GnRH Receptor</i>	N/A	N/A	+	-	N/A
<i>Gpr 39</i>	N/A	+	very weak?	-	+
<i>Gpr 120</i>	weak	-	strong	-	weak
<i>Grp</i>	+	-	strong	strong	+
<i>GrpR</i>	+	+	+	+	+
<i>Ht1b (5-Ht1b)</i>	+	+	+	+	+
<i>Htr2a (5-Htr2a)</i>	+	+	+	-	+
<i>Htr2c</i>	-	-	strong	strong	-
<i>IGF</i>	+	+	+	+	+
<i>IGF1R</i>	+	+	+	+	+
<i>IGFBP-1</i>	-	-	weak	-	-
<i>Insulin I</i>	-	-	?	N/A	-
<i>Insulin II</i>	-	-	+	N/A	-
<i>Insulin Receptor</i>	+	+	+	+	+
<i>Insulin receptor substrate 2</i>	-	+	+	+	+
<i>Kir6.1</i>	-	-	+	-	-
<i>Kir6.2</i>	?	?	+	+	+
<i>Kisspeptin</i>	-	+	+	-	-
<i>Kiss Receptor (GPR54)</i>	+	+	+	+	+
<i>Lep Receptor</i>	-	-	+	+	+
<i>Lipoprotein lipase (LPL)</i>	N/A	N/A	N/A	N/A	strong
<i>mc3R</i>	N/A	N/A	N/A	N/A	-
<i>mc4R</i>	-	+	+	+	-
<i>MCH</i>	+	+	+	+	+
<i>MCHR1</i>	+	+	+	+	+

MARKER	N29/4	N43/5	Hypothalamus	GT1-7	N41
<i>NPB</i>	+	+	+	+	+
<i>NPW</i>	weak	+	+	-	+
<i>NPY</i>	-	-	+	-	+
<i>NPY-Y1</i>	+	N/A	+	-	N/A
<i>NPY-Y2</i>	+	N/A	+	+	N/A
<i>NPY-Y4</i>	+	N/A	+	+	N/A
<i>NPY-Y5</i>	+	N/A	+	-	N/A
<i>NSE</i>	N/A	N/A	N/A	+	N/A
<i>NT</i>	+	+	+	+	+
<i>NTR1</i>	-	weak	+	-	-
<i>Opr1R</i>	+	+	+	+	+
<i>orexin</i>	-	-	+	-	-
<i>orexin R1</i>	+	+	+	weak	+
<i>orexin R2</i>	+	-	+	+	+
<i>Oxytocin</i>	N/A	N/A	+	+	N/A
<i>pAdcyap1</i>	-	weak	+	-	-
<i>POMC</i>	N/A	N/A	+	N/A	N/A
<i>proGlu</i>	-	-	+	+	+
<i>PTH2-R</i>	weak	weak	+	-	+
<i>resistin</i>	+	+	+	+	+
<i>Secretin</i>	-	weak	+	-	strong
<i>SF-1</i>	+	+	+	+	+
<i>Sim1 (S1)</i>	strong	strong	strong	strong	-
<i>Socs-3</i>	+	+	+	+	+
<i>somatostatin (som)</i>	+	?	strong	?	weak
<i>SSTY</i>	+	-	+	-	N/A
<i>STAT3</i>	+	+	+	+	+
<i>STAT5A</i>	+	+	+	weak	+
<i>STAT5B</i>	+	+	+	+	+
<i>Sur1</i>	-	-	+	+	+
<i>Sur2</i>	-	+	+	-	+
<i>Syndecan 3</i>	strong	strong	strong	+	strong
<i>T antigen</i>	+	+	N/A	+	+
<i>TAC2 (neurokinin B)</i>	-	-	strong	+	weak
<i>TH</i>	-	+	+	+	+
<i>Tph</i>	N/A	N/A	+	N/A	N/A
<i>THRalpha</i>	N/A	+	N/A	N/A	N/A
<i>THRbeta</i>	N/A	+	N/A	N/A	N/A
<i>TRH</i>	-	-	+	+	-
<i>Ucp2</i>	+	+	+	+	+
<i>VGF</i>	+	+	+	+	+
<i>VIP</i>	+	weak	strong	+	strong
<i>VIPR1</i>	?	+	+	-	+
<i>VIPR2</i>	weak	+	+	+	+

Primers for qRT-PCR detection and relative quantification of genes in rat

GENE	SEQUENCE
<i>AgRP for</i>	5'- AGCAGACCGAGCAGAAGATG
<i>AgRP rev</i>	5'- GACTCGTGCAGCCTTACACA
<i>NPY for</i>	5'- TATCCCTGCTCGTGTGTTG
<i>NPY rev</i>	5'- GTTCTGGGGCATTCTCTG
<i>POMC for</i>	5'- ACCTCACCCACGGAAAGCAA
<i>POMC rev</i>	5'- CGGGGATTTTCAGTCAAGG
<i>CART for</i>	5'- GCCAAGTCCCATGTGTGAC
<i>CART rev</i>	5'- CACCCCTTCACAAGCACTTCA
<i>VGLUT1 for</i>	5'- GATTCCGGGCGGATACAT
<i>VGLUT1 rev</i>	5'- TATGGCAGCCCAAAGAC
<i>VGLUT2 for</i>	5'- GCAGGAGGAGTTTCGGAAG
<i>VGLUT2 rev</i>	5'- CGCTCAGCTCCAATGTCTC
<i>VGLUT3 for</i>	5'- TTACGGCTGTGTCATGTGTGT
<i>VGLUT3 rev</i>	5'- GCAGGCTGGGTAGGTCAC
<i>VGAT for</i>	5'- GGGCTGGAACGTGACAAA
<i>VGAT rev</i>	5'- GGAGGATGGCGTAGGGTAG
<i>UCP2 for</i>	5'- GCGTGAGACCTCAAAGCAC
<i>UCP2 rev</i>	5'- GGGACCTTCAATCGTCAAGA
<i>Gpx3 for</i>	5'- ATTCTGGGCTTCCCTTGC
<i>Gpx3 rev</i>	5'- CACCCGGTCGAACGTACT
<i>SOD for</i>	5'- GGTCCAGCGGATGAAGAG
<i>SOD rev</i>	5'- GGACACATTGGCCACACC
<i>CAT for</i>	5'- ATCAGGGATGCCATGTTGTT
<i>CAT rev</i>	5'- GGGTCCTTCAGGTGAGTTTG
<i>Grp78/BIP for</i>	5'-CCGTAACAATCAAGGTCTACGA
<i>Grp78/BIP rev</i>	5'-AAGGTGACTTCAATCTGGGGTA
<i>PDI for</i>	5'-TACTTGTTCACCACGCAGA
<i>PDI rev</i>	5'-GCATACGACCCAGAACCATC
<i>CHOP for</i>	5'-CCAGCAGAGGTCACAAGCAC
<i>CHOP rev</i>	5'-CGCACTGACCACTCTGTTTC
<i>EDEM for</i>	5'-TGGAATTTGGGATTCTGAGC
<i>EDEM rev</i>	5'-TCTGGATGTTCAACATTGC
<i>BACTIN for</i>	5'- AAGTCCCTCACCTCCCAAAG
<i>BACTIN rev</i>	5'- AAGCAATGCTGTCACCTTCCC

Primers for qRT-PCR detection and relative quantification of genes in mouse

GENE	SEQUENCE
<i>CPT1A for</i>	5'- GACTCCGCTCGCTCATTTC
<i>CPT1A rev</i>	5'- AAGGCCACAGCTTGGTGA
<i>CPT1A (*) for</i>	5'- ACAATGGGACATTCCAGGAG
<i>CPT1A (*) rev</i>	5'- AAAGACTGGCGCTGCTCA
<i>CPT1C for</i>	5'- TATGCAGTCGCGCTTCTCT
<i>CPT1C rev</i>	5'- ACATCAATCAGGTGTGTCTGCT
<i>HMGCS2 for</i>	5'- GAGATGCAGCGGCTTTTGGC
<i>HMGCS2 rev</i>	5'- TCCTGGACCGAACAGAAGC
<i>AgRP for</i>	5'- TGCAGACCGAGCAGAAGAAG
<i>AgRP rev</i>	5'- GACTCGTGCAGCCTTACACA
<i>VGLUT1 for</i>	5'- AAAAGCAGCAGCCAAGTT
<i>VGLUT1 rev</i>	5'- CGCAGTTTAGCATTTCAGGAC
<i>VGLUT2 for</i>	5'- CTGGGGTCTTGTGCAGTAT
<i>VGLUT2 rev</i>	5'- CCGAAGCTGCCATAGACATAG
<i>VGLUT3 for</i>	5'- TAAGGAGTAGCATGTTGCTCAAA
<i>VGLUT3 rev</i>	5'- GGCAACCACCATGTACTCTTCT
<i>VGAT for</i>	5'- GGCAACCACCATGTACTCTTCT
<i>VGAT rev</i>	5'- TGAGGAACAACCCAGGTAG
<i>GAD1 for</i>	5'-ATACAACCTTTGGCTGCATGT
<i>GAD1 rev</i>	5'-TTCCGGGACATGAGCAGT
<i>GAD2 for</i>	5'-ACTAAAGAAAATGAGAGAAATCATTGG
<i>GAD2 rev</i>	5'-AGCATGGCATAACATGTTGGA
<i>GABAT for</i>	5'-TGCCTCCAGAGAACTTTGTG
<i>GABAT rev</i>	5'-TGATGAGCTGGGACATGC
<i>SSADH for</i>	5'-AACAGCTGGAAAGGGGTCTC
<i>SSADH rev</i>	5'-CATTAAGTCGTACCATTTACGGAGT

(*) Primers used to amplify both mouse CPT1A and overexpressed rat CPT1AM.

Solutions used for primary cortical cultures

Krebs-Ringer Buffer (KRB) 10x

35.35 g NaCl
1.8 g KCl
0.83 g KH₂PO₄
10.7 g NaHCO₃
12.85 g Glucose
qsp 500 mL milliQ Water

Magnesium stock

3.8 % MgSO₄·7H₂O

Calcium stock

1.2 % CaCl₂·2H₂O

Solution 1

50 mL KBS 1x
0.15 g BSA (Sigma 7906)
0.4 mL MgSO₄ 3.8%

Solution 2

10 mL Solution 1
2.5 mg trypsin (Sigma T9201)

Solution 3

10 mL Solution 1
0.8 mg DNase (Sigma D5025)
5.2 mg trypsin inhibitor (GIBCO 17075-029)
0.1 mL MgSO₄ 3.8%

Solution 4

8.4 mL Solution 1
1.6 mL Solution 3

Solution 5

5 mL Solution 1
40 uL MgSO₄ 3.8%
6 uL CaCl₂ 1.2%

PBE 1X

50 mL PBS 10X
10 mL Glucose 30% (w/v)
10 mL P/S
qsp 500 mL milliQ H₂O

PUBLICATIONS

*Serra D, Mera P, Malandrino MI, Mir JF, Herrero L. **Mitochondrial Fatty Acid Oxidation in Obesity.** Antioxid. Redox Signal. 2013 Jul 20;19(3):269-84. doi: 10.1089/ars.2012.4875. (Review article)*

Mera P, Mir JF*, Fabriàs G, Casas J, Costa ASH, Malandrino MI, Fernández-López JA, Remesar X, Gao S, Chohnan S, Rodríguez-Peña MS, Petry H, Asins G, Hegardt FG, Herrero L, Serra D. **Long-term increased CPT1A expression in ventromedial hypothalamus causes hyperphagia and alters the hypothalamic lipidomic profile.** PLOSOne. 2014 May. doi: 10.1371/journal.pone.0097195. (Research Article) *Both authors contributed equally to the article.*

*Malandrino MI, Fucho R, Weber M, Calderón-Domínguez M, Mir JF, Valcarcel L, Escoté X, Gómez-Serrano M, Peral B, Salvadó L, Fernández-Veledo S, Casals N, Vázquez-Carrera M, Villarroya F, Vendrell JJ, Serra D, Herrero L. **Enhanced fatty acid oxidation in adipocytes and macrophages reduces lipid-induced triglyceride accumulation and inflammation.** Am J Physiol Endocrinol Metab. 2015 May 1;308(9):E756-69. doi: 10.1152/ajpendo.00362.2014. (Research Article)*

*Herrero L, Mir JF, Weber M, Fucho R, Calderón M, Serra D. **Estratègies de modulació de l'oxidació d'àcids grassos com a tractament per combatre l'obesitat.** Revista de la Societat Catalana de Química. 2015 Dec, No. 14:16-24 doi: 10.2436/20.2003.01.61 (Review Articles)*

*Calderon-Dominguez M, Mir JF, Fucho R, Weber M, Serra D, Herrero L. **Fatty Acid Metabolism and the Basis of Brown Adipose Tissue Function.** Adipocyte. 2016, Vol. 0, No. 0, 1-21 doi:10.1080/21623945.2015.1122857 (Review Articles)*

Mitochondrial Fatty Acid Oxidation in Obesity

Dolors Serra, Paula Mera, Maria Ida Malandrino, Joan Francesc Mir, and Laura Herrero

Abstract

Significance: Current lifestyles with high-energy diets and little exercise are triggering an alarming growth in obesity. Excess of adiposity is leading to severe increases in associated pathologies, such as insulin resistance, type 2 diabetes, atherosclerosis, cancer, arthritis, asthma, and hypertension. This, together with the lack of efficient obesity drugs, is the driving force behind much research. **Recent Advances:** Traditional anti-obesity strategies focused on reducing food intake and increasing physical activity. However, recent results suggest that enhancing cellular energy expenditure may be an attractive alternative therapy. **Critical Issues:** This review evaluates recent discoveries regarding mitochondrial fatty acid oxidation (FAO) and its potential as a therapy for obesity. We focus on the still controversial beneficial effects of increased FAO in liver and muscle, recent studies on how to potentiate adipose tissue energy expenditure, and the different hypotheses involving FAO and the reactive oxygen species production in the hypothalamic control of food intake. **Future Directions:** The present review aims to provide an overview of novel anti-obesity strategies that target mitochondrial FAO and that will definitively be of high interest in the future research to fight against obesity-related disorders. *Antioxid. Redox Signal.* 19, 269–284.

Obesity: Molecular and Pathophysiological Features

OBESITY IS DEFINED AS abnormal or excessive fat accumulation in the adipose tissue and other organs. The World Health Organization (WHO) defines overweight as a body mass index (BMI; calculated as weight [kg] divided by height squared [m²]) equal to or greater than 25 kg/m² and obese as a BMI equal to or greater than 30 kg/m² (137). Current lifestyle trends and continuous nutrient excess are causing obesity to increase at alarming rates, especially in young people. There are more than 500 million obese people worldwide and, more importantly, overweight and obesity are the fifth leading risk for death globally (137). Humanity is facing a new epidemic already dubbed “Prosperity’s Plague” (160). Therefore, significant research is needed in the race to find effective therapies and to minimize the enormous costs of the related healthcare.

Weight gain is influenced by several factors, such as genetics, maternal and perinatal environment, energy-dense diets, and sedentary lifestyle (3). Of great concern are the concurrent and parallel increases in the prevalence of pathological conditions associated with obesity, which include insulin resistance, type 2 diabetes, cardiovascular disease, nonalcoholic fatty liver, polycystic ovary syndrome, asthma, Alzheimer’s disease, and some forms of cancer. Elucidating the causes involved in the pathophysiology of obesity-related

disorders is one of the most critical endeavors in modern medical research.

Several mechanisms have emerged in the past two decades, during which obesity and especially its connection to insulin resistance have become a top-interest research topic being studied by leading groups in the field.

Ectopic-fat deposition

When the adipose tissue cannot store excess fat, lipids accumulate inappropriately in the liver, muscle, and pancreas. This lipotoxic environment, mainly mediated by diacylglycerols (DAGs), blocks correct glucose transport and insulin signaling (145). Thus, it has been postulated that any strategy that could block the entry of fatty acids (FAs) into the cell, promote fatty acid oxidation (FAO), or convert DAGs into triglycerides (TGs) could prevent insulin resistance (160).

Inflammation

The pathophysiology of obesity-induced insulin resistance has also been correlated with an increase in circulation and tissue inflammation originating in the adipocyte damage and infiltration of immune cells (107, 151). As fat accumulates in adipose tissue, adipocytes overcome their healthy size limit (157, 169) and release inflammatory cytokines and molecules

Department of Biochemistry and Molecular Biology, Facultat de Farmàcia, Universitat de Barcelona, Institut de Biomedicina de la Universitat de Barcelona (IBUB), and CIBER Fisiopatología de la Obesidad y la Nutrición (CIBEROBN), Instituto de Salud Carlos III, Barcelona, Spain.

known as adipokines. The excessive accumulation of lipids in the adipose tissue leads to adipocyte hypoxia (73), endoplasmic reticulum (ER) stress (132), and cell death, and causes FA spillover (145). Infiltrated immune cells also contribute to this chronic low-grade inflammatory milieu, whereby the increase in inflammatory cytokines causes insulin resistance elsewhere in the body. Thus, anti-inflammatory strategies become central as possible new treatments of insulin resistance and other complications of obesity (56).

ER stress

The fundamental role of ER is the integration of multiple metabolic signals and the maintenance of cell homeostasis (26, 58). Under stress conditions that challenge its function, ER triggers an adaptive response called uncoupled protein response (UPR) (97, 178). To resolve ER stress, UPR promotes a decrease in protein synthesis, and at the same time, an increase in protein degradation and chaperone production for protein folding. During the chronic energy surplus associated with obesity, ER cannot recover its normal function and UPR activation contributes to the development of insulin resistance through several mechanisms, such as JNK-Ap1 and NF- κ -IKK signaling pathways, inflammation, and oxidative stress (74).

Food intake

The central nervous system, specifically the hypothalamus, is of crucial importance in obesity-induced pathologies, since it plays a major role in the control of food intake and regulation of body weight (177). The discovery of leptin was a major breakthrough for our current knowledge of energy homeostasis (179). This adipocyte-secreted hormone acts on the hypothalamus to inhibit food intake and control body weight and has proved essential in the interaction between the brain and other organs in obesity-related disorders (51). The alteration of the circadian rhythm has also been associated with an increased risk of obesity (63, 76), proving that it is not only what you eat, but also when you eat it. Thus, advances in understanding the molecular mechanisms linking circadian rhythms and metabolism may provide new therapies for obesity and other pathologies associated with the disruption of normal sleep-wake cycles.

Lack of Efficacy of Current Anti-Obesity Drugs

Obesity develops when energy intake exceeds energy expenditure. Thus, any treatment for obesity-induced disorders must reduce energy intake, increase energy expenditure, or have an effect on both. Attempting to lose weight only by caloric restriction comes up against the problem that mammals have evolved mechanisms to store energy to survive during periods of starvation. Such homeostatic mechanisms increase caloric efficiency, thus making further weight loss even more difficult. In recent years, several anti-obesity drugs designed to limit energy intake have been withdrawn from the market due to serious adverse effects (*i.e.*, fenfluramine, dexfenfluramine, sibutramine, and rimonabant) (36). Nowadays, only two drugs are approved specifically for weight loss by the US Food and Drug Administration (FDA): the lipase-inhibitor Orlistat that is also approved by the European Medicines Agency (EMA), but has a limited long-term effectiveness (36), and the recently approved serotonergic Lorca-

serin-Belviq (84, 126). Thus, more efforts are needed to develop new anti-obesity agents. In this regard, strategies designed to increase lipid mobilization and oxidation could be very useful in the treatment of obesity and associated diseases.

Mitochondrial FAO and Bioenergetics

Hormones, such as insulin, glucagon, and noradrenaline, control the extracellular uptake and intracellular release of the main cell fuels; namely, carbohydrates and FAs. Once inside the cell, FAs are esterified, metabolized to lipid second messengers, or β -oxidized in mitochondria. The first step of the oxidative pathway is the transport of long-chain FAs (LCFAs) into the mitochondrial matrix (Fig. 1). This step is controlled by the carnitine palmitoyltransferase (CPT) system, which consists of three proteins: CPT1, acylcarnitine translocase (CACT), and CPT2 (109). Malonyl-CoA, a molecule derived from glucose metabolism and the first intermediate in lipogenesis, regulates FAO by inhibiting CPT1, thus making this enzyme the rate-limiting step in mitochondrial oxidation of FAs. Mammal tissues express three isoforms of CPT1: CPT1A (41) (liver), CPT1B (175) (muscle and heart), and CPT1C (138) (brain). Acetyl-CoA carboxylase (ACC), which controls the synthesis of malonyl-CoA; malonyl-CoA decarboxylase

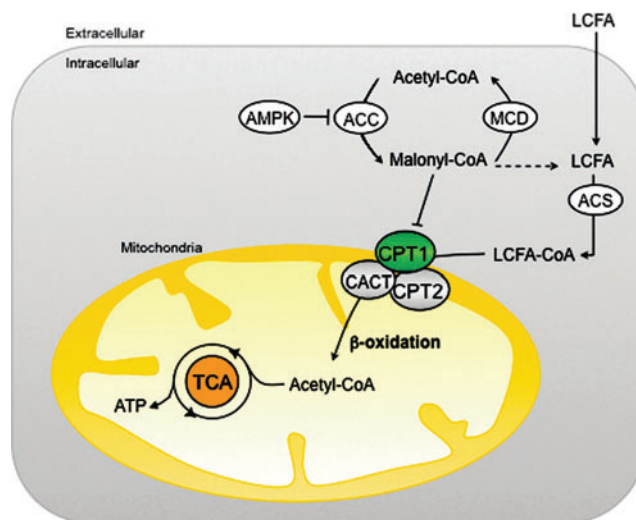


FIG. 1. Mitochondrial fatty acid oxidation (FAO). Long-chain fatty acid (LCFA) catalysis implies activation by acyl-CoA synthase (ACS) of LCFAs into LCFA-CoA, which is a substrate for the mitochondrial carnitine palmitoyltransferase 1 (CPT1) enzyme. The CPT system, which includes CPT1, acylcarnitine translocase (CACT), and CPT2, allows LCFA-CoA to enter the mitochondrial matrix, *via* transesterification reactions, to then be β -oxidized. CPT1 is the rate-limiting enzyme in FAO since its activity is tightly regulated by the glucose-derived malonyl-CoA, generated by acetyl-CoA carboxylase (ACC) during fatty acid (FA) *de novo* formation (in energetically abundant situations) or degraded by malonyl-CoA decarboxylase (MCD) in a process regulated by AMP-activated protein kinase (AMPK). Acetyl-CoA generated in FAO eventually enters the tricarboxylic acid (TCA) cycle to obtain reductive power for cellular respiration and produce ATP. To see this illustration in color, the reader is referred to the web version of this article at www.liebertpub.com/ars

(MCD), which catalyzes malonyl-CoA degradation; and CPT1, which is regulated by malonyl-CoA, are components of a metabolic signaling network that perceives the level of fuel stimuli (109).

One of the main regulators of this network is the AMP-activated protein kinase (AMPK). This protein is the downstream element of a kinase cascade, activated by its phosphorylation in the Thr172 residue of the catalytic subunit (174). In general, AMPK inhibits ATP-consuming processes, while activating catabolic pathways. Active AMPK phosphorylates and inhibits ACC and reduces the expression of FA synthase, thus decreasing the flux of substrates in the FA anabolic pathway (176). In consequence, the reduction in malonyl-CoA levels leads to an increase in CPT1 activity and FAO.

The regulation of AMPK by members of the sirtuin family of NAD^+ -dependent protein deacetylases and ADP-ribosyltransferases (sirtuins) has been reported (94). Sirtuin 1 (SIRT1) and SIRT3 stimulate AMPK by deacetylating its upstream activator, kinase LKB1 (94, 135). In turn, the AMPK activity leads to an increase in NAD^+ levels, thereby promoting deacetylation/activation of other SIRT1 targets involved in FAO, like peroxisome proliferator-activated receptor γ coactivator-1 α (PGC-1 α) (18). In recent years, sirtuins have emerged as critical modulators of lipid metabolism and specifically of FAO. In mammals, the seven identified members of the sirtuin family are differentially located within the cell: SIRT1, 6 and 7 are mainly located in the nucleus; SIRT3, 4 and 5 are located in the mitochondria; and SIRT2 is a cytosolic protein (111). In specific tissues, sirtuins act on different targets promoting FAO (liver and skeletal muscle [SkM]), mitochondrial respiration (brown adipose tissue [BAT]), lipolysis (white adipose tissue [WAT]), and food intake (hypothalamus) (148).

Energy flow in living cells (bioenergetics) takes place mainly in mitochondria. Energy is obtained from FAs and other nutrients in the form of ATP—the chemical currency of life—through the tricarboxylic acid (TCA) cycle, and the electron transport chain (ETC) in a process known as oxidative phosphorylation (162) (Fig. 2). This process is the main source of reactive oxygen species (ROS) in the cell. In the ETC, the energy of electrons from NADH and FADH_2 is used to pump protons (H^+) from the mitochondrial matrix to the intermembrane space and generate the electrochemical gradient necessary for ATP synthesis. However, when these electrons escape the ETC, ROS are produced in the mitochondria. Even under physiological conditions, the incomplete electron transfer to O_2 , resulting in ROS production, occurs with 0.2%–2% of oxygen molecules (21). Mitochondrial ROS production is highly regulated and important for various cell functions, as ROS can act as signaling molecules. However, high ROS levels are associated with significant cell damage and mitochondrial dysfunction in a process known as oxidative stress (122), usually associated with the etiology of obesity, insulin resistance, and type 2 diabetes (67).

In the mitochondria, the ETC complexes remain electron-bound when the proton gradient between the mitochondrial matrix and the intermembrane space is high, preventing the outward pumping of H^+ and increasing ROS production. Mitochondrial uncoupling proteins (UCPs) uncouple ATP production from mitochondrial respiration, thereby reducing the H^+ gradient across the inner mitochondrial membrane and relieving the formation of ROS (106). In BAT, UCP1 dis-

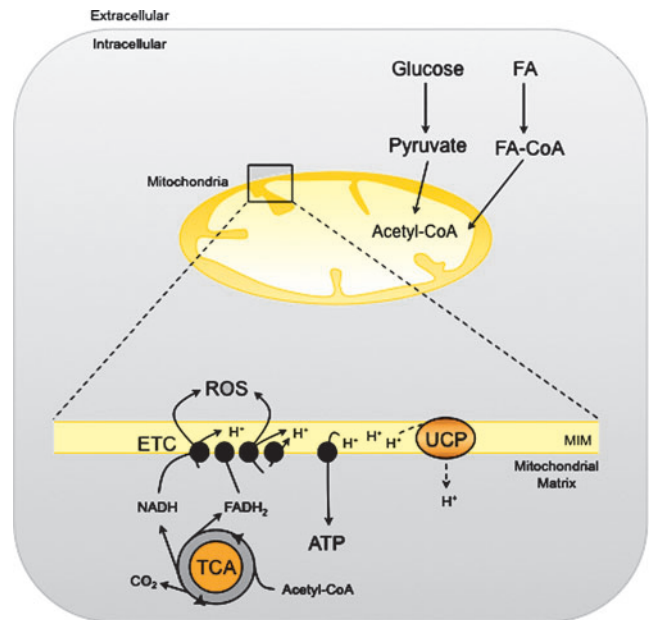


FIG. 2. Bioenergetics and mitochondrial metabolism. The mitochondrial fuels, glucose, and FAs, are converted to acetyl-CoA, which can be further metabolized to obtain energy. The TCA cycle generates protons (H^+) and electrons that are carried by NADH and FADH_2 to the electron transport chain (ETC), where the protons are transported to the mitochondrial intermembrane (MIM) space to generate energy as ATP. Highly reactive electrons may leak from the ETC and generate reactive oxygen species (ROS), which could act physiologically as signaling molecules, but can also cause significant cellular damage when overproduced. Uncoupling proteins (UCPs) dissipate the proton gradient and scavenge ROS accumulation, thus dissipating energy as heat. To see this illustration in color, the reader is referred to the web version of this article at www.liebertpub.com/ars

sipates energy as heat and plays a key role in adaptive thermogenesis. In other tissues, the UCP homologues (UCP2, 3, and 4) affect ROS production and have crucial roles in energy homeostasis (106).

The Central Role of Liver in Obesity

Fatty liver and nonalcoholic steatohepatitis

The liver plays a central role in both energy expenditure and lipid/glucose homeostasis. In conditions associated with prolonged excess of energy or impaired FA metabolism, the liver stores considerable amounts of lipids in a process that leads to nonalcoholic fatty liver disease (NAFLD). A hallmark of NAFLD is the accumulation of hepatic TGs, which originate in the increased availability of free FAs (FFAs; circulating and from *de novo* lipogenesis), altered FAO and inadequate synthesis and export of VLDL (37, 55). The imbalance between these inputs and outputs results in lipid accumulation in hepatocytes, which causes hepatosteatosis and insulin resistance. The progression of a more severe liver disease triggers nonalcoholic steatohepatitis (NASH), a serious condition of inflamed fatty liver that can further progress to liver fibrosis and cirrhosis (32, 155). The pathogenesis of NAFLD in human and animal models has been reviewed in seminal articles (27, 161). The mechanisms underlying NAFLD to NASH

progression are not completely understood. However, the alteration of FA metabolism and ROS production, which lead to mitochondrial dysfunction, and the induction of proinflammatory cytokines and fibrosis have emerged as key components that ultimately cause this liver disease (47).

Alterations of mitochondrial FAO and ROS production

Mitochondria play a vital role in the oxidation of FAs and ROS production. In the liver, mitochondrial FAO results either in complete oxidation to carbon dioxide or in partial oxidation to ketone bodies, which are exported to provide fuel for other tissues. The key step is catalyzed by CPT1A (109). Data on the rates of mitochondrial FAO and CPT1A activity in NAFLD/NASH are not conclusive, possibly because of the use of different models and parameters. *In vitro* and *in vivo* studies of liver or hepatocytes exposed to high FFA concentrations show both increased (25, 44, 112, 116) and decreased (43) mitochondrial FAO. Similarly controversial results were obtained with CPT1A expression and activity. An increase in CPT1A expression has been reported in several rodent models (14, 134). However, a considerable decrease in the expression of this enzyme was observed in NAFLD patients (123). Several mechanisms may explain these controversial data: (i) the variation of malonyl-CoA levels that depend on the expression and activity of AAC/MCD enzymes (24, 39); (ii) the loss of CPT1 sensitivity to malonyl-CoA, which alters CPT1 activity (29, 133); and (iii) the increased pool of FFAs or lipid derivatives in hepatocytes may activate transcription factors, such as PPARs (PPAR α , PPAR β/δ), which in turn may enhance CPT1 expression and FAO (19, 20, 22, 83). However, the transcriptional effect of PPAR α on liver CPT1 remains controversial, since some studies have suggested that long-chain FFA regulates CPT1 expression through a PPAR α -independent pathway (96, 101). Interestingly, another mechanism that modulates the CPT1 activity has recently been proposed (150). In this study, a NASH rat model fed a methionine-choline-deficient diet had a notable reduction in CPT1A activity and mitochondrial FAO despite increased CPT1A mRNA expression. The formation of a 4-hydroxynonenal-CPT1 adduct

caused by lipid peroxidation as a consequence of ROS overproduction is the main cause of impaired FAO and lipid removal from hepatocytes. ROS can attack polyunsaturated FAs, initiating lipid peroxidation and the formation of aldehyde by-products (4-hydroxy-2-nonenal [HNE] and malondialdehyde [MDA]), which have longer half-lives than ROS and are able to spread from their site of origin to reach distant intracellular and extracellular targets, thereby amplifying the effects of oxidative stress (44, 170). The observations listed above suggest that CPT1 overexpression and increased CPT1 activity occur in liver during the onset of steatosis as a mechanism to compensate for increased FA levels. Accelerated mitochondrial FAO might cause excessive electron flux in the ETC and ROS overproduction. As lipids, proteins, and mitochondrial DNA are the main ROS targets, increased ROS might initiate lipid peroxidation, damage mitochondrial DNA and proteins, and alter mitochondrial morphology and function. The post-translational modifications of CPT1 caused by lipid peroxidation could, subsequently, decrease CPT1 activity and reverse initially activated FAO. This notion raises the question of whether interventions aimed at promoting mitochondrial FAO in liver would be beneficial to the treatment of NAFLD/NASH.

Several strategies have been used to promote FAO, including the use of PPAR agonists (7, 114), AMPK agonists [metformin (180), AICAR (166)], and ACC antagonists (62, 108). Genetic approaches specifically promoting liver FAO are of considerable interest. An improvement in high-fat diet (HFD)-induced liver insulin resistance has been described in rodents, in which, FAO was indirectly enhanced by the reduction of malonyl-CoA levels through the modulation of ACC (146) and MCD (4). More interesting are the results obtained with a direct enhancement of mitochondrial FAO by increasing CPT1A expression in liver. Recent studies (117, 130) overexpressing an active and malonyl-CoA-insensitive mutant form of CPT1A (CPT1AM) (118) in obese rodents show that permanently enhanced liver FAO not only rescues impaired hepatic, muscle, and WAT insulin signaling in these animals, but also reduces steatosis, inflammation, and adiposity (Fig. 3). Furthermore, in these studies, enhanced

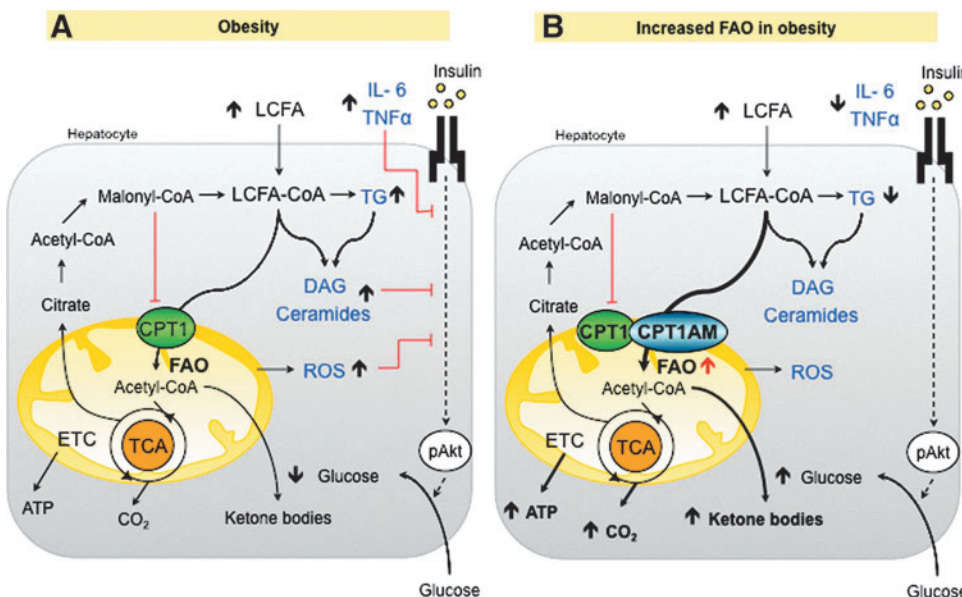


FIG. 3. Effects of enhanced FAO in fatty liver. (A) Obesity increases FA uptake, triglyceride (TG), diacylglycerol (DAG), ceramides, and other lipid derivatives that may inhibit insulin signaling. FA accumulation induces mitochondrial dysfunction and increased ROS production, oxidative stress, and inflammation that could also disrupt insulin signaling. (B) Enhancing FAO by the overexpression of CPT1AM (117, 130) increases the production of ketone bodies, ATP, and CO₂. The reduction of lipid content re-establishes lipid metabolism, insulin signaling, and decreases inflammation and ROS production.

mitochondrial FAO did not increase ROS derivatives or liver injury. Taken together, these results highlight an increase of CPT1A as a new strategy for the treatment of NAFLD/NASH pathologies. Alternatively, it has been reported that the administration of CPT1 inhibitors reduces gluconeogenesis and improves glucose homeostasis, although chronic treatments on HFD-treated mice caused hepatic steatosis (28, 53). This side effect has interrupted the development of other systemic inhibitors, such as etomoxir and 2-tetradecylglycidic acid, as a therapeutic tool. Taken together, these data support the idea that any strategy able to switch liver FA's fate from esterification toward oxidation produces a beneficial effect on the liver and on the whole body. It seems that the liver can deal with an increased flux of FA into the mitochondria, thus escaping from liver injury. This is due to the ability of liver to flip the balance from complete oxidation to ketone body production (88). The ketone bodies produced by enhanced FAO are easily consumed by other tissues, increasing the flux of carbons from liver to other organs. Recently, a new hepatic factor, fibroblast growth factor 21 (FGF21), has emerged as a key regulator in FAO and ketogenic activation. FGF21 is induced in the liver during fasting (136) and has been increasingly pointed to as a potential therapeutic agent in obesity-induced insulin-resistant states (78).

WAT Meets Inflammation and Metabolic Disorders in Obesity

WAT has long been recognized as the main storage site for lipids derived from food intake (142). This long-term energy reservoir stores lipids mainly in the form of TGs, which can be mobilized and used to generate ATP through the mitochondrial β -oxidation pathway in peripheral organs during periods of caloric need.

WAT is composed mainly by adipocytes, but also by immune cells, such as macrophages, T cells, and mast cells (68, 104). Thus, WAT is an active and endocrine organ that secretes a large number of adipokines, cytokines, and chemokines (*i.e.*, leptin, adiponectin, resistin, TNF α , IL-6, MCP-1,

and IL-10), and plays a key role in regulating whole-body glucose and lipid metabolism (46, 151).

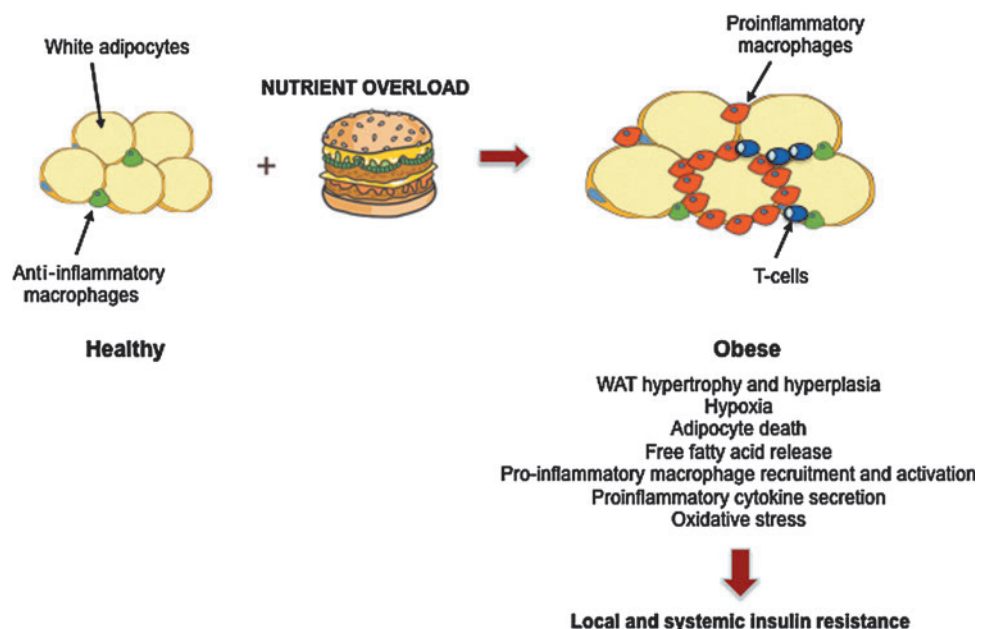
WAT, obesity, and inflammation

Obesity is characterized by the expansion of WAT mass due to an increase in both adipocyte number (hyperplasia) and size (hypertrophy), and it is closely associated with insulin resistance in peripheral tissues, such as SkM and liver. In fact, under excess caloric intake, WAT reaches its upper limit for further lipid storage (157, 169). Consequently, adipocytes exceed their oxygen diffusion limit, thereby promoting hypoxia (73), ER stress (132), and cell death, and increased circulating FFA and TG accumulation in ectopic sites is produced (145). The combination of microhypoxia and lipid overload triggers the recruitment of immune cells, such as macrophages in the adipose tissue and their activation (103, 129, 171). Obese adipocytes and infiltrated immune cells secrete a large amount of inflammatory mediators that promote a proinflammatory state through the activation of IKK β -NF- κ B and the JNK-Ap1 signaling pathways (151). The induction of JNK leads to serine phosphorylation of IRS-1 and 2, crucial molecules in insulin signaling, and consequently inhibits insulin action. These events cause insulin resistance in adipocytes, exacerbation of the inflammatory state, and systemic insulin resistance (59, 147) (Fig. 4).

FFAs, inflammation, and ROS

Physiological ROS production in adipocytes is a relevant cellular signaling mechanism in the insulin response and it depends mainly on the NADPH oxidase (NOX) family activity (9). In obesity, the excess of FFAs increases NOX-mediated ROS generation. Recently, it has been demonstrated that increased ROS in adipocytes exposed to an excess of FFAs does not depend on enhanced mitochondrial flux, but on high levels of TNF α and ER stress as well as the upregulation of aforementioned NOX enzymes (8, 60). ROS have the capacity to interfere with insulin signaling, since they activate several downstream pathways involving MAPK, JNK/IKK β , and

FIG. 4. White adipose tissue (WAT), obesity, and insulin resistance. Nutrient overload, weight gain, and obesity result in increased adipose tissue mass and adipocyte size. The expansion of the adipose tissue leads to adipocyte hypoxia, death, and free fatty acid (FFA) release into circulation. These events trigger the recruitment and activation of immune cells, such as macrophages and T cells, in the adipose tissue. Infiltrated and activated immune cells and adipocytes secrete large amounts of proinflammatory cytokines, which promote the inhibition of insulin signaling with an ensuing local and systemic resistance (147).



JAK/STAT, which are key contributors to the development of insulin resistance in obesity and type 2 diabetes (8, 75).

Enhanced FAO and improvement in insulin sensitivity

The imbalance between lipid storage and lipid utilization predisposes to adipocyte dysfunction and FFAs promote the proinflammatory response and ROS production involved in severe metabolic disorders. Although the exact physiological role of FAO in WAT remains to be determined, recent studies have shown beneficial effects of increased FAO and lipolysis in adipocytes, through direct CPT1A overexpression. In fact, this rise in lipid utilization improves insulin sensitivity in these cells and suppresses inflammatory signaling (50). However, there is still no evidence that increasing adipose tissue FAO would decrease FFA-induced ROS production. Thus, further research is required to elucidate these mechanisms and to evaluate the potential benefit of this strategy to prevent or reverse obesity and related metabolic diseases.

BAT, Turning Up the Heat

BAT morphology and function

In addition to energy-storing WAT, human fat consists of thermogenic controlling BAT. The latter has traditionally received less attention than WAT since it is less abundant and was considered exclusive to rodents and children. However, more recently, BAT have gained relevance in the mechanisms involved in obesity-related disorders.

BAT thermogenesis takes place in its numerous, densely packed mitochondria, which contain the BAT-specific UCP1. Activation of this protein uncouples aerobic respiration by producing heat instead of ATP (162). Brown adipocytes are also differentiated from white adipocytes because of their high expression of type 2 iodothyronine deiodinase (DIO2), the transcription coregulators, PRDM16 and PGC-1 α , and the lipolytic regulator, Cidea (52, 131). In rodents, BAT generates heat mainly for two reasons; namely, to protect against cold exposure *via* nonshivering thermogenesis and to burn the excess calories and reduce fat accumulation (54, 72). Therefore, BAT plays a crucial role in protecting mice from diet-induced obesity.

Rediscovery of human BAT

The fusion of positron emission tomography (PET) and computed tomography (CT) images allowed radiologists to see both functional and structural information in a single image. In the course of using PET-CT to detect and stage tumors in humans, active BAT was observed to increase after cold exposure (124).

However, the real breakthrough arrived in 2009 when five independent groups used PET-CT to identify the presence and study the relevance of BAT in adult humans (30, 143, 165, 168, 181). All the groups showed major depots of metabolically active fat in the cervical-supraclavicular region, a slightly different site from that in rodents and children, where BAT is found mainly situated in the interscapular area. The expression of UCP1, DIO2, and the β 3-adrenergic receptor was also reported, thereby indicating the potential responsiveness of human BAT to both hormonal and pharmacological stimuli.

Interestingly, human studies showed that BAT is reduced in obese and diabetic patients, thus indicating that this tissue participates in both cold-induced and diet-induced thermogenesis (30). These observations made BAT a major breakthrough, since any strategy able to increase the mass or activity of this tissue could potentially provide hope for obese and diabetic patients.

BAT bioenergetics and mitochondrial metabolism

BAT is the only tissue to express UCP1, a protein found in the inner mitochondrial membrane that orchestrates the uncoupled reaction of allowing protons to re-enter the mitochondrial matrix without generating ATP. The dissipation of energy as heat confers BAT with the capacity to control thermogenesis. In fact, altered UCP1 expression (UCP1-deficient or transgenic mice) leads to dysregulated sensitivity to cold exposure and body weight control (40, 42, 86, 87, 98).

Body temperature changes stimulate norepinephrine release by sympathetic nervous endings that activate β -adrenergic receptors and trigger a signal transduction cascade that converts nutrients into acetyl-CoA. The TCA cycle uses this mitochondrial fuel to produce protons and electrons, which generate ATP through the ETC. However, in BAT, UCP1 allows protons to enter the mitochondrial matrix without generating ATP, that is, uncoupled, and heat is produced in this process. Thus, BAT burning power intensely clears and oxidizes circulating lipids and glucose to generate heat (17). This observation thus highlights BAT thermogenesis as an attractive therapeutic anti-obesity target.

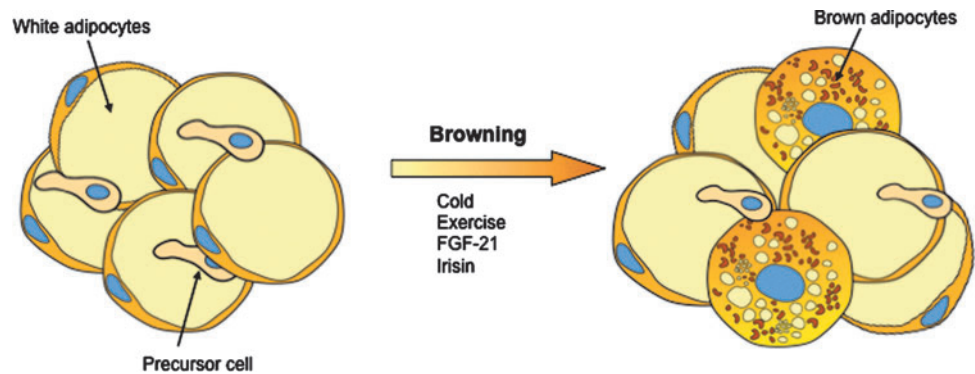
Enhancing BAT burning power and browning of WAT as an anti-obesity strategy

Recent landmark studies have identified novel secreted proteins, such as liver FGF21 (72), cardiac natriuretic peptides (11), and irisin (12), that stimulate brown adipocyte thermogenesis. Interestingly, a moderate increase (threefold) in irisin blood levels in mice enhanced energy expenditure and improved obesity and glucose homeostasis (12). In addition, recent articles reported that macrophages (125) and the bone morphogenetic protein BMP8B (172) have also the capacity to regulate BAT thermogenesis. Therefore, promoting BAT activation and/or brown adipocyte recruitment in white fat (browning) are approaches of considerable interest by which to develop pharmacological strategies to improve systemic metabolism by increasing energy expenditure (Fig. 5).

Role of FAO in Muscle Insulin Sensitivity During Obesity

SkM is vital for the maintenance of glucose homeostasis. It accounts for ~80% of total glucose uptake after insulin stimulation (34) and its transition to an insulin-resistant state is central for the pathogenesis of type 2 diabetes (152). Various pathways trigger obesity-induced insulin resistance (147). Both the action of fat-derived cytokines (adipocytokines) and ectopic accumulation of lipid deposition impair SkM function and play a critical role in insulin sensitivity. Obesity is characterized by a greater breakdown and uptake of FFAs. Parallel with the increase in circulating lipids, the intramyocellular (IMC) lipid content appears to increase proportionally in obese humans (105) and rodents (23). The lipotoxic hypothesis proposes that FFAs and their metabolites (such as DAG and

FIG. 5. Stimulation of brown adipose tissue (BAT) thermogenesis. Cold exposure, exercise, and some secreted proteins, such as fibroblast growth factor-21 (FGF-21) (72) and irisin (12), enhance BAT burning power by promoting brown adipocyte recruitment in white fat (browning).



ceramides) are important contributors to lipid-induced insulin resistance in SkM. These molecules activate proinflammatory and nutrient-sensing pathways that lead to the impairment of insulin action (Fig. 6A) [for further information, readers are referred to additional reviews (144, 159)].

Muscle FAO in obesity: two sides of the same coin

Several strategies have been designed to prevent IMC lipid accumulation and its deleterious effects. In SkM, these are mainly focused on the inhibition of FA uptake and esterification and/or the increase in FAO. However, whether the metabolic shift toward fat oxidation ameliorates lipid-induced SkM dysfunction is still open to debate.

Different laboratories have demonstrated that a decrease in the size and number of mitochondria, the activity of proteins in the ETC and, in general, impaired oxidative capacity in SkM are associated with obesity and insulin resistance in humans and animals (102, 139, 153). Given these observations, it is postulated that increased mitochondrial FAO could prevent lipid accumulation and, thus, improve insulin sensitivity in SkM (Fig. 6B). Several lines of evidence support this idea: (i) exercise in obese humans increases muscle mitochondrial FAO and improves glucose tolerance and insulin sensitivity (16). This effect is probably due to increased CPT1 expression and activity during exercise (163); (ii) direct CPT1 overexpression in animals and SkM cells protects muscle from FA-induced insulin resistance and apoptosis (15, 66, 149); and (iii) indirect SkM CPT1 activation, by the use of AMPK activators (77) or the ACC2 knockout (1), ameliorates insulin-stimulated glucose uptake in rodents.

Despite all the above points, the idea of mitochondrial deficiency as the main cause of diet-induced insulin resistance has been challenged in recent years. First, it is known that SkM's capacity to oxidize substrates is far in excess of what is needed to supply the energy demands of resting muscle (5). With this in mind, it seems clear that the mild ($\approx 30\%$) reduction in mitochondrial content observed in obese patients does not affect the ability of resting muscle to oxidize fat. Further, despite the reduction in the mitochondrial content, insulin-resistant SkM has normal mitochondrial function (13). Secondly, since FA and glucose compete as metabolic substrates, the decrease in FAO would produce enhanced glucose utilization instead of insulin resistance. In fact, patients with severe mitochondrial deficiency have an increase in glucose uptake despite the large accumulation of IMC lipids (61). And finally, a HFD causes insulin resistance in rodents, while inducing an increase in SkM mitochondrial biogenesis and β -

oxidation (164). This suggests that FAO might already be enhanced during obesity, contributing to the development of insulin resistance (121).

The main problems associated with an increase in FAO are: (i) the high rates of incomplete fat oxidation and (ii) the increase in oxidative stress associated with a mitochondrial overload (Fig. 6C) (89). Koves *et al.* (89) postulated that HFD induces the expression of FAO-related genes, but not those associated with the ETC and TCA cycle. This causes a mismatch between FAO and TCA cycle activity, thus leading to the accumulation of incomplete FAs and other intermediates (*i.e.*, acylcarnitines) that correlate negatively with glucose tolerance (2). How these intermediates mediate the onset of insulin resistance is still unknown. However, studies linking overnutrition with the acylation of mitochondrial proteins are relevant to this topic and suggest a role for acylcarnitines (70). Mitochondrial members of the sirtuin family are known to deacetylate/activate several proteins involved in fat oxidation. This along with the observation that SIRT3 knockout mice have high acylcarnitines and increased acylated mitochondrial proteins and develop metabolic syndrome, implies that mitochondrial accumulation of FAO intermediates triggers metabolic complications *via* protein modification (71, 80).

Role of ROS in muscle insulin signaling

FAO intermediates may also create an unfavorable environment in the mitochondria, which contributes to the formation of ROS and the development of oxidative stress (119, 120). High levels of ROS and systemic oxidative stress have been associated with obesity and insulin resistance (45). However, these molecules are produced normally during mitochondrial respiration and are essential signal transducers that regulate several cell processes in SkM (8), including the insulin pathway (64, 65). Due to its dual role in insulin sensitivity, modulation of redox balance is crucial for correct cell function. On the one hand, under physiological conditions, ROS are generated in response to insulin and are required for its action (69), since the activity of different enzymes that participate in the insulin cascade are dependent on their oxidation state. In particular, the phosphatases that negatively modulate the insulin pathway are the main targets for oxidative inhibition by ROS (35). It has also been reported that ROS enhance insulin sensitivity in HFD mice (100). These molecules are also crucial for the SkM remodeling that occurs in response to exercise (31). ROS show insulin-like effects, stimulating SkM glucose uptake during muscle contraction *via* the activation of AMPK (81) and the induction of PGC-1 α

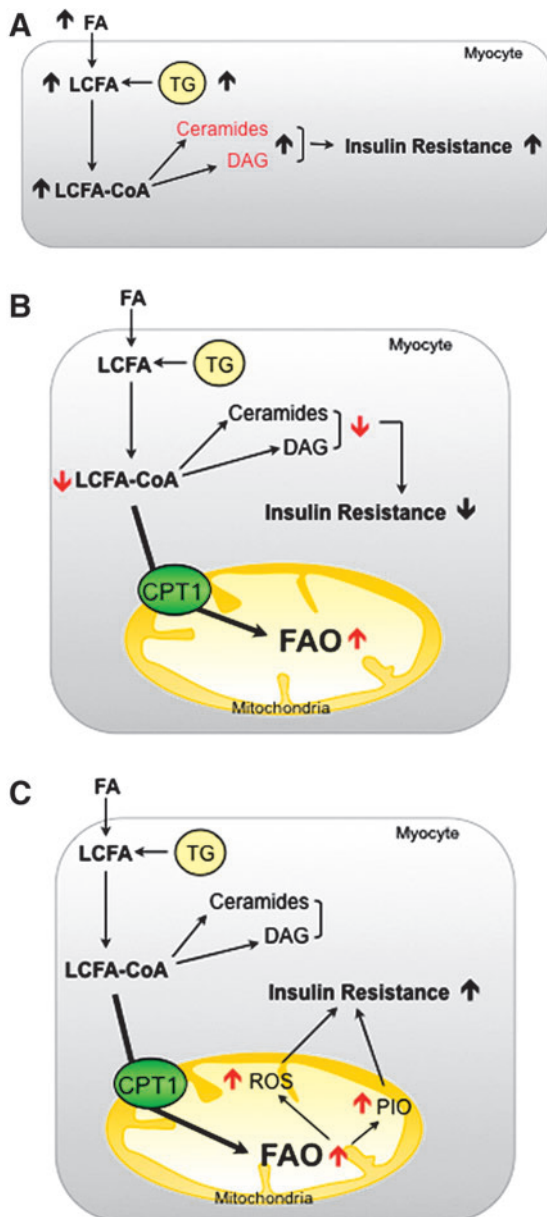


FIG. 6. Two hypotheses for the role of FAO in the development of obese-induced insulin resistance in skeletal muscle (SkM). (A) During obesity, intramyocellular lipid accumulation leads to a decrease in insulin-stimulated glucose uptake in SkM (144). (B) An increase in FAO may decrease LCFAs, ceramide, and DAG content, thus enhancing insulin action (15, 66, 149). (C) However, an increase in FAO may augment ROS production and enhance the accumulation of products of incomplete β -oxidation (PIO), which are hypothesized to decrease insulin signaling through the activation of various stress kinases (89).

expression *in vitro* and *in vivo* (57, 79). On the other hand, during a pathophysiological state, abundant evidence indicates that a large and sustained increase in ROS impairs insulin action, through the activation of stress signaling pathways (*i.e.*, MAPK and JNK) (85, 154), contributing to the pathogenesis of diet-induced insulin resistance (67). Therefore, clarifying the role of mitochondrial FAO, and the ROS

production derived from it, in diet-induced SkM insulin-resistance is crucial to the development of new therapeutic strategies to fight against obesity and its related metabolic complications.

Hypothalamic FAO in the Regulation of Food Intake

Excess food intake in obesity is related to behavioral processes controlled by the central nervous system. Specific hypothalamic nuclei, which sense nutrients and modify energy intake and expenditure to maintain a balance, are responsible for regulating this intake (48). The mechanisms for sensing the nutritional state have not been fully discovered and less is known about lipid than glucose sensing. Nonetheless, there are two classic hypotheses on nutritional state metabolic mediators, involving malonyl-CoA and LCFA-CoA.

CPT1A on food intake control: linking the malonyl-CoA and LCFA-CoA hypotheses

Strong evidence shows that increased malonyl-CoA levels, which are generated by activated (*i.e.*, dephosphorylated) ACC, act as abundance indicators, thereby diminishing food intake and consequently body weight (173). During starvation, ACC phosphorylation is mainly controlled by the well-known energy sensor, AMPK (115), which acts also as an important hub, integrating in-cell energetic state sensing and its modulation due to different circulating hormones. Concretely, ghrelin-mediated activation (*i.e.*, phosphorylation) of AMPK is done *via* SIRT1-mediated activation (*i.e.*, deacetylation) of p53. It is known that the SIRT1 activity is increased in hypothalamus during starvation with high ghrelin levels (167). The mechanism of leptin action also appears to be related to increases in physiological malonyl-CoA in the arcuate nucleus, which promotes a reduction in food intake and body weight, using different mechanisms to those previously reported for ghrelin action, during energetically wealthy states (49, 141).

In addition, LCFA-CoA levels have also been put forward as mediators in nutritional state sensing. During starvation, circulating FFA increase can be sensed in hypothalamic nuclei through in-cell activation to LCFA-CoA. This increase, previous to active ghrelin rise, is an early reporter of a deficient nutritional state (156). However, unfortunately, no cytoplasmic LCFA-CoA increase in hypothalamus has been found. Even so, in the last decade, pharmacological and genetic inhibition of hypothalamic CPT1A has been reported to reduce the food intake (10, 110, 127), potentially as a result of LCFA-CoA cytoplasmic accumulation. Furthermore, the role of malonyl-CoA as a CPT1 inhibitor is worth noting, to link the two hypotheses.

Regardless of whether malonyl-CoA or LCFA-CoA is the main actor, changes in feeding behavior and peripheral metabolism are conducted *via* the action of neuropeptides, such as agouti-related protein (AgRP), neuropeptide Y (NPY), and melanocortins. Transcription factors affected by changes in hypothalamic FAO, such as CREB, FoxO1, and BSX, are involved in ghrelin-induced expression of NPY and AgRP (92). However, it is still unknown whether high levels of LCFA-CoA trigger NPY and AgRP *via* BSX and subsequent transcription factors. Probably, neither malonyl-CoA nor LCFA-CoA act as key molecular mediators *per se* to induce the expression of the different food intake-controller neuropeptides,

but they are just two of the several pieces involved in the highly complex hypothalamic nutritional state sensing system, which is still not fully understood.

The relevance of FAO in neuronal cells is controversial because glucose is the brain's primary energy source. However, basal levels of FAO enzymes and FA transport proteins (such as FATP-1, FATP-4, and FAT/CD36) are expressed in hypothalamic neurons (93, 95). Additionally, the presence of such small, but functional FAO could be explained by its essential role in neuronal FA turnover and its action as a lipid-sensing mediator for energy homeostasis (113). There is also another controversy regarding fasting, because during fasting, high blood FFA levels presumably reach hypothalamic nuclei. This does not fit in with the satiety effect observed in early experiments with high LCFA concentration in the hypothalamus (128). Nonetheless, the direct correlation observed between fasting and FFA levels (156) and the capacity of hypothalamic neurons to sense glucose and FFA simultaneously and to integrate other nutritional and hormonal inputs (95, 99) seem to throw light on how important FAO really is in hypothalamic nuclei.

ROS, third in discord

Along with malonyl-CoA and LCFA-CoA, mitochondrial ROS have been put forward as a mediator in response to nutrient availability (140) (Fig. 7). ROS in the hypothalamus are produced chiefly in mitochondria ECT complexes. Concretely, some authors pointed to complex I as the most relevant site for single electron reduction in brain mitochondria (90). Various kinases and transcription factors, involved in neuropeptide regulation, have been reported to be modulated by redox signaling (33, 91). Further, the signaling under different levels of ROS may imply dissimilar pathophysiological changes in proteins, depending on their redox state (33). A

certain level of ROS, without being excessive, is probably required to trigger neuropeptide expression. This notion may explain the importance of UCP2 as a ROS scavenger to keep a physiological ROS level that allows correct NPY and AgRP expression in the hypothalamus (6). In addition to all these considerations, the recent finding that hypothalamic autophagy is a source of endogenous FFA to regulate AgRP levels (82) could be explained by increased mitochondrial FAO and ROS signaling. However, further research is needed to establish the contribution of ROS to the hypothalamic control of food intake.

Innovation

Recent results suggest that enhancing cellular energy expenditure may be an attractive therapy to prevent or reverse the exponential growth of obesity-related disorders. We reviewed those recent discoveries regarding mitochondrial FAO and its potential as a therapy for obesity.

Conclusions

Despite considerable current efforts, the prevalence of obesity and associated diseases is rising exponentially in both industrialized and developing countries worldwide. This is especially worrying in the young. Current therapeutic strategies, focused mainly on controlling food intake, have met limited success, probably due to the inherent resistance of the human body to weight loss. However, recent approaches targeting energy expenditure and mitochondrial FAO shed light on new therapies to fight obesity.

Mitochondrial FAO is the cell source of energy from FAs. Since an excess of lipids is found in obesity and associated pathologies, a lot of research studies how to eliminate them through an increase in FAO. Beneficial effects of an increase in energy expenditure in obesity have been described in several tissues, including liver, muscle, WAT, and BAT. On the contrary, FAO therapeutic inhibition in hypothalamus seems to reduce food intake. Whether or not FAO should be modulated in the above-mentioned tissues to improve insulin resistance or to lose weight is still a subject of debate. There is no doubt regarding the involvement of ROS in pathophysiological processes related to obesity, and CPT1 seems to be a good molecular target for ROS and FAO modulation. However, several questions still need to be answered before FAO can become an obesity therapy. First, it is not known whether a long-term increase in energy expenditure would cause an enhancement of appetite as a compensatory mechanism. Second, an increase in FAO could induce pathological levels of ROS and/or other incomplete oxidation products. Third, it is not known whether FAO enhancement might reach a limit in a specific tissue, such as in BAT, in which thermogenesis is tightly adjusted to the environmental temperature. Finally, since increasing flux through β -oxidation would only make sense together with a corresponding enhancement in energy demand (121), the physiological relevance of improved mitochondrial FAO might be questioned if the individual remains sedentary (muscle, WAT, or liver) or warm (BAT). Potential mechanisms to explain the beneficial effects of targeting mitochondrial FAO could be the concomitant enhancement of hepatic ketone bodies, CO₂, acid soluble products, ATP production, and endergonic processes (*e.g.*, gluconeogenesis) seen in previous publications (38, 130, 158).

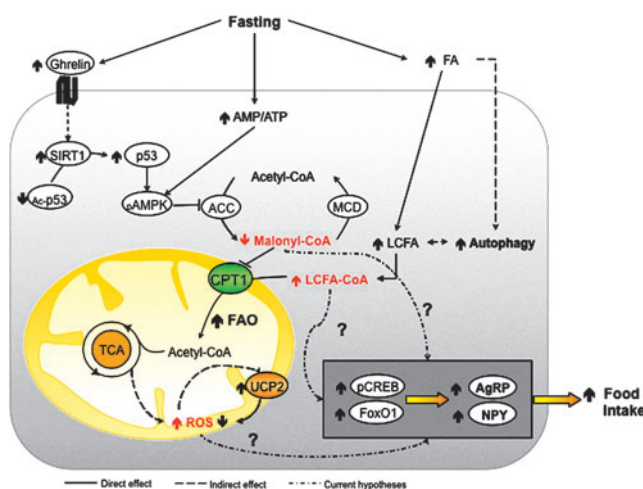


FIG. 7. Hypotheses involving FAO in the regulation of food intake. During fasting, the effects of ghrelin, AMP, and FAs act in hypothalamic nuclei to increase the expression of orexigenic neuropeptides (48). The mechanisms involved in this process appear to be related to an increase in LCFA-CoA, diminished malonyl-CoA, and a certain level of ROS. Excessive ROS production is controlled by UCP2 with a negative feed-back. CPT1A is postulated to be involved in all the three approaches.

Increased FAO may also decrease glucose oxidation to maintain energy homeostasis, augment mitochondrial burning capacity through an increase in the number of mitochondria and/or the increased expression of UCPs, and thus dissipate the excess of energy as heat and ATP. All of these could well alleviate the mitochondrial pressure found in lipid overload states. Thus, an increase in energy expenditure could indeed be the underlying protective mechanism against obesity-induced metabolic abnormalities.

Although more research is needed, we are encouraged that targeting of FAO and cell energy expenditure may be available in the near future as therapies to treat obesity and its associated severe diseases.

Acknowledgments

We thank Professor Fausto G. Hegardt for helpful, inspiring, and wise discussions and the Language Service of the University of Barcelona for valuable assistance in the preparation of the English manuscript. This study was supported by the Spanish Ministry of Science and Innovation (Grant SAF2010-20039 to L.H., Grant SAF2011-30520-C02-01 to D.S., and doctoral fellowships to M.I.M. and J.F.M.), by the CIBER Fisiopatología de la Obesidad y la Nutrición (CIBEROBN), Instituto de Salud Carlos III (Grant CB06/03/0026 to D.S. and research contract to P.M.), and by the EFSD/Lilly and EFSD/Janssen (research fellowships to L.H.).

References

1. Abu-Elheiga L, Oh W, Kordari P, and Wakil SJ. Acetyl-CoA carboxylase 2 mutant mice are protected against obesity and diabetes induced by high-fat/high-carbohydrate diets. *Proc Natl Acad Sci U S A* 100: 10207–10212, 2003.
2. Adams SH, Hoppel CL, Lok KH, Zhao L, Wong SW, Minkler PE, Hwang DH, Newman JW, and Garvey WT. Plasma acylcarnitine profiles suggest incomplete long-chain fatty acid beta-oxidation and altered tricarboxylic acid cycle activity in type 2 diabetic African-American women. *J Nutr* 139: 1073–1081, 2009.
3. Ahima RS. Digging deeper into obesity. *J Clin Invest* 121: 2076–2079, 2011.
4. An J, Muoio DM, Shiota M, Fujimoto Y, Cline GW, Shulman GI, Koves TR, Stevens R, Millington D, and Newgard CB. Hepatic expression of malonyl-CoA decarboxylase reverses muscle, liver and whole-animal insulin resistance. *Nat Med* 10: 268–274, 2004.
5. Andersen P and Saltin B. Maximal perfusion of skeletal muscle in man. *J Physiol* 366: 233–249, 1985.
6. Andrews ZB, Liu ZW, Wallingford N, Erion DM, Borok E, Friedman JM, Tschoop MH, Shanabrough M, Cline G, Shulman GI, Coppola A, Gao XB, Horvath TL, and Diano S. UCP2 mediates ghrelin's action on NPY/AgRP neurons by lowering free radicals. *Nature* 454: 846–851, 2008.
7. Barroso E, Rodriguez-Calvo R, Serrano-Marco L, Astudillo AM, Balsinde J, Palomer X, and Vazquez-Carrera M. The PPARbeta/delta activator GW501516 prevents the down-regulation of AMPK caused by a high-fat diet in liver and amplifies the PGC-1alpha-Lipin 1-PPARalpha pathway leading to increased fatty acid oxidation. *Endocrinology* 152: 1848–1859, 2011.
8. Bashan N, Kovsan J, Kachko I, Ovadia H, and Rudich A. Positive and negative regulation of insulin signaling by reactive oxygen and nitrogen species. *Physiol Rev* 89: 27–71, 2009.
9. Bedard K and Krause KH. The NOX family of ROS-generating NADPH oxidases: physiology and pathophysiology. *Physiol Rev* 87: 245–313, 2007.
10. Bentebibel A, Sebastian D, Herrero L, Lopez-Vinas E, Serra D, Asins G, Gomez-Puertas P, and Hegardt FG. Novel effect of C75 on carnitine palmitoyltransferase I activity and palmitate oxidation. *Biochemistry* 45: 4339–4350, 2006.
11. Bordicchia M, Liu D, Amri EZ, Ailhaud G, Dessi-Fulgheri P, Zhang C, Takahashi N, Sarzani R, and Collins S. Cardiac natriuretic peptides act via p38 MAPK to induce the brown fat thermogenic program in mouse and human adipocytes. *J Clin Invest* 122: 1022–1036, 2012.
12. Bostrom P, Wu J, Jedrychowski MP, Korde A, Ye L, Lo JC, Rasbach KA, Bostrom EA, Choi JH, Long JZ, Kajimura S, Zingaretti MC, Vind BF, Tu H, Cinti S, Hojlund K, Gygi SP, and Spiegelman BM. A PGC1-alpha-dependent myokine that drives brown-fat-like development of white fat and thermogenesis. *Nature* 481: 463–468, 2012.
13. Boushel R, Gnaiger E, Schjerling P, Skovbro M, Kraunsoe R, and Dela F. Patients with type 2 diabetes have normal mitochondrial function in skeletal muscle. *Diabetologia* 50: 790–796, 2007.
14. Brady LJ, Brady PS, Romsos DR, and Hoppel CL. Elevated hepatic mitochondrial and peroxisomal oxidative capacities in fed and starved adult obese (ob/ob) mice. *Biochem J* 231: 439–444, 1985.
15. Bruce CR, Hoy AJ, Turner N, Watt MJ, Allen TL, Carpenter K, Cooney GJ, Febbraio MA, and Kraegen EW. Over-expression of carnitine palmitoyltransferase-1 in skeletal muscle is sufficient to enhance fatty acid oxidation and improve high-fat diet-induced insulin resistance. *Diabetes* 58: 550–558, 2009.
16. Bruce CR, Thrush AB, Mertz VA, Bezaire V, Chabowski A, Heigenhauser GJ, and Dyck DJ. Endurance training in obese humans improves glucose tolerance and mitochondrial fatty acid oxidation and alters muscle lipid content. *Am J Physiol Endocrinol Metab* 291: E99–E107, 2006.
17. Cannon B and Nedergaard J. Brown adipose tissue: function and physiological significance. *Physiol Rev* 84: 277–359, 2004.
18. Canto C, Gerhart-Hines Z, Feige JN, Lagouge M, Noriega L, Milne JC, Elliott PJ, Puigserver P, and Auwerx J. AMPK regulates energy expenditure by modulating NAD+ metabolism and SIRT1 activity. *Nature* 458: 1056–1060, 2009.
19. Chakravarthy MV, Lodhi JJ, Yin L, Malapaka RR, Xu HE, Turk J, and Semenkovich CF. Identification of a physiologically relevant endogenous ligand for PPARalpha in liver. *Cell* 138: 476–488, 2009.
20. Chakravarthy MV, Pan Z, Zhu Y, Tordjman K, Schneider JG, Coleman T, Turk J, and Semenkovich CF. "New" hepatic fat activates PPARalpha to maintain glucose, lipid, and cholesterol homeostasis. *Cell Metab* 1: 309–322, 2005.
21. Chance B, Sies H, and Boveris A. Hydroperoxide metabolism in mammalian organs. *Physiol Rev* 59: 527–605, 1979.
22. Chatelain F, Kohl C, Esser V, McGarry JD, Girard J, and Pegorier JP. Cyclic AMP and fatty acids increase carnitine palmitoyltransferase I gene transcription in cultured fetal rat hepatocytes. *Eur J Biochem* 235: 789–798, 1996.
23. Chen MT, Kaufman LN, Spennetta T, and Shrago E. Effects of high fat-feeding to rats on the interrelationship of body weight, plasma insulin, and fatty acyl-coenzyme A esters in liver and skeletal muscle. *Metabolism* 41: 564–569, 1992.
24. Choi CS, Savage DB, Abu-Elheiga L, Liu ZX, Kim S, Kulkarni A, Distefano A, Hwang YJ, Reznick RM, Codella R, Zhang D, Cline GW, Wakil SJ, and Shulman GI. Con-

- tinuous fat oxidation in acetyl-CoA carboxylase 2 knockout mice increases total energy expenditure, reduces fat mass, and improves insulin sensitivity. *Proc Natl Acad Sci U S A* 104: 16480–16485, 2007.
25. Ciapaite J, van den Broek NM, Te Brinke H, Nicolay K, Jeneson JA, Houten SM, and Prompers JJ. Differential effects of short- and long-term high-fat diet feeding on hepatic fatty acid metabolism in rats. *Biochim Biophys Acta* 1811: 441–451, 2011.
 26. Cnop M, Foufelle F, and Velloso LA. Endoplasmic reticulum stress, obesity and diabetes. *Trends Mol Med* 18: 59–68, 2012.
 27. Cohen JC, Horton JD, and Hobbs HH. Human fatty liver disease: old questions and new insights. *Science* 332: 1519–1523, 2011.
 28. Conti R, Mannucci E, Pessotto P, Tassoni E, Carminati P, Giannessi F, and Arduini A. Selective reversible inhibition of liver carnitine palmitoyl-transferase 1 by teglicar reduces gluconeogenesis and improves glucose homeostasis. *Diabetes* 60: 644–651, 2011.
 29. Cook GA and Gamble MS. Regulation of carnitine palmitoyltransferase by insulin results in decreased activity and decreased apparent K_i values for malonyl-CoA. *J Biol Chem* 262: 2050–2055, 1987.
 30. Cypess AM, Lehman S, Williams G, Tal I, Rodman D, Goldfine AB, Kuo FC, Palmer EL, Tseng YH, Doria A, Kolodny GM, and Kahn CR. Identification and importance of brown adipose tissue in adult humans. *N Engl J Med* 360: 1509–1517, 2009.
 31. Davies KJ, Quintanilha AT, Brooks GA, and Packer L. Free radicals and tissue damage produced by exercise. *Biochem Biophys Res Commun* 107: 1198–1205, 1982.
 32. Day CP and James OF. Steatohepatitis: a tale of two “hits”? *Gastroenterology* 114: 842–845, 1998.
 33. de Keizer PL, Burgering BM, and Dansen TB. Forkhead box o as a sensor, mediator, and regulator of redox signaling. *Antioxid Redox Signal* 14: 1093–1106, 2010.
 34. DeFronzo RA, Jacot E, Jequier E, Maeder E, Wahren J, and Felber JP. The effect of insulin on the disposal of intravenous glucose. Results from indirect calorimetry and hepatic and femoral venous catheterization. *Diabetes* 30: 1000–1007, 1981.
 35. Denu JM and Tanner KG. Redox regulation of protein tyrosine phosphatases by hydrogen peroxide: detecting sulfenic acid intermediates and examining reversible inactivation. *Methods Enzymol* 348: 297–305, 2002.
 36. Derosa G and Maffioli P. Anti-obesity drugs: a review about their effects and their safety. *Expert Opin Drug Saf* 11: 459–471, 2012.
 37. Donnelly KL, Smith CI, Schwarzenberg SJ, Jessurun J, Boldt MD, and Parks EJ. Sources of fatty acids stored in liver and secreted via lipoproteins in patients with nonalcoholic fatty liver disease. *J Clin Invest* 115: 1343–1351, 2005.
 38. Drynan L, Quant PA, and Zammit VA. Flux control exerted by mitochondrial outer membrane carnitine palmitoyl-transferase over beta-oxidation, ketogenesis and tricarboxylic acid cycle activity in hepatocytes isolated from rats in different metabolic states. *Biochem J* 317: 791–795, 1996.
 39. Dyck JR, Berthiaume LG, Thomas PD, Kantor PF, Barr AJ, Barr R, Singh D, Hopkins TA, Voilley N, Prentki M, and Lopaschuk GD. Characterization of rat liver malonyl-CoA decarboxylase and the study of its role in regulating fatty acid metabolism. *Biochem J* 350: 599–608, 2000.
 40. Enerback S, Jacobsson A, Simpson EM, Guerra C, Yamashita H, Harper ME, and Kozak LP. Mice lacking mitochondrial uncoupling protein are cold-sensitive but not obese. *Nature* 387: 90–94, 1997.
 41. Esser V, Britton CH, Weis BC, Foster DW, and McGarry JD. Cloning, sequencing, and expression of a cDNA encoding rat liver carnitine palmitoyltransferase I. Direct evidence that a single polypeptide is involved in inhibitor interaction and catalytic function. *J Biol Chem* 268: 5817–5822, 1993.
 42. Feldmann HM, Golozoubova V, Cannon B, and Nedergaard J. UCP1 ablation induces obesity and abolishes diet-induced thermogenesis in mice exempt from thermal stress by living at thermoneutrality. *Cell Metab* 9: 203–209, 2009.
 43. Fromenty B and Pessayre D. Inhibition of mitochondrial beta-oxidation as a mechanism of hepatotoxicity. *Pharmacol Ther* 67: 101–154, 1995.
 44. Fromenty B, Robin MA, Igoudjil A, Mansouri A, and Pessayre D. The ins and outs of mitochondrial dysfunction in NASH. *Diabetes Metab* 30: 121–138, 2004.
 45. Furukawa S, Fujita T, Shimabukuro M, Iwaki M, Yamada Y, Nakajima Y, Nakayama O, Makishima M, Matsuda M, and Shimomura I. Increased oxidative stress in obesity and its impact on metabolic syndrome. *J Clin Invest* 114: 1752–1761, 2004.
 46. Galic S, Oakhill JS, and Steinberg GR. Adipose tissue as an endocrine organ. *Mol Cell Endocrinol* 316: 129–139, 2010.
 47. Gambino R, Musso G, and Cassader M. Redox balance in the pathogenesis of nonalcoholic fatty liver disease: mechanisms and therapeutic opportunities. *Antioxid Redox Signal* 15: 1325–1365, 2011.
 48. Gao Q and Horvath TL. Neurobiology of feeding and energy expenditure. *Annu Rev Neurosci* 30: 367–398, 2007.
 49. Gao S, Kinzig KP, Aja S, Scott KA, Keung W, Kelly S, Strynadka K, Chohnan S, Smith WW, Tamashiro KL, Ladenheim EE, Ronnett GV, Tu Y, Birnbaum MJ, Lopaschuk GD, and Moran TH. Leptin activates hypothalamic acetyl-CoA carboxylase to inhibit food intake. *Proc Natl Acad Sci U S A* 104: 17358–17363, 2007.
 50. Gao X, Li K, Hui X, Kong X, Sweeney G, Wang Y, Xu A, Teng M, Liu P, and Wu D. Carnitine palmitoyltransferase 1A prevents fatty acid-induced adipocyte dysfunction through suppression of c-Jun N-terminal kinase. *Biochem J* 435: 723–732, 2011.
 51. Gautron L and Elmquist JK. Sixteen years and counting: an update on leptin in energy balance. *J Clin Invest* 121: 2087–2093, 2011.
 52. Gesta S, Tseng YH, and Kahn CR. Developmental origin of fat: tracking obesity to its source. *Cell* 131: 242–256, 2007.
 53. Giannessi F, Pessotto P, Tassoni E, Chiodi P, Conti R, De Angelis F, Dell’Uomo N, Catini R, Deias R, Tinti MO, Carminati P, and Arduini A. Discovery of a long-chain carbamoyl aminocarnitine derivative, a reversible carnitine palmitoyltransferase inhibitor with antiketotic and antidiabetic activity. *J Med Chem* 46: 303–309, 2003.
 54. Giralt A, Hondares E, Villena JA, Ribas F, Diaz-Delfin J, Giralt M, Iglesias R, and Villarroya F. Peroxisome proliferator-activated receptor-gamma coactivator-1alpha controls transcription of the Sirt3 gene, an essential component of the thermogenic brown adipocyte phenotype. *J Biol Chem* 286: 16958–16966, 2011.
 55. Goldberg IJ and Ginsberg HN. Ins and outs modulating hepatic triglyceride and development of nonalcoholic fatty liver disease. *Gastroenterology* 130: 1343–1346, 2006.
 56. Goldfine AB, Fonseca V, and Shoelson SE. Therapeutic approaches to target inflammation in type 2 diabetes. *Clin Chem* 57: 162–167, 2011.

57. Gomez-Cabrera MC, Domenech E, Romagnoli M, Arduini A, Borrás C, Pallardo FV, Sastre J, and Vina J. Oral administration of vitamin C decreases muscle mitochondrial biogenesis and hampers training-induced adaptations in endurance performance. *Am J Clin Nutr* 87: 142–149, 2008.
58. Gregor MF and Hotamisligil GS. Thematic review series: Adipocyte Biology. Adipocyte stress: the endoplasmic reticulum and metabolic disease. *J Lipid Res* 48: 1905–1914, 2007.
59. Guilherme A, Virbasius JV, Puri V, and Czech MP. Adipocyte dysfunctions linking obesity to insulin resistance and type 2 diabetes. *Nat Rev Mol Cell Biol* 9: 367–377, 2008.
60. Han CY, Umemoto T, Omer M, Den Hartigh LJ, Chiba T, Leboeuf R, Buller CL, Sweet IR, Pennathur S, Abel ED, and Chait A. NADPH Oxidase-derived Reactive Oxygen Species Increases Expression of Monocyte Chemotactic Factor Genes in Cultured Adipocytes. *J Biol Chem* 287: 10379–10393, 2012.
61. Han DH, Nolte LA, Ju JS, Coleman T, Holloszy JO, and Semenkovich CF. UCP-mediated energy depletion in skeletal muscle increases glucose transport despite lipid accumulation and mitochondrial dysfunction. *Am J Physiol Endocrinol Metab* 286: E347–E353, 2004.
62. Harwood HJ, Jr., Petras SF, Shelly LD, Zaccaro LM, Perry DA, Makowski MR, Hargrove DM, Martin KA, Tracey WR, Chapman JG, Magee WP, Dalvie DK, Soliman VF, Martin WH, Mularski CJ, and Eisenbeis SA. Isozyme-nonspecific N-substituted bipiperidylcarboxamide acetyl-CoA carboxylase inhibitors reduce tissue malonyl-CoA concentrations, inhibit fatty acid synthesis, and increase fatty acid oxidation in cultured cells and in experimental animals. *J Biol Chem* 278: 37099–37111, 2003.
63. Hatori M, Vollmers C, Zarrinpar A, Dittacchio L, Bushong EA, Gill S, Leblanc M, Chaix A, Joens M, Fitzpatrick JA, Ellisman MH, and Panda S. Time-restricted feeding without reducing caloric intake prevents metabolic diseases in mice fed a high-fat diet. *Cell Metab* 15: 848–860, 2012.
64. Hayes GR and Lockwood DH. Role of insulin receptor phosphorylation in the insulinomimetic effects of hydrogen peroxide. *Proc Natl Acad Sci U S A* 84: 8115–8119, 1987.
65. Heffetz D, Bushkin I, Dror R, and Zick Y. The insulinomimetic agents H₂O₂ and vanadate stimulate protein tyrosine phosphorylation in intact cells. *J Biol Chem* 265: 2896–2902, 1990.
66. Henique C, Mansouri A, Fumey G, Lenoir V, Girard J, Bouillaud F, Prip-Buus C, and Cohen I. Increased mitochondrial fatty acid oxidation is sufficient to protect skeletal muscle cells from palmitate-induced apoptosis. *J Biol Chem* 285: 36818–36827, 2010.
67. Henriksen EJ, Diamond-Stanic MK, and Marchionne EM. Oxidative stress and the etiology of insulin resistance and type 2 diabetes. *Free Radic Biol Med* 51: 993–999, 2011.
68. Herrero L, Shapiro H, Nayer A, Lee J, and Shoelson SE. Inflammation and adipose tissue macrophages in lipodystrophic mice. *Proc Natl Acad Sci U S A* 107: 240–245, 2010.
69. Higaki Y, Mikami T, Fujii N, Hirshman MF, Koyama K, Seino T, Tanaka K, and Goodyear LJ. Oxidative stress stimulates skeletal muscle glucose uptake through a phosphatidylinositol 3-kinase-dependent pathway. *Am J Physiol Endocrinol Metab* 294: E889–E897, 2008.
70. Hirschey MD, Shimazu T, Huang JY, and Verdin E. Acetylation of mitochondrial proteins. *Methods Enzymol* 457: 137–147, 2009.
71. Hirschey MD, Shimazu T, Jing E, Grueter CA, Collins AM, Aouizerat B, Stancakova A, Goetzman E, Lam MM, Schwer B, Stevens RD, Muehlbauer MJ, Kakar S, Bass NM, Kuusisto J, Laakso M, Alt FW, Newgard CB, Farese RV Jr., Kahn CR, and Verdin E. SIRT3 deficiency and mitochondrial protein hyperacetylation accelerate the development of the metabolic syndrome. *Mol Cell* 44: 177–190, 2011.
72. Hondares E, Rosell M, Gonzalez FJ, Giralt M, Iglesias R, and Villarroya F. Hepatic FGF21 expression is induced at birth via PPARalpha in response to milk intake and contributes to thermogenic activation of neonatal brown fat. *Cell Metab* 11: 206–212, 2010.
73. Hosogai N, Fukuhara A, Oshima K, Miyata Y, Tanaka S, Segawa K, Furukawa S, Tochino Y, Komuro R, Matsuda M, and Shimomura I. Adipose tissue hypoxia in obesity and its impact on adipocytokine dysregulation. *Diabetes* 56: 901–911, 2007.
74. Hotamisligil GS. Endoplasmic reticulum stress and the inflammatory basis of metabolic disease. *Cell* 140: 900–917, 2010.
75. Houstis N, Rosen ED, and Lander ES. Reactive oxygen species have a causal role in multiple forms of insulin resistance. *Nature* 440: 944–948, 2006.
76. Huang W, Ramsey KM, Marcheva B, and Bass J. Circadian rhythms, sleep, and metabolism. *J Clin Invest* 121: 2133–2141, 2011.
77. Iglesias MA, Ye JM, Frangioudakis G, Saha AK, Tomas E, Ruderman NB, Cooney GJ, and Kraegen EW. AICAR administration causes an apparent enhancement of muscle and liver insulin action in insulin-resistant high-fat-fed rats. *Diabetes* 51: 2886–2894, 2002.
78. Iglesias P, Selgas R, Romero S, and Diez JJ. Biological role. Clinical significance and therapeutic possibilities of the recently discovered metabolic hormone fibroblastic growth factor 21. *Eur J Endocrinol* 167: 301–309, 2012.
79. Irrcher I, Ljubicic V, and Hood DA. Interactions between ROS and AMP kinase activity in the regulation of PGC-1alpha transcription in skeletal muscle cells. *Am J Physiol Cell Physiol* 296: C116–C123, 2009.
80. Jing E, Emanuelli B, Hirschey MD, Boucher J, Lee KY, Lombard D, Verdin EM, and Kahn CR. Sirtuin-3 (Sirt3) regulates skeletal muscle metabolism and insulin signaling via altered mitochondrial oxidation and reactive oxygen species production. *Proc Natl Acad Sci U S A* 108: 14608–14613, 2011.
81. Katz A. Modulation of glucose transport in skeletal muscle by reactive oxygen species. *J Appl Physiol* 102: 1671–1676, 2007.
82. Kaushik S, Rodriguez-Navarro JA, Arias E, Kiffin R, Sahu S, Schwartz GJ, Cuervo AM, and Singh R. Autophagy in hypothalamic AgRP neurons regulates food intake and energy balance. *Cell Metab* 14: 173–183, 2011.
83. Keller H, Dreyer C, Medin J, Mahfoudi A, Ozato K, and Wahli W. Fatty acids and retinoids control lipid metabolism through activation of peroxisome proliferator-activated receptor-retinoid X receptor heterodimers. *Proc Natl Acad Sci U S A* 90: 2160–2164, 1993.
84. Khan A, Raza S, Khan Y, Aksoy T, Khan M, Weinberger Y, and Goldman J. Current updates in the medical management of obesity. *Recent Pat Endocr Metab* 6: 117–128, 2012.
85. Kim JS, Saengsirisuwan V, Sloniger JA, Teachey MK, and Henriksen EJ. Oxidant stress and skeletal muscle glucose transport: roles of insulin signaling and p38 MAPK. *Free Radic Biol Med* 41: 818–824, 2006.
86. Kontani Y, Wang Y, Kimura K, Inokuma KI, Saito M, Suzuki-Miura T, Wang Z, Sato Y, Mori N, and Yamashita H. UCP1 deficiency increases susceptibility to diet-induced obesity with age. *Aging Cell* 4: 147–155, 2005.
87. Kopecky J, Clarke G, Enerback S, Spiegelman B, and Kozak LP. Expression of the mitochondrial uncoupling protein

- gene from the aP2 gene promoter prevents genetic obesity. *J Clin Invest* 96: 2914–2923, 1995.
88. Kotronen A, Seppala-Lindroos A, Vehkavaara S, Bergholm R, Frayn KN, Fielding BA, and Yki-Jarvinen H. Liver fat and lipid oxidation in humans. *Liver Int* 29: 1439–1446, 2009.
 89. Koves TR, Ussher JR, Noland RC, Slentz D, Mosedale M, Ilkayeva O, Bain J, Stevens R, Dyck JR, Newgard CB, Lopaschuk GD, and Muoio DM. Mitochondrial overload and incomplete fatty acid oxidation contribute to skeletal muscle insulin resistance. *Cell Metab* 7: 45–56, 2008.
 90. Kudin AP, Malinska D, and Kunz WS. Sites of generation of reactive oxygen species in homogenates of brain tissue determined with the use of respiratory substrates and inhibitors. *Biochim Biophys Acta* 1777: 689–695, 2008.
 91. Kuo DY, Chen PN, Yang SF, Chu SC, Chen CH, Kuo MH, Yu CH, and Hsieh YS. Role of reactive oxygen species-related enzymes in neuropeptide y and proopiomelanocortin-mediated appetite control: a study using atypical protein kinase C knockdown. *Antioxid Redox Signal* 15: 2147–2159, 2011.
 92. Lage R, Vazquez MJ, Varela L, Saha AK, Vidal-Puig A, Nogueiras R, Dieguez C, and Lopez M. Ghrelin effects on neuropeptides in the rat hypothalamus depend on fatty acid metabolism actions on BSX but not on gender. *FASEB J* 24: 2670–2679, 2010.
 93. Lam TK, Schwartz GJ, and Rossetti L. Hypothalamic sensing of fatty acids. *Nat Neurosci* 8: 579–584, 2005.
 94. Lan F, Cacicedo JM, Ruderman N, and Ido Y. SIRT1 modulation of the acetylation status, cytosolic localization, and activity of LKB1. Possible role in AMP-activated protein kinase activation. *J Biol Chem* 283: 27628–27635, 2008.
 95. Le Foll C, Irani BG, Magnan C, Dunn-Meynell AA, and Levin BE. Characteristics and mechanisms of hypothalamic neuronal fatty acid sensing. *Am J Physiol Regul Integr Comp Physiol* 297: R655–R664, 2009.
 96. Le May C, Cauzac M, Diradourian C, Perdereau D, Girard J, Burnol AF, and Pegorier JP. Fatty acids induce L-CPT I gene expression through a PPARalpha-independent mechanism in rat hepatoma cells. *J Nutr* 135: 2313–2319, 2005.
 97. Lee AH, Scapa EF, Cohen DE, and Glimcher LH. Regulation of hepatic lipogenesis by the transcription factor XBP1. *Science* 320: 1492–1496, 2008.
 98. Leonardsson G, Steel JH, Christian M, Pocock V, Milligan S, Bell J, So PW, Medina-Gomez G, Vidal-Puig A, White R, and Parker MG. Nuclear receptor corepressor RIP140 regulates fat accumulation. *Proc Natl Acad Sci U S A* 101: 8437–8442, 2004.
 99. Levin BE. Metabolic sensors: viewing glucosensing neurons from a broader perspective. *Physiol Behav* 76: 397–401, 2002.
 100. Loh K, Deng H, Fukushima A, Cai X, Boivin B, Galic S, Bruce C, Shields BJ, Skiba B, Ooms LM, Stepto N, Wu B, Mitchell CA, Tonks NK, Watt MJ, Febbraio MA, Crack PJ, Andrikopoulos S, and Tiganis T. Reactive oxygen species enhance insulin sensitivity. *Cell Metab* 10: 260–272, 2009.
 101. Louet JF, Chatelain F, Decaux JF, Park EA, Kohl C, Pineau T, Girard J, and Pegorier JP. Long-chain fatty acids regulate liver carnitine palmitoyltransferase I gene (L-CPT I) expression through a peroxisome-proliferator-activated receptor alpha (PPARalpha)-independent pathway. *Biochem J* 354: 189–197, 2001.
 102. Lowell BB and Shulman GI. Mitochondrial dysfunction and type 2 diabetes. *Science* 307: 384–387, 2005.
 103. Lumeng CN, Bodzin JL, and Saltiel AR. Obesity induces a phenotypic switch in adipose tissue macrophage polarization. *J Clin Invest* 117: 175–184, 2007.
 104. Lumeng CN, Maillard I, and Saltiel AR. T-ing up inflammation in fat. *Nat Med* 15: 846–847, 2009.
 105. Machann J, Bachmann OP, Brechtel K, Dahl DB, Wietek B, Klumpp B, Haring HU, Claussen CD, Jacob S, and Schick F. Lipid content in the musculature of the lower leg assessed by fat selective MRI: intra- and interindividual differences and correlation with anthropometric and metabolic data. *J Magn Reson Imaging* 17: 350–357, 2003.
 106. Mailloux RJ and Harper ME. Uncoupling proteins and the control of mitochondrial reactive oxygen species production. *Free Radic Biol Med* 51: 1106–1115, 2011.
 107. Mathis D and Shoelson SE. Immunometabolism: an emerging frontier. *Nat Rev Immunol* 11: 81, 2011.
 108. McCune SA and Harris RA. Mechanism responsible for 5-(tetradecyloxy)-2-furoic acid inhibition of hepatic lipogenesis. *J Biol Chem* 254: 10095–10101, 1979.
 109. McGarry JD and Brown NF. The mitochondrial carnitine palmitoyltransferase system. From concept to molecular analysis. *Eur J Biochem* 244: 1–14, 1997.
 110. Mera P, Bentebibel A, Lopez-Vinas E, Cordente AG, Gurnathan C, Sebastian D, Vazquez I, Herrero L, Ariza X, Gomez-Puertas P, Asins G, Serra D, Garcia J, and Hegardt FG. C75 is converted to C75-CoA in the hypothalamus, where it inhibits carnitine palmitoyltransferase 1 and decreases food intake and body weight. *Biochem Pharmacol* 77: 1084–1095, 2009.
 111. Michan S and Sinclair D. Sirtuins in mammals: insights into their biological function. *Biochem J* 404: 1–13, 2007.
 112. Miele L, Grieco A, Armuzzi A, Candelli M, Forgione A, Gasbarrini A, and Gasbarrini G. Hepatic mitochondrial beta-oxidation in patients with nonalcoholic steatohepatitis assessed by ¹³C-octanoate breath test. *Am J Gastroenterol* 98: 2335–2336, 2003.
 113. Migrenne S, Le Foll C, Levin BE, and Magnan C. Brain lipid sensing and nervous control of energy balance. *Diabetes Metab* 37: 83–88, 2011.
 114. Minnich A, Tian N, Byan L, and Bilder G. A potent PPARalpha agonist stimulates mitochondrial fatty acid beta-oxidation in liver and skeletal muscle. *Am J Physiol Endocrinol Metab* 280: E270–E279, 2001.
 115. Minokoshi Y, Alquier T, Furukawa N, Kim YB, Lee A, Xue B, Mu J, Fougelle F, Ferre P, Birnbaum MJ, Stuck BJ, and Kahn BB. AMP-kinase regulates food intake by responding to hormonal and nutrient signals in the hypothalamus. *Nature* 428: 569–574, 2004.
 116. Mollica MP, Iossa S, Liverini G, and Soboll S. Steady state changes in mitochondrial electrical potential and proton gradient in perfused liver from rats fed a high fat diet. *Mol Cell Biochem* 178: 213–217, 1998.
 117. Monsenego J, Mansouri A, Akkaoui M, Lenoir V, Esnous C, Fauveau V, Tavernier V, Girard J, and Prip-Buus C. Enhancing liver mitochondrial fatty acid oxidation capacity in obese mice improves insulin sensitivity independently of hepatic steatosis. *J Hepatol* 56: 632–639, 2012.
 118. Morillas M, Gomez-Puertas P, Bentebibel A, Selles E, Casals N, Valencia A, Hegardt FG, Asins G, and Serra D. Identification of conserved amino acid residues in rat liver carnitine palmitoyltransferase I critical for malonyl-CoA inhibition. Mutation of methionine 593 abolishes malonyl-CoA inhibition. *J Biol Chem* 278: 9058–9063, 2003.
 119. Muoio DM. Intramuscular triacylglycerol and insulin resistance: guilty as charged or wrongly accused? *Biochim Biophys Acta* 1801: 281–288, 2010.
 120. Muoio DM and Koves TR. Skeletal muscle adaptation to fatty acid depends on coordinated actions of the PPARs

- and PGC1 alpha: implications for metabolic disease. *Appl Physiol Nutr Metab* 32: 874–883, 2007.
121. Muoio DM and Neuffer PD. Lipid-induced mitochondrial stress and insulin action in muscle. *Cell Metab* 15: 595–605, 2012.
 122. Murphy MP. How mitochondria produce reactive oxygen species. *Biochem J* 417: 1–13, 2009.
 123. Nakamuta M, Kohjima M, Morizono S, Kotoh K, Yoshimoto T, Miyagi I, and Enjoji M. Evaluation of fatty acid metabolism-related gene expression in nonalcoholic fatty liver disease. *Int J Mol Med* 16: 631–635, 2005.
 124. Nedergaard J, Bengtsson T, and Cannon B. Unexpected evidence for active brown adipose tissue in adult humans. *Am J Physiol Endocrinol Metab* 293: E444–E452, 2007.
 125. Nguyen KD, Qiu Y, Cui X, Goh YP, Mwangi J, David T, Mukundan L, Brombacher F, Locksley RM, and Chawla A. Alternatively activated macrophages produce catecholamines to sustain adaptive thermogenesis. *Nature* 480: 104–108, 2011.
 126. O'Neil PM, Smith SR, Weissman NJ, Fidler MC, Sanchez M, Zhang J, Raether B, Anderson CM, and Shanahan WR. Randomized placebo-controlled clinical trial of lorcaserin for weight loss in type 2 diabetes mellitus: The BLOOM-DM Study. *Obesity* 20: 1426–1436, 2012.
 127. Obici S, Feng Z, Arduini A, Conti R, and Rossetti L. Inhibition of hypothalamic carnitine palmitoyltransferase-1 decreases food intake and glucose production. *Nat Med* 9: 756–761, 2003.
 128. Obici S, Feng Z, Morgan K, Stein D, Karkanas G, and Rossetti L. Central administration of oleic acid inhibits glucose production and food intake. *Diabetes* 51: 271–275, 2002.
 129. Olefsky JM and Glass CK. Macrophages, inflammation, and insulin resistance. *Annu Rev Physiol* 72: 219–246, 2010.
 130. Orellana-Gavalda JM, Herrero L, Malandrino MI, Paneda A, Sol Rodriguez-Pena M, Petry H, Asins G, Van Deventer S, Hegardt FG, and Serra D. Molecular therapy for obesity and diabetes based on a long-term increase in hepatic fatty acid oxidation. *Hepatology* 53: 821–832, 2011.
 131. Ortega FJ, Jilkova ZM, Moreno-Navarrete JM, Pavelka S, Rodriguez-Hermosa JJ, Kopeck Ygrave J, and Fernandez-Real JM. Type I iodothyronine 5'-deiodinase mRNA and activity is increased in adipose tissue of obese subjects. *Int J Obes* 36: 320–324, 2011.
 132. Ozcan U, Cao Q, Yilmaz E, Lee AH, Iwakoshi NN, Ozdelen E, Tuncman G, Gorgun C, Glimcher LH, and Hotamisligil GS. Endoplasmic reticulum stress links obesity, insulin action, and type 2 diabetes. *Science* 306: 457–461, 2004.
 133. Park EA, Mynatt RL, Cook GA, and Kashfi K. Insulin regulates enzyme activity, malonyl-CoA sensitivity and mRNA abundance of hepatic carnitine palmitoyltransferase-I. *Biochem J* 310: 853–858, 1995.
 134. Paterson JM, Morton NM, Fievet C, Kenyon CJ, Holmes MC, Staels B, Seckl JR, and Mullins JJ. Metabolic syndrome without obesity: Hepatic overexpression of 11beta-hydroxysteroid dehydrogenase type 1 in transgenic mice. *Proc Natl Acad Sci U S A* 101: 7088–7093, 2004.
 135. Pillai VB, Sundaresan NR, Kim G, Gupta M, Rajamohan SB, Pillai JB, Samant S, Ravindra PV, Isbatan A, and Gupta MP. Exogenous NAD blocks cardiac hypertrophic response via activation of the SIRT3-LKB1-AMP-activated kinase pathway. *J Biol Chem* 285: 3133–3144, 2010.
 136. Pissios P and Maratos-Flier E. More than satiety: central serotonin signaling and glucose homeostasis. *Cell Metab* 6: 345–347, 2007.
 137. Pizer ES, Jackisch C, Wood FD, Pasternack GR, Davidson NE, and Kuhajda FP. Inhibition of fatty acid synthesis induces programmed cell death in human breast cancer cells. *Cancer Res* 56: 2745–2747, 1996.
 138. Price N, van der Leij F, Jackson V, Corstorphine C, Thomson R, Sorensen A, and Zammit V. A novel brain-expressed protein related to carnitine palmitoyltransferase I. *Genomics* 80: 433–442, 2002.
 139. Ritov VB, Menshikova EV, Azuma K, Wood R, Toledo FG, Goodpaster BH, Ruderman NB, and Kelley DE. Deficiency of electron transport chain in human skeletal muscle mitochondria in type 2 diabetes mellitus and obesity. *Am J Physiol Endocrinol Metab* 298: E49–E58, 2009.
 140. Rochford JJ, Myers MG, Jr., and Heisler LK. Setting the tone: reactive oxygen species and the control of appetitive melanocortin neurons. *Cell Metab* 14: 573–574, 2011.
 141. Roman EA, Reis D, Romanatto T, Maimoni D, Ferreira EA, Santos GA, Torsoni AS, Velloso LA, and Torsoni MA. Central leptin action improves skeletal muscle AKT, AMPK, and PGC1 alpha activation by hypothalamic PI3K-dependent mechanism. *Mol Cell Endocrinol* 314: 62–69, 2010.
 142. Rosen ED and Spiegelman BM. Adipocytes as regulators of energy balance and glucose homeostasis. *Nature* 444: 847–853, 2006.
 143. Saito M, Okamatsu-Ogura Y, Matsushita M, Watanabe K, Yoneshiro T, Nio-Kobayashi J, Iwanaga T, Miyagawa M, Kameya T, Nakada K, Kawai Y, and Tsujisaki M. High incidence of metabolically active brown adipose tissue in healthy adult humans: effects of cold exposure and adiposity. *Diabetes* 58: 1526–1531, 2009.
 144. Samuel VT, Petersen KF, and Shulman GI. Lipid-induced insulin resistance: unravelling the mechanism. *Lancet* 375: 2267–2277, 2010.
 145. Samuel VT and Shulman GI. Mechanisms for insulin resistance: common threads and missing links. *Cell* 148: 852–871, 2012.
 146. Savage DB, Choi CS, Samuel VT, Liu ZX, Zhang D, Wang A, Zhang XM, Cline GW, Yu XX, Geisler JG, Bhanot S, Monia BP, and Shulman GI. Reversal of diet-induced hepatic steatosis and hepatic insulin resistance by antisense oligonucleotide inhibitors of acetyl-CoA carboxylases 1 and 2. *J Clin Invest* 116: 817–824, 2006.
 147. Schenk S, Saberi M, and Olefsky JM. Insulin sensitivity: modulation by nutrients and inflammation. *J Clin Invest* 118: 2992–3002, 2008.
 148. Schug TT and Li X. Sirtuin 1 in lipid metabolism and obesity. *Ann Med* 43: 198–211, 2011.
 149. Sebastian D, Herrero L, Serra D, Asins G, and Hegardt FG. CPT I overexpression protects L6E9 muscle cells from fatty acid-induced insulin resistance. *Am J Physiol Endocrinol Metab* 292: E677–E686, 2007.
 150. Serviddio G, Giudetti AM, Bellanti F, Priore P, Rollo T, Tamborra R, Siculella L, Vendemiale G, Altomare E, and Gnoni GV. Oxidation of hepatic carnitine palmitoyl transferase-I (CPT-I) impairs fatty acid beta-oxidation in rats fed a methionine-choline deficient diet. *PLoS One* 6: e24084, 2011.
 151. Shoelson SE, Herrero L, and Naaz A. Obesity, inflammation, and insulin resistance. *Gastroenterology* 132: 2169–2180, 2007.
 152. Shulman GI, Rothman DL, Jue T, Stein P, DeFronzo RA, and Shulman RG. Quantitation of muscle glycogen synthesis in normal subjects and subjects with non-insulin-dependent diabetes by ¹³C nuclear magnetic resonance spectroscopy. *N Engl J Med* 322: 223–228, 1990.

153. Simoneau JA, Veerkamp JH, Turcotte LP, and Kelley DE. Markers of capacity to utilize fatty acids in human skeletal muscle: relation to insulin resistance and obesity and effects of weight loss. *FASEB J* 13: 2051–2060, 1999.
154. Solinas G and Karin M. JNK1 and IKKbeta: molecular links between obesity and metabolic dysfunction. *FASEB J* 24: 2596–2611, 2010.
155. Starley BQ, Calcagno CJ, and Harrison SA. Nonalcoholic fatty liver disease and hepatocellular carcinoma: a weighty connection. *Hepatology* 51: 1820–1832, 2010.
156. Steyn FJ, Leong JW, Huang L, Tan HY, Xie TY, Nelson C, Waters MJ, Veldhuis JD, Epelbaum J, and Chen C. GH does not modulate the early fasting-induced release of free fatty acids in mice. *Endocrinology* 153: 273–282, 2012.
157. Sun K, Kusminski CM, and Scherer PE. Adipose tissue remodeling and obesity. *J Clin Invest* 121: 2094–2101, 2011.
158. Sunny NE, Parks EJ, Browning JD, and Burgess SC. Excessive hepatic mitochondrial TCA cycle and gluconeogenesis in humans with nonalcoholic fatty liver disease. *Cell Metab* 14: 804–810, 2011.
159. Taube A, Eckardt K, and Eckel J. Role of lipid-derived mediators in skeletal muscle insulin resistance. *Am J Physiol Endocrinol Metab* 297: E1004–E1012, 2009.
160. Taubes G. Insulin resistance. Prosperity's plague. *Science* 325: 256–260, 2009.
161. Tiniakos DG, Vos MB, and Brunt EM. Nonalcoholic fatty liver disease: pathology and pathogenesis. *Annu Rev Pathol* 5: 145–171, 2010.
162. Tseng YH, Cypess AM, and Kahn CR. Cellular bioenergetics as a target for obesity therapy. *Nat Rev Drug Discov* 9: 465–482, 2010.
163. Tunstall RJ, Mehan KA, Wadley GD, Collier GR, Bonen A, Hargreaves M, and Cameron-Smith D. Exercise training increases lipid metabolism gene expression in human skeletal muscle. *Am J Physiol Endocrinol Metab* 283: E66–E72, 2002.
164. Turner N, Bruce CR, Beale SM, Hoehn KL, So T, Rolph MS, and Cooney GJ. Excess lipid availability increases mitochondrial fatty acid oxidative capacity in muscle: evidence against a role for reduced fatty acid oxidation in lipid-induced insulin resistance in rodents. *Diabetes* 56: 2085–2092, 2007.
165. van Marken Lichtenbelt WD, Vanhomerig JW, Smulders NM, Drossaerts JM, Kemerink GJ, Bouvy ND, Schrauwen P, and Teule GJ. Cold-activated brown adipose tissue in healthy men. *N Engl J Med* 360: 1500–1508, 2009.
166. Velasco G, Geelen MJ, and Guzman M. Control of hepatic fatty acid oxidation by 5'-AMP-activated protein kinase involves a malonyl-CoA-dependent and a malonyl-CoA-independent mechanism. *Arch Biochem Biophys* 337: 169–175, 1997.
167. Velasquez DA, Martinez G, Romero A, Vazquez MJ, Boit KD, Dopeso-Reyes IG, Lopez M, Vidal A, Nogueiras R, and Dieguez C. The central Sirtuin 1/p53 pathway is essential for the orexigenic action of ghrelin. *Diabetes* 60: 1177–1185, 2011.
168. Virtanen KA, Lidell ME, Orava J, Heglind M, Westergren R, Niemi T, Taittonen M, Laine J, Savisto NJ, Enerback S, and Nuutila P. Functional brown adipose tissue in healthy adults. *N Engl J Med* 360: 1518–1525, 2009.
169. Virtue S and Vidal-Puig A. Adipose tissue expandability, lipotoxicity and the Metabolic Syndrome—an allostatic perspective. *Biochim Biophys Acta* 1801: 338–349, 2010.
170. Wagner BA, Buettner GR, and Burns CP. Free radical-mediated lipid peroxidation in cells: oxidizability is a function of cell lipid bis-allylic hydrogen content. *Biochemistry* 33: 4449–4453, 1994.
171. Weisberg SP, McCann D, Desai M, Rosenbaum M, Leibel RL, and Ferrante AW, Jr. Obesity is associated with macrophage accumulation in adipose tissue. *J Clin Invest* 112: 1796–1808, 2003.
172. Whittle AJ, Carobbio S, Martins L, Slawik M, Hondares E, Vazquez MJ, Morgan D, Csikasz RI, Gallego R, Rodriguez-Cuenca S, Dale M, Virtue S, Villarroya F, Cannon B, Rahmouni K, Lopez M, and Vidal-Puig A. BMP8B increases brown adipose tissue thermogenesis through both central and peripheral actions. *Cell* 149: 871–885, 2012.
173. Wolfgang MJ, Cha SH, Sidhaye A, Chohnan S, Cline G, Shulman GI, and Lane MD. Regulation of hypothalamic malonyl-CoA by central glucose and leptin. *Proc Natl Acad Sci U S A* 104: 19285–19290, 2007.
174. Woods A, Johnstone SR, Dickerson K, Leiper FC, Fryer LG, Neumann D, Schlattner U, Wallimann T, Carlson M, and Carling D. LKB1 is the upstream kinase in the AMP-activated protein kinase cascade. *Curr Biol* 13: 2004–2008, 2003.
175. Yamazaki N, Shinohara Y, Shima A, and Terada H. High expression of a novel carnitine palmitoyltransferase I like protein in rat brown adipose tissue and heart: isolation and characterization of its cDNA clone. *FEBS Lett* 363: 41–45, 1995.
176. Yeh LA, Lee KH, and Kim KH. Regulation of rat liver acetyl-CoA carboxylase. Regulation of phosphorylation and inactivation of acetyl-CoA carboxylase by the adenylate energy charge. *J Biol Chem* 255: 2308–2314, 1980.
177. Yue JT and Lam TK. Lipid sensing and insulin resistance in the brain. *Cell Metab* 15: 646–655, 2012.
178. Zeng L, Lu M, Mori K, Luo S, Lee AS, Zhu Y, and Shyy JY. ATF6 modulates SREBP2-mediated lipogenesis. *EMBO J* 23: 950–958, 2004.
179. Zhang Y, Proenca R, Maffei M, Barone M, Leopold L, and Friedman JM. Positional cloning of the mouse obese gene and its human homologue. *Nature* 372: 425–432, 1994.
180. Zhou G, Myers R, Li Y, Chen Y, Shen X, Fenyk-Melody J, Wu M, Ventre J, Doebber T, Fujii N, Musi N, Hirshman MF, Goodyear LJ, and Moller DE. Role of AMP-activated protein kinase in mechanism of metformin action. *J Clin Invest* 108: 1167–1174, 2001.
181. Zingaretti MC, Crosta F, Vitali A, Guerrieri M, Frontini A, Cannon B, Nedergaard J, and Cinti S. The presence of UCP1 demonstrates that metabolically active adipose tissue in the neck of adult humans truly represents brown adipose tissue. *FASEB J* 23: 3113–3120, 2009.

Address correspondence to:

Dr. Laura Herrero
 Department of Biochemistry and Molecular Biology
 School of Pharmacy
 University of Barcelona
 Av. Diagonal, 643
 E-08028 Barcelona
 Spain

E-mail: lherrero@ub.edu

Date of first submission to ARS Central, August 11, 2012; date of acceptance, August 19, 2012.

Abbreviations Used

ACC = acetyl-CoA carboxylase
AgRP = agouti-related protein
AMPK = AMP-activated protein kinase
BAT = brown adipose tissue
BMI = body mass index
CACT = acylcarnitine translocase
CPT1 = carnitine palmitoyltransferase 1
CPT1A = liver CPT1
CT = computed tomography
DAG = diacylglycerol
ETC = electron transport chain
FA = fatty acid
FAO = fatty acid oxidation
FAS = fatty acid synthase
FFA = free fatty acid

FGF21 = fibroblast growth factor 21
HFD = high-fat diet
IMC = intramyocellular
LCFA-CoA = long-chain fatty acid-CoA
MCD = malonyl-CoA decarboxylase
NAFLD = nonalcoholic fatty liver disease
NASH = nonalcoholic steatohepatitis
NPY = neuropeptide Y
PET = positron-emission tomography
ROS = reactive oxygen species
SkM = skeletal muscle
TCA = tricarboxylic acid
TG = triglyceride
UCPs = uncoupling proteins
UPR = uncoupled protein response
WAT = white adipose tissue



Long-Term Increased Carnitine Palmitoyltransferase 1A Expression in Ventromedial Hypothalamus Causes Hyperphagia and Alters the Hypothalamic Lipidomic Profile

Paula Mera¹*, Joan Francesc Mir¹*, Gemma Fabriàs², Josefina Casas², Ana S. H. Costa¹, Maria Ida Malandrino¹, José-Antonio Fernández-López³, Xavier Remesar³, Su Gao⁴, Shigeru Chohnan⁵, Maria Sol Rodríguez-Peña⁶, Harald Petry⁶, Guillermina Asins¹, Fausto G. Hegardt¹, Laura Herrero^{1*}, Dolors Serra^{1*}

1 Department of Biochemistry and Molecular Biology, Facultat de Farmàcia, Universitat de Barcelona and Institut de Biomedicina de la Universitat de Barcelona (IBUB) and CIBER Fisiopatología de la Obesidad y la Nutrición (CIBERObn), Instituto de Salud Carlos III, Barcelona, Spain, **2** Research Unit on BioActive Molecules, Department of Biomedical Chemistry, Institute of Advanced Chemistry of Catalonia (IQAC)/CSIC, Barcelona, Spain, **3** Department of Nutrition and Food Science, Facultat de Biologia, Universitat de Barcelona and Institut de Biomedicina de la Universitat de Barcelona (IBUB) and CIBER Fisiopatología de la Obesidad y la Nutrición (CIBERObn), Instituto de Salud Carlos III, Barcelona, Spain, **4** Scripps Research Institute, Jupiter, Florida, United States of America, **5** Department of Bioresource Science, College of Agriculture, Ibaraki University, Ibaraki, Japan, **6** UniQure, Amsterdam, The Netherlands

Abstract

Lipid metabolism in the ventromedial hypothalamus (VMH) has emerged as a crucial pathway in the regulation of feeding and energy homeostasis. Carnitine palmitoyltransferase (CPT) 1A is the rate-limiting enzyme in mitochondrial fatty acid β -oxidation and it has been proposed as a crucial mediator of fasting and ghrelin orexigenic signalling. However, the relationship between changes in CPT1A activity and the intracellular downstream effectors in the VMH that contribute to appetite modulation is not fully understood. To this end, we examined the effect of long-term expression of a permanently activated CPT1A isoform by using an adeno-associated viral vector injected into the VMH of rats. Peripherally, this procedure provoked hyperghrelinemia and hyperphagia, which led to overweight, hyperglycemia and insulin resistance. In the mediobasal hypothalamus (MBH), long-term CPT1A expression in the VMH did not modify acyl-CoA or malonyl-CoA levels. However, it altered the MBH lipidomic profile since ceramides and sphingolipids increased and phospholipids decreased. Furthermore, we detected increased vesicular γ -aminobutyric acid transporter (VGAT) and reduced vesicular glutamate transporter 2 (VGLUT2) expressions, both transporters involved in this orexigenic signal. Taken together, these observations indicate that CPT1A contributes to the regulation of feeding by modulating the expression of neurotransmitter transporters and lipid components that influence the orexigenic pathways in VMH.

Citation: Mera P, Mir JF, Fabriàs G, Casas J, Costa ASH, et al. (2014) Long-Term Increased Carnitine Palmitoyltransferase 1A Expression in Ventromedial Hypothalamus Causes Hyperphagia and Alters the Hypothalamic Lipidomic Profile. PLoS ONE 9(5): e97195. doi:10.1371/journal.pone.0097195

Editor: Marc Claret, Institut d'Investigacions Biomèdiques August Pi i Sunyer, Spain

Received: February 3, 2014; **Accepted:** April 16, 2014; **Published:** May 12, 2014

Copyright: © 2014 Mera et al. This is an open-access article distributed under the terms of the Creative Commons Attribution License, which permits unrestricted use, distribution, and reproduction in any medium, provided the original author and source are credited.

Funding: This study was supported by the Spanish Ministry of Economy and Competitiveness (Grant SAF2011-30520-C02-01 to D.S., Grant SAF2010-20039 to L.H. and doctoral fellowships to J.F.M. and M.I.M.), by the CIBER Fisiopatología de la Obesidad y la Nutrición (CIBEROBN), the Instituto de Salud Carlos III (Grant CB06/03/0026 to D.S. and X.R. and research contract to P.M.), and the European Foundation for the Study of Diabetes (EFSD)/Lilly and European Foundation for the Study of Diabetes (EFSD)/Janssen (research fellowships to L.H.), by Albert Renold Programme (Postdoctoral Fellowship to A.S.H.C.). UniQure provided support in the form of salaries for authors HP & MSRP, but did not have any additional role in the study design, data collection and analysis, decision to publish, or preparation of the manuscript. The specific roles of these authors are articulated in the 'author contributions' section.

Competing Interests: Harald Petry, PhD, is employed by uniQure B.V. in the function as Chief Scientific Officer. María Sol Rodríguez-Peña, PhD, used to be employed by UniQure B.V. in the function as Senior Researcher. Lilly and Janssen research grants assisted in the funding of this study through EFSD collaborations. There are no patents, products in development or marketed products to declare. This does not alter the authors' adherence to all the PLOS ONE policies on sharing data and materials.

* E-mail: lherrero@ub.edu (LH); dserra@ub.edu (DS)

† These authors contributed equally to this work.

Introduction

Current lifestyles are responsible for the alarming increase in the prevalence of obesity and the consequent development of insulin resistance and Type 2 diabetes. An imbalance between energy intake and expenditure can cause overweight, thus contributing to obesity and associated metabolic complications. The hypothalamus is crucial to the central control of appetite and energy

homeostasis [1,2]. This brain region consists of interconnected neuronal nuclei that respond to neuroendocrine and metabolic signals by modulating the production and release of specific neurotransmitters that control energy balance [3]. Hypothalamic lipid metabolism participates in this process and is linked to the molecular mechanisms by which hormones, such as leptin, ghrelin and insulin, exert their central effect on food intake [4–6].

Malonyl-CoA, the first intermediate in fatty acid (FA) biosynthesis, has emerged as a crucial player in the hypothalamic control of feeding [7,8]. On the one hand, decreased food intake and increased malonyl-CoA are observed after central treatment of drugs or anorectic hormones such as leptin. Leptin's anorectic pathway involves the inhibition of AMP-activated protein kinase (AMPK), which, in turn, activates acetyl-CoA carboxylase (ACC), key enzyme for malonyl-CoA synthesis [5]. Treatments with FAS inhibitors, such as C75 and cerulenin reduce food intake by an increase of hypothalamic malonyl-CoA level [8–10]. On the other hand, malonyl-CoA level decreases under fasting condition when ghrelin level is high. Orexigenic ghrelin pathway involves activation of AMPK, inhibition of ACC and a reduction of malonyl-CoA level [11,12]. One clear candidate for malonyl-CoA action is carnitine palmitoyltransferase (CPT) 1, a key enzyme regulating mitochondrial long chain fatty acyl-CoA (LCFA-CoA) β -oxidation [13], since CPT1 activity is physiologically inhibited by malonyl-CoA. An accumulation of LCFA-CoA in the hypothalamus was believed to signal reduction in food intake and hepatic gluconeogenesis in rodents. CPT1 is related to both metabolites and it has been implicated in the central control of both food intake and glucose metabolism [14–17]. Two CPT1 isoforms are expressed in the hypothalamus, CPT1A and CPT1C. The latter is found mainly in the endoplasmic reticulum of neurons and does not directly participate in mitochondrial FA β -oxidation (FAO) [18]. However, CPT1C binds malonyl-CoA and it may serve as a sensor for malonyl-CoA in the hypothalamic regulation of energy homeostasis [19,20]. Furthermore, we have recently shown that CPT1C mediates ghrelin central action by altering ceramide levels [21]. CPT1A also contributes to the central orexigenic action of ghrelin, since the molecular events derived from ghrelin binding to its receptor on hypothalamic neurons result in increased CPT1A activity and FAO [6,22,23]. It has been proposed that the derived metabolic changes, including the accumulation of reactive oxygen species (ROS) and the subsequent up-regulation of the mitochondrial uncoupling protein 2 (UCP2), contribute to the activation of arcuate (Arc) AgRP neurons [22]. Moreover, transcription factors such as brain-specific homeobox (Bsx), cAMP response-element binding protein (CREB), and forkhead box O1 (FoxO1) act as downstream mediators of CPT1A in the Arc nucleus for orexigenic neuropeptide synthesis [24]. These observations suggest a potential role of hypothalamic CPT1A in the control of feeding, however the exact mechanistic sequence and mediators involved are not yet revealed.

A growing body of evidence implicates the ventromedial hypothalamus (VMH) in the central control of food intake and regulation of energy homeostasis [17,25,26]. VMH neurons are reported to activate anorexigenic neuronal pathways in the Arc nucleus by projecting excitatory inputs into POMC neurons [27]. Moreover, some VMH neurons are GABAergic [28]. We have recently observed that CPT1A activity in the VMH changes concomitantly with fasting and refeeding states and that it is reinforced by the increase in appetite provoked by acute expression of a permanently activated CPT1A isoform [29]. Despite all the evidence, the exact mechanisms for the induction of feeding downstream of CPT1A in the VMH are unknown.

Here we examined the long-term effect of AAV-vectorized expression of a malonyl-CoA-insensitive CPT1A isoform [30], namely CPT1AM, in the VMH. This model allows us to uncouple malonyl-CoA effect on food intake and to activate permanently downstream effectors of CPT1A involved in feeding. We hypothesise that CPT1A modulates the lipidic and gene profile of the mediobasal hypothalamus (MBH, encompassing both Arc and the VMH), which may be involved in the central control of

feeding and glucose metabolism. Long-term CPT1AM expression led to alterations in MBH structural bioactive lipids, i.e. phospholipids, sphingolipids and ceramides. In addition, this CPT1AM expression altered the expression of glutamate and GABA vesicular transporters, which have been reported to control amino acid neurotransmitters which alter food intake. Moreover, hyperphagia, overweight and the later development of insulin resistance and hyperglycemia was also observed in the CPT1AM animals. All these results reinforce the notion that VMH CPT1A is involved in appetite modulation.

Materials and Methods

Adeno-associated vectors (AAVs)

Serotype 1-AAV, AAV-GFP and AAV-CPT1AM were constructed to express GFP and CPT1AM respectively. Vector plasmids carried: CMV promoter, cDNA sequence of GFP or CPT1AM [30], woodchuck posttranscriptional regulatory element (WPRE, acc #AY468–486) [31], and bovine growth hormone polyadenosine transcription termination signal (bases 2326–2533 GenBank acc #M57764). The expression cassette was flanked by two inverted terminal repeats (ITRs) derived from serotype 2-AAV. AAVs were produced in insect cells using a baculovirus [32]. The vector preparation used had the following titers: AAV-GFP, 5×10^{12} pfu/mL; and AAV-CPT1AM, $2.5 \cdot 10^{12}$ pfu/mL.

Animals

The *Comité Ètic d'Experimentació Animal de la Universitat de Barcelona (CEEA-UB)* and the *Generalitat de Catalunya Departament de Medi Ambient i Habitatge*, in accordance with current legislation, approved all experimental protocols from this work (Permit Numbers: 4068 and 5471). Sprague-Dawley male rats (260–290 g) (Harlan Co. Laboratories) were used in all the studies. Animals were housed in individual cages and maintained under a 12 h dark/light cycle with free access to food (2014, Harlan) and water. Rats were anaesthetised with intraperitoneal ketamine (Imalgene, 90 mg/kg) and xylazine (Rompun, 11 mg/kg) and immobilised in a stereotactic apparatus. Chronic catheters (26-gauge stainless steel guide cannulae (Plastic one)) were implanted bilaterally in the VMH (coordinates from Bregma: -2.8 mm posterior, ± 0.7 mm lateral and -10 mm ventral [33]). During the week after the surgery, animals received analgesics (buprenorphine, 0.3 mg/400 mL) and antibiotics (enrofloxacin, 10%) with water to aid recovery. Next, rats with VMH cannulae were given bilateral injections (1 μ L/each site) of AAV-GFP (control) or AAV-CPT1AM at a rate of 0.2 μ L/min. Food intake and body weight were measured in rats infected with AAV-CPT1AM (hereafter CPT1AM animals) and AAV-GFP (hereafter GFP animals) in the VMH.

Glucose Tolerance Test (GTT)

The GTT was performed in conscious rats 14 weeks after the AAV injection in the VMH. Glucose (2.0 g per kg body weight) was administered intraperitoneally after an overnight fast (16 h), and blood glucose concentrations were measured using a Glucometer Elite (Bayer) at baseline and 15, 30, 60, 90 and 120 min after glucose administration.

Measurement of circulating hormones and metabolites

Blood was collected from rats and processed to provide plasma and serum. Commercial kits were used to measure serum insulin (Rat/Mouse Insulin ELISA (Millipore)), leptin (Mouse/Rat Leptin ELISA (B-Bridge)), adiponectin (Rat Adiponectin ELISA (Millipore)), non-esterified FA (NEFA) (Wako Chemicals), plasma

acylated-ghrelin (Rat Acylated-Ghrelin ELISA (BioVendor)), T3, T4, and TSH (ELISA (DRG Diagnostics)). For the measurement of plasma amino acids, distilled water (100 μ L), 1000 μ M NLE (50 μ L) and (trifluoroacetic acid) 10% TFA acid (100 μ L) were added to 100 μ L plasma sample. After a 10-min incubation, tubes were centrifuged at 10000 \times g. The supernatant was filtered (Ultracel membrane 10 KDa filter (Millipore)), dried under a N₂ stream, and redissolved in lithium citrate pH 2.2 (400 μ L). Amino acids were measured at the Scientific-Technical Services of the University of Barcelona using an auto-analyser (Biochrom 30).

Determination of liver triacylglyceride (TAG) content

Pulverised frozen tissue from rats (\approx 100 mg) was homogenised in 500 μ L PBS. Lipids were extracted using chloroform, dried under a N₂ stream, and redissolved in n-propanol. TAGs were quantified using the Triglycerides Determination Kit (Sigma Aldrich).

Determination of malonyl-CoA, LCFA-CoA and acylcarnitine content

MBH wedges (encompassing Arc and VMH nuclei) and liver were quickly removed, frozen in liquid nitrogen, and stored at -80°C prior to malonyl-CoA or LCFA-CoA quantification. The former was measured using a malonyl-CoA recycling assay as described elsewhere [8,34]. LCFA-CoAs were extracted and measured by HPLC-MS/MS at the Scientific-Technical Services of the University of Barcelona, as previously described [35]. Acylcarnitines were analysed using an Acquity UPLC-TOF system (Waters) with an BEH C8 column (1.7 μ m particle size, 100 mm \times 2.1 mm, Waters). The two mobile phases were 1 mM ammonium formate in methanol (phase A) and 2 mM ammonium formate in H₂O (phase B), both phases with 0.05 mM formic acid. The following gradient was programmed: 0 min, 65% A; 10 min, 90% A; 15 min, 99% A; 17 min, 99% A; 20 min, 65% A, and a flow rate of 0.3 mL min⁻¹. Quantification was carried out using the extracted ion chromatogram of each compound, using 50-mDa windows. The linear dynamic range was determined by injecting standard mixtures. Positive identification of compounds was based on the accurate mass measurement with an error < 5 ppm and their LC retention time compared to that of a standard (\pm 2%).

Lipidomic analysis

MBH wedges were quickly removed, frozen in liquid nitrogen, and stored at -80°C prior to lipid analysis. Sphingolipid extraction and analysis by UPLC-TOF was carried out as described [36]. Phospholipid extracts were obtained using the same procedure but without the saponification step. Lipids were analysed by UPLC-TOF in positive or negative mode. The two mobile phases were 1 mM ammonium formate in methanol (phase A) and 2 mM ammonium formate in H₂O (phase B), both phases with 0.05 mM formic acid. The following gradient was programmed: 0 min, 80% A; 3 min, 90% A; 6 min, 90% A; 15 min, 99% A; 18 min, 99% A; 20 min, 80% A, and a flow rate of 0.3 mL min⁻¹.

Histological analysis

Brain histological examination was done using 50- μ m thick sections. Brains were excised and fixed overnight in 10% neutral-buffered formalin (Sigma). Next, they were immersed in 20% sucrose phosphate-buffered solution (PBS; pH 7.0) for 18–36 h at 4 $^{\circ}\text{C}$. Coronal sections were obtained using a freezing-sliding microtome and mounted onto microscope slides using

Immu-Mount (Thermo) to prevent fading. Examination of white adipose tissue (WAT), brown adipose tissue (BAT), and liver histology were done using 4- μ m thick formalin-fixed, paraffin-embedded tissue sections stained with hematoxylin and eosin (H&E) at the Pathology Department of *Hospital Clínic* of Barcelona.

mRNA expression analysis

The MBH, liver, WAT, and BAT from GFP and CPT1AM rats were excised, frozen, and stored at -80°C . Total RNA was isolated from frozen MBH, WAT, and BAT using RNeasy Lipid Tissue Mini-Kit (Qiagen) and from frozen liver using RNeasy Mini-Kit (Qiagen). cDNA was synthesised using the Transcriptor First Strand cDNA Synthesis Kit (Roche). qRT-PCR analyses were performed in a LightCycler 480 Instrument (Roche). To discern between the endogenous CPT1A (*CPT1Awt*) and the expressed isoform CPT1AM, we used specific primers and FRET probes and a LightCycler 480 Probes Master (Roche). The mRNA expression of other genes was determined using intron-skipping primers and SYBR Green Master Mix (Applied Biosystems). All sequences are available upon request.

Statistical analysis

Data are expressed as mean \pm SEM. Statistical significance was determined by ANOVA and Student's *t* test, using Microsoft Excel and GraphPad Prism 6 software. A *p* value < 0.05 was considered significant.

Results

AAV-mediated expression of GFP and CPT1AM

AAV carrying CPT1AM or GFP were obtained for long-term expression of the permanently active form of CPT1AM or GFP (Fig. 1A). AAV vectors were bilaterally injected into the VMH and several experiments were performed according to the showed scheme (Fig. 1B). Histological studies in GFP rats revealed that AAV-infected cells in the hypothalamus were limited mainly to the VMH (Fig. 1C). qRT-PCR analyses performed in MBH showed a robust 113 \pm 19.2-fold increase (p <0.0001) in the CPT1AM mRNA in CPT1AM rats with respect to GFP control rats (Fig. 1D). We analysed the levels of the long-chain acylcarnitines, as direct products of CPT1A activity in MBH samples. The levels of C18:0-acylcarnitine increased 3.3-fold in CPT1AM (298.4 \pm 72.62 pmol/ μ g) compared to GFP-expressing counterparts (90.46 \pm 12.69 pmol/ μ g, p <0.05). C14:0- and C16:0-acylcarnitine levels also increased, but not significantly (Fig. 1E).

CPT1AM expression in the VMH increased food intake and led to obesity, hyperglycemia and insulin resistance

We monitored the food intake and body weight of CPT1AM and GFP rats fed regular chow. The former group showed hyperphagia compared to GFP animals. Cumulative food intake was significantly higher 20 days after AAV injection (912 \pm 30.7 *vs.* 798 \pm 17.8 g, p <0.05) This increased food intake was maintained until the sacrifice (Fig. 1F). Furthermore a fast-refeeding test was performed to discern if this increased food intake may be due to impaired satiety. CPT1AM rats showed increased food intake in all measures performed after refeeding (Fig. 1G). Body weight was also measured. CPT1AM rats showed a significantly higher (83.8 \pm 13.7 g *vs.* 57 \pm 30.7 g, p <0.05) body weight change 20 days after AAV injection (Fig. 1H).

Glucose tolerance, blood glucose and serum insulin concentrations were examined in fasted CPT1AM and GFP rats. Fourteen weeks after the AAV injection, the GTT demonstrated glucose intolerance in the former (Fig. 1I). When sacrificed, CPT1AM rats

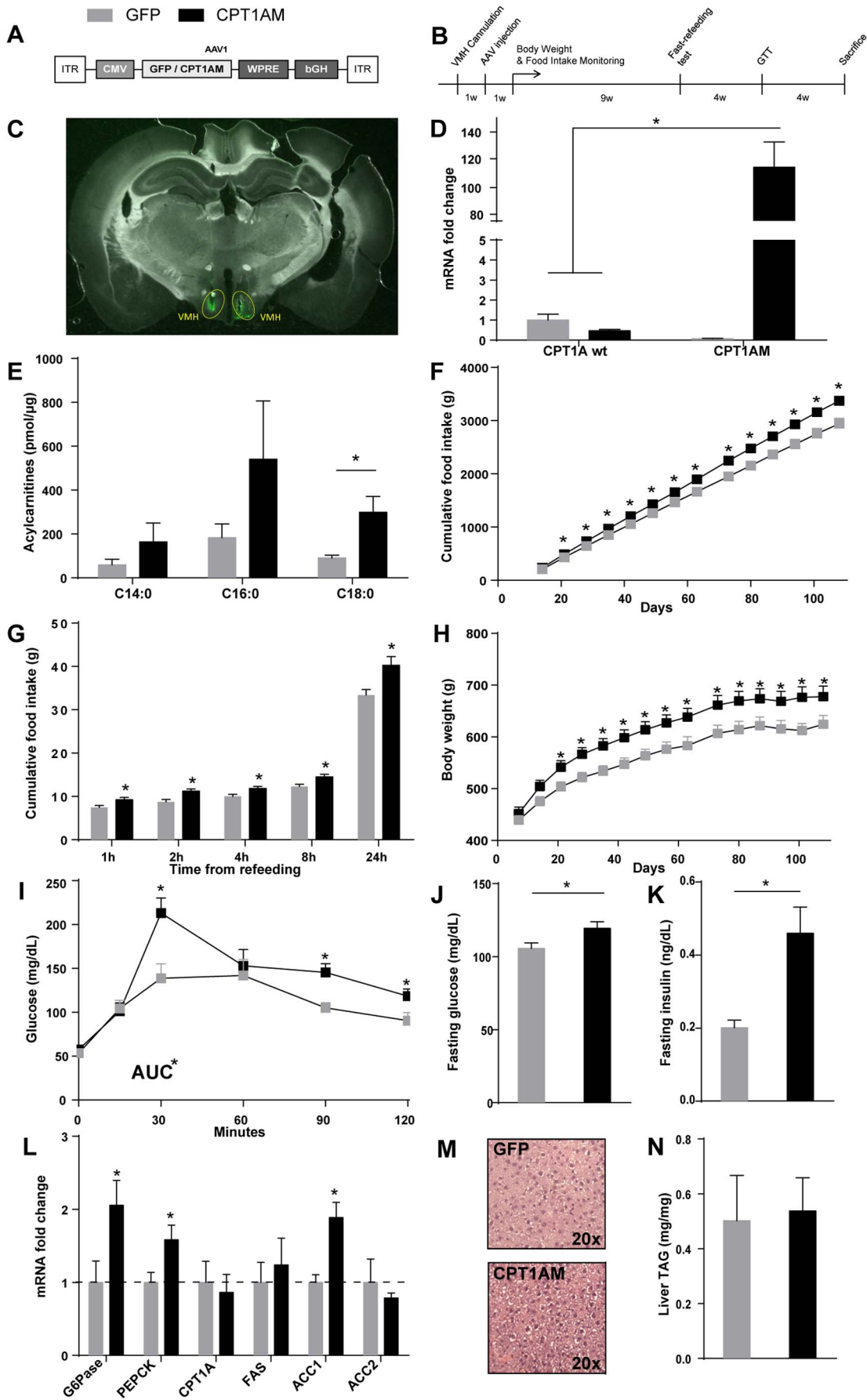


Figure 1. Analysis of the effect of VMH CPT1A expression on feeding behaviour and glucose homeostasis. (A) Scheme of the AAV vectors used in this study: AAV-GFP and AAV-CPT1AM. The cassettes contain the GFP or CPT1AM transgene driven by the cytomegalovirus (CMV) promoter. (B) Scheme of the time course of the experiment. (C) Representative histological section showing GFP in the VMH of GFP rats 2 weeks after the bilateral injection of AAV vector. (D) CPT1Awt and CPT1AM mRNA expression in the MBH (VMH + Arc) of GFP and CPT1AM rats. Measurements were performed 18 weeks after the bilateral injection of AAV vectors. Primers specifically recognise the sequence of wt or mutant CPT1A. (E) Acylcarnitines were measured as an indirect parameter of CPT1A activity. $n = 3$ (F) Cumulative food intake, (G) fast-refeeding test and (H) body weight change in rats fed a normal diet. $n = 11$. In E and G, X-axis represents days after the bilateral injection of AAV vectors into the VMH. (I) Intraperitoneal GTT in GFP and CPT1AM animals after an overnight fasting. The test was performed in animals 14 weeks after the AAV-injection into the VMH. (J) Blood fasting glucose and (K) serum fasting insulin levels measured in GFP and CPT1AM rats 18 weeks after the bilateral injection of AAV vectors into the VMH. The following analyses were performed 18 weeks after the AAV-injection into the VMH. (L) Liver relative mRNA expression of genes associated with gluconeogenesis and lipid metabolism in GFP and CPT1AM rats. (M) Liver histological sections (H & E staining) from representative GFP and CPT1AM rats. (N) Liver TAG content in GFP and CPT1AM animals. $n = 5-6$ animals in all cases. Error bars represent SEM. * $p < 0.05$. AUC: area under the curve.
doi:10.1371/journal.pone.0097195.g001

showed higher fasting glucose (increase of $16.4 \pm 3.3\%$, $p < 0.01$) and insulin (increase of $31.6 \pm 9.2\%$, $p < 0.01$) than GFP animals (Fig. 1J and 1K). Furthermore, the expression of key gluconeogenic enzymes, such as glucose-6-phosphatase (G-6-Pase) and phosphoenolpyruvate carboxykinase (PEPCK), was analysed in the liver of fasted GFP and CPT1AM animals (Fig. 1L). Results showed a 2 ± 0.3 -fold and 1.6 ± 0.5 -fold increase in G-6-Pase and PEPCK mRNA respectively in CPT1AM animals with respect to controls ($p < 0.05$). These results correlate with the hyperglycemia observed in the CPT1AM rats (Fig. 1J). The analysis of liver mRNA levels of lipid metabolism-related genes revealed a 2.1 ± 0.3 -fold increase in acetyl-CoA carboxylase 1 (ACC1) in CPT1AM rats ($p < 0.01$) (Fig. 1L). However, we found no significant changes in the hepatic concentration of TAG (Fig. 1N). In addition, histological liver examination revealed no major differences in the hepatic anatomy of between the two groups (Fig. 1M).

Next we studied the circulating metabolic and hormonal profile of GFP and CPT1AM rats. In parallel with the increase in food intake, fed CPT1AM animals presented a significant rise (3.3 ± 1.4 -fold increase, $p < 0.001$) in post-absorptive plasma levels of ghrelin (octanoylated/active form) (Fig. 2A). In addition, they exhibited high serum NEFA levels (2 ± 0.3 -fold increase, $p < 0.05$) (Fig. 2B) equivalent to those of fasted GFP and CPT1AM counterparts (data not shown). Levels of other hormones associated with energy metabolism, such as thyroid hormones (T3, T4 and TSH, data not shown), leptin and adiponectin, were unaltered between the two groups (Fig. 2C, 2D). In addition, we found significant differences in the plasma aminogram of the two groups of animals (Table 1). Interestingly, specific branched-chain amino acid (BCAA), such as Val and Ile, considered markers of obesity, increased by 18.8% and 19.8% respectively in CPT1AM animals (Table 1). Obesity is characterised by hyperplasia in WAT and browning of BAT. Histological examination of epididymal WAT revealed that white adipocytes from CPT1AM animals were significantly larger than those of the GFP controls (Fig. 2E and F). Analyses of the mRNA expression of pro-inflammatory cytokines showed an up-regulation of the monocyte chemoattractant protein-1 (MCP1) (1.6 ± 0.4 -fold increase, $p < 0.05$) in CPT1AM WAT with respect to GFP WAT (Fig. 2G). BAT showed a brown-to-white transformation in CPT1AM rats (Fig. 2H and I). We also determined the mRNA expression of genes associated with thermogenesis and FA metabolism in BAT. A moderate increase (1.2 ± 0.1 -fold, $p < 0.01$) in the expression of CPT1B in CPT1AM rats was detected with respect to GFP controls (Fig. 2J). All these results indicate that the expression of CPT1AM in the VMH impairs satiety and leads to an obesogenic phenotype.

CPT1AM expression in the VMH alters MBH mRNA levels of different genes involved in food intake

To discern the molecular mechanisms involved in the hyperphagia produced by CPT1AM expression in the VMH, we first analysed markers of excitatory inputs from the VMH to POMC neurons in Arc in fasted MBH of AAV-infected rats. We observed an 82% decrease ($p < 0.05$) in VGLUT2 mRNA levels in CPT1AM rats, without any change in VGLUT1 or VGLUT3. This observation correlates with the finding of unaltered POMC and CART mRNA levels (Fig. 3A) and indicates that the anorexigenic response was not activated.

Vesicular GABA transporter (VGAT) showed a 2.2 ± 0.4 -fold increase ($p < 0.05$) in the MBH in CPT1AM rats. However, no changes were observed in the mRNA levels of other orexigenic neurotransmitters (such as NPY, AgRP) (Fig. 3A). Interestingly, the mRNA levels of three key transcription factors involved in the expression of the aforementioned orexigenic neuropeptides [21,37,38], namely Bsx, CREB and FoxO1, were up-regulated in fasted CPT1AM rats (Fig. 3A) (Bsx: 1.8 ± 0.2 -fold increase, $p < 0.05$; CREB: 1.3 ± 0.1 -fold increase, $p < 0.01$ and FoxO1: 1.5 ± 0.2 -fold increase, $p < 0.01$). Taking into account that the orexigenic neuropeptide NPY exerts its effect on food intake mainly by binding to receptors Y1 (NPY1R) and Y5 (NPY5R), we measured the mRNA levels of these receptors. The NPY1R mRNA level was higher in CPT1AM animals than in controls (2.7 ± 0.5 , $p < 0.05$) (Fig. 3B), and no changes were observed in NPY5R. Since serum levels of ghrelin were increased in CPT1AM rats, we analysed the mRNA levels of ghrelin receptor (GHS-R), which is known to be induced in fasting conditions [39]. A 1.6 ± 0.2 -fold increase in GHS-R ($p < 0.05$) was detected, while no changes in mRNA levels of other receptors, such as MC3R, MC4R and ObRb, were observed (Fig. 3B). All these results show that increased VMH CPT1A alters different pathways involved in the control of food intake.

GABAergic transmission is modulated by ROS [40]. Given that CPT1AM expression putatively increases mitochondrial FAO and ROS, we measured the mRNA expression of antioxidant enzymes and UCP2 (Fig. 3C). A moderate increase in the mRNA levels of catalase (CAT), glutathione peroxidase 3 (Gpx3), superoxide dismutase (SOD) (1.2 ± 0.04 , 1.5 ± 0.1 and 1.2 ± 0.03 -fold increase respectively, $p < 0.01$) and UCP2 (1.4 ± 0.1 -fold increase, $p < 0.05$) was detected in CPT1AM animals with respect to GFP controls. However, the markers of ER stress were not induced in VMH CPT1AM rats (Fig. 3C). These data suggest that increased ROS production in the VMH of CPT1AM rats may modulate GABAergic vesicular transporter.

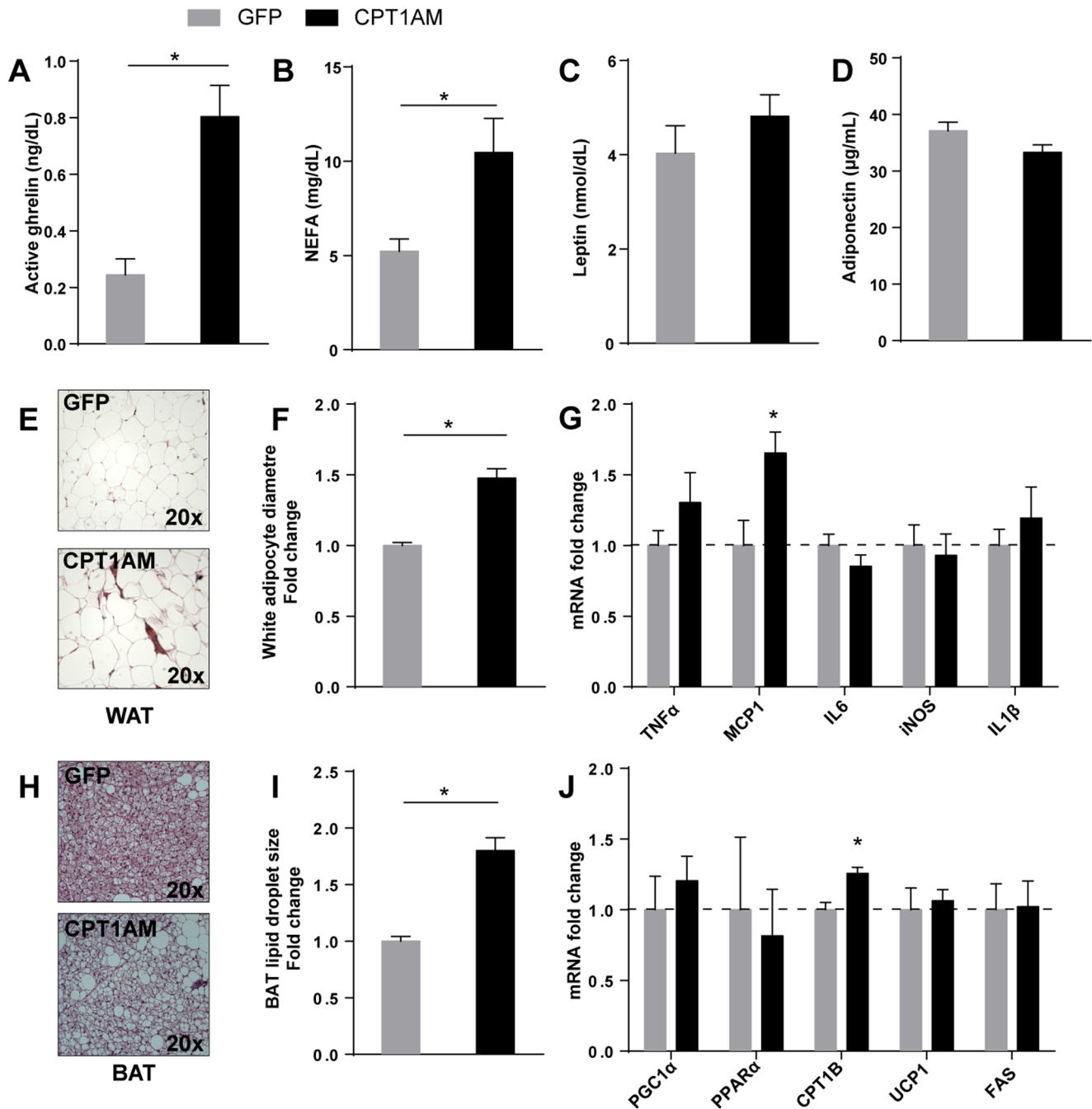


Figure 2. Analysis of postprandial metabolic and hormonal profile, adipose tissue histology, and mRNA expression in GFP and CPT1AM rats. Serum and plasma samples from fed GFP and CPT1AM rats were used for all the analyses. (A) Plasma active ghrelin. (B) Serum non-esterified fatty acids (NEFA). (C) Serum leptin. (D) Serum adiponectin. $n=6-10$ animals per group. (E) Epididymal WAT histological sections (H & E staining) from representative GFP and CPT1AM rats. (F) White adipocyte diameter scored using ImageJ software and expressed as a fold change respect to GFP animals (5 high power field counted per rat, $n=3$ rats per group). (G) mRNA expression of pro-inflammatory markers in WAT from GFP and CPT1AM rats. $n=5-7$ animals per group. (H) Interscapular BAT histological sections (H & E staining) from representative GFP and CPT1AM rats. (I) Lipid droplet size scored using ImageJ software and expressed as a fold change respect to GFP animals (4 high power field counted per rat, $n=3$ rats per group). (J) mRNA expression of genes associated with lipid metabolism and thermogenesis in BAT from GFP and CPT1AM animals. $n=10$ animals per group. Error bars indicate SEM. $*p<0.05$. doi:10.1371/journal.pone.0097195.g002

CPT1AM expression in the VMH alters fatty acid metabolism and the lipidomic profile in the MBH

Previous reports indicate that LCFA-CoA levels in the hypothalamus act as a signal in the pathways that modulate food

intake. Interestingly, animals with long-term CPT1AM expression in the VMH did not show a reduction of total LCFA-CoA in the MBH (Fig. 4A), in contrast to animals with short-term expression of this isoform [29]. In fact, the levels of C18:0 LCFA-CoA increased in the former (Table 2). We then analysed the mRNA

Table 1. Analysis of plasma amino acids from CPT1AM and GFP rats.

	GFP-expressing rats	CPT1AM-expressing rats	
Amino acids (μM)	<i>n</i> = 6	<i>n</i> = 6	<i>p</i> value
Taur	132 \pm 9	128 \pm 10.1	<i>ns</i>
Asp	23.7 \pm 0.8	26.7 \pm 1.2	<i>ns</i>
Hypro	1.6 \pm 0.2	1.7 \pm 0.1	<i>ns</i>
Thr	198.5 \pm 11.1	216.7 \pm 9.6	<i>ns</i>
Ser	216.2 \pm 6	221.4 \pm 5.6	<i>ns</i>
Asn	30.4 \pm 1.1	30.5 \pm 2.3	<i>ns</i>
Glu	192.4 \pm 15.8	265.1 \pm 12.3	<i>ns</i>
Gln	103.1 \pm 9.8	91.3 \pm 10.1	<i>ns</i>
Pro	70.8 \pm 1.5	67.5 \pm 2.7	<i>ns</i>
Gly	251 \pm 7.4	223.1 \pm 8.3	0.04
Ala	335 \pm 11.3	324.3 \pm 10.7	<i>ns</i>
Citr	66.4 \pm 3.5	71.2 \pm 3.8	<i>ns</i>
Val	159.4 \pm 6.2	189 \pm 5.8	0.006
Cyst	50 \pm 1.4	57.1 \pm 3.1	<i>ns</i>
Met	78.5 \pm 2.4	77.1 \pm 4.5	<i>ns</i>
Ile	66.1 \pm 2.5	79.2 \pm 2.2	0.003
Leu	194.3 \pm 6.9	204.9 \pm 3	<i>ns</i>
Tyr	127.5 \pm 8.4	144.7 \pm 8	<i>ns</i>
Phe	75 \pm 2.8	79.7 \pm 0.9	<i>ns</i>
Orn	115.5 \pm 3.2	163 \pm 7.1	0.004
Lys	632 \pm 9.1	696.1 \pm 25	0.05
His	101.3 \pm 2.7	122.4 \pm 2.8	0.001
Trp	21.9 \pm 1.5	20.8 \pm 2	<i>ns</i>
Arg	215.4 \pm 9.4	225.9 \pm 6.3	<i>ns</i>

Analysis was performed on plasma obtained at 18 weeks after AAV injection. Data indicated as Mean \pm SEM.
doi:10.1371/journal.pone.0097195.t001

levels of key genes involved in *de novo* FA synthesis (Fig. 4B). CPT1AM animals showed a 2.1 \pm 0.1-fold increase in FA synthase (FAS) mRNA ($p < 0.05$). Since hypothalamic malonyl-CoA levels have been proposed to regulate feeding, we also measured the concentration of this compound in the MBH of the two experimental groups. Concentrations of this metabolite showed no differences between groups (Fig. 4C). This finding is consistent with the absence of changes in ACC1 and ACC2 between the two groups in the MBH (Fig. 4B). On the basis of these observations, we conclude that the hyperphagic phenotype observed in our model is independent of the variations of these two metabolites.

To find out whether other bioactive lipids are involved in the orexigenic effect of VMH CPT1AM expression, we performed a lipidomic study of the MBH. Recent evidence has linked ceramide concentration in the hypothalamus to appetite modulation [20,21]. In our model, total ceramide levels were not significantly different; however, an analysis by species showed an increase in 14:0-ceramide (AAV-GFP, 5.3 \pm 0.7 pmol/mg, AAV-CPT1AM, 8.3 \pm 1.0 pmol/mg, $p < 0.01$) and 18:1-ceramide (AAV-GFP, 170.4 \pm 18.8 pmol/mg, AAV-CPT1AM, 250.5 \pm 31.9 pmol/mg, $p < 0.02$) levels (Fig. 4D, Table 2). We also observed a 36.1% increase in total lactosylceramides (LacCer) in CPT1AM rats (Fig. 4D). Furthermore, other sphingolipids related to ceramides, such as sphingomyelin (SM) and dihydrosphingomyelin (DHSM), were analysed. Total concentrations of SMs and DHSMs were

increased by 30.8% and 30.6%, respectively in the MBH of CPT1AM animals.

Membrane traffic and vesicular fusion are especially sensitive to the amount of phosphatidylethanolamine (PE) [41]. We determined the total levels of lysophosphatidylethanolamine (LPE), plasmalogen-phosphatidylethanolamine (PlasPE), and lysoplasmalogen (LPlasPE) and found them to be decreased by 38.5%, 29.0%, 45.8% respectively in CPT1AM rats with respect to controls. The concentration of lysophosphatidylserine (LPS) was also analysed in the MBH, finding it to be decreased by 39% in CPT1A animals (Fig. 4E). Interestingly, the amount of lysophosphatidylcholine (LPC) was 30.0% higher in CPT1AM animals than in controls, even though no changes were observed in total phosphatidylcholine (PC) and plasmalogenphosphatidylcholine (PlasPC). Neutral lipids (TAG, DAG and cholesterol esters) were not significantly different between groups (data not shown). All these observations indicate that CPT1A expression in the VMH changes lipid metabolic flows and alters the profile of structural and bioactive complex lipids in the MBH, which may be involved in the hyperphagic phenotype observed.

Discussion

The hypothalamus is a critical site in the regulation of food intake and energy homeostasis. The VMH has been considered a satiety centre, since lesion of the nucleus induces hyperphagia and

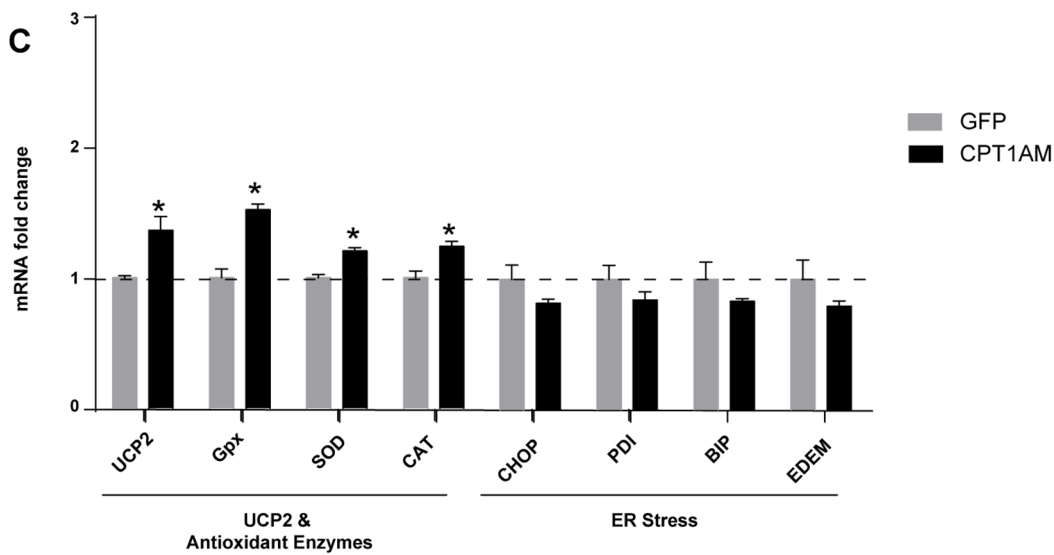
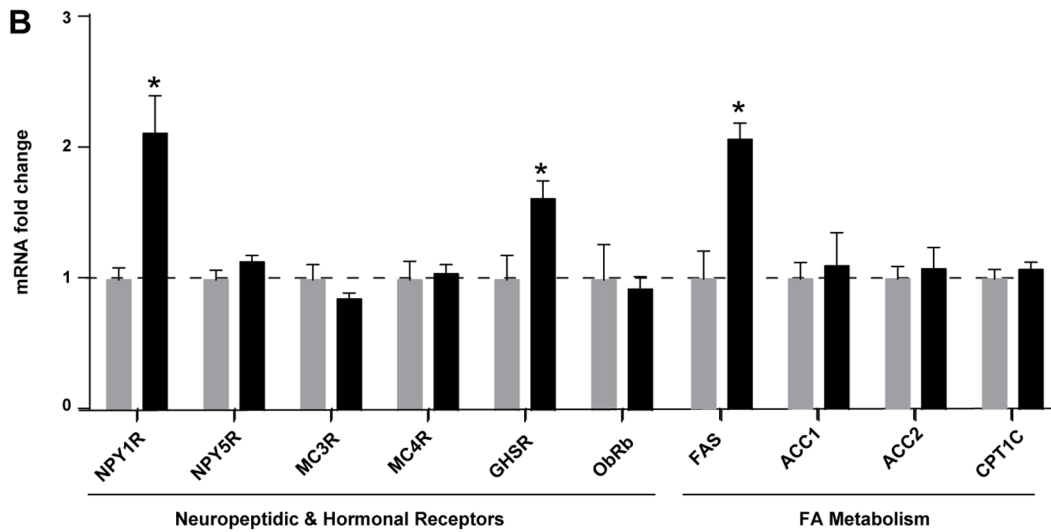
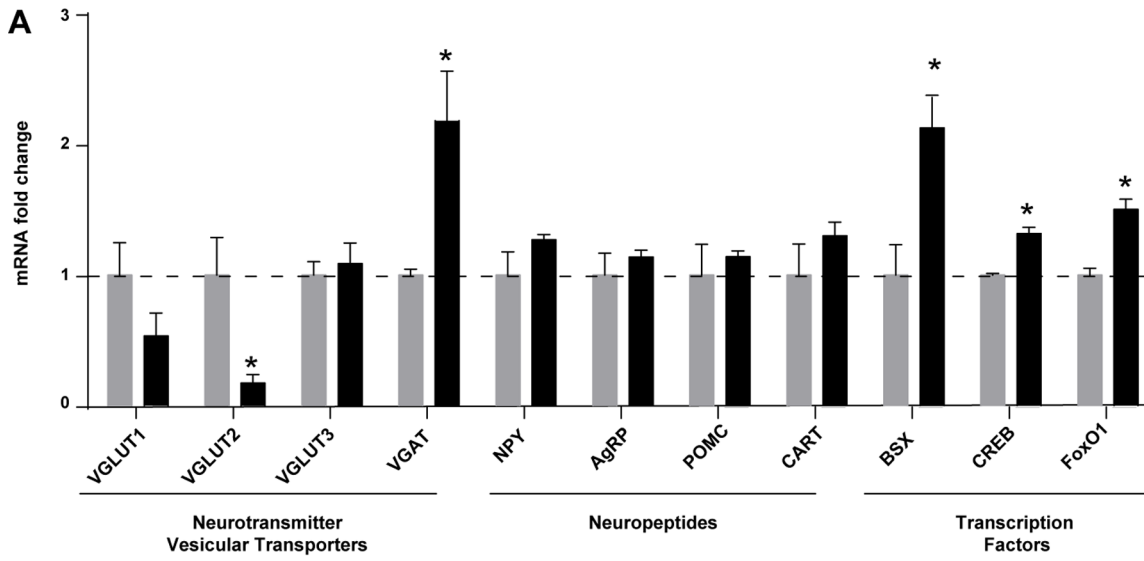


Figure 3. Analysis of MBH gene expression of GFP and CPT1AM rats. All analyses were performed 18 weeks after the AAV-injection into the VMH. (A) MBH relative mRNA expression of hypothalamic vesicular classical neurotransmitter transporters, hypothalamic neuropeptides, transcription factors. (B) Receptors for neuropeptides and hormones involved in feeding regulation and genes associated with fatty acid metabolism. (C) UCP2 and anti-oxidant enzymes and ER stress-related genes. $n = 6-7$ animals per group in all panels. Error bars indicate SEM. $*p < 0.05$. doi:10.1371/journal.pone.0097195.g003

obesity [26,42]. Several years ago, the focus of research into food intake control shifted from the VMH to the Arc with the development of cell-specific molecular tools to study its impact [22,43,44]. Nonetheless, the critical role of the VMH in the control of food intake and energy homeostasis has attracted renewed attention. This has arisen as a result of recent studies in knock-out mice in VMH-specific SF1 cells [26,45], the discovery of neuronal connections between the various hypothalamic nuclei [27], and the crucial role of the Arc- and VMH-originated classical amino acid neurotransmitters in the control of food intake [46–50]. FA metabolism is a key component in the regulation of food intake. We have recently reported that acute expression of CPT1AM, which is insensitive to malonyl-CoA, produces hyperphagia [29]. In the present study we have taken advantage of AAV vectors to demonstrate for the first time that long-term increased CPT1A expression in the VMH produces a chronic hyperphagia and body weight gain. Amongst others, this might be a result of the alteration of vesicular amino acid transporters expression, which are involved in the glutamatergic and

GABAergic neurotransmission. Moreover, the alteration on the lipidomic profile found in CPT1AM rats could explain these effects too. These findings emphasise the key role of VMH CPT1A expression in the hypothalamic control of appetite and body weight.

Our data confirm that CPT1AM expression in the VMH produces hyperphagia, as seen by the unsated state of CPT1AM rats. Such chronic over-feeding may contribute to the phenotype observed: CPT1AM rats present overweight and a progression towards insulin resistance, glucose intolerance and hyperglycemia. However, this hyperglycemia may be caused by the direct action of VMH CPT1AM expression. It has been reported that glutamatergic outputs from the VMH exert their effect on liver and thus control gluconeogenesis [51]. This observation is consistent with the observed up-regulation of liver gluconeogenic genes in CPT1AM rats, which show a decreased expression of the glutamatergic VGLUT2. In addition, these animals showed increased adiposity. This centrally driven direct effect may also be involved in the brown-to-white modification of BAT of VMH

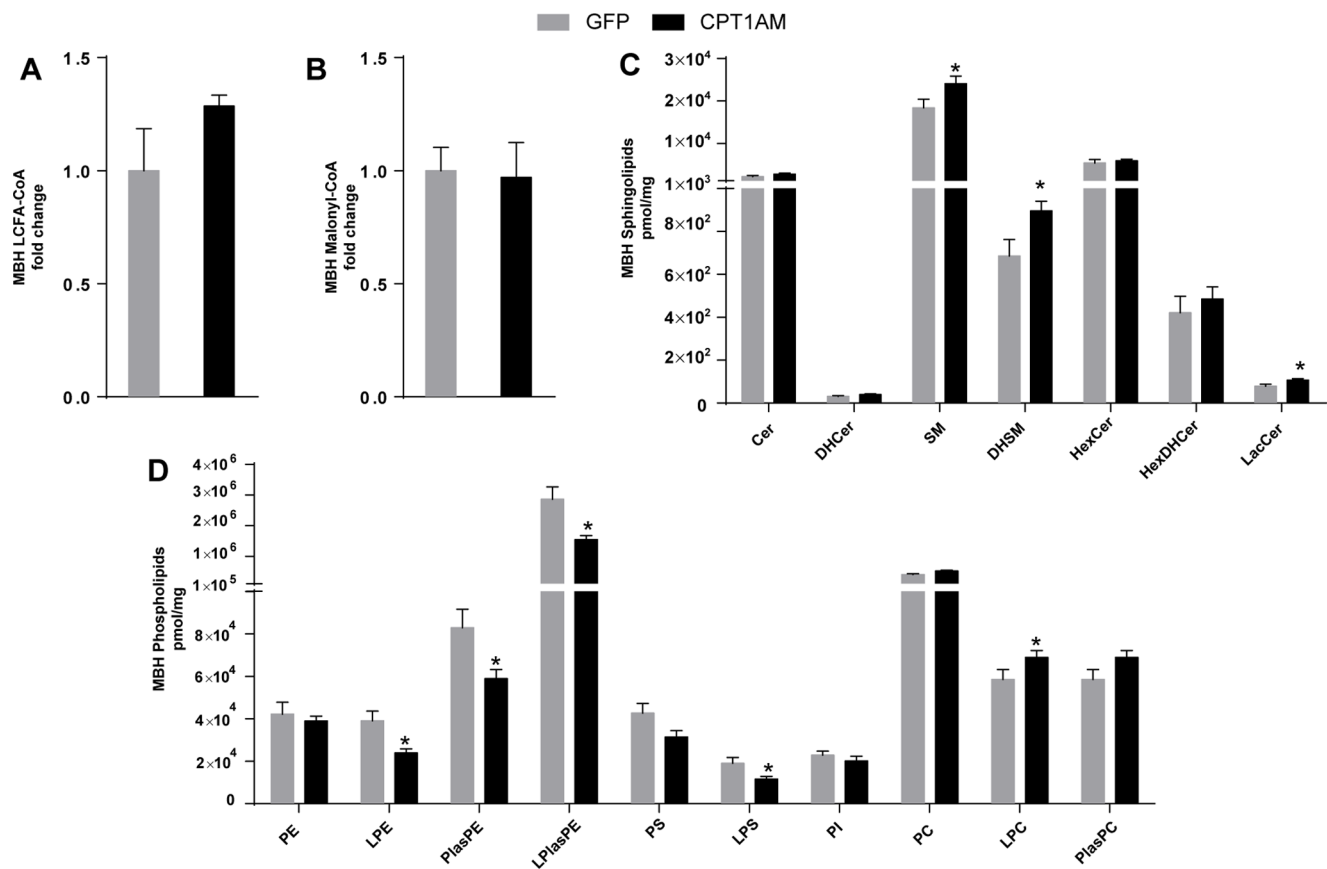


Figure 4. Lipid profile analysis in the MBH of GFP and CPT1AM rats. (A) Relative LCFA-CoA and (B) malonyl-CoA content in the MBH. (C) Sphingolipid (SLs) and (D) phospholipid (PLs) levels in the MBH. $n = 5-8$ animals per group in panels A and B. $n = 10$ animals per group in panels C, D and E. Error bars represent SEM. $*p < 0.05$. DAG: diacylglycerol; TAG: triacylglycerol; Cho-E: cholesterol ester; Cer: ceramide; DHCer: dihydroceramide; SM: sphingomyelin; DHSM: dihydro sphingomyelin; GlucCer: glucosylceramide; GlucDHCer: glucosyldihydroceramide; LacCer: lactosylceramide; PE: phosphatidylethanolamine; LPE: lysophosphatidylethanolamine; PlasPE: plasminogen phosphatidylethanolamine; PS: phosphatidylserine; LPS: lysophosphatidylserine; PI: phosphatidylinositol. doi:10.1371/journal.pone.0097195.g004

Table 2. LCFA-CoA and ceramides levels in MBH from CPT1AM and GFP rats.

	GFP-expressing rats	CPT1AM-expressing rats	
LCFA-CoA (pg/mg protein)	<i>n</i> = 5	<i>n</i> = 7	<i>p</i> value
16:0	1±0.2	1.2±0.1	<i>ns</i>
18:0	0.19±0.04	0.3±0.02	0.02
18:1			<i>ns</i>
Ceramides (pmol/mg protein)	<i>n</i> = 10	<i>n</i> = 10	<i>p</i> value
14:0	5.3±0.7	8.3±1	0.01
14:1	2.7±0.4	4±0.7	<i>ns</i>
16:0	66.3±9.6	84.9±13.1	<i>ns</i>
16:1	7.3±1.1	9.5±1	<i>ns</i>
18:0	1479.9±177.9	1880.8±165.9	<i>ns</i>
18:1	170.4±18.8	250.5±31.9	0.02
20:0	246.9±41.3	312.4±23.9	<i>ns</i>
22:0	40.3±6.9	51±7.1	<i>ns</i>
22:1	10.6±1.3	12.5±1.2	<i>ns</i>
24:0	61.2±9.4	67.1±13.5	<i>ns</i>
24:1	65±7.8	67.5±10.5	<i>ns</i>
24:2	24.3±3.5	29.1±3.6	<i>ns</i>

Analysis was performed on MBH extracts obtained at 18 weeks after AAV injection. Data indicated as Mean ± SEM.
doi:10.1371/journal.pone.0097195.t002

CPT1AM rats. In support of this notion, VMH has been implicated in the modulation of BAT thermogenesis through parasympathetic innervation [52,53]. We detected lipid accumulation and hypertrophy in WAT. Although these conditions may be a direct effect of CPT1AM expression in the VMH, we cannot discard indirect mechanisms such as the effect of ghrelin on peripheral tissues [54–56].

In our hands, fed VMH CPT1AM rats showed increased circulating levels of the appetite-stimulating hormone ghrelin and NEFA, thus mimicking the metabolic status of fasting animals during the postprandial phase. The relationship between ghrelin hypothalamic signalling and CPT1A activity is well established [22,23,29,56]. Nevertheless, the observation of increased ghrelin levels as a result of VMH CPT1AM expression is striking, since it may indicate a connection between the VMH and the stomach, which is the main producer of octanoylated ghrelin. This notion is reinforced by the observation of reduced ghrelin levels in response to icv administration of C75 [57], a compound that inhibits FAS and CPT1A [35]. Nonetheless, further research is required to confirm these physiological findings.

The molecular mediators in the orexigenic signalling triggered by CPT1A in the VMH are not clear. Although little attention has been given to amino acid neurotransmitters in the control of food intake, their role in hunger signalling has been recently highlighted. Glutamatergic outputs from the VMH have been described to activate anorexigenic POMC/CART neurons to stimulate satiety signalling [27]. In the MBH of rats expressing CPT1AM in the VMH, we observed diminished mRNA levels of VGLUT2, which is the main vesicular glutamate transporter in that nucleus (Fig. 3). Such a decrease may lead to a reduction in glutamate quantal size in the VMH, which would in turn attenuate the activation of anorexigenic neurons. Moreover, optogenetic stimulation on NPY/AgRP neurons produces an orexigenic effect that is blocked using GABA antagonists. This finding indicates that the orexigenic signalling was not dependent on peptidergic neurotransmission [50]. We observed an increase in VGAT

expression, which may produce a rise in GABAergic signalling. This inhibitory signalling may come from the VMH [58] and/or from NPY/AgRP neurons [59] to anorexigenic POMC/CART neurons. This notion is consistent with the experiments in which injections of the GABA agonist muscimol markedly increased food intake [60]. Although we do not know how the vesicular transporters are modulated in our model, ROS signalling has been reported to boost GABA release [40]. For this reason, we hypothesise that CPT1AM expression in the VMH, which increases ROS, might be responsible for this higher inhibitory output. Although we did not monitor ROS directly, we observed an increase in the transcription of ROS-buffering enzymes.

Alternatively, the lipidomic profile modification driven by CPT1AM expression could be responsible for the increased food intake. CPT1A alters the lipid profile in neurons [61], and membrane composition is crucial to maintain the structure and functionality of embedded proteins [62–65]. In some physiopathological states, neurotransmission is modified by alterations in membrane lipid composition [66]. In the synaptic vesicular model developed by Takamori *et al.*, transmembrane proteins encompass one fourth of the whole vesicular surface [64]. Among them, vesicular amino acid transporters, such as VGAT and VGLUT2, require their phospholipidic rims to be anchored to the lipid bilayer and to have a correct functionality [63,64]. The reduction in phospholipids observed in our model may affect the functionality of these transporters, thus impairing their transcription in some way, at least in the case of VGLUT2. Notwithstanding, we hypothesise that the putative increased VGAT mRNA levels occurs as a result of other factors, such as an indirect effect on other regions within the MBH, mainly Arc, or the aforementioned ROS-induced up-regulation. Both changes in lipid composition and expression of glutamatergic and GABAergic transporters may be implicated in the increase of food intake in animals with CPT1AM expression in the VMH (Fig. 5). Accordingly, we did not observe changes in POMC or CART expression in this animal model or an increase in NPY or AgRP mRNA levels. This could

be attributed to the fact that we measured these transcripts in fasting conditions, where both CPT1AM and control GFP rats may express high levels of these orexigenic neuropeptides. However, the transcription factors BSX, CREB and FoxO1, involved in NPY and AgRP expression, were induced in CPT1AM rats [21,37,38].

In addition, our results indicate that long-term expression of CPT1AM raises sphingolipid levels in the MBH. It has recently been demonstrated that hypothalamic ceramide metabolism participates in feeding regulation [20]. In particular, the brain-specific CPT1C is required for the fasting-induced increase in hypothalamic ceramides [21]. The present data also implicate CPT1A in ceramide metabolism, as CPT1AM rats showed a significant increase in the hypothalamic concentrations of 18:1 and 14:0-ceramides. Sphingolipids act as signalling molecules in a variety of physiological processes, including neuronal development and plasticity. The formation and transport of specific axonal

vesicles has been reported to be coupled to sphingolipid synthesis [67]. Here we observed that CPT1AM expression alters sphingolipid metabolism by increasing SM and DHSM, and it may lead to the modification of hypothalamic synaptic plasticity and energy balance. However, further research is required to test this notion and to clarify the contribution of CPT1A and CPT1C isoforms to hypothalamic sphingolipid metabolism and feeding modulation. In addition, CPT1A expression in the VMH reduces phospholipids in MBH. Although concrete lipid metabolic flows were not the objective of this study, we hypothesise that phospholipids may serve as fuel for increased FAO in CPT1AM-expressing neurons.

Previous hypotheses assume that LCFA-CoAs signal nutrient availability in the hypothalamus and modulate food intake control [14,15]. Accordingly, in collaboration with Lopaschuck's group [29], we observed that short-term expression of CPT1AM in the VMH produces hyperphagia and reduced LCFA-CoA concentration in MBH neurons. Nonetheless, here we show that total

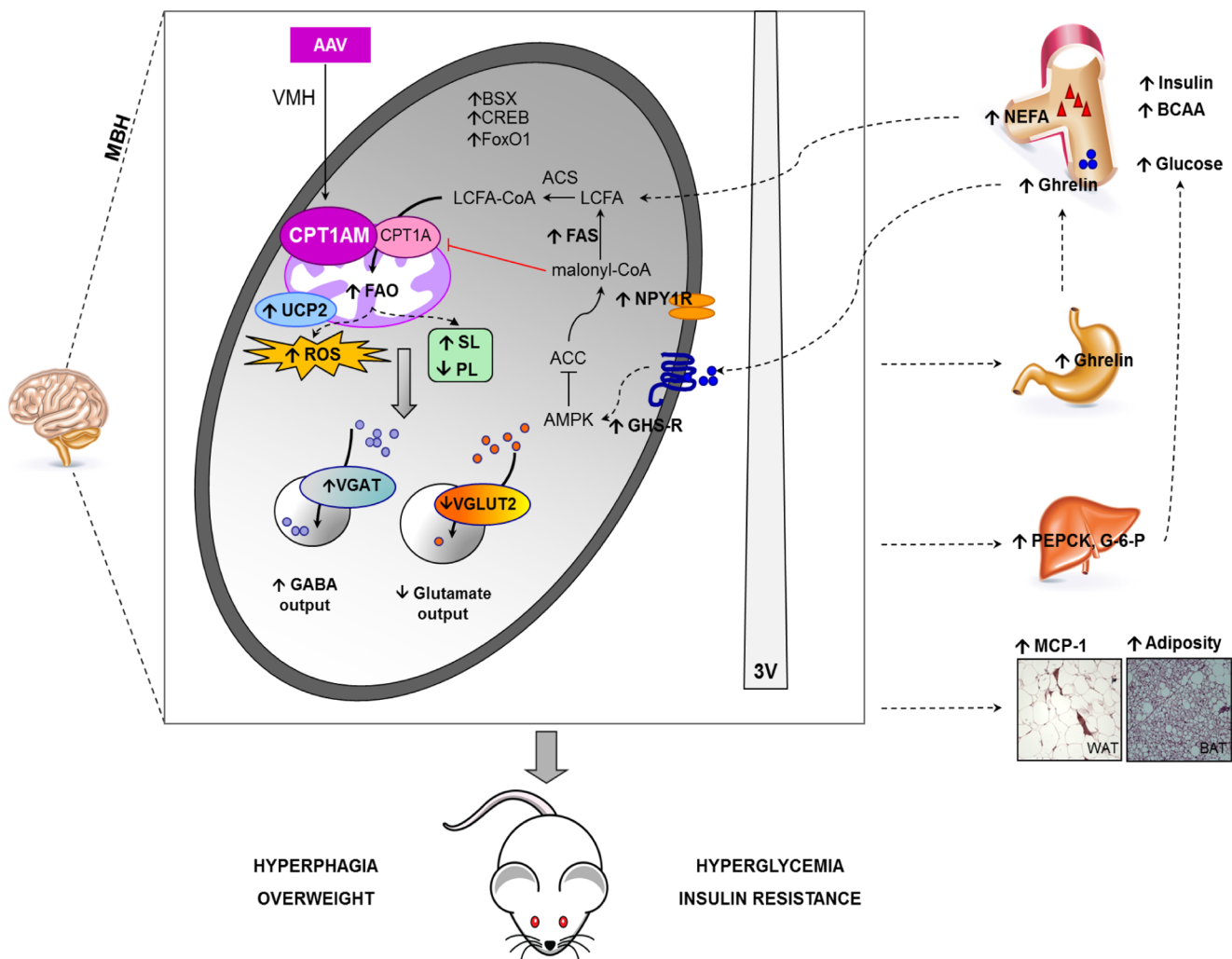


Figure 5. Proposed role of VMH CPT1A in the hypothalamic control of satiety. AAV-mediated CPT1AM expression in the VMH would increase FAO and modulate ROS production and the cellular profile of SLs and PLs. The derived molecular changes in the hypothalamus include the up-regulation of the mitochondrial protein UCP2, the enzyme FAS, and the receptors NPY1R and GHS-R, which indicate an enhanced response to orexigenic NPY and ghrelin. Moreover, an up-regulation of VGAT transporter and a decrease in VGLUT2 may indicate enhanced inhibitory signalling which has been described to promote food intake. The long-term de-regulation of hypothalamic energy sensing induces systemic modifications, including increased circulating levels of BCAA, NEFA, ghrelin, insulin and glucose, the up-regulation of hepatic gluconeogenic genes, increased adiposity, and MCP1 expression in WAT. These central and systemic changes derived from VMH CPT1AM expression promote an increase in food intake and the development of associated metabolic complications.

doi:10.1371/journal.pone.0097195.g005

hypothalamic LCFA-CoA content in hyperphagic long-term CPT1A-expressing animals was similar to GFP control rats and, specifically, the concentration of 18:0-LCFA-CoA was significantly higher in the former. This discrepancy with our previous study might be a consequence of the adaptability of FA metabolism to long-term CPT1A expression and poses the question as to whether hyperphagia is dependent on LCFA-CoAs levels or whether it relies only on CPT1A activity.

In conclusion, our results indicate that CPT1A expression in the VMH plays a key role in the regulation of food intake and glucose homeostasis (Fig. 5). Mechanistically, our findings suggest that CPT1A modulates mRNA levels of glutamatergic and GABAergic neurotransmission markers and transcription factors controlling orexigenic neuropeptides. Since CPT1A modifies the composition of sphingolipids and phospholipids and also boosts ROS formation, we cannot discard a mechanistic involvement of these

species. Taken together, these data shed light on the central molecular mechanism controlling appetite and highlight mitochondrial FAO in the hypothalamus as a potential target for the treatment of obesity and other eating disorders.

Acknowledgments

We thank Robin Rycroft and Tanya Yates for valuable assistance in preparing the English manuscript and Eva Dalmau, from IQAC/CSIC, Barcelona, for excellent technical assistance with lipid analyses.

Author Contributions

Conceived and designed the experiments: LH DS. Performed the experiments: PM JFM GF JC MIM JAF LR. Analyzed the data: ASHG GA FGH. Contributed reagents/materials/analysis tools: SG SC MSRP HP. Wrote the paper: PM JFM LH DS.

References

- Schwartz MW, Woods SC, Porte D Jr, Seeley RJ, Baskin DG (2000) Central nervous system control of food intake. *Nature* 404: 661–671.
- Williams G, Bing C, Cai XJ, Harrold JA, King PJ, et al. (2001) The hypothalamus and the control of energy homeostasis: different circuits, different purposes. *Physiology & behavior* 74: 683–701.
- Woods SC, D'Alessio DA (2008) Central control of body weight and appetite. *The Journal of clinical endocrinology and metabolism* 93: S37–50.
- Lopez M, Lelliott CJ, Vidal-Puig A (2007) Hypothalamic fatty acid metabolism: a housekeeping pathway that regulates food intake. *Bioessays* 29: 248–261.
- Gao S, Kinzig KP, Aja S, Scott KA, Keung W, et al. (2007) Leptin activates hypothalamic acetyl-CoA carboxylase to inhibit food intake. *Proceedings of the National Academy of Sciences of the United States of America* 104: 17358–17363.
- Lopez M, Lage R, Saha AK, Perez-Tilve D, Vazquez MJ, et al. (2008) Hypothalamic fatty acid metabolism mediates the orexigenic action of ghrelin. *Cell metabolism* 7: 389–399.
- Hu Z, Dai Y, Prentki M, Chohan S, Lane MD (2005) A role for hypothalamic malonyl-CoA in the control of food intake. *The Journal of biological chemistry* 280: 39681–39683.
- Hu Z, Cha SH, Chohan S, Lane MD (2003) Hypothalamic malonyl-CoA as a mediator of feeding behavior. *Proceedings of the National Academy of Sciences of the United States of America* 100: 12624–12629.
- Loftus TM (2000) Reduced Food Intake and Body Weight in Mice Treated with Fatty Acid Synthase Inhibitors. *Science* 288: 2379–2381.
- Lopez M, Lelliott CJ, Tovar S, Kimber W, Gallego R, et al. (2006) Tamoxifen-Induced Anorexia Is Associated With Fatty Acid Synthase Inhibition in the Ventromedial Nucleus of the Hypothalamus and Accumulation of Malonyl-CoA. *Diabetes* 55: 1327–1336.
- Lopez M, Lage R, Saha AK, Pérez-Tilve D, Vázquez MJ, et al. (2008) Hypothalamic fatty acid metabolism mediates the orexigenic action of ghrelin. *Cell metabolism* 7: 389–399.
- Gao S, Casals N, Keung W, Moran TH, Lopaschuk GD (2013) Differential effects of central ghrelin on fatty acid metabolism in hypothalamic ventral medial and arcuate nuclei. *Physiology & behavior* 118: 165–170.
- McGarry JD, Brown NF (1997) The mitochondrial carnitine palmitoyltransferase system. From concept to molecular analysis. *European journal of biochemistry/FEBS* 244: 1–14.
- Obici S, Feng Z, Morgan K, Stein D, Karkhanian G, et al. (2002) Central administration of oleic acid inhibits glucose production and food intake. *Diabetes* 51: 271–275.
- Obici S, Feng Z, Arduini A, Conti R, Rossetti L (2003) Inhibition of hypothalamic carnitine palmitoyltransferase-1 decreases food intake and glucose production. *Nature medicine* 9: 756–761.
- Pocai A, Lam TK, Obici S, Gutierrez-Juarez R, Muse ED, et al. (2006) Restoration of hypothalamic lipid sensing normalizes energy and glucose homeostasis in overfed rats. *The Journal of clinical investigation* 116: 1081–1091.
- Kang L, Routh VH, Kuzhikandathil EV, Gaspers LD, Levin BE (2004) Physiological and molecular characteristics of rat hypothalamic ventromedial nucleus glucosensing neurons. *Diabetes* 53: 549–559.
- Sierra AY, Gratacos E, Carrasco P, Clotet J, Urena J, et al. (2008) CPT1c is localized in endoplasmic reticulum of neurons and has carnitine palmitoyltransferase activity. *The Journal of biological chemistry* 283: 6878–6885.
- Price N, van der Leij F, Jackson V, Corstorphine C, Thomson R, et al. (2002) A novel brain-expressed protein related to carnitine palmitoyltransferase I. *Genomics* 80: 433–442.
- Gao S, Zhu G, Gao X, Wu D, Carrasco P, et al. (2011) Important roles of brain-specific carnitine palmitoyltransferase and ceramide metabolism in leptin hypothalamic control of feeding. *Proceedings of the National Academy of Sciences of the United States of America* 108(23): 9691–9696.
- Ramirez S, Martins L, Jacas J, Carrasco P, Pozo M, et al. (2013) Hypothalamic ceramide levels regulated by CPT1C mediate the orexigenic effect of ghrelin. *Diabetes*.
- Andrews ZB, Liu ZW, Wallingford N, Erion DM, Borok E, et al. (2008) UCP2 mediates ghrelin's action on NPY/AgRP neurons by lowering free radicals. *Nature* 454: 846–851.
- Varela L, Vázquez MJ, Cordido F, Nogueiras R, Vidal-Puig A, et al. (2011) Ghrelin and lipid metabolism: key partners in energy balance. *Journal of molecular endocrinology* 46: R43–63.
- Lage R, Vazquez MJ, Varela L, Saha AK, Vidal-Puig A, et al. (2010) Ghrelin effects on neuropeptides in the rat hypothalamus depend on fatty acid metabolism actions on BSX but not on gender. *FASEB J* 24: 2670–2679.
- Kernie SG, Liebl DJ, Parada LF (2000) BDNF regulates eating behavior and locomotor activity in mice. *Embo J* 19: 1290–1300.
- King BM (2006) The rise, fall, and resurrection of the ventromedial hypothalamus in the regulation of feeding behavior and body weight. *Physiology & behavior* 87: 221–244.
- Sternson SM, Shepherd GMG, Friedman JM (2005) Topographic mapping of VMH → arcuate nucleus microcircuits and their reorganization by fasting. *Nature neuroscience* 8: 1356–1363.
- Jo YH (2012) Endogenous BDNF regulates inhibitory synaptic transmission in the ventromedial nucleus of the hypothalamus. *Journal of neurophysiology* 107: 42–49.
- Gao S, Serra D, Keung W, Hegardt FG, Lopaschuk GD (2013) Important role of ventromedial hypothalamic carnitine palmitoyltransferase-1a in the control of food intake. *Am J Physiol Endocrinol Metab*.
- Morillas M, Gomez-Puertas P, Bentebibel A, Selles E, Casals N, et al. (2003) Identification of conserved amino acid residues in rat liver carnitine palmitoyltransferase I critical for malonyl-CoA inhibition. Mutation of methionine 593 abolishes malonyl-CoA inhibition. *The Journal of biological chemistry* 278: 9058–9063.
- Grimm D, Kern A, Rittner K, Kleinschmidt JA (1998) Novel tools for production and purification of recombinant adenoassociated virus vectors. *Human gene therapy* 9: 2745–2760.
- Dentin R, Pegorier JP, Benhamed F, Foulfelle F, Ferre P, et al. (2004) Hepatic glucokinase is required for the synergistic action of ChREBP and SREBP-1c on glycolytic and lipogenic gene expression. *The Journal of biological chemistry* 279: 20314–20326.
- Paxinos G, Watson C (1998) *The rat brain in stereotaxic coordinates*. San Diego; London: Academic. xxvi, [236]p. p.
- Takamura Y, Kitayama Y, Arakawa A, Yamanaka S, Tosaki M, et al. (1985) Malonyl-CoA: acetyl-CoA cycling. A new micromethod for determination of acyl-CoAs with malonate decarboxylase. *Biochimica et biophysica acta* 834: 1–7.
- Mera P, Bentebibel A, Lopez-Vinas E, Cordente AG, Gurunathan C, et al. (2009) C75 is converted to C75-CoA in the hypothalamus, where it inhibits carnitine palmitoyltransferase 1 and decreases food intake and body weight. *Biochem Pharmacol* 77: 1084–1095.
- Canals D, Mormeneo D, Fabrias G, Llebaria A, Casas J, et al. (2009) Synthesis and biological properties of Pachastriamine (jaspine B) and diastereoisomeric jaspines. *Bioorganic & medicinal chemistry* 17: 235–241.
- Sakkou M, Wiedmer P, Anlag K, Hamm A, Seuntjens E, et al. (2007) A role for brain-specific homeobox factor Bsx in the control of hyperphagia and locomotor behavior. *Cell metabolism* 5: 450–463.
- Sasaki T, Kitamura T (2010) Roles of FoxO1 and Sirt1 in the central regulation of food intake. *Endocrine journal* 57: 939–946.
- Nogueiras R, Tovar S, Mitchell SE, Rayner DV, Archer ZA, et al. (2004) Regulation of growth hormone secretagogue receptor gene expression in the arcuate nuclei of the rat by leptin and ghrelin. *Diabetes* 53: 2552–2558.

40. Tarasenko A, Krupko O, Himmelreich N (2012) Reactive oxygen species induced by presynaptic glutamate receptor activation is involved in [(3)H]GABA release from rat brain cortical nerve terminals. *Neurochemistry international* 61: 1044–1051.
41. Thai TP, Rodemer C, Jauch A, Hunziker A, Moser A, et al. (2001) Impaired membrane traffic in defective ether lipid biosynthesis. *Human molecular genetics* 10: 127–136.
42. Hetherington A, Ranson S (1942) The relation of various hypothalamic lesions to adiposity in the rat. *J Comp Neurol* 76: 475–499.
43. Lane MD, Wolfgang M, Cha SH, Dai Y (2008) Regulation of food intake and energy expenditure by hypothalamic malonyl-CoA. *Int J Obes (Lond)* 32 Suppl 4: S49–54.
44. Swierczynski J, Goyke E, Korczynska J, Jankowski Z (2008) Acetyl-CoA carboxylase and fatty acid synthase activities in human hypothalamus. *Neuroscience letters* 444: 209–211.
45. Choi YH, Fujikawa T, Lee J, Reuter A, Kim KW (2013) Revisiting the Ventral Medial Nucleus of the Hypothalamus: The Roles of SF-1 Neurons in Energy Homeostasis. *Frontiers in neuroscience* 7: 71.
46. Wittmann G, Hrabovszky E, Lechan RM (2013) Distinct glutamatergic and GABAergic subsets of hypothalamic pro-opiomelanocortin neurons revealed by in situ hybridization in male rats and mice. *The Journal of comparative neurology* 521: 3287–3302.
47. Schöne C, Burdakov D (2012) Glutamate and GABA as rapid effectors of hypothalamic “peptidergic” neurons. *Frontiers in behavioral neuroscience* 6: 81.
48. Delgado TC (2013) Glutamate and GABA in Appetite Regulation. *Frontiers in endocrinology* 4: 103.
49. van den Pol AN (2012) Neuropeptide transmission in brain circuits. *Neuron* 76: 98–115.
50. Atasoy D, Aponte Y, Su HH, Sternson SM (2008) A FLEX switch targets Channelrhodopsin-2 to multiple cell types for imaging and long-range circuit mapping. *J Neurosci* 28: 7025–7030.
51. Tong Q, Ye C, McCrimmon RJ, Dhillon H, Choi B, et al. (2007) Synaptic glutamate release by ventromedial hypothalamic neurons is part of the neurocircuitry that prevents hypoglycemia. *Cell metabolism* 5: 383–393.
52. López M, Varela L, Vázquez MJ, Rodríguez-Cuenca S, González CR, et al. (2010) Hypothalamic AMPK and fatty acid metabolism mediate thyroid regulation of energy balance. *Nature medicine* 16: 1001–1008.
53. Martínez de Morentin PB, Whittle AJ, Ferno J, Nogueiras R, Dieguez C, et al. (2012) Nicotine induces negative energy balance through hypothalamic AMP-activated protein kinase. *Diabetes* 61: 807–817.
54. Tschöp M, Smiley DL, Heiman ML (2000) Ghrelin induces adiposity in rodents. *Nature* 407: 908–913.
55. Theander-Carrillo C, Wiedmer P, Cettour-Rose P, Nogueiras R, Perez-Tilve D, et al. (2006) Ghrelin action in the brain controls adipocyte metabolism. *The Journal of clinical investigation* 116: 1983–1993.
56. Sangiao-Alvarellos S, Vazquez MJ, Varela L, Nogueiras R, Saha AK, et al. (2009) Central ghrelin regulates peripheral lipid metabolism in a growth hormone-independent fashion. *Endocrinology* 150: 4562–4574.
57. Hu Z, Cha SH, van Haasteren G, Wang J, Lane MD (2005) Effect of centrally administered C75, a fatty acid synthase inhibitor, on ghrelin secretion and its downstream effects. *Proceedings of the National Academy of Sciences of the United States of America* 102: 3972–3977.
58. Zhu W, Czyzyk D, Paranjape SA, Zhou L, Horblitt A, et al. (2010) Glucose prevents the fall in ventromedial hypothalamic GABA that is required for full activation of glucose counterregulatory responses during hypoglycemia. *American journal of physiology* 298: E971–977.
59. Wu Q, Palmiter RD (2011) GABAergic signaling by AgRP neurons prevents anorexia via a melanocortin-independent mechanism. *European journal of pharmacology* 660: 21–27.
60. Kelly J, Rothstein J, Grossman SP (1979) GABA and hypothalamic feeding systems. I. Topographic analysis of the effects of microinjections of muscimol. *Physiology & behavior* 23: 1123–1134.
61. Arduini A, Denisova N, Virmani A, Avrova N, Federici G, et al. (1994) Evidence for the involvement of carnitine-dependent long-chain acyltransferases in neuronal triglyceride and phospholipid fatty acid turnover. *Journal of neurochemistry* 62: 1530–1538.
62. Schug ZT, Frezza C, Galbraith LC, Gottlieb E (2012) The music of lipids: how lipid composition orchestrates cellular behaviour. *Acta oncologica (Stockholm, Sweden)* 51: 301–310.
63. Lundback JA (2006) Regulation of membrane protein function by lipid bilayer elasticity—a single molecule technology to measure the bilayer properties experienced by an embedded protein. *J Phys Condens Matter* 18: S1305–1344.
64. Takamori S, Holt M, Stenius K, Lemke EA, Grønborg M, et al. (2006) Molecular anatomy of a trafficking organelle. *Cell* 127: 831–846.
65. Sprong H, van der Sluijs P, van Meer G (2001) How proteins move lipids and lipids move proteins. *Nature reviews* 2: 504–513.
66. du Bois TM, Deng C, Huang XF (2005) Membrane phospholipid composition, alterations in neurotransmitter systems and schizophrenia. *Progress in neuro-psychopharmacology & biological psychiatry* 29: 878–888.
67. Chang MC, Wisco D, Ewers H, Norden C, Winckler B (2006) Inhibition of sphingolipid synthesis affects kinetics but not fidelity of L1/NgCAM transport along direct but not transcytotic axonal pathways. *Molecular and cellular neurosciences* 31: 525–538.

Enhanced fatty acid oxidation in adipocytes and macrophages reduces lipid-induced triglyceride accumulation and inflammation

Maria Ida Malandrino,^{1,2} Raquel Fucho,^{1,2} Minéia Weber,^{1,2} María Calderon-Dominguez,^{1,2} Joan Francesc Mir,^{1,2} Lorea Valcarcel,^{1,2} Xavier Escoté,^{3,4} María Gómez-Serrano,^{2,5} Belén Peral,^{2,5} Laia Salvadó,^{4,6} Sonia Fernández-Veledo,^{3,4} Núria Casals,^{2,7} Manuel Vázquez-Carrera,^{4,6} Francesc Villarroya,^{1,2} Joan J Vendrell,^{3,4} Dolors Serra,^{1,2} and Laura Herrero^{1,2}

¹Department of Biochemistry and Molecular Biology, Institut de Biomedicina de la Universitat de Barcelona, Universitat de Barcelona, Barcelona, Spain; ²Institut de Biomedicina de la Universitat de Barcelona Fisiopatología de la Obesidad y la Nutrición, Instituto de Salud Carlos III, Madrid, Spain; ³Endocrinology and Diabetes Unit, Joan XXIII University Hospital, Institut d'Investigació Sanitària Pere i Virgili, Universitat Rovira i Virgili, Tarragona, Spain; ⁴Institut de Biomedicina de la Universitat de Barcelona de Diabetes y Enfermedades Metabólicas Asociadas, Instituto de Salud Carlos III, Madrid, Spain; ⁵Instituto de Investigaciones Biomédicas Alberto Sols, Consejo Superior de Investigaciones Científicas and Universidad Autónoma de Madrid, Madrid, Spain; ⁶Pharmacology Unit, Department of Pharmacology and Therapeutic Chemistry and Institut de Biomedicina de la Universitat de Barcelona, Faculty of Pharmacy, University of Barcelona, Barcelona, Spain; and ⁷Basic Sciences Department, Faculty of Medicine and Health Sciences, Universitat Internacional de Catalunya, Barcelona, Spain

Submitted 30 July 2014; accepted in final form 19 February 2015

Malandrino MI, Fucho R, Weber M, Calderon-Dominguez M, Mir JF, Valcarcel L, Escoté X, Gómez-Serrano M, Peral B, Salvadó L, Fernández-Veledo S, Casals N, Vázquez-Carrera M, Villarroya F, Vendrell JJ, Serra D, Herrero L. Enhanced fatty acid oxidation in adipocytes and macrophages reduces lipid-induced triglyceride accumulation and inflammation. *Am J Physiol Endocrinol Metab* 308: E756–E769, 2015. First published February 24, 2015; doi:10.1152/ajpendo.00362.2014.—Lipid overload in obesity and type 2 diabetes is associated with adipocyte dysfunction, inflammation, macrophage infiltration, and decreased fatty acid oxidation (FAO). Here, we report that the expression of carnitine palmitoyl-transferase 1A (CPT1A), the rate-limiting enzyme in mitochondrial FAO, is higher in human adipose tissue macrophages than in adipocytes and that it is differentially expressed in visceral vs. subcutaneous adipose tissue in both an obese and a type 2 diabetes cohort. These observations led us to further investigate the potential role of CPT1A in adipocytes and macrophages. We expressed CPT1AM, a permanently active mutant form of CPT1A, in 3T3-L1 CARΔ1 adipocytes and RAW 264.7 macrophages through adenoviral infection. Enhanced FAO in palmitate-incubated adipocytes and macrophages reduced triglyceride content and inflammation, improved insulin sensitivity in adipocytes, and reduced endoplasmic reticulum stress and ROS damage in macrophages. We conclude that increasing FAO in adipocytes and macrophages improves palmitate-induced derangements. This indicates that enhancing FAO in metabolically relevant cells such as adipocytes and macrophages may be a promising strategy for the treatment of chronic inflammatory pathologies such as obesity and type 2 diabetes.

obesity; type 2 diabetes; adipocytes; macrophages; inflammation; fatty acid oxidation; CPT1

OBESITY HAS REACHED EPIDEMIC PROPORTIONS worldwide, leading to severe associated pathologies such as insulin resistance, type 2 diabetes (T2D), cardiovascular disease, Alzheimer's disease, hypertension, hypercholesterolemia, hypertriglyceri-

demia, nonalcoholic fatty liver disease, arthritis, asthma, and certain forms of cancer (12).

Over the last two decades, adipose tissue has gained crucial importance in the mechanisms involved in obesity-related disorders. The energy-storing white adipose tissue (WAT) is well vascularized and contains adipocytes, connective tissue, and numerous immune cells such as macrophages, T and B cells, mast cells, and neutrophils that infiltrate and increase their presence during obesity (22). Macrophages were the first immune cells reported to participate in obesity-induced insulin resistance (56). This highlights their pathological role in adipose tissue in addition to their traditional involvement in tissue repair and in response to dead and dying adipocytes (5, 14). Fat is an active endocrine tissue that secretes hormones such as leptin, adiponectin, or resistin and inflammatory cytokines such as TNF- α , IL-6, IL-1 β , etc. in response to several stimuli. It is therefore a complex organ controlling energy expenditure, appetite, insulin sensitivity, endocrine and reproductive functions, inflammation, and immunity (53).

The pathophysiology of obesity-induced insulin resistance has been attributed to ectopic fat deposition (39), increased inflammation, endoplasmic reticulum (ER) stress (16, 42), adipose tissue hypoxia (15) and mitochondrial dysfunction (32), and impaired adipocyte expansion and angiogenesis (50, 51, 54). In obesity, fatty acids (FA) together with other stimuli such as ceramide, various PKC isoforms, proinflammatory cytokines and reactive oxygen species (ROS), and ER stresses activate JNK, NF- κ B, RAGE, and TLR pathways both in adipocytes and macrophages triggering inflammation and insulin resistance (43).

Strenuous efforts are being made by the research community to elucidate the mechanisms involved in the pathophysiology of obesity-related disorders. However, an alternative strategy could be to act upstream by preventing the accumulation of lipids and the progression of obesity. In addition to reducing caloric intake, a potential effective approach to combating obesity would be to increase energy expenditure in key metabolic organs such as adipose tissue. Obese individuals and

Address for reprint requests and other correspondence: L. Herrero, Dept. of Biochemistry and Molecular Biology, IBUB, School of Pharmacy, Univ. of Barcelona, Av. Diagonal, 643, E-08028 Barcelona, Spain (e-mail: lherrero@ub.edu).

those with T2D are known to have lower fatty acid oxidation (FAO) rates and lower electron transport chain activity in muscle (17, 19, 37), together with higher glycolytic capacities and enhanced cellular FA uptake compared with nonobese and nondiabetic individuals (44). Thus, any strategy able to eliminate the excess of lipids found in obesity could be beneficial for health. Lipid levels can be reduced by inhibiting synthesis and transport or by increasing oxidation; here, we focus on the latter.

Malonyl-CoA, derived from glucose metabolism and the first intermediate in lipogenesis, regulates FAO by inhibiting carnitine palmitoyltransferase 1 (CPT1). This makes CPT1 the rate-limiting step in mitochondrial FA β -oxidation. Thus, in high-energy conditions, malonyl-CoA inhibits oxidation, diverting FAs' fate into TG accumulation. There are three CPT1 isoforms, with different tissue expressions: CPT1A (liver, kidney, intestine, pancreas, ovary, and mouse and human WAT), CPT1B (brown adipose tissue, skeletal muscle, heart, and rat and human WAT), and CPT1C (brain and testis) (2, 36). The fact that CPT1 controls FAO makes it a very attractive target to reduce lipid levels and fight against obesity and T2D. Despite their excess fat, obese individuals have reduced visceral WAT CPT1 mRNA and protein levels (20). This prompted our group and others to overexpress CPT1 in liver (26, 29, 45), muscle (3, 33, 40), and white adipocytes (9), which led to a decrease in triglyceride (TG) content and an improvement in insulin sensitivity.

Here, we show that CPT1A expression was higher in human adipose tissue macrophages than in mature adipocytes and that it was differentially expressed in visceral vs. subcutaneous adipose tissue. To further investigate the role of CPT1A in both adipocytes and macrophages, we used a permanently active mutant form of CPT1A, CPT1AM, which is insensitive to its inhibitor malonyl-CoA (27), to achieve continuous oxidation of lipids. When cells were incubated with palmitate to mimic obesity, CPT1AM restored most of the palmitate-induced imbalances. An increase in FAO in adipocytes and macrophages reduced TG content and inflammatory levels, improved insulin sensitivity in adipocytes, and reduced ER stress and ROS damage in macrophages.

MATERIALS AND METHODS

Human cohorts: selection of patients. Adipose tissue was selected from an adipose tissue biobank collection of the University Hospital Joan XXII (Tarragona, Spain). All subjects were of Caucasian origin and reported that their body weight had been stable for at least 3 mo before the study. They had no systemic disease other than obesity or T2D, and all had been free of any infections in the previous month before the study. Liver and renal diseases were specifically excluded by biochemical work-up. Appropriate Institutional Review Board approval and adequate biobank informed consent were obtained from all participants. Biobanking samples included plasma and total and fractionated adipose tissue from subcutaneous and visceral origin. All patients had fasted overnight before collection of blood and adipose tissue samples. Visceral adipose tissue (VAT) and subcutaneous adipose tissue (SAT) samples were obtained during surgical procedures that included laparoscopic surgery for hiatus hernia repair or cholecystectomy. Samples were selected according stratification by age, sex, and BMI and grouped into two cohorts:

Obesity cohort. Subjects were classified by BMI according to the World Health Organization criteria (WHO, 2000). The study included 19 lean, 28 overweight, and 15 obese nondiabetic subjects matched for age and sex (Table 1).

T2D cohort. Patients were classified as having T2D according to American Diabetes Association criteria (1997). Variability in metabolic control was assessed by stable glycated hemoglobin A_{1c} (HbA_{1c}) values during the previous 6 mo. These criteria having been gathered, there were 11 T2D subjects. As a control group, we selected 36 subjects without diabetes from the obesity cohort, matched for age, BMI, and sex (Table 2). No patient was being treated with thiazolidinedione.

Anthropometric measurements. Height was measured to the nearest 0.5 cm and body weight to the nearest 0.1 kg. BMI was calculated as weight (kilograms) divided by height (meters) squared. Waist circumference was measured midway between the lowest rib margin and the iliac crest.

Collection and processing of human samples. Samples from VAT (omental) and SAT (anterior abdominal wall) from the same individual were obtained during abdominal elective surgical procedures (cholecystectomy or surgery for abdominal hernia). All patients had fasted overnight at least 12 h before the surgical procedure. Blood samples were collected before the surgical procedure from the antecubital vein, 20 ml of blood with EDTA (1 mg/ml), and 10 ml of blood in silicone tubes. Collected blood (15 ml) was used for the

Table 1. Clinical, analytic, and CPT1A gene expression analysis of the obesity cohort

	Lean BMI <25 (13 M; 6 F)	Overweight 25 ≤ BMI <30 (16 M; 12 F)	Obese BMI ≥30 (9 M; 6 F)
Age, yr	51.7 ± 16.0	57.1 ± 15.0	57.4 ± 12.8
BMI, kg/m ²	23.6 (22.1–24.2)	27.2 (26.5–27.9)*	32.1 (30.8–33.6)*#
Waist, cm	83.0 (79.0–90.0)	97.0 (90.5–100.0)*	107.0 (100.0–117.2)*#
Cholesterol, mM	5.2 ± 1.2	4.9 ± 1.0	5.2 ± 0.8
HDL-cholesterol, mM	1.5 ± 0.5	1.3 ± 0.3	1.4 ± 0.3
Triglycerides, mM	1.0 (0.7–1.6)	1.1 (0.8–1.5)	1.0 (0.7–1.3)
Glucose, mM	4.8 ± 0.7	5.5 ± 0.5*	5.6 ± 0.5*
Insulin, μ IU/ml	3.4 (2.1–6.7)	4.0 (2.8–7.2)	6.6 (4.5–16.5)¶
HOMA-IR	0.75 (0.54–1.83)	1.01 (0.52–2.09)	1.60 (1.19–4.79)¶
sIL-6, pg/ml	1.4 (1.1–2.5)	1.0 (0.7–2.2)	2.5 (1.4–5.2)§
SBP, mmHg	120 (120–127)	130 (121–140)	145 (130–160)*§
DBP, mmHg	70 (60–80)	70 (70–80)	80 (78–90)¶
SAT CPT1A	0.85 (0.66–1.14)†	1.15 (0.85–1.60)†	0.86 (0.72–1.81)
VAT CPT1A	1.31 (1.07–2.50)	1.42 (0.97–3.00)	1.07 (0.84–1.76)

Values are expressed as means ± SD or median (interquartile range) for non-Gaussian distributed variables. CPT1A, carnitine palmitoyltransferase 1A; BMI, body mass index; HOMA-IR, homeostasis model assessment of insulin resistance; sIL-6, soluble interleukin-6; SBP, systolic blood pressure; DBP, diastolic blood pressure; SAT, subcutaneous adipose tissue; VAT, visceral adipose tissue. Differences vs. Lean: * $P < 0.001$; ¶ $P < 0.05$. Differences vs. Overweight: # $P < 0.001$; § $P < 0.05$. † $P < 0.05$ SAT vs. VAT expression.

Table 2. Clinical, analytic, and CPT1A gene expression analysis of the T2D cohort

	Control (21 M, 15 F)	Type 2 Diabetes (5 M, 6 F)
Age, yr	61.6 ± 10.6	66.1 ± 8.6
BMI, kg/m ²	28.6 (27.0–31.5)	28.7 (26.9–30.4)
Waist, cm	100.0 (94.0–107.0)	97.0 (94.0–102.0)
Cholesterol, mM	5.1 ± 0.9	4.7 ± 1.2
HDL-chole., mM	1.4 (1.2–1.6)	1.2 (1.0–1.9)
Triglycerides, mM	1.0 (0.7–1.5)	1.7 (1.2–2.3)¶
NEFA, μM	775.5 ± 275.1	926.4 ± 412.3
Glycerol, μM	135.2 (117.2–222.3)	301.6 (209.6–465.3)¶¶
Glucose, mM	5.6 (5.3–5.8)	8.3 (7.0–10.1)*
Insulin, μIU/ml	4.5 (3.5–7.7)	10.2 (3.5–21.4)
HOMA-IR	1.22 (0.89–2.10)	3.66 (1.71–23.66)¶¶
sIL-6, pg/ml	1.4 (1.0–2.6)	1.5 (1.0–2.4)
SBP, mmHg	140 (130–150)	140 (124–156)
DBP, mmHg	80 (70–80)	80 (63–83)
SAT CPT1A	1.08 (0.79–1.59)†	1.70 (1.03–2.18)
VAT CPT1A	1.39 (0.87–2.28)	1.57 (0.98–1.96)

Values are expressed as means ± SD or median (interquartile range) for non-Gaussian distributed variables. Differences vs. controls: * $P < 0.001$; ¶ $P < 0.05$. Differences between SAT and VAT in the same group: † $P = 0.03$.

separation of plasma. Plasma samples were stored at -80°C until analytic measurements were performed; 5 ml of blood with EDTA was used for the determination of HbA_{1c}. Adipose tissue samples were collected, washed in PBS, immediately frozen in liquid N₂ and stored at -80°C .

Adipose tissue fractionation. Adipose tissue biopsies were processed immediately. The adipose tissue was finely diced into small pieces (10–30 mg), washed in PBS, and incubated in Medium 199 (Life Technologies) supplemented with 4% BSA plus 2 mg/ml collagenase type I (Sigma) for 1 h in a shaking water bath at 37°C . After digestion, mature adipocytes (ADI) were separated from tissue matrix by filtration through a 200-μm mesh fabric (Spectrum Laboratories). The filtrated solution was centrifuged for 5 min at 1,500 g. The mature adipocytes were removed from the top layer and the stromal vascular fraction (SVF) cells remained in the pellet. Cells were washed four times in PBS and processed for RNA and protein extraction.

Analytic methods. Glucose, cholesterol, and TG plasma levels were determined in an autoanalyzer (Hitachi 737, Boehringer Mannheim) using the standard enzyme methods. High-density lipoprotein (HDL) cholesterol was quantified after precipitation with polyethylene glycol at room temperature (PEG-6000). Plasma insulin was determined by radioimmunoassay (Coat-A-Count insulin; Diagnostic Products). Nonesterified free fatty acid (NEFA) serum levels were determined in an autoanalyzer (Advia 1200, Siemens) using an enzymatic method developed by Wako Chemicals. Plasma glycerol levels were analyzed by using a free glycerol determination kit, a quantitative enzymatic determination assay (Sigma-Aldrich). Intra- and interassay CVs were less than 6% and less than 9.1%, respectively. The degree of insulin resistance was determined by homeostasis model assessment (HOMA), as $[\text{glucose (mmol/l)} \times \text{insulin (mIU/l)}] / 22.5$. (24).

Immunohistochemistry. Five-micrometer sections of formalin-fixed paraffin-embedded adipose tissue were deparaffinized and rehydrated prior to antigen unmasking by boiling in 1 mM EDTA, pH 8. Sections were blocked in normal serum and incubated overnight with rabbit anti-CPT1A (Sigma-Aldrich) at 1:50 dilution. Secondary antibody staining was performed using a VECTASTAIN ABC kit (Vector Laboratories) and detected with diaminobenzidine (Vector Laboratories). Sections were counterstained with hematoxylin prior to dehydration and coverslip placement and examined under a Nikon Eclipse 90i microscope. As a negative control, the procedure was performed in the absence of primary antibody.

Immunofluorescence. Five-micrometer sections of formalin-fixed paraffin-embedded adipose tissue were blocked in normal serum and

incubated overnight with rabbit anti-CPT1A antibody (Sigma-Aldrich) at 1:50 dilution and with mouse anti-CD68 (Santa Cruz Biotechnology) at 1:50 dilution, and visualized using Alexa fluor 546 goat anti-rabbit, and Alexa fluor 488 goat anti-mouse antibodies, respectively (1:500, Molecular Probes). The slides were counterstained with DAPI (4,6-diamidino-2-phenylindole) to reveal nuclei and were examined under a Nikon Eclipse 90i fluorescent microscope. As a negative control, the assay was performed in the absence of primary antibody.

Materials. Sodium palmitate, sodium oleate, BSA, and L-carnitine hydrochloride were purchased from Sigma Aldrich. DMEM, FBS, and penicillin-streptomycin mixture were purchased from Life Technologies.

Cell culture. Murine 3T3-L1 CARΔ1 preadipocytes, kindly given by Dr. Orlicky (Department of Pathology, UCHSC at Fitzsimons, Aurora, CO), were cultured and differentiated into mature adipocytes following the published protocol (31). Mature adipocytes were used for experiments at day 8 postdifferentiation. Murine RAW 264.7 macrophages were obtained from ATCC and were maintained in DMEM supplemented with 10% heat-inactivated FBS and 1% penicillin-streptomycin mixture. Simpson-Golabi-Behmel Syndrome (SGBS) human cells were cultured and differentiated to adipocytes as previously described (55).

Adenovirus infection. At day 8 of differentiation, 3T3-L1 CARΔ1 cells were infected with adenoviruses AdGFP [100 moi (multiplicity of infection)] and AdCPT1AM (13) (100 moi) for 24 h in serum-free DMEM, and then the medium was replaced with complete DMEM for additional 24 h. RAW 264.7 macrophages were infected with AdGFP (100 moi) and AdCPT1AM (100 moi) for 2 h in serum-free DMEM and then replaced with complete medium for an additional 72 h. Adenovirus infection efficiency was assessed in AdGFP-infected cells (see Fig. 3, A and B). The same batch of adenoviruses stored in 50-μl aliquots was used throughout the experiments.

FA treatment. Sodium palmitate was conjugated with FA-free BSA in a 5:1 ratio to yield a stock solution of 2.5 mM (40). Cells were incubated with 0.3 or 1 mM of this solution for 24 h (3T3-L1 CARΔ1 adipocytes) or 0.3, 0.5, or 0.75 mM for 24, 18, or 8 h (RAW 264.7 macrophages), respectively.

Adipocyte and macrophage viability. 3T3-L1 CARΔ1 adipocytes and RAW 264.7 macrophages were infected as previously described and incubated for 24 h with 1 or 0.3 mM palmitate, respectively. Cells were washed twice with PBS and lifted from the surface with trypsin followed by 2 min of incubation at 37°C . Trypsinization was stopped with 10% FBS-containing medium, and equal volumes of cell suspension were mixed with 0.4% Trypan blue staining. Trypan blue-positive and -negative cells were counted using a Neubauer chamber for adipocytes and a Countess Automated Cell Counter (Invitrogen) for macrophages. Percentage of viability was determined normalizing viable cells of each group to viable cells of BSA GFP group. Statistical significance was assessed using two-way ANOVA of three individual experiments (* $P < 0.05$).

CPT1 activity. Mitochondria-enriched fractions were obtained from cell culture grown in 10-cm² dishes, and CPT1 activity was measured by a radiometric method as described (13).

FA oxidation. Total oleate oxidation was measured in 3T3-L1 CARΔ1 adipocytes and RAW 264.7 macrophages grown in 25-ml flasks, differentiated, and infected as described above. The day of the assay, cells were washed in KRBH-0.1% BSA, preincubated at 37°C for 30 min in KRBH-1% BSA, and washed again in KRBH-0.1% BSA. Cells were then incubated for 3 h (3T3-L1 CARΔ1 adipocytes) or 2 h (RAW 264.7 macrophages) at 37°C with fresh KRBH containing 11 mM glucose, 0.8 mM carnitine, and 0.2 mM [¹⁻¹⁴C]oleate (PerkinElmer). Oxidation was measured as described (29). The scintillation values were normalized to the protein content of each flask.

TG content. Cells were grown in 12-well plates, differentiated, and infected as described above. After 24 h (3T3-L1 CARΔ1 adipocytes) or 18 h (RAW 264.7 macrophages) of FA treatment, cells were

collected for lipid extraction following a protocol of Gesta et al. (10) with minor modifications: after cell lysis with 0.1% SDS, 1/2/0.12 (vol/vol/vol) methanol-chloroform-0.5 M KCl solution was added, the two phases were separated by centrifugation, and the upper phase was dried with N₂. Finally, lipids were resuspended in 100% isopropanol, and TGs were quantified using a TG Triglyceride kit (Sigma) according to the manufacturer's instructions. Protein concentrations were used to normalize sample values.

Oil red O staining. RAW 264.7 macrophages grown on coverslips were infected as described above and incubated with 0.75 mM palmitate for 18 h. After this time, cells were rinsed twice with PBS, fixed in 10% paraformaldehyde for 30 min at room temperature, and washed again with PBS. Then, cells were rinsed with 60% isopropanol for 5 min to facilitate the staining of neutral lipids and were stained with filtered Oil red O working solution (0.3% Oil red O in isopropanol) for 15 min. After several washes with distilled water, the coverslips were removed and mounted on a drop of mount medium. The intracellular lipid vesicles stained with Oil red O were identified by their bright red color under the microscope.

Analysis of intracellular protein oxidation. RAW 264.7 macrophages were cultured in 12-well plates and infected as described before. After FA treatment, cell extracts were prepared and analyzed for protein oxidative modifications (i.e., carbonyl group content) with a OxyBlot Protein Oxidation Detection kit (Millipore), following the manufacturer's instructions.

Western blot analysis. 3T3-L1 CARΔ1 adipocytes and RAW 264.7 macrophages were cultured in 12-well plates, differentiated, and infected as described above. Cells were collected in lysis buffer (RIPA), and protein concentration was determined using a BCA protein assay kit (ThermoScientific). An equal amount of protein from whole cell lysates was resolved by 8% SDS-PAGE and transferred to PVDF membranes (Millipore). Signal detection was carried out with the ECL immunoblotting detection system (GE Healthcare), and the results were quantitatively analyzed using Image Quant LAS4000 Mini (GE Healthcare). The following antibodies were used: CPT1A [1/6,000 (13)], β-actin (1-19; 1/4,000, Santa Cruz), Akt and pAkt (Ser⁴⁷³; 1/1,000, Cell Signaling), C/EBP homologous protein (CHOP; GADD 153, 1/200; Santa Cruz) and insulin receptor-β (IRβ; 1/1,000; Santa Cruz). Human fat tissue was homogenized in RIPA buffer as previously described (34). Protein extracts (10–20 μg) were loaded, resolved on 10% SDS-PAGE, and transferred to Hybond ECL nitrocellulose membranes. Membranes were stained with 0.15% Ponceau red (Sigma-Aldrich) to ensure equal loading after transfer and then blocked with 5% (wt/vol) BSA in TBS buffer with 0.1% Tween 20. Immunoblotting was performed with 1:2,000 goat anti-human CPT1A (Abcam). Blots were incubated with the appropriate IgG-HRP-conjugated secondary antibody. Immunoreactive bands were visualized with an ECL-plus reagent kit (GE Healthcare). Optical densities of the immunoreactive bands were measured using Image J analysis software.

Analysis of mRNA expression by quantitative real-time PCR. Total RNA was extracted from cultured cells grown in 12-well plates using

Illustra Mini RNA Spin kit (GE Healthcare), and cDNA was obtained using a Transcriptor First Strand cDNA Synthesis kit (Roche). Quantitative real-time PCR was performed using a SYBR Green PCR Master Mix Reagent Kit (Life Technologies). Levels of mRNA were normalized to those of β-actin and expressed as fold change. Forward/reverse primers for several genes were used (Table 3; other sequences are available upon request):

Frozen human adipose tissue (400–500 mg) was homogenized with an Ultra-Turrax 8 (Ika). Total RNA from adipose biopsies, SVF, and isolated adipocytes were extracted by using an RNeasy Lipid Tissue Midi Kit (QIAGEN) following the manufacturer's instructions, and total RNA was treated with 55 U of RNase-free DNase (QIAGEN) to avoid contamination with genomic DNA. Between 0.2 and 1 μg of total RNA was reverse-transcribed to cDNA using TaqMan reverse transcription reagents (Applied Biosystems) and subsequently diluted with nuclease-free water (Sigma) to 20 ng/μl cDNA. For adipose tissue gene expression analysis, real-time quantitative PCR was performed, with duplicates, on a 7900HT Fast Real-Time PCR System using commercial Taqman Assays (Applied Biosystems). SDS software 2.3 and RQ Manager 1.2 (Applied Biosystems) were used to analyze the results with the comparative threshold cycle (C_T) method (2^{ΔΔC_T}). C_T values for each sample were normalized with an optimal reference gene (cyclophilin) after testing of three additional house-keeping genes: β-actin and RNA 18S. A panel of genes involved in the adipocyte differentiation and metabolism was selected in the study of CPT1A gene expression (Table 4).

Cytokine measurement in culture media. Cytokine protein levels in culture medium of 3T3-L1 CARΔ1 adipocytes and RAW 264.7 macrophages were measured by Luminex technology with a MILLIPLEX Analyzer Luminex 200x Ponenet System (MCYTOMAG-70K-08 Mouse Cytokine MAGNETIC Kit; Merck Millipore).

Analysis of cellular redox status. To detect ROS (superoxide) formation, MitoSOX Red (M36008, Life Technologies) fluorescence was measured by flow cytometry. RAW 264 cells were infected with 100 moi AdCPT1AM (or AdGFP as control) for 48 h; then, 16 h prior to ROS measurement, macrophages were treated with 0.75 mM palmitate BSA-conjugated (or with BSA as control). Medium was removed, and cells were incubated for 30 min with PBS containing 5 μM MitoSOX Red. The labeled macrophages were washed three times with HBSS-Ca-Mg, pelleted, resuspended in 300 μl of HBSS-Ca-Mg, and fixed by adding 1.2 ml of absolute ethanol and keeping them at –20°C for 5 min. Cells were pelleted again and resuspended in HBSS-Ca-Mg containing 3 μM DAPI to mark their nuclei. Then macrophages were analyzed by flow cytometry (Gallios Cytometer, Beckman-Coulter). The fluorescence intensity of MitoSOX Red was measured using excitation at 510 nm and emission at 580 nm.

Statistical analysis. Data are expressed as means ± SE and analyzed statistically using Student's *t*-test (column analysis) or two-way ANOVA (grouped analysis). All figures and statistical analyses were generated using GraphPad Prism 6. *P* < 0.05 was considered statistically significant. For human data, statistical analyses were performed with SPSS 12.0. Results are expressed as means ± SD. The nonnor-

Table 3. Forward and reverse primers

	Forward	Reverse
β-Actin	5'-AGGTGACAGCATTGCTTCTG-3'	5'-GCTGCCTCAACACCTCAAC-3'
CHOP	5'-CCCTGCCTTTACCTTGG-3'	5'-CCGGCTCGTTCTCCTGCTC-3'
CPT1A*	5'-GCAGCAGATGCAGCAGATCC-3'	5'-TCAGGATCCTCCTCTGTATCCG-3'
EDEM	5'-AAGCCCTCTGGAACCTGCG-3'	5'-AACCCAAATGGCCTGTCTGG-3'
GRP78	5'-ACTTGGGGACACCTATTCT-3'	5'-ATCGCCAATCAGACGCTCC-3'
IL-1β	5'-GCCCATCCTCTGTGACTCAT-3'	5'-AGGCCACAGGTATTTTGTCC-3'
MCP-1	5'-TCCCAATGAGTAGGCTGGAG-3'	5'-AAGTGCTTGAGGTGGTTGTG-3'
PDI	5'-ACCTGCTGGTGGAGTTCTATG-3'	5'-CGGCAGCTTGGCATACT-3'
TLR-4	5'-GGACTCTGATCATGGCACTG-3'	5'-CTGATCCATGCATTGGTAGGT-3'
TNF-α	5'-ACGGCATGGATCTCAAAGAC-3'	5'-AGATAGCAAATCGCTGAACG-3'

*Recognizes both carnitine palmitoyltransferase 1A (CPT1A) and the active mutant CPT1AM. See text for other definitions.

Table 4. Gene symbols, denominations, and assay ID numbers

Gene Symbol	Gene Denomination	Assay ID
ACC1	(acetyl-coenzyme carboxylase 1) ACACA	Hs00167385_m1
PCK2	(phosphoenolpyruvate carboxylase 2)	Hs00388934_m1
PPAR α	(peroxisome proliferator-activated receptor- α)	Hs00231882_m1
PPAR γ	(peroxisome proliferator-activated receptor- γ)	Hs00234592_m1
AGPAT3	(1-acyl- <i>sn</i> -glycerol-3-phosphate acyltransferase- γ /LPAAT-g1)	Hs00987571_m1
AGPAT4	(1-acyl- <i>sn</i> -glycerol-3-phosphate acyltransferase/LPAAT-d)	Hs00220031_m1
AGPAT5	(1-acyl- <i>sn</i> -glycerol-3-phosphate acyltransferase/LPAAT-e)	Hs00218010_m1
AGPAT9	(1-acylglycerol-3-phosphate <i>O</i> -acyltransferase 9/LPAAT- θ)	Hs00262010_m1
CDS1	(phosphatidate cytidylyltransferase)	Hs00181633_m1
PCYT1A	(choline-phosphate cytidylyltransferase)	Hs00192339_m1
PCYT2	(ethanolamine-phosphate cytidylyltransferase)	Hs00161098_m1
PDE3B	(phosphodiesterase type 3)	Hs01057215_m1
FDFT1	(farnesyl-diphosphate farnesyltransferase 1)	Hs00926054_m1
SREBF1	(sterol regulatory element binding transcription factor 1)	Hs01088691_m1
BCL2	(B cell CLL/lymphoma 2)	Hs99999018_m1
CD163	Macrophage and monocyte marker	Hs01016661_m1
CPT1A	(carnitine palmitoyltransferase 1A)	Hs00912676_m1

mally distributed variables are represented as the median (interquartile range). Categorical variables are reported by number (percentages). Student's *t*-test analysis was used to compare the mean value of normally distributed continuous variables. Variables with a non-Gaussian distribution were analyzed using a nonparametric test (Kruskal-Wallis or Mann-Whitney test for independent samples or Wilcoxon test for related samples when necessary). Associations between continuous variables were sought by correlation analyses. Finally a stepwise multiple linear regression analysis was performed to determine independent variables associated with CPT1A gene expression levels in SAT and VAT depots. Results are expressed as unstandardized coefficient (B), and 95% confidence interval for B [95% CI(B)]. Differences are considered significant if a computed two-tailed probability value (*P*) is < 0.05.

RESULTS

CPT1A expression pattern in human adipose tissue from obese and diabetic patients. Visceral and subcutaneous adipose tissue (VAT and SAT, respectively) were analyzed from both an obesity cohort (lean, overweight and obese patients) and a T2D cohort (control and T2D patients). Tables 1 and 2 show the phenotypic and metabolic characteristics and CPT1A expression levels of the subjects. No differences in CPT1A gene expression levels either in SAT or in VAT depots were observed when comparing with the nonobese or the nondiabetic counterparts (Fig. 1, A and B; Tables 1 and 2). However, in the obesity cohort, CPT1A mRNA expression was significantly higher in lean and overweight VAT than in SAT (Fig. 1A); this difference was lost in the obese patients. These results were corroborated by Western blot with human adipose tissue of several lean and obese individuals (Fig. 1, C and D, *P* = 0.015). Similar results were obtained in the T2D cohort, where control subjects showed significantly higher CPT1A mRNA levels in VAT vs. SAT (Fig. 1B); however, this difference disappeared in T2D patients. Despite T2D patients showing a trend to express higher CPT1A levels in SAT and VAT compared with controls (the opposite of that in the obese subjects), this difference was nonsignificant. Since the CPT1B isoform is also expressed in human adipose tissue, we analyzed CPT1B mRNA (Fig. 1, E and F) and protein (data not shown) levels in human VAT and SAT of the

obesity and the T2D cohort. No differences were seen among the groups.

To establish the main relationship between CPT1A gene expression and key adipocyte genes involved in differentiation and metabolic pathways, we explored a panel of genes (see MATERIALS AND METHODS) both in SAT and in VAT depots of the obesity cohort. Results are shown from those genes that changed the most (up or down; Tables 5 and 6). Simple association analysis showed an inverse correlation between CPT1A and peroxisome proliferator-activated receptor- γ (PPAR γ) in SAT ($r = -0.38$, $P = 0.002$; Table 5). Positive CPT1A correlation in both VAT and SAT was found with 1-acylglycerol-3-phosphate *O*-acyltransferase 5 (AGPAT5; phospholipid biosynthesis), sterol regulatory element binding transcription factor 1 (SREBF1; glucose and lipid metabolism), B cell CLL/lymphoma 2 (BCL2; antiapoptosis), and CD163 (macrophage marker) (Table 5).

To study the main determinants of CPT1A gene expression levels, a stepwise multiple regression analysis was performed, including the aforementioned bivariate associations and confounding factors such as BMI, age and sex. This model showed that SAT CPT1A was positively associated with AGPAT5, SREBF1, and CD163 and that VAT CPT1A was positively correlated with SREBF1 and CD163 and negatively with age and PPAR γ (Table 6). The inverse relationship between CPT1A and PPAR γ was corroborated with the human adipocyte cell line SGBS. CPT1A mRNA expression dropped to a new steady state in adipocytes that was 11% of its expression in fibroblasts (data not shown).

CPT1A is highly expressed in human adipose tissue macrophages. To determine the cellular distribution of CPT1A gene and protein in human adipose tissue biopsies, we performed qRT-PCR and immunostaining analysis on both adipose and SVF. CPT1A mRNA levels were 42.6- and 43.4-fold increased in the SVF compared with mature adipocytes in both human SAT ($P < 0.05$) and VAT ($P < 0.05$), respectively (Fig. 2A). Immunohistological examination of SAT from obese subjects revealed CPT1A+ cells mostly in the SVF (Fig. 2B). Immunofluorescence detection showed a bright staining pattern in cells resembling adipose tissue macrophages. Costaining analysis using CPT1A and

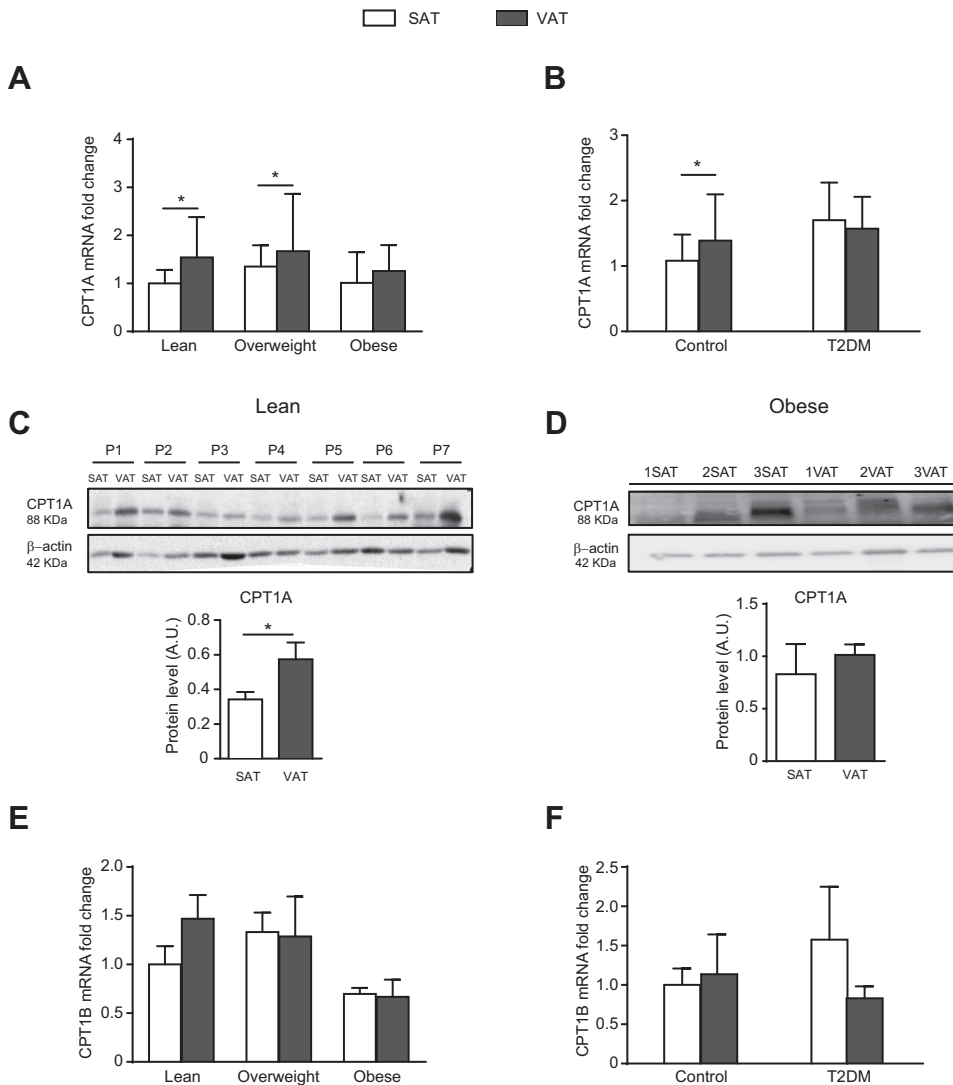


Fig. 1. Carnitine palmitoyltransferase 1A (CPT1A) gene and protein expression in human adipose tissue. *A* and *B*: CPT1A relative mRNA levels in human visceral (VAT) and subcutaneous adipose tissue (SAT) of the obesity (*A*) or the type 2 diabetes (T2D; *B*) cohort. Numbers of individuals: 19 lean, 28 overweight, 15 obese, 36 control, and 11 T2D (see Tables 1 and 2 for more details). *C* and *D*: CPT1A protein levels in human VAT and SAT of 7 lean individuals (P1-P7; *C*) and 3 obese individuals (*D*). *E* and *F*: CPT1B relative mRNA levels in human VAT and SAT of the obesity (*E*) or the T2D (*F*) cohort. **P* < 0.05.

CD68 (a macrophage marker) antibodies confirmed the expression of CPT1A in macrophages (Fig. 2C). Macrophages seemed to localize forming the so-called “crown-like structures” surrounding the adipocytes.

CPT1A-expressing adipocytes show enhanced FA oxidation and reduced TG content. To further study the role of CPT1A in adipocytes and macrophages, we decided to con-

tinue with in vitro studies. Since 3T3-L1 adipocytes are inefficiently infected with adenovirus, we decided to use the high-infection efficiency white adipocyte cell culture line, 3T3-L1 CARΔ1 adipocytes (31) (Fig. 3A). Cells were transduced for the first time with adenoviruses carrying the CPT1A gene or GFP as a control. Interestingly, CPT1A-

Table 5. Bivariate correlation analysis of CPT1A gene expression levels with several genes in human VAT and SAT of the obesity cohort

	CPT1A	
	SAT R	VAT R
PPAR γ	-0.382	
AGPAT5	0.639	0.714
SREBF1	0.525	0.757
BCL2	0.639	0.580
CD163	0.731	0.716

PPAR γ , peroxisome proliferator-activated receptor- γ ; AGPAT5, 1-acylglycerol-3-phosphate *O*-acyltransferase-5; SREBF1, sterol regulatory element-binding transcription factor 1; BCL2, B cell CLL/lymphoma 2; CD163, macrophage and monocyte marker. *P* < 0.005 for all correlations.

Table 6. Multiple regression analysis for CPT1A in VAT and SAT as dependent variable in the obesity cohort

Independent Variables	B (95% CI)	β st	<i>P</i>
SAT (<i>r</i> ² of the model: 0.71)			
CD163	0.34 (0.20–0.49)	0.446	<0.0001
AGPAT5	0.64 (0.33–0.95)	0.345	<0.0001
SREBF1	0.19 (0.06–0.33)	0.245	0.006
VAT (<i>r</i> ² of the model: 0.70)			
CD163	0.34 (0.21–0.48)	0.569	<0.0001
Age	-0.15 (-0.025–0.004)	-0.22	0.006
SREBF1	0.413 (0.13–0.69)	0.323	0.005
PPAR γ	-0.29 (-0.53–0.05)	-0.19	0.017

Independent variables included in the model: age, sex, BMI, PPAR α , PPAR γ , AGPAT5, SREBF1, BCL2, and macrophage and monocyte marker (CD163) gene expression levels. β st, standardized β -coefficient. CI, confidence interval.

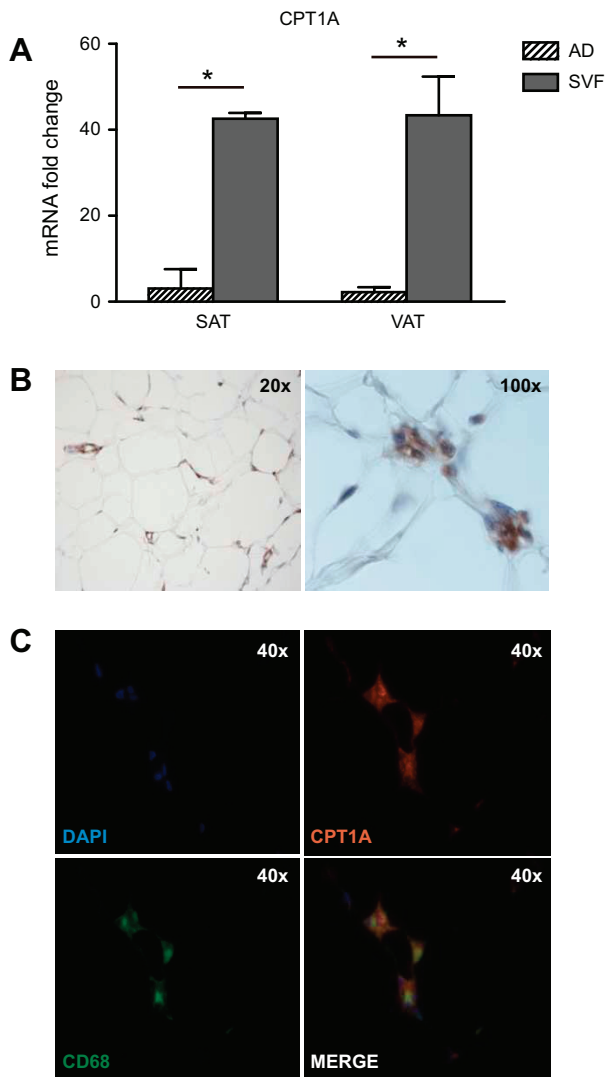


Fig. 2. CPT1A is highly expressed in human adipose tissue macrophages. *A*: CPT1A mRNA levels in both adipose (Ad) and stromal-vascular fraction (SVF) of human VAT and SAT; $n = 4$, $*P < 0.05$. *B*: immunohistochemical detection of CPT1A (brown) in SAT of obese subjects. *C*: immunofluorescence staining of CPT1A (red) and CD68 (green) proteins in SAT of obese individuals. Counterstaining of nuclei (DAPI) is shown in blue. Images are representative of adipose tissue preparations collected from 3 subjects.

expressing adipocytes were partially protected from palmitate-induced cell death (Fig. 3C).

CPT1A mRNA, protein, and activity levels were increased in CPT1AM-expressing adipocytes compared with GFP control cells (Fig. 4, A–C). CPT1AM-expressing adipocytes retained most of the CPT1 activity after incubation with the CPT1A inhibitor malonyl-CoA (Fig. 4C). The FA oxidation (FAO) rate was concordantly enhanced (1.37-fold increase, $P < 0.05$) in CPT1AM-expressing adipocytes (Fig. 4D). FA undergoing β -oxidation yield acetyl-CoA moieties that have two main possible fates: 1) complete oxidation to CO_2 and ATP production or 2) conversion to ketone bodies (mainly in the liver). Here, the total FAO rate was calculated as the sum of acid-soluble products plus CO_2 oxidation. CPT1AM expression blocked the palmitate-induced increase in TG content (Fig. 4E).

Enhanced adipocyte FAO improves insulin sensitivity and reduces inflammation. We examined the effect of increased FAO on insulin sensitivity and inflammatory responses in 3T3-L1 CAR Δ 1 adipocytes infected with AdCPT1AM. Palmitate-induced decrease in insulin-stimulated Akt phosphorylation and insulin receptor- β (IR β) protein levels was partially restored in CPT1AM-expressing adipocytes (Fig. 4, F–H). Palmitate-induced increase of proinflammatory markers [IL-1 β , monocyte chemoattractant protein-1 (MCP-1), and IL-1 α] mRNA and protein levels was blunted in CPT1AM-expressing adipocytes (Fig. 4, I–K). Several palmitate concentrations and times of incubation were used to better fit the different dose and time responses of the cytokines and parameters measured. Consistent with previous studies (9, 11), palmitate incubation raised cytokines expression two- to threefold.

Increased FAO in CPT1AM-expressing macrophages protects from palmitate-induced TG accumulation. Since CPT1A was highly expressed in the SVF, and particularly in macrophages, of human adipose tissue, we decided to further analyze the effect of increased FAO on cultured macrophages. RAW 264.7 macrophages were efficiently infected with AdCPT1AM (Fig. 3B). CPT1AM-expressing macrophages were protected from palmitate induced cell death (Fig. 3D). CPT1AM-expressing macrophages showed a 2.4-fold ($P < 0.01$) increase in CPT1A mRNA levels, a 6.6-fold ($P < 0.01$) increase in protein levels, and a 2.2-fold ($P < 0.05$) increase in activity levels (Fig. 5, A–C). In addition, we showed that malonyl-CoA did not inhibit CPT1 activity in CPT1AM-expressing macrophages (Fig. 5C). CPT1AM-expressing macrophages showed a 1.5-fold increase in FAO rate compared with GFP control cells (Fig. 5D, $P < 0.05$) and a total restoration in palmitate-induced enhancement of TG content (Fig. 5, E and F).

Enhanced macrophage FAO reduced inflammation, ER stress, and ROS damage. Palmitate-induced increase in proinflammatory cytokines [TNF- α , MCP-1, IL-1 β , Toll-like receptor 4 (TLR-4), and IL-12p40], and ER stress markers (CHOP, GRP78, protein disulfide isomerase (PDI), and ER degradation enhancing α -mannosidase-like protein (EDEM)] mRNA and protein levels were blunted in CPT1AM-expressing macrophages (Fig. 6, A, B, D, and E). Consistent with previous studies (18, 47, 48), palmitate incubation raised cytokines expression two- to threefold. No differences were seen in anti-inflammatory markers such as IL-10, Mgl-1, and IL-4 in CPT1AM-expressing cells incubated with or without palmitate (Fig. 6C). Incubation with etomoxir, a permanent inhibitor of CPT1A, counteracted the reduction of MCP-1 expression seen in CPT1AM-expressing cells incubated with palmitate (data not shown). We also studied the effect of enhanced FAO in RAW 264.7 macrophages on palmitate-induced ROS damage by protein carbonyl content analysis. Palmitate-induced ROS damage was reduced in CPT1AM-expressing macrophages (Fig. 6F). This reduction was not detected when ROS (superoxide) was directly measured using the MitoSOX Red probe (Fig. 6G).

DISCUSSION

The obesity epidemic has put a spotlight on adipose tissue as a key player in obesity-induced insulin resistance (38). Obese individuals and those with T2D have lower FAO rates (17, 19, 37). Although these data were reported in skeletal muscle, we expected to see reduced CPT1A expression levels in the

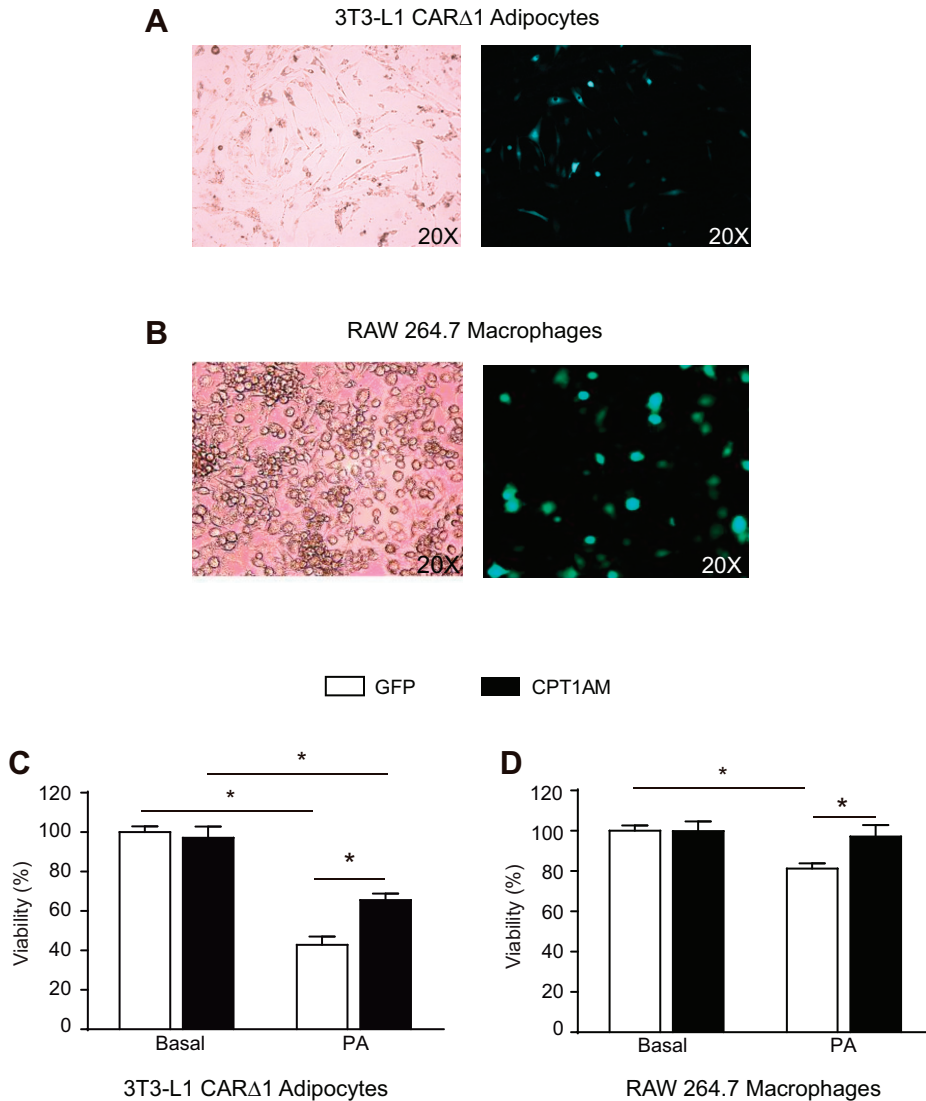


Fig. 3. Adenovirus infection efficiency and viability in 3T3-L1 CAR Δ 1 adipocytes and RAW 264.7 macrophages. Images were taken from AdGFP-infected 3T3-L1 CAR Δ 1 adipocytes (50% infection; A) or RAW 264.7 macrophages (70% infection; B) 48 or 72 h after infection, respectively. C and D: cCell viability of 3T3-L1 CAR Δ 1 adipocytes (C) or RAW 264.7 macrophages (D) infected with AdGFP or AdCPT1AM and incubated for 24 h with 1 or 0.3 mM palmitate (PA), respectively.

adipose tissue of both obese and T2D patients. However, no differences were seen in CPT1A mRNA expression between the obese or T2D patients and their respective controls either in VAT or in SAT. Other authors have reported a decrease in VAT CPT1 mRNA and protein levels in obese individuals (20). However, those authors did not specify which of the CPT1 isoforms was measured in VAT, CPT1A or CPT1B. We showed that CPT1A expression is higher in adipose tissue macrophages than in mature adipocytes. Since the obese adipose tissue has higher infiltration of immune cells such as macrophages, we postulate that the putative decrement of CPT1A expression in obese individuals could be compensated for by increased expression from the infiltrated macrophages and thus that no differences are seen between the groups. The CPT1B isoform is also expressed in human adipose tissue, and it has been shown to raise FAO in metabolic tissues such as skeletal muscle (3). Thus, we measured mRNA and protein levels in the obese and T2D cohorts. However, no differences were seen among the groups, indicating that CPT1B expression is not changed by obesity and T2D.

We found that, in insulin-sensitive individuals (control and overweight patients from the obese cohort and control patients

from the T2D cohort), CPT1A mRNA expression was higher in VAT than in SAT. However, no differences between VAT and SAT were seen in the more insulin-resistant individuals with a more proinflammatory environment: obese and T2D patients. A similar phenomenon was described for T regulatory cells, described to have anti-inflammatory properties and to improve obesity-induced insulin resistance (7). Those authors reported that the VAT and SAT of healthy individuals had similar low numbers of T regulatory cells at birth, with a progressive accumulation over time in the VAT, though not in the SAT. Our results suggest a CPT1A expression balance between SAT and VAT depots that may be disturbed in obese and T2D patients. The difference in CPT1A expression between these two fat depots is potentially crucial, given the association of VAT, but not SAT, with insulin resistance (1, 52). It might indicate, in healthy individuals, a potential protective role of CPT1A in the more insulin-resistant associated VAT.

Gene expression analysis revealed a negative association between CPT1A and the adipocyte marker of differentiation PPAR γ . This is consistent with the fact that while white adipocytes mature they shift their lipid preferences to storage rather than oxidation. Aging was associated with reduced

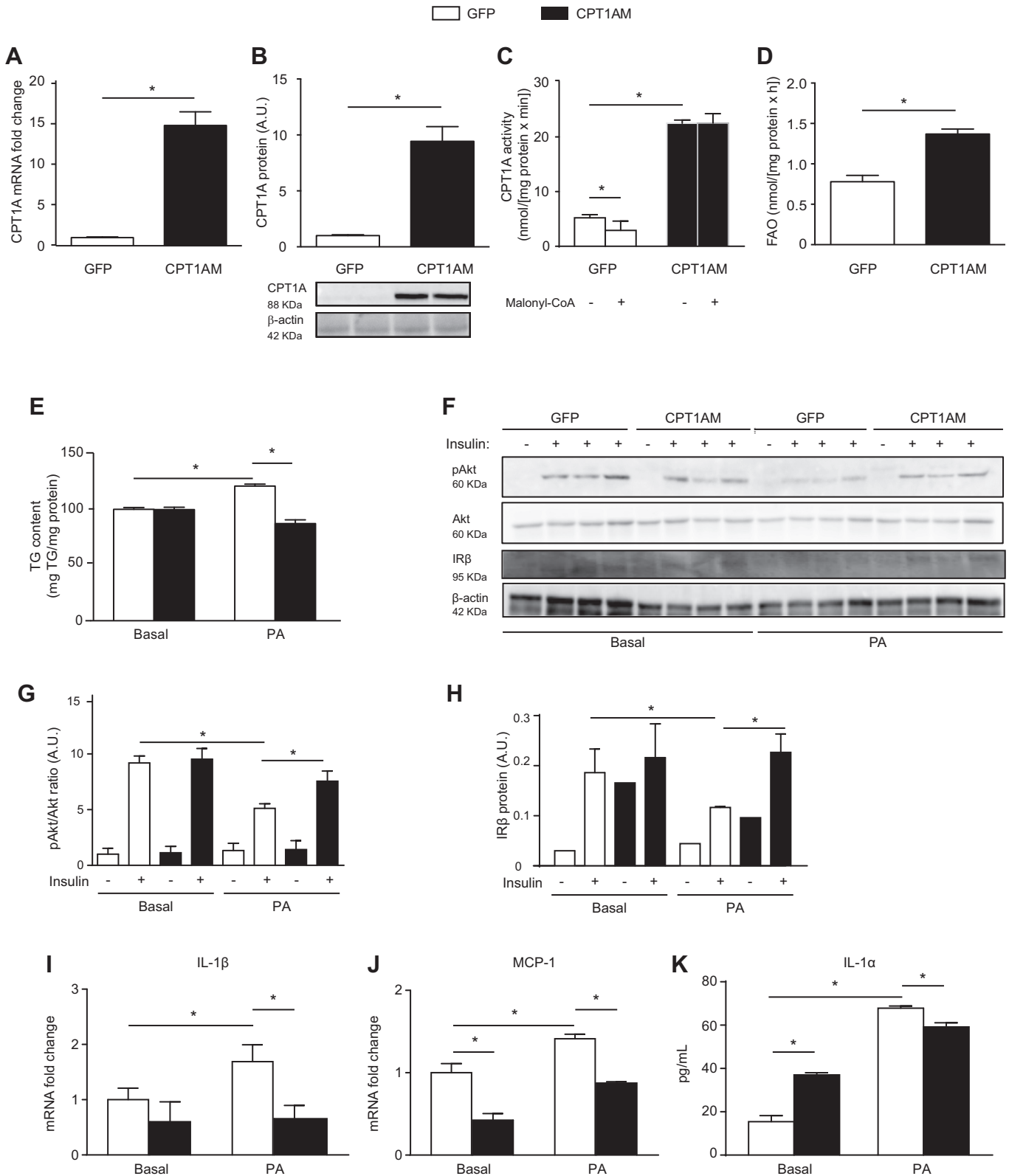


Fig. 4. Enhanced fatty acid oxidation (FAO) in 3T3-L1 CARΔ1 adipocytes improves lipid-induced triglyceride (TG) accumulation, insulin sensitivity, and inflammation. Relative CPT1A mRNA expression (A) and protein levels (B) in AdGFP- or AdCPT1AM-infected 3T3-L1 CARΔ1 adipocytes. C: CPT1A activity from mitochondria-enriched cell fractions incubated (or not) with 100 μM malonyl-CoA. D: total FAO rate represented as the sum of acid-soluble products plus CO₂ oxidation. E: TG content of adipocytes treated for 24 h with 1 mM PA. F: insulin signaling in GFP- and CPT1AM-expressing adipocytes incubated with 0.3 mM PA for 24 h, indicated by Western blotting of insulin-induced Akt phosphorylation (pAkt) and insulin receptor-β (IRβ). G: quantification of pAkt normalized by total Akt (fold change of arbitrary units, AU). H: quantification of IRβ normalized by β-actin. I and J: relative mRNA expression from GFP- or CPT1A-expressing adipocytes incubated with 1 mM PA for 24 h. K: protein levels of IL-1α in culture media of GFP- or CPT1A-expressing adipocytes incubated with 1 mM PA for 6 h. Shown are representative experiments out of 3; n = 3–6, *P < 0.05.

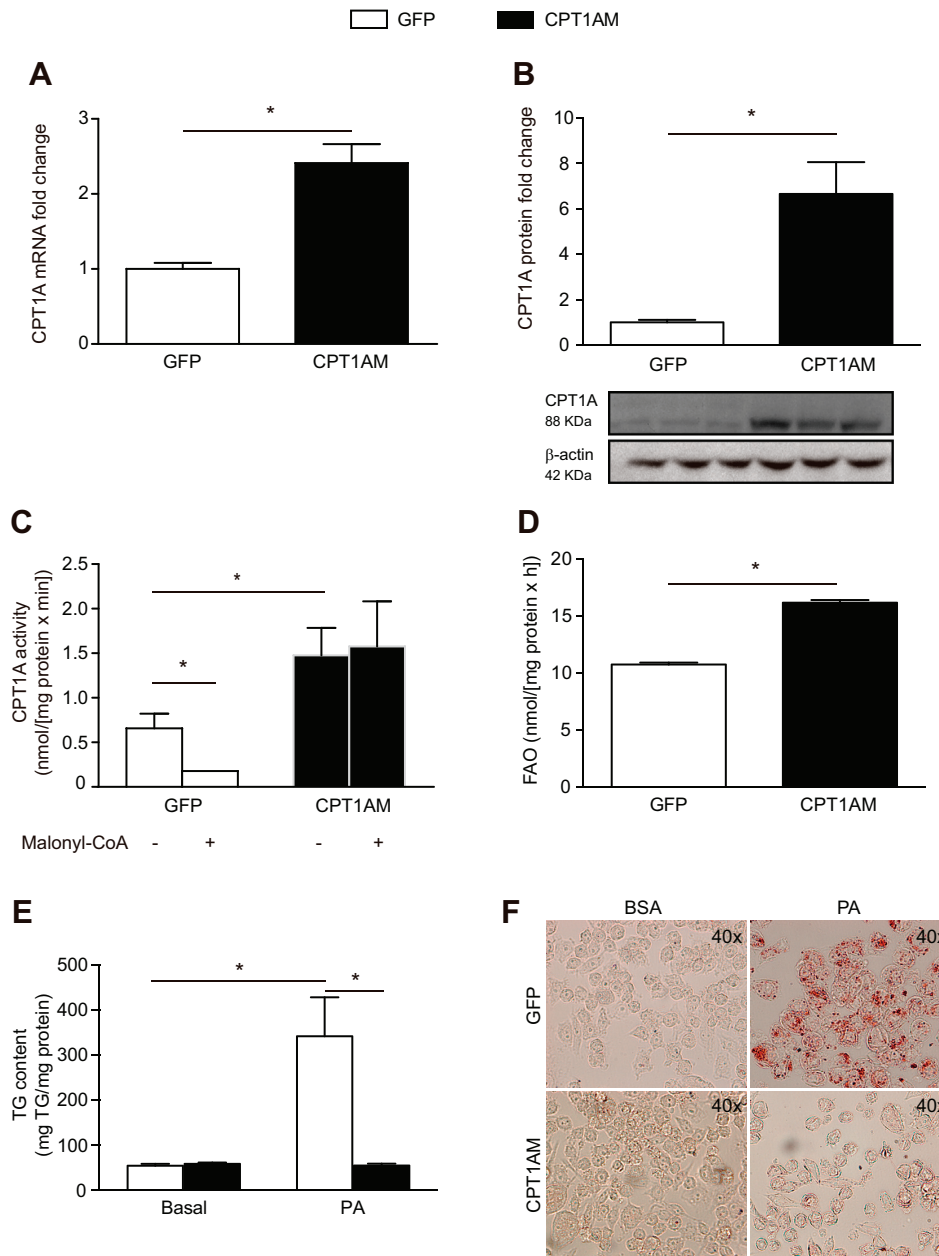


Fig. 5. Enhanced FAO and reduced TG content in CPT1AM-expressing RAW 264.7 macrophages. Relative CPT1A mRNA expression (A) and protein levels (B) in AdGFP- or AdCPT1AM-infected macrophages. C: CPT1 activity from mitochondria-enriched cell fractions incubated (or not) with 100 μ M malonyl-CoA. D: total FAO rate measured as the sum of acid-soluble products plus CO₂ oxidation. TG content (E) and Oil red O staining (F) of macrophages treated for 18 h with 0.75 mM PA. Shown are representative experiments out of 3; n = 3–6, *P < 0.05.

CPT1A expression in VAT. This might reflect a potential protective role of CPT1A expression in VAT that is lost with age. Considering that VAT accretion is a hallmark of aging and especially that it is a stronger risk factor for comorbidities and mortality (23), we speculate a favorable role of enhanced CPT1A expression in age metabolic decline and related pathological conditions. Positive correlation in both VAT and SAT CPT1A was found with AGPAT5, SREBF1, Bcl2, and CD163. These results may indicate a potential role of CPT1A in lipid biosynthesis processes (AGPAT5), glucose and lipid metabolism (SREBF1), and protecting adipose tissue from apoptosis (Bcl2). The positive association between CPT1A and CD163 (macrophage marker) was not surprising given the higher CPT1A expression in macrophages than in adipocytes (Fig. 2).

We are aware that many of the aforementioned associations may be secondary to obesity or T2D and that no causal

relationship may be inferred with this study design. To prove the causality of some of these observations, we performed in vitro studies directly targeting adipocytes and macrophages to burn off the excess lipids through an increase in FAO. We used the high-infection efficiency adipocyte cell line 3T3-L1 CARΔ1 (31) to express for the first time CPT1AM through adenoviral infection. Noteworthy, white adipocytes are designed to store lipids rather than to oxidize them. Thus, CPT1 activity in WAT is lower than in other tissues (6). However, CPT1AM-expressing adipocytes showed a 4.3-fold increase in CPT1 activity that was not inhibited despite incubation with high concentrations of malonyl-CoA. Since increased lipid accumulation, inflammation, ER stress, and ROS-induced protein damage trigger metabolic diseases, we decided to measure TG content, inflammation, ER stress, and ROS damage as important mechanisms that could explain the potential protec-

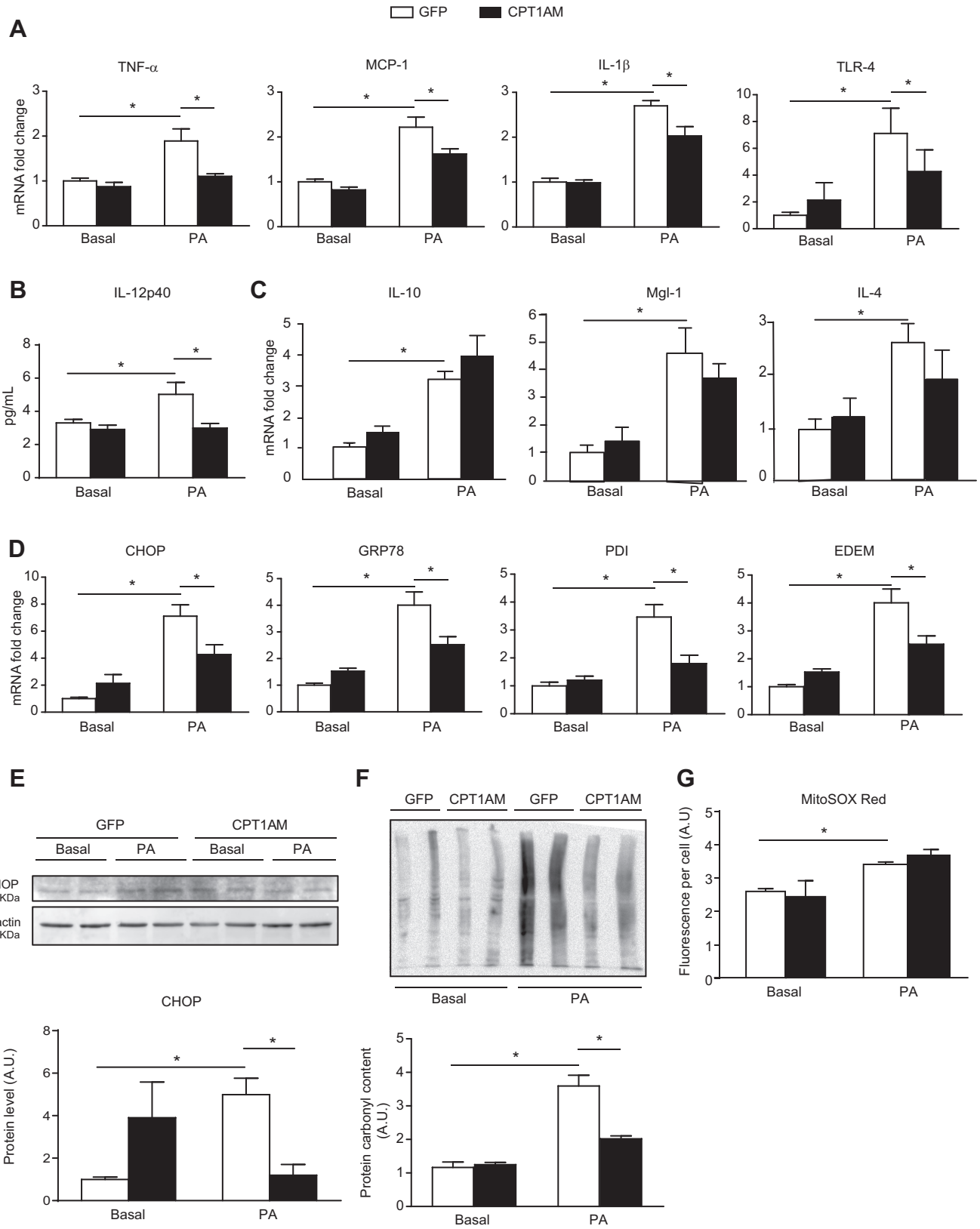


Fig. 6. CPT1AM expression reduced inflammation, ER stress, and ROS damage in RAW 264.7 macrophages. **A, C, D**: relative mRNA gene expression from macrophages incubated with 0.5 mM PA for 8 h (TNF- α and MCP-1) or 0.3 mM PA for 24 h (IL-10, Mgl-1, IL-4, IL-1 β , TLR-4, CHOP, GRP78, PDI, and EDEM). **B**: protein levels of IL-12p40 in culture media of macrophages incubated with 0.3 mM PA for 24 h. **E**: CHOP protein levels and quantification in macrophages incubated with 0.5 mM PA for 8 h. **F**: protein carbonyl content analysis and quantification in macrophages incubated with 0.75 mM PA for 18 h. **G**: measurement of ROS (superoxide) using the MitoSOX Red probe. Shown are representative experiments out of 3; $n = 3-4$, * $P < 0.05$.

tive effect of CPT1AM expression. Enhanced FAO led to complete restoration of TG content, improved insulin signaling (measured as pAkt), increased IR β expression and cell viability, and reduced inflammation in palmitate-incubated CPT1AM-expressing adipocytes. CPT1AM-expressing adipocytes showed a general improvement in lipid-induced derangements as a consequence of increased FA flux through mitochondria. However, enhanced FA flux in the absence of a concomitant dissipation of FAO metabolites has been associated with increased ROS damage (35) and inflammation (8, 21, 43). Interestingly, although no differences were seen in ER or oxidative stress (data not shown), CPT1AM-expressing adipocytes showed a significant decrease in proinflammatory mediators such as IL-1 β and MCP-1. The favorable role of CPT1A in adipocytes to attenuate FA-evoked insulin resistance and inflammation has been also described to act via suppression of JNK (9). These results suggest that factors other than a FAO increase per se are responsible for ROS production and inflammation. Accumulation of toxic substances (diacylglycerol or ceramides) (49), hypoxia (15), as well as cytokines (42) might participate in the induction of ROS damage and the inflammatory state. Several researchers have demonstrated that enhanced FAO through CPT1A or CPT1AM expression results in a decrease in relevant lipid mediators involved in inflammation and insulin resistance such as diacylglycerol, intracellular NEFAs, free FA, ceramides, and TG (3, 9, 13, 26, 29, 40, 45). Although some authors (3) did not see changes in skeletal muscle acylcarnitines' profile, our group has shown an increase in several acylcarnitines in CPT1AM-expressing neurons (25).

FA undergoing β -oxidation yield acetyl-CoA moieties that have two main possible fates: 1) entry to the TCA cycle for complete oxidation and ATP production or 2) conversion to ketone bodies (mainly in the liver). We observed increased FAO to CO₂ and acid-soluble products in CPT1AM-expressing adipocytes and macrophages. CPT1AM expression in liver has been shown to enhance ATP and ketone body production with no changes in glucose oxidation (13, 29). All together, this indicates a metabolic rate switch toward FA.

Monocytes were the first immune cells reported to infiltrate obese adipose tissue, differentiate to macrophages, produce inflammatory cytokines, and trigger insulin resistance (56, 57). Thus, we examined whether CPT1AM expression could play a protective role in obesity-induced macrophage derangements. We found that, in human WAT, CPT1A is highly expressed in SVF compared with adipocytes. This happened in both human VAT and SAT. A closer histological and immunofluorescence examination showed that macrophages present in the adipose tissue expressed CPT1A. This does not rule out CPT1A expression in other immune cells also present in the adipose tissue such as T and B cells, T regulatory cells, and mast cells.

Given the high CPT1A expression in human adipose tissue macrophages, we decided to study the effect of CPT1AM in RAW 264.7 macrophages. A permanently enhanced FAO rate in CPT1AM-expressing macrophages led to a complete restoration of palmitate-induced increase in TG content and a decrease in inflammation and ER and oxidative stress without affecting cell viability. Recent data show that FAO is capable of regulating the degree of acyl chain saturation in ER phospholipids (28). Since increasing the degree of saturation in ER phospholipids has been described to directly activate ER stress and inflammation (28), this might provide a mechanistic link to

how FAO alleviates ER stress under palmitate loading. Thus, enhancing CPT1A expression in macrophages may be a potential approach to fight against obesity-induced disorders.

In conclusion, we have shown that CPT1A expression was higher in human adipose tissue macrophages than in mature adipocytes and that it was differentially expressed in VAT vs. SAT. Further in vitro studies demonstrated that an increase in FAO in lipid-treated adipocytes and macrophages reduced TG content and inflammatory levels, improved insulin sensitivity in adipocytes, and reduced ER stress and ROS damage in macrophages. Adipocyte-specific knockout or transgenic animal models for CPT1A would be especially relevant to elucidate its potential protection against obesity-induced insulin resistance in vivo. Our data support the hypothesis that pharmacological or genetic strategies to enhance FAO may be beneficial for the treatment of chronic inflammatory pathologies such as obesity and T2D.

ACKNOWLEDGMENTS

We thank Prof. F. G. Hegardt and Dr. G. Asins for helpful comments and suggestions, A. Orozco for technical assistance, and R. Rycroft from the Language Service of the University of Barcelona for valuable assistance in the preparation of the English manuscript. We also thank D. Orlicky for kindly providing 3T3-L1 CARA1 adipocytes.

GRANTS

This study was supported by the Spanish Ministry of Science and Innovation (Grants SAF2010-20039 and SAF2013-45887-R to L. Herrero, SAF2011-30520-C02-01 to D. Serra, PI11/00085 to J. J. Vendrell, SAF2012-33014 to B. Peral, SAF2012-36186 to S. Fernández-Veledo, SAF2012-30708 to M. Vázquez-Carrera, SAF2011-23626 to F. Villarroya, and doctoral fellowships to M. I. Malandrino and J. F. Mir, by the CIBER Fisiopatología de la Obesidad y la Nutrición (Grant CB06/03/0001 to D. Serra), and CIBER Diabetes y Enfermedades Metabólicas Asociadas (Grant CB07/08/0003 to M. Vázquez-Carrera), Instituto de Salud Carlos III, by the European Union (BetaBat project FP7-277713 to F. Villarroya), by the European Foundation for the Study of Diabetes (EFSD)/Lilly and EFSD/Janssen-Rising Star research fellowships to L. Herrero, and by a L'Oréal-UNESCO "For Women in Science" research fellowship to L. Herrero. S. Fernández-Veledo acknowledges support from the "Miguel Servet" tenure track program (CP10/00438) from the Fondo de Investigación Sanitaria and cofinanced by the European Regional Development Fund. M. Weber is a recipient of the Ciência sem Fronteiras-CNPq fellowship (237976/2012-9).

DISCLOSURES

No conflicts of interest, financial or otherwise, are declared by the author(s).

AUTHOR CONTRIBUTIONS

Author contributions: M.I.M., R.F., M.W., M.C.-D., J.F.M., L.V., X.E., M.G.-S., B.P., L.S., S.F.-V., N.C., M.V.-C., F.V., J.J.V., D.S., and L.H. conception and design of research; M.I.M., R.F., M.W., M.C.-D., J.F.M., L.V., X.E., M.G.-S., B.P., and L.S. performed experiments; M.I.M., R.F., M.W., M.C.-D., J.F.M., L.V., X.E., M.G.-S., B.P., L.S., M.V.-C., F.V., J.J.V., D.S., and L.H. analyzed data; M.I.M., R.F., M.W., M.C.-D., J.F.M., L.V., X.E., M.G.-S., B.P., L.S., S.F.-V., N.C., M.V.-C., F.V., J.J.V., D.S., and L.H. interpreted results of experiments; M.I.M., R.F., M.W., M.C.-D., L.V., X.E., M.G.-S., B.P., L.S., J.J.V., and L.H. prepared figures; M.I.M., R.F., M.C.-D., J.F.M., X.E., B.P., J.J.V., and L.H. drafted manuscript; M.I.M., R.F., M.C.-D., J.F.M., X.E., B.P., N.C., J.J.V., D.S., and L.H. edited and revised manuscript; M.I.M., R.F., M.W., M.C.-D., J.F.M., L.V., X.E., M.G.-S., B.P., L.S., S.F.-V., N.C., M.V.-C., F.V., J.J.V., D.S., and L.H. approved final version of manuscript.

REFERENCES

1. **Bosello O, Zamboni M.** Visceral obesity and metabolic syndrome. *Obes Rev* 1: 47–56, 2000.
2. **Brown NF, Hill JK, Esser V, Kirkland JL, Corkey BE, Foster DW, Garry JDMC.** Mouse white adipocytes and 3T3-L1 cells display an

- anomalous pattern of carnitine palmitoyltransferase (CPT) I isoform expression during differentiation. *Biochem J* 231: 225–231, 1997.
3. Bruce CR, Hoy AJ, Turner N, Watt MJ, Allen TL, Carpenter K, Cooney GJ, Febbraio M, Kraegen EW. Overexpression of carnitine palmitoyltransferase-1 in skeletal muscle is sufficient to enhance fatty acid oxidation and improve high-fat diet-induced insulin resistance. *Diabetes* 58: 550–558, 2009.
 5. Davies LC, Jenkins SJ, Allen JE, Taylor PR. Tissue-resident macrophages. *Nat Immunol* 14: 986–995, 2013.
 6. Doh KO, Kim YW, Park SY, Lee SK, Park JS, Kim JY. Interrelation between long-chain fatty acid oxidation rate and carnitine palmitoyltransferase I activity with different isoforms in rat tissues. *Life Sci* 77: 435–443, 2005.
 7. Feuerer M, Herrero L, Cipolletta D, Naaz A, Wong J, Nayer A, Lee J, Goldfine AB, Benoist C, Shoelson S, Mathis D. Lean, but not obese, fat is enriched for a unique population of regulatory T cells that affect metabolic parameters. *Nat Med* 15: 930–939, 2009.
 8. Furukawa S, Fujita T, Shimabukuro M, Iwaki M, Yamada Y, Nakajima Y, Nakayama O, Makishima M, Matsuda M, Shimomura I. Increased oxidative stress in obesity and its impact on metabolic syndrome. *J Clin Invest* 114: 1752–1761, 2004.
 9. Gao X, Li K, Hui X, Kong X, Sweeney G, Wang Y, Xu A, Teng M, Liu P, Wu D. Carnitine palmitoyltransferase 1A prevents fatty acid-induced adipocyte dysfunction through suppression of c-Jun N-terminal kinase. *Biochem J* 435: 723–732, 2011.
 10. Gesta S, Bezy O, Mori MA, Macotela Y, Lee KY, Kahn CR. Mesodermal developmental gene Tbx15 impairs adipocyte differentiation and mitochondrial respiration. *Proc Natl Acad Sci USA* 108: 2771–2776, 2011.
 11. Hamada Y, Nagasaki H, Fujiya A, Seino Y, Shang QL, Suzuki T, Hashimoto H, Oiso Y. Involvement of de novo ceramide synthesis in pro-inflammatory adipokine secretion and adipocyte-macrophage interaction. *J Nutr Biochem* 25: 1309–1316, 2014.
 12. Haslam DW, James WPT. Obesity. *Lancet* 366: 1197–1209, 2005.
 13. Herrero L, Rubí B, Sebastián D, Serra D, Asins G, Maechler P, Prentki M, Hegardt FG. Alteration of the malonyl-CoA/carnitine palmitoyltransferase I interaction in the beta-cell impairs glucose-induced insulin secretion. *Diabetes* 54: 462–471, 2005.
 14. Herrero L, Shapiro H, Nayer A, Lee J, Shoelson SE. Inflammation and adipose tissue macrophages in lipodystrophic mice. *Proc Natl Acad Sci USA* 107: 240–245, 2010.
 15. Hosogai N, Fukuhara A, Oshima K, Miyata Y, Tanaka S, Segawa K, Furukawa S, Tochino Y, Komuro R, Matsuda M, Shimomura I. Adipose tissue hypoxia in obesity and its impact on adipocytokine dysregulation. *Diabetes* 56: 901–911, 2007.
 16. Hotamisligil GS. Endoplasmic reticulum stress and the inflammatory basis of metabolic disease. *Cell* 140: 900–917, 2010.
 17. Houmard JA. Intramuscular lipid oxidation and obesity. *Am J Physiol Regul Integr Comp Physiol* 294: R1111–R1116, 2008.
 18. Huang S, Rutkowski JM, Snodgrass RG, Ono-Moore KD, Schneider DA, Newman JW, Adams SH, Hwang DH. Saturated fatty acids activate TLR-mediated proinflammatory signaling pathways. *J Lipid Res* 53: 2002–2013, 2012.
 19. Kelley DE, He J, Menshikova EV, Ritov VB. Dysfunction of mitochondria in human skeletal muscle in type 2 diabetes. *Diabetes* 51: 2944–2950, 2002.
 20. Krishnan J, Danzer C, Simka T, Ukropec J, Walter KM, Kumpf S, Mirtschink P, Ukropcova B, Gasperikova D, Pedrazzini T, Krek W. Dietary obesity-associated Hif1 α activation in adipocytes restricts fatty acid oxidation and energy expenditure via suppression of the Sirt2-NAD⁺ system. *Genes Dev* 26: 259–270, 2012.
 21. Lin Y, Berg AH, Iyengar P, Lam TK, Giacca A, Combs TP, Rajala MW, Du X, Rollman B, Li W, Hawkins M, Barzilai N, Rhodes CJ, Fantus IG, Brownlee M, Scherer PE. The hyperglycemia-induced inflammatory response in adipocytes: the role of reactive oxygen species. *J Biol Chem* 280: 4617–4626, 2005.
 22. Mathis D. Immunological goings-on in visceral adipose tissue. *Cell Metab* 17: 851–859, 2013.
 23. Matsuzawa Y, Shimomura I, Nakamura T, Keno Y, Tokunaga K. Pathophysiology and pathogenesis of visceral fat obesity. *Ann NY Acad Sci* 748: 399–406, 1995.
 24. Matthews DR, Hosker JP, Rudenski AS, Naylor BA, Treacher DF, Turner RC. Homeostasis model assessment: insulin resistance and beta-cell function from fasting plasma glucose and insulin concentrations in man. *Diabetologia* 28: 412–419, 1985.
 25. Mera P, Mir JF, Fabriàs G, Casas J, Costa ASH, Malandrino MI, Fernández-López JA, Remesar X, Gao S, Chohann S, Rodríguez-Peña MS, Petry H, Asins G, Hegardt FG, Herrero L, Serra D. Long-term increased carnitine palmitoyltransferase 1A expression in ventromedial hypothalamus causes hyperphagia and alters the hypothalamic lipidomic profile. *PLoS One* 9: e97195, 2014.
 26. Monsénigo J, Mansouri A, Akkaoui M, Lenoir V, Esnous C, Fauveau V, Tavernier V, Girard J, Prip-Buus C. Enhancing liver mitochondrial fatty acid oxidation capacity in obese mice improves insulin sensitivity independently of hepatic steatosis. *J Hepatol* 56: 632–639, 2012.
 27. Morillas M, Gómez-Puertas P, Bentebibel A, Sellés E, Casals N, Valencia A, Hegardt FG, Asins G, Serra D. Identification of conserved amino acid residues in rat liver carnitine palmitoyltransferase I critical for malonyl-CoA inhibition. Mutation of methionine 593 abolishes malonyl-CoA inhibition. *J Biol Chem* 278: 9058–9063, 2003.
 28. Namgaladze D, Lips S, Leiker TJ, Murphy RC, Ekroos K, Ferreiros N, Geisslinger G, Brüne B. Inhibition of macrophage fatty acid β -oxidation exacerbates palmitate-induced inflammatory and endoplasmic reticulum stress responses. *Diabetologia* 57: 1067–1077, 2014.
 29. Orellana-Gavalda JM, Herrero L, Malandrino MI, Paneda A, Sol Rodríguez-Pena M, Petry H, Asins G, Van Deventer S, Hegardt FG, Serra D. Molecular therapy for obesity and diabetes based on a long-term increase in hepatic fatty-acid oxidation. *Hepatology* 53: 821–832, 2011.
 31. Orlicky DJ, DeGregori J, Schaack J. Construction of stable coxsackievirus and adenovirus receptor-expressing 3T3-L1 cells. *J Lipid Res* 42: 910–915, 2001.
 32. Patti ME, Corvera S. The role of mitochondria in the pathogenesis of type 2 diabetes. *Endocr Rev* 31: 364–395, 2010.
 33. Perdomo G, Commerford SR, Richard AMT, Adams SH, Corkey BE, O'Doherty RM, Brown NF. Increased beta-oxidation in muscle cells enhances insulin-stimulated glucose metabolism and protects against fatty acid-induced insulin resistance despite intramyocellular lipid accumulation. *J Biol Chem* 279: 27177–27186, 2004.
 34. Pérez-Pérez R, García-Santos E, Ortega-Delgado FJ, López JA, Camafeita E, Ricart W, Fernández-Real JM, Peral B. Attenuated metabolism is a hallmark of obesity as revealed by comparative proteomic analysis of human omental adipose tissue. *J Proteomics* 75: 783–795, 2012.
 35. Pessayre D, Fromenty B, Mansouri A. Mitochondrial injury in steatohepatitis. *Eur J Gastroenterol Hepatol* 16: 1095–1105, 2004.
 36. Price N, van der Leij F, Jackson V, Corstorphine C, Thomson R, Sorensen A, Zammit V. A novel brain-expressed protein related to carnitine palmitoyltransferase I. *Genomics* 80: 433–442, 2002.
 37. Ritov VB, Menshikova EV, He J, Ferrell RE, Goodpaster BH, Kelley DE. Deficiency of subsarcolemmal mitochondria in obesity and type 2 diabetes. *Diabetes* 54: 8–14, 2004.
 38. Rosen ED, Spiegelman BM. What we talk about when we talk about fat. *Cell* 156: 20–44, 2014.
 39. Samuel VT, Shulman GI. Mechanisms for insulin resistance: common threads and missing links. *Cell* 148: 852–871, 2012.
 40. Sebastian D, Herrero L, Serra D, Asins G, Hegardt FG. CPT I overexpression protects L6E9 muscle cells from fatty acid-induced insulin resistance. *Am J Physiol Endocrinol Metab* 292: E677–E686, 2007.
 42. Shoelson SE, Herrero L, Naaz A. Obesity, inflammation, and insulin resistance. *Gastroenterology* 132: 2169–2180, 2007.
 43. Shoelson SE, Lee J, Goldfine AB. Inflammation and insulin resistance. *J Clin Invest* 116: 1793–1801, 2006.
 44. Simoneau JA, Veerkamp JH, Turcotte LP, Kelley DE. Markers of capacity to utilize fatty acids in human skeletal muscle: relation to insulin resistance and obesity and effects of weight loss. *FASEB J* 13: 2051–2060, 1999.
 45. Stefanovic-Racic M, Perdomo G, Mantell BS, Sipula IJ, Brown NF, O'Doherty RM. A moderate increase in carnitine palmitoyltransferase 1a activity is sufficient to substantially reduce hepatic triglyceride levels. *Am J Physiol Endocrinol Metab* 294: E969–E977, 2008.
 47. Suganami T, Nishida J, Ogawa Y. A paracrine loop between adipocytes and macrophages aggravates inflammatory changes: role of free fatty acids and tumor necrosis factor alpha. *Arterioscler Thromb Vasc Biol* 25: 2062–2068, 2005.
 48. Suganami T, Tanimoto-Koyama K, Nishida J, Itoh M, Yuan X, Mizuarai S, Kotani H, Yamaoka S, Miyake K, Aoe S, Kamei Y, Ogawa Y. Role of the Toll-like receptor 4/NF- κ B pathway in saturated fatty acid-induced inflammatory changes in the interaction between adipocytes and macrophages. *Arterioscler Thromb Vasc Biol* 27: 84–91, 2007.

49. **Summers SA.** Ceramides in insulin resistance and lipotoxicity. *Prog Lipid Res* 45: 42–72, 2006.
50. **Sun K, Kusminski CM, Scherer PE.** Adipose tissue remodeling and obesity. *J Clin Invest* 121: 2094–2101, 2011.
51. **Sun K, Wernstedt Asterholm I, Kusminski CM, Bueno AC, Wang ZV, Pollard JW, Brekken a R, Scherer PE.** Dichotomous effects of VEGF-A on adipose tissue dysfunction. *Proc Natl Acad Sci USA* 109: 5874–5879, 2012.
52. **Tran TT, Yamamoto Y, Gesta S, Kahn CR.** Beneficial effects of subcutaneous fat transplantation on metabolism. *Cell Metab* 7: 410–420, 2008.
53. **Villarroya F, Domingo P, Giralt M.** Lipodystrophy in HIV 1-infected patients: lessons for obesity research. *Int J Obes (Lond)* 31: 1763–1776, 2007.
54. **Virtue S, Vidal-Puig A.** Adipose tissue expandability, lipotoxicity and the Metabolic Syndrome—an allostatic perspective. *Biochim Biophys Acta* 1801: 338–349, 2010.
55. **Wabitsch M, Brenner RE, Melzner I, Braun M, Moller P, Heinze E, Debatin KM, Hauner H.** Characterization of a human preadipocyte cell strain with high capacity for adipose differentiation. *Int J Obes Relat Metab Disord* 25: 8–15, 2001.
56. **Weisberg SP, McCann D, Desai M, Rosenbaum M, Leibel RL, Ferrante AW.** Obesity is associated with macrophage accumulation in adipose tissue. *J Clin Invest* 112: 1796–1808, 2003.
57. **Xu H, Barnes GT, Yang Q, Tan G, Yang D, Chou CJ, Sole J, Nichols A, Ross JS, Tartaglia LA, Chen H.** Chronic inflammation in fat plays a crucial role in the development of obesity-related insulin resistance. *J Clin Invest* 112: 1821–1830, 2003.



Estratègies de modulació de l'oxidació d'àcids grassos com a tractament per combatre l'obesitat

Fatty acid oxidation regulation strategies to treat obesity

Laura Herrero,^{1,2,3} Joan Francesc Mir,^{1,2} Minéia Weber,^{1,2} Raquel Fucho,^{1,2} María Calderón^{1,2,3} i Dolors Serra^{1,2,3}

¹ Universitat de Barcelona. Facultat de Farmàcia. Departament de Bioquímica i Biologia Molecular

² Institut de Biomedicina de la Universitat de Barcelona (IBUB)

³ CIBER Fisiopatología de la Obesidad y la Nutrición (CIBERObn)

Resum: L'estil de vida actual, amb dietes d'alt contingut calòric i falta d'exercici físic, fa que la incidència d'obesitat s'incrementi notablement. Augmentar la degradació de greixos o bé reduir la ingesta calòrica poden ser potencials estratègies terapèutiques. L'enzim carnitina palmitoiltransferasa I (CPT1) és el pas limitant de l'oxidació dels àcids grassos. En aquest article, es mostra com la modulació de la seva activitat en diferents teixits, com el fetge, el teixit adipós o l'hipotàlem, pot ser clau a l'hora d'augmentar la despesa energètica i controlar la ingesta d'aliments.

Paraules clau: Obesitat, ingesta, oxidació d'àcids grassos, CPT1.

Abstract: Current lifestyles, with high-energy diets and little exercise, are triggering an alarming growth in obesity. Strategies that enhance fat degradation or reduce caloric food intake could be considered therapeutic interventions to reduce not only obesity, but also its associated disorders. The enzyme carnitine palmitoyltransferase I (CPT1) is the critical rate-determining regulator of fatty acid oxidation. In this paper, we show that this enzyme might play a key role in different tissues, such as liver, adipose tissue and hypothalamus, increasing energy expenditure and controlling food intake.

Keywords: Obesity, food intake, fatty acid oxidation, CPT1.

Introducció

L'obesitat i els trastorns metabòlics associats, com ara la resistència a la insulina, la diabetis de tipus 2, les malalties cardiovasculars, el càncer i altres patologies, són un dels greus problemes de salut pública del segle XXI. Segons l'Organització Mundial de la Salut, hi ha més de sis-cents milions de persones obeses a tot el món i, més important encara, el sobrepès i l'obesitat són la cinquena causa de mort en l'àmbit mundial. En els últims anys, s'està fent un gran esforç per entendre la fisiopatologia de l'obesitat i, en particular, la seva associació amb la resistència a la insulina [1]. S'han proposat diversos mecanismes que podrien explicar aquesta relació causal:

a) Deposició de greix ectòpica: durant l'obesitat falla la capacitat d'expandir del teixit adipós i d'emmagatzemar l'excés de greix, i això comporta un augment del depòsit de lípids en altres òrgans perifèrics com el fetge, el múscul esquelètic i el

pàncrees. Aquesta acumulació excessiva de lípids crea un ambient lipotòxic que bloqueja el transport de glucosa i la correcta senyalització de la insulina.

b) Inflamació: l'excés de lípids acumulats en el teixit adipós durant l'obesitat causa hipòxia en els adipòcits i, a la vegada, el reclutament i l'activació de les cèl·lules immunes en aquest teixit. Els adipòcits engrandits per l'acumulació de lípids i les cèl·lules immunes infiltrades secreten moltes citocines inflammatòries que promouen un estat proinflamatori que contribueix a la resistència a la insulina local i també sistèmica.

c) La ingesta d'aliments: el sistema nerviós central, específicament l'hipotàlem, és extremament important en les patologies induïdes per l'obesitat, ja que desenvolupa un paper crucial en el control de la ingesta i la regulació del pes corporal. De fet, la leptina, una hormona secretada pels adipòcits, actua sobre l'hipotàlem inhibint la ingesta d'aliments i controlant el pes corporal. En els trastorns relacionats amb l'obesitat, aquesta hormona és essencial en les interrelacions entre el cervell i els altres òrgans.

Les estratègies terapèutiques actuals per combatre l'obesitat se centren en l'augment de la despesa energètica mitjançant l'exercici regular i/o en la reducció del consum d'energia. Però modificar i mantenir aquest estil de vida més saludable du-

Correspondència: Dolors Serra
Universitat de Barcelona. Facultat de Farmàcia. Departament de Bioquímica i Biologia Molecular
Av. de Joan XXIII, 27-31. 08028 Barcelona
Tel.: +34 934 024 522. Fax: +34 934 024 520
A/e: dserra@ub.edu

rant llargs períodes de temps és difícil, ja que requereix una gran força de voluntat i el pacient acaba abandonant moltes de les mesures adoptades. Tots els medicaments que es troben en el mercat contra l'obesitat van dirigits a limitar el consum d'energia. Tot i els grans esforços fets fins al moment per combatre l'obesitat, la llista de medicaments retirats del mercat per raons de seguretat sembla ser cada vegada més gran: fenfluramina, dexfenfluramina, sibutramina i rimonabant. Actualment, només l'orlistat i la lorcaserina tenen una indicació clínica aprovada per al tractament de l'obesitat. Les agències del medicament europea, EMA (European Medicines Agency), i americana, FDA (Food and Drug Administration), han aprovat l'ús de l'orlistat, i només la FDA, l'ús de la lorcaserina [2, 3]. La liraglutida, un fàrmac anteriorment aprovat com a antidiabètic, ha estat aprovada per les dues institucions com a fàrmac contra l'obesitat [4, 5]. Altres fàrmacs existents en el mercat, com la combinació de bupropiò/naltrexona, que actuen en el sistema nerviós central augmentant l'activitat de les neurones POMC, han estat aprovats per la FDA, però no per l'agència europea EMA, ja que aquesta última és molt més restrictiva a l'hora d'aprovar medicaments per al control del pes que estiguin dirigits al sistema nerviós central. A causa, doncs, de la pandèmia de malalties relacionades amb l'obesitat (diabetis, resistència a la insulina, malalties cardiovasculars, asma, alguns tipus de càncer, Alzheimer, etc.), hi ha una gran necessitat de trobar nous fàrmacs que presentin un perfil més segur per optimitzar i individualitzar teràpies contra l'obesitat. Per tant, és imperatiu desenvolupar noves estratègies per abordar el problema i, entre elles, les destinades a augmentar la mobilització de lípids i l'oxidació de greixos són algunes de les més atractives.

Mobilització i oxidació dels àcids grassos

L'oxidació d'àcids grassos de cadena llarga es produeix en els mitocondris i duu a terme un paper clau en el desenvolupament de l'obesitat. El transport de lípids en el mitocondri es realitza a través del sistema carnitina palmitoïltransferasa (CPT). Aquest sistema està integrat per tres proteïnes: CPT1, acilcarnitina translocasa i CPT2. CPT1 catalitza l'etapa limitant de l'oxidació mitocondrial d'àcids grassos i està regulada pels canvis en els nivells de malonil-CoA. Aquests nivells estan controlats per l'acetil-CoA carboxilasa (ACC), que catalitza la síntesi de malonil-CoA i per malonil-CoA descarboxilasa (MCD), que en catalitza la degradació. Junts, aquests compo-

nents actuen com una xarxa metabòlica que detecta l'estat energètic de la cèl·lula. Un cop els àcids grassos de cadena llarga s'han degradat a acetil-CoA dins del mitocondri, es transformen en ATP a través del cicle de Krebs i la fosforilació oxidativa. Els teixits de mamífers expressen tres isoformes de CPT1: CPT1A, descoberta originalment al fetge, però que està present gairebé de forma ubíqua [6]; CPT1B, que es troba en múscul, cor i teixit adipós marró [7], i CPT1C, l'última isoforma descoberta, que s'expressa principalment en el cervell [8].

La nostra investigació indica que la modulació de la bioenergètica mitocondrial (i, en particular, l'oxidació d'àcids grassos) és un bon objectiu com a teràpia contra l'obesitat. La nostra estratègia es basa en dues intervencions: l'acció sobre teixits perifèrics, com ara el fetge i el teixit adipós, i l'acció central a l'hipotàlem. Per dur a terme la primera intervenció, el nostre grup ha obtingut una forma mutada de CPT1A, M593S-CPT1A (CPT1AM), que és una proteïna completament activa però totalment insensible a la inhibició per malonil-CoA [9]. La sobreexpressió de CPT1AM permet desconnectar el metabolisme de la glucosa, que augmenta els nivells de malonil-CoA, del dels àcids grassos, amb la qual cosa s'accelera la degradació d'aquests últims. Per tant, la reducció dels lípids cel·lulars es produeix d'una forma molt més eficient. En l'àmbit central, la nostra estratègia es basa en la inhibició de l'activitat CPT1, ja que sembla que està implicada en la via de senyalització d'hormones que controlen la ingesta d'aliments.

L'augment d'oxidació d'àcids grassos al mitocondri de fetge millora la resistència a la insulina i l'obesitat induïda per una dieta rica en greix en ratolins

Al fetge, en condicions associades a un excés d'energia crònica o a alteracions del metabolisme lipídic, hi ha una considerable acumulació de lípids. Això desencadena el desenvolupament de la malaltia del fetge gras no alcohòlica. Aquesta malaltia produeix una acumulació anormal de lípids i inflamació. També comporta un augment de la gluconeogènesi hepàtica, que deixa de ser sensible a la insulina. Aquest sol ser el començament de la diabetis, que pot conduir, en etapes posteriors, al desenvolupament d'alteracions més greus, com l'esteatohepatitis, la cirrosi i el carcinoma hepatocel·lular. Te-

nint en compte que el fetge gras és, en última instància, el resultat d'un desequilibri entre l'entrada i la sortida de lípids dels hepatòcits, qualsevol intervenció que estimuli l'oxidació hepàtica d'àcids grassos ha de donar lloc a una reducció de l'esteatosi hepàtica. S'han descrit diverses aproximacions farmacològiques que activen l'oxidació d'àcids grassos al fetge. Per exemple, l'ús d'agonistes de PPAR [10] i AMPK [11, 12] i d'antagonistes de l'ACC [13]. Més interessants són els estudis en rosegadors en els quals s'intenta reduir l'esteatosi augmentant l'oxidació d'àcids grassos específicament al fetge. En aquests estudis, la modulació a curt termini de l'expressió dels gens ACC [14] i MCD [15] produeix una reducció en els nivells de malonil-CoA i un augment de l'oxidació d'àcids grassos. A més a més, en aquests estudis, es va observar una disminució hepàtica del contingut de triglicèrids i una millora de la sensibilitat a la insulina dels animals obesos. Tot i els bons resultats, cal tenir en compte que aquests gens estan implicats en altres rutes metabòliques, i això planteja la qüestió sobre la seva eficàcia en tractaments a llarg termini.

Tenint en compte que l'enzim clau i limitant de l'oxidació dels àcids grassos és CPT1A, la seva sobreexpressió sembla una estratègia més adient a l'hora de reduir el contingut de lípids i aconseguir una millora general del metabolisme hepàtic. La sobreexpressió hepàtica de CPT1A mitjançant adenovirus s'ha dut a terme en rates obeses per Stefanovic-Racic *et al.* [16]. Aquests autors van observar que un lleuger augment de l'oxidació d'àcids grassos produïa una reducció dels nivells de triglicèrids hepàtics, però això no va suposar cap millora en la sensibilitat a la insulina. Aquest efecte moderat podria ser degut a l'augment dels nivells de malonil-CoA induïts per una

dieta alta en greixos, que podria limitar l'activitat de CPT1A *in vivo*, tot i haver-la sobreexpressat.

Per evitar la inhibició pel malonil-CoA, el nostre grup va generar fa temps una isoforma mutant de CPT1A, CPT1AM [9], que és insensible al malonil-CoA. Els resultats publicats pel nostre grup confirmen en la línia cel·lular pancreàtica INS-1 [17] i en la línia de cèl·lules de múscul L6E9 [18] que la sobreexpressió de CPT1AM mitjançant adenovirus és més eficient a l'hora d'augmentar l'oxidació d'àcids grassos que la forma de CPT1A salvatge. A més a més, la sobreexpressió de CPT1AM en les cèl·lules L6E9 produeix un augment de dues vegades l'oxidació de palmitat, i disminueix la seva esterificació cap a altres lípids cel·lulars. Resultats similars han estat obtinguts en cultius primaris d'hepatòcits pel grup de la doctora Prip-Buus [19] i també pel nostre grup.

A més dels estudis *in vitro*, s'han realitzat experiments *in vivo* en ratolins alimentats amb una dieta grassa [20]. Mitjançant la injecció per la vena de la cua de ratolins de virus adenoassociats (AAV) que contenen la CPT1AM dirigida per un promotor específic de fetge, es va obtenir una sobreexpressió hepàtica perllongada de CPT1AM. Això va permetre avaluar l'impacte metabòlic i mecanismes subjacents de l'augment de l'oxidació d'àcids grassos en ratolins amb obesitat induïda per una dieta alta en greixos, així com en ratolins genèticament obesos *db/db*. En aquests estudis, es va observar que els ratolins que expressaven CPT1AM en fetge mostraven una millora general del metabolisme hepàtic de la glucosa i dels lípids a causa de l'augment del flux d'àcids grassos cap al mitocondri. Això evitava l'acumulació intracel·lular de lípids al fetge i la producció de ROS i rescatava la malmesa senyalització de la insulina (figura 1). Aquesta capacitat del fetge per fer front a un augment del flux dels àcids grassos cap al mitocondri, de manera que s'escapava d'una possible lesió hepàtica, podria ser explicada en part per la capacitat del fetge de formar cossos cetònics. Els cossos cetònics produïts per una major β -oxidació són fàcilment consumits per altres teixits, de manera que augmenta el flux de carbonis des del fetge cap a altres òrgans. A més a més, en aquests ratolins s'observà una reducció dels lípids acumulats en el teixit adipós blanc i un menor pes corporal, comparat amb el dels ratolins control, alimentats també amb una dieta rica en greixos. La senyalització de la insulina, deteriorada en teixits com ara el múscul o el teixit adipós blanc, també va millorar (figura 1). Aquests resultats han estat confirmats per un estudi posterior que van dur a terme Monsenego *et al.* [21].

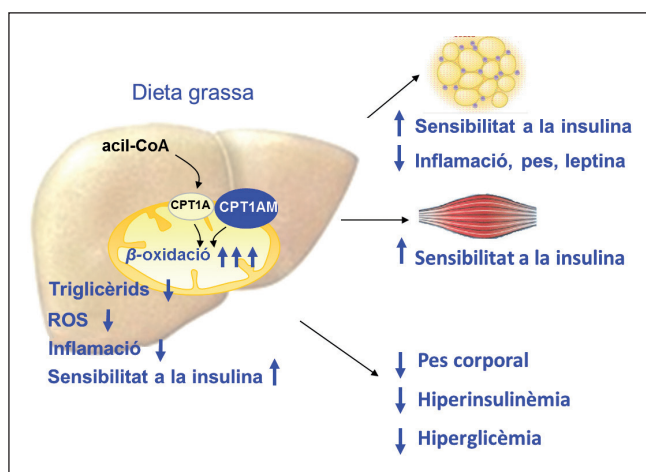


FIGURA 1. Efecte de la sobreexpressió de CPT1AM en fetge de ratolí amb obesitat induïda per dieta grassa.

En els ratolins genèticament obesos *db/db* que expressaven CPT1AM, també es va observar una millora de la hiperglucèmia i la hiperinsulinèmia que pateixen aquests animals. En conjunt, tots aquests resultats fan palès que un augment de la CPT1AM hepàtica pot ser una nova estratègia per al tractament de patologies del fetge gras i de l'obesitat.

L'augment de l'oxidació d'àcids grassos en adipòcits i en macròfags redueix el contingut en triglicèrids i la inflamació

Durant les dues últimes dècades, el teixit adipós ha guanyat importància com a responsable dels mecanismes implicats en els trastorns relacionats amb l'obesitat. El teixit adipós blanc és el responsable de l'emmagatzematge d'energia i conté adipòcits, teixit connectiu i nombroses cèl·lules immunes, com els macròfags, cèl·lules T i B, els mastòcits i els neutròfils, que s'infiltra i augmenten la seva presència durant l'obesitat. Els macròfags van ser les primeres cèl·lules immunes descrites implicades en la resistència a la insulina derivada de l'obesitat. Això mostrà que, a més del seu paper convencional en la reparació de teixits i en la resposta a adipòcits moribunds, aquests poden desenvolupar un paper patològic en el teixit adipós [22]. El teixit adipós és també un teixit endocrí que secreta hormones com la leptina, l'adiponectina i la resistina i citocines inflamatòries com ara TNF- α , IL-6, IL-1 β , etc., en resposta a diversos estímuls. Per tant, és un òrgan complex que controla la despesa d'energia, la gana, la sensibilitat a la insulina, la inflamació i la immunitat.

La fisiopatologia de la resistència a la insulina induïda per l'obesitat s'ha atribuït a diversos factors, com ara la deposició de greix ectòpica, l'augment de la inflamació i l'estrès del reticle endoplasmàtic (RE), la hipòxia del teixit adipós i la disfunció mitocondrial, l'expansió dels adipòcits deteriorats i l'angiogènesi. En l'obesitat, els àcids grassos, juntament amb altres estímuls, com ara les ceramides, diverses isoformes de PKC, citocines proinflamatòries, ROS i estrès de RE, activen les vies de senyalització de JNK, NF- κ B, RAGE i TLR, tant en adipòcits com en macròfags, la qual cosa desencadena la inflamació i la resistència a la insulina [23].

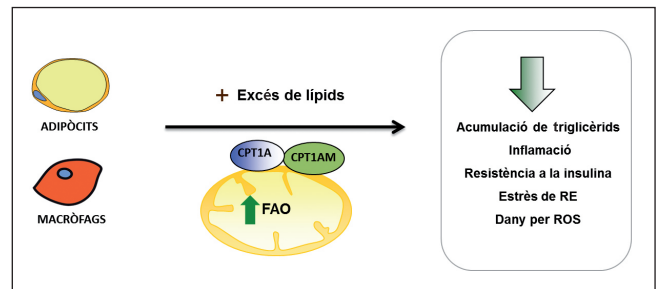


FIGURA 2. Efecte de l'augment de l'oxidació d'àcids grassos en adipòcits i macròfags incubats amb palmitat per sobreexpressió de CPT1AM.

S'ha descrit que les persones obeses i les persones amb diabetis de tipus 2 presenten nivells d'oxidació d'àcids grassos inferiors en diversos teixits. Així, s'ha observat que les persones obeses tenen reduïts els nivells d'expressió de CPT1 en el teixit adipós visceral [24]. Un estudi recent mostra que la sobreexpressió de CPT1A en adipòcits blancs disminueix el contingut de triglicèrids i millora la sensibilitat a la insulina [25]. En un estudi realitzat pel nostre grup, vam observar que l'expressió de CPT1A és major en els macròfags del teixit adipós humà que en adipòcits i que s'expressa diferencialment en teixit adipós visceral vs subcutani tant en una cohort d'obesos com en una de diabetis de tipus 2 [26]. Aquestes observacions ens van portar a investigar més a fons el paper potencial de CPT1A en adipòcits i macròfags. Quan vam expressar la CPT1AM en una línia cel·lular d'adipòcits 3T3-L1 CARD1 i en macròfags RAW 264,7 mitjançant adenovirus, vam observar un augment de l'oxidació d'àcids grassos en ambdós tipus cel·lulars. Quan les cèl·lules es van incubar amb palmitat per simular una situació d'obesitat, vam observar una disminució del contingut de triglicèrids, de la inflamació i de la sensibilitat a la insulina en adipòcits i una reducció d'estrès de RE i ROS en macròfags (figura 2). Tots aquests resultats indiquen que un augment de la mobilització i l'oxidació d'àcids grassos en cèl·lules metabòlicament rellevants, com ara adipòcits i macròfags, pot ser una estratègia prometedora per al tractament de patologies inflamatòries cròniques com l'obesitat i la diabetis de tipus 2.

La modulació de l'activitat CPT1 a l'hipotàlem regula la ingesta i el pes

El sistema nerviós central desenvolupa un paper important en l'avaluació i el control de l'homeòstasi energètica. L'hipotàlem és un òrgan complex organitzat en diferents nuclis formats per

agrupacions de neurones especialitzades que són sensibles a canvis en l'estatus energètic. Aquestes neurones responen als canvis energètics alterant l'expressió de neuromoduladors i neurotransmissors específics que, a la vegada, modifiquen la ingesta d'aliments i la despesa energètica. El metabolisme hipotalàmic dels àcids grassos participa en aquest procés i actua com a intermediari dels mecanismes moleculars de l'acció central d'hormones com la leptina, la grelina i els nutrients en el control de la ingesta i el balanç energètic [27].

Alguns estudis suggereixen que el malonil-CoA actua en aquests processos com a missatger molecular de l'estat nutricional [28]. Així, la leptina, hormona de la sacietat, realitza la seva acció anorexigènica augmentant els nivells de malonil-CoA a l'hipotàlem. També hi ha evidències clares del procés invers, és a dir, una disminució hipotalàmica dels nivells de malonil-CoA senyalitza un dèficit energètic que causa un augment de la ingesta i del pes [29]. Un clar candidat de l'acció del malonil-CoA és la CPT1. Al cervell hi ha dues isoformes de CPT1: CPT1A (en el mitocondri) i CPT1C (en el RE). Les dues isoformes tenen un lloc d'unió a malonil-CoA. No obstant això, les seves notables diferències en la localització subcel·lular i en l'activitat suggereixen una funció neuronal diferent per a cada isoforma.

S'ha proposat que, en situacions d'augment de malonil-CoA, aquest actuaria inhibint la CPT1A, la qual cosa limitaria l'oxidació dels acil-CoA de cadena llarga. L'acumulació d'acil-CoA o altres derivats lipídics permetria la seva interacció amb proteïnes que regularien l'expressió dels neuropèptids orexigènics (NPY i AgRP) i anorexigènics (POMC i CART). Donen suport a aquest mecanisme les observacions fetes amb la injecció intracerebroventricular (icv) d'una ribosonda que causa inhibició genètica de la CPT1A hipotalàmica i redueix la ingesta [30]. D'altra banda, s'ha observat que l'acció orexigènica de la grelina es dona a través d'una activació de la cinasa activada per AMP (AMPK), que, a la vegada, inactiva ACC, la qual cosa impedeix la síntesi de malonil-CoA i, en conseqüència, augmenta l'activitat CPT1A [29]. Aquest augment d'activitat CPT1A produeix un augment de ROS que podria ser responsable, en part, de l'activació de la senyalització de la resposta orexigènica.

Estudis recents realitzats pel nostre grup mostren que una sobreexpressió de CPT1AM en el nucli ventromedial (VMN) (nucli de sacietat) de l'hipotàlem produeix hiperfàgia (figura 3). Això va associat a canvis notables del perfil lipídic de la regió mediobasal (MBH), que comprèn els nuclis arquat (ARC)

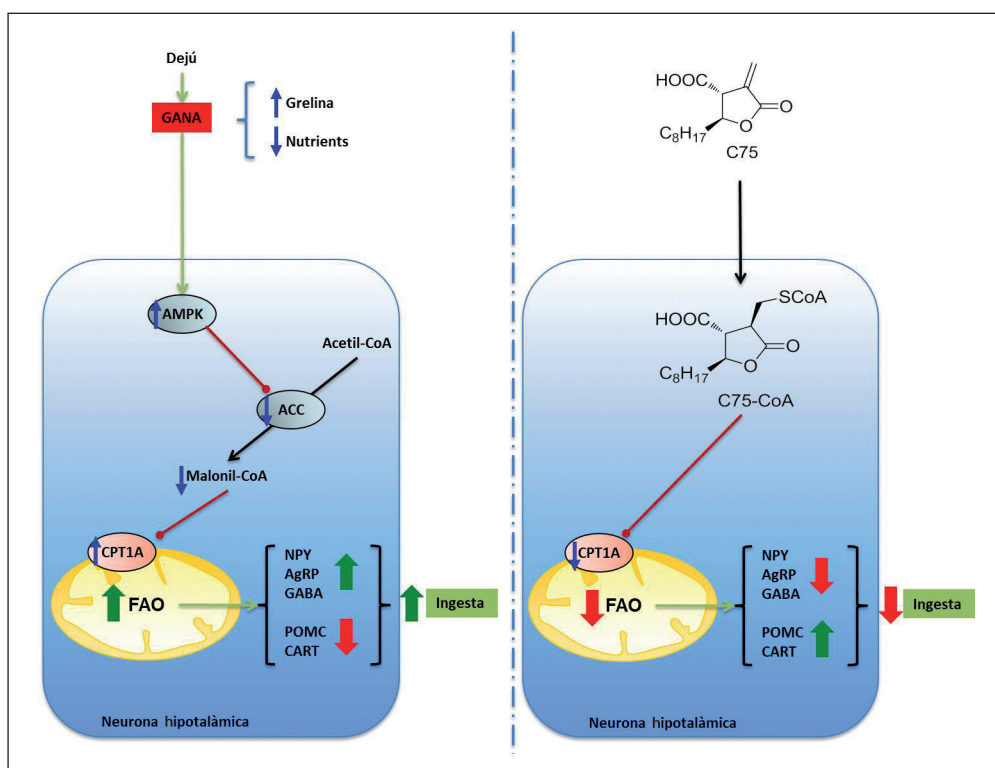


FIGURA 3. Modulació de l'activitat CPT1A a hipotàlem. L'augment de l'activitat CPT1A produeix un augment de la ingesta. La inhibició de l'activitat CPT1A per acció del C75 redueix la ingesta.

i VMN de l'hipotàlem, i a canvis en els nivells d'expressió dels transportadors de glutamat i GABA [31]. En canvi, al nucli ARC, aquesta mateixa sobreexpressió de CPT1A no altera la ingesta en resposta a la leptina [32]. Tot això apunta a un paper clau de CPT1A en el control de la ingesta. Malgrat totes aquestes evidències, encara no es coneixen exactament quins són els esdeveniments per sota de CPT1A en els diferents nuclis hipotalàmics que porten a la resposta orexigènica.

D'altra banda, s'ha realitzat un esforç important per dissenyar nous fàrmacs contra l'obesitat dirigits a augmentar els nivells de malonil-CoA en l'àmbit hipotalàmic. L'enzim àcid gras sintasa (AGS) catalitza la síntesi de palmitat a partir d'acetil-CoA i malonil-CoA. S'ha descrit que la inhibició d'AGS a l'hipotàlem suprimeix la ingesta d'aliments a través de l'acumulació de malonil-CoA [33]. El C75 és un inhibidor sintètic de l'AGS i s'ha proposat com un agent antiobesitat. La seva administració disminueix la gana i el pes corporal en rosegadors [34]. El nostre grup ha demostrat que el coenzim-A adducte de C75 (C75-CoA) és un potent inhibidor de la CPT1 [35] i que una part de la resposta anorexigènica del C75 pot ser deguda a la potent inhibició d'aquest producte sobre CPT1A. Totes aquestes dades indiquen que la CPT1A podria ser considerada una bona diana per al control de la gana amb vista a possibles accions terapèutiques contra l'obesitat.

Conclusions

La comunitat investigadora és conscient del fet que s'han de buscar nous tractaments per lluitar contra l'epidèmia actual de l'obesitat i de les malalties relacionades. Un canvi en la dieta i l'exercici físic regular són dues estratègies clàssiques i efectives per disminuir la sobrecàrrega de nutrients. Tot i així, el seu manteniment a llarg termini depèn de la voluntat del pacient. És per això que calen noves aproximacions que permetin reduir la càrrega de lípids i augmentar la despesa d'energia. D'altra banda, per modular la conducta alimentària, cal també desenvolupar nous medicaments que permetin reduir la ingesta. Els resultats del nostre grup i d'altres demostren que un augment sistèmic o una disminució en l'àmbit central de l'oxidació de lípids és una estratègia prometedora per lluitar contra l'obesitat i les malalties relacionades.

Agraïments

Voldriem agrair al Ministeri de Ciència i Innovació el finançament rebut pels projectes SAF2013-45887-R, de LH; SAF2014-52223-C2-1-R, de DS, i la beca doctoral de JFM. El CIBER Fisiopatología de la Obesidad y la Nutrición (CIBERObn) CB06/03/0001, de DS. Els ajuts a la recerca de la European Foundation for the Study of Diabetes, de LH; (EFSD)/Lilly i EFSD/Janssen-Rising Star, de LH, i L'Oréal-UNESCO «For Women in Science», de LH. L'ajut a la recerca de la Generalitat de Catalunya 2014SGR465, de DS. Els autors també agraeixen la beca doctoral «Ciencia sin fronteras» del Brasil de MW.

Referències

- [1] AHIMA, R. S. «Digging deeper into obesity». *J. Clin. Invest.*, núm. 121 (2011), p. 2076-2079.
- [2] O'NEIL, P. M.; SMITH, S. R.; WEISSMAN, N. J.; FIDLER, M. C.; SÁNCHEZ, M.; ZHANG, J.; RAETHER, B.; ANDERSON, C. M.; SHANAHAN, W. R. «Randomized placebo-controlled clinical trial of lorcaserin for weight loss in type 2 diabetes mellitus: the BLOOM-DM study». *Obes.*, núm. 20 (2012), p. 1426-1436.
- [3] KHAN, A.; RAZA, S.; KHAN, Y.; AKSOY, T.; KHAN, M.; WEINBERGER, Y.; GOLDMAN, J. «Current updates in the medical management of obesity». *Recent Pat. Endocr. Metab. Immune Drug Discov.*, núm. 6 (2012), p. 117-128.
- [4] NOVO NORDISK. *Liraglutide 3.0 mg for weight management: NDA 206-321: Briefing document* [en línia]. Silver Spring: US Food and Drug Administration. Endocrinologic and Metabolic Drugs Advisory Committee, 2014. <<http://www.fda.gov/downloads/advisorycommittees/committeesmeetingmaterials/drugs/endocrinologicandmetabolicdrugsadvisorycommittee/ucm413318.pdf>>.
- [5] EUROPEAN MEDICINES AGENCY (EMA). «Saxenda recommended for approval in weight management in adults: medicine to be used in addition to reduced-calorie diet and physical activity». Londres, 2015.
- [6] ESSER, V.; BRITTONSO, C. H.; WEIS, B. C.; FOSTER, D. W.; MCGARRY, J. D. «Cloning, sequencing, and expression of a cDNA encoding rat liver carnitine palmitoyltransferase I. Direct evidence that a single polypeptide is involved in inhibitor interaction and catalytic function». *J. Biol. Chem.*, núm. 268 (1993), p. 5817-5822.
- [7] YAMAZAKI, N.; SHINOHARA, Y.; SHIMA, A.; TERADA, H. «High expression of a novel carnitine palmitoyltransferase I like pro-

tein in rat brown adipose tissue and heart: isolation and characterization of its cDNA clone». *FEBS Lett.*, núm. 363 (1995), p. 41-45.

[8] PRICE, N.; LEIJ, F. van der; JACKSON, V.; CORSTORPHINE, C.; THOMSON, R.; SORENSEN, A.; ZAMMIT, V. «A novel brain-expressed protein related to carnitine palmitoyltransferase I». *Genomics*, núm. 80 (2002), p. 433-442.

[9] MORILLAS, M.; GÓMEZ-PUERTAS, P.; BENTEBIBEL, A.; SELLÉS, E.; CASALS, N.; VALENCIA, A.; HEGARDT, F. G.; ASINS, G.; SERRA, D. «Identification of conserved amino acid residues in rat liver carnitine palmitoyltransferase I critical for malonyl-CoA inhibition. Mutation of methionine 593 abolishes malonyl-CoA inhibition». *J. Biol. Chem.*, núm. 278 (2003), p. 9058-9063.

[10] BARROSO, E.; RODRÍGUEZ-CALVO, R.; SERRANO-MARCO, L.; ASTUDILLO, A. M.; BALSINDE, J.; PALOMER, X.; VÁZQUEZ-CARRERA, M. «The PPAR β/δ activator GW501516 prevents the down-regulation of AMPK caused by a high-fat diet in liver and amplifies the PGC-1 α -Lipin 1-PPAR α pathway leading to increased fatty acid oxidation». *Endocrinology*, núm. 152 (2011), p. 1848-1859.

[11] ZHOU, G.; MYERS, R.; LI, Y.; CHEN, Y.; SHEN, X.; FENYK-MELODY, J.; WU, M.; VENTRE, J.; DOEBBER, T.; FUJII, N.; MUSI, N.; HIRSHMAN, M. F.; GOODYEAR, L. J.; MOLLER, D. E. «Role of AMP-activated protein kinase in mechanism of metformin action». *J. Clin. Invest.*, núm. 108 (2001), p. 1167-1174.

[12] VELASCO, G.; GEELLEN, M. J.; GUZMÁN, M. «Control of hepatic fatty acid oxidation by 5'-AMP-activated protein kinase involves a malonyl-CoA-dependent and a malonyl-CoA-independent mechanism». *Arch. Biochem. Biophys.*, núm. 337 (1997), p. 169-175.

[13] HARWOOD, H. J.; PETRAS, S. F.; SHELLY, L. D.; ZACCARO, L. M.; PERRY, D. A.; MAKOWSKI, M. R.; HARGROVE, D. M.; MARTIN, K. A.; TRACEY, W. R.; CHAPMAN, J. G.; MAGEE, W. P.; DALVIE, D. K.; SOLIMAN, V. F.; MARTIN, W. H.; MULARSKI, C. J.; EISENBEIS, S. A. «Isozyme-nonspecific N-substituted bipiperidylcarboxamide acetyl-CoA carboxylase inhibitors reduce tissue malonyl-CoA concentrations, inhibit fatty acid synthesis, and increase fatty acid oxidation in cultured cells and in experimental animals». *J. Biol. Chem.*, núm. 278 (2003), p. 37099-37111.

[14] SAVAGE, D. B.; CHOI, C. S.; SAMUEL, V. T.; LIU, Z.-X.; ZHANG, D.; WANG, A.; ZHANG, X. M.; CLINE, G. W.; YU, X. X.; GEISLER, J. G.; BHANOT, S.; MONIA, B. P.; SHULMAN, G. I. «Reversal of diet-induced hepatic steatosis and hepatic insulin resistance by antisense oligonucleotide inhibitors of acetyl-CoA carboxylases 1 and 2». *J. Clin. Invest.*, núm. 116 (2006), p. 817-824.

[15] AN, J.; MUOIO, D. M.; SHIOTA, M.; FUJIMOTO, Y.; CLINE, G. W.; SHULMAN, G. I.; KOVES, T. R.; STEVENS, R.; MILLINGTON, D.; NEWGARD, C. B.

«Hepatic expression of malonyl-CoA decarboxylase reverses muscle, liver and whole-animal insulin resistance». *Nat. Med.*, núm. 10 (2004), p. 268-274.

[16] STEFANOVIC-RACIC, M.; PERDOMO, G.; MANTELL, B. S.; SIPULA, I. J.; BROWN, N. F.; O'DOHERTY, R. M. «A moderate increase in carnitine palmitoyltransferase 1 α activity is sufficient to substantially reduce hepatic triglyceride levels». *Am. J. Physiol. Endocrinol. Metab.*, núm. 294 (2008), p. E969-E977.

[17] HERRERO, L.; RUBÍ, B.; SEBASTIÁN, D.; SERRA, D.; ASINS, G.; MAECHLER, P.; PRENTKI, M.; HEGARDT, F. G. «Alteration of the malonyl-CoA/carnitine palmitoyltransferase I interaction in the β -cell impairs glucose-induced insulin secretion». *Diabetes*, núm. 54 (2005), p. 462-471.

[18] SEBASTIÁN, D.; HERRERO, L.; SERRA, D.; ASINS, G.; HEGARDT, F. G. «CPT I overexpression protects L6E9 muscle cells from fatty acid-induced insulin resistance». *Am. J. Physiol. Endocrinol. Metab.*, núm. 292 (2007), p. E677-E686.

[19] AKKAQUI, M.; COHEN, I.; ESNOUS, C.; LENOIR, V.; SOURNAC, M.; GIRARD, J.; PRIP-BUUS, C. «Modulation of the hepatic malonyl-CoA-carnitine palmitoyltransferase 1A partnership creates a metabolic switch allowing oxidation of *de novo* fatty acids». *Biochem. J.*, núm. 420 (2009), p. 429-438.

[20] ORELLANA-GAVALDA, J. M.; HERRERO, L.; MALANDRINO, M. I.; PAÑEDA, A.; RODRÍGUEZ-PEÑA, M. S.; PETRY, H.; ASINS, G.; DEVENTER, S. van; HEGARDT, F. G.; SERRA, D. «Molecular therapy for obesity and diabetes based on a long-term increase in hepatic fatty-acid oxidation». *Hepatology*, núm. 53 (2011), p. 821-832.

[21] MONSÉNÉGO, J.; MANSOURI, A.; AKKAQUI, M.; LENOIR, V.; ESNOUS, C.; FAUVEAU, V.; TAVERNIER, V.; GIRARD, J.; PRIP-BUUS, C. «Enhancing liver mitochondrial fatty acid oxidation capacity in obese mice improves insulin sensitivity independently of hepatic steatosis». *J. Hepatol.*, núm. 56 (2012), p. 632-639.

[22] DAVIES, L. C.; JENKINS, S. J.; ALLEN, J. E.; TAYLOR, P. R. «Tissue-resident macrophages». *Nat. Immunol.*, núm. 14 (2013), p. 986-995.

[23] HERRERO, L.; SHAPIRO, H.; NAYER, A.; LEE, J.; SHOELSON, S. E. «Inflammation and adipose tissue macrophages in lipodystrophic mice». *Proc. Natl. Acad. Sci. USA*, núm. 107 (2010), p. 240-245.

[24] KRISHNAN, J.; DANZER, C.; SIMKA, T.; UKROPEC, J.; WALTER, K. M.; KUMPF, S.; MIRTSCHINK, P.; UKROPCOVA, B.; GASPERIKOVA, D.; PEDRAZZINI, T.; KREK, W. «Dietary obesity-associated Hif1 α activation in adipocytes restricts fatty acid oxidation and energy expenditure via suppression of the Sirt2-NAD⁺ system». *Genes Dev.*, núm. 26 (2012), p. 259-270.

[25] GAO, X.; LI, K.; HUI, X.; KONG, X.; SWEENEY, G.; WANG, Y.; XU, A.; TENG, M.; LIU, P.; WU, D. «Carnitine palmitoyltransferase 1A pre-

vents fatty acid-induced adipocyte dysfunction through suppression of c-Jun N-terminal kinase». *Biochem. J.*, núm. 435 (2011), p. 723-732.

[26] MALANDRINO, M. I.; FUCHO, R.; WEBER, M.; CALDERÓN-DOMÍNGUEZ, M.; MIR, J. F.; VALCÁRCEL, L.; ESCOTÉ, X.; GÓMEZ-SERRANO, M.; PERAL, B.; SALVADÓ, L.; FERNÁNDEZ-VELEDO, S.; CASALS, N.; VÁZQUEZ-CARRERA, M.; VILLARROYA, F.; VENDRELL, J. J.; SERRA, D.; HERRERO, L. «Enhanced fatty acid oxidation in adipocytes and macrophages reduces lipid-induced triglyceride accumulation and inflammation». *Am. J. Physiol. Endocrinol. Metab.*, núm. 308 (2015), p. E756-E769.

[27] LÓPEZ, M.; LELLIOTT, C. J.; VIDAL-PUIG, A. «Hypothalamic fatty acid metabolism: a housekeeping pathway that regulates food intake». *Bioessays*, núm. 29 (2007), p. 248-261.

[28] HU, Z.; CHA, S. H.; CHOHNAN, S.; LANE, M. D. «Hypothalamic malonyl-CoA as a mediator of feeding behavior». *Proc. Natl. Acad. Sci. USA*, núm. 100 (2003), p. 12624-12629.

[29] LÓPEZ, M.; LAGE, R.; SAHA, A. K.; PÉREZ-TILVE, D.; VÁZQUEZ, M. J.; VARELA, L.; SANGIAO-ALVARELLOS, S.; TOVAR, S.; RAGHAY, K.; RODRÍGUEZ-CUENCA, S.; DEOLIVEIRA, R. M.; CASTAÑEDA, T.; DATTA, R.; DONG, J. Z.; CULLER, M.; SLEEMAN, M. W.; ÁLVAREZ, C. V.; GALLEGO, R.; LELLIOTT, C. J.; CARLING, D.; TSCHÖP, M. H.; DIÉGUEZ, C.; VIDAL-PUIG, A. «Hypothalamic fatty acid metabolism mediates the orexigenic action of ghrelin». *Cell. Metab.*, núm. 7 (2008), p. 389-399.

[30] OBICI, S.; FENG, Z.; ARDUINI, A.; CONTI, R.; ROSSETTI, L. «Inhibition of hypothalamic carnitine palmitoyltransferase-1 decreases food intake and glucose production». *Nat. Med.*, núm. 9 (2003), p. 756-761.

[31] MERA, P.; MIR, J. F.; FABRIÁS, G.; CASAS, J.; COSTA, A. S. H.; MALANDRINO, M. I.; FERNÁNDEZ-LÓPEZ, J. A.; REMESAR, X.; GAO, S.; CHOHNAN, S.; RODRÍGUEZ-PEÑA, M. S.; PETRY, H.; ASINS, G.; HEGARDT, F. G.; HERRERO, L.; SERRA, D. «Long-term increased carnitine palmitoyltransferase 1A expression in ventromedial hypothalamus causes hyperphagia and alters the hypothalamic lipidomic profile». *PLoS One*, núm. 9 (2014), p. e97195.

[32] GAO, S.; KEUNG, W.; SERRA, D.; WANG, W.; CARRASCO, P.; CASALS, N.; HEGARDT, F. G.; MORAN, T. H.; LOPASCHUK, G. D. «Malonyl-CoA mediates leptin hypothalamic control of feeding independent of inhibition of CPT-1 α ». *Am. J. Physiol. Regul. Integr. Comp. Physiol.*, núm. 301 (2011), p. R209-R217.

[33] GAO, S.; LANE, M. D. «Effect of the anorectic fatty acid synthase inhibitor C75 on neuronal activity in the hypothalamus and brainstem». *Proc. Natl. Acad. Sci. USA*, núm. 100 (2003), p. 5628-5633.

[34] LOFTUS, T. M.; JAWORSKY, D. E.; FREHYWOT, G. L.; TOWNSEND, C. A.; RONNETT, G. V.; LANE, M. D.; KUHAJDA, F. P. «Reduced food intake and body weight in mice treated with fatty acid synthase inhibitors». *Science*, núm. 288 (2000), p. 2379-2381.

[35] MERA, P.; BENTEBIBEL, A.; LÓPEZ-VIÑAS, E.; CORDENTE, A. G.; GURUNATHAN, C.; SEBASTIÁN, D.; VÁZQUEZ, I.; HERRERO, L.; ARIZA, X.; GÓMEZ-PUERTAS, P.; ASINS, G.; SERRA, D.; GARCÍA, J.; HEGARDT, F. G. «C75 is converted to C75-CoA in the hypothalamus, where it inhibits carnitine palmitoyltransferase 1 and decreases food intake and body weight». *Biochem. Pharmacol.*, núm. 77 (2009), p. 1084-1095.

Fatty acid metabolism and the basis of brown adipose tissue function

María Calderon-Dominguez^{a,b}, Joan F. Mir^{a,b}, Raquel Fucho^{a,b}, Minéia Weber^{a,b}, Dolors Serra^{a,b}, and Laura Herrero^{a,b}

^aDepartment of Biochemistry and Molecular Biology, School of Pharmacy, Institut de Biomedicina de la Universitat de Barcelona (IBUB), Universitat de Barcelona, Barcelona, Spain; ^bCIBER Fisiopatología de la Obesidad y la Nutrición (CIBEROBN), Instituto de Salud Carlos III, Madrid, Spain

ABSTRACT

Obesity has reached epidemic proportions, leading to severe associated pathologies such as insulin resistance, cardiovascular disease, cancer and type 2 diabetes. Adipose tissue has become crucial due to its involvement in the pathogenesis of obesity-induced insulin resistance, and traditionally white adipose tissue has captured the most attention. However in the last decade the presence and activity of heat-generating brown adipose tissue (BAT) in adult humans has been rediscovered. BAT decreases with age and in obese and diabetic patients. It has thus attracted strong scientific interest, and any strategy to increase its mass or activity might lead to new therapeutic approaches to obesity and associated metabolic diseases. In this review we highlight the mechanisms of fatty acid uptake, trafficking and oxidation in brown fat thermogenesis. We focus on BAT's morphological and functional characteristics and fatty acid synthesis, storage, oxidation and use as a source of energy.

ARTICLE HISTORY

Received 13 August 2015
Revised 13 October 2015
Accepted 12 November 2015

KEYWORDS

brown adipose tissue; fatty acid oxidation; lipid metabolism; obesity

Introduction

Importance of adipose tissue in obesity

Current life styles and continuous nutrient excess are increasing the incidence of obesity at an alarming rate, especially at younger ages. Worldwide there are more than 600 million obese subjects and, importantly, most of the world's population live in countries where overweight and obesity kills more people than underweight.¹ Very worrisome are the concurrent and parallel increases in the prevalence of pathologic conditions associated with obesity such as insulin resistance, cardiovascular and Alzheimer disease, cancer, and type 2 diabetes.

Over the last 2 decades the obesity epidemic has put a spotlight on the adipose tissue as a key player in the mechanisms involved in obesity-related disorders. Human fat consists of energy-storing white adipose tissue (WAT) and brown adipose tissue (BAT), which controls thermogenesis by dissipating energy to produce heat. In addition to adipocytes, adipose tissue is well vascularized and contains connective tissue and numerous immune cells such as macrophages, T and B cells, mast cells and neutrophils.² It has been demonstrated that obesity-induced insulin resistance is due to several factors: ectopic fat deposition,³ increased inflammation and endoplasmic reticulum

(ER) stress,^{4,5} adipose tissue hypoxia and mitochondrial dysfunction,^{6,7} and impaired adipocyte expansion and angiogenesis.^{8–10} Fat is also an active endocrine tissue that secretes hormones such as leptin, adiponectin or resistin and inflammatory cytokines such as tumor necrosis factor α (TNF α), interleukin (IL)-6, IL-1 β , etc. in response to several stimuli. Adipose tissue is therefore a complex and active organ controlling very important metabolic pathways such as energy expenditure, appetite, insulin sensitivity, endocrine and reproductive functions, inflammation and immunity.

Rediscovery of human active BAT

The fusion of positron-emission tomography (PET) and computed tomography (CT) images has allowed radiologists to retrieve both functional and structural information from a single image. In the course of using PET-CT to detect and stage tumors in humans, active BAT that increased after cold exposure was rediscovered.^{11,12} Until that moment BAT was considered exclusive to rodents and human neonates. However, the breakthrough came in 2009, when 5 independent research groups used PET-CT to identify the presence

CONTACT Laura Herrero  lherrero@ub.edu  Department of Biochemistry and Molecular Biology, School of Pharmacy, Institut de Biomedicina de la Universitat de Barcelona (IBUB), Universitat de Barcelona, Av. Diagonal, 643, Barcelona 08028, Spain.

© María Calderon-Dominguez, Joan F. Mir, Raquel Fucho, Minéia Weber, Dolors Serra and Laura Herrero
This is an Open Access article distributed under the terms of the Creative Commons Attribution-Non-Commercial license (<http://creativecommons.org/licenses/by-nc/3.0/>), which permits unrestricted non-commercial use, distribution, and reproduction in any medium, provided the original work is properly cited. The moral rights of the named author(s) have been properly cited. Published with license by Taylor & Francis Group, LLC

and relevance of BAT in adult humans.¹³⁻¹⁷ All showed major depots of metabolically active fat in the cervical-supravicular region. Furthermore, these depots expressed type 2 iodothyronine deiodinase (DIO2), the β 3-adrenergic receptor, and the brown adipocyte-specific protein, uncoupling protein 1 (UCP1), which physiologically uncouples ATP production from mitochondrial respiration, thereby dissipating energy as heat.¹⁸ The expression of these proteins indicated the potential responsiveness of human BAT to both hormonal and pharmacological stimuli. Here, we review the possibility that BAT could be induced to enhance its lipid-burning function even further and thus be an effective target to fight against obesity and associated metabolic disorders.

Brown adipose tissue characteristics

BAT localization and morphology

Our knowledge of BAT has been significantly influenced by studies in rodent models. There, BAT is situated at the interscapular, cervical, mediastinal and retroperitoneal regions.¹⁹ While in infants BAT is mainly found in the interscapular area, in adult humans BAT is localized in a region extending from the anterior neck to the thorax.²⁰

In contrast to white adipocytes, which are unilocular, with polygonal morphology that optimizes their fat storing capacity, brown adipocytes are multiloculate and their color is due to their high mitochondrion content and vascular supply.²¹ BAT thermogenesis takes place in its numerous, densely-packed mitochondria containing the BAT-specific inner membrane protein UCP1. Multilocular lipid stores provide a rapid source of fatty acids (FAs) for activated mitochondria. FAs released into the circulation by the WAT are also an important source of FAs for brown adipocytes. Thermogenesis is classified into: 1) Obligatory thermogenesis, which takes into account the standard metabolic rate (energy used for basic function of cells and organs) and the heat generated during food metabolism (digestion, absorption, processing and storing of energy); and 2) Adaptive thermogenesis or heat production in response to environmental temperature and diet. Adaptive thermogenesis can be further divided into: cold-induced shivering thermogenesis, which takes place in skeletal muscle; cold-induced non-shivering thermogenesis, which takes place mainly in brown fat; and diet-induced thermogenesis triggered by overfeeding, which also takes place in BAT.²² Thus, BAT generates heat, with 2 main consequences: protection against cold exposure via non-shivering thermogenesis; and dissipation of the excess of energy from food. Therefore, BAT can be considered as

an organ that burns off excess lipids, and further examination of this property may lead to the development of novel strategies against diet-induced obesity.

Molecular BAT signature: beige and brown adipocytes

Comprehensive research is being done to define the still under debate cellular heterogeneity of human fat.²³ At least 2 types of thermogenic adipocyte exist in rodents and humans: classical brown adipocytes and beige (also called brite) adipocytes. They have both anatomical and developmental differences. While brown adipocytes are mainly located in the above-mentioned BAT depots, beige adipocytes co-locate with white adipocytes in WAT near vascular and neural innervation and appear in response to certain stimuli, such as chronic cold exposure or β 3-adrenergic signaling. In adult humans the ratio of brown to beige increases as one moves deeper within the neck and back.^{20,24-27}

BAT releases endocrine factors such as insulin-like growth factor I (IGF-1), IL-6 or fibroblast growth factor 21 (FGF21).²⁸ Brown adipocytes differ from white adipocytes due to their high expression of DIO2, the lipolytic regulator cell death-inducing DNA fragmentation factor- α -like effector A (CIDEA), and the transcription co-regulators PR domain-containing 16 (PRDM16) and peroxisome proliferator activated receptor gamma coactivator 1 α (PGC1 α).^{29,30} Beige and brown adipocytes have overlapping but distinct gene expression patterns.³¹ Both express the main thermogenic and mitochondrial genes, including *Ucp1*. However, some surface markers such as CD137, TBX1 and TMEM26 seem to be specific to murine beige adipocytes^{24,27} while other genes, like *Zic1* and *Lhx8*, appear to specifically mark classic brown adipocytes.^{20,32} Basal UCP1 expression and uncoupled respiration before hormonal stimulation are highest in brown fat cells and lower in beige cells, the lowest being found in white fat cells.²⁷ However, stimulation with a β 3-adrenergic agonist elevates UCP1 expression in beige cells to levels seen in brown fat cells (fold-change compared to white cells).^{27,33} This suggests that beige cells have a unique molecular signature with a dual role. They store energy in the absence of thermogenic stimuli but initiate heat production when appropriate signals are received.²⁷ White-to-beige conversion of adipocytes is a potential therapeutic approach to targeting obesity; however, the signals involved in this process still remain unclear.

Brown adipocytes arise from mesenchymal precursor cells common to the myogenic cell lineage and express myogenic factor 5 (*Myf5*).³⁴ Beige adipocytes derive from precursor cells that differ from those in classical BAT and are closer to the white adipocyte cell lineage.

Thus, while brown adipocytes come from a Pax7⁺/Myf5⁺ lineage shared with skeletal muscle, white and beige adipocytes derive from Pax7⁻/Myf5⁻ cells via distinct precursor cells. Beige adipocytes differentiate following activation by cold or other stimuli, and when the cold challenge is ceased, they become inactive, taking on the morphology of a white adipocyte.³⁵ However, the cell lineage and developmental origin of the adipose tissue is not so simple. Individual brown and white fats contain a mixture of adipocyte progenitor cells derived from Myf5⁺ and Myf5⁻ lineages, with numbers varying depending on the depot location. In fact, beige adipocytes in the retroperitoneal WAT are Myf5⁺.³⁶ For further information about the developmental origin of white, beige and brown adipocytes see other excellent reviews.^{34,37,38}

At least 2 mechanisms have been postulated to occur during the browning process: transdifferentiation of white into beige adipocytes vs. *de novo* brown adipogenesis. The transdifferentiation process is the conversion of a differentiated somatic cell type into another one.³⁹ The transdifferentiation of white into beige adipocytes has been reported in several studies.⁴⁰⁻⁴³ On the other hand, Lee *et al.* have shown that β 3-adrenergic stimulation induces the proliferation and further differentiation of precursors in WAT.⁴⁴ Furthermore, Myf5⁺ precursors have also been reported to differentiate into white adipocytes.^{36,45} Thus, whether the browning process arises from transdifferentiation or *de novo* brown adipogenesis is far from being fully understood. One could hypothesize that the 2 processes might take place simultaneously and to a different extent depending on the adipose depot or browning stimuli.

BAT activity in pathological conditions

Human studies showed that BAT was reduced in aging and in obese and diabetic patients, indicating that BAT participates in both cold-induced and diet-induced thermogenesis.¹³ This significant discovery highlights that any strategy able to increase the mass or activity of BAT could potentially be a promising therapy for obese and diabetic patients. In contrast, enhanced BAT activation has been described as a negative effect on cancer cachexia.⁴⁶ In this study, mice with cachexia-inducing colorectal tumor showed increased BAT activity despite thermoneutrality, indicating that BAT activation may contribute to impaired energy balance in cancer cachexia. Hibernoma is another BAT pathological condition. A hibernoma is a benign tumor of BAT that up to date has no clear explanation of its cause. It is very rare in humans and it is successfully treated by complete surgical excision.^{47,48} It has shown to

express UCP1 and thus potentially contribute to whole-body energy balance.

Activators of thermogenesis

Despite some controversy, a large body of evidence indicates that browning entails the enhancement of thermogenesis within WAT, i.e. increased expression and activity of UCP1 in what are normally considered WAT depots.⁴⁹ Several factors have been described to activate the browning of the adipose tissue such as irisin,⁵⁰ natriuretic peptides,⁵¹ bone morphogenetic protein 7 (BMP7)⁵² and BMP8b,⁵³ norepinephrine,⁵⁴ meteorin-like,⁵⁵ bile acids,⁵⁶ adenosine,⁵⁷ or FGF21.⁵⁸ Interestingly, recent studies have shown activation of human BAT by the β 3-adrenergic receptor agonist mirabegron.⁵⁹ β 3-adrenergic receptor is expressed in humans on the surfaces of brown and white adipocytes and urinary bladder. Cypess *et al.* administered 200 mg of oral mirabegron, currently approved to treat overactive bladder, to healthy and young humans. Mirabegron acutely stimulated human BAT thermogenesis and increased resting metabolic rate. Further studies would be needed to explore the specificity of mirabegron's mechanism of action, possible adverse effects such as tachycardia, and the dose used, which was 4-fold higher than that prescribed for overactive bladder.

Although a large number of browning agents have been described (extensively reviewed elsewhere)^{60,61} some studies showed that browning was a secondary consequence of enhanced heat loss, e.g. because of fur disruption in rodents.⁴⁹ The search for potential therapeutic browning agents to increase metabolism at thermoneutrality, to function through mechanisms other than those affecting heat loss and to finally decrease obesity should thus continue.

Fatty acid storage

FA synthesis, storage and metabolism are essential during thermogenesis because they are required for UCP1 proton transport activity in BAT.^{62,63} Fundamentally, brown adipocytes have 2 mechanisms to obtain lipids: FA uptake via lipoproteins carriers and *de novo* FA synthesis, also known as lipogenesis.

Fatty acid uptake

While brown adipocytes synthesize FAs, the enzyme lipoprotein lipase (LPL), bound at the endothelial cell surface, is the major source of FAs in BAT.⁶⁴ After a meal, dietary lipids are transported by chylomicrons and very low density proteins (VLDL) via lymphatic vessels into the bloodstream. Once triglyceride (TG) rich-

lipoproteins reach the bloodstream, LPL hydrolyzes them into free FAs (FFAs) and monoacylglycerol (MG) for BAT uptake. Indeed, BAT is an efficient modulator of triglyceridemia and it is contemplated as a major plasma lipid-clearing organ in rodents.⁶⁵⁻⁶⁷ In fact, FA uptake under cold exposure is higher in BAT than in skeletal muscle.⁶⁵ Under cold exposure, the β 3-adrenergic pathway enhances BAT FA flux and clearance via increased expression and activity of LPL.⁶⁵ However, the increase in LPL activity has also been shown to trigger adiposity and insulin resistance.⁶⁸ Adipocyte-specific LPL KO animals show an increase in FAs derived from lipogenesis and a decrease in polyunsaturated FAs, accompanied by an increase in the expression of lipogenic genes.⁶⁹ Glycosylphosphatidylinositol-anchored high density lipoprotein binding protein 1 (GPIHBP1) transports LPL across capillary endothelial cells, and GPIHBP1 KO mice show mislocated LPL in many tissues, including BAT,⁷⁰ decreased TG content and deficient lipolysis.⁷¹ Administration of PPAR γ agonists, such as rosiglitazone, in rodents increases BAT TG clearance and LPL activity, while lipogenesis is not increased. This suggests that under rosiglitazone treatment brown adipocytes metabolize FAs derived from TG hydrolyzed from lipoproteins or recycled from lipolysis.⁷²

Fatty acid transport

Once FAs are released by LPL, they are taken up into cells by plasmatic membrane receptors and transported for further utilization or storage.^{65,73-75} The most important FA transporters in BAT are the following (Fig. 1):

Cluster of differentiation 36 (CD36)

This integral membrane protein is expressed in BAT among other tissues.⁷³ CD36 belongs to the class B scavenger receptor family of cell surface proteins, whose main function is to translocate FAs, released by LPL activity, across the plasmatic membrane and thus provide a substrate for BAT thermogenesis.⁶⁵ Under cold exposure, CD36 expression and activity increase (Fig. 1).⁶⁵ However, CD36 is not a simple translocase; it is considered a lipid sensor and a regulator of FA uptake and transport in adipocytes.⁷⁶⁻⁷⁸ CD36 KO mice die after 24 hours of cold exposure, which implicates CD36 in thermogenesis.⁶⁵ In addition, CD36 genetic variability has been associated with body weight differences in humans.⁷⁹

FA transport proteins (FATPs)

There are 6 isoforms of FATPs. FATP1 and 4 can be found specifically in BAT (extensively reviewed

elsewhere).⁸⁰ These proteins translocate FAs into cells.⁸¹ They display very long-chain acyl-CoA synthetase activity,^{64,82} and their overexpression increases FA uptake.⁸³

G-protein-coupled receptors (GPCRs)

GPCRs comprise a family of proteins that respond to several ligands, and trigger a cascade of intracellular signaling (extensively reviewed elsewhere).⁸⁴ GPR41 (also known as FFA3) and GPR120 are activated by medium and long-chain FFA in BAT, and they are considered as sensors that maintain cell lipid homeostasis.⁸⁵ Interestingly, GPR120 mRNA expression increases under cold exposure (3).⁸⁶

Fatty acid binding proteins (FABPs)

Once in the cytoplasm, FFAs are minimally soluble. To prevent disruption of membrane or lipotoxicity, cells have soluble proteins that bind FFAs and transport them.⁸⁷ Brown adipocytes harbour 3 different isoforms: FABP3, FABP4 and FABP5.⁸⁸ FABP4, commonly known as adipocyte protein 2 (aP2), has been extensively used as a marker of adipocyte differentiation.⁸⁹ Although FABP4 is the most abundantly expressed isoform in BAT, only FABP3 and FABP5 are increased by cold exposure in rats.^{88,90} Interestingly, FABP3 is overexpressed in mice with diet-induced obesity and in UCP1 KO mice, and it is associated with increased thermogenesis.⁹¹ Thus, FFAs bind to FABPs present in brown adipocytes and are either stored or utilized to maintain thermogenesis (Fig. 1).

Lipogenesis

De novo FA synthesis or lipogenesis is the metabolic pathway that synthesizes FAs and ultimately induces TG synthesis.^{92,93} Excellent studies on WAT report that glucose uptake, a preliminary step in *de novo* FA synthesis, is also involved in the regulation of lipogenesis.^{94,95} Whether BAT contributes to this process is still unclear. A recent study examined the dynamics of *de novo* lipogenesis and lipolysis in classic brown, subcutaneous beige and classic white adipose tissues during chronic β 3-adrenergic receptor stimulation.⁹⁶ Sustained β 3-adrenergic stimulation increased *de novo* lipogenesis, TG turnover, and the expression of genes involved in FA synthesis and oxidation similarly in all adipose depots indicating that FA synthesis and FAO are tightly coupled during chronic β 3-adrenergic stimulation.

Lipogenesis takes place in the cytosol and it can be summarized in 3 steps: synthesis of FAs from acetyl-CoA,

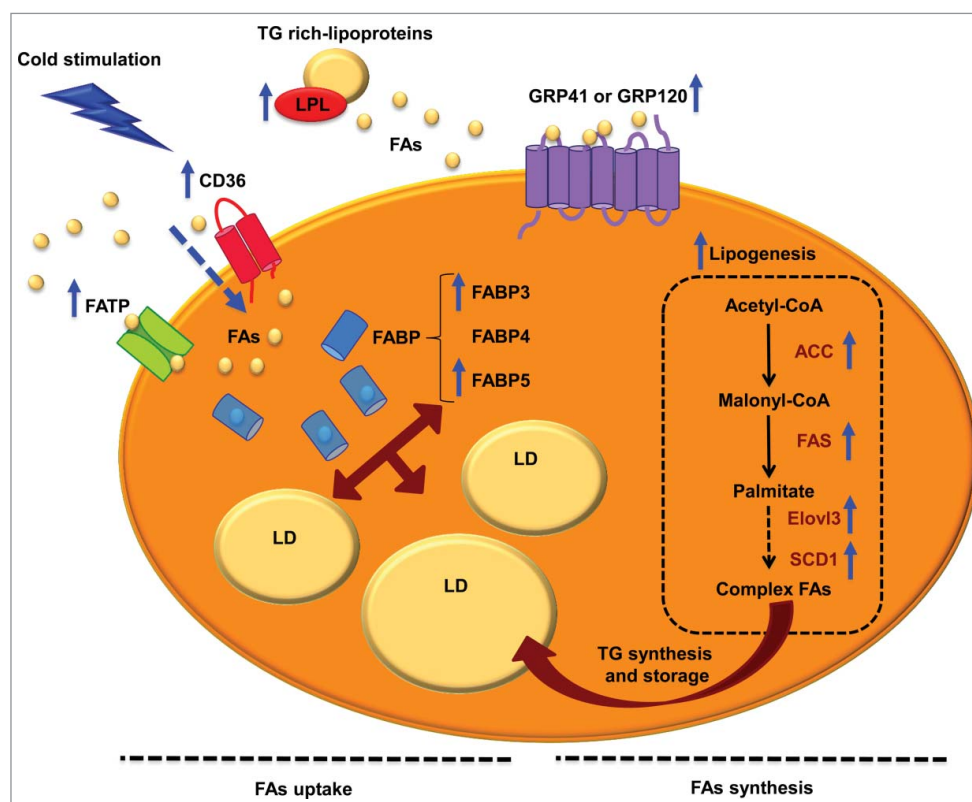


Figure 1. FA uptake and lipogenesis in brown adipocytes. Schematic representation of FA uptake, transport, synthesis and storage in brown adipocytes, which provide substrate to mitochondria for thermogenesis. While brown adipocytes synthesize FAs, the enzyme lipoprotein lipase (LPL) is the major source of FAs in BAT. Once triglyceride (TG) rich-lipoproteins reach the bloodstream, LPL hydrolyzes them into FFAs for BAT uptake. FAs are sensed and taken up by FFAs 3 (FFA3) proteins, cluster of differentiation 36 (CD36) and/or FA transport proteins (FATPs). Inside the cytoplasm, FAs are transported by FA binding proteins (FABP). On the other hand, FAs can be synthesized by lipogenesis. This process takes place in the cytosol, and the first phase begins with the formation of malonyl-CoA from acetyl-CoA by the action acetyl-CoA carboxylase (ACC). Then, FA synthetase (FAS) catalyzes various reactions to finally generate palmitate, a 16-carbon saturated FA. In BAT, the last phases of lipogenesis are carried out by very long chain FA 3 (ELOVL3) and stearoyl-CoA desaturase 1 (SCD1). Once FAs are synthesized they can be esterified, becoming available for FAO or stored as TG in lipid droplets (LD). Blue arrows indicate enhanced processes or expression of proteins after cold stimulation and β 3-adrenergic receptor activation.

elongation and desaturation. Lipogenesis begins with the carboxylation of acetyl-CoA to malonyl-CoA, the committed step catalyzed by acetyl-CoA carboxylase (ACC), which requires biotin cofactor.^{97,98} Finally, FA synthetase (FAS), a multifunctional cytosolic protein, catalyzes different reactions to form palmitate, a 16-carbon saturated FA.⁹³ It has been shown that adipose-specific FAS KO mice have increased energy expenditure, which comes from the browning of subcutaneous WAT.⁹⁹

In the second phase of lipogenesis, FAs derived from the FAS enzymatic reaction, are elongated by membrane-bound enzymes mostly localized in the ER.⁹³ This process is induced by the elongation of very long chain FA (ELOVL) proteins, which have 7 members in mice and humans.¹⁰⁰ Among them, Elov13 is expressed in BAT,¹⁰¹ and its expression and activity are upregulated under cold conditions to re-establish the intracellular pool of TG and preserve lipid homeostasis.¹⁰²⁻¹⁰⁴

ELOVL3 KO mice are resistant to diet-induced obesity, showing an increase in energy expenditure.¹⁰⁴

The final phase of lipogenesis is the desaturation of FAs. This process is catalyzed by desaturases, such as stearoyl-CoA desaturases (SCDs), which introduce double bonds at a specific position in a FA chain.^{93,97} SCD1 is the predominant isoform in adipose tissue and liver, and its downregulation in liver prevents diet-induced obesity.^{105,106} SCD1 KO mice show an increase in glucose uptake and glycogen metabolism, higher energy expenditure and basal thermogenesis in BAT.¹⁰⁷

Once FAs have been synthesized they can be esterified to be used for fatty acid oxidation (FAO) or stored as TG in lipid droplets. In BAT, the proper levels of TG are associated with thermogenic activity.¹⁰⁸ Since TG are composed of molecules of glycerol and 3 esterified FAs, TG synthesis depends on intracellular levels of glycerol-3-phosphate (G3P), the activated form of glycerol and

first intermediary in TG synthesis. Thus, G3P levels are preserved under rigorous control in brown adipocytes.⁶⁶ It has been shown that rosiglitazone, a PPAR γ agonist, increases BAT glycerolkinase activity, which phosphorylates glycerol generating G3P.⁶⁷ Since G3P comes from glucose, glucose metabolism plays a key role in BAT, as an important glucose-clearing organ, specifically under sympathetic activation.⁶⁵ In fact, G3P is a major substrate for BAT respiration.¹⁰⁹

In conclusion, coordinated FA uptake, transport and synthesis contribute to thermogenesis in BAT (Fig. 1). For this reason, the maintenance of the intracellular pool of TG to preserve lipid homeostasis in brown adipocytes is so important.^{110,111} Indeed, any of these processes might be a potential target in the treatment of obesity-related disorders, such as insulin resistance and diabetes.

Fatty acid storage

Cells package the excess of intracellular lipids in a phylogenetically conserved organelle called lipid droplet, preventing the lipotoxicity of lipids and cholesterol in the cytoplasm.^{112,113} Lipid droplets are composed of a neutral lipid core (cholesteryl ester and TGs) covered by a phospholipid monolayer, which contains proteins that regulate lipolysis. Among the lipid droplet membrane proteins found in brown adipocytes we will highlight fat storage-inducing transmembrane protein 2 (FITM2/FIT2), CIDEA and fat-specific protein 27 (FSP27 or CIDEC).

FITM2/FIT2 is strongly expressed in brown adipocytes and it determines the number of new lipid droplets formed in these cells.¹¹⁴ FIT2 KO mice show few but larger lipid droplets in interscapular BAT without changes in cellular TG levels.¹¹⁵ Thus, FIT2 is not essential for lipid droplet formation but it is required for normal storage of TG *in vivo*.

CIDEA is one of the 3 members of cell death-inducing DFF45-like effector (CIDE) family of proteins, which has emerged as an important regulator for various aspects of metabolism.¹¹⁶ CIDEA is highly expressed in lipid droplet membranes and mitochondria of brown adipocytes. It is involved in the browning phenomenon and it is considered as a BAT differentiation marker.^{117,118} CIDEA plays an inhibitory role during thermogenesis because it negatively modulates the activity of UCPI1, being the first protein known to interact directly with an uncoupler protein.¹¹⁹⁻¹²¹ Moreover, CIDEA mRNA and protein are down-regulated after cold exposure¹²¹ and CIDEA-null mice are resistant to diet-induced obesity.¹¹⁸

FSP27 also belongs to the CIDE family, and it is over-expressed during adipogenesis in BAT. It has been

proposed as a novel lipid droplet protein that promotes TG storage and inhibits lipolysis, playing a key role in body energy homeostasis.^{122,123} FSP27 interacts directly with another lipid droplet protein, perilipin 1, which is involved in lipolysis by indirect activation of the adipose triglyceride lipase (ATGL) at the lipid droplet surface.¹²³ Furthermore, FSP27 KO mice have larger lipid droplets and higher TG serum levels.¹²⁴

Thus, the above-mentioned proteins involved in FA storage contribute to the multilocular phenotype of brown adipocytes. Lipid droplets prevent lipotoxicity and provide FAs as substrates for mitochondrial thermogenesis. Therefore, the regulation and function of these proteins might be a target for enhancing BAT activity.

Fatty acids as a source of energy

Lipolysis

Intracellular lipolysis is the catabolic process that allows cells to obtain FAs and glycerol from the breakdown of TG stored in lipid droplets. Cells use these FAs and glycerol endogenously in times of metabolic need with the exception of WAT, which can also export them to circulation so they can reach other tissues in fasting or exercise periods.¹²⁵ In BAT, lipolysis is vital to its main physiological function, the cold response. To raise body temperature BAT dissipates energy as heat and mobilizes FAs from the breakdown of TGs stored in lipid droplets to mitochondria for thermogenesis.¹⁰⁸ Lipolysis can be classified in 2 types depending on the pH-optimum of action of the enzymes involved. Accordingly, there is neutral lipolysis, which relies on 3 key enzymes that work at a pH-optimum of 7, and acid lipolysis that depends on lysosomal degradation of TG by acidic lipases. Next we will focus on neutral lipolysis.

Neutral lipolysis

Neutral lipolysis takes place in the cytosol and it is the result of the action of 3 consecutive lipases that hydrolyze each ester bond of TG to obtain 3 FAs and glycerol. The 3 major lipases are ATGL, hormone sensitive lipase (HSL) and monoacylglycerol lipase (MGL).

ATGL/Desnutrin/calcium-independent phospholipase A2 ζ (iPLA2 ζ) was discovered in 2004 by 3 independent laboratories.¹²⁶⁻¹²⁸ It is strongly expressed in both WAT and BAT and performs the first step of TG lipolysis, the hydrolysis of TG into diacylglycerides (DG) and FAs (Fig. 2).¹²⁹ It exhibits high substrate specificity for TG and it is associated with lipid droplets.¹²⁶ ATGL regulation is complex and mRNA or protein levels of the enzyme do not always correlate with enzyme activity.

This happens because ATGL has strong post translational regulation that often requires accessory proteins.¹³⁰ CGI-58 (Comparative gene identification-58) is a coactivator of ATGL that is necessary for full hydrolase activity.¹³¹ On the other hand, G0S2 (G0/G1 switch gene 2) inactivates ATGL.¹³² ATGL deficient mice accumulate TGs in all organs and have enlarged fat depots, especially BAT, which also displays defective thermogenesis.¹³³ Moreover, aP2-ATGL overexpressing mice display increased lipolysis and FAO in WAT and increased thermogenesis, resulting in higher energy expenditure and resistance to obesity.¹³⁴ Microarrays from ATGL KO BAT indicate a decrease in mRNA expression of genes involved in FAO and down-regulation of PPAR α target genes.^{135,136} In addition, a study using ATGL knock down brown adipocytes demonstrated that ATGL is required for the maximal induction of genes involved in

FAO and mitochondrial electron transport.¹³⁷ All together, these results point to the crucial role of lipolysis and its first step, TG hydrolysis by ATGL, in thermogenesis.

HSL performs the second step in TG lipolysis, hydrolyzing DG into MG and FAs (Fig. 2).¹³⁸ Similarly to ATGL, HSL mRNA and protein expression are highest in WAT and BAT.^{139,140} Although DG are its preferred substrate, HSL can also hydrolyze TG, cholesterol esters, MGs and retinyl esters.¹⁴¹ Before ATGL was known, HSL was believed to be the rate-limiting enzyme for TG hydrolysis. However, HSL $^{-/-}$ mice efficiently hydrolyze TG and accumulate large amounts of DG, indicating that, *in vivo*, HSL has a more important role as a DG than as a TG hydrolase.¹⁴² Activation of HSL occurs in 2 steps: protein phosphorylation and binding to perilipins.¹⁴³ HSL has 5 putative phosphorylation sites and

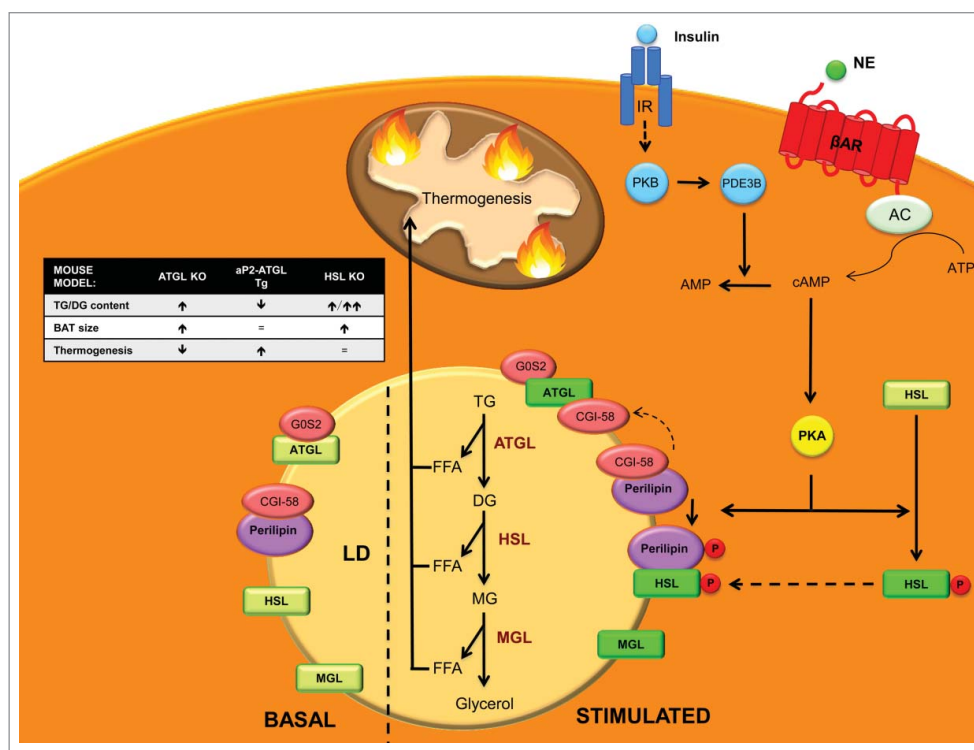


Figure 2. Neutral lipolysis players and regulation in BAT. Neutral lipolysis allows cells to obtain 3 free fatty acids (FFAs) and glycerol from the hydrolysis of triglycerides (TG). Three enzymes control this process: adipose triglyceride lipase (ATGL), which hydrolyzes TG into diacylglycerol (DG), hormone sensitive lipase (HSL), which has high affinity for DG and converts them into monoacylglycerols (MG) and monoacylglycerol lipase (MGL), which finalizes the hydrolysis of MG into glycerol and FFA that are used as a fuel for thermogenesis. In basal state ATGL is inhibited by G0/G1 switch gene 2 (G0S2) and ATGL co-activator comparative gene identification-58 (CGI-58) is kidnapped by perilipin. In addition, HSL is located in the cytosol and thus unable to reach its substrates. Upon β 3-adrenergic stimulation, adenyl cyclase (AC) increases cAMP levels that activate protein kinase A (PKA), which phosphorylates HSL promoting its translocation to the membrane of lipid droplets (LD). PKA also phosphorylates perilipin, which releases CGI-58 that can then fully activate ATGL. Phosphorylated perilipin also enhances HSL activity. On the other hand, insulin stimulation, through protein kinase B (PKB) activates phosphodiesterase 3B (PDE3B) which converts cAMP into AMP decreasing PKA activation and its lipolytic action. Figure insert: mouse models of the enzymes involved in neutral lipolysis. ATGL KO mice accumulate TGs and have enlarged BAT, which displays defective thermogenesis.¹³³ aP2-ATGL overexpressing mice show a reduction in TGs and increased thermogenesis.¹³⁴ HSL KO mice accumulate TGs and specially large amounts of DG leading to an enlarged BAT.¹⁴²

one of the most widely studied kinases that regulate its activity is cAMP-dependent Protein Kinase (PKA). Other kinases include AMPK, extracellular signal-regulated kinase (ERK), glycogen synthase kinase-4 and Ca²⁺/calmoduline dependent kinase II.¹³⁰

Glucagon, adrenaline or β 3-adrenergic agonist stimulation, through adenylyl cyclase (AC) activation increases cyclic AMP (cAMP) levels within the cell. This activates PKA that in turn phosphorylates HSL on serines 659 and 660, promoting its translocation from the cytoplasm to lipid droplets, where it acts on its substrates (Fig. 2).¹⁴⁴ Perilipins have an important role mediating this translocation, and PKA-mediated phosphorylation of perilipin is necessary for HSL translocation to lipid droplets and full induction of HSL activity. On the other hand, insulin activates cAMP phosphodiesterase, promoting cAMP hydrolysis, lowering PKA activity, HSL activation and lipolysis.¹⁴⁴ Mice lacking HSL display normal thermogenesis¹⁴⁵ and are not cold sensitive despite a lipolytic defect that results in brown adipocyte hypertrophy due to TG and DG accumulation. Apparently, during HSL deficiency sufficient amounts of FAs that are not HSL-dependent are mobilized for mitochondrial heat production. Later work on HSL null mice established that HSL KO mice are resistant to high-fat diet (HFD) effects due to an increase in energy expenditure.¹⁴⁶ This was linked to increased UCP1 and carnitine palmitoyltransferase (CPT) 1 expression levels in white adipocytes as well as an increase in white adipocyte mitochondrial size (see section 4.2.1 for more information). White adipocytes had increased basal O₂ consumption and increased uncoupling. In addition, HSL is required to sustain normal expression levels of retinoblastoma protein (pRb) and receptor interacting protein 140 (RIP140), which both promote differentiation into the white, rather than the brown, adipocyte lineage. Thus, HSL may be involved in the determination of white versus brown adipocytes during adipocyte differentiation.¹⁴⁶

MGL specifically hydrolyzes MG derived from intracellular and extracellular TG hydrolysis and phospholipid hydrolysis into FAs and glycerol, culminating the lipolysis process (Fig. 2). It is ubiquitously expressed in tissues and localizes in cell membrane, cytoplasm and lipid droplets.¹⁴⁷ MGL has been implicated in the degradation of the bioactive MG 2-arachidonoyl glycerol, which is a potent endogenous agonist of cannabinoid receptors.¹⁴⁸

Upon lipolysis stimulation the most important mechanisms regulating lipolysis are: 1) Activation of ATGL by CGI-58; and 2) PKA-mediated phosphorylation of HSL and perilipin 1 (Fig. 2). In basal state, CGI-58 is bound and kidnaped by perilipin 1, and thus unable to activate ATGL. In addition, HSL is located in the cytosol far

from its substrates. Upon hormonal stimulation, PKA phosphorylates HSL, promoting its translocation to the lipid droplet surface, where it hydrolyzes its substrates.^{149,150} In addition, PKA phosphorylates perilipin 1, liberating CGI-58, which is then available to bind and activate ATGL.¹⁵¹

The final result of lipolysis is the provision of energy to the cell in the form of FFAs and glycerol. Elevated levels of FFAs can be toxic for cells.⁸ Brown adipocytes can prevent this lipotoxicity by matching this increment in FFAs with an increase in oxidative capacity. β 3-adrenergic stimulation triggers lipase activation, resulting in a rise of lipolytic products that act as ligands of PPAR α and PPAR δ . PPAR activation promotes expression of oxidative genes such as UCP1 or PGC1 α and as a result expands the oxidative capacity to match FA supply.¹³⁷ These findings highlight the importance of coupling lipolysis with increased oxidative capacity, which ultimately depends on the uptake of FAs to the mitochondria for FAO by carnitine acyltransferases.

Fatty acid oxidation

Consistent with its physiological role, BAT presents one of the highest FAO rates in the body.¹⁵² Most of the oxidation of longchain fatty acids (LCFAs) to acetyl-CoA takes place in the mitochondrial matrix, although peroxisomal FAO has also been implicated in thermogenesis.

Mitochondrial fatty acid oxidation

Traditionally, research on the regulation of BAT thermogenesis has focused on the central role of UCP1 in maximizing rates of proton leak and heat production. In fact, FAs and HFD activate UCP1 and diet-induced thermogenesis.¹⁵³⁻¹⁵⁵ However, studies by Yu *et al.*¹⁵⁶ support the hypothesis that additional systems and genes cooperate in the thermogenic system. These authors demonstrated that cold induces simultaneous FA synthesis and FAO in murine BAT. Similar conclusions were obtained by Mottillo *et al.*⁹⁶ In addition, it has recently been reported in primary brown adipocyte culture that intracellular FA levels are critical for thermogenesis¹⁵⁷ and that in rodents maximal BAT thermogenesis relies on the levels of LCFA pool, which activates entry to the mitochondria.¹⁵⁸ Acyl-CoA synthetase-1 (ACSL) mediates the conversion of FAs to acyl-CoA and specifically directs them toward mitochondrial FAO via the CPT1 system (Fig. 3). Experiments with ACSL KO mice showed that ACSL is required for cold thermogenesis.¹⁵⁹

The CPT system permits the entry of LCFAs into the mitochondrial matrix, where they can undergo FAO.

The first component of the system, CPT1 is located on the mitochondrial outer membrane (Fig. 3). This enzyme catalyzes the *trans* esterification of a fatty acyl group from CoA to carnitine, which is considered the rate-limiting step in the regulation of mitochondrial FAO of FAs.^{160,161} Acylcarnitines are shuttled to the mitochondrial matrix by the transporter carnitine/acylcarnitine translocase (CACT). Once inside the mitochondria, acylcarnitines are converted to acyl-CoA by CPT2, located in the inner mitochondrial membrane, and can thus enter the FAO cycle. There are 3 isoforms of CPT1, denoted CPT1A,^{162,163} CPT1B¹⁶⁴ and CPT1C.¹⁶⁵ They differ in their sequence, tissue distribution, intracellular location, kinetics and malonyl-CoA sensitivity. CPT1B is strongly expressed in BAT, skeletal muscle, heart, testis and, in some species, in WAT (human, rat and hamster)^{108,166} while CPT1A is predominant in other tissues such as liver, kidney, lung, ovary, spleen, brain, intestine, mouse WAT and pancreas. CPT1C appears to be expressed exclusively in the neurons and testis. While CPT1A and B are located on the mitochondrial outer membrane and both isoforms are involved in the regulation of the flux

of FAs into the mitochondria, CPT1C has been found on the ER membrane¹⁶⁷ and its function seems to be related with ceramide metabolism rather than FAO.^{168,169}

CPT1A and B isoforms have high sequence similarity but show important kinetic differences. In particular, they differ in their affinities for the substrate carnitine and their physiological inhibitor malonyl-CoA,¹⁷⁰ which is synthesized from acetyl-CoA by ACC and is degraded by malonyl-CoA decarboxylase.¹⁷¹ CPT1B has higher affinity for the inhibitor malonyl-CoA and lower affinity for carnitine than CPT1A.^{172,173} Doh et al.¹⁵² examined the relation between the long-chain FAO rate and the CPT1A and CPT1B activity in different tissues. They found that all the tissues containing CPT1B showed a strong positive correlation between palmitate oxidation rate and the CPT1 activity and, among the tissues with CPT1B (heart, red and white gastrocnemius and BAT), BAT showed the highest palmitate oxidation and CPT1 activity. In addition, mice lacking CPT1B die during cold-exposure as a result of their inability to perform thermogenesis.¹⁷⁴ These observations indicate that CPT1B may play an important role in enhancing BAT

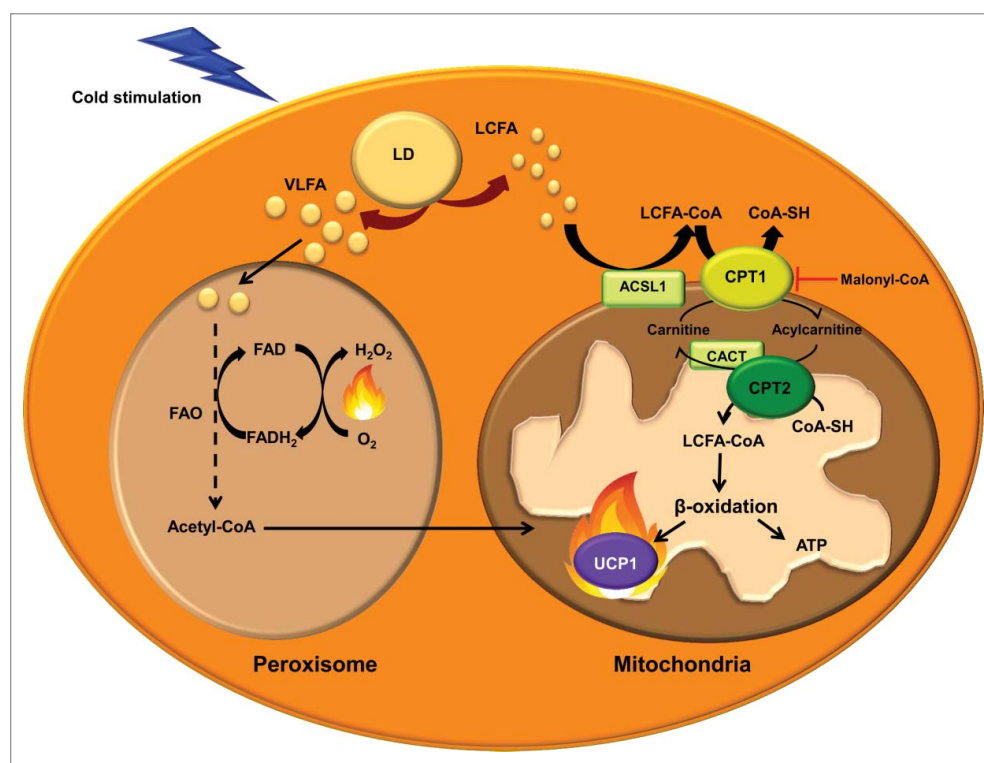


Figure 3. Mitochondrial and peroxisomal fatty acid oxidation. Transport of long-chain fatty acids (LCFAs) from the cytosol to the mitochondrial matrix for FAO involves the activation to acyl-CoA by acyl-CoA synthetase-1 (ACSL), conversion of LCFA-CoA to LCFA-carnitines by carnitine palmitoyltransferase (CPT) 1, translocation across the inner mitochondrial membrane by the carnitine/acylcarnitine translocase (CACT) and reconversion to LCFA-CoA by CPT2. These acyl-CoAs are β -oxidized and render acetyl-CoA. The entry of acetyl-CoA to the tricarboxylic acid cycle generates NADH and FADH. These cofactors transfer the electrons to the electron transport chain, where the protons are transported to the mitochondrial intermembrane space to generate energy as ATP. UCP1 dissipates the proton gradient, releasing energy as heat. Very long chain fatty acids (VLFA) enter the peroxisome to be shortened by peroxisomal FAO. Shortened acyl-CoAs and acetyl-CoA are transported to the mitochondria to be completely oxidized.

thermogenesis. Indeed, inhibitors of CPT1 also inhibit mitochondrial respiration driven by LCFA in murine BAT.¹⁵⁸ Interestingly, BAT of diabetic rats showed decreased CPT1 activity and FAO.¹⁷⁵ Further, a recent study in adipose CPT2 KO mice demonstrated that FAO is required for both acute cold adaptation and the induction of thermogenic genes in BAT.¹⁷⁶ Taking into account the effect that this and other mitochondrial FAO alterations¹⁷⁷ produce in thermogenesis and cold intolerance, it could be an appealing strategy to enhance FAO in BAT mitochondria to increase energy expenditure and fight against obesity-induced metabolic disorders. Studies enhancing FAO by CPT1 overexpression in the context of obesity have shown a decrease in TG content and an improvement in insulin sensitivity.¹⁷⁸⁻¹⁸⁸ These results indicate that activation of FAO may provide the basis for the development of novel treatment options for obesity.¹⁸⁹

Peroxisomal fatty acid oxidation

Oxidation of very long chain FAs preferentially occurs in peroxisomes rather than in mitochondria (Fig. 3).¹⁹⁰ However, FAO in peroxisomes is not carried to completion. Since peroxisomes, unlike mitochondria, lack a citric-acid cycle and respiratory chain, shorter FAs can be shuttled to the mitochondria to be oxidized. During cold exposure peroxisomal FAO is also activated in BAT.¹⁹¹ Furthermore, catalase protein, a marker of the quantity of peroxisomes, is dramatically increased in rat BAT under cold exposure.¹⁹² However, the contribution of peroxisomal FAO to thermogenesis is not well established. Acetyl-CoAs produced by peroxisomal FAO may enter the mitochondria to fuel UCP1-mediated thermogenesis. Alternatively, a recent review by Lodhi *et al.*¹⁹³ suggests that peroxisomal FAO may contribute to adaptive thermogenesis independently of UCP1 by the generation of heat instead of ATP. Peroxisomes do not have a respiratory chain and the electrons from FADH₂, obtained in the first step of peroxisomal FAO, are transferred by the flavoprotein acyl-CoA oxidase directly to O₂ producing H₂O₂, and energy is released as heat.

In summary, mitochondrial and peroxisomal FAO are necessary for thermogenesis in BAT, and enhancing these catabolic processes is an unexplored strategy in our fight against the current obesity epidemic.

Future directions: BAT fat-burning power as a potential therapy against obesity

Despite the considerable current effort made worldwide, the prevalence of obesity and associated metabolic diseases is rising exponentially, jointly with their healthcare costs. The first line therapy is based on behavioral

modifications, including healthy eating and exercise. However, this meets limited success when it comes to long-term maintenance of weight loss. Bariatric surgery achieves a sustained weight loss over the years, but its cost and associated dangers reduce its clinical indication to morbidly obese patients.¹⁹⁴ Moreover, the endocrine effects of bariatric surgery seem to be more important than the mechanically induced food restriction, which has led many researchers to assess obesity treatments based on the endocrine modifications derived from it.¹⁹⁵ Interestingly, bariatric surgery also leads to alterations in the microbiome.¹⁹⁶

Even though the list of potential anti-obesity drugs is increasing, the approval of new anti-obesity drugs has met relatively limited success. This is due to the history of withdrawals of anti-obesity drugs from the market due to serious adverse effects (i.e., dinitrophenol, fenfluramine, dexfenfluramine, phenylpropranolamine, sibutramine and rimonabant).^{197,198} This has led US Food and Drug Administration (FDA) and European Medicines Agency (EMA) to make it harder for pharmaceutical corporations to market new anti-obesity drugs, especially in the case of the European regulator.¹⁹⁹ Today, the lipase inhibitor orlistat is approved by both FDA and EMA but it has shown limited long-term effectiveness.²⁰⁰ In the US, the serotonergic lorcaserin is also approved,^{201,202} but its European marketing authorization application has been withdrawn because of the lack of evidence regarding safety in tumorigenesis in long-term use.²⁰³ Liraglutide, a previously approved antidiabetic drug, has recently been approved by both regulators for an anti-obesity indication.^{204,205} Nonetheless, the fixed-dose combination of bupropion/naltrexone, which is described to act in the central nervous system (CNS) by increasing POMC neuron activity, has obtained marketing approval as an anti-obesity drug by the FDA,²⁰⁶ but the EMA seems to be much more conservative regarding the approval of weight-management drug with effect on the CNS.²⁰⁷

The mechanisms of action of obesity-management drugs are classified into 3 groups:²⁰⁸ 1) centrally acting medications impairing dietary intake (including bupropion/naltrexone and lorcaserin); 2) medications that act peripherally to impair dietary absorption (e.g., orlistat); and 3) medications that increase energy expenditure, whose effect is mediated by CNS. We propose that the increase in energy expenditure is a promising way to manage obesity, but only if this could be achieved via a direct effect on peripheral tissues without involving the CNS. Thus, some of the collateral effects, which caused other drugs to be withdrawn, would be overcome. Here we highlight an increase in FAO as a potential approach to enhance energy expenditure in peripheral tissues.

Several studies enhancing FAO by CPT1 overexpression in the context of obesity have shown an improved metabolic phenotype.¹⁷⁸⁻¹⁸⁷ Thus, an increasing body of evidence highlights FAO activation as a potential target to develop novel anti-obesity strategies.

The pathogenesis of obesity is multifactorial and complex. However, the rediscovery of active BAT in adult humans and its relevance in metabolism has put a spotlight on this tissue as a potential target for therapies against obesity and metabolic diseases. A large number of activators of thermogenesis are increasingly being identified. This year, the β 3-adrenergic receptor agonist mirabegron, the first compound able to stimulate human BAT thermogenesis and to increase resting metabolic rate, has been described.⁵⁹ Although further studies are needed to explore the specificity of its mechanism of action and potential adverse effects, mirabegron provides the first evidence of human BAT thermogenesis stimulation.

As a controller of thermogenesis BAT is a good modulator of triglyceridemia, an important consumer of glucose and the major plasma lipid-clearing organ in rodents. Furthermore, diabetes has been shown to decrease CPT1 activity and FAO in rat BAT.¹⁷⁵ Thus, strategies designed to enhance the fat-burning power of BAT and to increase lipid mobilization and oxidation could be very useful in the treatment of obesity and associated pathologies. Traditionally, most research has focused on the activation of BAT thermogenesis through UCP1. However, recent studies have shown that cold stimulates both FA synthesis and FAO in murine BAT.^{96,156} Moreover, BAT peroxisomal FAO may generate heat independently of UCP1.¹⁹³ BAT transplantation is another strategy proving BAT's lipid-burning capacity in obesity. BAT transplantation to HFD-induced obese mice has shown a beneficial effect improving whole-body energy metabolism by increasing FAO-related genes such as PPAR α , PGC1 α , CPT1B and UCP1 in endogenous BAT.²⁰⁹ Although the present review is focused on obesity, it is noteworthy to mention the role of BAT in atherosclerosis. Data showing both a positive and negative effect of BAT activation in the development of atherosclerosis have been reported.^{210,211} On the one hand, Dong et al.²¹⁰ showed that sustained cold exposure accelerated the atherosclerotic plaque development by increasing plasma levels of small low-density lipoproteins (LDL) in apolipoprotein E (*ApoE*) and LDL receptor (*LDLr*) deficient atherosclerosis mouse models. On the other hand, Berbee et al.²¹¹ reported that APOE*3-Leiden.CETP mice (a model for human-like lipoprotein metabolism) treated with Western diet, to induce hyperlipidaemia and atherosclerosis, plus CL316243 (a β 3-adrenergic receptor agonist) had fewer atherosclerotic lesions. In this case BAT activation lead to enhanced uptake of FAs from

TG-rich lipoproteins into BAT and increased hepatic clearance of cholesterol-enriched remnants and lower plasma cholesterol levels. The apparent opposite effects between the 2 studies could be explained by the different mouse model used. ApoE and LDL receptor are essential for hepatic clearance of TG-rich lipoprotein remnants. Thus, this pathway is blocked in *ApoE* (-/-) or *LDLr* (-/-) mice but not in APOE*3-Leiden.CETP mice. In fact, the antiatherogenic effect seen by Berbee *et al.* was blunted in *ApoE* (-/-) or *LDLr* (-/-) mice. Importantly, mice treated with the β 3-receptor agonist lost weight and had increased FAO. This indicates that the beneficial effect of BAT activation on atherosclerosis could be the consequence of decreased obesity and enhanced FAO shedding light into FAO as a potential target to fight against obesity-induced metabolic disorders such as atherosclerosis.

At least 3 questions still need to be answered before increased BAT FAO can become an effective approach for obesity therapy. First, it is not known whether FAO enhancement might reach a limit in BAT, in which thermogenesis is tightly adjusted to the environmental temperature. Second, since increasing flux through FAO would only make sense together with a corresponding enhancement of energy demand,²¹² the physiological relevance of this strategy might be questioned if the individual is at thermoneutrality. Third, secondary effects of BAT pharmacological activation may include excessive body temperature or increased food intake as a compensatory effect to re-establish energy balance. Increased BAT FAO may augment mitochondrial burning capacity through an increase in the number of mitochondria and/or the increased expression of UCPs, and thus dissipate the excess of energy as heat and ATP. These could well alleviate the mitochondrial pressure found in lipid overload states.

In summary, an increase in FAO and BAT mass and/or activity could indeed be one of the underlying protective mechanisms against obesity-induced metabolic abnormalities. Although more research is needed, we strongly believe that enhancing BAT thermogenic power through increased FAO may be available in the near future as a therapy to treat obesity and its associated severe diseases.

Abbreviations

AC	adenyl cyclase
ACC	acetyl-CoA carboxylase
AMPK	AMP-dependent protein kinase
ATG	autophagy-related protein
ATGL	adipose triglyceride lipase
BAT	brown adipose tissue

BMP8b	bone morphogenetic protein 8b
cAMP	cyclic AMP
CIDEA	cell death-inducing DNA fragmentation factor- α -like effector A
CGI-58	comparative gene identification-58
CNS	central nervous system
CPT	carnitine palmitoyltransferase
DG	diacylglycerol
DIO2	type 2 iodothyronine deiodinase
ELOVL	elongation of very long chain FA
ER	endoplasmic reticulum
FA	fatty acid
FAO	fatty acid oxidation
FFA	free fatty acids
FGF21	fibroblast growth factor 21
G0S2	G0/G1 switch gene 2
GPCRs	G-protein-coupled receptors
HFD	high-fat diet
HSL	hormone-sensitive lipase
IGF-1	insulin-like growth factor I
IL-1 β	interleukin-1 β
IL-6	interleukin-6
KO	knockout
LAL	lysosomal acid lipase
MEFs	primary mouse fibroblasts
MG	monoacylglycerol
MGL	monoacylglycerol lipase
Myf5+	myogenic factor 5-positive
iPLA2 ζ	calcium-independent phospholipase A2 ζ
PGC1 α	peroxisome proliferator activated receptor gamma coactivator 1 alpha
PKA	protein kinase A
PKB	protein kinase B
PRDM16	PR domain-containing 16
pRb	retinoblastoma protein
RIP140	receptor interacting protein 140
TG	triglyceride
TNF α	tumor necrosis factor α
UCP1	uncoupling protein-1
WAT	white adipose tissue

Disclosure of potential conflicts of interest

No potential conflicts of interest were disclosed.

Acknowledgment

We thank Robin Rycroft for valuable assistance in the preparation of the English manuscript.

Funding

This work was supported by the Ministry of Spain (SAF2013-45887-R to LH, SAF2014-52223-C2-1-R to DS

(grant cofounded by Fondos Europeos de Desarrollo Regional de la Unión Europea (FEDER)) and doctoral fellowship to JFM), by the Centro de Investigación Biomédica en Red Fisiopatología de la Obesidad y la Nutrición (CIBEROBN) (Grant CB06/03/0001 to DS), by Generalitat de Catalunya (2014SGR465 to DS), and by the European Foundation for the Study of Diabetes (EFSD)/Janssen-Rising Star and L'Oréal-UNESCO "For Women in Science" research fellowships to LH. MW is a recipient of the Ciència sem Fronteiras-CNPq fellowship (237976/2012-9).

References

1. World Health Organization. Obesity and overweight. Available from: <http://www.who.int/mediacentre/factsheets/fs311/en/> (accessed 1 October 2015)
2. Mathis D. Immunological goings-on in visceral adipose tissue. *Cell Metab* 2013; 17:851-9; PMID:23747244; <http://dx.doi.org/10.1016/j.cmet.2013.05.008>
3. Samuel VT, Shulman GI. Mechanisms for insulin resistance: common threads and missing links. *Cell* 2012; 148:852-71; PMID:22385956; <http://dx.doi.org/10.1016/j.cell.2012.02.017>
4. Shoelson SE, Herrero L, Naaz A. Obesity, inflammation, and insulin resistance. *Gastroenterology* 2007; 132:2169-80; PMID:17498510; <http://dx.doi.org/10.1053/j.gastro.2007.03.059>
5. Hotamisligil GS. Endoplasmic reticulum stress and the inflammatory basis of metabolic disease. *Cell* 2010; 140:900-17; PMID:20303879; <http://dx.doi.org/10.1016/j.cell.2010.02.034>
6. Hosogai N, Fukuhara A, Oshima K, Miyata Y, Tanaka S, Segawa K, Furukawa S, Tochino Y, Komuro R, Matsuda M, et al. Adipose tissue hypoxia in obesity and its impact on adipocytokine dysregulation. *Diabetes* 2007; 56:901-11; PMID:17395738; <http://dx.doi.org/10.2337/db06-0911>
7. Patti M-E, Corvera S. The role of mitochondria in the pathogenesis of type 2 diabetes. *Endocr Rev* 2010; 31:364-95; PMID:20156986; <http://dx.doi.org/10.1210/er.2009-0027>
8. Virtue S, Vidal-Puig A. Adipose tissue expandability, lipotoxicity and the Metabolic Syndrome—an allostatic perspective. *Biochim Biophys Acta* 2010; 1801:338-49; PMID:20056169; <http://dx.doi.org/10.1016/j.bbali.2009.12.006>
9. Sun K, Kusminski CM, Scherer PE. Adipose tissue remodeling and obesity. *J Clin Invest* 2011; 121:2094-101; PMID:21633177; <http://dx.doi.org/10.1172/JCI45887>
10. Sun K, Wernstedt Asterholm I, Kusminski CM, Bueno AC, Wang ZV, Pollard JW, Brekken RA, Scherer PE. Dichotomous effects of VEGF-A on adipose tissue dysfunction. *Proc Natl Acad Sci U S A* 2012; 109:5874-9; PMID:22451920; <http://dx.doi.org/10.1073/pnas.1200447109>
11. Hany TF, Gharehpapagh E, Kamel EM, Buck A, Himmshagen J, Von Schulthess GK. Brown adipose tissue: a factor to consider in symmetrical tracer uptake in the neck and upper chest region. *Eur J Nucl Med* 2002; 29:1393-8; PMID:12271425; <http://dx.doi.org/10.1007/s00259-002-0902-6>

12. Nedergaard J, Bengtsson T, Cannon B. Unexpected evidence for active brown adipose tissue in adult humans. *Am J Physiol Endocrinol Metab* 2007; 293:E444-52; PMID:17473055; <http://dx.doi.org/10.1152/ajpendo.00691.2006>
13. Cypess AM, Lehman S, Williams G, Tal I, Rodman D, Goldfine AB, Kuo FC, Palmer EL, Tseng YH, Doria A, et al. Identification and importance of brown adipose tissue in adult humans. *N Engl J Med* 2009; 360:1509-17; PMID:19357406; <http://dx.doi.org/10.1056/NEJMoa0810780>
14. Virtanen KA, Lidell ME, Orava J, Heglind M, Westergren R, Niemi T, Taittonen M, Laine J, Savisto NJ, Enerback S, et al. Functional brown adipose tissue in healthy adults. *N Engl J Med* 2009; 360:1518-25; PMID:19357407; <http://dx.doi.org/10.1056/NEJMoa0808949>
15. Zingaretti MC, Crosta F, Vitali A, Guerrieri M, Frontini A, Cannon B, Nedergaard J, Cinti S. The presence of UCP1 demonstrates that metabolically active adipose tissue in the neck of adult humans truly represents brown adipose tissue. *Faseb J* 2009; 23:3113-20; PMID:19417078; <http://dx.doi.org/10.1096/fj.09-133546>
16. Saito M, Okamatsu-Ogura Y, Matsushita M, Watanabe K, Yoneshiro T, Nio-Kobayashi J, Iwanaga T, Miyagawa M, Kameya T, Nakada K, et al. High incidence of metabolically active brown adipose tissue in healthy adult humans: effects of cold exposure and adiposity. *Diabetes* 2009; 58:1526-31; PMID:19401428; <http://dx.doi.org/10.2337/db09-0530>
17. Van Marken Lichtenbelt WD, Vanhomerig JW, Smulders NM, Drossaerts JM, Kemerink GJ, Bouvy ND, Schrauwen P, Teule GJ. Cold-activated brown adipose tissue in healthy men. *N Engl J Med* 2009; 360:1500-8; PMID:19357405; <http://dx.doi.org/10.1056/NEJMoa0808718>
18. Mailloux RJ, Harper M-E. Uncoupling proteins and the control of mitochondrial reactive oxygen species production. *Free Radic Biol Med* 2011; 51:1106-15; PMID:21762777; <http://dx.doi.org/10.1016/j.freeradbiomed.2011.06.022>
19. Frontini A, Cinti S. Distribution and development of brown adipocytes in the murine and human adipose organ. *Cell Metab* 2010; 11:253-6; PMID:20374956; <http://dx.doi.org/10.1016/j.cmet.2010.03.004>
20. Cypess AM, White AP, Vernochet C, Schulz TJ, Xue R, Sass CA, Huang TL, Roberts-Toler C, Weiner LS, Sze C, et al. Anatomical localization, gene expression profiling and functional characterization of adult human neck brown fat. *Nat Med* 2013; 19:635-9; PMID:23603815; <http://dx.doi.org/10.1038/nm.3112>
21. Cinti S. Between brown and white: novel aspects of adipocyte differentiation. *Ann Med* 2011; 43:104-15; PMID:21254898; <http://dx.doi.org/10.3109/07853890.2010.535557>
22. Tseng YH, Cypess AM, Kahn CR. Cellular bioenergetics as a target for obesity therapy. *Nat Rev Drug Discov* 2010; 9:465-82; PMID:20514071; <http://dx.doi.org/10.1038/nrd3138>
23. Xue R, Lynes MD, Dreyfuss JM, Shamsi F, Schulz TJ, Zhang H, Huang TL, Townsend KL, Li Y, Takahashi H, et al. Clonal analyses and gene profiling identify genetic biomarkers of the thermogenic potential of human brown and white preadipocytes. *Nat Med* 2015; 21:760-8; PMID:26076036; <http://dx.doi.org/10.1038/nm.3881>
24. Jespersen NZ, Larsen TJ, Peijs L, Dagaard S, Homøe P, Loft A, de Jong J, Mathur N, Cannon B, Nedergaard J, et al. A classical brown adipose tissue mRNA signature partly overlaps with brite in the supraclavicular region of adult humans. *Cell Metab* 2013; 17:798-805; PMID:23663743; <http://dx.doi.org/10.1016/j.cmet.2013.04.011>
25. Lidell ME, Betz MJ, Dahlqvist Leinhard O, Heglind M, Elander L, Slawik M, Mussack T, Nilsson D, Romu T, Nuutila P, et al. Evidence for two types of brown adipose tissue in humans. *Nat Med* 2013; 19:631-4; PMID:23603813; <http://dx.doi.org/10.1038/nm.3017>
26. Sharp LZ, Shinoda K, Ohno H, Scheel DW, Tomoda E, Ruiz L, Hu H, Wang L, Pavlova Z, Gilsanz V, et al. Human BAT possesses molecular signatures that resemble beige/brite cells. *PLoS One* 2012; 7:e49452; PMID:23166672; <http://dx.doi.org/10.1371/journal.pone.0049452>
27. Wu J, Boström P, Sparks LM, Ye L, Choi JH, Giang A-H, Khandekar M, Virtanen KA, Nuutila P, Schaart G, et al. Beige adipocytes are a distinct type of thermogenic fat cell in mouse and human. *Cell* 2012; 150:366-76; PMID:22796012; <http://dx.doi.org/10.1016/j.cell.2012.05.016>
28. Villarroya J, Cereijo R, Villarroya F. An endocrine role for brown adipose tissue? *Am J Physiol Endocrinol Metab* 2013; 305:E567-72; PMID:23839524; <http://dx.doi.org/10.1152/ajpendo.00250.2013>
29. Gesta S, Tseng YH, Kahn CR. Developmental origin of fat: tracking obesity to its source. *Cell* 2007; 131:242-56; PMID:17956727; <http://dx.doi.org/10.1016/j.cell.2007.10.004>
30. Ortega FJ, Jilkova ZM, Moreno-Navarrete JM, Pavelka S, Rodriguez-Hermosa JI, Kopeck Ygrave J, Fernandez-Real JM. Type I iodothyronine 5'-deiodinase mRNA and activity is increased in adipose tissue of obese subjects. *Int J Obes* 2011; 36:320-4; PMID:21610697; <http://dx.doi.org/10.1038/ijo.2011.101>
31. Peirce V, Carobbio S, Vidal-Puig A. The different shades of fat. *Nature* 2014; 510:76-83; PMID:24899307; <http://dx.doi.org/10.1038/nature13477>
32. Waldén TB, Hansen IR, Timmons JA, Cannon B, Nedergaard J. Recruited vs. nonrecruited molecular signatures of brown, "brite," and white adipose tissues. *Am J Physiol Endocrinol Metab* 2012; 302:E19-31; PMID:21828341; <http://dx.doi.org/10.1152/ajpendo.00249.2011>
33. Bartelt A, Heeren J. Adipose tissue browning and metabolic health. *Nat Rev Endocrinol* 2014; 10:24-36; PMID:24146030; <http://dx.doi.org/10.1038/nrendo.2013.204>
34. Rosenwald M, Wolfrum C. The origin and definition of brite versus white and classical brown adipocytes. *Adipocyte* 2014; 3:4-9; PMID:24575363; <http://dx.doi.org/10.4161/adip.26232>
35. Timmons JA, Wennmalm K, Larsson O, Walden TB, Lassmann T, Petrovic N, Hamilton DL, Gimeno RE, Wahlestedt C, Baar K, et al. Myogenic gene expression signature establishes that brown and white adipocytes originate from distinct cell lineages. *Proc Natl Acad Sci*

- U S A 2007; 104:4401-6; PMID:17360536; <http://dx.doi.org/10.1073/pnas.0610615104>
36. Sanchez-Gurmaches J, Hung C-M, Sparks CA, Tang Y, Li H, Guertin DA. PTEN loss in the Myf5 lineage redistributes body fat and reveals subsets of white adipocytes that arise from Myf5 precursors. *Cell Metab* 2012; 16:348-62; PMID:22940198; <http://dx.doi.org/10.1016/j.cmet.2012.08.003>
 37. Tseng Y-H, Cypess AM, Kahn CR. Cellular bioenergetics as a target for obesity therapy. *Nat Rev Drug Discov* 2010; 9:465-82; PMID:20514071; <http://dx.doi.org/10.1038/nrd3138>
 38. Kajimura S, Spiegelman BM, Seale P. Brown and beige fat: physiological roles beyond heat generation. *Cell Metab* 2015; 22:546-59; PMID:26445512; <http://dx.doi.org/10.1016/j.cmet.2015.09.007>
 39. Zhou Q, Melton DA. Extreme makeover: converting one cell into another. *Cell Stem Cell* 2008; 3:382-8; PMID:18940730; <http://dx.doi.org/10.1016/j.stem.2008.09.015>
 40. Barbatelli G, Murano I, Madsen L, Hao Q, Jimenez M, Kristiansen K, Giacobino JP, De Matteis R, Cinti S. The emergence of cold-induced brown adipocytes in mouse white fat depots is determined predominantly by white to brown adipocyte transdifferentiation. *Am J Physiol Endocrinol Metab* 2010; 298:E1244-53; PMID:20354155; <http://dx.doi.org/10.1152/ajpendo.00600.2009>
 41. Barbatelli G, Morroni M, Vinesi P, Cinti S, Michetti F. S-100 protein in rat brown adipose tissue under different functional conditions: a morphological, immunocytochemical, and immunochemical study. *Exp Cell Res* 1993; 208:226-31; PMID:8359217; <http://dx.doi.org/10.1006/excr.1993.1241>
 42. Himms-Hagen J, Melnyk A, Zingaretti MC, Ceresi E, Barbatelli G, Cinti S. Multilocular fat cells in WAT of CL-316243-treated rats derive directly from white adipocytes. *Am J Physiol Cell Physiol* 2000; 279:C670-81; PMID:10942717
 43. Rosenwald M, Perdikari A, Rüllicke T, Wolfrum C. Bidirectional interconversion of brite and white adipocytes. *Nat Cell Biol* 2013; 15:659-67; PMID:23624403; <http://dx.doi.org/10.1038/ncb2740>
 44. Lee Y-H, Petkova AP, Mottillo EP, Granneman JG. In vivo identification of bipotential adipocyte progenitors recruited by β 3-adrenoceptor activation and high-fat feeding. *Cell Metab* 2012; 15:480-91; PMID:22482730; <http://dx.doi.org/10.1016/j.cmet.2012.03.009>
 45. Schulz TJ, Huang P, Huang TL, Xue R, McDougall LE, Townsend KL, Cypess AM, Mishina Y, Gussoni E, Tseng Y-H. Brown-fat paucity due to impaired BMP signalling induces compensatory browning of white fat. *Nature* 2013; 495:379-83; PMID:23485971; <http://dx.doi.org/10.1038/nature11943>
 46. Tsoi M, Moore M, Burg D, Painter A, Taylor R, Lockie SH, Turner N, Warren A, Cooney G, Oldfield B, et al. Activation of thermogenesis in brown adipose tissue and dysregulated lipid metabolism associated with cancer cachexia in mice. *Cancer Res* 2012; 72:4372-82; PMID:22719069; <http://dx.doi.org/10.1158/0008-5472.CAN-11-3536>
 47. Vijgen GHEJ, Bouvy ND, Smidt M, Kooreman L, Schaart G, van Marken Lichtenbelt W. Hibernoma with metabolic impact? *BMJ Case Rep* 2012; 2012:bcr2012006325-bcr2012006325; PMID:22914232
 48. Radi Z, Bartholomew P, Elwell M, Vogel WM. Comparative pathophysiology, toxicology, and human cancer risk assessment of pharmaceutical-induced hibernoma. *Toxicol Appl Pharmacol* 2013; 273:456-63; PMID:24141031; <http://dx.doi.org/10.1016/j.taap.2013.10.011>
 49. Nedergaard J, Cannon B. The browning of white adipose tissue: some burning issues. *Cell Metab* 2014; 20:396-407; PMID:25127354; <http://dx.doi.org/10.1016/j.cmet.2014.07.005>
 50. Lo JC, Cinti S, Tu H, Kajimura S, Korde A, Choi JH, Wu J, Zingaretti MC, Rasbach KA, Vind BF, et al. A PGC1- α -dependent myokine that drives brown-fat-like development of white fat and thermogenesis. *Nature* 2012; 481:463-8; PMID:22237023; <http://dx.doi.org/10.1038/nature10777>
 51. Bordicchia M, Liu D, Amri EZ, Ailhaud G, Dessi-Fulgheri P, Zhang C, Takahashi N, Sarzani R, Collins S. Cardiac natriuretic peptides act via p38 MAPK to induce the brown fat thermogenic program in mouse and human adipocytes. *J Clin Invest* 2012; 122:1022-36; PMID:22307324; <http://dx.doi.org/10.1172/JCI59701>
 52. Boon MR, van den Berg SAA, Wang Y, van den Bossche J, Karkampouna S, Bauwens M, De Saint-Hubert M, van der Horst G, Vukicevic S, de Winther MPJ, et al. BMP7 activates brown adipose tissue and reduces diet-induced obesity only at subthermoneutrality. *PLoS One* 2013; 8:e74083; PMID:24066098; <http://dx.doi.org/10.1371/journal.pone.0074083>
 53. Whittle AJ, Carobbio S, Martins L, Slawik M, Hondares E, Vazquez MJ, Morgan D, Csikasz RI, Gallego R, Rodriguez-Cuenca S, et al. BMP8B increases brown adipose tissue thermogenesis through both central and peripheral actions. *Cell* 2012; 149:871-85; PMID:22579288; <http://dx.doi.org/10.1016/j.cell.2012.02.066>
 54. Villarroya F, Vidal-Puig A. Beyond the sympathetic tone: the new brown fat activators. *Cell Metab* 2013; 17:638-43; PMID:23583169; <http://dx.doi.org/10.1016/j.cmet.2013.02.020>
 55. Rao RR, Long JZ, White JP, Svensson KJ, Lou J, Lokurkar I, Jedrychowski MP, Ruas JL, Wrann CD, Lo JC, et al. Meteorin-like is a hormone that regulates immune-adipose interactions to increase beige fat thermogenesis. *Cell* 2014; 157:1279-91; PMID:24906147; <http://dx.doi.org/10.1016/j.cell.2014.03.065>
 56. Watanabe M, Houten SM, Matakı C, Christoffolete MA, Kim BW, Sato H, Messaddeq N, Harney JW, Ezaki O, Kodama T, et al. Bile acids induce energy expenditure by promoting intracellular thyroid hormone activation. *Nature* 2006; 439:484-9; PMID:16400329; <http://dx.doi.org/10.1038/nature04330>
 57. Gnad T, Scheibler S, von Kügelgen I, Scheele C, Kilić A, Glöde A, Hoffmann LS, Reverte-Salisa L, Horn P, Mutlu S, et al. Adenosine activates brown adipose tissue and recruits beige adipocytes via A2A receptors. *Nature* 2014; PMID:25317558; PMID:25317558
 58. Hondares E, Rosell M, Gonzalez FJ, Giralto M, Iglesias R, Villarroya F. Hepatic FGF21 expression is induced at birth via PPARalpha in response to milk intake and contributes to thermogenic activation of neonatal brown fat.

- Cell Metab 2010; 11:206-12; PMID:20197053; <http://dx.doi.org/10.1016/j.cmet.2010.02.001>
59. Cypess AM, Weiner LS, Roberts-Toler C, Elia EF, Kessler SH, Kahn PA, English J, Chatman K, Trauger SA, Doria A, et al. Activation of human brown adipose tissue by a β 3-adrenergic receptor agonist. *Cell Metab* 2015; 21:33-8; PMID:25565203; <http://dx.doi.org/10.1016/j.cmet.2014.12.009>
 60. Wu J, Cohen P, Spiegelman BM. Adaptive thermogenesis in adipocytes: is beige the new brown? *Genes Dev* 2013; 27:234-50; PMID:23388824; <http://dx.doi.org/10.1101/gad.211649.112>
 61. Bonet ML, Oliver P, Palou A. Pharmacological and nutritional agents promoting browning of white adipose tissue. *Biochim Biophys Acta - Mol Cell Biol Lipids* 2013; 1831:969-85; PMID:23246573; <http://dx.doi.org/10.1016/j.bbailip.2012.12.002>
 62. Divakaruni AS, Humphrey DM, Brand MD. Fatty acids change the conformation of uncoupling protein 1 (UCP1). *J Biol Chem* 2012; 287:36845-53; PMID:22952235; <http://dx.doi.org/10.1074/jbc.M112.381780>
 63. Fedorenko A, Lishko PV, Kirichok Y. Mechanism of fatty-acid-dependent UCP1 uncoupling in brown fat mitochondria. *Cell* 2012; 151:400-13; PMID:23063128; <http://dx.doi.org/10.1016/j.cell.2012.09.010>
 64. Bartelt A, Merkel M, Heeren J. A new, powerful player in lipoprotein metabolism: brown adipose tissue. *J Mol Med (Berl)* 2012; 90:887-93; PMID:22231746; <http://dx.doi.org/10.1007/s00109-012-0858-3>
 65. Bartelt A, Bruns OT, Reimer R, Hohenberg H, Itrich H, Peldschus K, Kaul MG, Tromsdorf UI, Weller H, Waurisch C, et al. Brown adipose tissue activity controls triglyceride clearance. *Nat Med* 2011; 17:200-5; PMID:21258337; <http://dx.doi.org/10.1038/nm.2297>
 66. Festuccia WT, Blanchard P-G, Deshaies Y. Control of brown adipose tissue glucose and lipid metabolism by PPAR γ . *Front Endocrinol (Lausanne)* 2011; 2:84; PMID:22654830
 67. Festuccia WT, Blanchard P-G, Turcotte V, Laplante M, Sariahmetoglu M, Brindley DN, Richard D, Deshaies Y. The PPAR γ agonist rosiglitazone enhances rat brown adipose tissue lipogenesis from glucose without altering glucose uptake. *Am J Physiol Regul Integr Comp Physiol* 2009; 296:R1327-35; PMID:19211718; <http://dx.doi.org/10.1152/ajpregu.91012.2008>
 68. Duivenvoorden I, Teusink B, Rensen PC, Romijn JA, Havekes LM, Voshol PJ. Apolipoprotein C3 deficiency results in diet-induced obesity and aggravated insulin resistance in mice. *Diabetes* 2005; 54:664-71; PMID:15734841; <http://dx.doi.org/10.2337/diabetes.54.3.664>
 69. Bartelt A, Weigelt C, Cherradi ML, Niemeier A, Tödter K, Heeren J, Scheja L. Effects of adipocyte lipoprotein lipase on de novo lipogenesis and white adipose tissue browning. *Biochim Biophys Acta* 2013; 1831:934-42; PMID:23228690; <http://dx.doi.org/10.1016/j.bbailip.2012.11.011>
 70. Davies BSJ, Beigneux AP, Barnes RH, Tu Y, Gin P, Weinstein MM, Nobumori C, Nyrén R, Goldberg I, Olivecrona G, et al. GPIHBP1 is responsible for the entry of lipoprotein lipase into capillaries. *Cell Metab* 2010; 12:42-52; PMID:20620994; <http://dx.doi.org/10.1016/j.cmet.2010.04.016>
 71. Weinstein MM, Goulbourne CN, Davies BSJ, Tu Y, Barnes RH, Watkins SM, Davis R, Reue K, Tontonoz P, Beigneux AP, et al. Reciprocal metabolic perturbations in the adipose tissue and liver of GPIHBP1-deficient mice. *Arterioscler Thromb Vasc Biol* 2012; 32:230-5; PMID:22173228; <http://dx.doi.org/10.1161/ATVBAHA.111.241406>
 72. Laplante M, Festuccia WT, Soucy G, Gélinas Y, Lalonde J, Deshaies Y. Involvement of adipose tissues in the early hypolipidemic action of PPAR γ agonism in the rat. *Am J Physiol Regul Integr Comp Physiol* 2007; 292:R1408-17; PMID:17170230; <http://dx.doi.org/10.1152/ajpregu.00761.2006>
 73. Glatz JFC, Luiken JJFP, Bonen A. Membrane fatty acid transporters as regulators of lipid metabolism: implications for metabolic disease. *Physiol Rev* 2010; 90:367-417; PMID:20086080; <http://dx.doi.org/10.1152/physrev.00003.2009>
 74. McArthur MJ, Atshaves BP, Frolov A, Foxworth WD, Kier AB, Schroeder F. Cellular uptake and intracellular trafficking of long chain fatty acids. *J Lipid Res* 1999; 40:1371-83; PMID:10428973
 75. Sasaki A, Sivaram P, Goldberg IJ. Lipoprotein lipase binding to adipocytes: evidence for the presence of a heparin-sensitive binding protein. *Am J Physiol* 1993; 265:E880-8; PMID:8279543
 76. Baillie AG, Coburn CT, Abumrad NA. Reversible binding of long-chain fatty acids to purified FAT, the adipose CD36 homolog. *J Membr Biol* 1996; 153:75-81; PMID:8694909; <http://dx.doi.org/10.1007/s002329900111>
 77. Jochen AL, Hays J, Mick G. Inhibitory effects of cerulenin on protein palmitoylation and insulin internalization in rat adipocytes. *Biochim Biophys Acta* 1995; 1259:65-72; PMID:7492617; [http://dx.doi.org/10.1016/0005-2760\(95\)00147-5](http://dx.doi.org/10.1016/0005-2760(95)00147-5)
 78. Martin C, Passilly-Degrace P, Gaillard D, Merlin J-F, Chevrot M, Besnard P. The lipid-sensor candidates CD36 and GPR120 are differentially regulated by dietary lipids in mouse taste buds: impact on spontaneous fat preference. *PLoS One* 2011; 6:e24014.
 79. Bokor S, Legry V, Meirhaeghe A, Ruiz JR, Mauro B, Widhalm K, Manios Y, Amouyel P, Moreno LA, Molnár D, et al. Single-nucleotide polymorphism of CD36 locus and obesity in European adolescents. *Obesity (Silver Spring)* 2010; 18:1398-403; PMID:19893500; <http://dx.doi.org/10.1038/oby.2009.412>
 80. Gimeno RE. Fatty acid transport proteins. *Curr Opin Lipidol* 2007; 18:271-6; PMID:17495600; <http://dx.doi.org/10.1097/MOL.0b013e3281338558>
 81. Hagberg CE, Falkevall A, Wang X, Larsson E, Huusko J, Nilsson I, van Meeteren LA, Samen E, Lu L, Vanwildermeersch M, et al. Vascular endothelial growth factor B controls endothelial fatty acid uptake. *Nature* 2010; 464:917-21; PMID:20228789; <http://dx.doi.org/10.1038/nature08945>
 82. Stienstra R, Haim Y, Riahi Y, Netea M, Rudich A, Leibowitz G. Autophagy in adipose tissue and the beta cell: implications for obesity and diabetes. *Diabetologia* 2014;

- 57:1505-16; PMID:24795087; <http://dx.doi.org/10.1007/s00125-014-3255-3>
83. Doege H, Stahl A. Protein-mediated fatty acid uptake: novel insights from in vivo models. *Physiology (Bethesda)* 2006; 21:259-68; PMID:16868315; <http://dx.doi.org/10.1152/physiol.00014.2006>
 84. Milligan G, Stoddart LA, Brown AJ. G protein-coupled receptors for free fatty acids. *Cell Signal* 2006; 18:1360-5; PMID:16716567; <http://dx.doi.org/10.1016/j.cellsig.2006.03.011>
 85. Ulven T. Short-chain free fatty acid receptors FFA2/GPR43 and FFA3/GPR41 as new potential therapeutic targets. *Front Endocrinol (Lausanne)* 2012; 3:111; PMID:23060857
 86. Rosell M, Kaforou M, Frontini A, Okolo A, Chan Y-W, Nikolopoulou E, Millership S, Fenech ME, MacIntyre D, Turner JO, et al. Brown and white adipose tissues: intrinsic differences in gene expression and response to cold exposure in mice. *Am J Physiol Endocrinol Metab* 2014; 306:E945-64; PMID:24549398; <http://dx.doi.org/10.1152/ajpendo.00473.2013>
 87. LaLonde JM, Bernlohr DA, Banaszak LJ. The up-and-down beta-barrel proteins. *FASEB J* 1994; 8:1240-7; PMID:8001736
 88. Yamamoto T, Yamamoto A, Watanabe M, Matsuo T, Yamazaki N, Kataoka M, Terada H, Shinohara Y. Classification of FABP isoforms and tissues based on quantitative evaluation of transcript levels of these isoforms in various rat tissues. *Biotechnol Lett* 2009; 31:1695-701; PMID:19565192; <http://dx.doi.org/10.1007/s10529-009-0065-7>
 89. Shan T, Liu W, Kuang S. Fatty acid binding protein 4 expression marks a population of adipocyte progenitors in white and brown adipose tissues. *FASEB J* 2013; 27:277-87; PMID:23047894; <http://dx.doi.org/10.1096/fj.12-211516>
 90. Nakamura Y, Sato T, Shiimura Y, Miura Y, Kojima M. FABP3 and brown adipocyte-characteristic mitochondrial fatty acid oxidation enzymes are induced in beige cells in a different pathway from UCP1. *Biochem Biophys Res Commun* 2013; 441:42-6; PMID:24129192; <http://dx.doi.org/10.1016/j.bbrc.2013.10.014>
 91. Yamashita H, Wang Z, Wang Y, Segawa M, Kusudo T, Kontani Y. Induction of fatty acid-binding protein 3 in brown adipose tissue correlates with increased demand for adaptive thermogenesis in rodents. *Biochem Biophys Res Commun* 2008; 377:632-5; PMID:18938135; <http://dx.doi.org/10.1016/j.bbrc.2008.10.041>
 92. Ameer F, Scandiuzzi L, Hasnain S, Kalbacher H, Zaidi N. De novo lipogenesis in health and disease. *Metabolism* 2014; 63:895-902; PMID:24814684; <http://dx.doi.org/10.1016/j.metabol.2014.04.003>
 93. Lodhi IJ, Wei X, Semenkovich CF. Lipoexpediency: de novo lipogenesis as a metabolic signal transmitter. *Trends Endocrinol Metab* 2011; 22:1-8; PMID:20889351; <http://dx.doi.org/10.1016/j.tem.2010.09.002>
 94. Herman MA, Peroni OD, Villoria J, Schön MR, Abumrad NA, Blüher M, Klein S, Kahn BB. A novel ChREBP isoform in adipose tissue regulates systemic glucose metabolism. *Nature* 2012; 484:333-8; PMID:22466288; <http://dx.doi.org/10.1038/nature10986>
 95. Eissing L, Scherer T, Tödter K, Knippschild U, Greve JW, Buurman WA, Pinnschmidt HO, Rensen SS, Wolf AM, Bartelt A, et al. De novo lipogenesis in human fat and liver is linked to ChREBP- β and metabolic health. *Nat Commun* 2013; 4:1528; PMID:23443556; <http://dx.doi.org/10.1038/ncomms2537>
 96. Mottillo EP, Balasubramanian P, Lee Y-H, Weng C, Kershaw EE, Granneman JG. Coupling of lipolysis and de novo lipogenesis in brown, beige, and white adipose tissues during chronic β 3-adrenergic receptor activation. *J Lipid Res* 2014; 55:2276-86; PMID:25193997; <http://dx.doi.org/10.1194/jlr.M050005>
 97. Berg JM, Tymoczko JL, Stryer L. *Biochemistry*. 7th edition. New York: WH Freeman; 2012.
 98. Bianchi A, Evans JL, Iverson AJ, Nordlund AC, Watts TD, Witters LA. Identification of an isozymic form of acetyl-CoA carboxylase. *J Biol Chem* 1990; 265:1502-9; PMID:1967254
 99. Lodhi IJ, Yin L, Jensen-Urstad APL, Funai K, Coleman T, Baird JH, El Ramahi MK, Razani B, Song H, Fu-Hsu F, et al. Inhibiting adipose tissue lipogenesis reprograms thermogenesis and PPAR γ activation to decrease diet-induced obesity. *Cell Metab* 2012; 16:189-201; PMID:22863804; <http://dx.doi.org/10.1016/j.cmet.2012.06.013>
 100. Kihara A. Very long-chain fatty acids: elongation, physiology and related disorders. *J Biochem* 2012; 152:387-95; PMID:22984005; <http://dx.doi.org/10.1093/jb/mvs105>
 101. Tvrdik P, Westerberg R, Silve S, Asadi A, Jakobsson A, Cannon B, Loison G, Jakobsson A. Role of a new mammalian gene family in the biosynthesis of very long chain fatty acids and sphingolipids. *J Cell Biol* 2000; 149:707-18; PMID:10791983; <http://dx.doi.org/10.1083/jcb.149.3.707>
 102. Jakobsson A, Jörgensen JA, Jakobsson A. Differential regulation of fatty acid elongation enzymes in brown adipocytes implies a unique role for Elovl3 during increased fatty acid oxidation. *Am J Physiol Endocrinol Metab* 2005; 289:E517-26; PMID:15855229; <http://dx.doi.org/10.1152/ajpendo.00045.2005>
 103. Tvrdik P, Asadi A, Kozak LP, Nedergaard J, Cannon B, Jakobsson A. Cig30, a mouse member of a novel membrane protein gene family, is involved in the recruitment of brown adipose tissue. *J Biol Chem* 1997; 272:31738-46; PMID:9395518; <http://dx.doi.org/10.1074/jbc.272.50.31738>
 104. Zadavec D, Brolinson A, Fisher RM, Carneheim C, Csikasz RI, Bertrand-Michel J, Borén J, Guillou H, Rudling M, Jakobsson A. Ablation of the very-long-chain fatty acid elongase ELOVL3 in mice leads to constrained lipid storage and resistance to diet-induced obesity. *FASEB J* 2010; 24:4366-77; PMID:20605947; <http://dx.doi.org/10.1096/fj.09-152298>
 105. Miyazaki M, Flowers MT, Sampath H, Chu K, Oztelberger C, Liu X, Ntambi JM. Hepatic stearoyl-CoA desaturase-1 deficiency protects mice from carbohydrate-induced adiposity and hepatic steatosis. *Cell Metab* 2007; 6:484-96; PMID:18054317; <http://dx.doi.org/10.1016/j.cmet.2007.10.014>
 106. Ntambi JM, Miyazaki M, Stoehr JP, Lan H, Kendzierski CM, Yandell BS, Song Y, Cohen P, Friedman JM, Attie AD. Loss of stearoyl-CoA desaturase-1 function protects

- mice against adiposity. *Proc Natl Acad Sci U S A* 2002; 99:11482-6; PMID:12177411; <http://dx.doi.org/10.1073/pnas.132384699>
107. Rahman SM, Dobrzyn A, Lee S, Dobrzyn P, Miyazaki M, Ntambi JM. Stearoyl-CoA desaturase 1 deficiency increases insulin signaling and glycogen accumulation in brown adipose tissue. *Am J Physiol Endocrinol Metab* October 2005; 53706:381-7
 108. Townsend KL, Tseng Y-H. Brown fat fuel utilization and thermogenesis. *Trends Endocrinol Metab* 2014; 25:168-77; PMID:24389130; <http://dx.doi.org/10.1016/j.tem.2013.12.004>
 109. Orr AL, Quinlan CL, Perevoshchikova IV, Brand MD. A refined analysis of superoxide production by mitochondrial sn-glycerol 3-phosphate dehydrogenase. *J Biol Chem* 2012; 287:42921-35; PMID:23124204; <http://dx.doi.org/10.1074/jbc.M112.397828>
 110. Cannon B, Nedergaard J. Brown adipose tissue: function and physiological significance. *Physiol Rev* 2004; 84:277-359; PMID:14715917; <http://dx.doi.org/10.1152/physrev.00015.2003>
 111. Moura MAF, Festuccia WTL, Kawashita NH, Garófalo MAR, Brito SRC, Kettelhut IC, Migliorini RH. Brown adipose tissue glyceroneogenesis is activated in rats exposed to cold. *Pflugers Arch* 2005; 449:463-9; PMID:15688247; <http://dx.doi.org/10.1007/s00424-004-1353-7>
 112. Brasaemle DL, Wolins NE. Packaging of fat: an evolving model of lipid droplet assembly and expansion. *J Biol Chem* 2012; 287:2273-9; PMID:22090029; <http://dx.doi.org/10.1074/jbc.R111.309088>
 113. Walther TC, Farese RV. Lipid droplets and cellular lipid metabolism. *Annu Rev Biochem* 2012; 81:687-714; PMID:22524315; <http://dx.doi.org/10.1146/annurev-biochem-061009-102430>
 114. Beller M, Thiel K, Thul PJ, Jäckle H. Lipid droplets: a dynamic organelle moves into focus. *FEBS Lett* 2010; 584:2176-82; PMID:20303960; <http://dx.doi.org/10.1016/j.febslet.2010.03.022>
 115. Miranda DA, Kim J-H, Nguyen LN, Cheng W, Tan BC, Goh VJ, Tan JSY, Yaligar J, Kn BP, Velan SS, et al. Fat storage-inducing transmembrane protein 2 is required for normal fat storage in adipose tissue. *J Biol Chem* 2014; 289:9560-72; PMID:24519944; <http://dx.doi.org/10.1074/jbc.M114.547687>
 116. Gong J, Sun Z, Li P. CIDE proteins and metabolic disorders. *Curr Opin Lipidol* 2009; 20:121-6; PMID:19276890; <http://dx.doi.org/10.1097/MOL.0b013e328328d0bb>
 117. Cinti S. Transdifferentiation properties of adipocytes in the adipose organ. *Am J Physiol Endocrinol Metab* 2009; 297(5):E977-86; PMID:19458063; <http://dx.doi.org/10.1152/ajpendo.00183.2009>
 118. Zhou Z, Yon Toh S, Chen Z, Guo K, Ng CP, Ponniah S, Lin S-C, Hong W, Li P. Cidea-deficient mice have lean phenotype and are resistant to obesity. *Nat Genet* 2003; 35:49-56; PMID:12910269; <http://dx.doi.org/10.1038/ng1225>
 119. Li P. Cidea, brown fat and obesity. *Mech Ageing Dev* 2004; 125:337-8; PMID:15063110; <http://dx.doi.org/10.1016/j.mad.2004.01.002>
 120. Qi J, Gong J, Zhao T, Zhao J, Lam P, Ye J, Li JZ, Wu J, Zhou H-M, Li P. Downregulation of AMP-activated protein kinase by Cidea-mediated ubiquitination and degradation in brown adipose tissue. *EMBO J* 2008; 27:1537-48; PMID:18480843; <http://dx.doi.org/10.1038/emboj.2008.92>
 121. Shimizu T, Yokotani K. Acute cold exposure-induced down-regulation of CIDEA, cell death-inducing DNA fragmentation factor-alpha-like effector A, in rat interscapular brown adipose tissue by sympathetically activated beta3-adrenoreceptors. *Biochem Biophys Res Commun* 2009; 387:294-9; PMID:19577538; <http://dx.doi.org/10.1016/j.bbrc.2009.06.147>
 122. Grahn THM, Kaur R, Yin J, Schweiger M, Sharma VM, Lee M-J, Ido Y, Smas CM, Zechner R, Lass A, et al. Fat-specific protein 27 (FSP27) interacts with adipose triglyceride lipase (ATGL) to regulate lipolysis and insulin sensitivity in human adipocytes. *J Biol Chem* 2014; 289:12029-39; PMID:24627478; <http://dx.doi.org/10.1074/jbc.M113.539890>
 123. Puri V, Konda S, Ranjit S, Aouadi M, Chawla A, Chouinard M, Chakladar A, Czech MP. Fat-specific protein 27, a novel lipid droplet protein that enhances triglyceride storage. *J Biol Chem* 2007; 282:34213-8; PMID:17884815; <http://dx.doi.org/10.1074/jbc.M707404200>
 124. Toh SY, Gong J, Du G, Li JZ, Yang S, Ye J, Yao H, Zhang Y, Xue B, Li Q, et al. Up-regulation of mitochondrial activity and acquirement of brown adipose tissue-like property in the white adipose tissue of fsp27 deficient mice. *PLoS One* 2008; 3:e2890; PMID:18682832; <http://dx.doi.org/10.1371/journal.pone.0002890>
 125. Lafontan M, Langin D. Lipolysis and lipid mobilization in human adipose tissue. *Prog Lipid Res* 2009; 48:275-97; PMID:19464318; <http://dx.doi.org/10.1016/j.plipres.2009.05.001>
 126. Zimmermann R, Strauss JG, Haemmerle G, Schoiswohl G, Birner-Gruenberger R, Riederer M, Lass A, Neuberger G, Eisenhaber F, Hermetter A, et al. Fat mobilization in adipose tissue is promoted by adipose triglyceride lipase. *Science* 2004; 306:1383-6; PMID:15550674; <http://dx.doi.org/10.1126/science.1100747>
 127. Villena JA, Roy S, Sarkadi-Nagy E, Kim K-H, Sul HS. Desnutrin, an adipocyte gene encoding a novel patatin domain-containing protein, is induced by fasting and glucocorticoids: ectopic expression of desnutrin increases triglyceride hydrolysis. *J Biol Chem* 2004; 279:47066-75; PMID:15337759; <http://dx.doi.org/10.1074/jbc.M403855200>
 128. Jenkins CM, Mancuso DJ, Yan W, Sims HF, Gibson B, Gross RW. Identification, cloning, expression, and purification of three novel human calcium-independent phospholipase A2 family members possessing triacylglycerol lipase and acylglycerol transacylase activities. *J Biol Chem* 2004; 279:48968-75; PMID:15364929; <http://dx.doi.org/10.1074/jbc.M407841200>
 129. Zechner R, Kienesberger PC, Haemmerle G, Zimmermann R, Lass A. Adipose triglyceride lipase and the lipolytic catabolism of cellular fat stores. *J Lipid Res* 2009; 50:3-21; PMID:18952573; <http://dx.doi.org/10.1194/jlr.R800031-JLR200>
 130. Lass A, Zimmermann R, Oberer M, Zechner R. Lipolysis - a highly regulated multi-enzyme complex mediates the catabolism of cellular fat stores. *Prog Lipid Res* 2011; 50:14-27; PMID:21087632; <http://dx.doi.org/10.1016/j.plipres.2010.10.004>

131. Lass A, Zimmermann R, Haemmerle G, Riederer M, Schoiswohl G, Schweiger M, Kienesberger P, Strauss JG, Gorkiewicz G, Zechner R. Adipose triglyceride lipase-mediated lipolysis of cellular fat stores is activated by CGI-58 and defective in Chanarin-Dorfman Syndrome. *Cell Metab* 2006; 3:309-19; PMID:16679289; <http://dx.doi.org/10.1016/j.cmet.2006.03.005>
132. Yang X, Lu X, Lombès M, Rha GB, Chi Y-I, Guerin TM, Smart EJ, Liu J. The G(0)/G(1) switch gene 2 regulates adipose lipolysis through association with adipose triglyceride lipase. *Cell Metab* 2010; 11:194-205; PMID:20197052; <http://dx.doi.org/10.1016/j.cmet.2010.02.003>
133. Haemmerle G, Lass A, Zimmermann R, Gorkiewicz G, Meyer C, Rozman J, Heldmaier G, Maier R, Theussl C, Eder S, et al. Defective lipolysis and altered energy metabolism in mice lacking adipose triglyceride lipase. *Science* 2006; 312:734-7; PMID:16675698; <http://dx.doi.org/10.1126/science.1123965>
134. Ahmadian M, Duncan RE, Varady KA, Frasson D, Hellerstein MK, Birkenfeld AL, Samuel VT, Shulman GI, Wang Y, Kang C. Adipose overexpression of desnutrin promotes fatty acid use and attenuates diet-induced obesity. 2009; 58.
135. Pinent M, Hackl H, Burkard TR, Prokesch A, Papak C, Scheideler M, Hämmerle G, Zechner R, Trajanoski Z, Strauss JG. Differential transcriptional modulation of biological processes in adipocyte triglyceride lipase and hormone-sensitive lipase-deficient mice. *Genomics* 2008; 92:26-32; PMID:18572100; <http://dx.doi.org/10.1016/j.ygeno.2008.03.010>
136. Ahmadian M, Abbott MJ, Tang T, Hudak CSS, Kim Y, Bruss M, Hellerstein MK, Lee H-Y, Samuel VT, Shulman GI, et al. Desnutrin/ATGL is regulated by AMPK and is required for a brown adipose phenotype. *Cell Metab* 2011; 13:739-48; PMID:21641555; <http://dx.doi.org/10.1016/j.cmet.2011.05.002>
137. Mottillo EP, Bloch AE, Leff T, Granneman JG. Lipolytic products activate peroxisome proliferator-activated receptor (PPAR) α and δ in brown adipocytes to match fatty acid oxidation with supply. *J Biol Chem* 2012; 287:25038-48; PMID:22685301; <http://dx.doi.org/10.1074/jbc.M112.374041>
138. Vaughan M, Berger J, Steinberg D. Hormone-sensitive lipase and tissue hormone-sensitive lipase and monoglyceride activities in adipose tissue. *J Biol Chem* 1964; 239:401-9; PMID:14169138
139. Holm C, Osterlund T, Laurell H, Contreras JA. Molecular mechanisms regulating hormone-sensitive lipase and lipolysis. *Annu Rev Nutr* 2000; 20:365-93; PMID:10940339; <http://dx.doi.org/10.1146/annurev.nutr.20.1.365>
140. Holm C, Fredrikson G, Cannon B, Belfrage P. Hormone-sensitive lipase in brown adipose tissue: identification and effect of cold exposure. *Biosci Rep* 1987; 7:897-904; PMID:3329536; <http://dx.doi.org/10.1007/BF01119481>
141. Fredrikson G, Belfrage P. Positional specificity of hormone-sensitive lipase from rat adipose tissue. *J Biol Chem* 1983; 258:14253-6; PMID:6643478
142. Haemmerle G, Zimmermann R, Hayn M, Theussl C, Waeg G, Wagner E, Sattler W, Magin TM, Wagner EF, Zechner R. Hormone-sensitive lipase deficiency in mice causes diglyceride accumulation in adipose tissue, muscle, and testis. *J Biol Chem* 2002; 277:4806-15; PMID:11717312; <http://dx.doi.org/10.1074/jbc.M110355200>
143. Wang H, Hu L, Dalen K, Dorward H, Marcinkiewicz A, Russell D, Gong D, Londos C, Yamaguchi T, Holm C, et al. Activation of hormone-sensitive lipase requires two steps, protein phosphorylation and binding to the PAT-1 domain of lipid droplet coat proteins. *J Biol Chem* 2009; 284:32116-25; PMID:19717842; <http://dx.doi.org/10.1074/jbc.M109.006726>
144. Holm C. Molecular mechanisms regulating hormone-sensitive lipase and lipolysis. *Biochem Soc Trans* 2003; 31:1120; PMID:14641008; <http://dx.doi.org/10.1042/bst0311120>
145. Osuga J -I, Ishibashi S, Oka T, Yagyu H, Tozawa R, Fujimoto A, Shionoiri F, Yahagi N, Kraemer FB, Tsutsumi O, et al. Targeted disruption of hormone-sensitive lipase results in male sterility and adipocyte hypertrophy, but not in obesity. *Proc Natl Acad Sci* 2000; 97:787-92; PMID:10639158; <http://dx.doi.org/10.1073/pnas.97.2.787>
146. Ström K, Hansson O, Lucas S, Nevsten P, Fernandez C, Klint C, Movérare-Skrtic S, Sundler F, Ohlsson C, Holm C. Attainment of brown adipocyte features in white adipocytes of hormone-sensitive lipase null mice. *PLoS One* 2008; 3:e1793; PMID:18335062; <http://dx.doi.org/10.1371/journal.pone.0001793>
147. Sakurada T, Noma A. Subcellular localization and some properties of monoacylglycerol lipase in rat adipocytes. *J Biochem* 1981; 90:1413-9; PMID:7338512
148. Zechner R, Zimmermann R, Eichmann TO, Kohlwein SD, Haemmerle G, Lass A, Madeo F. FAT SIGNALS—lipases and lipolysis in lipid metabolism and signaling. *Cell Metab* 2012; 15:279-91; PMID:22405066; <http://dx.doi.org/10.1016/j.cmet.2011.12.018>
149. Egan JJ, Greenberg AS, Chang M, Wek SA, Moos MC, Londos C. Mechanism of hormone-stimulated lipolysis in adipocytes: Translocation of hormone-sensitive lipase to the lipid storage droplet. 1992; 89:8537-41; PMID:1528859
150. Clifford GM. Translocation of Hormone-sensitive Lipase and Perilipin upon Lipolytic Stimulation of Rat Adipocytes. *J Biol Chem* 2000; 275:5011-5; PMID:10671541; <http://dx.doi.org/10.1074/jbc.275.7.5011>
151. Granneman JG, Moore H-PH, Granneman RL, Greenberg AS, Obin MS, Zhu Z. Analysis of lipolytic protein trafficking and interactions in adipocytes. *J Biol Chem* 2007; 282:5726-35; PMID:17189257; <http://dx.doi.org/10.1074/jbc.M610580200>
152. Doh K-O, Kim Y-W, Park S-Y, Lee S-K, Park JS, Kim J-Y. Interrelation between long-chain fatty acid oxidation rate and carnitine palmitoyltransferase 1 activity with different isoforms in rat tissues. *Life Sci* 2005; 77:435-43; PMID:15894012; <http://dx.doi.org/10.1016/j.lfs.2004.11.032>
153. Feldmann HM, Golozoubova V, Cannon B, Nedergaard J. UCP1 ablation induces obesity and abolishes diet-induced thermogenesis in mice exempt from thermal stress by living at thermoneutrality. *Cell Metab* 2009; 9:203-9; PMID:19187776; <http://dx.doi.org/10.1016/j.cmet.2008.12.014>
154. Ueta CB, Fernandes GW, Capelo LP, Fonseca TL, Maculan FD, Gouveia CHA, Brum PC, Christoffoleto MA,

- Aoki MS, Lancellotti CL, et al. $\beta(1)$ Adrenergic receptor is key to cold- and diet-induced thermogenesis in mice. *J Endocrinol* 2012; 214:359-65; PMID:22728333; <http://dx.doi.org/10.1530/JOE-12-0155>
155. Rothwell NJ, Stock MJ. A role for brown adipose tissue in diet-induced thermogenesis. *Nature* 1979; 281:31-5; PMID:551265; <http://dx.doi.org/10.1038/281031a0>
 156. Yu XX, Lewin DA, Forrest W, Adams SH. Cold elicits the simultaneous induction of fatty acid synthesis and beta-oxidation in murine brown adipose tissue: prediction from differential gene expression and confirmation in vivo. *FASEB J* 2002; 16:155-68; PMID:11818363; <http://dx.doi.org/10.1096/fj.01-0568com>
 157. Li Y, Fromme T, Schweizer S, Schöttl T, Klingenspor M. Taking control over intracellular fatty acid levels is essential for the analysis of thermogenic function in cultured primary brown and brite / beige adipocytes. *EMBO Rep* 2014; 15:1069-76.
 158. Bukowiecki LJ, Folllea N, Lupien J, Paradis A. Metabolic relationships between lipolysis and respiration in rat brown. *Respiration* 1981; 256:12840-8
 159. Ellis JM, Li LO, Wu P-C, Koves TR, Ilkayeva O, Stevens RD, Watkins SM, Muoio DM, Coleman RA. Adipose acyl-CoA synthetase-1 directs fatty acids toward beta-oxidation and is required for cold thermogenesis. *Cell Metab* 2010; 12:53-64; PMID:20620995; <http://dx.doi.org/10.1016/j.cmet.2010.05.012>
 160. McGarry JD, Foster DW. Regulation of hepatic fatty acid oxidation and ketone body production. *Annu Rev Biochem* 1980; 49:395-420; PMID:6157353; <http://dx.doi.org/10.1146/annurev.bi.49.070180.002143>
 161. McGarry JD, Woeltje KF, Kuwajima M, Foster DW. Regulation of ketogenesis and the renaissance of carnitine palmitoyltransferase. *Diabetes Metab Rev* 1989; 5:271-84; PMID:2656156; <http://dx.doi.org/10.1002/dmr.5610050305>
 162. Curtis DE, Sukumaran S, Shao X, Parameswara V, Rashid S, Corte A, Smith AR, Ren J, Esser V, Hammer RE, et al. Article Molecular Mechanisms of Hepatic Steatosis and Insulin Resistance in the AGPAT2-Deficient Mouse Model of Congenital Generalized Lipodystrophy. 2009; 165-76.
 163. Esser V, Britton CH, Weis BC, Foster DW, McGarry JD. Cloning, sequencing, and expression of a cDNA encoding rat liver carnitine palmitoyltransferase I: Direct evidence that a single polypeptide is involved in inhibitor interaction and catalytic function. *J Biol Chem* 1993; 268:5817-22; PMID:8449948
 164. Yamazaki N, Shinohara Y, Shima A, Terada H. High expression of a novel carnitine palmitoyltransferase I like protein in rat brown adipose tissue and heart: isolation and characterization of its cDNA clone. *FEBS Lett* 1995; 363:41-5; PMID:7729550; [http://dx.doi.org/10.1016/0014-5793\(95\)00277-G](http://dx.doi.org/10.1016/0014-5793(95)00277-G)
 165. Price N, van der Leij F, Jackson V, Corstorphine C, Thomson R, Sorensen A, Zammit V. A novel brain-expressed protein related to carnitine palmitoyltransferase I. *Genomics* 2002; 80:433-42; PMID:12376098; <http://dx.doi.org/10.1006/geno.2002.6845>
 166. Brown NF, Hill JK, Esser V, Kirkland JL, Corkey BE, Foster DW, McGarry JD. Mouse white adipocytes and 3T3-L1 cells display an anomalous pattern of carnitine palmitoyltransferase (CPT) I isoform expression during differentiation. Inter-tissue and inter-species expression of CPT I and CPT II enzymes. *Biochem J* 1997; 327 (Pt 1):225-31; PMID:9355756; <http://dx.doi.org/10.1042/bj3270225>
 167. Sierra AY, Gratacós E, Carrasco P, Clotet J, Ureña J, Serra D, Asins G, Hegardt FG, Casals N. CPT1c is localized in endoplasmic reticulum of neurons and has carnitine palmitoyltransferase activity. *J Biol Chem* 2008; 283:6878-85; PMID:18192268; <http://dx.doi.org/10.1074/jbc.M707965200>
 168. Gao S, Zhu G, Gao X, Wu D, Carrasco P, Casals N, Hegardt FG, Moran TH, Lopaschuk GD. Important roles of brain-specific carnitine palmitoyltransferase and ceramide metabolism in leptin hypothalamic control of feeding. *Proc Natl Acad Sci U S A* 2011; 108:9691-6; PMID:21593415; <http://dx.doi.org/10.1073/pnas.1103267108>
 169. Ramírez S, Martins L, Jacas J, Carrasco P, Pozo M, Clotet J, Serra D, Hegardt FG, Diéguez C, López M, et al. Hypothalamic ceramide levels regulated by CPT1C mediate the orexigenic effect of ghrelin. *Diabetes* 2013; 62:2329-37; PMID:23493572; <http://dx.doi.org/10.2337/db12-1451>
 170. Ramsay RR, Gandour RD, Van Der Leij FR. Molecular enzymology of carnitine transfer and transport. *Biochim Biophys Acta - Protein Struct Mol Enzymol* 2001; 1546:21-43; PMID:11257506; [http://dx.doi.org/10.1016/S0167-4838\(01\)00147-9](http://dx.doi.org/10.1016/S0167-4838(01)00147-9)
 171. Alam A, Saggerson E. Malonyl-CoA and the regulation of fatty acid oxidation in soleus muscle. *Biochem J* 1998; 241:233-41; PMID:9693125; <http://dx.doi.org/10.1042/bj3340233>
 172. Esser V, Brown NF, Cowan AT, Foster DW, McGarry JD, Lett HF. Expression of a cDNA Isolated from Rat Brown Adipose Tissue and Heart Identifies the Product as the Muscle Isoform of Carnitine Palmitoyltransferase I (M-CPT I) isolated from rat brown adipose tissue (BAT) by. *Biochemistry* 1996; 271:6972-7
 173. Morillas M, Gómez-Puertas P, Bentebibel A, Sellés E, Casals N, Valencia A, Hegardt FG, Asins G, Serra D. Identification of conserved amino acid residues in rat liver carnitine palmitoyltransferase I critical for malonyl-CoA inhibition: Mutation of methionine 593 abolishes malonyl-CoA inhibition. *J Biol Chem* 2003; 278:9058-63; PMID:12499375; <http://dx.doi.org/10.1074/jbc.M209999200>
 174. Ji S, You Y, Kerner J, Hoppel CL, Schoeb TR, Chick WSH, Hamm DA, Sharer JD, Wood PA. Homozygous carnitine palmitoyltransferase 1b (muscle isoform) deficiency is lethal in the mouse. *Mol Genet Metab* 2008; 93:314-22; PMID:18023382; <http://dx.doi.org/10.1016/j.ymgme.2007.10.006>
 175. Jamal Z, Saggerson ED. Changes in brown-adipose-tissue mitochondrial processes in streptozotocin-diabetes. *Biochem J* 1988; 252:293-6; PMID:3421907; <http://dx.doi.org/10.1042/bj2520293>
 176. Lee J, Ellis JM, Wolfgang MJ. Adipose fatty acid oxidation is required for thermogenesis and potentiates oxidative stress-induced inflammation. *Cell Rep* 2015; 10:266-79; PMID:25578732; <http://dx.doi.org/10.1016/j.celrep.2014.12.023>

177. Schuler AM, Gower BA, Matern D, Rinaldo P, Vockley J, Wood PA. Synergistic heterozygosity in mice with inherited enzyme deficiencies of mitochondrial fatty acid beta-oxidation. *Mol Genet Metab* 2005; 85:7-11; PMID:15862275; <http://dx.doi.org/10.1016/j.ymgme.2004.09.006>
178. Bruce CR, Hoy AJ, Turner N, Watt MJ, Allen TL, Carpenter K, Cooney GJ, Febbraio MA, Kraegen EW. Overexpression of carnitine palmitoyltransferase-1 in skeletal muscle is sufficient to enhance fatty acid oxidation and improve high-fat diet-induced insulin resistance. *Diabetes* 2009; 58:550-8; PMID:19073774; <http://dx.doi.org/10.2337/db08-1078>
179. Perdomo G, Commerford SR, Richard A-MT, Adams SH, Corkey BE, O'Doherty RM, Brown NF. Increased beta-oxidation in muscle cells enhances insulin-stimulated glucose metabolism and protects against fatty acid-induced insulin resistance despite intramyocellular lipid accumulation. *J Biol Chem* 2004; 279:27177-86; PMID:15105415; <http://dx.doi.org/10.1074/jbc.M403566200>
180. Stefanovic-Racic M, Perdomo G, Mantell BS, Sipula IJ, Brown NF, O'Doherty RM. A moderate increase in carnitine palmitoyltransferase 1a activity is sufficient to substantially reduce hepatic triglyceride levels. *Am J Physiol Endocrinol Metab* 2008; 294:E969-77; PMID:18349115; <http://dx.doi.org/10.1152/ajpendo.00497.2007>
181. Orellana-Gavaldà JM, Herrero L, Malandrino MI, Pañeda A, Sol Rodríguez-Peña M, Petry H, Asins G, Van Deventer S, Hegardt FG, Serra D, et al. Molecular therapy for obesity and diabetes based on a long-term increase in hepatic fatty-acid oxidation. *Hepatology* 2011; 53:821-32; PMID:21319201; <http://dx.doi.org/10.1002/hep.24140>
182. Monsenego J, Mansouri A, Akkaoui M, Lenoir V, Esnous C, Fauveau V, Tavernier V, Girard J, Prip-Buus C, Monsénego J, et al. Enhancing liver mitochondrial fatty acid oxidation capacity in obese mice improves insulin sensitivity independently of hepatic steatosis. *J Hepatol* 2012; 56:632-9; PMID:22037024; <http://dx.doi.org/10.1016/j.jhep.2011.10.008>
183. Sebastián D, Herrero L, Serra D, Asins G, Hegardt FG, Sebastian D, Herrero L, Serra D, Asins G, Hegardt FG. CPT I overexpression protects L6E9 muscle cells from fatty acid-induced insulin resistance. *Am J Physiol Endocrinol Metab* 2007; 292:E677-86; PMID:17062841; <http://dx.doi.org/10.1152/ajpendo.00360.2006>
184. Namgaladze D, Lips S, Leiker TJ, Murphy RC, Ekroos K, Ferreiros N, Geisslinger G, Brüne B. Inhibition of macrophage fatty acid β -oxidation exacerbates palmitate-induced inflammatory and endoplasmic reticulum stress responses. *Diabetologia* 2014; 57:1067-77; PMID:24488024; <http://dx.doi.org/10.1007/s00125-014-3173-4>
185. Gao X, Li K, Hui X, Kong X, Sweeney G, Wang Y, Xu A, Teng M, Liu P, Wu D. Carnitine palmitoyltransferase 1A prevents fatty acid-induced adipocyte dysfunction through suppression of c-Jun N-terminal kinase. *Biochem J* 2011; 435:723-32; PMID:21348853; <http://dx.doi.org/10.1042/BJ20101680>
186. Malandrino MI, Fucho R, Weber M, Calderon-Dominguez M, Mir JF, Valcarcel L, Escoté X, Gómez-Serrano M, Peral B, Salvadó L, et al. Enhanced fatty acid oxidation in adipocytes and macrophages reduces lipid-induced triglyceride accumulation and inflammation. *Am J Physiol Endocrinol Metab* 2015; 308:E756-69; PMID:25714670; <http://dx.doi.org/10.1152/ajpendo.00362.2014>
187. Herrero L, Rubí B, Sebastián D, Serra D, Asins G, Maechler P, Prentki M, Hegardt FG. Alteration of the malonyl-CoA/carnitine palmitoyltransferase I interaction in the beta-cell impairs glucose-induced insulin secretion. *Diabetes* 2005; 54:462-71; PMID:15677504; <http://dx.doi.org/10.2337/diabetes.54.2.462>
188. Mera P, Mir JF, Fabriás G, Casas J, Costa ASH, Malandrino MI, Fernández-López J-A, Remesar X, Gao S, Chohann S, et al. Long-term increased carnitine palmitoyltransferase 1A expression in ventromedial hypothalamus causes hyperphagia and alters the hypothalamic lipidomic profile. *PLoS One* 2014; 9:e97195; PMID:24819600; <http://dx.doi.org/10.1371/journal.pone.0097195>
189. Serra D, Mera P, Malandrino MI, Mir JF, Herrero L. Mitochondrial fatty acid oxidation in obesity. *Antioxid Redox Signal* 2013; 19:269-84; PMID:22900819; <http://dx.doi.org/10.1089/ars.2012.4875>
190. Singh I, Moser AE, Goldfischer S, Moser HW. Lignoceric acid is oxidized in the peroxisome: implications for the Zellweger cerebro-hepato-renal syndrome and adrenoleukodystrophy. *Proc Natl Acad Sci U S A* 1984; 81:4203-7; PMID:6588384; <http://dx.doi.org/10.1073/pnas.81.13.4203>
191. Nedergaard J, Alexson S, Cannon B. Cold adaptation in the rat: increased brown fat peroxisomal beta-oxidation relative to maximal mitochondrial oxidative capacity. *Am J Physiol Cell Physiol* 1980; 239:C208-16
192. Ahlaba I, Barnard T. Observations on peroxisomes in brown adipose tissue of the rat. *J Histochem Cytochem* 1971; 19:670-5; PMID:4107748; <http://dx.doi.org/10.1177/19.11.670>
193. Lodhi IJ, Semenkovich CF. Peroxisomes: a nexus for lipid metabolism and cellular signaling. *Cell Metab* 2014; 19:380-92; PMID:24508507; <http://dx.doi.org/10.1016/j.cmet.2014.01.002>
194. Schneider BE, Mun EC. Surgical management of morbid obesity. *Diabetes Care* 2005; 28:475-80; PMID:15677820; <http://dx.doi.org/10.2337/diacare.28.2.475>
195. Mumphrey MB, Patterson LM, Zheng H, Berthoud H-R. Roux-en-Y gastric bypass surgery increases number but not density of CCK-, GLP-1-, 5-HT-, and neurotensin-expressing enteroendocrine cells in rats. *Neurogastroenterol Motil* 2013; 25:e70-9; PMID:23095091; <http://dx.doi.org/10.1111/nmo.12034>
196. Tremaroli V, Karlsson F, Werling M, Ståhlman M, Kovatcheva-Datchary P, Olbers T, Fändriks L, le Roux CW, Nielsen J, Bäckhed F. Roux-en-Y gastric bypass and vertical banded gastroplasty induce long-term changes on the human Gut microbiome contributing to fat mass regulation. *Cell Metab* 2015; 22:228-38; PMID:26244932; <http://dx.doi.org/10.1016/j.cmet.2015.07.009>
197. Hurt RT, Edakkanambeth Varayil J, Ebbert JO. New pharmacological treatments for the management of obesity. *Curr Gastroenterol Rep* 2014; 16:394; PMID:24828101; <http://dx.doi.org/10.1007/s11894-014-0394-0>

198. Jackson VM, Price DA, Carpino PA. Investigational drugs in Phase II clinical trials for the treatment of obesity: implications for future development of novel therapies. *Expert Opin Investig Drugs* 2014; 23:1055-66; PMID:25000213; <http://dx.doi.org/10.1517/13543784.2014.918952>
199. EMA. Guideline on clinical evaluation of medicinal products used in weight control. London: 2014. Available from: http://www.ema.europa.eu/docs/en_GB/document_library/Scientific_guideline/2014/07/WC500170278.pdf
200. Derosa G, Maffioli P. Anti-obesity drugs: a review about their effects and their safety. *Expert Opin Drug Saf* 2012; 11:459-71; PMID:22439841; <http://dx.doi.org/10.1517/14740338.2012.675326>
201. O'Neil PM, Smith SR, Weissman NJ, Fidler MC, Sanchez M, Zhang J, Raether B, Anderson CM, Shanahan WR. Randomized Placebo-Controlled Clinical Trial of Lorcaserin for Weight Loss in Type 2 Diabetes Mellitus: The BLOOM-DM Study. *Obes (Silver Spring)* 2012; 20:1426-36; PMID:22421927; <http://dx.doi.org/10.1038/oby.2012.66>
202. Khan A, Raza S, Khan Y, Aksoy T, Khan M, Weinberger Y, Goldman J. Current updates in the medical management of obesity. *Recent Pat Endocr Metab Immune Drug Discov* 2012; 6:117-28; PMID:22435392; <http://dx.doi.org/10.2174/187221412800604644>
203. EMA. Withdrawal of the marketing authorisation application for Belviq (lorcaserin). London: 2013. Available from: http://www.ema.europa.eu/docs/en_GB/document_library/Medicine_QA/2013/05/WC500143811.pdf
204. FDA. Liraglutide 3.0 mg for Weight Management NDA 206-321 Briefing Document Endocrinologic and Metabolic Drug Advisory Committee. Silver Spring, MD: 2014. Available from: <http://www.fda.gov/downloads/advisorycommittees/committeesmeetingmaterials/drugs/endocrinologicandmetabolicdrugsadvisorycommittee/ucm413318.pdf>
205. EMA. Saxenda recommended for approval in weight management in adults Medicine to be used in addition to reduced-calorie diet and physical activity. London: 2015. Available from: http://www.ema.europa.eu/docs/en_GB/document_library/Press_release/2015/01/WC500180857.pdf
206. Jeon WS, Park CY. Antiobesity pharmacotherapy for patients with type 2 diabetes: focus on long-term management. *Endocrinol Metab (Seoul, Korea)* 2014; 29:410-7; PMID:25559569; <http://dx.doi.org/10.3803/EnM.2014.29.4.410>
207. Caixàs A, Albert L, Capel I, Rigla M. Naltrexone sustained-release/bupropion sustained-release for the management of obesity: review of the data to date. *Drug Des Devel Ther* 2014; 8:1419-27; PMID:25258511; <http://dx.doi.org/10.2147/DDDT.S55587>
208. Hamdy O, Uwaifo GI, Oral EA. Obesity Medication. *Medscape* 2015; Available from: <http://emedicine.medscape.com/article/123702-medication>
209. Zhu Z, Spicer EG, Gavini CK, Goudjo-Ako AJ, Novak CM, Shi H. Enhanced sympathetic activity in mice with brown adipose tissue transplantation (transBATation). *Physiol Behav* 2014; 125:21-9; PMID:24291381; <http://dx.doi.org/10.1016/j.physbeh.2013.11.008>
210. Dong M, Yang X, Lim S, Cao Z, Honek J, Lu H, Zhang C, Seki T, Hosaka K, Wahlberg E, et al. Cold exposure promotes atherosclerotic plaque growth and instability via UCP1-dependent lipolysis. *Cell Metab* 2013; 18:118-29; PMID:23823482; <http://dx.doi.org/10.1016/j.cmet.2013.06.003>
211. Berbée JFP, Boon MR, Khedoe PPSJ, Bartelt A, Schlein C, Worthmann A, Kooijman S, Hoeke G, Mol IM, John C, et al. Brown fat activation reduces hypercholesterolaemia and protects from atherosclerosis development. *Nat Commun* 2015; 6:6356; PMID:25754609; <http://dx.doi.org/10.1038/ncomms7356>
212. Muoio DM, Neuffer PD. Lipid-induced mitochondrial stress and insulin action in muscle. *Cell Metab* 2012; 15:595-605; PMID:22560212; <http://dx.doi.org/10.1016/j.cmet.2012.04.010>